

DEVELOPMENT OF A NEW METHODOLOGY FOR THE SYNTHESIS OF
HALOCONDURITOLS AND GOLD CATALYZED ALKYNE
CYCLIZATIONS OF *N*-PROPARGYL SUBSTITUTED INDOLE
DERIVATIVES

A THESIS SUBMITTED TO
THE GRADUATE SCHOOL OF NATURAL AND APPLIED SCIENCES
OF
MIDDLE EAST TECHNICAL UNIVERSITY

BY

SERDAL KAYA

IN PARTIAL FULFILLMENT OF THE REQUIREMENTS
FOR
THE DEGREE OF DOCTOR OF PHILOSOPHY
IN
CHEMISTRY

DECEMBER 2015

Approval of the thesis:

**DEVELOPMENT OF A NEW METHODOLOGY FOR THE SYNTHESIS
OF HALOCONDURITOLS AND GOLD CATALYZED ALKYNE
CYCLIZATIONS OF *N*-PROPARGYL SUBSTITUTED INDOLE
DERIVATIVES**

submitted by **SERDAL KAYA** in partial fulfillment of the requirements for the degree of **Doctor of Philosophy in Department of Chemistry, Middle East Technical University** by,

Prof. Dr. Gülbin Dural Ünver
Dean, Graduate School of **Natural and Applied Sciences**

Prof. Dr. Cihangir Tanyeli
Head of Department, **Chemistry**

Prof. Dr. Metin Balcı
Supervisor, **Chemistry Dept., METU**

Examining Committee Members:

Prof. Dr. Mustafa Güllü
Chemistry Dept., Ankara University

Prof. Dr. Metin Balcı
Chemistry Dept., METU

Prof. Dr. Cihangir Tanyeli
Chemistry Dept., METU

Prof. Dr. Metin Zora
Chemistry Dept., METU

Prof. Dr. Yunus Kara
Chemistry Dept., Atatürk University

Date: December 18, 2015

I hereby declare that all information in this document has been obtained and presented in accordance with academic rules and ethical conduct. I also declare that, as required by these rules and conduct, I have fully cited and referenced all material and results that are not original to this work.

Name, Last name: Serdal Kaya

Signature:

ABSTRACT

DEVELOPMENT OF A NEW METHODOLOGY FOR THE SYNTHESIS OF HALOCONDURITOLS AND GOLD CATALYZED ALKYNE CYCLIZATIONS OF *N*-PROPARGYL SUBSTITUTED INDOLE DERIVATIVES

Kaya, Serdal

PhD, Department of Chemistry

Supervisor: Prof. Dr. Metin Balcı

December 2015, 323 pages

Because of the biological properties and being useful intermediates, haloconduritols became synthetically important molecules. During the last decades, some methodologies have been developed for the construction of haloconduritol derivatives. Our synthetic strategy was based on stereospecific hydroxylation of one of the double bonds of commercially available cyclopentadiene. After protection of the hydroxyl groups as a ketal, the remaining double bond was submitted to the dibromocarbene addition reaction. Silver-promoted ring opening reaction of the tricyclic compound resulted in the formation of a six-membered ring with a double bond having a bromine atom. Removal of the ketal group under the acidic conditions gave bromocyclo-hexenetriols

In the second part of the thesis, the main interest was concentrated on the synthesis of nitrogen containing heterocycles. For this purpose, starting from *N*-propargyl-2-indole carbaldehyde or *N*-propargyl-2-indole carboxylic acid, the synthesis of the nitrogen containing heterocycles, such as pyrazino-indole-*N*-oxide, pyrazolo-pyrazino-indole, diazepino-indole and pyrazolo-diazepino-indole derivatives, were planned. Ring cyclization was carried out in the presence of Au(III) salt and NaH. Cyclization of oxime derivative derived from *N*-propargyl-indole aldehyde gave the corresponding pyrazine oxides. In case of substituted alkynes, an oxime-oxime rearrangement was observed which was unprecedented in the literature. Gold-catalyzed cyclization of *N*-propargyl indoles having a pyrazole ring attached to the

C-2 carbon atom underwent *6-exo-dig* and *7-endo-dig* cyclization reactions depending on the nature of the substituents attached to the terminal alkyne group. However, NaH-supported cyclization resulted in the formation of six-membered rings.

Keywords: Haloconduritols, carbene addition, gold catalyst, alkyne cyclization reaction, DFT calculations.

ÖZ

HALOKONDURİTOL SENTEZİ İÇİN YENİ BİR YÖNTEM GELİŞTİRİLMESİ VE *N*-PROPARGİL SÜBSTİTÜE İNDOL TÜREVLERİNİN ALTIN KATALİZÖRLÜĞÜNDE HALKALAŞMA TEPKİMELERİ

Kaya, Serdal

Doktora, Kimya Bölümü

Tez Yöneticisi: Prof. Dr. Metin Balcı

Aralık 2015, 323 sayfa

Halokonduritoller göstermiş oldukları biyolojik aktivite ve karmaşık yapılı bileşiklerin sentezlerinde ara kademe olmaları bakımından önemli bileşiklerdir. Son yıllarda halokonduritol türevlerinin sentezi için bazı metotlar geliştirilmiştir. Yapmış olduğumuz bu çalışma çerçevesinde ticari olarak temin edilebilen siklopentadien molekülü ve bu molekülün stereospesifik hidroksilasyon reaksiyonu başlangıç basamağı olarak seçildi. Oluşturulan diol grubu ketal olarak korunduktan sonra siklopentadien molekülünün diğer çift bağına dibromokarben katıldı. Elde edilen bu üç halkalı yapının gümüş iyonları varlığında halka açılma reaksiyonu ile çift bağa brom bağlı 6-üyelik halkalar sentezlendi. Ketal gruplarının yapıdan uzaklaştırılması ile de bromosikloheksentrioller elde edildi.

Çalışmanın ikinci bölümünde ise azot atomu içeren heterosiklik bileşiklerin sentezleri amaçlanmıştır. Bu amaç doğrultusunda, pirazino-indol-*N*-oksit, pirazolo-pirazino-indol, diazepino-indole ve pirazolo-diazepino-indol bileşiklerinin sentezleri *N*-propargil-indol-2-karbaldehit veya *N*-propargil-indol-2-karboksilik asitten başlayarak gerçekleştirildi. Halkalaşma reaksiyonları Au(III) tuzları veya NaH varlığında yapıldı. *N*-propargil-indol-2-karbaldoxim bileşiklerinin halkalaşma reaksiyonu ile ilgili pirazin-*N*-oksit bileşikleri sentezlendi. Sübstitüe alkin grubu içeren oksim bileşikleri ise literatürde daha önce bilinmeyen bir oksim-oksime düzenlenme reaksiyonu ile sonuçlandı. C-2 konumunda pirazol halkası içeren indol türevlerinin halkalaşma reaksiyonları ise alkin grubunun elektronik

yapısına baęlı olarak 6-*ekzo*-dig veya 7-*endo*-dig halkalařma ürünlerini oluřturdu. NaH varlıęında gerekleřtirilen halkalařma reaksiyonları ile ilgili 6-üyeliler halkaların oluřtuęu gözlemlendi.

Anahtar Kelimeler: Halokonduritoller, karben katılma reaksiyonları, altın katalizörü, alkin halkalařma reaksiyonları, DFT hesaplamaları.

To my precious family...

ACKNOWLEDGEMENT

I would like to express my deep thanks to my supervisor Prof. Dr. Metin Balcı for his continuous guidance, endless support, valuable advices, patience and encouragements. It was a great chance for me to be a student of Prof. Dr. Metin Balcı.

I would like to thank Dr. Nurettin Mengeş, Dr. Gani Koza, Dr. Sinan Başçeken, Dr. Dilem Doğan and Dr. Benan Kılbaş for their sincere assistance, sharing experience and advices through this research.

I would like to thank Özlem Sarı for her contribution during the theoretical calculations.

I would like to thank to NMR specialist Zehra Uzunoğlu and Betül Eymur for the NMR experiments.

I am particularly grateful for working with all SYNTHOR Research Group members, Selbi Keskin, Yasemin Altun, Nurettin Mengeş, Merve Gökçen Bekarlar, Emrah Karahan, Emre Hoplamaz, Çağatay Dengiz, Yasin Çetinkaya, Raşit Çalışkan, Melek Sermin Özer, Dilem Doğan, Zeynep Ekmekçi, Benan Kılbaş, Gani Koza, Nalan Korkmaz Çokol, Özlem Sarı, Işıl Yenice, Sultan Aslan, Merve Sinem Özer, Sinem Güven, Kadir Deliömeroğlu, Yasemin Dinçoflaz, Furgan Aslanoğlu, Başak Öztürk, Selin Ceyhan, Merve Ergun, Fatih Şeybek, Dilgeş Baskın, Tolga Kaptı, Kübra Kılıç, Meltem Tan, Sinan Başçeken, Burak Südemen, Alper Kılıklı, Berk Müjde, Erol Can Vatansever, Saniye Yazıcı, Özgür Yılmaz, Kıvılcım Şendil and Yusif Abdullayev. Without their warm friendship, great support and assistance, this research process would have been difficult.

I would like to thank all of the members of the Department of Chemistry of METU for their support and guidance, especially the organic staff. I have been learnt by valuable knowledge from them.

I would like to thank Middle East Technical University (METU), Giresun University and Faculty Development Program (ÖYP) for giving me a chance to study in METU.

I would like to thank TÜBİTAK (Scientific and Technological Research Council of Turkey, Project no: TBAG 112T360), Undersecretariat for Defense Industries & ROKETSAN and ÖYP for their financial support.

Finally, my special appreciation and great gratitude is devoted to my family; my wife, daughter, mother, father and brother for their endless love, and encouragement in every moment of my life. Without their support, it would be impossible to achieve this study and being successful as psychological and physiological.

TABLE OF CONTENTS

ABSTRACT	i
ÖZ.....	vii
ACKNOWLEDGEMENT.....	x
TABLE OF CONTENTS	xii
LIST OF FIGURES	xvii
LIST OF SCHEMES	xxvii
LIST OF TABLES	xxxii
LIST OF ABBREVIATIONS	xxxii
CHAPTERS	
1. DEVELOPMENT OF A NEW METHODOLOGY FOR THE SYNTHESIS OF HALOCONDURITOLS	1
1.1 Introduction	1
1.1.1 Cyclitols.....	2
1.1.2 Inositols	2
1.1.3 Quercitols	3
1.1.4 Conduritols	4
1.1.5 Synthesis of Conduritol Derivatives.....	6
1.1.6 Haloconduritols	27
1.1.7 Biological Importance of Conduritol Derivatives	32
1.1.8 Aim of the Study	34
1.2 Results and Discussion.....	35
1.2.1 Synthesis of cyclopent-3-ene-1,2-diol (207)	35
1.2.2 Synthesis of cyclopent-3-ene-1,2-diyl diacetate (213)	37
1.2.3 Attempted Oxidation of 207, 213, and 220 with Singlet Oxygen: Ene Reaction	38
1.2.4 Carbene Addition Reaction	40
1.2.5 Electrophilic Ring Opening Reaction of 231	46
1.2.6 Acetylation Reaction of the Major Ring-Opening product 234.	52

1.2.7	Allylic Oxidation Reaction of the Major Ring-Opening Product	234.
	53
1.2.8	α -Acetoxylation Reaction of 240 with Mn(OAc) ₃
		53
1.2.9	Reduction of α,β -Unsaturated Compound: The Luche Reduction	..
		56
1.2.10	Synthesis of Bromotriols 248-251: Deprotection of 234-237
		57
2.	GOLD CATALYZED ALKYNE CYCLIZATIONS OF THE <i>N</i> -PROPARGYL SUBSTITUTED INDOLE DERIVATIVES
		59
2.1	Introduction
		59
2.1.1	Indole
		60
2.1.2	Pyrazines
		63
2.1.3	Synthesis of Pyrazine Rings
		65
2.1.4	Diazepines
		67
2.1.5	Ring-Junction Nitrogen Containing Heterocyclic Molecules
		71
2.1.6	Gold Catalyzed Alkyne Cyclization Reactions
		72
2.1.7	Aim of the Study
		73
2.2	Results and Discussions
		75
2.2.1	Synthetic Applications of <i>N</i> -Alkyne Substituted Indole-2- carbaldoximes: Synthesis of Pyrazino[1,2- <i>a</i>]indole- <i>N</i> -oxide and Oxime- Oxime Rearrangement
		76
2.2.2	Intramolecular Gold-catalyzed and NaH-supported Cyclization Reactions of <i>N</i> -propargyl Indole Derivatives with Pyrazole Ring: Synthesis of Pyrazolo-pyrazino-indoles and Pyrazolo-diazepino-indoles
		91
3.	CONCLUSION
		105
4.	EXPERIMENTAL
		111
4.1	General
		111
4.2	Synthesis of cyclopent-3-ene-1,2-diol (207)
		112
4.3	Synthesis of cyclopent-3-ene-1,2-diyl diacetate (213)
		112
4.4	2,2-Dimethyl-4,6a-dihydro-3a <i>H</i> -cyclopenta[<i>d</i>][1,3]dioxole (220)
		113
4.5	4,4-Dibromo-2,2-dimethylhexahydrocyclopropa[3,4]cyclopenta[1,2- <i>d</i>][1,3]di-oxole (231)
		114
4.6	(3a <i>R</i> ,5 <i>S</i> ,7a <i>S</i>)-6-bromo-2,2-dimethyl-3a,4,5,7a-tetrahydrobenzo[<i>d</i>][1,3]- diox-ol-5-ol (234)
		115
4.7	(3a <i>R</i> ,5 <i>S</i> ,7a <i>S</i>)-6-bromo-2,2-dimethyl-3a,4,5,7a-tetrahydrobenzo[<i>d</i>][1,3]- diox-ol-5-yl acetate (239)
		117

4.8(3a <i>R</i> ,7a <i>S</i>)-6-bromo-2,2-dimethyl-3a,4-dihydrobenzo[<i>d</i>][1,3]dioxol-5(7a <i>H</i>)-one (240)	117
4.9(3a <i>S</i> , 4 <i>R</i> , 7a <i>S</i>)-6-bromo-2,2-dimethyl-5-oxo-3a,4,5,7a-tetrahydrobenzo[<i>d</i>]-[1,3]dioxol-4-yl acetate (241)	118
4.10 (1 <i>S</i> ,2 <i>R</i> ,4 <i>S</i>)-5-bromocyclohex-5-ene-1,2,4-triol (248)	119
4.11 (1 <i>S</i> ,2 <i>R</i> ,4 <i>R</i>)-5-bromocyclohex-5-ene-1,2,4-triol (249).....	119
4.12 (1 <i>R</i> ,2 <i>R</i> ,3 <i>R</i>)-4-bromocyclohex-4-ene-1,2,3-triol (250)	120
4.13 (1 <i>R</i> ,2 <i>R</i> ,3 <i>S</i>)-4-bromocyclohex-4-ene-1,2,3-triol (251).....	120
4.14 Ethyl-1 <i>H</i> -indole-2-carboxylate (353).....	121
4.15 1 <i>H</i> -indol-2-ylmethanol (354)	122
4.16 1 <i>H</i> -indole-2-carboxaldehyde (355)	122
4.17 1-Prop-2-ynyl-1 <i>H</i> -indole-2-carbaldehyde (357)	123
4.18 (<i>E/Z</i>)-1-(1-prop-2-ynyl-1 <i>H</i> -indol-2-yl)ethanone oxime (358 and 359).....	123
4.19 3-Methylpyrazino[1,2- <i>a</i>]indole-2-oxide (360).....	124
4.20 3-Methylpyrazino[1,2- <i>a</i>]indole (364).....	125
4.21 1-But-2-ynyl-1 <i>H</i> -indole-2-carbaldehyde (366).....	125
4.22 1-(3-Phenylprop-2-ynyl)-1 <i>H</i> -indole-2-carbaldehyde (367a).....	126
4.23 1-[3-(4-Methoxyphenyl)prop-2-ynyl]-1 <i>H</i> -indole-2-carb-aldehyde (367b)	127
4.24 1-[3-(3-nitrophenyl)prop-2-ynyl]-1 <i>H</i> -indole-2-carbaldehyde (367c) .	128
4.25 (<i>E/Z</i>)-1-(1-prop-2-ynyl-1 <i>H</i> -indol-2-yl)ethanone oxime (376a).	129
4.26 1-(3-Phenylprop-2-ynyl)-1 <i>H</i> -indole-2-carbaldehyde oxime (376b) ...	129
4.27 1-[3-(4-Methoxyphenyl)prop-2-ynyl]-1 <i>H</i> -indole-2-carbaldehyde oxime (376c).....	130
4.28 1-[(3 <i>E/Z</i>)-3-(hydroxyimino)butyl]-1 <i>H</i> -indole-2-carbaldehyde (378a)	131
4.29 1-[(3 <i>E/Z</i>)-3-(hydroxyimino)-3-phenylpropyl]-1 <i>H</i> -indole-2-carbaldehyde (378b)	132
4.30 1-[(3 <i>Z</i>)-3-(hydroxyimino)-3-(4-methoxyphenyl)propyl]-1 <i>H</i> -indole-2-carbaldehyde (378c)	133
4.31 Ethyl 1-(prop-2-yn-1-yl)-1 <i>H</i> -indole-2-carboxylate (390a)	133
4.32 Ethyl 1-(but-2-yn-1-yl)-1 <i>H</i> -indole-2-carboxylate (390b).	134
4.33 1-(Prop-2-yn-1-yl)-1 <i>H</i> -indole-2-carboxylic acid (391a).....	135
4.34 1-(But-2-yn-1-yl)-1 <i>H</i> -indole-2-carboxylic acid (391b).	135

4.35	Trimethyl(phenylethynyl)silane (394)	136
4.36	3-Phenyl-1-(1-(prop-2-yn-1-yl)-1 <i>H</i> -indol-2-yl)prop-2-yn-1-one (393a)	136
4.37	1-(1-(But-2-yn-1-yl)-1 <i>H</i> -indol-2-yl)-3-phenylprop-2-yn-1-one (393b)	137
4.38	3-Phenyl-1-(1-(3-phenylprop-2-yn-1-yl)-1 <i>H</i> -indol-2-yl)prop-2-yn-1-one (395a)	138
4.39	3-phenyl-1-(1-(3-(<i>p</i> -tolyl)prop-2-yn-1-yl)-1 <i>H</i> -indol-2-yl)prop-2-yn-1- one (395b)	139
4.40	1-(1-(3-(3-nitrophenyl)prop-2-yn-1-yl)-1 <i>H</i> -indol-2-yl)-3-phenylprop-2- yn-1-one (395c)	140
4.41	2-(3-phenyl-1 <i>H</i> -pyrazol-5-yl)-1-(prop-2-yn-1-yl)-1 <i>H</i> -indole (396a) ..	141
4.42	1-(but-2-yn-1-yl)-2-(3-phenyl-1 <i>H</i> -pyrazol-5-yl)-1 <i>H</i> -indole (396b)	141
4.43	2-(3-Phenyl-1 <i>H</i> -pyrazol-5-yl)-1-(3-phenylprop-2-yn-1-yl)-1 <i>H</i> -indole (396c)	142
4.44	2-(3-Phenyl-1 <i>H</i> -pyrazol-5-yl)-1-(3-(<i>p</i> -tolyl)prop-2-yn-1-yl)-1 <i>H</i> -indole (396d)	143
4.45	1-(3-(3-Nitrophenyl)prop-2-yn-1-yl)-2-(3-phenyl-1 <i>H</i> -pyrazol-5-yl)-1 <i>H</i> - indole (396e)	144
4.46	5-Methyl-2-phenylpyrazolo[5',1':3,4]pyrazino[1,2- <i>a</i>]indole (404a)....	144
4.47	2-phenylpyrazolo[5',1':3,4]pyrazino[1,2- <i>a</i>]indole (407).....	145
4.48	5-Benzyl-2-phenylpyrazolo[5',1':3,4]pyrazino[1,2- <i>a</i>]indole (404c)....	146
4.49	5-(4-methylbenzyl)-2-phenylpyrazolo[5',1':3,4]pyrazino[1,2- <i>a</i>]indole (404d)	147
4.50	5-(3-nitrobenzyl)-2-phenylpyrazolo[5',1':3,4]pyrazino[1,2- <i>a</i>]indole (404e)	147
4.51	5-methyl-2-phenylpyrazolo[5',1':3,4]pyrazino[1,2- <i>a</i>]indole (404a)	148
4.52	5-Methyl-2-phenyl-7 <i>H</i> -pyrazolo[5',1':3,4][1,4]diazepino[1,2- <i>a</i>]indole (408b)	149
4.53	2,5-diphenyl-7 <i>H</i> -pyrazolo[5',1':3,4][1,4]diazepino[1,2- <i>a</i>]indole (408c)	150
4.54	2-phenyl-5-(<i>p</i> -tolyl)-7 <i>H</i> -pyrazolo[5',1':3,4][1,4]diazepino[1,2- <i>a</i>]indole (408d)	150
4.55	5-(3-nitrophenyl)-2-phenyl-7 <i>H</i> -pyrazolo[5',1':3,4][1,4]diazepino[1,2- <i>a</i>]indole (408e).....	151

REFERENCES	153
APPENDICES	
A. SPECTRAL DATA.....	163
B. CARTESIAN COORDINATES FOR THE OPTIMIZED STRUCTURES	291
C. ABSOLUTE ENERGIES OF OPTIMIZED STRUCTURES IN GAS PHASE [DFT(B3LYP)/6-31+G(D,P)]	319
CURRICULUM VITAE	321

LIST OF FIGURES

FIGURES

Figure 1. Haloconduuritols	1
Figure 2. General structures of inositols, quercitols and conduuritols.....	2
Figure 3. Structures of inositol isomers 6-14.....	3
Figure 4. Quercitol isomers.....	4
Figure 5. Structures of conduuritol isomers 25-30.....	5
Figure 6. Haloconduuritols	28
Figure 7. Structures of Pancratistatine (194) and Lycoridicine (195).....	33
Figure 8. Structures of halichondrin-B (197) and hexol 198	33
Figure 9. The optimized geometry of the <i>cis</i> -cyclopent-3-ene-1,2-diol	37
Figure 10. Structures of singlet and triplet carbenes.....	40
Figure 11. Phase transfer catalyst mechanism for carbene generation	41
Figure 12. COSY spectrum of compound 231.....	44
Figure 13. The optimized geometry of the carbene-adduct 231	45
Figure 14. ¹³ C-NMR and DEPT-135 NMR spectrum of the compound 231.....	46
Figure 15. COSY spectrum of the compound 234.....	47
Figure 16. Optimized geometry of compounds 234, 235, 236 and 237.....	49
Figure 17. IR and Mass spectrum of compound 238	51
Figure 18. COSY spectrum of compound 238.....	51
Figure 19. Optimized geometry of possible configurations of 238	52
Figure 20. Optimized geometry of compounds 241	54
Figure 21. ¹ H-NMR of compound 242 and corresponding possible couplings	55
Figure 22. Heterocyclic compounds 252 and 253.....	59
Figure 23. Benzene, pyrrole, and indole structures.....	60
Figure 24. Indole containing bioactive molecules	61
Figure 25. Structures of isomeric diazines.....	63
Figure 26. Structures of some biologically active pyrazine derivatives	64

Figure 27. Structures of some biologically active pyrazino-indole derivatives	64
Figure 28. Structures of some pyrazine and indole <i>N</i> -oxide derivatives.....	65
Figure 29. Synthetic methods for pyrazine rings.....	66
Figure 30. Structures of isomeric diazepine derivatives	67
Figure 31. General structure of benzodiazepines	67
Figure 32. Structures of commercial available diazepine derivatives	68
Figure 33. Ring-junction nitrogen containing heterocycles	71
Figure 34. Hydrogen bonding of oximes.....	79
Figure 35. The potential energy profile for the formation of <i>N</i> -oxide 360	82
Figure 36. HMBC spectrum of compound 378e	87
Figure 37. Geometry optimized structure of 358+AuCl ₃ and 376b+ AuCl ₃ complexes. NBO charges and distances (in Å). DFT/B3LYP; Basis Set: GEN (combination of the 6-31+G(d,p) basis set with the LANL2DZ).....	90
Figure 38. HSQC spectrum of compound 407	99
Figure 39. Geometry optimized structures of 409a+AuCl ₃ and 409c+AuCl ₃ complexes; NBO charges and distances in Å.....	101
Figure 40. Possible cyclization pathways.....	102
Figure 41. HMBC spectrum of compound 408b	103
Figure 42. ¹ H-NMR Spectrum of Crude Mixture of <i>cis</i> -hydroxylation Reaction	163
Figure 43. ¹ H-NMR Spectrum of Compound 207.....	164
Figure 44. ¹³ C-NMR Spectrum of Compound 207	164
Figure 45. IR Spectrum of Compound 207	165
Figure 46. ¹ H-NMR Spectrum of Compound 213.....	165
Figure 47. ¹³ C-NMR Spectrum of Compound 213	166
Figure 48. IR Spectrum of Compound 213	166
Figure 49. ¹ H-NMR Spectrum of Compound 220.....	167
Figure 50. ¹³ C-NMR Spectrum of Compound 220	167
Figure 51. IR Spectrum of Compound 220	168
Figure 52. ¹ H-NMR Spectrum of Compound 231.....	168
Figure 53. ¹³ C-NMR Spectrum of Compound 231	169
Figure 54. DEPT-90 Spectrum of Compound 231	169
Figure 55. DEPT-135 Spectrum of Compound 231	170

Figure 56. COSY Spectrum of Compound 231	170
Figure 57. IR Spectrum of Compound 231	171
Figure 58. HRMS Spectrum of Compound 231	171
Figure 59. GC-MS Spectrum of Compound 231	172
Figure 60. ¹ H-NMR Spectrum of Compound 234	172
Figure 61. ¹ H-NMR Spectrum of D ₂ O Exchange Reaction of Compound 234....	173
Figure 62. ¹³ C-NMR Spectrum of Compound 234	173
Figure 63. DEPT-90 Spectrum of Compound 234.....	174
Figure 64. DEPT-135 Spectrum of Compound 234.....	174
Figure 65. COSY Spectrum of Compound 234	175
Figure 66. HSQC Spectrum of Compound 234	175
Figure 67. HMBC Spectrum of Compound 234	176
Figure 68. ¹ H-NMR Spectrum of Compound 235	177
Figure 69. ¹³ C-NMR Spectrum of Compound 235	177
Figure 70. COSY Spectrum of Compound 235	178
Figure 71. HSQC Spectrum of Compound 235	178
Figure 72. IR Spectrum of Compound 235.....	179
Figure 73. ¹ H-NMR Spectrum of Compound 236	179
Figure 74. ¹³ C-NMR Spectrum of Compound 236.....	180
Figure 75. IR Spectrum of Compound 236.....	180
Figure 76. Mass Spectrum of Compound 236	181
Figure 77. ¹ H-NMR Spectrum of Compound 237	181
Figure 78. ¹ H-NMR Spectrum of Compound 238	182
Figure 79. ¹³ C-NMR Spectrum of Compound 238.....	182
Figure 80. DEPT-135 Spectrum of Compound 238.....	183
Figure 81. COSY Spectrum of Compound 238	183
Figure 82. HSQC Spectrum of Compound 238	184
Figure 83. HMBC Spectrum of Compound 238.....	184
Figure 84. IR Spectrum of Compound 238.....	185
Figure 85. Mass Spectrum of Compound 238	185
Figure 86. ¹ H-NMR Spectrum of Compound 239	186
Figure 87. ¹³ C-NMR Spectrum of Compound 239	186

Figure 88. IR Spectrum of Compound 239	187
Figure 89. HRMS Spectrum of Compound 239	187
Figure 90. ¹ H-NMR Spectrum of Compound 240.....	188
Figure 91. ¹³ C-NMR Spectrum of Compound 240	188
Figure 92. ¹ H-NMR Spectrum of Compound 241.....	189
Figure 93. IR Spectrum of Compound 241	189
Figure 94. Mass Spectrum of Compound 241	190
Figure 95. ¹ H-NMR Spectrum of Compound 242.....	190
Figure 96. ¹ H-NMR Spectrum of Compound 242.....	191
Figure 97. HMBC Spectrum of Compound 242	191
Figure 98. Mass Spectrum of Compound 242.....	192
Figure 99. ¹ H-NMR Spectrum of Compound 248.....	192
Figure 100. ¹³ C-NMR Spectrum of Compound 248.....	193
Figure 101. IR Spectrum of Compound 248	193
Figure 102. ¹ H-NMR Spectrum of Compound 249.....	194
Figure 103. ¹³ C-NMR Spectrum of Compound 249.....	194
Figure 104. IR Spectrum of Compound 249	195
Figure 105. ¹ H-NMR Spectrum of Compound 250.....	195
Figure 106. ¹³ C-NMR Spectrum of Compound 250.....	196
Figure 107. IR Spectrum of Compound 250	196
Figure 108. ¹ H-NMR Spectrum of Compound 251.....	197
Figure 109. ¹³ C-NMR Spectrum of Compound 251.....	197
Figure 110. DEPT-90 Spectrum of Compound 251	198
Figure 111. DEPT-135 Spectrum of Compound 251	198
Figure 112. COSY Spectrum of Compound 251.....	199
Figure 113. HSQC Spectrum of Compound 251.....	199
Figure 114. HMBC Spectrum of Compound 251	200
Figure 115. IR Spectrum of Compound 251	200
Figure 116. ¹ H-NMR Spectrum of Compound 353.....	201
Figure 117. ¹³ C-NMR Spectrum of Compound 353.....	201
Figure 118. IR Spectrum of Compound 353	202
Figure 119. ¹ H-NMR Spectrum of Compound 354.....	202

Figure 120. ¹³ C-NMR Spectrum of Compound 354	203
Figure 121. IR Spectrum of Compound 354	203
Figure 122. ¹ H-NMR Spectrum of Compound 355	204
Figure 123. ¹³ C-NMR Spectrum of Compound 355	204
Figure 124. IR Spectrum of Compound 355	205
Figure 125. ¹ H-NMR Spectrum of Compound 357	205
Figure 126. ¹³ C-NMR Spectrum of Compound 357	206
Figure 127. IR Spectrum of Compound 357	206
Figure 128. HRMS Spectrum of Compound 357	207
Figure 129. Crude ¹ H-NMR Spectrum of Compounds 358 and 359	207
Figure 130. ¹ H-NMR Spectrum of Compound 359	208
Figure 131. ¹³ C-NMR Spectrum of Compound 359	208
Figure 132. IR Spectrum of Compound 359	209
Figure 133. HRMS Spectrum of Compound 359	209
Figure 134. ¹ H-NMR Spectrum of Compound 360	210
Figure 135. ¹³ C-NMR Spectrum of Compound 360	210
Figure 136. IR Spectrum of Compound 360	211
Figure 137. HRMS Spectrum of Compound 360	211
Figure 138. ¹ H-NMR Spectrum of Compound 360	212
Figure 139. ¹³ C-NMR Spectrum of Compound 360	212
Figure 140. DEPT-135 Spectrum of Compound 360	213
Figure 141. ¹ H-NMR Spectrum of Compound 366	213
Figure 142. ¹³ C-NMR Spectrum of Compound 366	214
Figure 143. IR Spectrum of Compound 366	214
Figure 144. HRMS Spectrum of Compound 366	215
Figure 145. ¹ H-NMR Spectrum of Compound 367a	215
Figure 146. ¹³ C-NMR Spectrum of Compound 367a	216
Figure 147. IR Spectrum of Compound 367a	216
Figure 148. HRMS Spectrum of Compound 367a	217
Figure 149. ¹ H-NMR Spectrum of Compound 367b	217
Figure 150. ¹³ C-NMR Spectrum of Compound 367b	218
Figure 151. DEPT-135 Spectrum of Compound 367b	218

Figure 152. IR Spectrum of Compound 367b	219
Figure 153. HRMS Spectrum of Compound 367b	219
Figure 154. ¹ H-NMR Spectrum of Compound 367c	220
Figure 155. ¹³ C-NMR Spectrum of Compound 367c	220
Figure 156. DEPT-135 Spectrum of Compound 367c	221
Figure 157. IR Spectrum of Compound 367c	221
Figure 158. HRMS Spectrum of Compound 367c	222
Figure 159. ¹ H-NMR Spectrum of Compound 376a (<i>E</i> -isomer)	222
Figure 160. ¹³ C-NMR Spectrum of Compound 376a (<i>E</i> -isomer)	223
Figure 161. IR Spectrum of Compound 376a (<i>E</i> -isomer)	223
Figure 162. HRMS Spectrum of Compound 376a (<i>E</i> -isomer)	224
Figure 163. ¹ H-NMR Spectrum of Crude Mixture of 376a (<i>E</i> - and <i>Z</i> -isomer) ...	224
Figure 164. ¹ H-NMR Spectrum of Compound 376b (<i>E</i> -isomer)	225
Figure 165. ¹³ C-NMR Spectrum of Compound 376b (<i>E</i> -isomer)	225
Figure 166. IR Spectrum of Compound 376b (<i>E</i> -isomer)	226
Figure 167. HRMS Spectrum of Compound 376b (<i>E</i> -isomer)	226
Figure 168. ¹ H-NMR Spectrum of Crude Mixture of 376c (<i>E</i> - and <i>Z</i> -isomer) ...	227
Figure 169. ¹ H-NMR Spectrum of Compound 376c (<i>E</i> -isomer)	227
Figure 170. ¹³ C-NMR Spectrum of Compound 376c (<i>E</i> -isomer)	228
Figure 171. IR Spectrum of Compound 376c (<i>E</i> -isomer)	228
Figure 172. HRMS Spectrum of Compound 376c (<i>E</i> -isomer)	229
Figure 173. ¹ H-NMR Spectrum of Crude Mixture of 378a (<i>E</i> - and <i>Z</i> -isomer) ...	229
Figure 174. ¹ H-NMR Spectrum of Compound 378e	230
Figure 175. ¹³ C-NMR Spectrum of Compound 378e	230
Figure 176. HSQC Spectrum of Compound 378e	231
Figure 177. HMBC Spectrum of Compound 378e	231
Figure 178. IR Spectrum of Compound 378e	232
Figure 179. HRMS Spectrum of Compound 378e	232
Figure 180. ¹ H-NMR Spectrum of Crude Mixture of 378b (<i>E</i> - and <i>Z</i> -isomer) ...	233
Figure 181. ¹ H-NMR Spectrum of Compound 378b (<i>E</i> -isomer)	233
Figure 182. ¹³ C-NMR Spectrum of Compound 378b (<i>E</i> -isomer)	234
Figure 183. IR Spectrum of Compound 378b (<i>E</i> -isomer)	234

Figure 184. HRMS Spectrum of Compound 378b (<i>E</i> -isomer)	235
Figure 185. ¹ H-NMR Spectrum of Compound 378c (<i>E</i> -isomer)	235
Figure 186. ¹³ C-NMR Spectrum of Compound 378c (<i>E</i> -isomer)	236
Figure 187. IR Spectrum of Compound 378c (<i>E</i> -isomer)	236
Figure 188. HRMS Spectrum of Compound 378c (<i>E</i> -isomer)	237
Figure 189. ¹ H-NMR Spectrum of Compound 390a	237
Figure 190. ¹³ C-NMR Spectrum of Compound 390a	238
Figure 191. ¹ H-NMR Spectrum of Compound 390b	238
Figure 192. ¹³ C-NMR Spectrum of Compound 390b	239
Figure 193. DEPT-135 Spectrum of Compound 390b.....	239
Figure 194. IR Spectrum of Compound 390b	240
Figure 195. HRMS Spectrum of Compound 390b	240
Figure 196. ¹ H-NMR Spectrum of Compound 391a	241
Figure 197. ¹³ C-NMR Spectrum of Compound 391a	241
Figure 198. ¹ H-NMR Spectrum of Compound 391b	242
Figure 199. ¹³ C-NMR Spectrum of Compound 391b	242
Figure 200. DEPT-135 Spectrum of Compound 391b.....	243
Figure 201. IR Spectrum of Compound 391b	243
Figure 202. HRMS Spectrum of Compound 391b	244
Figure 203. ¹ H-NMR Spectrum of Compound 394	244
Figure 204. ¹³ C-NMR Spectrum of Compound 394	245
Figure 205. ¹ H-NMR Spectrum of Compound 393a	245
Figure 206. ¹³ C-NMR Spectrum of Compound 393a	246
Figure 207. DEPT-135 Spectrum of Compound 393a.....	246
Figure 208. IR Spectrum of Compound 393a	247
Figure 209. HRMS Spectrum of Compound 393a.....	247
Figure 210. ¹ H-NMR Spectrum of Compound 393b	248
Figure 211. ¹³ C-NMR Spectrum of Compound 393b	248
Figure 212. DEPT-135 Spectrum of Compound 393b.....	249
Figure 213. IR Spectrum of Compound 393b	249
Figure 214. HRMS Spectrum of Compound 393b	250
Figure 215. ¹ H-NMR Spectrum of Compound 395a	250

Figure 216. ¹³ C-NMR Spectrum of Compound 395a.....	251
Figure 217. IR Spectrum of Compound 395a.....	251
Figure 218. HRMS Spectrum of Compound 395a	252
Figure 219. ¹ H-NMR Spectrum of Compound 395b.....	252
Figure 220. ¹³ C-NMR Spectrum of Compound 395b.....	253
Figure 221. DEPT-135 Spectrum of Compound 395b	253
Figure 222. IR Spectrum of Compound 395b	254
Figure 223. HRMS Spectrum of Compound 395b	254
Figure 224. ¹ H-NMR Spectrum of Compound 395c	255
Figure 225. ¹³ C-NMR Spectrum of Compound 395c.....	255
Figure 226. IR Spectrum of Compound 395c.....	256
Figure 227. HRMS Spectrum of Compound 395c	256
Figure 228. ¹ H-NMR Spectrum of Compound 396a.....	257
Figure 229. ¹³ C-NMR Spectrum of Compound 396a.....	257
Figure 230. IR Spectrum of Compound 396a.....	258
Figure 231. HRMS Spectrum of Compound 396a	258
Figure 232. ¹ H-NMR Spectrum of Compound 396b.....	259
Figure 233. ¹³ C-NMR Spectrum of Compound 396b.....	259
Figure 234. DEPT-135 Spectrum of Compound 396b	260
Figure 235. IR Spectrum of Compound 396b	260
Figure 236. HRMS Spectrum of Compound 396b	261
Figure 237. ¹ H-NMR Spectrum of Compound 396c	261
Figure 238. ¹³ C-NMR Spectrum of Compound 396c.....	262
Figure 239. IR Spectrum of Compound 396c.....	262
Figure 240. HRMS Spectrum of Compound 396c	263
Figure 241. ¹ H-NMR Spectrum of Compound 396d.....	263
Figure 242. ¹³ C-NMR Spectrum of Compound 396d.....	264
Figure 243. IR Spectrum of Compound 396d	264
Figure 244. HRMS Spectrum of Compound 396d	265
Figure 245. ¹ H-NMR Spectrum of Compound 396e.....	265
Figure 246. ¹³ C-NMR Spectrum of Compound 396e.....	266
Figure 247. IR Spectrum of Compound 396e.....	266

Figure 248. HRMS Spectrum of Compound 396e.....	267
Figure 249. ¹ H-NMR Spectrum of Compound 404a	267
Figure 250. ¹³ C-NMR Spectrum of Compound 404a	268
Figure 251. IR Spectrum of Compound 404a	268
Figure 252. HRMS Spectrum of Compound 404a.....	269
Figure 253. ¹ H-NMR Spectrum of Compound 404b	269
Figure 254. ¹ H-NMR Spectrum of Compound 407	270
Figure 255. ¹³ C-NMR Spectrum of Compound 407	270
Figure 256. DEPT-135 Spectrum of Compound 407.....	271
Figure 257. HSQC Spectrum of Compound 407	271
Figure 258. ¹ H-NMR Spectrum of Compound 404c	272
Figure 259. ¹³ C-NMR Spectrum of Compound 404c	272
Figure 260. IR Spectrum of Compound 404c.....	273
Figure 261. HRMS Spectrum of Compound 404c.....	273
Figure 262. ¹ H-NMR Spectrum of Compound 404d	274
Figure 263. ¹³ C-NMR Spectrum of Compound 404d	274
Figure 264. IR Spectrum of Compound 404d.....	275
Figure 265. HRMS Spectrum of Compound 404d	275
Figure 266. ¹ H-NMR Spectrum of Compound 404e	276
Figure 267. ¹³ C-NMR Spectrum of Compound 404e	276
Figure 268. IR Spectrum of Compound 404e	277
Figure 269. HRMS Spectrum of Compound 404e.....	277
Figure 270. ¹ H-NMR Spectrum of Compound 408b	278
Figure 271. ¹³ C-NMR Spectrum of Compound 408b	278
Figure 272. DEPT-90 Spectrum of Compound 408b.....	279
Figure 273. DEPT-135 Spectrum of Compound 408b.....	279
Figure 274. COSY Spectrum of Compound 408b	280
Figure 275. HSQC Spectrum of Compound 408b	280
Figure 276. HMBC Spectrum of Compound 408b	281
Figure 277. IR Spectrum of Compound 408b.....	281
Figure 278. HMBC Spectrum of Compound 408b	282
Figure 279. ¹ H-NMR Spectrum of Compound 408c	282

Figure 280. ¹³ C-NMR Spectrum of Compound 408c.....	283
Figure 281. APT Spectrum of Compound 408c.....	283
Figure 282. DEPT-135 Spectrum of Compound 408c.....	284
Figure 283. HSQC Spectrum of Compound 408c.....	284
Figure 284. HMBC Spectrum of Compound 408c.....	285
Figure 285. IR Spectrum of Compound 408c.....	285
Figure 286. HRMS Spectrum of Compound 408c.....	286
Figure 287. ¹ H-NMR Spectrum of Compound 408d.....	286
Figure 288. ¹³ C-NMR Spectrum of Compound 408d.....	287
Figure 289. IR Spectrum of Compound 408d.....	287
Figure 290. HRMS Spectrum of Compound 408d.....	288
Figure 291. ¹ H-NMR Spectrum of Compound 408e.....	288
Figure 292. ¹³ C-NMR Spectrum of Compound 408e.....	289
Figure 293. IR Spectrum of Compound 408e.....	289
Figure 294. HRMS Spectrum of Compound 408e.....	290

LIST OF SCHEMES

SCHEMES

Scheme 1. Constitution and configuration determination of conduritol-A (25).....	6
Scheme 2. The first synthesis of conduritol-A (25).....	7
Scheme 3. Stereoselective synthesis of conduritol-A (25).....	8
Scheme 4. Synthesis of conduritol-A (25) by singlet oxygen reaction.....	8
Scheme 5. Ring closure metathesis for the synthesis of conduritol-A (25).....	9
Scheme 6. Synthesis of bis-homoconduritol-A (54) and -D (55).....	9
Scheme 7. The first synthesis of conduritol-B (26).....	10
Scheme 8. Synthesis of conduritol-B by thiocarbonyldiimidazole protection.....	11
Scheme 9. Synthesis of conduritol-B (26).....	11
Scheme 10. Synthesis of conduritol-B by photooxygenation of oxepine-benzeneoxide system $65 \rightleftharpoons 66$	12
Scheme 11. The first synthesis of (+)-conduritol-B.....	13
Scheme 12. Sulfur mediated synthesis of conduritol-B (26).....	13
Scheme 13. Synthesis of phenyl substituted conduritol-B derivative 82.....	14
Scheme 14. Synthesis of conduritol-C.....	14
Scheme 15. Synthesis of conduritol-C (27).....	15
Scheme 16. Synthesis of conduritol-C (27).....	15
Scheme 17. Synthesis of conduritol-C (27).....	16
Scheme 18. Synthesis of (+) and (-)-conduritol-C (27).....	16
Scheme 19. Synthesis of conduritol-C (27).....	17
Scheme 20. The first synthesis of conduritol-D (28).....	18
Scheme 21. Synthesis of conduritol-D.....	18
Scheme 22. Synthesis of conduritol-D.....	19
Scheme 23. Synthesis of conduritol-D (28).....	20
Scheme 24. Synthesis bis-homo-conduritol-D (123).....	20
Scheme 25. Synthesis of conduritol-E.....	21
Scheme 26. Synthesis of conduritol-E (29).....	21
Scheme 27. Synthesis of conduritol-E (29).....	22

Scheme 28. Synthesis of conduritol-E (29)	22
Scheme 29. Synthesis of conduritol-E.....	23
Scheme 30. Synthesis of (-)-conduritol-E (29) by Hudlicky <i>et al.</i>	23
Scheme 31. The first synthesis of conduritol-F	24
Scheme 32. Synthesis of conduritol-F (30)	25
Scheme 33. Synthesis of conduritol-F (30)	26
Scheme 34. Synthesis of oligomer of conduritol-F (30)	26
Scheme 35. Synthesis of diamino analogous of conduritol-F (165).....	27
Scheme 36. The first synthesis of bromoconduritol-B and -F	28
Scheme 37. Synthesis of haloconduritols	29
Scheme 38. Synthesis of haloconduritol derivatives 176, 177, 178 and 179	29
Scheme 39. Synthesis of bromoconduritol derivatives 181 and 182.....	30
Scheme 40. Synthesis of haloconduritol derivatives 185	30
Scheme 41. Synthesis of haloconduritol derivatives 187	31
Scheme 42. Synthesis of bromoconduritol-B 193.	31
Scheme 43. Retrosynthetic plan for bromoconduritol 201	34
Scheme 44. Synthesis of <i>cis</i> -diol 207	35
Scheme 45. Pb(OAc) ₄ mediated <i>cis</i> -hydroxylation reaction mechanism.....	36
Scheme 46. Acetylation reaction of compound 207	37
Scheme 47. The mechanism of the singlet oxygen ene reaction	39
Scheme 48. Synthetic attempts for ene reaction.....	39
Scheme 49. Stereospecific carbene addition by α -elimination.....	42
Scheme 50. Attempted carbene addition to 207 and 213.	42
Scheme 51. Ketal formation	43
Scheme 52. Dibromocarbene addition reaction to 220.....	44
Scheme 53. Electrophilic ring opening reaction.....	47
Scheme 54. Formation of nitro-substituted side product 238.....	50
Scheme 55. Acetylation reaction of compound 234.....	52
Scheme 56. Allylic oxidation reaction of the compound 234	53
Scheme 57. α -Acetoxylation reaction of the compound 240	54
Scheme 58. Possible reaction pathways	56
Scheme 59. The reduction of 240.....	56

Scheme 60. Deprotection reactions of 234-237	57
Scheme 61. Structures of the intermediates formed during substitution at the C-2 and C-3 carbon atoms of indole	62
Scheme 62. Mechanism for substitution at the C-2 position.	62
Scheme 63. Mechanism for the formation of indoles by Fischer indole synthesis	63
Scheme 64. Pyrazine synthesis by electrocyclic ring closure reaction	66
Scheme 65. Alkyne cyclization method for the synthesis of pyrazines	66
Scheme 66. Synthesis of diazepinone derivative 313	68
Scheme 67. Synthesis of benzodiazepine- <i>N</i> -oxide ring 315	69
Scheme 68. Synthesis of diazepine ring by the Ugi four-component condensation	69
Scheme 69. Formation of diazepine derivatives with terminal alkynes	70
Scheme 70. Formation of diazepine derivatives starting from alkynes	70
Scheme 71. Nucleophilic addition to gold catalyzed alkyne	72
Scheme 72. Application of gold catalyzed alkyne cyclization reaction to the synthesis of 337 and 339.	73
Scheme 73. Synthetic Plan	74
Scheme 74. Retro-synthesis of the <i>N</i> -oxides 345 and 346.	75
Scheme 75. Synthetic plan for pyrazolo-pyrazino(diazepino)-indoles	75
Scheme 76. Esterification of indole-2-carboxylic acid 352	77
Scheme 77. Propargylation reaction of 355	78
Scheme 78. Synthesis of oximes 358 and 359.	79
Scheme 79. Metal-catalyzed cyclization reaction of oxime mixture 358/359.	80
Scheme 80. Mechanism for gold-catalyzed cyclization reaction of 358/359.	81
Scheme 81. Attempted synthesis of <i>N</i> -oxide 360 by oxidation of 364.	83
Scheme 82. Derivatization of alkyne unit in 357	84
Scheme 83. Catalytic cycle of the Sonogashira cross-coupling reaction	84
Scheme 84. The oxime-oxime rearrangement of 376 to 378	85
Scheme 85. Mechanism of the “ <i>the oxime-oxime rearrangement</i> ”	88
Scheme 86. Independent synthesis of rearranged product 389	89
Scheme 87. Synthesis of <i>N</i> -propargyl substituted indole-2-carboxylic acids 391a,b	91

Scheme 88. Synthesis of α,β -alkynyl ketones	92
Scheme 89. Derivatization of α,β -unsaturated alkynyl ketones	93
Scheme 90. Synthesis Pyrazole derivatives 396.....	94
Scheme 91. Mechanism of the formation of pyrazoles 396.	95
Scheme 92. Possible cyclization modes	96
Scheme 93. NaH induced cyclization reactions of 396.....	97
Scheme 94. Mechanism for the formation of pyrazine rings	97
Scheme 95. Formation of compound 407.....	98
Scheme 96. Gold catalyzed cyclization reactions of 396.	100
Scheme 97. Mechanism of the gold-catalyzed cyclizations of 396.....	101
Scheme 98. Synthesis of bromocyclohexenetriol derivatives 234-237	105
Scheme 99. α -Acetoxylation attempt and reduction reaction.....	106
Scheme 100. Deprotection reactions	107
Scheme 101. Gold catalyzed cyclization attempts of oximes 358, 366 and 367.	107
Scheme 102. Synthesis of pyrazoles 396 with hydrazine.....	108
Scheme 103. Gold catalyzed cyclization reactions of pyrazoles 396.....	109

LIST OF TABLES

TABLES

Table 1. <i>N</i> -oxide formation with different metal catalysis	80
Table 2. Oxime-oxime rearrangement with different metal catalysis.....	86
Table 3: TS1	319
Table 4. TS2	320

LIST OF ABBREVIATIONS

aq	Aqueous
ATR	Attenuated total reflectance
B3LYP	Becke-3-parameter functional and Lee, Yang, Parr correlation functional
δ	Chemical shift
DCPD	Dicyclopentadiene
DFT	Density functional theory
DMP	2,2 Dimethoxypropane
LANL2DZ	Los Alamos National Laboratory 2 double ζ
<i>m</i> CPBA	<i>m</i> -Chloroperoxybenzoic acid
MS	Molecular sieve
NBO	Natural bond orbital analysis
NBS	N-bromosuccinimide
NMO	N-methylmorpholine N-oxide
PTC	Phase transfer catalyst
PTSA	<i>p</i> -Toluenesulphonic acid
RCM	Ring closure metathesis
TBAF	Tetra- <i>n</i> -butylammonium fluoride
TBDPS	<i>tert</i> -Buthyldiphenylsilyl
TFA	Trifluoroacetic acid
THF	Tetrahydrofuran
TPP	Tetraphenylporphyne
TS	Transition structure

CHAPTER 1

DEVELOPMENT OF A NEW METHODOLOGY FOR THE SYNTHESIS OF HALOCONDURITOLS

1.1 Introduction

Cyclitols, polyhydroxy-substituted cyclohexene derivatives are biologically active compounds and their pharmaceutical activities such as antibiotic, antifungal, antifeedant and growth regulation effects are known.¹ As a member of this group, haloconduritols (Figure 1), halogen substituted derivatives of conduritols, gained synthetic importance during the last two decades because of being biologically active compounds like conduritols. For example, bromoconduritols are active site directed covalent inhibitor of α -glycosidase and therefore, they are interesting molecules in Acquired Immune Deficiency Syndrome (AIDS) research.²

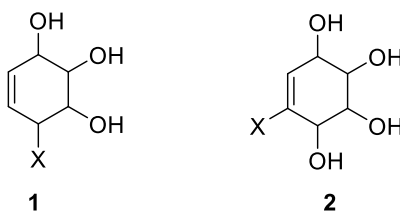


Figure 1. Haloconduritols

In the light of this information, haloconduritol derivatives have potential to be biologically active molecules. For this reason, the synthesis of haloconduritols gained great importance by synthetic organic chemists.

1.1.1 Cyclitols

Cyclitols are cyclic compounds containing at least three hydroxyl groups in their structures attached to the different carbons atoms.^{3,4} They are also called as carbasugars generated by replacing *endo*-oxygen atom in sugars with a methylene group. Cyclitol derivatives have some biological activities ranging from being inhibitors of α -glycosidase enzyme to having glycomimetic effect. For example, they are used in the treatment of metabolic disorders and carbohydrates related diseases such as diabetes, cancer, AIDS and viral infections.⁵ The most common types of cyclitols are inositols (**3**), quercitols (**4**) and conduritols (**5**) (Figure 2).

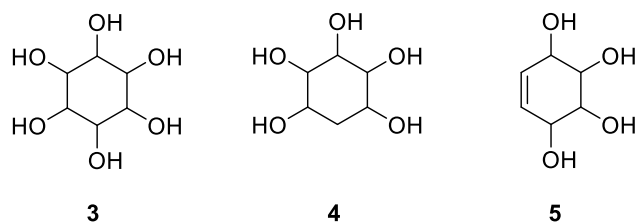


Figure 2. General structures of inositols, quercitols and conduritols

1.1.2 Inositols

Inositols are hexahydroxy-substituted cyclohexane derivatives. The first isolation of *myo*-inositols was done by Scherer in 1850 from muscular tissue. Because of the fact that the '*inos*' is the Greek name of muscle, these cyclohexanehexol derivatives were named as inositol and this nomenclature was used for the other isomers.⁶ Inositols have nine possible stereoisomers (Figure 3). Five of them are naturally occurring ones, *myo*- (**6**), *scyllo*- (**7**), *muco*- (**8**), *neo*- (**9**) and *D-chiro*-inositol (**10**), the other four isomers (**11-14**) are unnaturally synthetic isomers of inositols.⁷ The

most plentiful inositol isomer is the *myo*-inositol (**6**) which is found in eukaryotic cells in phosphate form and also commercially available molecule.

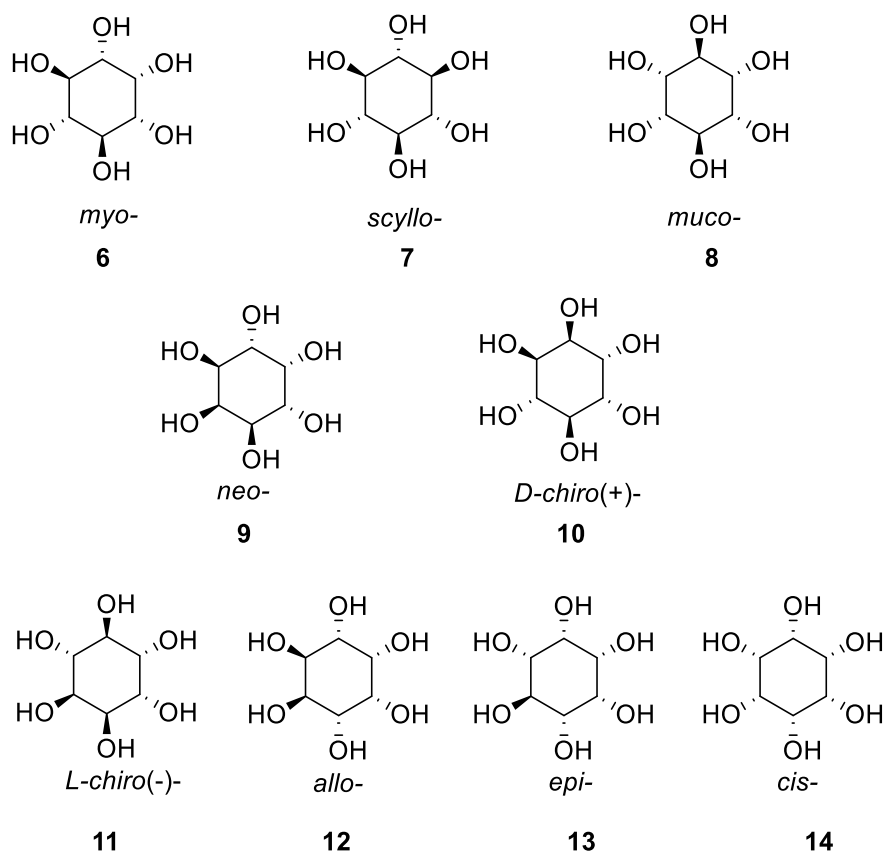


Figure 3. Structures of inositol isomers **6-14**

Inositols are sugar like molecules and some of them are used as sweetener. They are also biologically active molecules and their therapeutic properties ranging from panic disorder and bulimia nervosa to adjusting the insulin action and controlling the intercellular Ca^{2+} concentration.^{7,8}

1.1.3 Quercitols

Quercitols, also known as deoxyinositol, are cyclohexanepentols. The first isolated species of quercitols is (+)-*proto*-quercitol (**15**) from the acorn of *Quercus*, oak species, by Braconnot.⁹ The quercitols family is the one of the largest all-known family of the diastereomers. They have theoretically 16 diastereomers. Four of them

are symmetric, and the other twelve isomers are being the pair of 6 mirror images. Only three of them, (+)-*proto*-, (-)-*proto*-quercitol (**15**) and (-)-*vibo*-quercitol (**17**) are optically active and found in the nature.^{10,11}

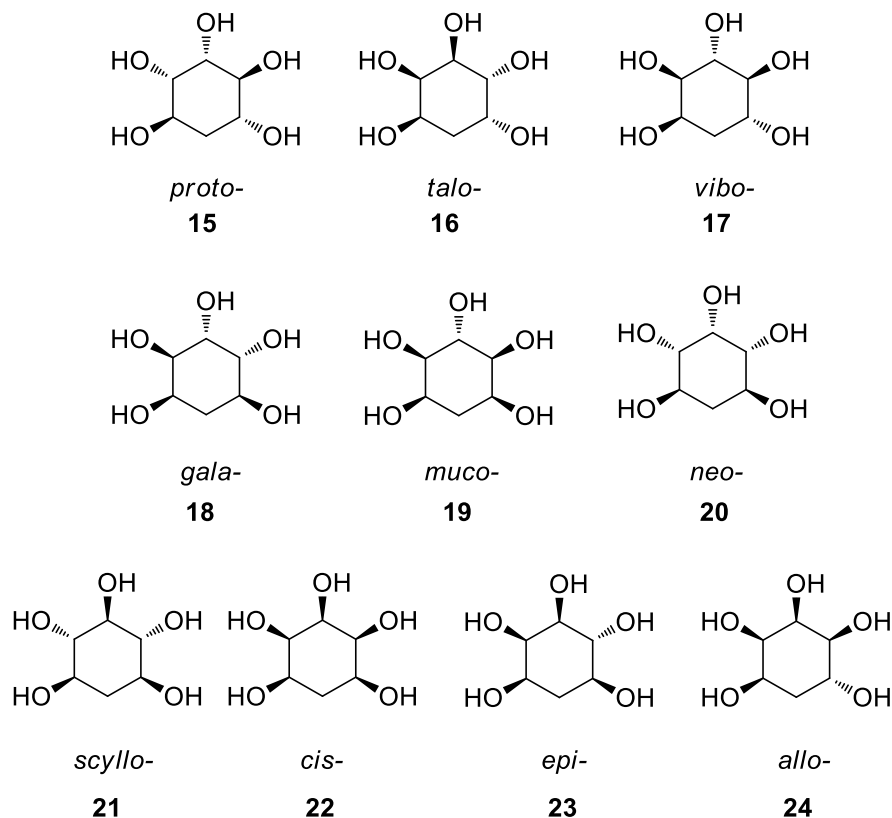


Figure 4. Quercitol isomers

1.1.4 Conduritols

Conduritols are cyclohex-5-ene-1,2,3,4-tetrol derivatives. There are theoretically ten possible stereoisomeric forms, although, two of them are *meso*- (**25** and **28**) and four of them are *DL*-pairs (**26**, **27**, **29** and **30**). These isomers can be found in the nature. To avoid an ambiguousness, they are labelled with letter as conduritol-A (**25**), conduritol-B (**26**), conduritol-C (**27**), conduritol-D (**28**), conduritol-E (**29**) and as conduritol-F (**30**) (Figure 5).

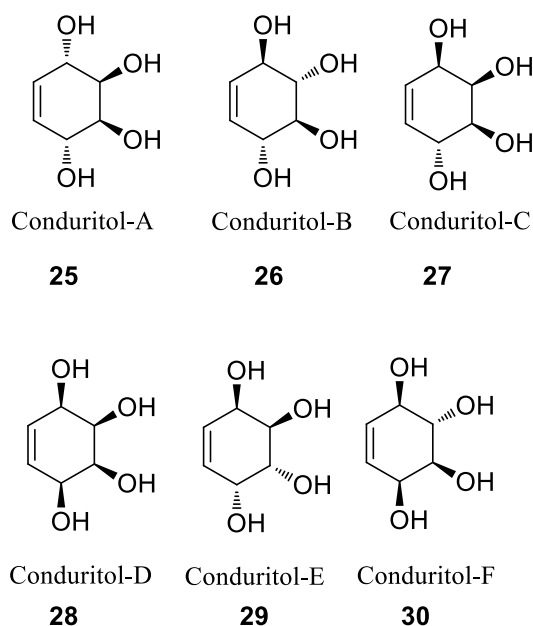
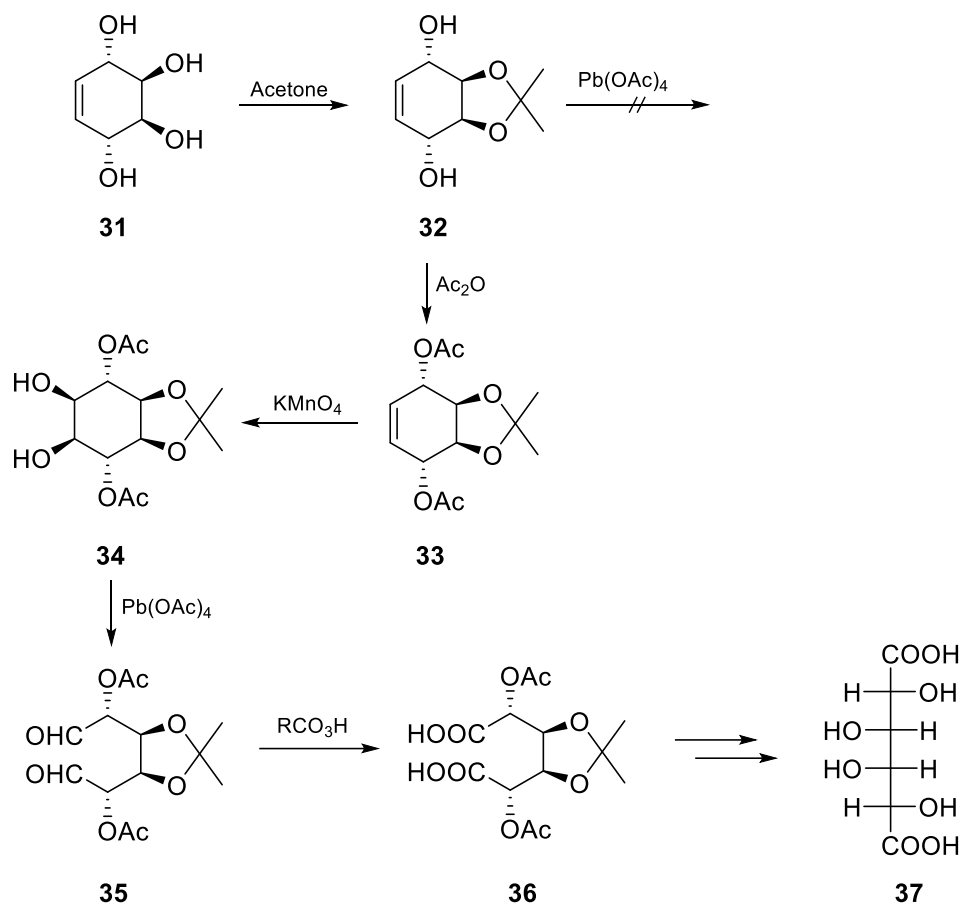


Figure 5. Structures of conduritol isomers **25-30**.

First conduritol isomer was isolated from the bark of vine *Marsdenia condurango* by Kübler in 1908. At that time, they could not determine the constitution of conduritol; however, they showed that conduritol was optically inactive and an unsaturated cyclic compound.^{1,12} After 30 years later the configuration and constitution of this compound were established by Dangschat and Fischer as conduritol-A (**25**) by the evidence of the oxidative ring opening reaction to yield *meso*-hexaric acid.¹³ According to their study, treatment of molecule **31** with acetone gave corresponding mono-acetonide **32**. The following acetylation reaction yielded compound **33**. After getting the corresponding *cis*-hydroxylated compound **34**, following oxidative ring opening reaction furnished the corresponding dialdehyde **35**. Further oxidation and deprotection reaction of this aldehyde to the known molecule galactaric (mucic) acid (**37**) showed the constitution and configuration of conduritol isomer to be conduritol-A (**25**)¹⁴ (Scheme 1).



Scheme 1. Constitution and configuration determination of conduritol-A (**25**)

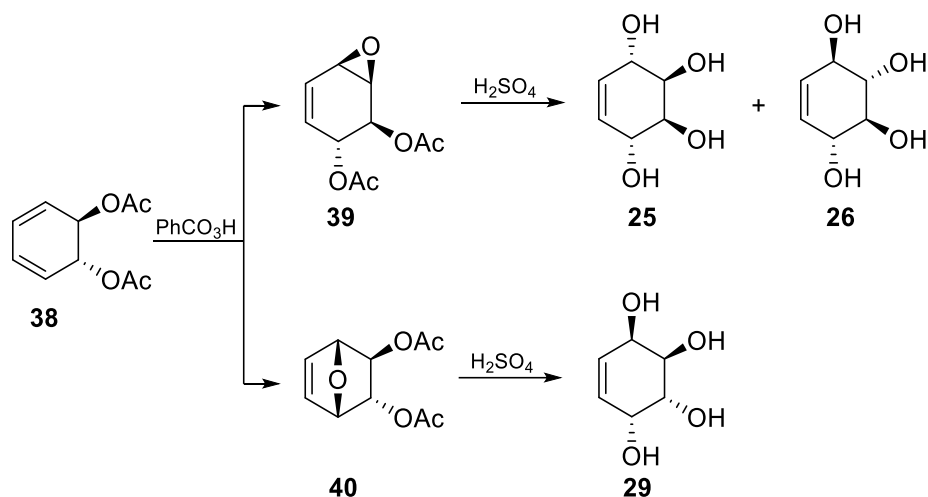
Among all conduritol derivatives (Figure 5), conduritol-A (**25**) and conduritol-F (**30**) are found almost in every green plants and the rests are the synthetic isomers. Because of the diverse biological activities of the conduritol derivatives, their synthesis gained great importance by synthetic organic chemists.

1.1.5 Synthesis of Conduritol Derivatives

1.1.5.1 Synthesis of Conduritol-A

After the discovery of the correct stereochemistry of the conduritol-A (**25**), it was first synthesized non-stereospecifically by Nakajima *et al.*¹⁵ in 1957. According to their synthetic strategy, diacetate **38** was used as the starting material. The

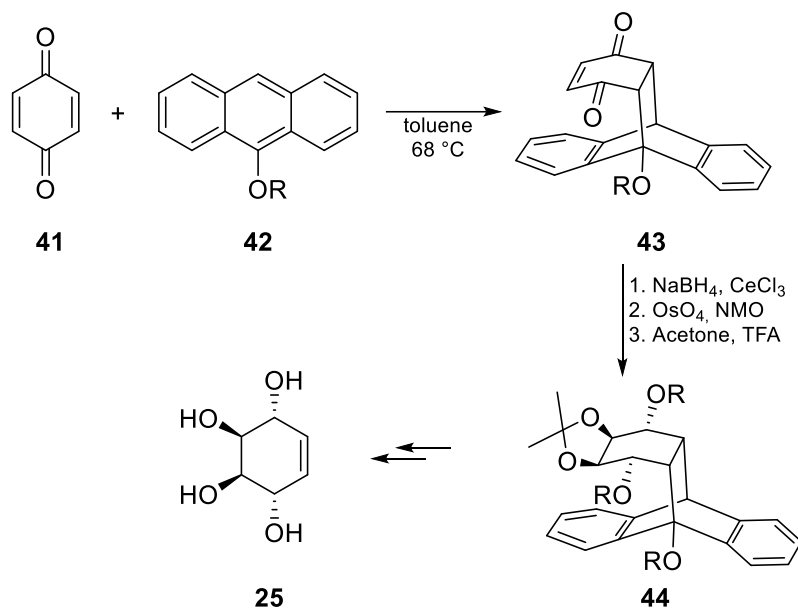
epoxidation reaction of corresponding diacetate **38** with peracid yielded a mixture of compounds **39** and **40**. The following ring opening reaction of these epoxides gave the corresponding conduritol derivatives, namely, conduritol-A (**25**), conduritol-B (**26**) and conduritol-E (**29**) as a mixture (Scheme 2).



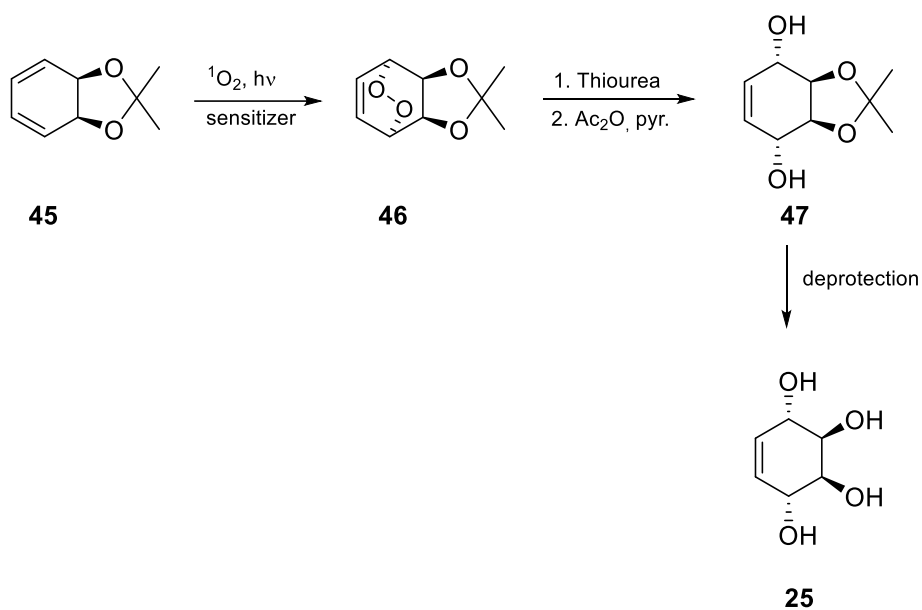
Scheme 2. The first synthesis of conduritol-A (**25**)

After 30 years later, Knapp *et al.*¹⁶ reported the stereospecific synthesis of the conduritol-A (**25**). For this purpose, *p*-benzoquinone (**41**) was used as the starting material. One of double bonds was protected with anthracene derivative by Diels-Alder reaction as adduct **43**. Then, the selective *cis*-reduction of the carbonyl carbons furnished 1,4-*cis*-enediol. The remaining double bond was submitted to *cis*-hydroxylation reaction using OsO₄ and protected as a ketal unit to furnish **44** with the correct configuration which is required by conduritol-A (**25**). As a next step, the retro-Diels-Alder reaction and following deprotection reactions were applied to obtain conduritol-A (**25**) (Scheme 3).

Balci *et al.*¹⁷ reported a facile synthesis of conduritol-A (**25**) with a new, efficient and stereospecific method by applying the singlet oxygen addition to the isopropylidene protected *cis*-diol **45**. After the formation of corresponding *endo*-peroxide **46**, the oxygen-oxygen bond was selectively cleaved by thiourea and successive deprotection of compound **47** gave the conduritol-A (**25**) (Scheme 4).



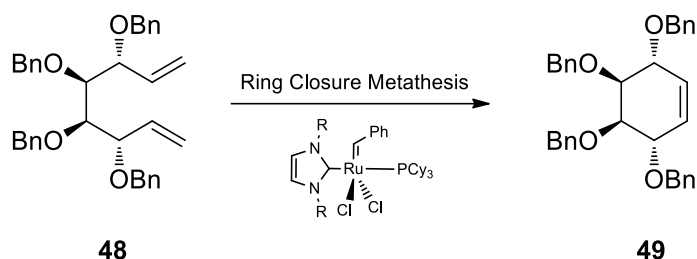
Scheme 3. Stereoselective synthesis of conduritol-A (**25**)



Scheme 4. Synthesis of conduritol-A (**25**) by singlet oxygen reaction

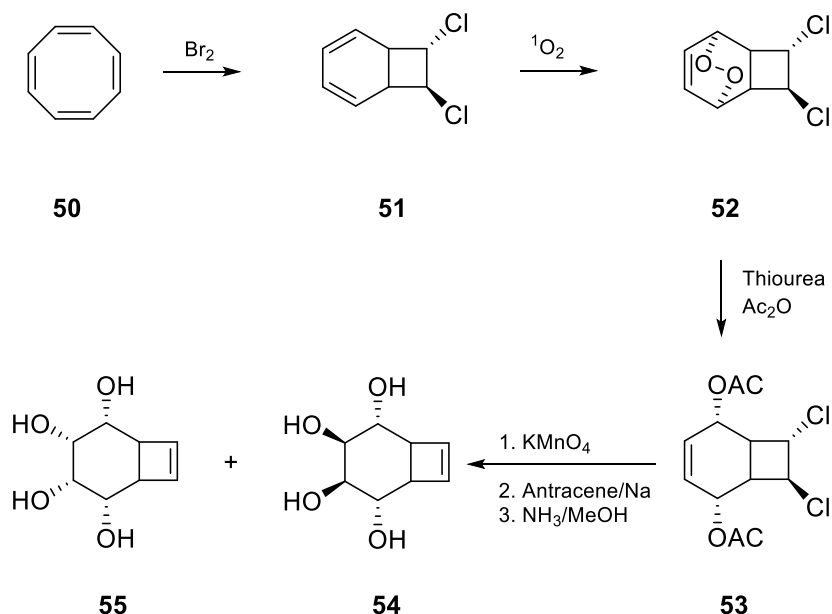
A new approach to the preparation of conduritol derivatives, the ring closure metathesis (RCM), was applied by Fürstner *et al.*¹⁸ to the synthesis of conduritol-A (**25**). According to their results, the ring closure metathesis was accomplished with

diene **48** by the ruthenium carbene ligands of imidazole-2-ylidene to furnish the benzoyl protected analogous of conduritol-A (**49**) (Scheme 5).



Scheme 5. Ring closure metathesis for the synthesis of conduritol-A (**25**)

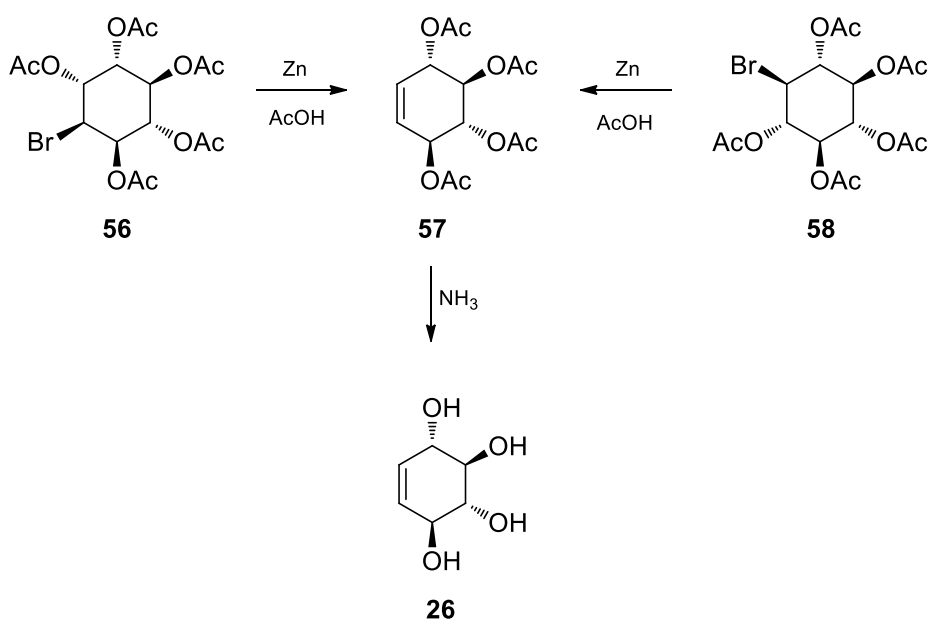
Bis-homoconduritol derivatives of conduritol-A, -D and -F were synthesized by Balci *et al.*¹⁹ in 2005 starting from cyclooctatetraene (**50**) by applying the photooxygenation reaction to *trans*- and *cis*-7,8-dichlorobicyclo[4.2.0]octa-2,4-dienes forming bicyclic endoperoxide (**52**). The ring opening reaction of the resulting endoperoxide and further *cis*-dihydroxylation reaction of the corresponding molecule **53** gave the bis-homoconduritol-A (**54**) and bis-homoconduritol-D (**55**) (Scheme 6).



Scheme 6. Synthesis of bis-homoconduritol-A (**54**) and -D (**55**)

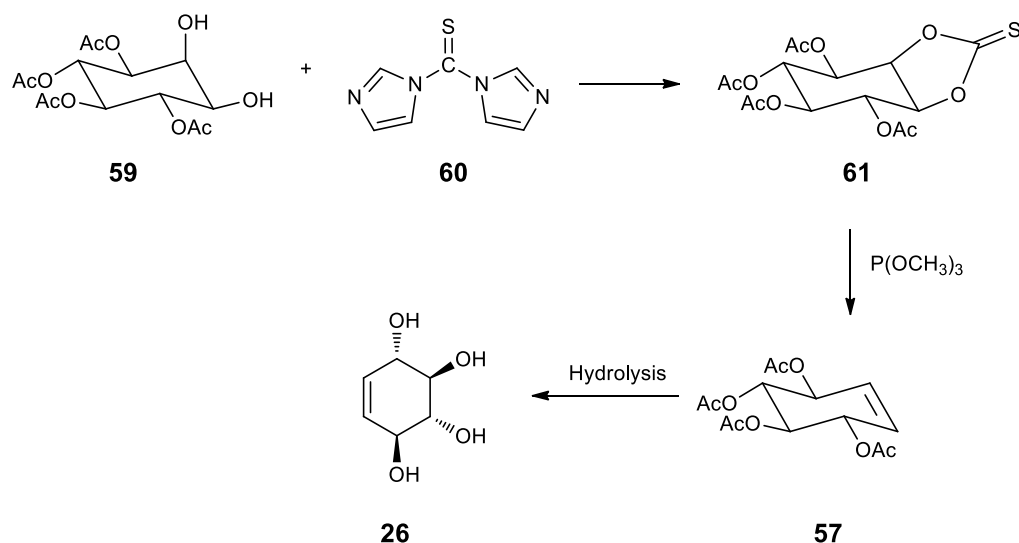
1.1.5.2 Synthesis of Conduritol-B

The first attempt to synthesize conduritol-B (**26**) was done by Müller in 1907.²⁰ According to his strategy, debromination of 6-bromoquercitol derivative (**56** and **58**) with zinc in acetic acid gave the compound with molecular formula C₁₄H₁₈O₈. To clarify this result, in 1953 McCasland and Horswill repeated Müller's debromination reaction and characterized this new unsaturated product **57** as tetraacetylated derivative of conduritol-B (**26**)²¹ (Scheme 7).



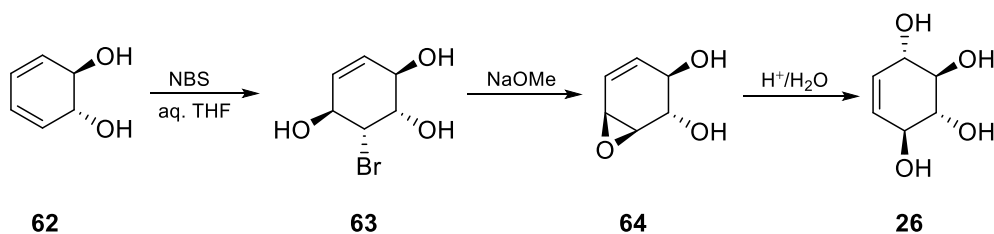
Scheme 7. The first synthesis of conduritol-B (**26**)

Conduritol-B (**26**) was also synthesized as a byproduct by Nakajima *et al.* during the preparation of conduritol-A (**25**) starting from *myo*-inositol (**6**).¹⁵ Nagabhushan *et al.*²² synthesized the conduritol-B (**26**) by reacting 1,4,5,6-tetra-*O*-acetyl-*myo*-inositol (**59**) with *N,N'*-thiocarbonyldiimidazole (**60**). The intermediate 1,4,5,6-tetra-*O*-acetyl-*myo*-inositol-2,3-(3)-thionocarbonate (**61**) was subsequently deprotected by trimethylphosphite and hydrolyzed to give conduritol-B (**26**) as a racemic mixture (Scheme 8).



Scheme 8. Synthesis of conduritol-B (**26**) by thiocarbonyldiimidazole protection

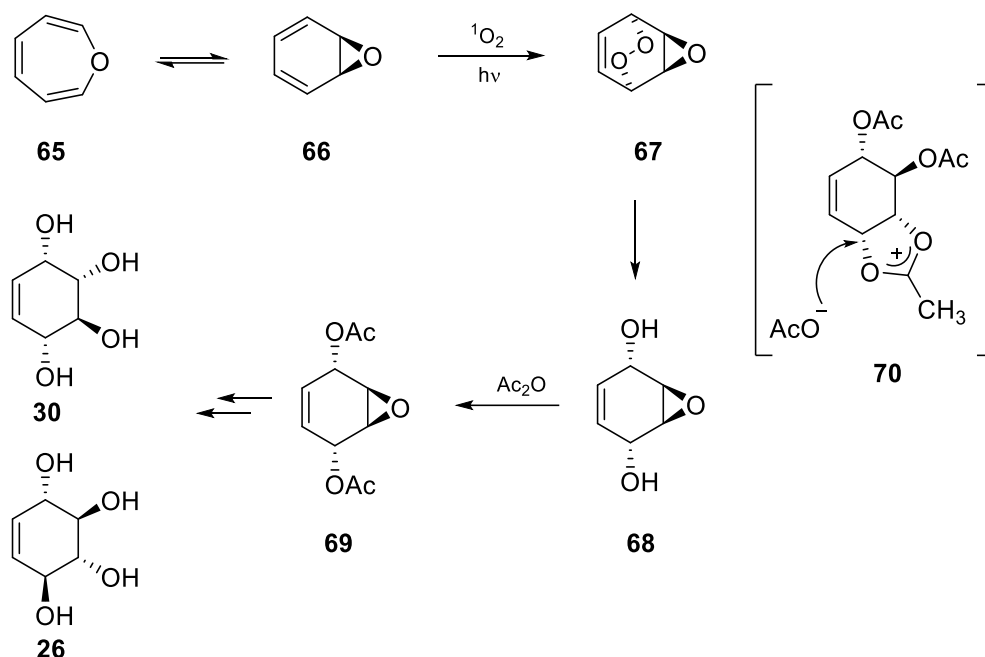
Short and efficient synthesis of conduritol-B (**26**) was described by Berchtold *et al.*²³ Treatment of diol (**62**) with *N*-bromosuccinimide in aqueous tetrahydrofuran yielded the compound **63** which was converted to epoxide **64** by dehydrobromination. The acidic ring-opening reaction of **64** in water gave the corresponding conduritol-B (**26**) (Scheme 9).



Scheme 9. Synthesis of conduritol-B (**26**)

Balcı *et al.* reported a stereospecific synthesis of conduritol-B (**26**) by photooxygenation of oxepine-benzene oxide (**65** \rightleftharpoons **66**) system.²⁴ According to this short and stereospecific synthetic pathway, first endoperoxide **67** was synthesized by reacting of oxepine-benzeneoxide system **65** \rightleftharpoons **66** with singlet oxygen. Then, the cleavage of the oxygen-oxygen bond by thiourea yielded the corresponding diol **68**. As a next step, the acetylation reaction was performed. After that, the epoxide functionality was subjected to acid catalyzed ring-opening reaction. During this

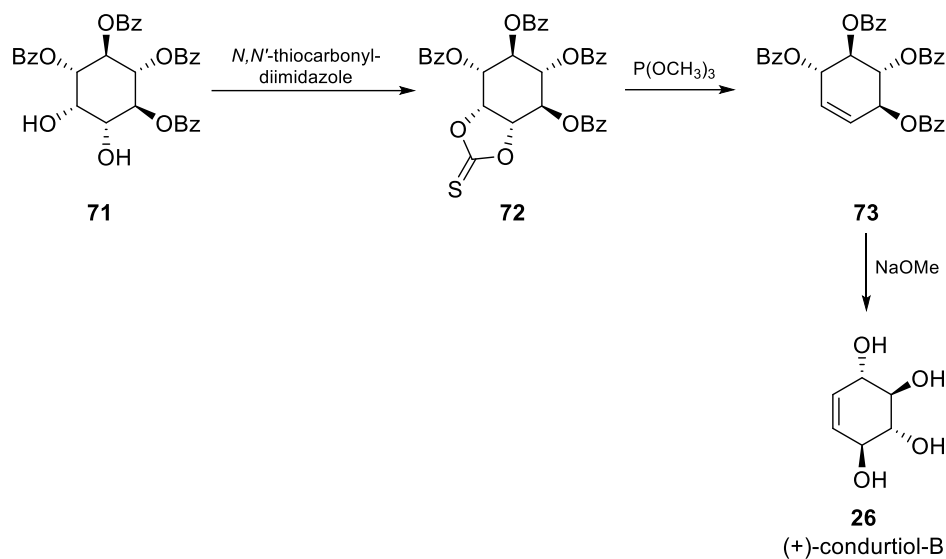
conversion, the neighboring group participation took place which helped to form the core structure of the conduritol-B (**26**) through the intermediate **70** (Scheme 10).



Scheme 10. Synthesis of conduritol-B by photooxygenation of oxepine-benzeneoxide system $65 \rightleftharpoons 66$

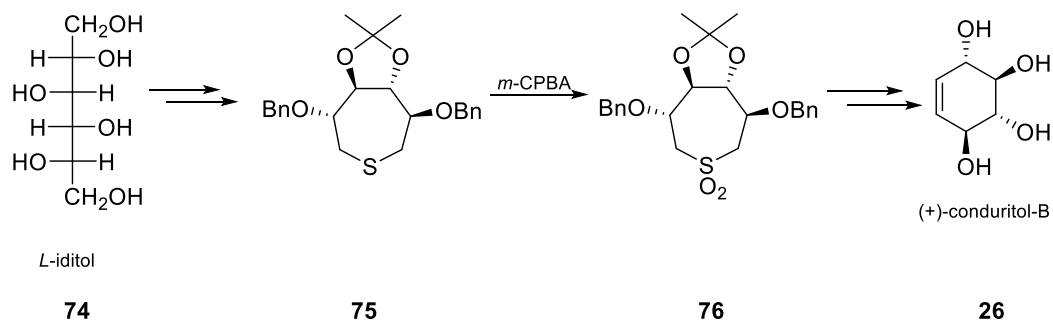
Three years later, in 1993, Ozaki and Akiyama *et al.*²⁵ described a chiral synthesis of the (+)-conduritol-B (**26**) starting from *D*-3,4,5,6-tetra-*O*-benzoyl-*myo*-inositol (**71**). According to this procedure, the treatment of **71** with *N,N'*-thiocarbonyldiimidazole (**60**) gave the compound **72** which subsequently subjected to elimination reaction with trimethylphosphite to furnish the compound **73**. After that, the methanolysis of the benzoyl groups resulted in the formation of (+)-conduritol-B (**26**) (Scheme 11).

In 2000, Cerè *et al.*²⁶ presented a new way to synthesize conduritol derivatives from acyclic sugar **74** which have the same configuration with targeted cyclitol derivatives.



Scheme 11. The first synthesis of (+)-conduritol-B

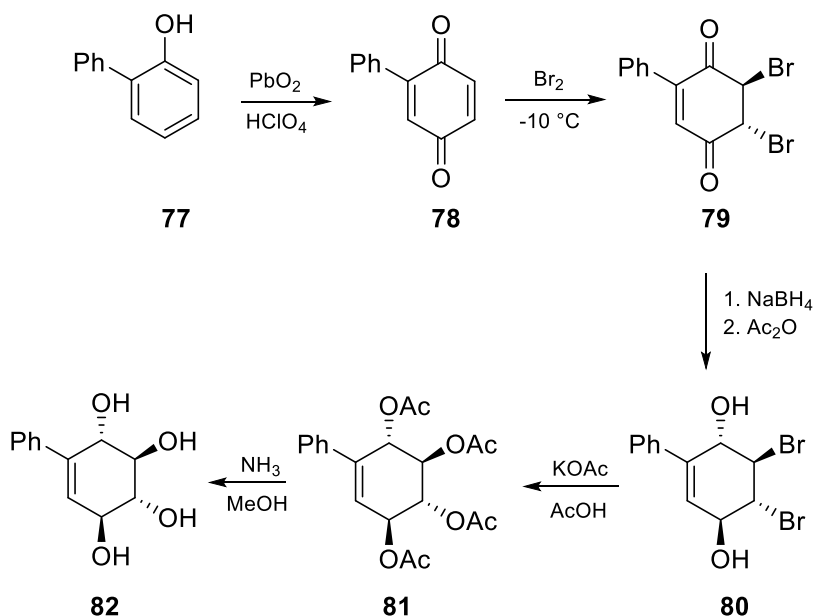
According to their procedure, the intramolecular thiacyclization reaction of the sugar molecule followed by the oxidation reaction gave the corresponding sulfone **76**. After synthesis of the sulfone derivative, the Ramberg-Bäcklund reaction was performed to form double bond by the elimination of SO_2 in basic medium (Scheme 12).



Scheme 12. Sulfur mediated synthesis of conduritol-B (**26**)

Phenyl substituted conduritol-B **82** derivative was also synthesized by Balci *et al.*²⁷ in 2007. In this context, the double bond of the conduritol-B (**26**) was substituted by phenyl ring which might show valuable properties. According to this strategy, they started from the commercially available compound, 1,1'-biphenyl-2-ol (**77**). After the oxidation of compound **77** to **78**, they performed the low temperature

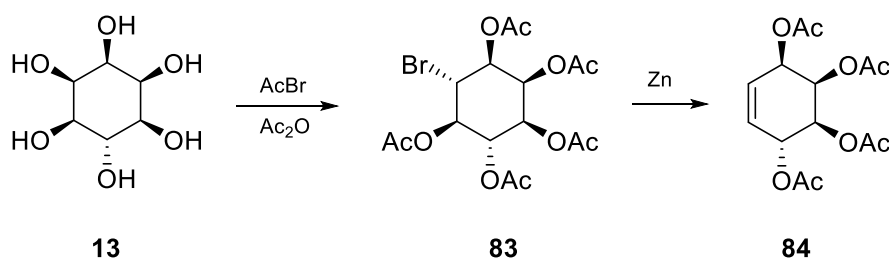
bromination reaction to get regiospecifically *trans* brominated compound **79**. In the next step, the carbonyl groups were reduced to **80**. Substitution of bromine atoms with acetate groups followed by the hydrolysis reaction afforded the target conduritol-B derivative **82** (Scheme 13).



Scheme 13. Synthesis of phenyl substituted conduritol-B derivative **82**

1.1.5.3 Synthesis of Conduritol-C

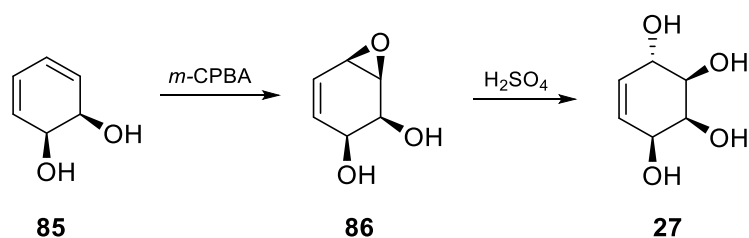
Conduritol-C was first synthesized by McCasland and Reeves in 1955.²⁸ Treatment of the *epi*-inositol (**13**) with acetylbromide and acetic anhydride afforded the bromoquercitol derivative **83**. After Zn-promoted elimination reaction of this



Scheme 14. Synthesis of conduritol-C (**27**)

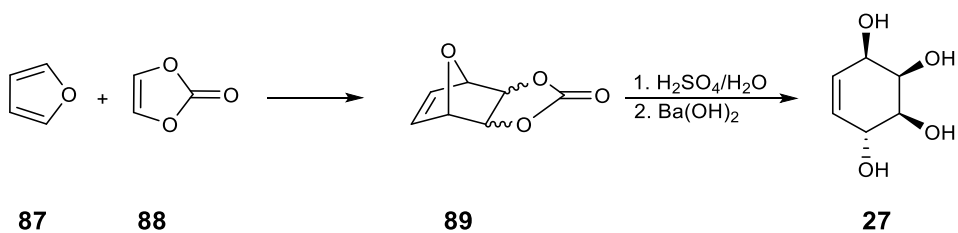
bromoquercitol derivative **84** and then successive hydrolysis furnished the conduritol-C (**27**) (Scheme 14).

One year later, Nakijama *et al.*¹⁵ synthesized conduritol-C from *cis*-diol (**85**) by epoxidation and successive *trans* ring-opening reaction of epoxide **86** in acidic medium (Scheme 15).



Scheme 15. Synthesis of conduritol-C (**27**)

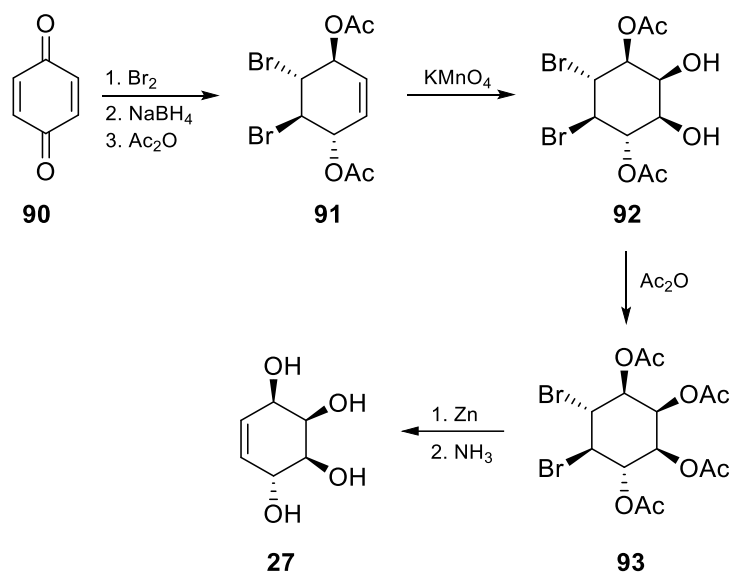
In 1961, Yurev and Zafirov discovered a new synthetic pathway for the synthesis of the conduritol-C (**27**) starting from adduct **89** formed by Diels-Alder reaction between furan (**87**) and vinylene carbonate (**88**).²⁹ After formation of the both *endo*- and *exo*-cyclic products **89**, the ring opening procedure was performed in acidic medium followed by the basic cleavage of the carbonate with Ba(OH)₂ to form the conduritol-C (**27**) (Scheme 16).



Scheme 16. Synthesis of conduritol-C (**27**)

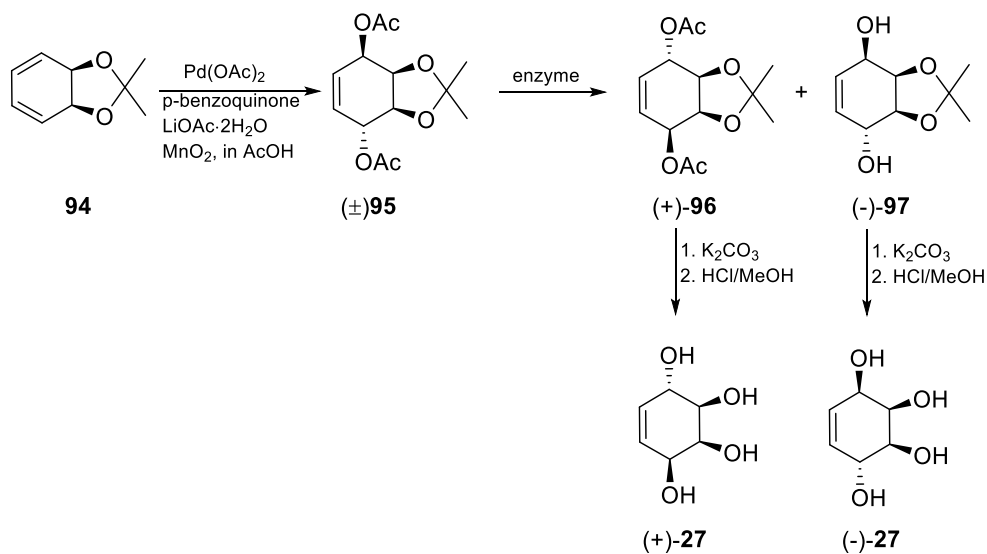
In 1992, Balci *et al.*³⁰ demonstrated a new method for the synthesis of conduritol-C (**27**) starting from benzoquinone **90**. One of double bonds in benzoquinone was first brominated and the carbonyl groups were reduced to the corresponding alcohols which were then protected with acetyl groups. After synthesis of **91**, *cis*-hydroxylation reaction was performed to form the compound **92**. The following

debromination with zinc and deprotection of the protecting groups gave the corresponding conduritol-C (**27**) (Scheme 17).



Scheme 17. Synthesis of conduritol-C (**27**)

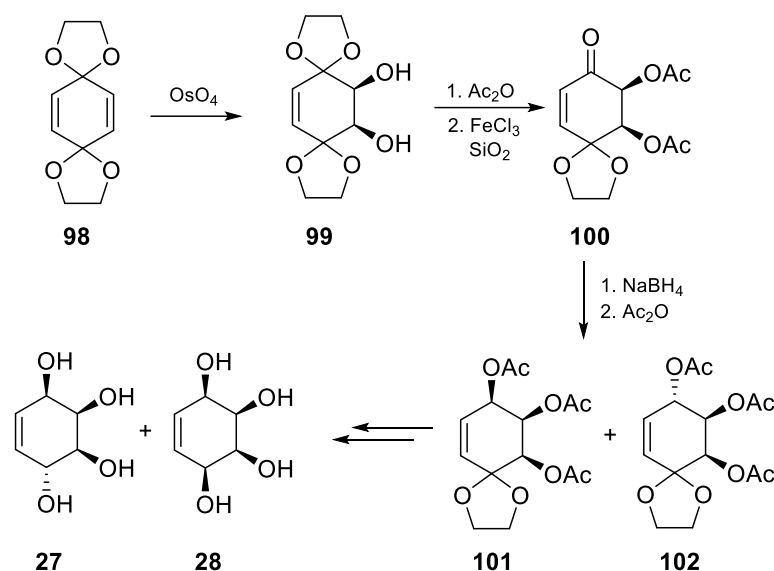
Bäckvall *et al.*³¹ carried out the synthesis of (+) and (-)-conduritol-C (**27**) by the Pd(OAc)₂ catalyzed stereoselective 1,4-diacetoxylation reaction of commercially available *cis*-1,2-dihydrocatechol (**94**). After successful synthesis of the *rac*-diacetoxyated compound **95**, hydrolysis in the presence of the *lipase* enzyme gave



Scheme 18. Synthesis of (+) and (-)-conduritol-C (**27**)

a mixture of compounds (+)-**96** and (-)-**97**. Purification and successive deprotection afforded the enantiomerically pure (+)- and (-)-conduritol-C (**27**) (Scheme 18).

Recently, Ziegler *et al.*³² synthesized (+)- and (-)-conduritol-C (**27**) by *cis*-hydroxylation reaction of benzoquinone(bisethylene acetal) (**98**) with OsO₄. After selective removal of one of the protecting groups of **99** and reduction of the carbonyl group gave a mixture of compound **101** and **102** which were successively separated from each other. Final deprotection and reduction of the carbonyl group gave conduritol-C (**27**) as a racemic mixture. The kinetic resolution of this mixture afforded both enantiomers of conduritol-C (**27**) (Scheme 19).

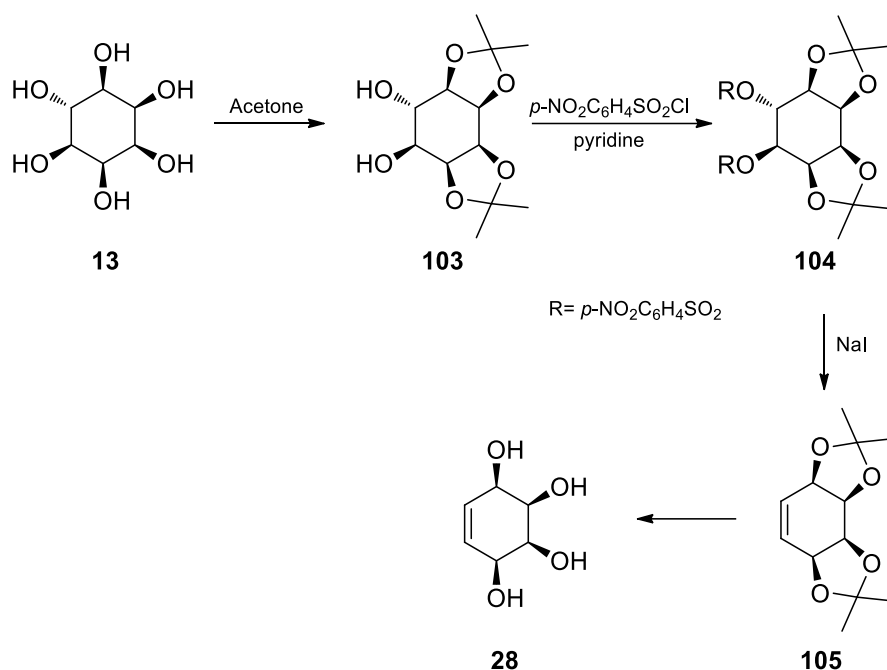


Scheme 19. Synthesis of conduritol-C (**27**)

1.1.5.4 Synthesis of Conduritol-D

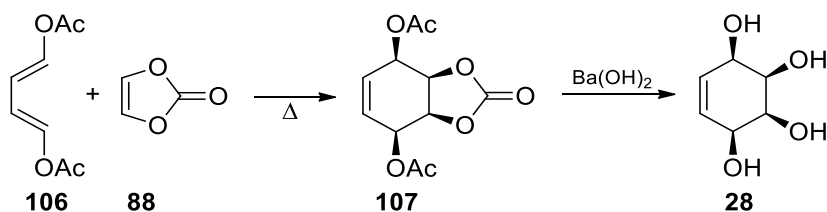
Among the conduritol derivatives, conduritol-D (**28**) is the less accessible isomer because of the all *cis*-stereochemistry of the hydroxyl groups. Conduritol-D (**28**) was first synthesized by Angyal and Gilham in 1958.³³ According to this method; after the ketalization of the *epi*-inositol (**13**), the remaining two vicinal hydroxyl groups were converted to sulphonyloxy groups. The elimination of this groups with NaI, yielded the protected conduritol-D derivative (**105**) with proper configuration.

The hydrolysis of the ketal groups gave the corresponding conduritol-D (**28**) (Scheme 20).



Scheme 20. The first synthesis of conduritol-D (**28**)

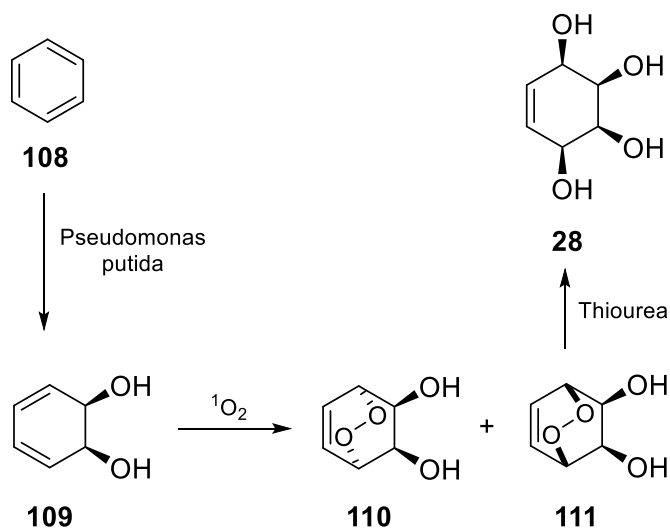
At the same time, Criegee and Becher³⁴ synthesized conduritol-D (**28**) starting from the adduct generated by Diels-Alder reaction of *trans-trans*-diacetoxybutadiene (**106**) and vinilenecarbonate (**88**) at elevated temperature and pressure. The hydrolysis of the compound **107** with $\text{Ba}(\text{OH})_2$ gave the conduritol-D (**28**) (Scheme 21).



Scheme 21. Synthesis of conduritol-D

In 1989, Carless *et al.*³⁵ synthesized conduritol-D (**28**) starting from benzene by applying the microbial oxidation with *pseudomonas putida*. After stereospecific synthesis of compound **109**, photooxygenation reaction gave a mixture of *endo*-

peroxides **110** and **111**. The cleavage of the corresponding *endo*-peroxide linkage of the compound **111** formed the targeted conduritol-D (**28**) (Scheme 22).

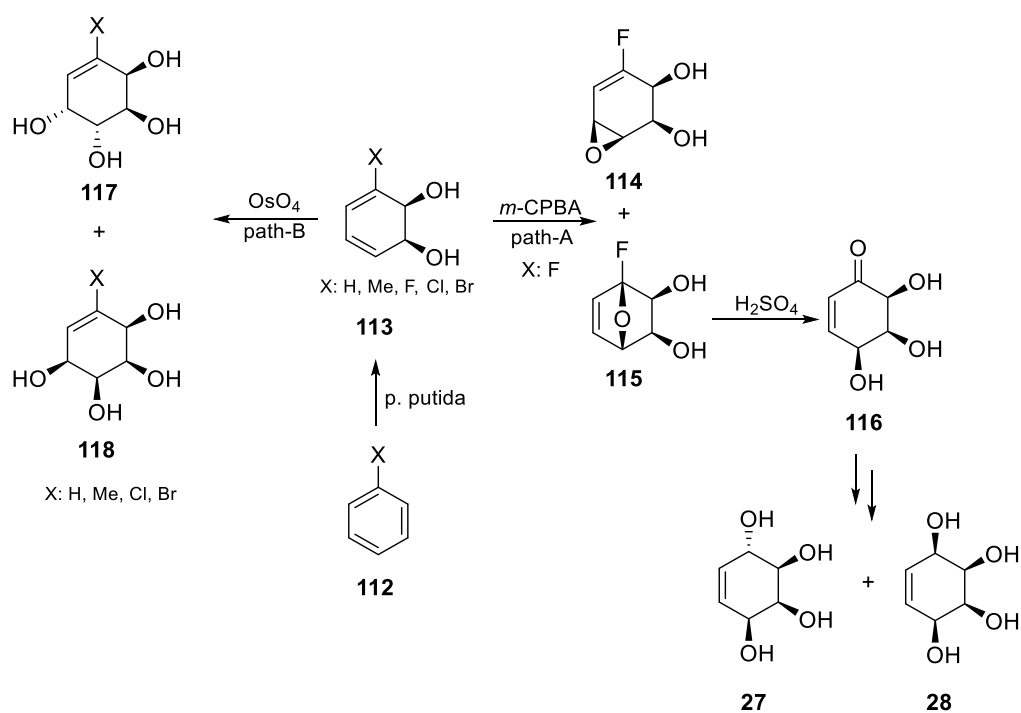


Scheme 22. Synthesis of conduritol-D

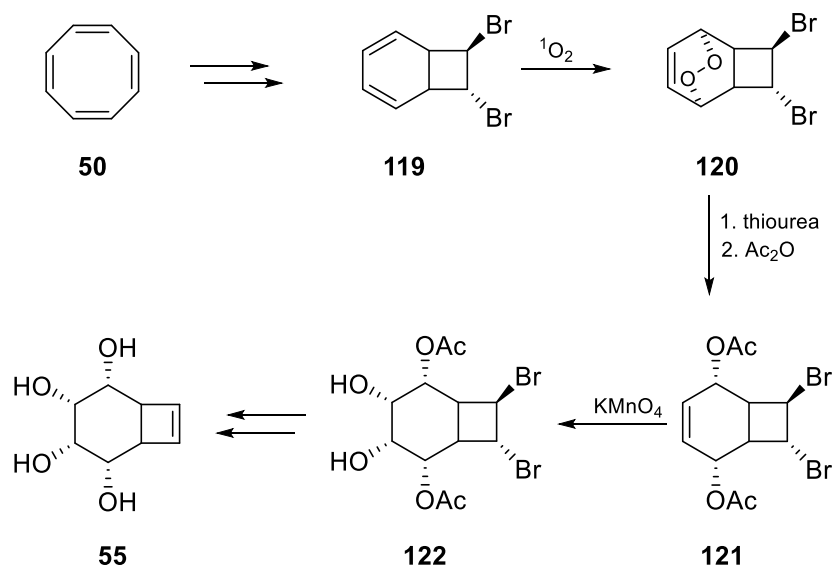
Carless *et al.* have developed two additional methods for the synthesis of conduritol-D (**28**).^{36,37} They started with the microbial *cis*-hydroxylation of halobenzenes (**112**). After formation of halosubstituted *cis*-diol **113**, the epoxidation reaction was performed and the resultant mixture was separated. The oxygen bridge in **115** was opened in acidic medium and compound **116** was formed. The reduction of the carbonyl group in **116** afforded two isomers; conduritol-C (**27**) and conduritol-D (**28**) (path-A). In the second route, Carless *et al.* synthesized conduritol-D (**28**) by stereospecific *cis*-hydroxylation of compound **113** with osmylation reaction. After formation of two diastereomers of tetrahydroxylated halobenzene derivatives **117** and **118**, separation and successive dehalogenation afforded the corresponding conduritol-D (**28**) (path-B) (Scheme 23).

In 1994, Balci *et al.*³⁸ synthesized a new conduritol analogous, bis-homo-conduritol-D **55**, starting from cyclooctatetraene (**50**). For this purpose, they first synthesized dibromobicyclooctadiene **119**. The photooxygenation reaction of compound **119** gave the corresponding *endo*-peroxide **120**. The reduction of *endo*-peroxide and successive acetylation led to diacetate **121**. The final *cis*-

hydroxylation and debromination reaction with Zn metal gave the corresponding bis-homo-conduritol-D derivative **55** (Scheme 24).



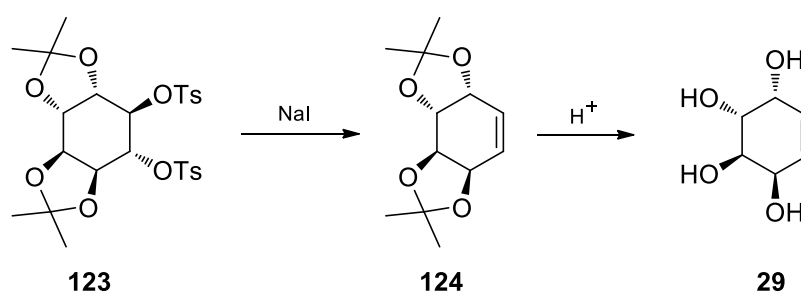
Scheme 23. Synthesis of conduritol-D (**28**)



Scheme 24. Synthesis bis-homo-conduritol-D (**123**)

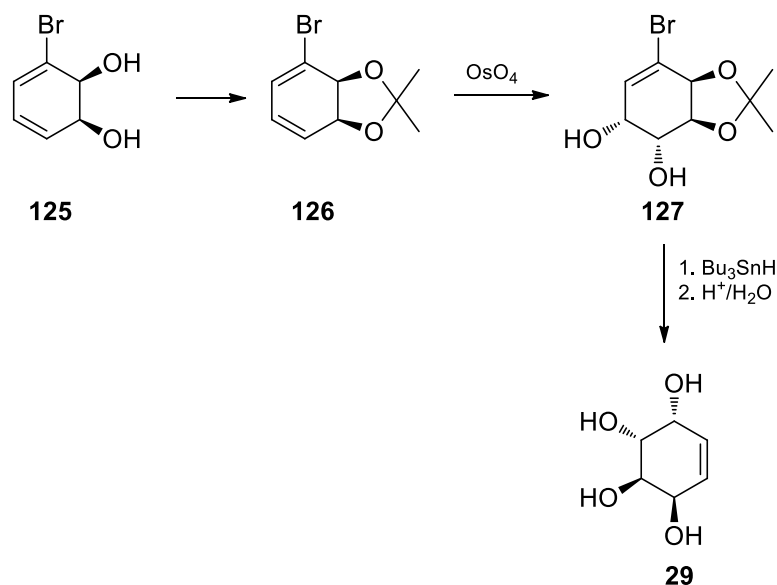
1.1.5.5 Synthesis of Conduritol-E

The first synthesis of the conduritol-E (**29**) was achieved by Nakajima *et al.*¹⁵ in 1957; however, it was not stereospecific. In 1958, Angyal and Gilham³³ suggested a methodology for a stereospecific synthesis of conduritol-E (**29**) starting from suitable inositol derivatives. Protection of *cis*-configured hydroxyl groups of inositol by di-*O*-isopropylidene followed by the elimination of vicinal sulphonyloxy groups by iodide gave the corresponding conduritol-E (**29**) (Scheme 25).



Scheme 25. Synthesis of conduritol-E

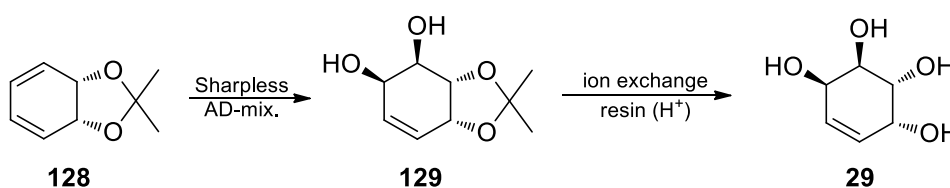
To reach enantiomerically controlled synthesis of conduritol-E (**29**), Hudlicky *et al.*³⁹ suggested a synthetic pathway. According to their methodology, bromo-*cis*-



Scheme 26. Synthesis of conduritol-E (**29**)

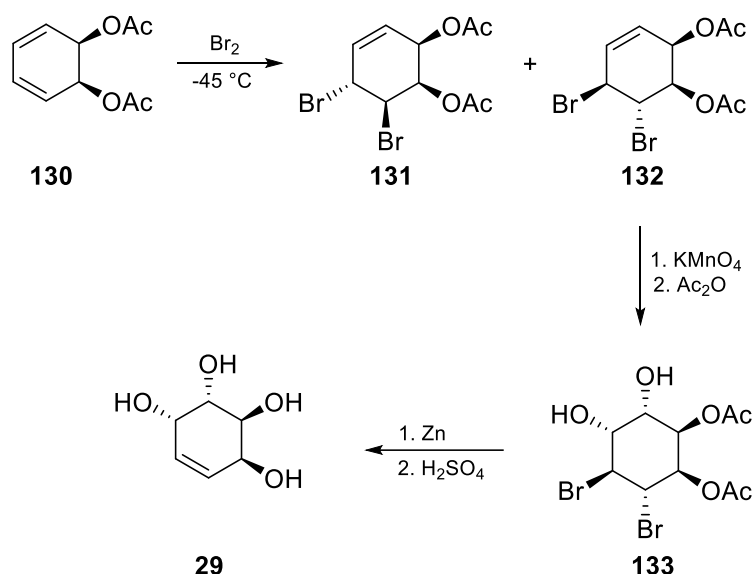
diol **125** was firstly protected and then the *cis*-hydroxylation reaction with OsO₄ was performed to obtain **127** as a single diastereomer. Reduction of bromine atom with tributyltin hydride and removal of the isopropylidene group gave the conduritol-E (**29**) (Scheme 26).

In 1994, Takano *et al.*⁴⁰ used Sharpless oxidation methodology⁴¹ by using the reagent, Sharpless AD-mix., to produce conduritol-E (**29**). In this synthetic pathway, the enantioselective oxidation of **128** was followed by acidic hydrolysis to give the conduritol-E (**29**) (Scheme 27).



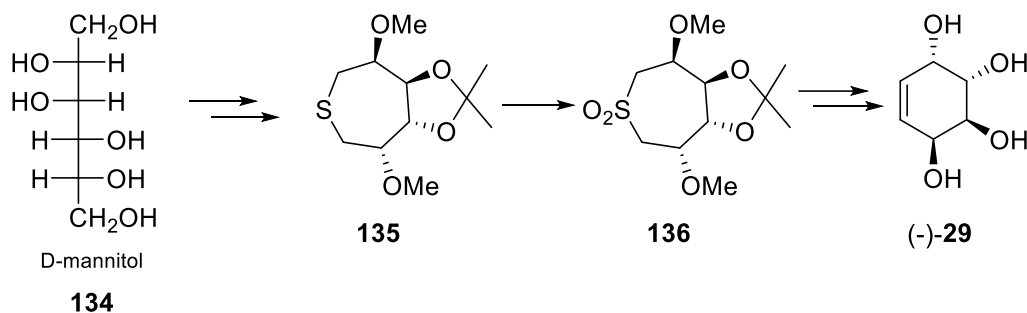
Scheme 27. Synthesis of conduritol-E (**29**)

Balci *et al.*⁴² synthesized conduritol-E (**29**) starting from 1,2-*cis*-diacetate **130**. Bromination of compound **130** gave a mixture of compounds **131** and **132**. After separation of the main product **132**, it was submitted to *cis*-hydroxylation reaction. Elimination of bromine atoms by Zn and successive hydrolysis gave the conduritol-E (**29**) (Scheme 28).



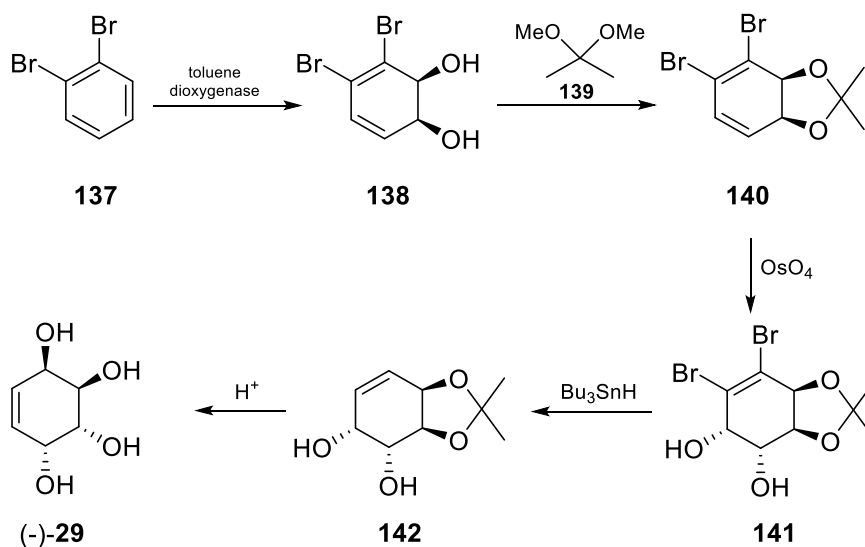
Scheme 28. Synthesis of conduritol-E (**29**)

As indicated in the synthesis of conduritol-B (**26**) section, Cerè *et al.*²⁶ used suitable sugar molecules for the synthesis of conduritol-E (**29**). For this purpose, *D*-mannitol (**156**) was used as the starting material. After intramolecular thiacyclization of *D*-mannitol (**134**), the formed thiepane **135** was oxidized to the corresponding sulfone **136**. The conduritol-E (**29**) was then manufactured via the formation of double bond by means of the Ramberg-Bäcklund procedure (Scheme 29).



Scheme 29. Synthesis of conduritol-E

Hudlicky *et al.*⁴³ revealed another work for the synthesis of conduritol-E (**29**) in 2006. They reacted 1,2-dibromobenzene (**137**) with toluene oxygenase enzyme



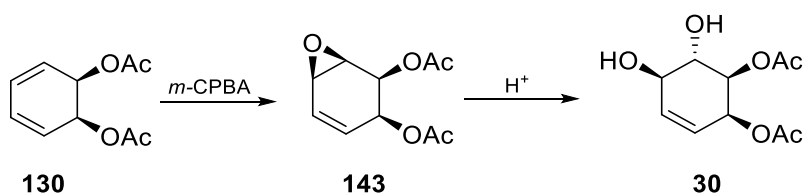
Scheme 30. Synthesis of (-)-conduritol-E (**29**) by Hudlicky *et al.*

and obtained diol **138**. After protection of the diol unit, the *cis*-hydroxylation reaction with OsO₄ was performed. The successive debromination and deprotection gave the (–)-conduritol-E (**29**) (Scheme 30).

1.1.5.6 Synthesis of Conduritol-F

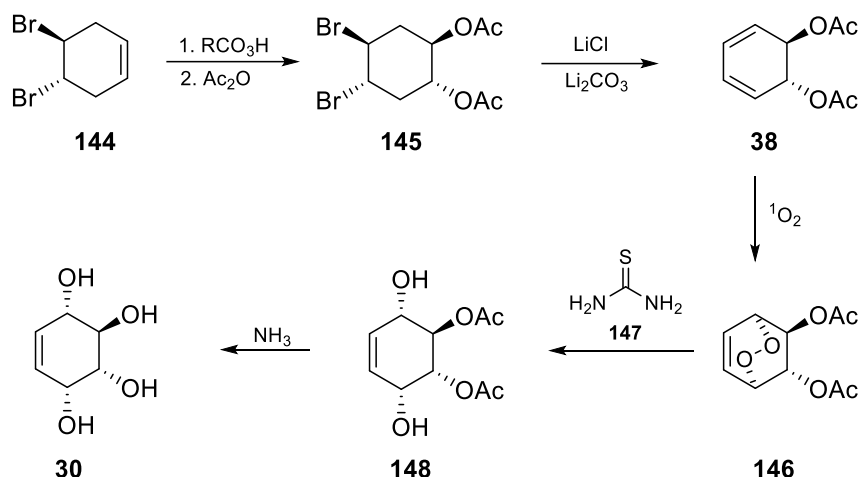
Conduritol-F (**30**) is one of two naturally occurring conduritol isomers. The first isolation of the conduritol-F (**30**) was carried out from *Chrysanthemum leucanthemum* by Plouvier⁴⁴ in 1962. They realized that this newly isolated alcohol was an isomer of conduritol-A (**25**) and named as *L*-luecanthemitol. Conduritol-F (**30**) is found in almost all green plants.

It was first synthesized by Nakajima *et al.*¹⁵ Epoxidation of 1,2-diacetate (**130**) followed by successive ring-opening reaction of the epoxide **143** in the acidic medium gave the targeted molecule **30** (Scheme 31).



Scheme 31. The first synthesis of conduritol-F

Balci *et al.*²⁴ discovered a new method for the stereospecific synthesis of conduritol-F (**30**) in 1990. They selected dibromocyclohexene derivative **144** as the starting material. After conversion of compound **144** into the dibromo-1,2-diacetate **145** followed by removal of bromine atoms by dehydrobromination reaction, the desired diene diacetate **38** was formed. Photooxygenation of diene unit in **146** gave the corresponding bicyclic endoperoxide **146**, which was submitted to reduction reaction with thiourea (**147**) to cleave the endoperoxide linkage under mild conditions to give the compound **148**. The following deprotection of the acetate groups yielded the conduritol-F (**30**) (Scheme 32).

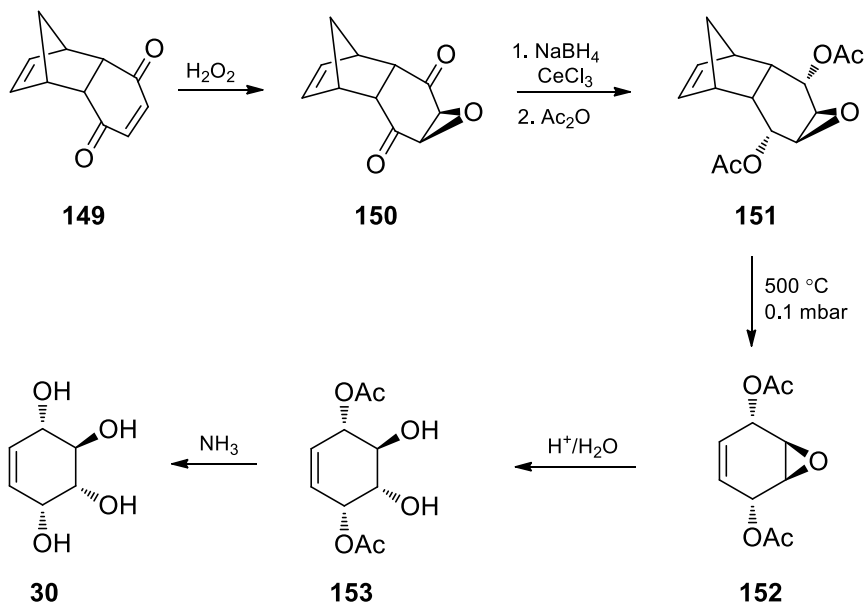


Scheme 32. Synthesis of conduritol-F (**30**)

Furthermore, they also used the oxepine-benzeneoxide (**65** \rightleftharpoons **66**) system for the synthesis of conduritol-B (**26**). Photooxygenation of **65** \rightleftharpoons **66** system followed by epoxidation gave epoxyendoperoxide **67**. Cleavage of the epoxide linkage by thiourea and acetylation of the hydroxyl groups gave epoxy diacetate **69**. *trans*-Ring opening reaction of epoxide ring and removal of acetate groups in acidic medium led to the formation of conduritol-F (**30**) (Scheme 10).

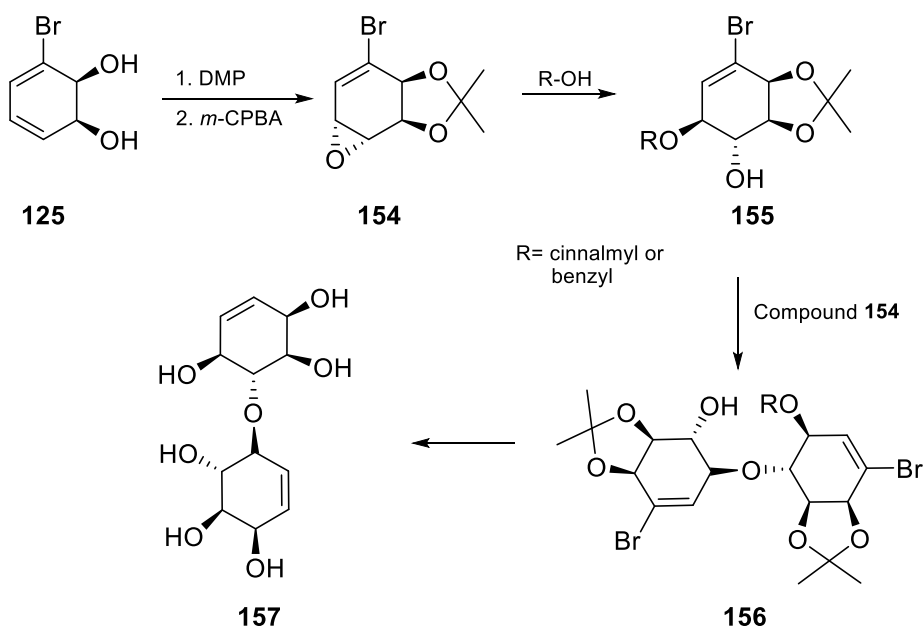
In 1995 Klunder and Zwanenburg *et al.*⁴⁵ achieved the synthesis of conduritol-F (**30**) by using the Diels-Alder adduct of cyclopentadiene and benzoquinone **149** as the starting material. This adduct was first subjected to the epoxidation reaction to furnish the compound **150**. Successive reduction and acetylation reaction of compound **150** was followed by the application of the retro Diels-Alder reaction to give epoxy diacetate **152**. The following ring opening and hydrolysis reaction of the compound **152** gave the conduritol-F (**30**) (Scheme 33).

In 2004, Hudlicky *et al.*⁴⁶ synthesized the glycosidically stable oligomer of conduritol-F (**157**) which has similar structure with oligosaccharides. For this purpose, they selected known diol **125** as the starting material. The epoxidation



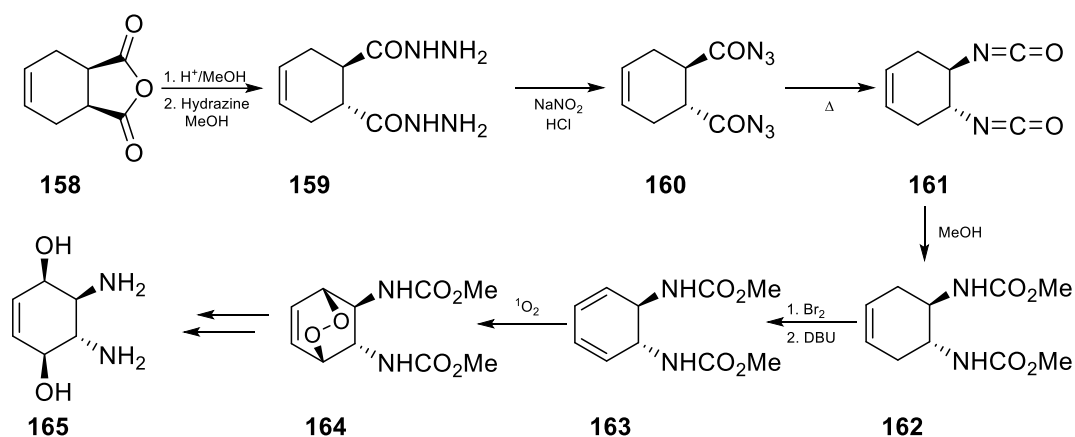
Scheme 33. Synthesis of conduritol-F (**30**)

reaction of compound **125** was followed by the epoxide-opening reaction with cinnamyl or benzyl alcohol to obtain corresponding conduritol-F analogous **155** which were used as a nucleophilic reagent in the next step to produce conduritol-F dimer **157** after the electrochemical deprotection and hydrolysis reaction (Scheme 34).



Scheme 34. Synthesis of oligomer of conduritol-F (**30**)

In a recent publication Balci, *et al.*⁴⁷ reported the synthesis of diaminoconduritol derivative **165** which has the same configuration as in the conduritol-F (**30**). For incorporation of the diamino groups into the cyclohexene ring Curtius rearrangement was used as the key step. After the successful synthesis of diisocyanate **161**, it was converted to bis-carbamate **162**. For introduction of hydroxyl groups in the *cis*-configuration, the photooxygenation reaction was selected. To achieve this, diene **163** was formed by bromination and elimination reaction of **162**. The formation of bicyclic endoperoxide **164** was followed by the conversion into the corresponding diol unit by treatment with thiourea. The successive hydrolysis reaction gave the 2,3-diaminoconduritol **165** which has the conduritol-F (**30**) configuration (Scheme 35).



Scheme 35. Synthesis of diamino analogous of conduritol-F (**165**)

1.1.6 Haloconduritols

Haloconduritols are halogen substituted analogous of the conduritols (Figure 6). They are important molecules due to having biological activities such as inhibition of α -glycosidase enzyme and useful intermediates for the synthesis of more hydroxylated cyclitol derivatives and natural products. In the last decades, synthesis of haloconduritol derivatives has been found valuable by synthetic organic chemists because of their bioactivities. Haloconduritol derivatives have been prepared by different procedures in the literature.^{48,49}

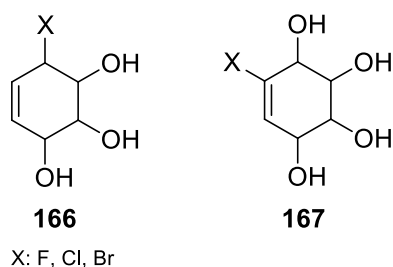
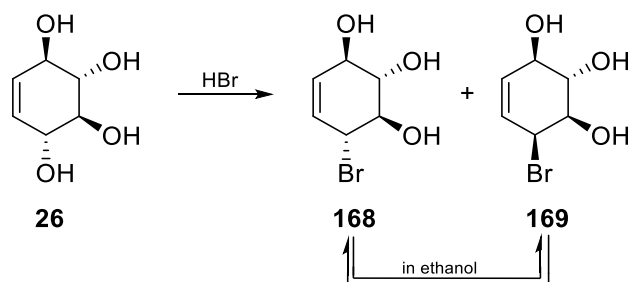


Figure 6. Haloconduritols

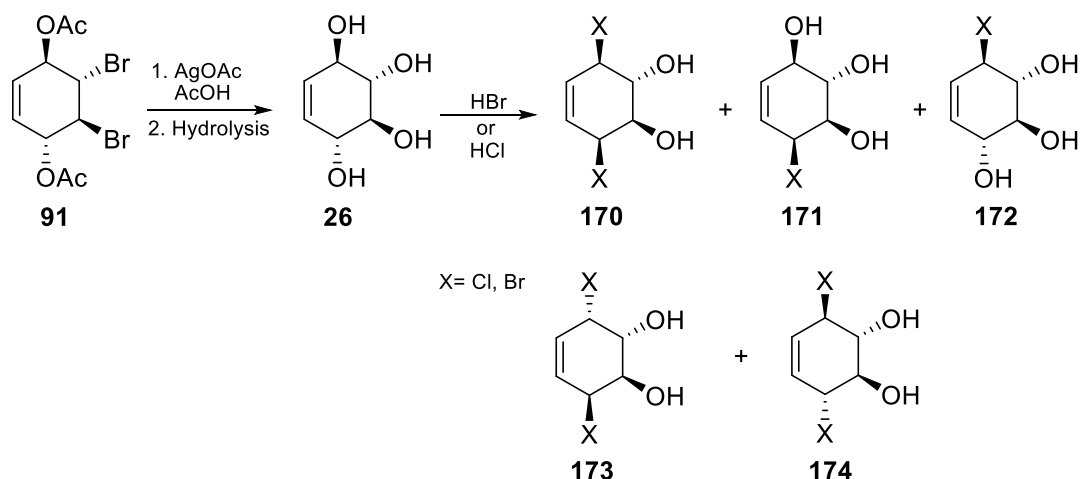
The first synthesis of a haloconduritol derivative was achieved by Legler *et al.*⁵⁰ in 1977. According to this method, treatment of conduritol-B (**26**) with HBr solution (48%) yielded a mixture of bromoconduritol derivatives **168** and **169**. During the crystallization procedure, they also realized that the epimerization reaction of these isomers took place which means the conversion of two isomers to each other (Scheme 36).



Scheme 36. The first synthesis of bromoconduritol-B and -F

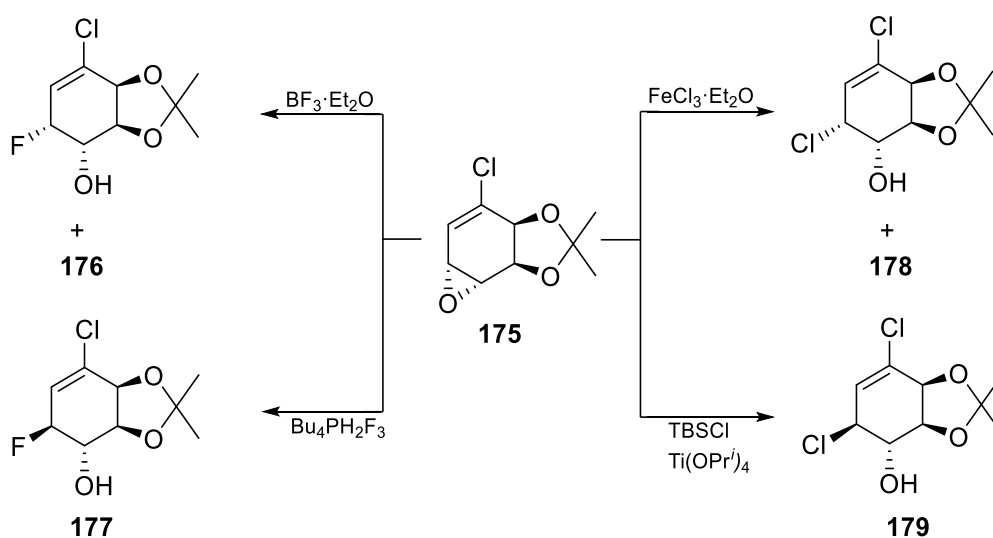
In 1994 Taylor and Haines *et al.*⁵¹ developed a method for the preparation of haloconduritol derivatives. In this study, they aimed the preparation of conduritol-B (**26**) from dibromodiacete **91** molecule. The conduritol-B (**26**), was treated with HBr or HCl solution to get the haloconduritol derivatives. Although the target products were formed, various dihalogenated compounds such as **170**, **173** and **174** were also observed as the byproducts (Scheme 37).

Hudlicky *et al.*⁵² reported the formation of haloconduritols during the synthesis of the conduritol-E (**29**). According to their results, the ring-opening reaction of the epoxide **175** furnished the corresponding haloconduritol derivatives. For this



Scheme 37. Synthesis of haloconduritol

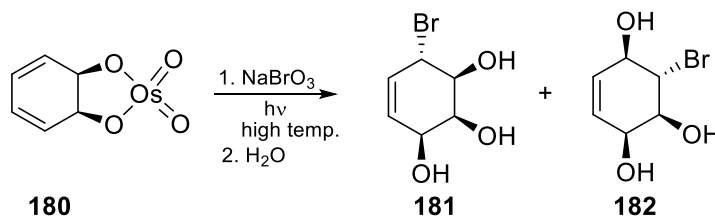
conversion, the reaction proceeded through S_N1 -type mechanism forming an allylic carbocation which can be captured by halides to result in the formation of diastereomers (Scheme 38).



Scheme 38. Synthesis of haloconduritol derivatives **176**, **177**, **178** and **179**

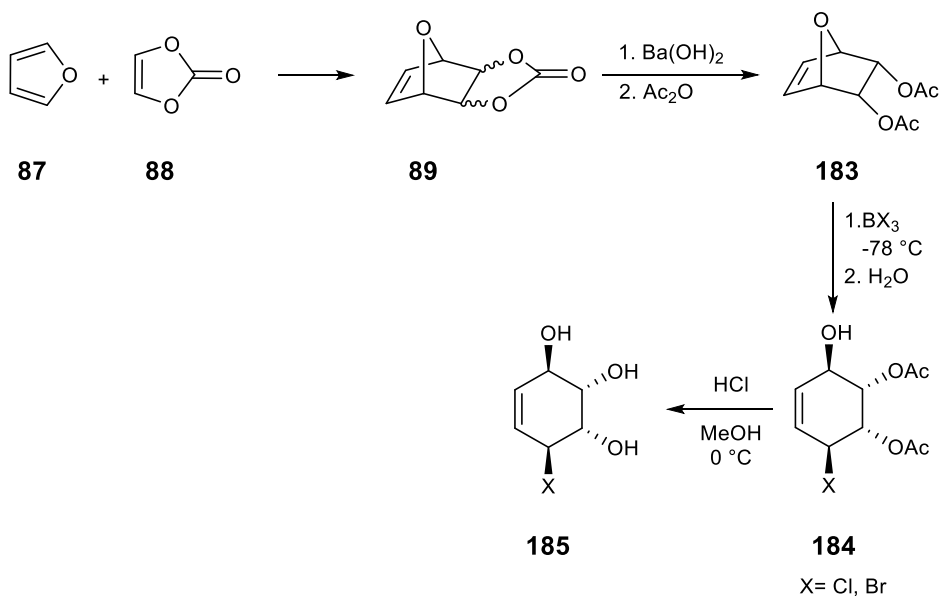
In 1997, Motherwell *et al.*⁵³ developed a methodology for the synthesis of bromoconduritol derivatives. The osmylated product **180** was reacted with sodium bromate in the presence of light. During this procedure, *trans*-addition of

hypobromous acid to the osmylated product **180** took place and bromoconduritol derivatives **181** and **182** were formed (Scheme 39).



Scheme 39. Synthesis of bromoconduritol derivatives **181** and **182**

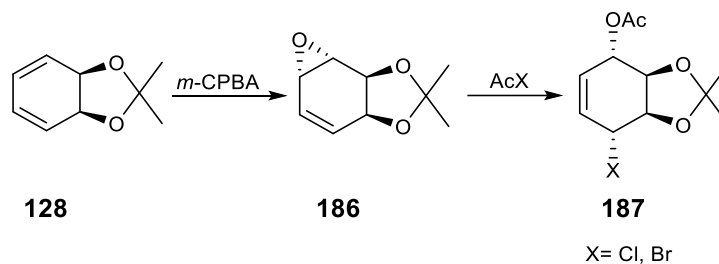
In 2003, Seçen and Sütbeyaz *et al.*⁵⁴ synthesized haloconduritol derivatives by the modification of the methodology published by Yurev and Zafirov. According to this method, the Diels-Alder reaction of furan (**87**) and vinylene carbonate (**88**) gave a mixture of *endo*- and *exo*-cycloadducts **89** as the major and minor products. The major product was converted to diacetate **183** followed by treatment with boron tribromide or boron chloride to afford the haloconduritol derivatives **184** by a stereospecific cleavage of the etheric linkage (Scheme 40).



Scheme 40. Synthesis of haloconduritol derivatives **185**

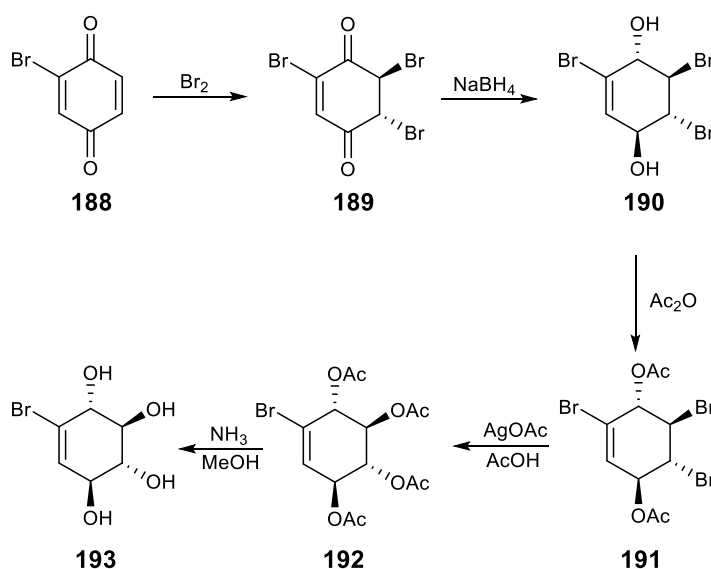
One year later, the same group revealed another synthetic pathway for the formation of haloconduritol derivatives.⁵⁵ According to their study, the ring opening reaction

of the epoxide **186** synthesized from the *cis*-diol **128** gave the targeted haloconduritol **187** by the treatment with the acyl halides without using any catalyst (Scheme 41).



Scheme 41. Synthesis of haloconduritol derivatives **187**

In a recent study, Balci *et al.*⁵⁶ synthesized bromoconduritol-B starting from bromobenzoquinone (**188**). The regioselective bromination of quinone **188** and successive reduction of carbonyl groups with NaBH_4 gave the corresponding diol **190**. After the acetylation of the hydroxyl groups, the compound **191** was treated with AgOAc and AcOH to substitute bromine atoms by acetoxyl groups. Hydrolysis of the acetates in **192** gave the bromoconduritol-B **193** (Scheme 42).



Scheme 42. Synthesis of bromoconduritol-B **193**

1.1.7 Biological Importance of Conduritol Derivatives

Conduritols are important molecules because of their applications in view of their biological activities. In addition to their usefulness in the synthesis of cyclitols such as inositols, their biological applications have gained great importance during last decades. Although the biological activities of conduritol derivatives have been studied during the last decades, their usage for medical purposes was seen on the ancient time. For example, the antidiabetic properties of conduritols were known in 1930s. At that time, the medical shrub of *Gymnena syvestre*, which is a tropical herb, was used to cure diabetic diseases. In 1990, Kensho *et al.*⁵⁷ determined that leaves of *Gymnena syvestre* contain conduritol-A (**25**) and isolated it from the leaves. In addition to this, Billington *et al.*⁵⁸ examined the effect of the conduritol derivatives onto the insulin level and detected regulation properties of conduritol-A (**25**) and conduritol-B (**26**). They also suggested that conduritol derivatives had a potential to be a drug for the treatment of diabetes.⁵⁹

Glycosidase enzymes are the enzyme that break the N- or S-glycoside bonds. They have special positions during the synthesis of glycoproteins which play important role in the processes of transformation of normal cell to the cancer cell and have trigger effect of the immune defense towards viral infections. Inhibition effect of the conduritols to glycosidase enzyme have been also known. In 1990, Fellows and Nash⁶⁰ showed that conduritols, especially the bromoconduritols, have inhibition effect for the formation of the cancer cell.⁴⁹ In the light of these information, conduritols have a potential to show an anticancer properties and inhibit human immunodeficiency virus (HIV).^{61,62}

Conduritol derivatives have also antifeedant, antibiotic, antileukemic and growth-regulating effects.² They are also used as building blocks of some biologically significant molecules. For example, *pancratium littorale*, found as an herbal medicine in the past time. Pancratistatine (**194**), which is found in *pancratium littorale*, has an inhibition effect towards protein synthesis and antineoplastic activities in ovarian sarcoma or lymphotic leukemia. It is synthesized from Lycoridine (**195**). Lycoridine, synthesized starting from conduramine-A (**196**)

in nine steps, also shows inhibition effect towards oligosaccharide-processing enzymes, and is a chemotherapeutic agent (Figure 7).⁶³

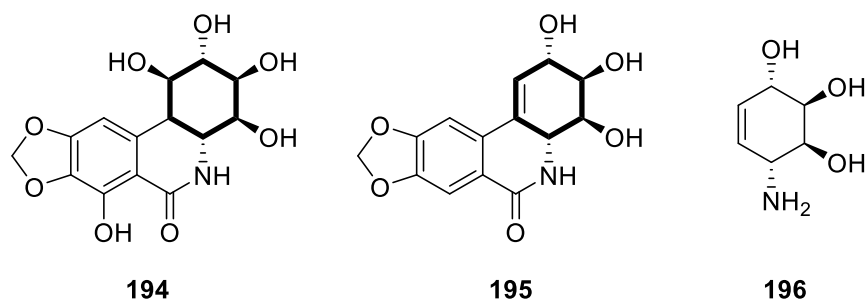


Figure 7. Structures of Pancratistatine (**194**) and Lycoridicine (**195**)

Some complex molecules were synthesized starting from conduritol derivatives. The C1-C22 subunit of halichondrin B (**197**) which has 11 asymmetric center and six rings in its structure was synthesized by Burke *et al.*⁶⁴ starting from the (+)-conduritol-E (**29**) in 18 steps. In addition to this, the total synthesis of the hexol **198** was achieved by Billington *et al.*⁵⁸ starting from the conduritol-A (**25**) because of its modulation effect releasing of insulin in both stimulatory and an inhibitory conditions (Figure 8).

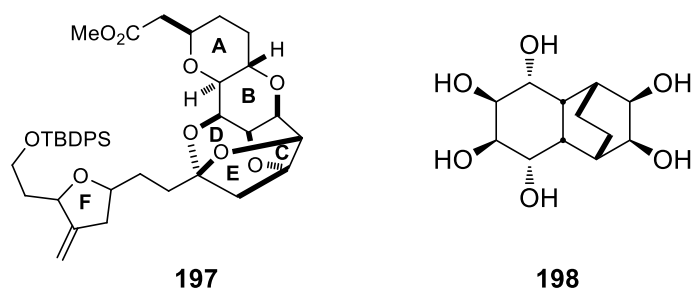
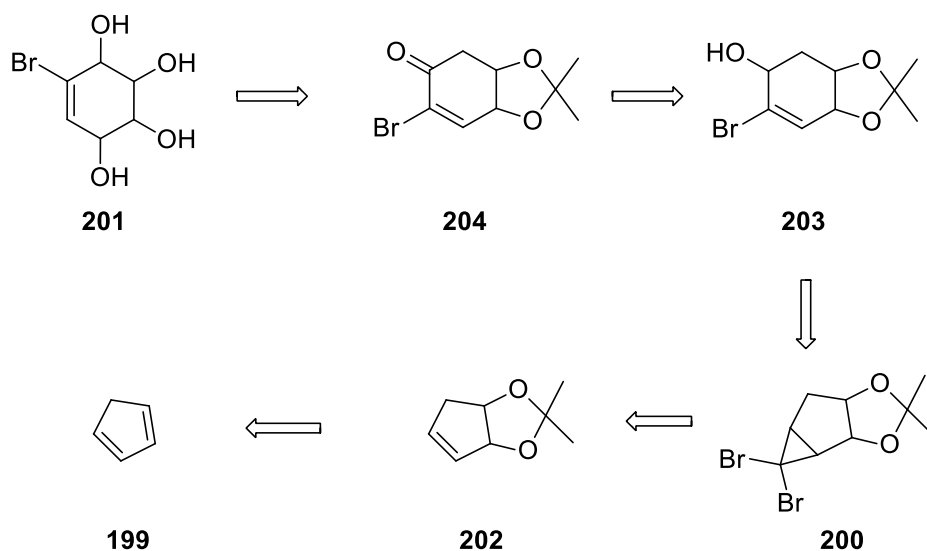


Figure 8. Structures of halichondrin-B (**197**) and hexol **198**

Haloconduritols have also the similar effect as conduritols and their some biological activities are known in the literature. Datema *et al.*⁶⁵ found that bromoconduritols affect the release of the virus of influenza. In addition to this, Legler *et al.*⁶⁶ claimed that bromoconduritols were the active site directed and covalent inhibitors of α -glycosidase enzyme and therefore, they attracted interests in AIDS research area.^{2,56}

1.1.8 Aim of the Study

Because of the biological properties and being useful intermediates of haloconduritol, they became synthetically important molecules. During the last decades, some methodologies were developed for construction of haloconduritol derivatives. The aim of this thesis was to develop a new synthetic method for the synthesis of haloconduritol. Retro-synthetic analysis of haloconduritol derivatives is given in Scheme 43. For the synthesis of bromoconduritol derivative **201**, cyclopentadiene (**199**) was chosen as the starting material because of its low price and easy availability. To introduce the hydroxyl functionalities into the molecule, the stereospecific *cis*-hydroxylation reaction of one of the double bonds was preferred. After protection of *cis*-diol as a ketal **202**, we intended to apply a carbene addition using Makozsa method to synthesize the tricyclic molecule **200** which should be a precursor of compound **203**. For the introducing the final hydroxyl group, Mn(OAc)₃ mediated α -acetoxylation reaction of the α,β -unsaturated cyclohexene derivative **204** was planned to obtain **201** (Scheme 43).

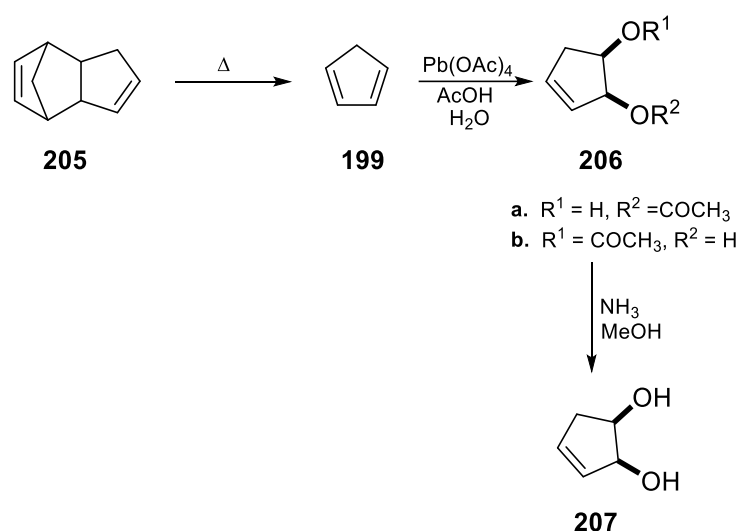


Scheme 43. Retrosynthetic plan for bromoconduritol **201**

1.2 Results and Discussion

1.2.1 Synthesis of cyclopent-3-ene-1,2-diol (**207**)

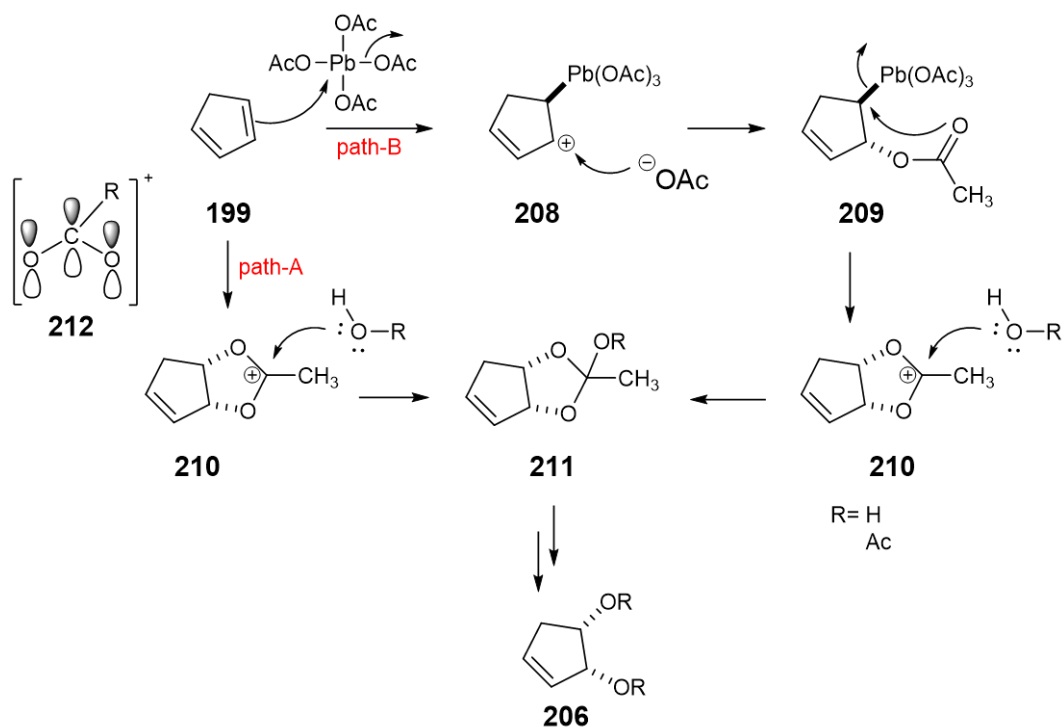
The *cis*-diol **207** was synthesized starting from cyclopentadiene (**199**). Cyclopentadiene occurs at room temperature as dicyclopentadiene (DCPD) **205** which is a dimeric form of cyclopentadiene. Over 150 °C, dicyclopentadiene undergoes retro Diels-Alder reaction to give the cyclopentadiene (**199**). Therefore, dicyclopentadiene was first cracked to produce cyclopentadiene (**199**). Twice distilled cyclopentadiene (**199**) was then subjected to the stereospecific *cis*-hydroxylation reaction in the presence of lead (IV) acetate in acetic acid (Scheme 44).



Scheme 44. Synthesis of *cis*-diol **207**

Two different mechanisms for the formation of *cis*-diol **207** are postulated in the literature⁶⁷ which are presented in Scheme 45. According to the first mechanism (path-A) the intermediate **212** or its equivalent is formed by direct addition of acetate to cyclopentadiene (**199**). The formation of the intermediate **210** was followed by the nucleophilic addition of acetic acid or water on the α -position of the oxolonium ion **210** to form glycolic ester **211**. The ring-opening of **211** results in the formation of **206**. Second mechanism (path-B) first proceeds by the attacking

of the double bond on the central metal atom forming free acetate anion and the (allylic) carbocation which can be captured by free acetate anion from the back side attack forming the *trans*-addition product **209**. The formation of compound **209** is followed by the departure of the lead(III) acetate by substitution of the carbonyl oxygen and forming the intermediate **210** which is the same glycolic ester discussed in the path-A. The hydrolysis of compound **211** gives a mixture of regio isomers of mono-acetylated cyclopentene derivatives **206**. To furnish the targeted *cis*-hydroxylated product, compound **206** was hydrolyzed by the ammonia in methanol to give **207** (Scheme 44). Over the all steps, the *cis*-hydroxylation reaction yielded the racemic mixture of the compound **206** in moderate yield (65%).



Scheme 45. $\text{Pb}(\text{OAc})_4$ mediated *cis*-hydroxylation reaction mechanism

The NMR spectral data were in agreement with the structure of **207**.⁶⁸ The ^1H -NMR spectrum shows two olefinic proton signals at 5.85 and 5.71 ppm with coupling constants of $J = 5.6$ Hz. Additionally two alkoxy proton resonances are observed at 4.48 and in the range of 4.30 – 4.09 ppm with a coupling constant of $J = 4.8$ Hz. Geometry optimized calculations showed that the dihedral angle between two alkoxy protons should be about 58.2° (Figure 9). According to the Karplus-Conroy

curve^{69,70}, this angle shows that the corresponding coupling constant value should be between 3.5 – 6.0 Hz. The coupling constant determined supports the *cis*-configuration of hydroxyl groups. The AB system at 2.51 and 2.28 ppm shows the presence of two diastereomeric –CH₂– protons in the cyclopentene ring.

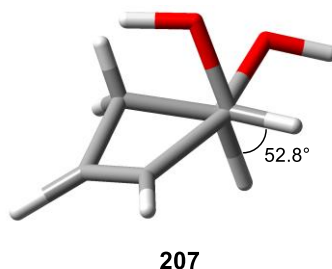
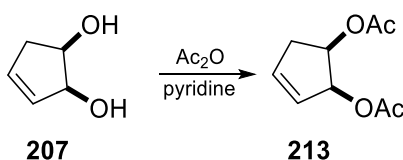


Figure 9. The optimized geometry of the *cis*-cyclopent-3-ene-1,2-diol **207**

The ¹³C-NMR spectrum has five different signals. Two of them appear in the range of sp²-hybridized carbon atoms, at 132.8 and 131.6 ppm, and the other two are observed at 75.8 and 70.9 ppm, showing the connection to electronegative oxygen atoms. The resonance signal at 39.4 ppm belongs to the –CH₂– carbon atom. In addition to this, the IR spectrum shows a broad signal at 3345 cm⁻¹ which supports the presence of the hydroxyl groups.

1.2.2 Synthesis of cyclopent-3-ene-1,2-diyl diacetate (**213**)

After synthesis of the *cis*-hydroxylated cyclopentene **207**, for further characterization of the compound and to protect the hydroxyl groups for the next reactions, diol **207** was submitted to acetylation reaction with acetic anhydride in pyridine at room temperature (Scheme 46).

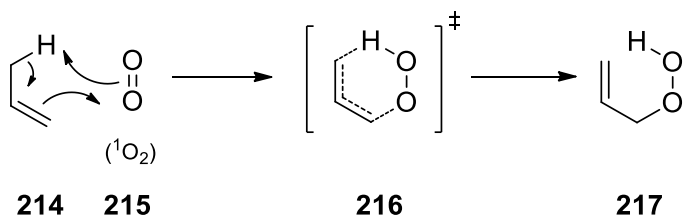


Scheme 46. Acetylation reaction of compound **207**

The ^1H -NMR spectrum of the compound **213** shows two olefinic proton resonances as multiplet in the range of 6.02 – 5.98 ppm and doublet of quartets at 5.76 ppm. Additionally, two resonance signals appear at 5.61 and 5.29 ppm which are shifted to the lower field with respect to the diol **207**. This low field of the acetoxy protons are due to the electron withdrawing effects of acetate groups. The methylene protons appear again as an AB-system. The A-part of the AB system resonates at 2.65 ppm and the B-part at 2.43 ppm. Also there is a singlet at 2.0 ppm with six integration value which belongs to $-\text{COCH}_3$ protons of the acetyl groups. In the ^{13}C -NMR spectrum, there are nine signals. Four new carbon signals support the introducing of the acetyl groups. Two of them belong to the carbonyl carbon atoms of the acetyl group and they resonate at 170.3 and 170.2 ppm. The olefinic carbons resonate at 134.7 and 128.2 ppm. Tertiary carbons are shifted to the lower field as observed in the ^1H -NMR spectrum and they appear at 75.6 and 71.2 ppm. The methylene carbon resonates at 36.6 ppm. Methyl groups resonate at 20.8 and 20.7 ppm. In addition to the NMR spectra, IR spectrum supports our result with having the carbonyl group absorption at 1721 cm^{-1} and disappearing the hydroxyl group signal at 3345 cm^{-1} .

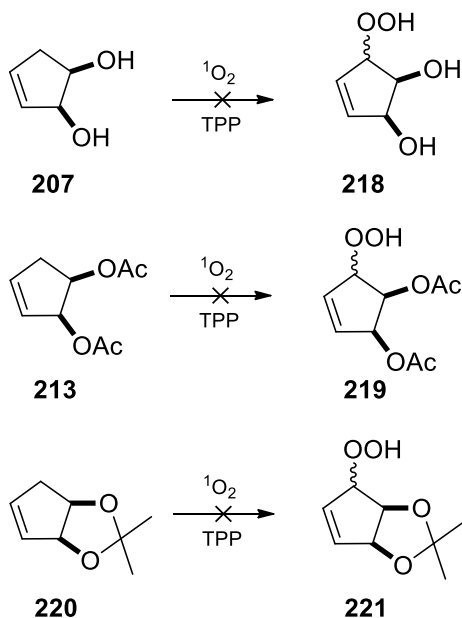
1.2.3 Attempted Oxidation of **207**, **213**, and **220** with Singlet Oxygen: Ene Reaction

The further oxidation of the cyclopentene ring, introduction of an additional hydroxyl group into the molecule, was aimed by ene-reaction of the singlet oxygen. The ene reaction, also known as the Alder-ene reaction, is a pericyclic reaction in which four π -electron system of double bond and allylic hydrogen bond (ene) interact an olefin (enophile) to form a new C–O bond and C=C double bond through the intermediate **216**. Hydrogen atom is shifted to the enophile (singlet oxygen) where an allylic shift of the double bond occurs. Finally, an unsaturated hydroperoxide is formed. This reaction was discovered by Schenk in 1953.⁷¹ The ene-reaction can be ensued by different intermediates which determines the regioselectivity and stereoselectivity of the reaction in the asymmetric double bonds (Scheme 47).^{72,73}



Scheme 47. The mechanism of the singlet oxygen ene reaction

The oxidation of the cyclopentene derivatives with singlet oxygen was attempted in the presence of photosensitizer, tetraphenylporphyrin (TPP). The reaction proceeding was followed by TLC. Although the long reaction time, the expected product, the hydroperoxide was not formed. After this unsuccessful result, our attention turned out to protection of the hydroxyl functionalities in **207**. The diol protected derivatives **213** and **220** were also subjected to the photooxygenation reaction, unfortunately the corresponding hydroperoxides were not formed (Scheme 48).



Scheme 48. Synthetic attempts for ene reaction

1.2.4 Carbene Addition Reaction

To generate a six membered ring starting from a five membered, the ring enlargement reaction of the cyclopentene was required. Carbene addition to a double bond for the formation of cyclopropane ring and following ring opening reaction is one of the ring enlargement strategy.

Carbenes have generally sp^2 hybridized central carbon atom. The two sp^2 hybridized hybrid orbital make bond with the substituents and the other two orbitals, sp^2 and p orbitals, are empty. Unpaired two electrons are located in these orbitals. Because of the location of these two electrons, carbenes can be singlet if two electrons are located in the same orbitals, or triplet where two electrons are located in two different orbitals in terms of the Hund's rule. This difference is caused from the energy difference of the σ - and π -orbitals. If the energy difference is high enough, electrons prefer to populate the same orbital and so the electronic configuration of the carbene is singlet. If the energy difference is low, then the electrons can go in two different orbitals and the electronic configuration of the carbene is then triplet. The substituents affect the electronic configuration of the carbenes. If carbene is attached by the electron withdrawing groups, the electronic configuration of the carbene is singlet because the attached group makes the σ -bond of the carbene more stable and increase the energy difference between σ - and π -bonds by inductively and electrons are located in the same orbital or vice versa. On the other hand, if the carbene substituted by atoms, having unpaired electrons, like halogens, because of the donating of electrons mesomerically to locate one of the empty orbitals carbenes are singlet (Figure 10).⁷⁴

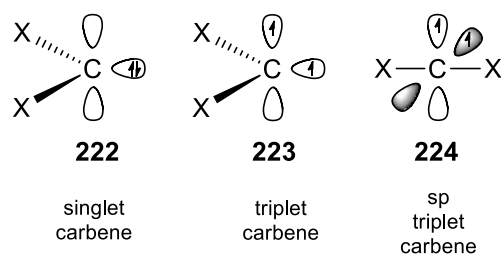


Figure 10. Structures of singlet and triplet carbenes

Carbenes are generated by different methods. One of the generation methods of carbenes is α -elimination reaction of haloforms by strong bases in aprotic solvents. Since carbenes are reactive intermediates, the reaction medium should not contain any water. In other words, carbenes can be generated in the dry reaction medium or solvents.

In 1969, Makozsa *et al.* revealed a work showing the generation of the carbene in the biphasic system by using the phase transfer catalyst (PTC) and sat. NaOH solution in water.⁷⁵ Phase transfer catalysts are generally tetrasubstituted ammonium salts. For this reason it helps the transfer of the carbene precursor anion from aqueous phase to organic phase. As soon as carbene is in situ formed in the organic phase, it is easily added to the double bond (Figure 11).

The most common reactions of carbenes are cyclopropanation reactions by [2+2] cycloaddition mechanism. The electronic configuration of the carbenes determine the stereochemical outcome of the cycloaddition products.

According to Skell and Woodward singlet carbenes generally give the stereospecific addition to the double bonds yielding *syn*-addition product with

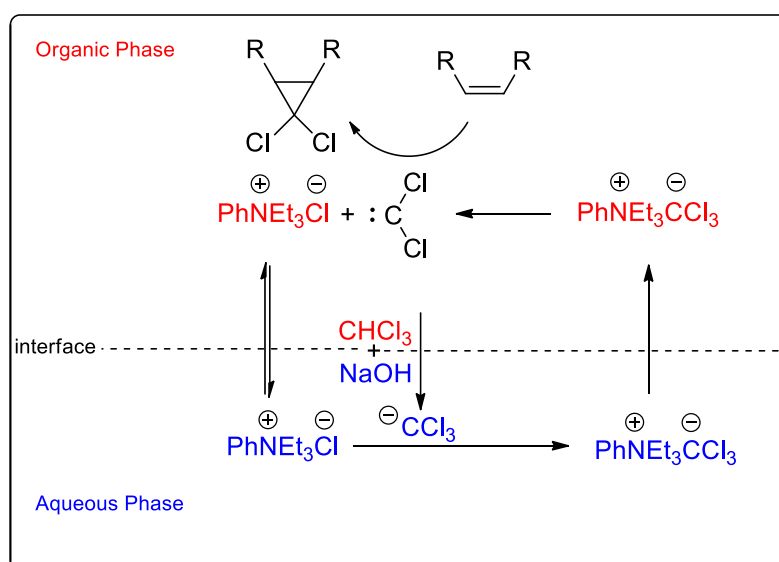
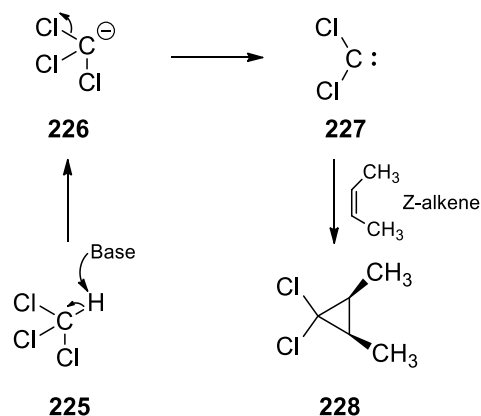


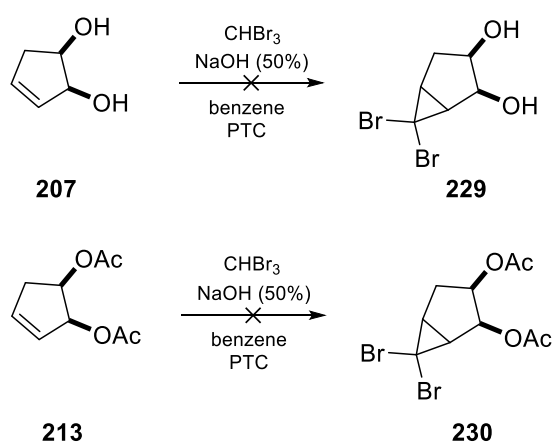
Figure 11. Phase transfer catalyst mechanism for carbene generation



Scheme 49. Stereospecific carbene addition by α -elimination

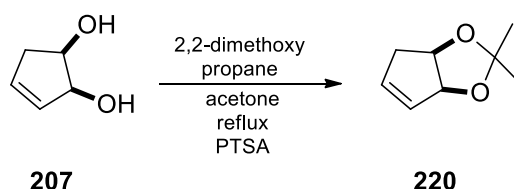
a synchron process.⁷⁶ This type cyclopropanation by carbene addition reaction is the most used method to construct cyclopropane ring (Scheme 49).

In our synthetic strategy, the carbene addition reaction to the double bond of the cyclopentene was performed to generate bicyclic compound **229**. Although different reaction conditions were tried, the carbene addition reaction to diol **207** could not be achieved because of the solubility of diol **207** in water phase. Then our attention turned out to protect the hydroxyl group with acetate groups. After acetylation of the hydroxyl groups, the carbene addition was performed but it was not successful. The hydrolysis of the acetate groups in strong basic medium took place and the protected compound **213** was converted to the corresponding diol **207** (Scheme 50).



Scheme 50. Attempted carbene addition to **207** and **213**

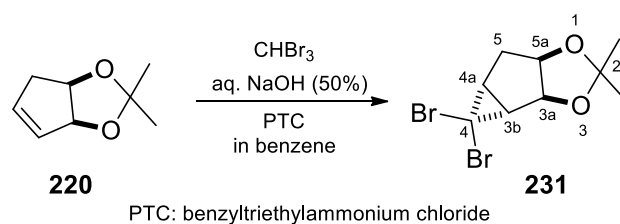
After unsuccessful results, we decided to protect the hydroxyl groups so that they should be stable in the basic medium. The ketal protected groups are generally stable in the basic reaction medium. So, we tried to protect the diol unit as a ketal group. For this purpose, diol **207** was treated with 2,2-dimethoxypropane to yield compound **220** (Scheme 51).



Scheme 51. Ketal formation

The ^1H -NMR and ^{13}C -NMR spectral data are in agreement with the structure **220**. The ^1H -NMR spectrum shows two olefinic proton resonances appearing as a doublet of triplets at 5.76 ppm and doublet of quartets at 5.71 ppm. The alkoxy proton next to the double bond resonates at 5.04 ppm as a broad doublet with a coupling constant of $J = 5.9$ Hz. The other alkoxy proton resonates at 4.69 ppm as a doublet of triplets. Doublet splitting ($J = 1.8$ Hz) is arising from the coupling with one of the methylene protons. Triplet splitting ($J = 5.9$) is due to the coupling with the other methylene proton and adjacent alkoxy proton. The methylene protons resonate as an AB-system between 2.56 ppm and 2.40 ppm having main geminal coupling constant of $J = 18.0$ Hz. The ^{13}C -NMR spectrum shows eight resonance signals as expected. The resonance signals at 109.7, 85.5, and 77.7 ppm are in agreement with the ketal structure

Carbene addition to **220** was performed by using the Makozsa procedure.⁷⁵ For this purpose, compound **220** was reacted with dibromocarbene which was formed in situ by the α -elimination of bromoform in the presence of aqueous NaOH (50%) solution and benzyltriethylammonium chloride as phase transfer catalyst (PTC) to give dibromocarbene adduct **231**. (Scheme 52).



Scheme 52. Dibromocarbene addition reaction to **220**

The structure of tricyclic compound **231** was determined by means of the 1D- and 2D-NMR spectra which were also supported by HRMS analysis. The ¹H-NMR spectrum shows eight different resonances. Two of them are arising from methyl protons, four of them from tertiary protons and the remaining resonances belong to two diastereotopic methylene protons which appear as an AB-system. The disappearance of the olefinic proton signals in **220** appearing at around 5.76 ppm and 5.71 ppm and formation of the aliphatic proton signals at around 2.42 ppm and

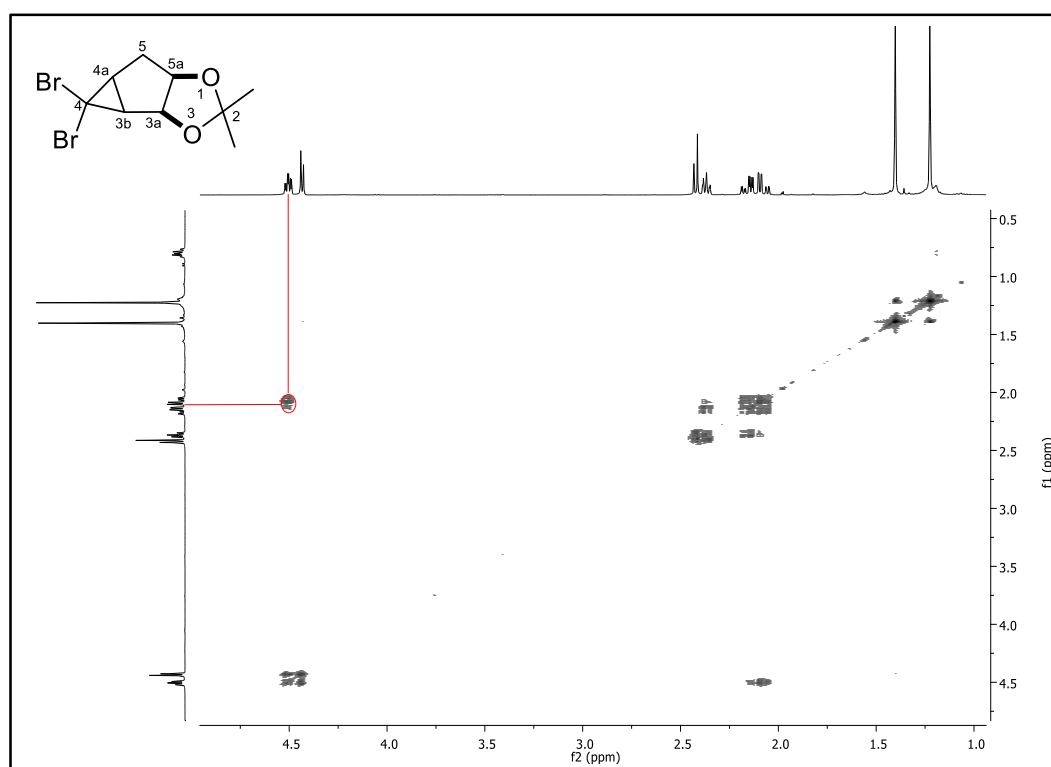


Figure 12. COSY spectrum of compound **231**

2.37 ppm clearly show the addition of dibromocarbene to the double bond. The alkoxy protons (H-3a and H-5a) appear as an AB-system at around 4.51 and 4.43 ppm. The low field resonance belongs to the alkoxy proton H-5a which is adjacent to the methylene group (determined by the COSY spectrum) and is split into the doublet of triplets by two methylene protons and H-3a (Figure 12). The H-3a proton resonates as doublet although it has two adjacent protons. This is due to the dihedral angle between H-3a and H-3b protons. According to the geometry optimized DFT calculations of *anti*-addition product, the dihedral angle between these two protons is approximately 88.1° and this coupling constant should be near to zero with respect to the Karplus-Conroy curve. In the COSY spectrum, it can be easily seen that there is no correlation between these two protons. This result also supports the *anti*-addition of the carbene to the double bond with respect to the ketal unit (Figure 13).

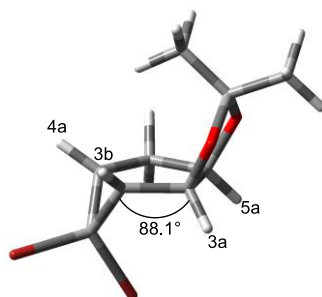
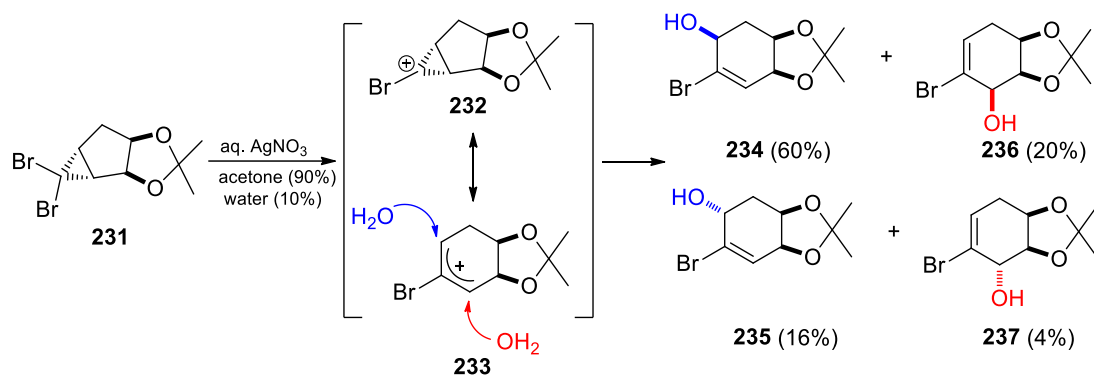


Figure 13. The optimized geometry of the carbene-adduct **231**

The ^{13}C -NMR spectrum shows nine distinct signals. Olefinic carbon resonances disappeared and new three different aliphatic signals belonging the cyclopropane ring appeared. The quaternary carbon atom connected two oxygen atoms resonates at 111.8 ppm. Alkoxy carbon atoms appear at 85.0 and 84.7 ppm. The cyclopropane carbons resonances appear at 41.6, 38.0, and 35.2 ppm. According to the DEPT-135 NMR spectrum, methylene carbon atom resonates at 36.6 ppm. The remaining methyl carbon resonance signals appear at 27.1 and 24.9 ppm. The HRMS spectrum supports the formation of the molecule (Figure 14).



Scheme 53. Electrophilic ring opening reaction

$^1\text{H-NMR}$ spectrum of the major product **234** shows nine different proton resonances. The olefinic proton resonance appears at 6.01 ppm as doublet of doublets with coupling constants of $J = 3.2$ and 1.1 Hz. The COSY spectrum of **234** shows that there is no coupling between the olefinic proton and the methylene protons (Figure 15). There is strong correlation between the olefinic protons and the neighboring alkoxy proton. On the basis of this finding we were able to

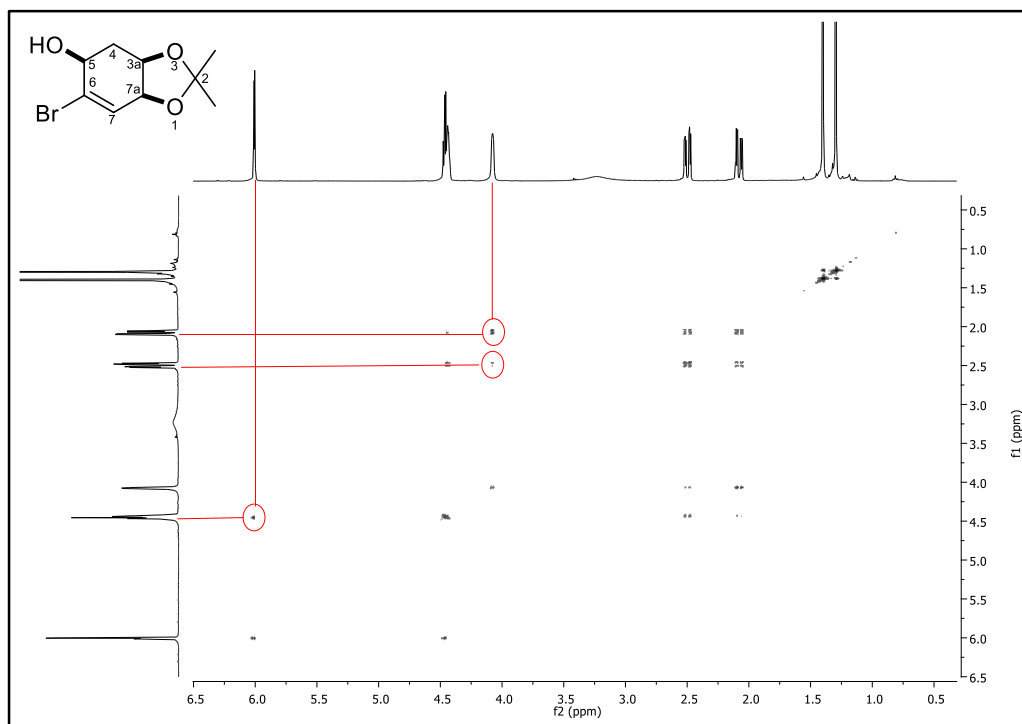


Figure 15. COSY spectrum of the compound **234**

distinguish between two different constitution **234** and **236** and assigned the structure **234** as the major product. The coupling constant, $J = 1.1$ Hz, shows that this is an allylic coupling. Additionally, the proton resonance appearing at 4.47 ppm which belongs to the tertiary proton, next to the double bond in **234** and **235**, also support this arrangement by splitting into doublet of doublets with the coupling constants of $J = 4.9$ Hz and $J = 3.2$ Hz. Additionally, the $-\text{CH}_2-$ protons resonate as an AB-system. The A-part of this system appears at 2.50 ppm and the B-part appears at 2.08 ppm as doublet of doublets of doublets. The main coupling between these two methylenic protons, geminal coupling, ${}^2J = 15.3$ Hz is in agreement with the structure.

In addition to this, the resonance assigned belonging to the $-\text{OH}$ signal at 3.23 ppm was confirmed by deuterium exchange experiment.

The ${}^{13}\text{C}$ -NMR of the major product has nine resonance signals. In the sp^2 region, there are two olefinic resonance appearing at 128.7 and 128.2 ppm. The quaternary carbon connected by two oxygen atoms resonates at 110.2 ppm. Three tertiary carbons which are next to the oxygen atoms appear at 74.0, 71.9 and 69.4 ppm. According to the HSQC spectrum, the resonance signal at 69.4 ppm belongs to the carbon atom connected by hydroxyl group. The DEPT-135 spectrum shows the resonance signal at 32.4 ppm belongs to the $-\text{CH}_2-$ carbon. The rest two carbon resonance signals at 28.1 and 26.5 belong to the methyl carbons.

Having ascertained the constitution of the major product as **234** or **235**, the correct configurations were determined again by means of the ${}^1\text{H}$ -NMR spectra. The resonance of the alkoxy proton appeared at 4.08 ppm is split into broad doublet with a coupling constant of $J_{(5,4a)} = 2.3$ Hz arising from the coupling of one of $-\text{CH}_2-$ protons. The magnitude of this coupling constant shows that the dihedral angle between this alkoxy proton and $-\text{CH}_2-$ protons must be in between 50° and 80° according to the Karplus-Conroy curve.⁶⁹ The geometry optimization calculations of two products **234** and **235** showed that the dihedral angles between the alkoxy proton and methylene protons are about 46° and 71° in the *syn*-configured product **234**. According to these calculations the corresponding coupling constants should have a value of 0 – 3.0 Hz (Figure 16).

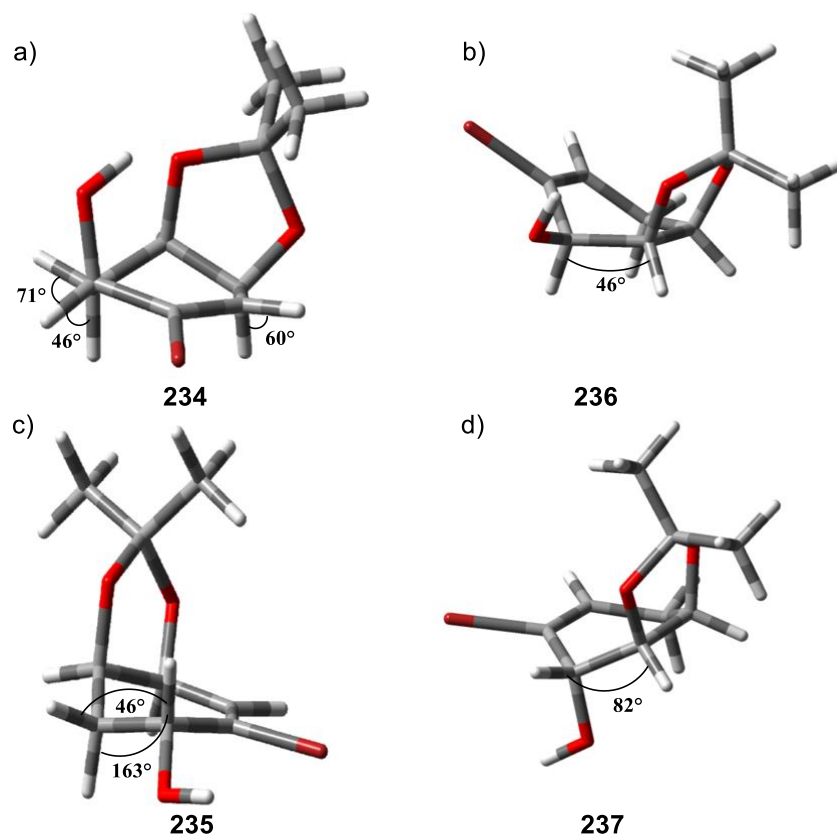


Figure 16. Optimized geometry of compounds **234**, **235**, **236** and **237**

Experimentally determined value, $J_{(5,4a)} = 2.3$ Hz, is in good agreement with the calculations. Therefore, *syn*-configuration (with respect to the ketal functionality) of the hydroxyl group in **234** was assigned. In the case of the *anti*-configured product, the corresponding angles were calculated as 46° and 163° (Figure 16). The dihedral angle of 163° between one of the $-\text{CH}_2-$ protons and alkoxy proton should have the coupling constant $8.5 - 11.0$ Hz with respect to the Karplus-Conroy curve. In the case of **235**, the coupling constant between the alkoxy proton and one of the methylene protons was found to be $J = 8.4$ Hz. This result, furtherly confirm our finding. Therefore, *anti*-configuration to the hydroxyl group in **235** was assigned.

The constitution of the other isomers **236** and **237** was determined mainly by the coupling constants. Strong correlation between the olefinic proton and the methylene protons supported the proposed constitution for **236** and **237**. To distinguish between these two configurational isomers, again geometry optimization calculations were carried out. The dihedral angle between the alkoxy

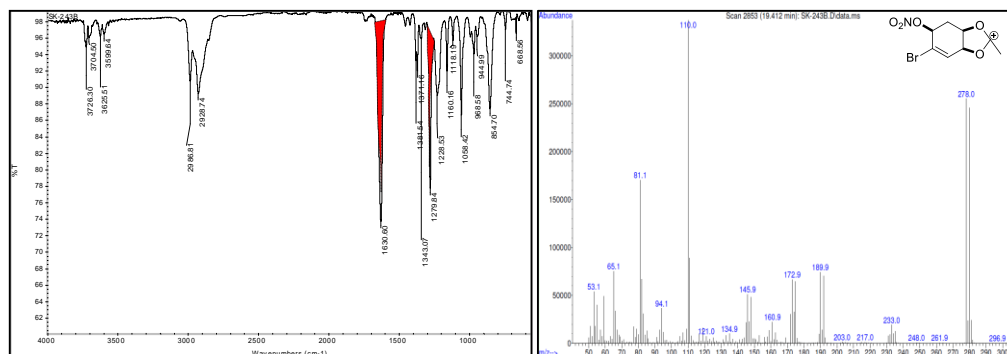


Figure 17. IR and Mass spectrum of compound **238**

resonating at 2.56 ppm and 2.23 ppm, which supports the exact location of $-\text{ONO}_2$ group in **238** (Figure 18).

$^1\text{H-NMR}$ spectrum of the compound **238** also gives information about the configuration of the molecule. The tertiary proton next to $-\text{ONO}_2$ group resonates as doublet of doublets ($J = 5.0$ and 2.6 Hz) due to the coupling with methylene protons. The theoretical calculations show that in the molecule having *syn*-configured $-\text{ONO}_2$ group, the dihedral angle between tertiary proton and methylene protons should be around 73.9° and 41.5° (Figure 19a). According to the Karplus-Conroy curve, estimated coupling constants should be in between 2.0

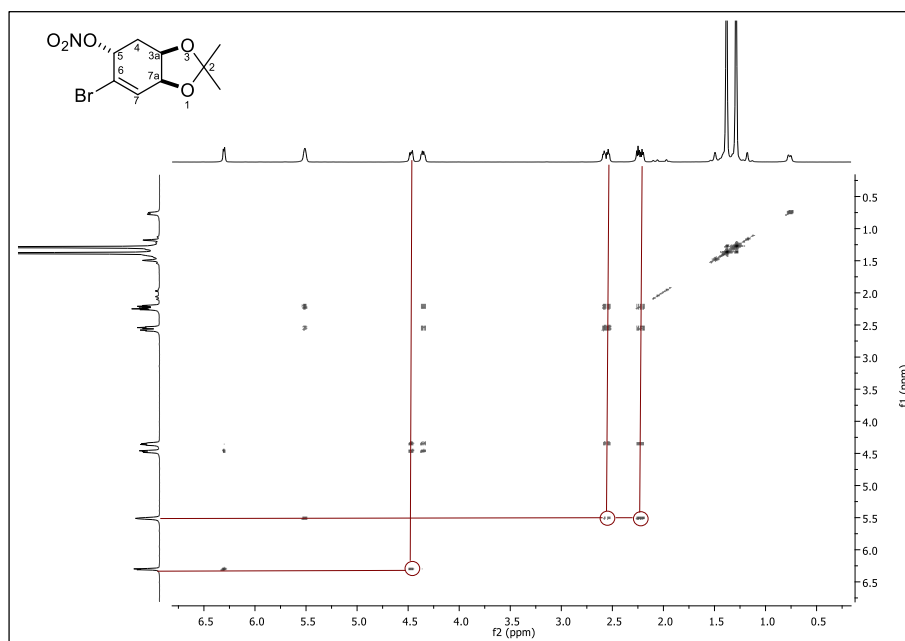


Figure 18. COSY spectrum of compound **238**

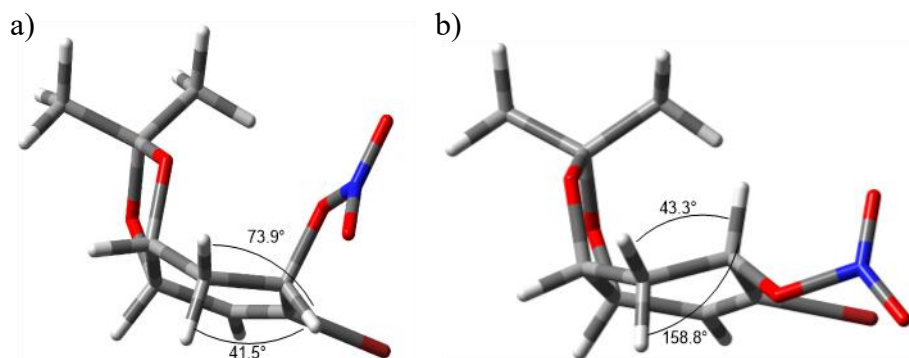
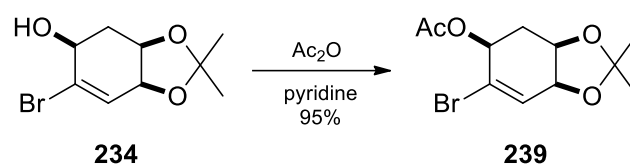


Figure 19. Optimized geometry of possible configurations of **238**

– 8.0 Hz. Experimental values of coupling constants, $J = 5.0$ and 2.6 Hz, refers to the *syn*-configuration of $-\text{ONO}_2$ group. According to our calculations, the related coupling constants in the case of *anti*-configuration should be $8.5 - 10.0$ Hz (Figure 19).

1.2.6 Acetylation Reaction of the Major Ring-Opening product **234**.

The major product **234** was submitted to acetylation reaction. For this purpose, compound **234** was treated with acetic anhydride in pyridine at room temperature and acetylated product **239** was isolated in 95% yield and characterized without any additional purification (Scheme 55).



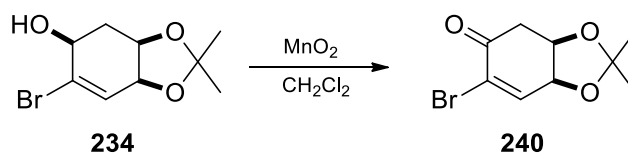
Scheme 55. Acetylation reaction of compound **234**

In the $^1\text{H-NMR}$ spectrum, olefinic proton resonates at 6.22 ppm as a doublet. The alkoxy proton resonance signal of the starting material at 4.08 ppm was shifted to the lower field (5.36 ppm) because of the presence of the electron-withdrawing acetate group. Additionally, a new methyl resonance at 2.13 ppm also showed the introduction of the acetyl group into the molecule. $^{13}\text{C-NMR}$ spectrum of molecule

239 has eleven carbon resonance signals. The carbonyl carbon resonance appearing at 170.0 ppm which is a characteristic chemical shift for the ester carbons and a new methyl carbon resonance signal in the aliphatic region also show the introduction of the acetyl group.

1.2.7 Allylic Oxidation Reaction of the Major Ring-Opening Product **234**.

For the synthesis of haloconduritol derivatives, α -acetoxylation reaction of **240** was necessary to introduce the final hydroxyl group. To perform the α -acetoxylation reaction, oxidation of the allylic hydroxyl group in **234** was required. For this purpose, allylic alcohol **234** was treated with activated MnO_2 in CH_2Cl_2 to give the desired α,β -unsaturated bromoenone **240** in quantitative yield (Scheme 56).

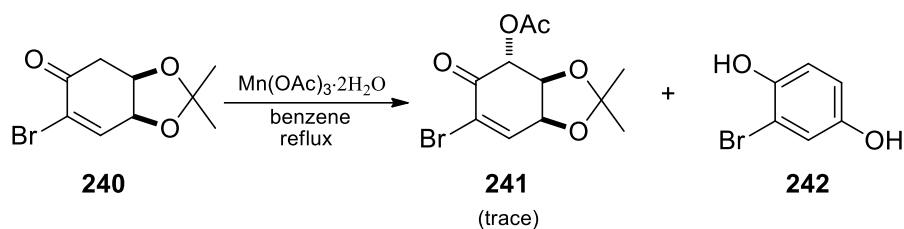


Scheme 56. Allylic oxidation reaction of the compound **234**

The compound **240** was characterized by means of the $^1\text{H-NMR}$ and $^{13}\text{C-NMR}$ spectra. The formation of the α,β -unsaturated ketone was easily recognized by shifting of the olefinic resonance signal to the aromatic region (7.03 ppm). In addition to this, the resonance signal of the methylene protons were also shifted to lower field (3.11 and 2.71 ppm). The geminal coupling constant between the methylene protons was increased up to 17.5 Hz which is specific value for being adjacent to the carbonyl group. In the $^{13}\text{C-NMR}$ spectrum, the newly formed carbonyl resonance signal at 187.3 ppm shows the achievement of the allylic oxidation.

1.2.8 α -Acetoxylation Reaction of **240** with $\text{Mn}(\text{OAc})_3$

In our synthetic pathway, $\text{Mn}(\text{OAc})_3$ mediated α -acetoxylation reaction was performed for the final oxidation of the cyclohexene ring and incorporate the final



Scheme 57. α -Acetoxylation reaction of the compound **240**

hydroxyl group which is required for the haloconduritol skeleton. This procedure is one of the well-known and applicable method to introduce acetoxy group to the α -position of a ketone.⁷⁸ (Scheme 57).

Reaction of **240** with Mn(OAc)_3 in benzene as described in the literature⁷⁸ formed the aromatized product **242**, a trisubstituted benzene derivative almost in quantitative yield (98%). Then, the reaction conditions were changed. First, the Dean-Stark apparatus was used to remove the water from the reaction medium. After unsuccessful results, the reaction temperature was decreased and the water was removed from the Mn(OAc)_3 before the addition to the reaction medium. All these attempts failed and the targeted α -acetoxyated compound **241** was isolated in trace amount (1%). From the $^1\text{H-NMR}$ spectrum of **241**, incorporation of the acetoxy group was observed. A new methyl resonance signal at 2.15 ppm and a new proton resonance signal at 5.50 ppm showed the presence of the acetoxy group in **241**. The doublet splitting of this resonance signal with a coupling constant of $J = 8.3$ Hz gave additional information about the *anti*-configuration of the acetoxy

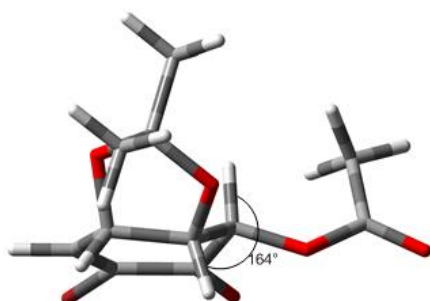


Figure 20. Optimized geometry of compounds **241**

group. The geometry optimized structure of the compound **241** showed that the dihedral angle between these protons should be about 164° . According to the Karplus-Conroy curve, the estimated coupling constant should be between 8.5 – 12.0 Hz (Figure 20). This value is in agreement with the *anti*-configuration.

The major product, 2-bromohydroquinone (**242**), was characterized by the $^1\text{H-NMR}$ spectrum, which showed three different aromatic signals (Figure 21a). Coupling constants show that there are one proton having only meta coupling, one proton having only ortho coupling and one proton having meta and ortho couplings. On the basis of the recorded coupling constants, we determined the benzene ring is substituted at 1,2,4 positions (Figure 21b). According to the proposed mechanism which is depicted in Scheme 58, there are two possible structures **242** or **246**. In order to distinguish between these two possible isomers, we recorded 2D-NMR spectra. The HMBC spectrum showed that there is no correlation between the carbon atom bearing the bromine and the proton which resonates as doublet of doublets. After determination of the exact position of the bromine atom, we assigned the structure **242** as the major product which was in agreement with the literature.^{79,80}

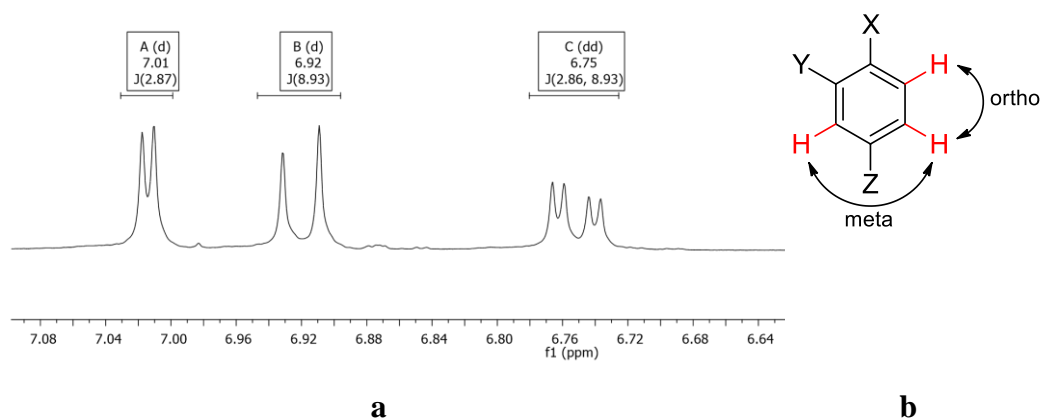
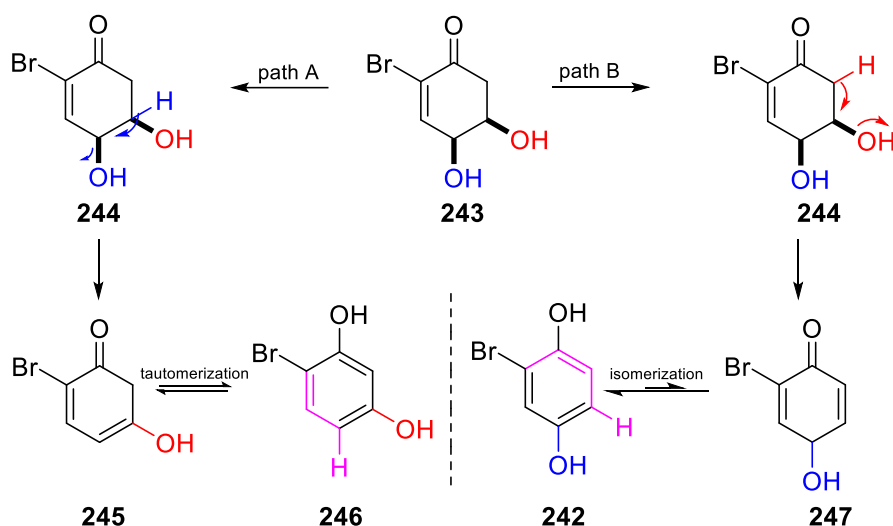


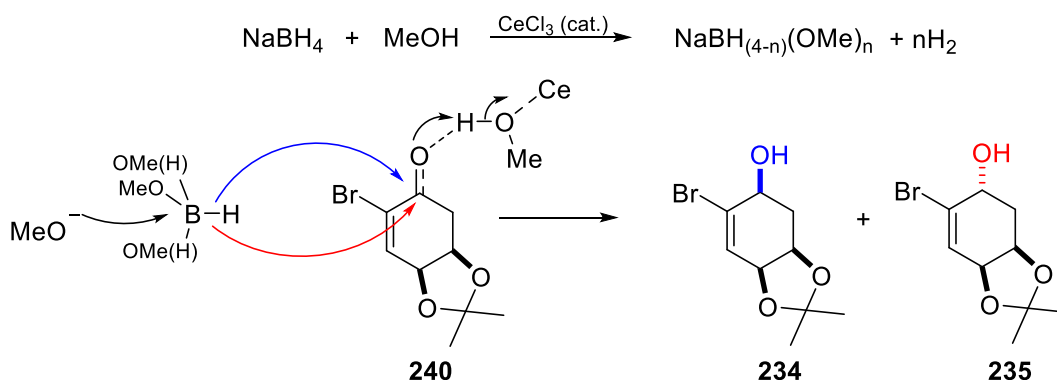
Figure 21. $^1\text{H-NMR}$ of compound **242** and corresponding possible couplings



Scheme 58. Possible reaction pathways

1.2.9 Reduction of α,β -Unsaturated Compound: The Luche Reduction

After unsuccessful results for the synthesis of α -acetoxyated compound **240**, we decided to reduce the carbonyl group to get the corresponding three hydroxylated compounds **234** and **235**. For this purpose, “Luche Reduction” conditions were applied. According to this procedure, in the presence of CeCl_3 , a selective catalyst for methanolysis of NaBH_4 , a harder reducing agent is produced for selective 1,2-reduction reaction of the α,β -unsaturated systems (Scheme 59).^{81,82}

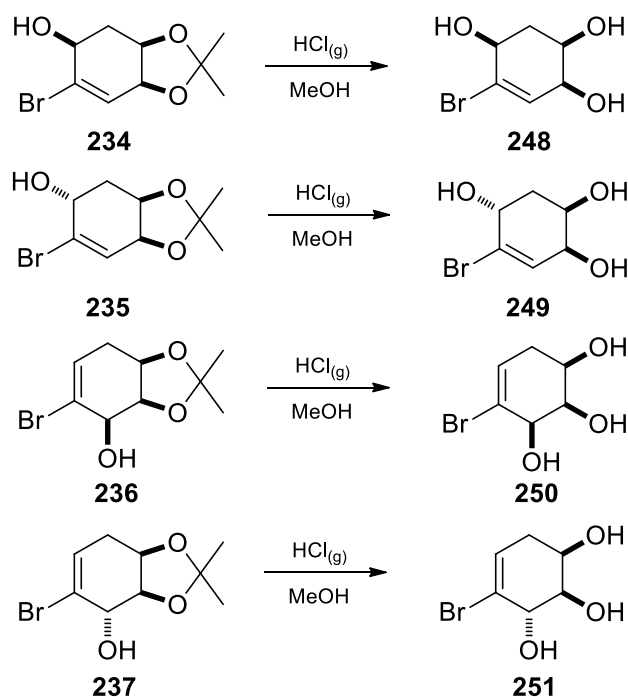


Scheme 59. The reduction of **240**.

The Luche reduction of the compound **240** gave a mixture of **234** and **235** in a ratio of 1.6:1 determined from the crude $^1\text{H-NMR}$ spectrum. Spectroscopic data, $^1\text{H-NMR}$ and $^{13}\text{C-NMR}$ are also in agreement with the data reported in the literature.⁸³

1.2.10 Synthesis of Bromotriols 248-251: Deprotection of 234-237

Deprotection reaction of the bromohexenes **234-237** were performed to get the corresponding triols **248-251**. For this purpose ketal protected diol functionalities **234-237** were separately subjected to the acid catalyzed deprotection reaction because of ketal units are sensitive towards acidic conditions. Ketal groups in **234-237** were removed with $\text{HCl}_{(\text{g})}$ in MeOH. After completion of the reaction solvents were removed to get the corresponding compounds **248-251** almost in quantitative yield (Scheme 60).



Scheme 60. Deprotection reactions of **234-237**

After synthesis of bromotriols **248-251**, characterizations were done with $^1\text{H-NMR}$, $^{13}\text{C-NMR}$ and IR spectroscopy. The $^1\text{H-NMR}$ spectrum of the compound **248** shows one olefinic resonance signal at 6.21 ppm and three alkoxy proton resonance

signal between 4.27 – 3.77 ppm and one AB-system arising from the methylenic protons at 2.13 – 2.03 ppm. In the ^{13}C -NMR spectrum, there are six resonance signals. Two of them belong to the olefinic protons at 131.4 and 130.2 ppm. Three alkoxy carbons are resonating between 68.7 – 66.0 ppm. The methylene carbon appears at 34.0 ppm. Moreover, an additional proof of the removal of the protecting groups was the solubility changes of compounds **248-251** from organic solvents to water.

CHAPTER 2

GOLD CATALYZED ALKYNE CYCLIZATIONS OF THE *N*-PROPARGYL SUBSTITUTED INDOLE DERIVATIVES

2.1 Introduction

Heterocyclic compounds are one of the most important part of the organic molecules because of their pharmacological properties and being precursor of the complex structures. Cyclic compounds containing carbon and hydrogen are called as carbocyclic molecules. In the ring, if one of carbon atom is replaced by heteroatom, generally; nitrogen, oxygen or sulfur atom, this ring is called as heterocyclic compound. There are two different definition of the heterocyclic molecules. According to first one; heterocyclic compounds are defined as; “cyclic compounds having as ring member atoms at least two different elements, e.g. 1,2-thiazole (**252**), bicyclo[3.3.1]tetrasiloxane (**253**)” in *The IUPAC Gold Book*.⁸⁴ In the *Encyclopedia Britannica*, heterocyclic compounds are described as; “heterocyclic compounds, also called as heterocycles, any of major class of organic

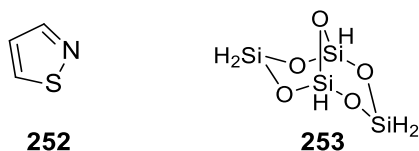


Figure 22. Heterocyclic compounds **252** and **253**

compounds having at least one atom of an element other than carbon (C) atom as a heteroatom".⁸⁵ Although heterocyclic compound can be inorganic, most of them have carbon atom on their structure (Figure 22).

Heterocyclic compounds are one of the most important class of the chemical compounds, that are found in all drugs, biomolecules, agrochemicals, natural products, and pharmaceuticals.⁸⁶ In fact, it is estimated that the most of pharmaceutical products, more than 70%, are heterocyclic molecules and showing biological activities.⁸⁷ In addition to this, most of heterocyclic molecules have found application field in material science because of their electronic structure.

2.1.1 Indole

Indole (**255**), a benzopyrrole, is a bicyclic aromatic heterocyclic compound and formed by the combination of benzene (**108**) and pyrrole (**254**) at the C-2 and C-3 position of the pyrrole ring. It is a one of the important heterocyclic compounds because it is found in wide range of the natural products and biologically active molecules. In addition to this, indole has driven attention in material science because of its electronic structure. Therefore, efficient synthesis of indole derivatives were extensively studied by heterocyclic chemists (Figure 23).

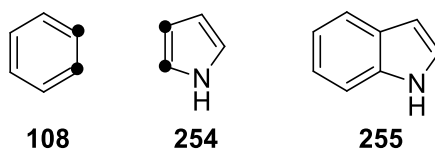


Figure 23. Benzene, pyrrole, and indole structures

Up to date, over 200 indole derivative are known as drugs and undergoing trials. For example, indole is found in *L*-tryptophan (**256**) which is an essential amino acid and natural product used in the derivation of complex molecules in living cells. Another example for the indole containing bioactive molecules is serotonin (**257**), which is a member of tryptamines acting neurotransmitter in the human body. Melatonin (**258**), another indole containing natural hormone, has the circadian

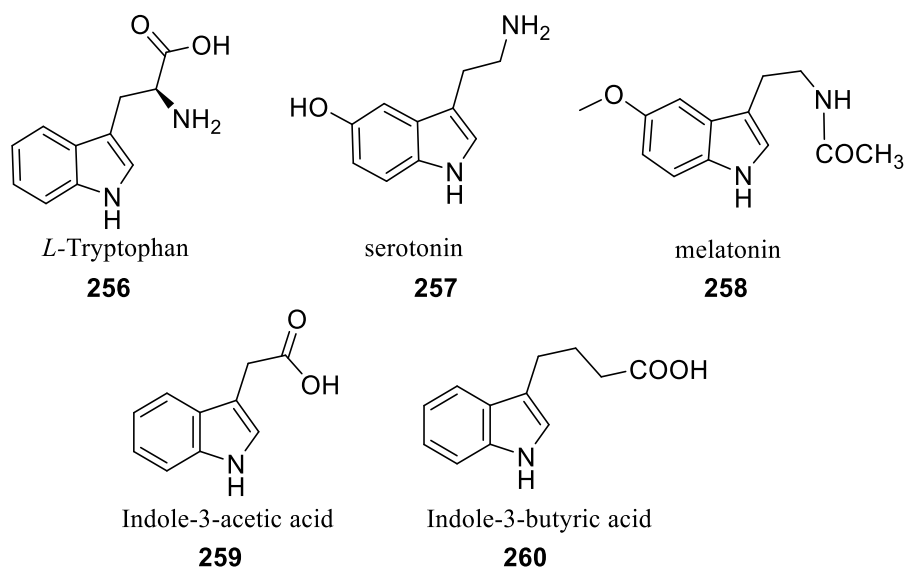
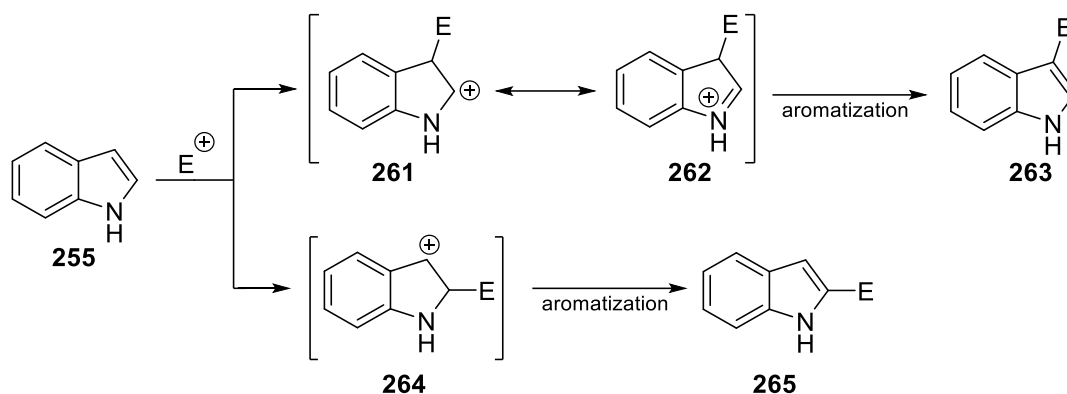


Figure 24. Indole containing bioactive molecules

rhythms regulation effect for the sleep-wake actions. The *auxin* derivatives, for example, natural indole-3-acetic acid (**259**) and synthetic indole-3-butyric acid (**260**) are the growth regulating substances in plants. In view of these information, indole molecule can be considered as one of the special or privileged structure in all heterocyclic compounds (Figure 24).^{87,88}

Indole is an aromatic heterocyclic molecule. It is also considered as a π -excessive molecule having 10- π electrons. Therefore, the electrophilic aromatic substitution reaction is the most characteristic properties of indole ring. Indole is reactive towards the electrophiles at the C-3 position because of the stabilization ability of the intermediate **262** by the unpaired electrons of the nitrogen atom. In case of substitution at the C-2 position this stabilization is not possible because of the disruption of the aromaticity of the benzene ring (Scheme 61).

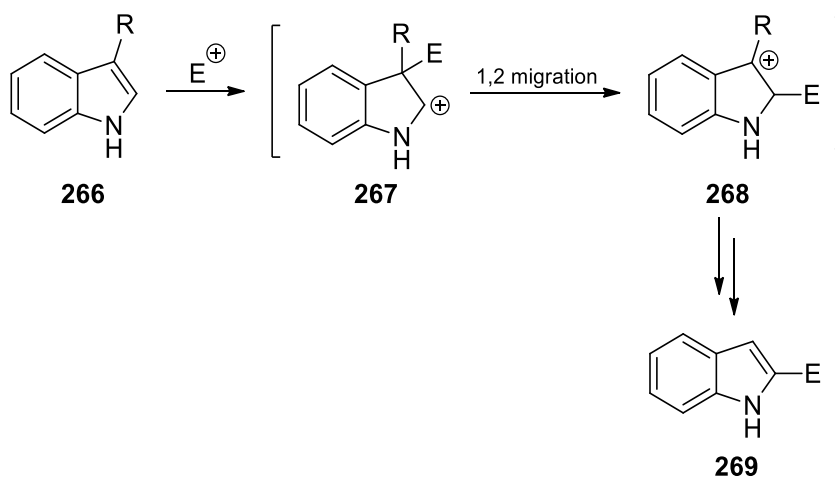
For the synthesis of substituted indole derivatives there are two main strategical ways. The first one is the direct substitution at C-3 position of the required substituent as shown in Scheme 61. However, if a substitution at the C-2 carbon atom is required, the C-3 position must be blocked by a protecting group and then the compound can be submitted to electrophilic substitution reaction. Finally,



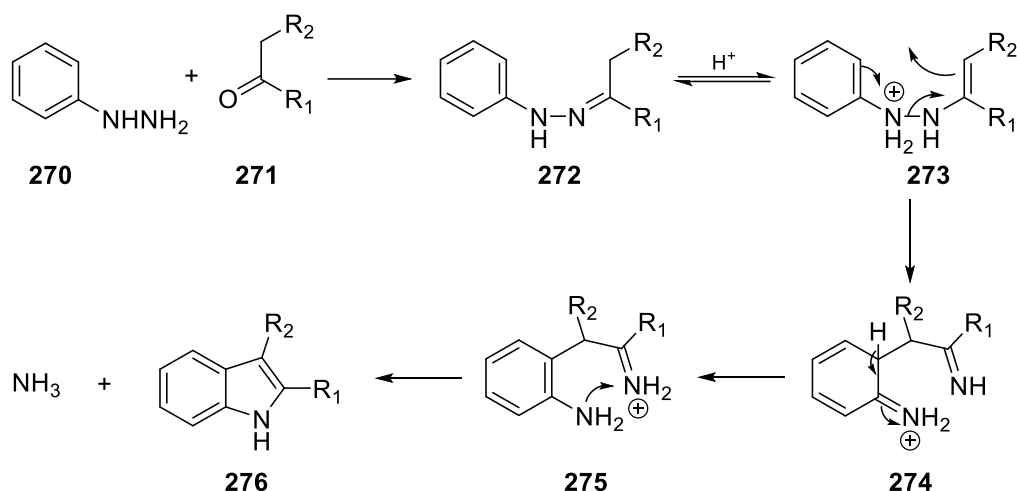
Scheme 61. Structures of the intermediates formed during substitution at the C-2 and C-3 carbon atoms of indole

deprotection would give the desired indole derivative substituted at the C-2 carbon atom (Scheme 62).⁸⁸

In the case of second method, substituted indole derivatives can be synthesized by cyclization reactions starting from acyclic molecules having the required substituents. The most applicable method is the Fischer indole synthesis, which is the condensation reaction of aromatic hydrazines **270** with ketones **271**. In the mechanistic view, as the first, the hydrazone **272** molecule is formed. In the acidic



Scheme 62. Mechanism for substitution at the C-2 position.



Scheme 63. Mechanism for the formation of indoles by Fischer indole synthesis

medium, an electrocyclic process takes place to give the intermediate **275**. Finally, cyclization yields the indole derivative **276** (Scheme 63).⁸⁹

2.1.2 Pyrazines

Pyrazine (1,4-diazine) (**277**) is one of three isomers of diazines; pyrimidines (1,3-diazines) (**278**) and pyridazines (1,2-diazines) (**279**). They are six membered heterocyclic molecules having two sp^2 hybridized nitrogen atoms on the ring (Figure 25).

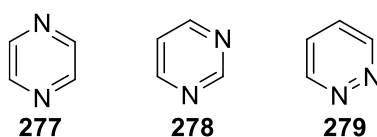


Figure 25. Structures of isomeric diazines

Biological activities of diazine derivatives are known in the literature. For example, the pyrimidines, also known pyrimidine bases such as uracil (**280**), thymine (**281**) and cytosine (**282**), are the naturally occurring diazine derivatives and they are the nucleoside building blocks in DNA (deoxyribonucleic acid) and RNA (ribonucleic

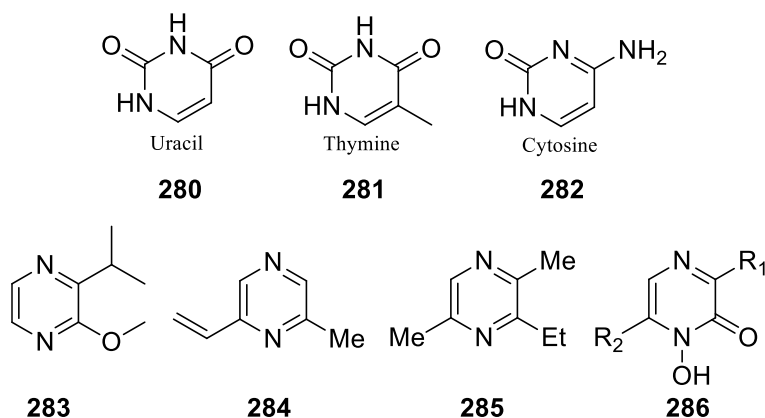


Figure 26. Structures of some biologically active pyrazine derivatives

acid). Pyrazines have also important properties such as; alkyl substituted derivatives **283** are found in green peas, and **284** is found in coffee and used as foodstuffs; **285** is also found in ant and acts as alarm pheromone. Furthermore, some pyrazinone derivatives such as **286** are known as antibiotic (Figure 26).⁸⁸

2.1.2.1 Pyrazino-indole and Pyrazine-*N*-oxides

Indole and pyrazine molecules are the heteroaromatic compounds having nitrogen atom in the ring. Among the bioactive molecules, heterocyclic compounds having sulfur, oxygen and nitrogen are the most common molecules. Because of these biological importance of indole and pyrazine rings, it can be easily estimated that heterocyclic molecules having these two rings in their structure would be important molecules having biological activity. For example, the pyrazino[1,2-*a*]indole (**287**) derivatives show antibacterial properties.^{90,91} Another example is Dragmacidin D

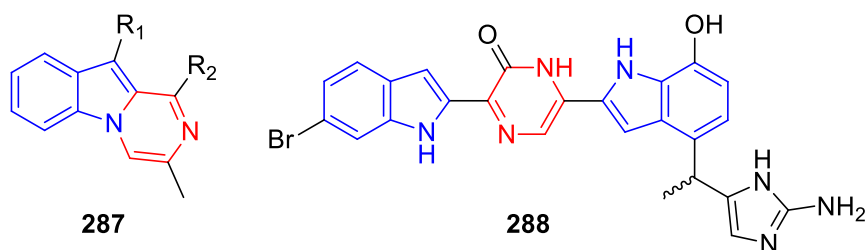


Figure 27. Structures of some biologically active pyrazino-indole derivatives

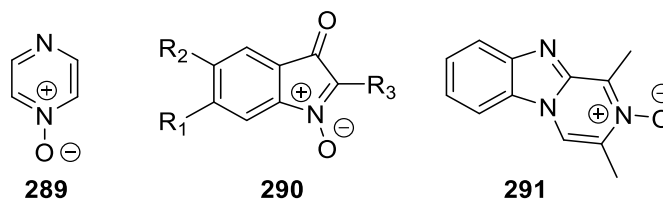


Figure 28. Structures of some pyrazine and indole *N*-oxide derivatives

(**288**) isolated from the marine sponge of the deep-water and having properties of treatment of Alzheimer's, Parkinson's and Huntington's diseases (Figure 27).⁹²

In addition to the pyrazino-indole derivatives; antibiotic, antimicrobial and antifungal properties of pyrazine-*N*-oxide (**289**) are known in the literature.⁹⁰ In recent years, the antiprotozoal and antimicrobial activity of indolone-*N*-oxide **290**⁹³ and antiviral effect of pyrazino-benzimidazole **291** have been reported (Figure 28).⁹⁴

2.1.3 Synthesis of Pyrazine Rings

Various methods for the synthesis of the pyrazine ring are described in the literature. There are four popular fashions to construct this ring by using two components. The self-condensation reaction of two α -aminocarbonyl groups **292** and reaction of 1,2-dicarbonyl **294** with 1,2-diamines **295** forming imine intermediates are two different common ways to synthesize pyrazine derivatives.^{88,95-96} The dimerization reactions of nitrile ylides **296** formed by Beckmann rearrangement is another method for the formation of pyrazine rings.^{97,98} The oxidative ring closure reaction of bis(acetylmethyl)amines **297** by ammonia is also a methodology to construct pyrazine molecules (Figure 29).⁸⁸

Pyrazine derivatives can also be synthesized by electrocyclic ring closure reactions. Buchi *et al.* reported the synthesis of alkyl substituted pyrazine derivatives by electrocyclic ring closure reaction of **298** obtained from the condensation reaction of α -hydroxyaminoketones and allylamines. After *O*-acetylation of compound **298**, electrocyclization reaction and following CO₂ extrusion gave the corresponding pyrazine derivatives **300** (Scheme 64).⁹⁹

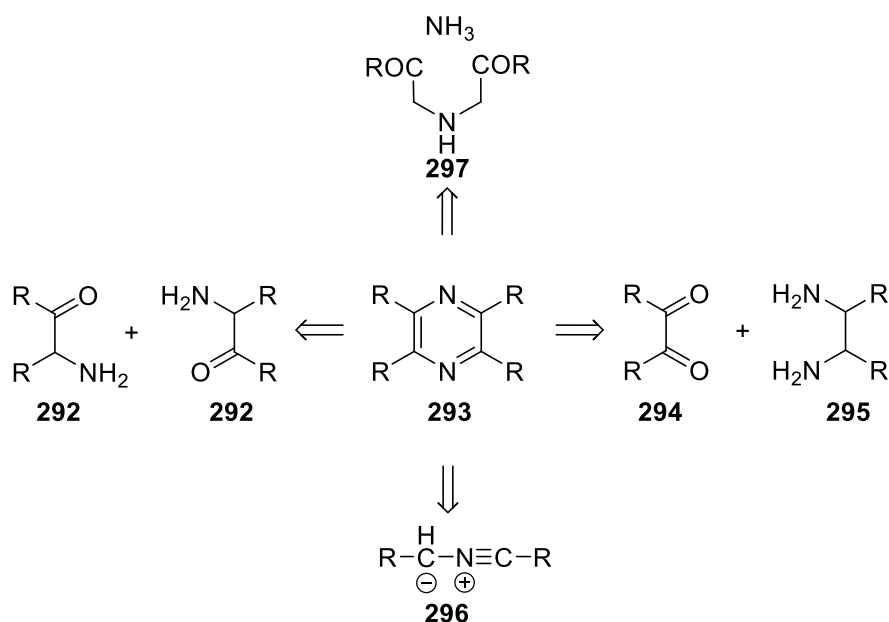
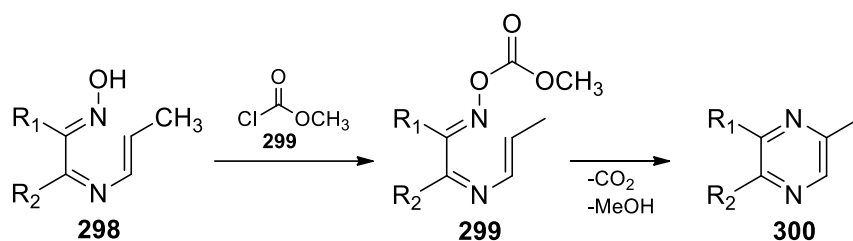
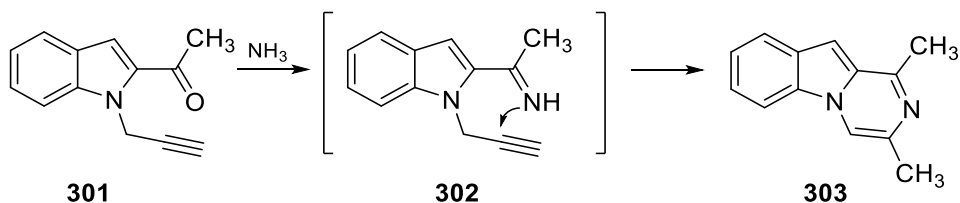


Figure 29. Synthetic methods for pyrazine rings



Scheme 64. Pyrazine synthesis by electrocyclic ring closure reaction

Another important synthetic method for pyrazines is intramolecular electrophilic cyclization reactions of alkynes in the presence of ammonia. Abbiati *et al.* applied this methodology to the synthesis of pyrazine fused indole molecules. The imine **302** formed by the condensation of ketone **301** with ammonia underwent a 6-*exo*-dig cyclization reaction to give **303**.¹⁰⁰



Scheme 65. Alkyne cyclization method for the synthesis of pyrazines

2.1.4 Diazepines

Diazepines are seven-membered heterocyclic molecules containing two sp^2 - and sp^3 - hybridized nitrogen atoms on the ring. There are three possible diazepine derivatives; namely, 1,2-diazepine (**304**), 1,3-diazepine (**305**) and 1,4-diazepine (**306**) (Figure 30).

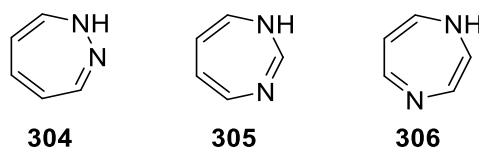


Figure 30. Structures of isomeric diazepine derivatives

Among the seven membered rings, diazepine derivatives have an important position because of their biological activities. Pharmaceutical ability about anxiety and related disorders of diazepines are known in the literature.¹⁰¹ In addition to this, biological activity of diazepines on the treatment of cancer, human immunodeficiency virus (HIV) and cardiac arrhythmia have been under the research.¹⁰²

As a derivative of diazepines, 1,4-benzodiazepines **307** are the most widely searched one, due to their known biological activities. Up to date, for diazepine derivatives **307**; Thurston *et al.* showed their anti-cancer properties,¹⁰³ Volsky *et al.* found their inhibition effect on the replication of human immunodeficiency virus (HIV),¹⁰⁴ and the anti-Alzheimer activities were discovered by Audia *et al.* (Figure 31).¹⁰⁵

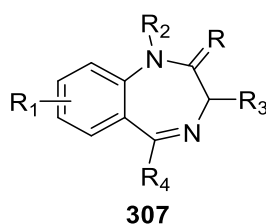


Figure 31. General structure of benzodiazepines

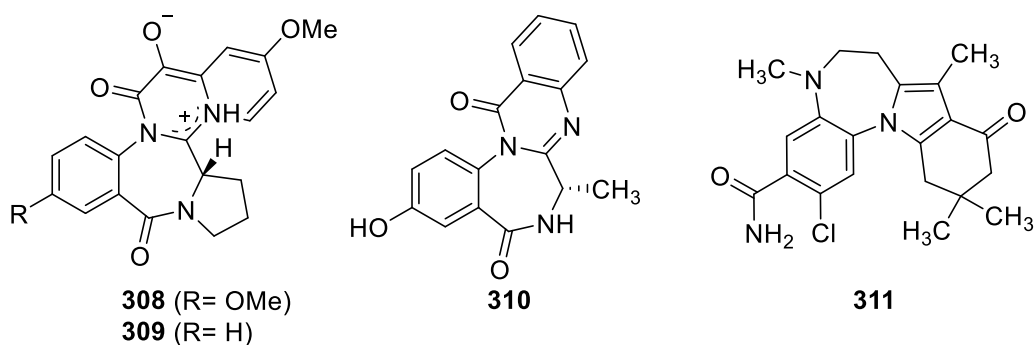
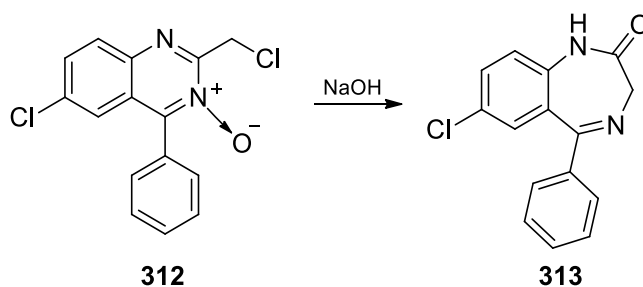


Figure 32. Structures of commercial available diazepine derivatives

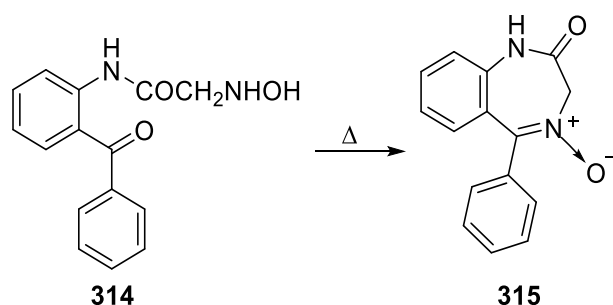
The marketed isomers of the benzodiazepine derivatives are the benzodiazepinic alkaloids; circumdatin-A (**308**), circumdatin-B (**309**) and circumdatin-C (**310**) which are used in the treatment of the gastrointestinal disorders.⁸⁸ In addition to this, Neubert *et al.* recently described benzodiazepine derivative **311** as heat shock protein 90 inhibitors having a potential for the lung cancer therapy (Figure 32).¹⁰⁶

2.1.4.1 Synthesis of Diazepines

Diazepine derivatives gained great importance because of their biological activities described above. For this reason, approaches to the synthesis of diazepine molecules have been under the main goal by synthetic organic chemistry during the last few decades. There are some synthetic pathways to form the diazepine rings. In 1961, Sternbach and Reeder synthesized diazepinone derivative **313**, known as demoxepam a special anticonvulsant drug, starting from 2-chloromethyl-quinazoline-*N*-oxide (**312**) in basic medium (Scheme 66).¹⁰⁷



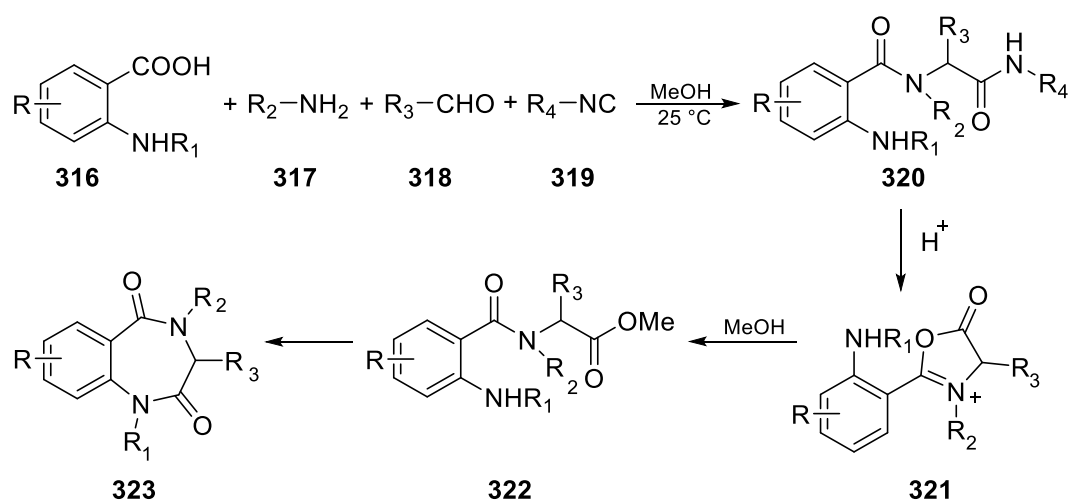
Scheme 66. Synthesis of diazepinone derivative **313**



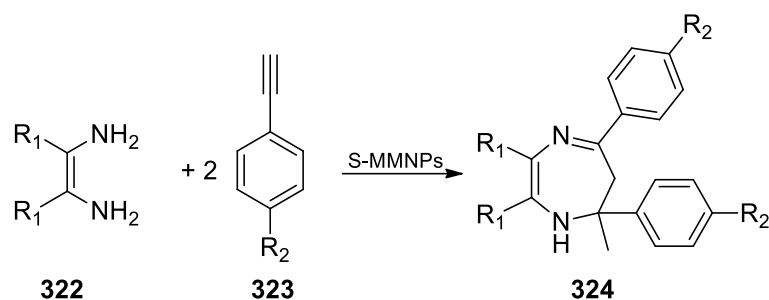
Scheme 67. Synthesis of benzodiazepine-*N*-oxide ring **315**

For the synthesis of diazepine skeleton, Evans *et al.* applied an intramolecular cyclization methodology using hydroxyamido acetamide derivative **314** to obtain benzodiazepinone-*N*-oxide ring **315** in (Scheme 67).¹⁰⁸

In a different way, Armstrong *et al.* used the Ugi four-component condensation (4CC) reaction to synthesize diazepine skeleton. The Ugi 4CC reaction consists of four different reagent, e.g. a carboxylic acid, an isocyanide, a carbonyl compound and an amine.¹⁰⁹ According to this synthetic pathway, an anthranilic acid derivative **316** gave α -acylaminoamide derivative **320** in the presence of amine **317**, aldehyde **318** and cyanide **319**. After formation of the diazepine precursor **320**, the cyanide moiety was activated by acid and successively removal from the molecule resulted



Scheme 68. Synthesis of diazepine ring by the Ugi four-component condensation

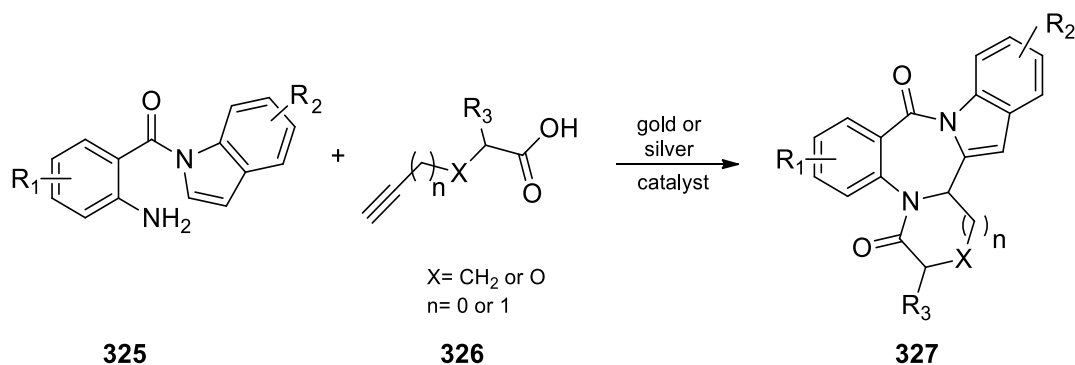


Scheme 69. Formation of diazepine derivatives with terminal alkynes

in the formation of reactive azomethine ylide **321**. The nucleophilic addition of the methoxide group reopens the ring and produces the compound **322**. The following ring closure reaction gave the diazepine derivatives **323** (Scheme 68).^{110,111}

In recent years, Maleki *et al.* showed the one-pot multicomponent synthesis of diazepine derivative **324** starting from 1,2-diamines **322** and terminal alkynes **323** in the presence of catalytic amount of silica supported on iron oxide (Fe₃O₄/Silica) nanoparticles (S-MMNPs) (Scheme 69).¹¹²

Liu *et al.* generated diazepine structures **327** by the activation of the alkyne functionality with the help of transition metals especially gold and silver salts. By this protocol, they have prepared various diazepine derivatives **327** with various alkyne units **326** using gold and silver catalyzed cascade reactions (Scheme 70).¹¹³



Scheme 70. Formation of diazepine derivatives starting from alkynes in the presence of transition metals

2.1.5 Ring-Junction Nitrogen Containing Heterocyclic Molecules

The ring-junction nitrogen containing heterocycles which means having nitrogen atom sharing by two different rings are also known and most of them are biologically important compounds. Although these type compounds have wide variety of pharmaceutical properties, they do not occur naturally.⁸⁸

As a member of these type compounds, biological activities of indole fused heterocycles such as pyrazino-indole **328**, pyrazolo-pyrazino-indole **331** are known. For example, pyrazino-indole **328** or its substituted analogous have been found in variety complex structures showing antiproliferative agent against the human chronic myelogenous leukemia K562 cell line and potent antibacterial activity.^{114,115} In addition to this, the pyrazolo-pyrazine **329** and pyrrolo-pyrazine **330** also show biological activity towards Vasopressin_{1b} receptor which control the water, glucose and salt level in the blood.^{116,117}

Under the light of these information, it can be easily foreseen that heterocyclic molecules such as pyrazolo-pyrazino-indole **331**, pyrrolo-pyrazino-indole **332** and pyrazolo-diazepino-indole **333** or their derivatives bearing these type ring in their skeleton have a potential to be biologically active molecule (Figure 33).⁹¹

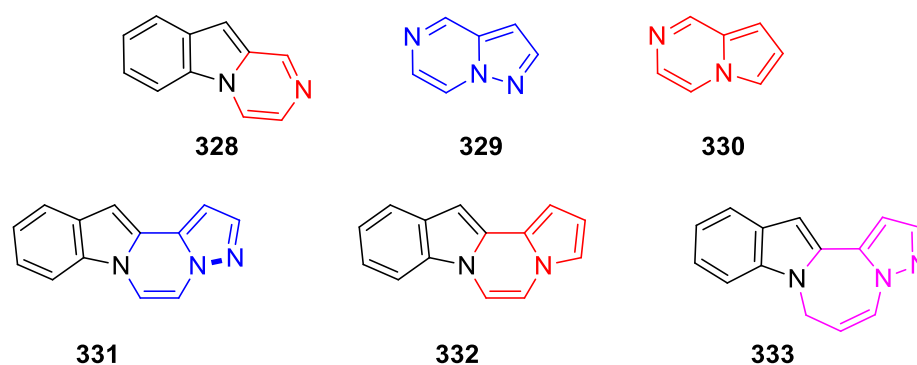
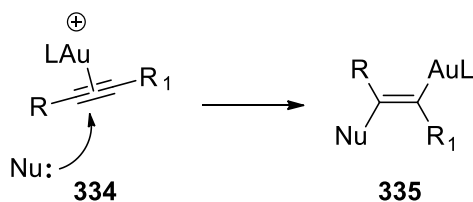


Figure 33. Ring-junction nitrogen containing heterocycles

2.1.6 Gold Catalyzed Alkyne Cyclization Reactions

Cyclization methodologies ranging from condensation reactions to electrocyclic processes are the most applicable way to produce carbocycles as well as the heterocyclic molecules. Among the cyclization reactions, electrophilic alkyne cyclization methodologies are the new popular method that produce cyclic molecules. During this process, to achieve cyclization reaction, alkyne moiety must be activated. Transition metal catalyzed activation of alkyne functionality is one way applied for this purpose. During the last decade, gold salts are one of the common catalysts used for this purpose. Until the discovery of these utilities of gold, at the early of 1980s, it was known as unreactive metal. After the confirmation of the catalytic activity of Au^{3+} ion, the usage of gold as a catalyst started to increase.¹¹⁸ The electronic effects of alkyne-gold complexes such as being strong σ - and weak π -acceptor make them attractive towards the nucleophiles. These unusual reactivity of that complexes have become the powerful method for the synthetic applications. Additionally, the high oxidation potential of gold(I) to gold(III) in aqueous solutions, gold(I) is disproportionated to gold(III) and gold(0), offers the practicality usage of gold catalyst and becomes them don't require air-water exclusion precautions. For this reason, despite the other transition metals, gold catalyst are alkynophilic, selective towards alkynes but not oxophilic.^{119,120}

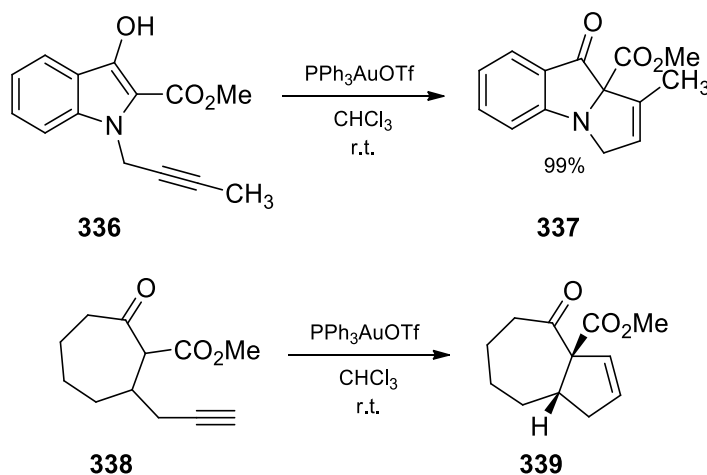
There are wide range of usage of gold catalyzed alkyne cyclizations. During these cyclization reaction, the reaction proceeds by the activation of alkyne functionality by gold catalyst and formation of intermediate **334**. After coordination of the ligand with gold catalyst, the nucleophilic attack occurs and the *trans*-alkenyl gold



Scheme 71. Nucleophilic addition to gold catalyzed alkyne

complex **335** is produced. The formation of complex **335** can be followed by decomplexation or formation of non-classical carbocation and/or carbenoid formation which caused a rearrangement. This phenomenon is a common way among the gold-catalyzed alkyne reactions (Scheme 71).^{119,121}

Synthesis of carbocycles and heterocycles over the gold catalyzed alkyne complexes have found a broad range of application fields. The gold-catalyzed alkyne cyclization reaction was performed by Toste *et al.* to synthesize bicyclic heterocycles **337** and **339** (Scheme 72). In the first reaction of the internal alkyne **336**, 5-*exo*-dig cyclization product **337** was formed as the sole product. Gold-catalyzed cyclization reaction of **338** resulted in the formation of the 5-*endo*-dig cyclization product **339**.¹²²

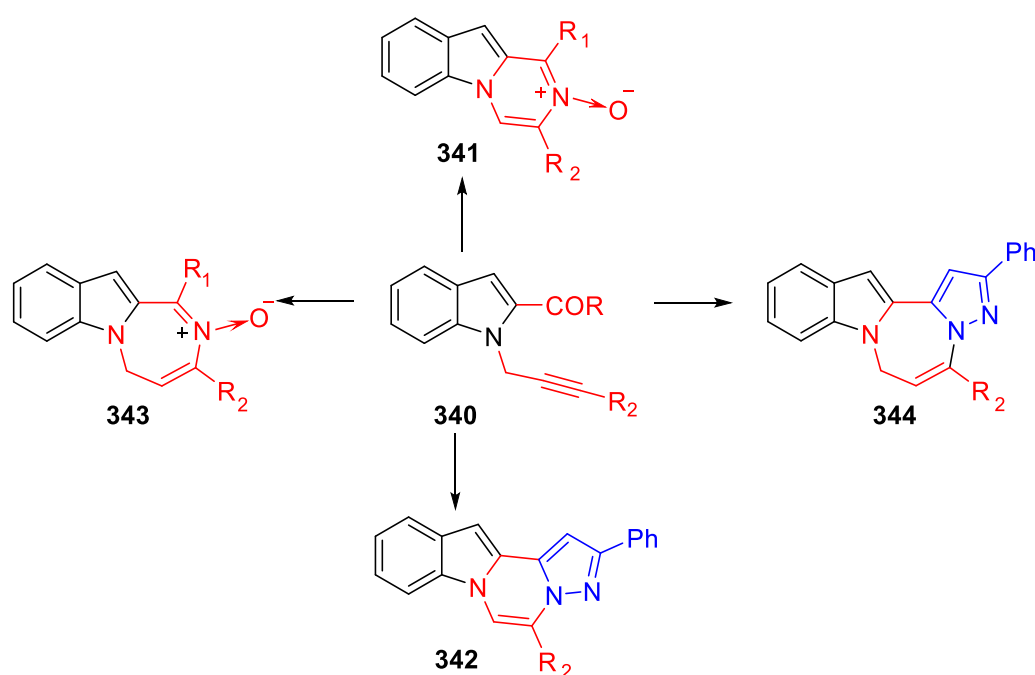


Scheme 72. Application of gold catalyzed alkyne cyclization reaction to the synthesis of **337** and **339**.

2.1.7 Aim of the Study

Among the biologically active molecules and commercial drugs, nitrogen-containing heterocyclic molecules occupy a respectful place. The discovery of synthetic approaches to produce these molecules is the major interest of the synthetic organic chemists. Herein, the main aim of this chapter was the synthesis of new heterocycles having a nitrogen atom on the ring-junction position by the cyclization of the alkyne functionality. Gold catalysts are the most preferred ones

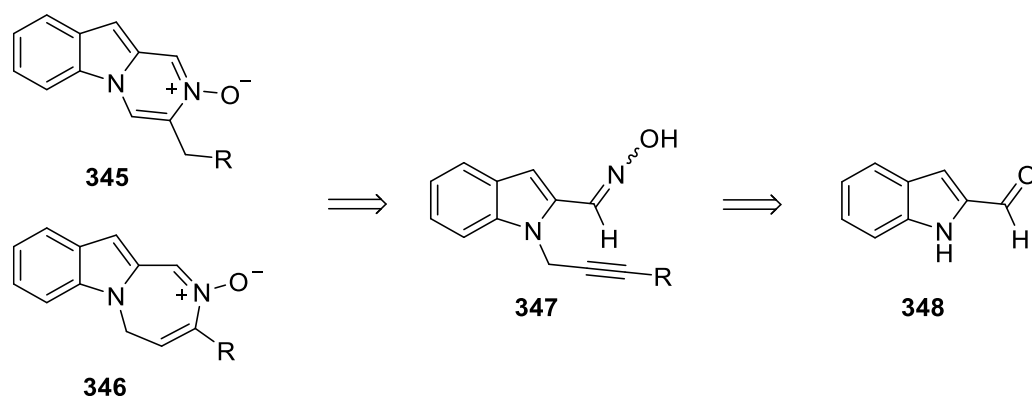
because of their stability and easy of usage mentioned above. The main objective of the thesis was to investigate the reactivity or to understand the behavior of the alkyne unit in the presence of the gold catalyst. For this purpose, starting from *N*-propargyl-indole-2-carbonyl derivatives **340**, synthesis of the nitrogen containing heterocycles such as; pyrazino-indole-*N*-oxide **341**, pyrazolo-pyrazino-indole **342**, diazepino-indole **343** and pyrazolo-diazepino-indole **344** derivatives were planned (Scheme 73).



Scheme 73. Synthetic Plan

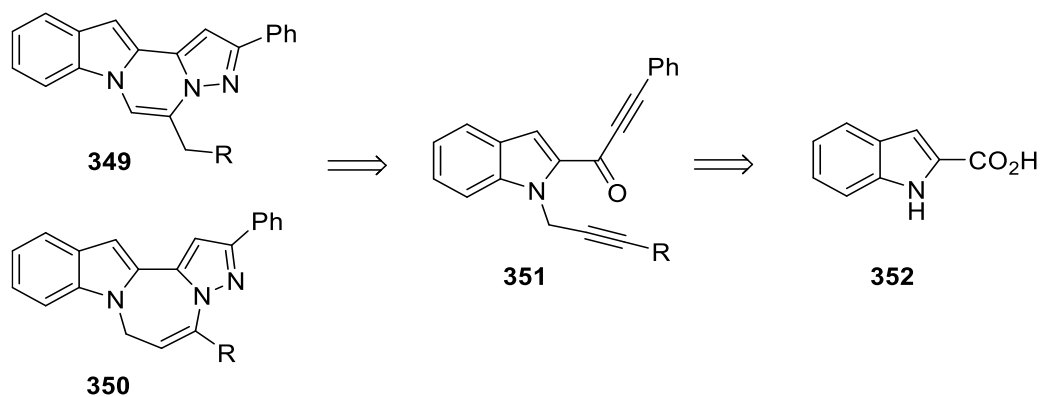
2.2 Results and Discussions

In the first part of the study, the synthesis of pyrazine-*N*-oxide **345** derivatives and the synthetic attempts for the formation of diazepine-*N*-oxide **346** were performed with gold salts as the catalyst. For this purpose, the oximes **347** was synthesized from *N*-propargylindole-2-carbaldehyde (Scheme 74).



Scheme 74. Retro-synthesis of the *N*-oxides **345** and **346**.

In the second part of the study, pyrazolo-pyrazino-indole **349** derivatives and pyrazolo-diazepino-indole **350** derivatives were synthesized by gold catalyzed alkyne cyclization as well as the base supported, especially NaH-induced electrophilic cyclization reactions starting from indole-2-carboxylic acid (**352**).



Scheme 75. Synthetic plan for pyrazolo-pyrazino(diazepino)-indoles

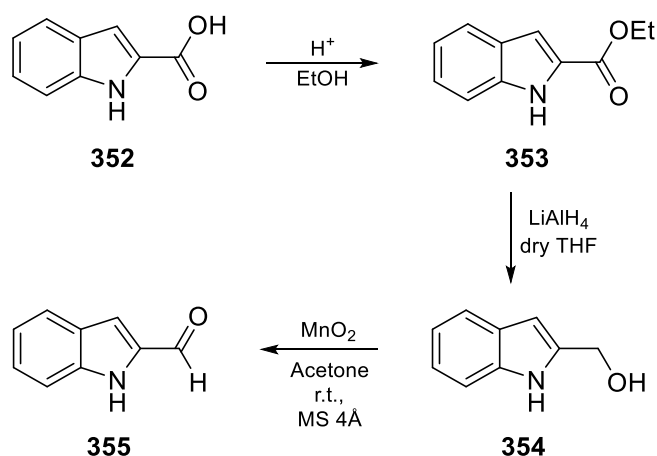
Pyrazole ring was formed by the condensation reaction of the phenyl substituted α,β -alkynyl ketones with hydrazine. Second alkyne functionality was incorporated by *N*-propargylation reaction of the nitrogen atom of indole ring in the presence of propargyl bromide (Scheme 75).

2.2.1 Synthetic Applications of *N*-Alkyne Substituted Indole-2-carbaldoximes: Synthesis of Pyrazino[1,2-*a*]indole-*N*-oxide and Oxime-Oxime Rearrangement

2.2.1.1 Synthesis of Ethyl 1*H*-indole-2-carboxyaldehyde (355)

The starting material indole-2-carboxaldehyde (**355**) was synthesized in three steps in 89% overall yield (Scheme 76). In the first step, indole-2-carboxylic acid (**352**) was subjected to Fischer esterification reaction. This procedure is well known method for the esterification reaction of the carboxylic acids.¹²³ The basic work-up procedure gave ethyl 1*H*-indole-2-carboxylate (**353**)¹²⁴ in high yield. The characterization was done by ¹H-NMR and ¹³C-NMR spectra. Ethyl protons resonance at 4.42 ppm and 1.42 ppm and carbonyl carbon resonances at 159.6 ppm which is specific chemical shift for the ester group; 58.6 ppm and 11.9 ppm show incorporation of ethyl group into the molecule. After getting ethyl ester **353**, the reduction procedure was applied for the synthesis of alcohol **354**. For this reason, the reduction of ester **353** was achieved by LiAlH₄ in quantitative yield. At this stage one may raise the question whether alcohol **354** could be synthesized in one step by the direct reduction of acid **352**. However, the yield for reduction of the ester group in **353** was significantly higher as compared to that of carboxylic acid functionality in **352**. The formation of alcohol was proven by means of NMR spectroscopy. In the ¹H-NMR spectrum of alcohol **354**, the resonance signals of the ethyl unit disappeared, and a new singlet at 4.69 ppm for the methylenic protons appeared. In the ¹³C-NMR spectrum of alcohol **354**, the carbonyl signal of the ethyl unit disappeared as well as the aliphatic signals. Additionally, a new carbon signal at 58.5 ppm belonging to the methylene carbon appeared. In the IR spectrum, the disappearance of carbonyl signal at 1697 cm⁻¹ of compound **353**, and the

appearance of the broad –OH signal at 3239 cm^{-1} also support the formation of alcohol **354**. To synthesize aldehyde **355**, the allylic oxidation of alcohol **354** was performed with MnO_2 . This procedure is one of the most applicable method for the synthesis of the α,β -unsaturated systems. For this purpose, the alcohol was treated with MnO_2 in dry acetone in the presence of the molecular sieve (MS 4Å) which removes the water formed during the reaction. The aldehyde **355**¹²⁵ was formed in good yield (93%) (Scheme 76).



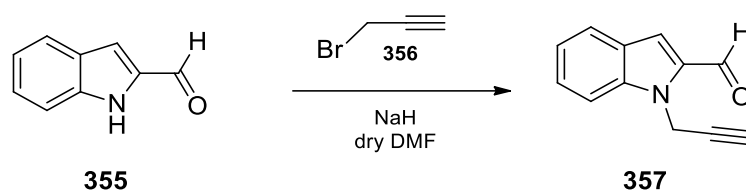
Scheme 76. Esterification of indole-2-carboxylic acid **352**

Characterization of aldehyde **355** was done by the ^1H -NMR and ^{13}C -NMR spectra. In the ^1H -NMR spectrum, methylenic signal at 4.69 ppm disappeared and the aldehyde peak appeared at 9.85 ppm. These prove the formation of the aldehyde **355**. In the ^{13}C -NMR spectrum, carbonyl peak of aldehyde group at 182.1 ppm confirmed the allylic oxidation. As a result of these synthetic pathway, 1H-indole-2-carboxaldehyde (**355**) was synthesized successively in three steps in 89% yield.¹²⁵

2.2.1.2 Synthesis of *N*-propargyl Substituted Indole-2-carbaldehyde (**357**)

After successful synthesis of aldehyde **355**, the aim was the synthesis of *N*-propargyl-1H-indole-2-carbaldehyde (**357**). For this purpose, the literature method¹²⁶ was applied for the direct propargylation of aldehyde **355**. According to the method, aldehyde **355** was treated with NaH in dry DMF. After the abstraction

of nitrogen proton of the indole unit, propargyl bromide (**356**) solution in dry DMF was added. The completion of the reaction was followed by TLC (Scheme 77).¹²⁷



Scheme 77. Propargylation reaction of **355**

The ¹H-NMR spectrum of **357** shows additional two peaks which belong to the methylenic protons (5.39 ppm) and terminal alkyne proton (2.20 ppm). The doublet splitting of the methylene proton resonance by a coupling constant of $J = 2.50$ Hz is arising from the long range coupling (⁴ J) with the alkyne proton. This coupling is also observed in the terminal alkyne proton resonance signal at 2.20 ppm. In addition to this, in the ¹³C-NMR spectrum of molecule **357**, three new resonance signals are observed. The most informative ones of these three are the carbon signals of the alkyne unit at 78.2 and 72.5 ppm because this region is the specific area for the alkyne resonance signals. The methylene carbon resonates at 33.9 ppm. The incorporation of the alkyne unit was proven by these NMR data. The IR spectrum, with specific signals at the 3238 cm⁻¹ (–C≡C–H stretching) and 2120 cm⁻¹ (–C≡C– stretching) also supported the formation of **357**.

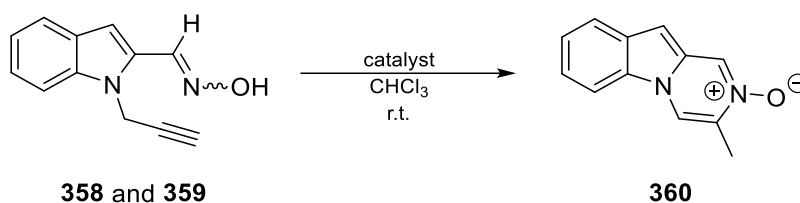
2.2.1.3 Synthesis of *N*-propargyl Substituted Indole-2-carbaldoximes

After the successful propargylation reaction of indole-2-carbaldehyde, *N*-propargyl aldehyde **357** was treated with hydroxyl amine salt (NH₂OH·HCl) in dry EtOH in the presence of anhydrous sodium carbonate to yield indole-2-carbaldoximes **358** and **359**. The oxime formation reaction gave the theoretically expected mixture of *E*- and *Z*-oximes **358** and **359** in quantitative yield (Scheme 78).

carbon are the main indicators of the formation of oxime unit. In some cases, the major component of the oxime could be isolated, and in some cases a mixture of *E*- and *Z*-oximes was used for further reactions.

2.2.1.4 Gold Catalyzed Alkyne Cyclization Reactions of Oximes

After synthesis of the oximes, our attention turned to the alkyne cyclization reactions with various catalysts at room temperature in chloroform. For this purpose, oximes **358** and **359** were treated with some metal catalyst which are widely used for the activation of the alkyne unit (Scheme 79 and Table 1).



Scheme 79. Metal-catalyzed cyclization reaction of oxime mixture **358/359**.

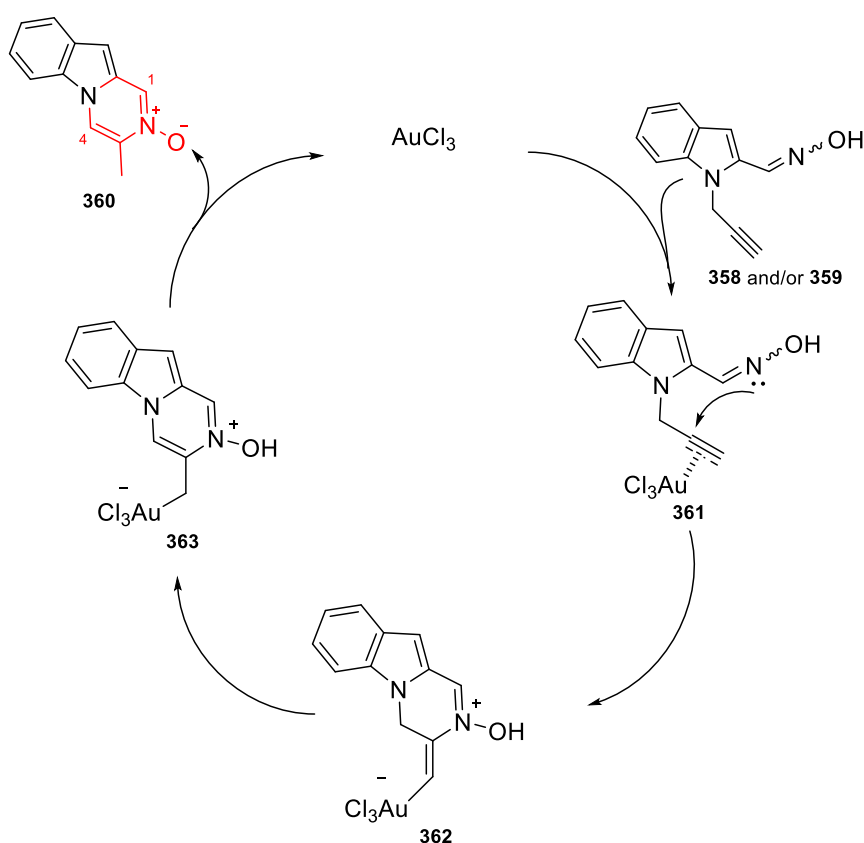
Alkyne cyclization reactions are carried out by the activation of the alkyne with metal catalysts. There are many catalysts that are used for this purpose. Among them, gold and silver catalysts are two of most used catalysts. We tried cyclization reactions with some catalysis listed below in the Table 1 and observed the formation of the corresponding pyrazine-*N*-oxide **360** in different yields. As seen from the Table 1, gold(III) chloride gave the highest yield (95%), whereas the CuI catalyst gave the lowest yield (35%).

Table 1. *N*-oxide formation with different metal catalysis

<i>Catalyst (3 mol %)</i>	<i>NMR Yield (%)</i>
AuCl ₃	95
AuBr ₃	90
CF ₃ SO ₂ OAg	65
CuI	35

To test the effect of configuration of the oxime derivatives on the mode of the cyclization reaction, we examined the reactions of the isomers of the oximes. For this purpose, separated (*E*)- and (*Z*)-isomers **358** and **359** were submitted to cyclization reactions. Consequently, both isomers smoothly underwent cyclization reactions and gave the product **360** in almost same yields.

Mechanistically, the reaction starts with the activation of alkyne unit by the gold-catalyst to form the intermediate **361** (Scheme 80). Then, it is followed by the nucleophilic attack of oxime nitrogen atom to form 6-*exo*-dig cyclization product **362**. After isomerization of intermediate **362** to the *endo*-cyclic product **363** which has lower energy (Figure 35) and following decomplexation of the gold metal gives the corresponding pyrazino-indole-*N*-oxide **360** (Figure 35).



Scheme 80. Mechanism for gold-catalyzed cyclization reaction of **358/359**.

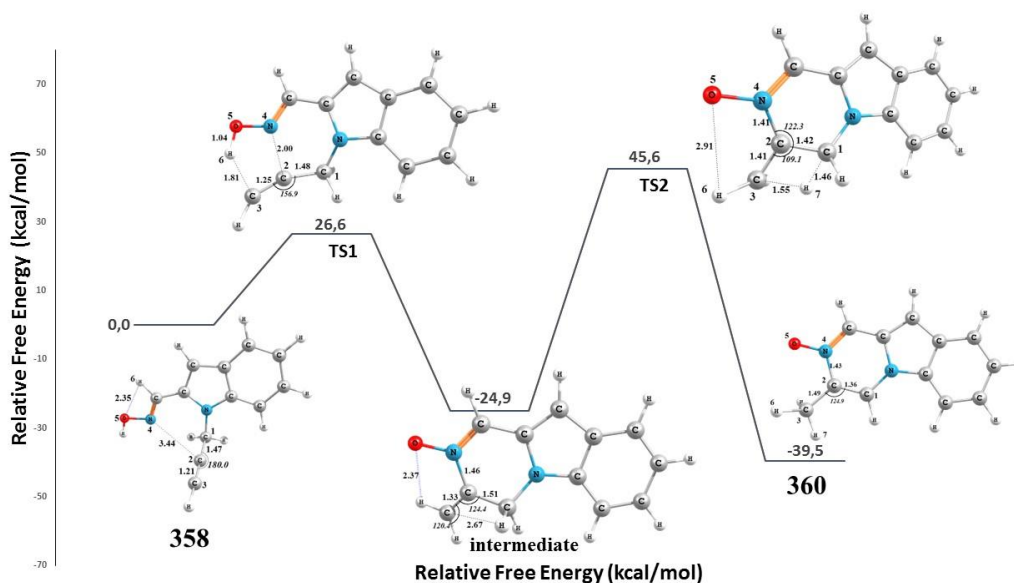


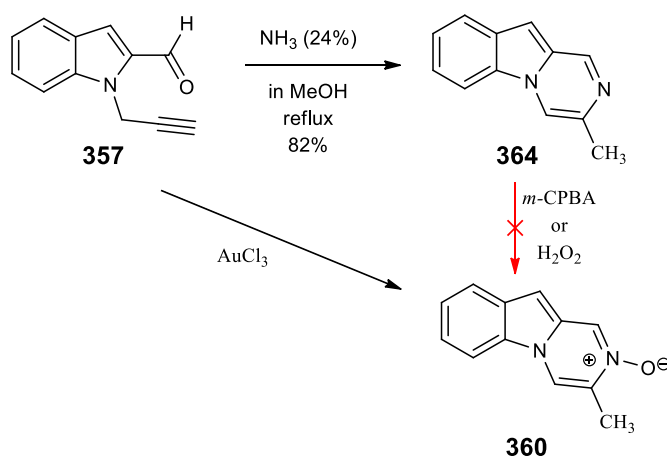
Figure 35. The potential energy profile for the formation of *N*-oxide **360**

The formation of *N*-oxide ring was confirmed by the spectroscopic methods. In the $^1\text{H-NMR}$ spectrum of compound **360**, it is clearly seen that peaks arising from propargyl unit at 5.21 ppm ($-\text{CH}_2-$) and 2.19 ppm ($\equiv\text{C-H}$) are disappeared. In addition to this, a new singlet at 2.48 ppm ($-\text{CH}_3$) appeared. The proton resonance signals at 8.60 ppm and 8.10 ppm belong to H-1 and H-4 protons adjacent to the nitrogen atom of the *N*-oxide group. This chemical shifts are low for a regular aromatic protons. Because of the positive charge on the nitrogen atom, the electron density around these protons are decreased and chemical shifts are moved to the lower field.

In the $^{13}\text{C-NMR}$ spectrum of compound **360**, the resonance signal of the C-1 adjacent to the nitrogen atom of *N*-oxide group is shifted to 171.8 ppm which is also quite low for an aromatic carbon. Additionally, a new methyl carbon resonance was observed at 29.7 ppm. In the IR spectrum of this compound, there is a specific C–H stretching at 2919 cm^{-1} belonging to the *N*-oxides ring.^{129,130}

Heterocyclic *N*-oxides were synthesized by different ways in the literature. One of them is the oxidation of *N*-atom with H_2O_2 or *m*-CPBA to form *N*-oxide heterocycles. We decided to synthesize the compound **360** by an independent way;

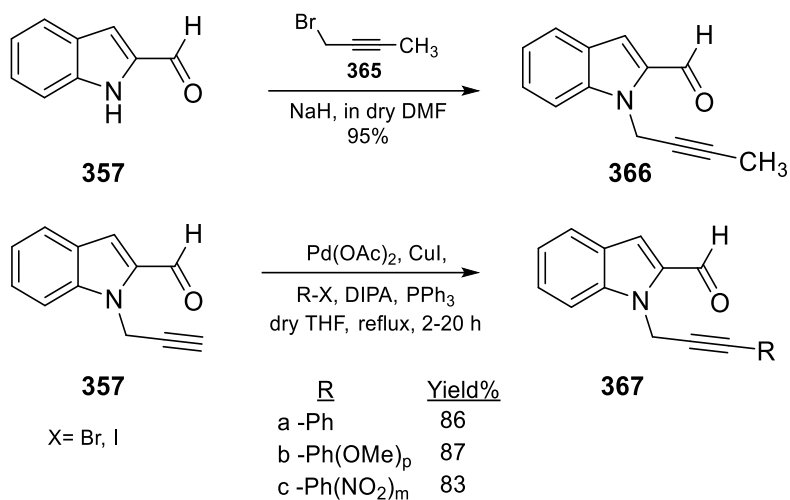
by oxidation of the corresponding heterocycle **364** in the presence of H₂O₂ or *m*-CPBA (Scheme 81). For this purpose, we first synthesized the precursor **364** by cyclization reaction of aldehyde **357** with ammonia in methanol.¹⁰⁰ Then, **364** was submitted under the different reaction conditions to oxidation reaction. Unfortunately, we were not able to observe any trace amount of oxidized product **360**. This unsuccessful results also show the superiority of our method for the formation of pyrazino-indole-*N*-oxide as a simple and efficient method (Scheme 81).



Scheme 81. Attempted synthesis of *N*-oxide **360** by oxidation of **364**.

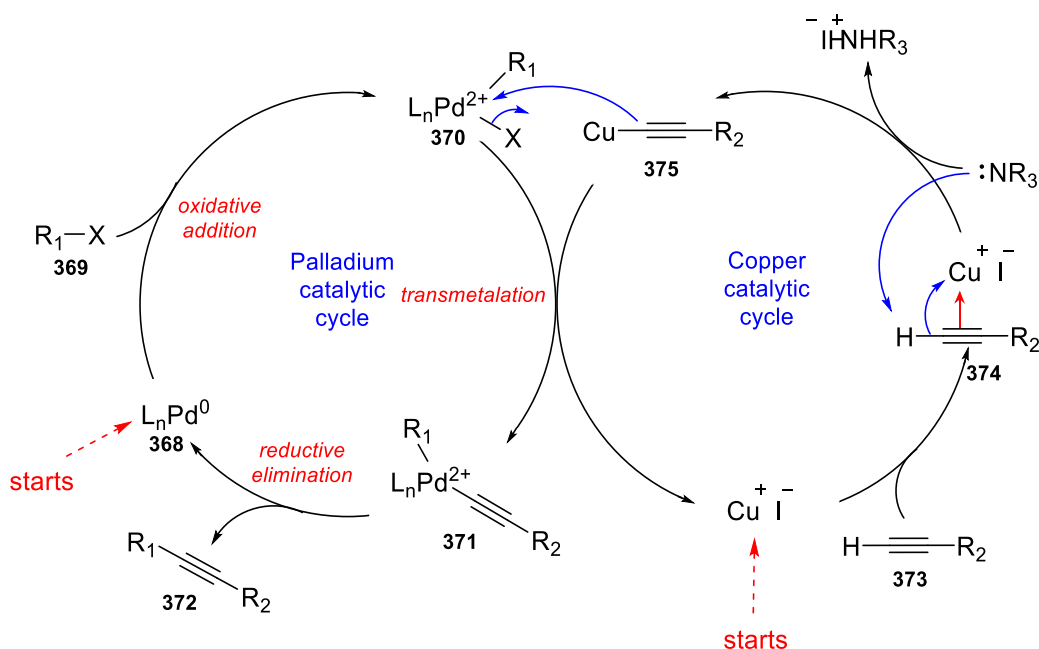
2.2.1.5 Derivatization Reaction *N*-Propargyl Aldehydes by Sonogashira Cross-Coupling Reaction

To generalize and examine the electronic effects of the substituent on the gold-catalyzed cyclization reactions of *N*-substituted-aldoximes, we decided to derivatize the alkyne unit of **357** (Scheme 82). For this reason, alkyne unit was substituted by some aromatic and aliphatic groups. To synthesize substituted alkyne, first compound **357** was reacted with 1-bromo-2-butyne (**365**) to give the methyl substituted alkyne **366**. For the synthesis of aryl-substituted alkyne derivatives, Sonogashira cross-coupling reaction was applied. By the application of the Sonogashira reaction, benzene rings having electron withdrawing and electron donating groups were attached to the terminal alkyne unit in good yields.



Scheme 82. Derivatization of alkyne unit in **357**

Sonogashira reaction is an organometallic reaction of terminal alkynes **373** with aryl halides (R_1-X) in the presence of palladium catalyst **368**, a copper salt (CuI) as a cocatalyst and bases (N_3R or NHR_2) to give the C-C coupled product **372**. This reaction starts by oxidative addition of aryl halide to palladium to form the oxidized palladium(II) complex **370**. At the same time, in the reaction medium, the



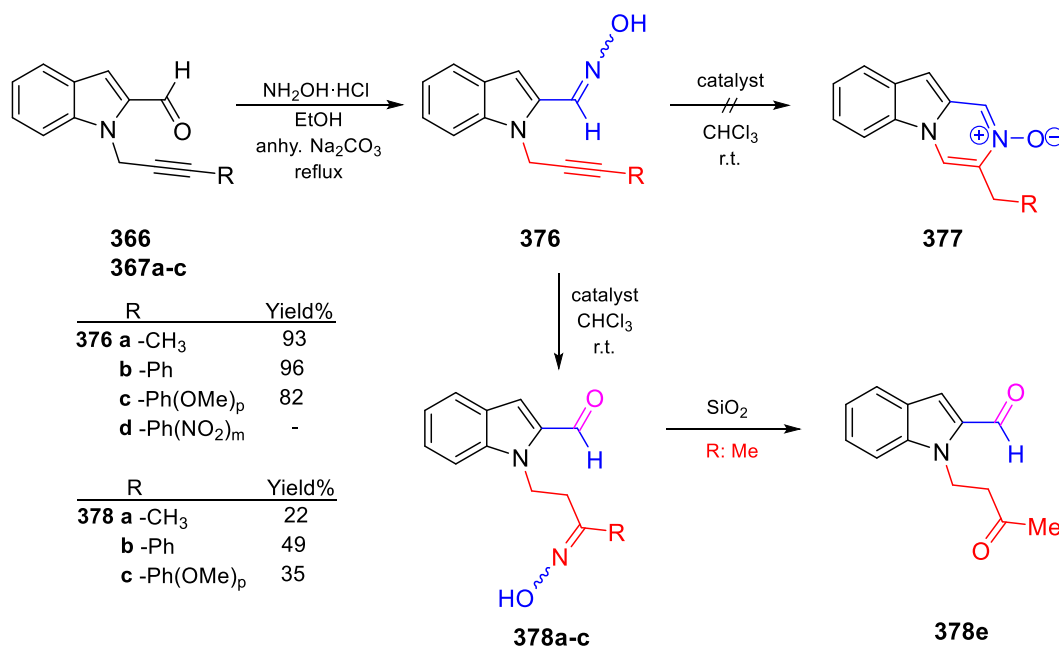
Scheme 83. Catalytic cycle of the Sonogashira cross-coupling reaction

organocopper reagent **375** is formed by terminal alkyne **373** and copper salt (CuI). After that, the formed alkynyl anion **375** is replaced by the halide bonded to the palladium complex followed by the reductive elimination to give the final coupled product **372**. During this process, the copper halide and palladium catalyst are regenerated and starts the catalytic cycle again (Scheme 83).¹³¹

2.2.1.6 Gold Catalyzed Heterocyclization of Internal Alkynes

After successful derivatization, we converted the aldehydes to oximes with the defined methodology discussed in the previous section. The oxime having substituted alkyne derivatives (**376a-c**) were synthesized in good yields, however, the $-(\text{NO}_2)_m\text{-Ph}$ substituted alkyne did not give the corresponding oxime molecule **376d**. Instead of this, it gave an unidentified complex mixture.

As a next step, the gold catalyzed cyclization methodology was applied to get the desired *N*-oxides **377a-c** from the oximes **376a-c**. Unfortunately, the expected cyclization products, *N*-oxides **377**, were not formed according to the spectroscopic



Scheme 84. The oxime-oxime rearrangement of **376** to **378**

Table 2. Oxime-oxime rearrangement with different metal catalysis

<i>Catalyst (3 mol %)</i>	<i>NMR Yield (%)</i>
AuCl ₃	90-95
AuBr ₃	85-90
HAuCl ₄ ·3H ₂ O	85-90
LAuCl*/AgOTf	60-72
CF ₃ SO ₂ OAg	60-65

*Chloro[1,3-bis(2,4,6-trimethylphenyl)imidazol-2-ylidene]gold(I)

analysis. To our surprise, the gold catalyzed reactions smoothly gave rearranged products **378a-c** having the (*E*)- and (*Z*)-isomers under the same reaction conditions with different catalysis as shown in Table 2 (Scheme 84).

The newly formed products **378a-c** were characterized properly with the help of spectral data. According to the ¹H- NMR spectrum of **378b**, it is seen that the –CH₂– proton resonances of alkyne unit disappeared. Instead of these signals, two new adjacent triplets belonging two different –CH₂– protons appeared at 4.86 ppm and 3.30 ppm. Additionally, a new aldehyde resonance signal was observed at 9.89 ppm in the ¹H- NMR spectrum. In the ¹³C-NMR spectrum, aldehyde carbon resonate at 182.6 ppm and imine carbon resonate at 157.0 ppm. In addition to this, two methyl carbons resonances at 41.3 and 27.8 ppm were observed. According to these data, the oxime unit was transferred from one carbon atom to another carbon atom and new aldehyde functionality was formed

During the purification attempts, the oxime functionality of one of these rearranged product **378a** was hydrolyzed to **378e** (Scheme 84). For the further characterization, 1D- and 2D-NMR techniques were applied to determine the correct structure of **378e**. In the ¹H- NMR spectrum of **378e**, we observe two triplets belonging two adjacent –CH₂– protons resonating at 4.78 and 2.96 ppm. Additionally, an aldehyde resonance signal was observed at 9.89 ppm. In the ¹³C-NMR spectrum, two carbonyl signals appeared at 206.5 and 182.5 ppm. According to the HSQC spectrum, the carbon signal at 182.5 ppm belongs to the aldehyde group. The resonance signal at 206.5 may arise from a carbonyl group substituted with alkyl

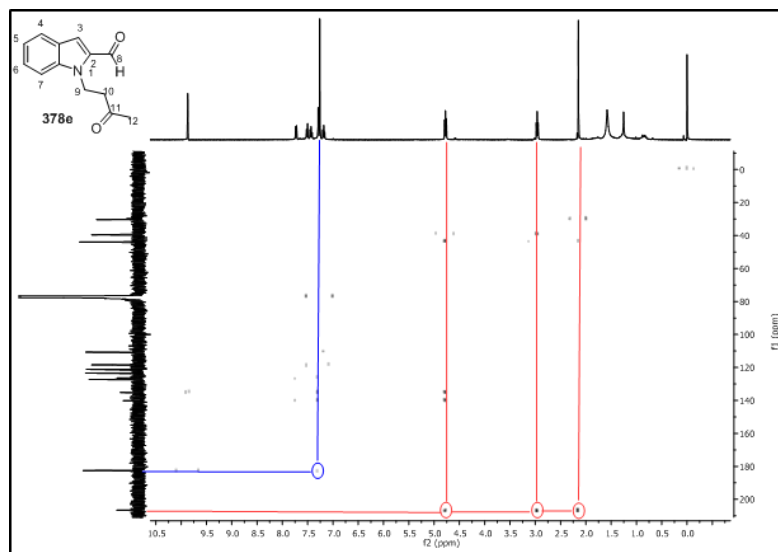
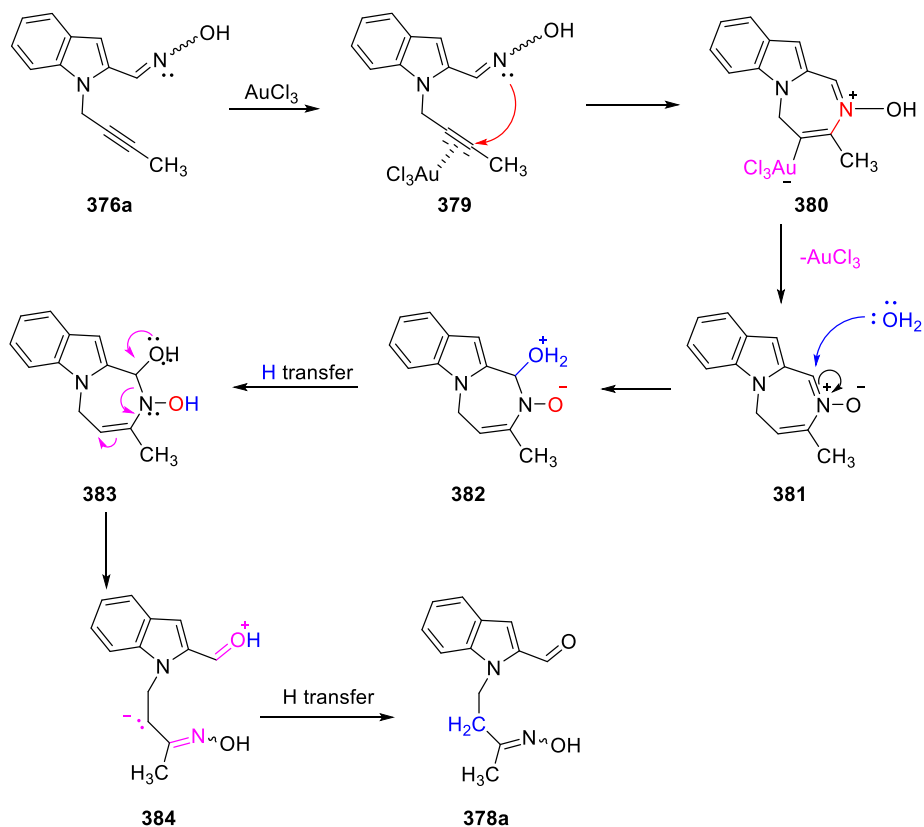


Figure 36. HMBC spectrum of compound **378e**

groups. We propose that the primarily formed oxime functionality underwent hydrolysis reaction during column chromatography to give **378e**. Additionally, two methylene and one methyl carbon signals appearing at 43.9, 39.6 ppm and 30.3 ppm, support our proposed structure.

According to the HMBC spectrum of **378e**, $-\text{CH}_2-$ protons and methyl protons have strong correlations with the carbonyl carbon signal. This clearly shows that the carbonyl group is located between the ethylene and methyl units. Additionally, aldehyde proton has a correlation with the singlet proton resonance (H-3) of the indole ring (Figure 36).

After confirmation of the structure of rearranged products **378a-c** and **378e**, a mechanism for the formation of the oxime-oxime rearrangement was proposed (Scheme 85). According to this mechanism, firstly gold undergoes a coordination with alkyne unit to form complex **379**. At this stage, the formed intermediate **379** can be attacked at two alkyne carbon atoms. Since the positive charge next to the methyl group can be better stabilized, the attack on this carbon atom in **379** is preferred to form a seven membered ring intermediate **380**. Water molecule present in the reaction medium attacks the imine carbon atom of **381** to form intermediate **382**. After H-transfer and formation of intermediate **383**, ring opening reaction

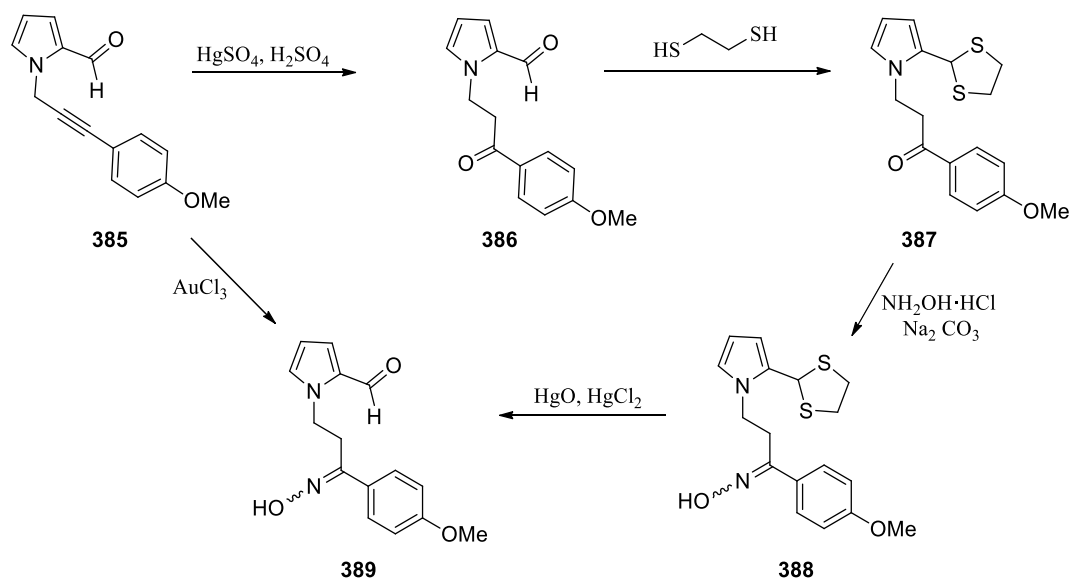


Scheme 85. Mechanism of the “the oxime-oxime rearrangement”

followed by second H–transfer of intermediate **384** results in the formation of final product **378a** (Scheme 85).

Overall this reaction, the oxime functionality attached to the indole ring was transferred intramolecularly from one carbon atom to another carbon atom next to methyl group. This rearrangement was called as “the oxime-oxime rearrangement”. To the best of our knowledge, this reaction is unprecedented in the literature.

During the oxime-oxime rearrangement studies of the pyrrole analogous in our laboratory, rearranged product **389** was independently synthesized to support the structure of the rearranged product. For this purpose compound **385** was subjected to the hydration reaction in the acidic medium yielding the compound **386**. After selective protection of the aldehyde functionality, the oxime **388** was synthesized.



Scheme 86. Independent synthesis of rearranged product **389**

The targeted product **389** was then formed by the deprotection reaction of the compound **388**. The comparison of this product with that one synthesized by the gold-catalyzed cyclization reaction of the compound **385** showed that they are the same product (Scheme 86).¹³²

The mode of the cyclization is determined by the electronic nature of substituents attached to the triple bonds. To gain more insight into the chemoselectivity, we conducted some calculations to understand the formation of the products arising from 7-*endo*-dig as well as 6-*exo*-dig cyclization processes. The optimization and the successive NBO analysis of the corresponding gold-coordinated complexes **358** and **376b** showed the origin of this selectivity. According to the calculations, in the unsubstituted case, after the coordination of gold to the alkyne unit, the bond distances between the gold and the alkyne carbon atoms are different. The distance between the terminal carbon atom and the gold atom (2.31 Å) is shorter than the distance between the internal alkyne carbon atom and gold (2.51 Å). This shows that the gold atom is tightly connected to the terminal alkyne carbon atom, whereas the positive charge is located on the internal carbon atom. As a consequence of this unsymmetrical coordination of the gold atom, the nucleophile, *N*-atom of oxime group attacks the internal alkyne carbon atom and form 6-*exo*-dig intermediate (

Figure 37a). This finding is completely in agreement with our experimental results. On the other hand, in the case of substituted gold-alkyne complexes we observed that the distance between the internal alkyne carbon atom and the gold atom is shorter (2.18 Å) than the distance between the carbon atom next to the substituents and the gold atom (2.67 Å) (

Figure 37b). This clearly indicates that the positive charge is more concentrated on the alkyne carbon atom which is next to the substituents because of better stabilization ability of the aromatic substituents. In this case, an attack on this carbon forming a 7-endo-dig ring intermediate is preferred (

Figure 37b).

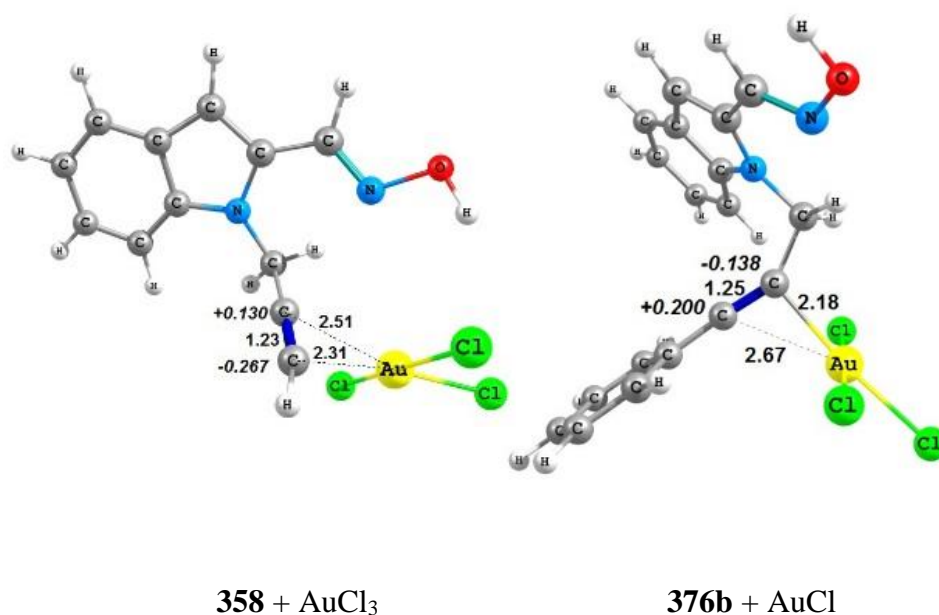
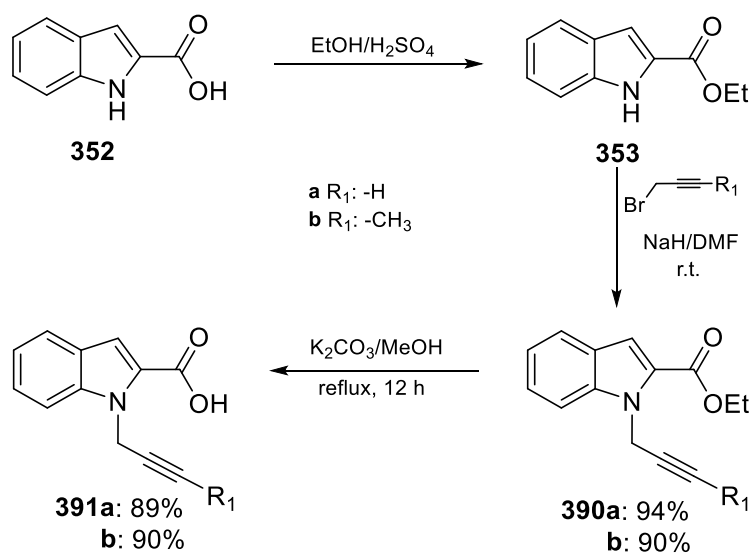


Figure 37. Geometry optimized structure of **358**+AuCl₃ and **376b**+ AuCl₃ complexes. NBO charges and distances (in Å). DFT/B3LYP; Basis Set: GEN (combination of the 6-31+G(d,p) basis set with the LANL2DZ)

2.2.2 Intramolecular Gold-catalyzed and NaH-supported Cyclization Reactions of *N*-propargyl Indole Derivatives with Pyrazole Ring: Synthesis of Pyrazolo-pyrazino-indoles and Pyrazolo-diazepino-indoles

2.2.2.1 Synthesis of *N*-propargyl Substituted 1*H*-indole-2-carboxylic acids

N-propargyl substituted 1*H*-indole-2-carboxylic acids **391a** and **391b** are the key compounds for the preparation of pyrazolo-indoles (**396a-e**). These carboxylic acids were prepared starting from commercially available 1*H*-indole-2-carboxylic acid (**352**) in three steps. For this purpose, indole-2-carboxylic acid was first converted to ethyl ester derivative **353** in quantitative yield as mentioned in the previous section. *N*-propargyl substituted esters **390a** and **390b** were synthesized by treatment of compound **353** with propargyl bromide (**356**) or 1-bromo-2-butyne (**365**) in dry DMF in the presence of NaH. After successful synthesis of compounds **390a** and **390b**, they were hydrolyzed by K₂CO₃ in MeOH to give the corresponding carboxylic acids **391a** and **391b** in 89% and 90% yields, respectively (Scheme 87).



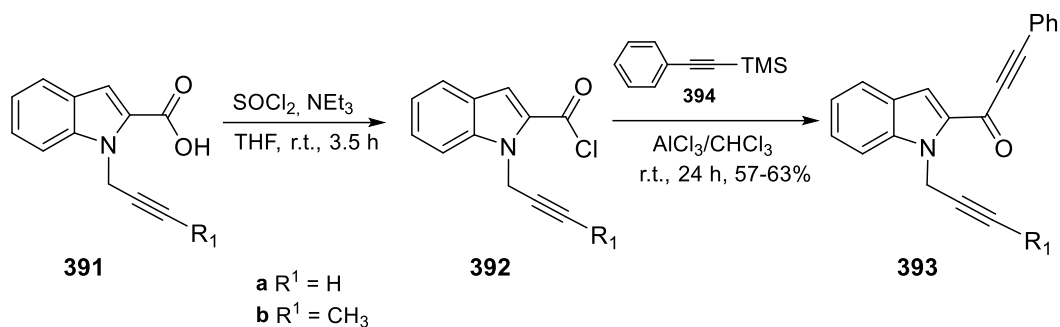
Scheme 87. Synthesis of *N*-propargyl substituted indole-2-carboxylic acids **391a,b**

The formation of the targeted compounds were confirmed by means of the $^1\text{H-NMR}$ and $^{13}\text{C-NMR}$ spectra. For the formation of the propargyl substituted compounds **390a** and **390b**, the main indicator was the disappearing the $-\text{NH}$ resonance signal and accordingly observation of the $-\text{CH}_2-$ and acetylenic resonances of the propargyl group.

Additionally, in the $^{13}\text{C-NMR}$ spectrum, alkyne carbons resonance signals around 70 – 85 ppm also clearly show incorporation of the propargyl group into the molecules. The hydrolysis to form carboxylic acids **391a** and **391b** were confirmed by the disappearance of the ester group resonances in the $^1\text{H-NMR}$ spectrum around 4.30 ppm and 1.40 ppm as well as in the $^{13}\text{C-NMR}$ spectrum around 60.0 and 15.0 ppm.

2.2.2.2 Synthesis of α,β -Alkynyl Ketones

After successful synthesis of carboxylic acid **391a** and **391b**, the next step was the synthesis of α,β -alkynyl ketones **393a** and **393b**. For this purpose, the prior activation of carboxylic acid as the acyl chlorides **392** was necessary. This was accomplished by treatment of **391a** and **391b** with thionyl chloride in the presence of triethylamine in THF at room temperature. The resulting acid chlorides **392a** and **392b** were then reacted in situ with trimethylsilylphenylacetylene (**394**) to furnish the corresponding alkynyl products **393a** and **393b** in 63% and 57% yields,

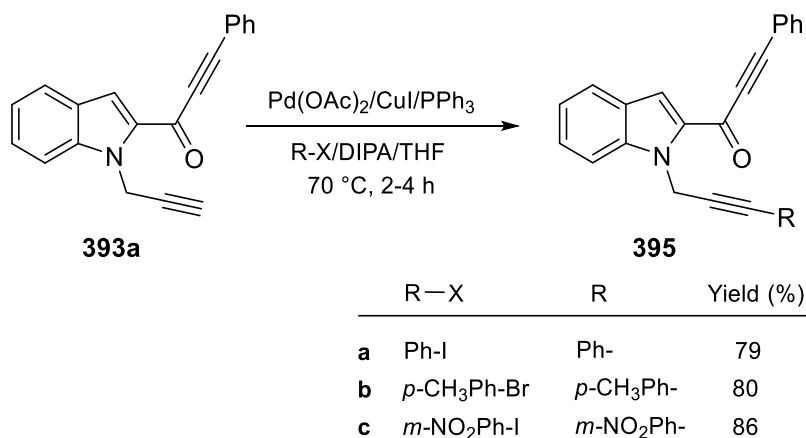


Scheme 88. Synthesis of α,β -alkynyl ketones

respectively. Trimethylsilylphenylacetylene (**394**) was prepared by the substitution reaction of phenylacetylene with trimethylsilyl chloride in the presence of *n*-BuLi.¹³³ (Scheme 88).

The incorporation of phenylacetylenyl group was characterized by means of the NMR spectra. The proton resonances in ¹H-NMR spectrum of the newly substituted phenyl group was not clear, because of the collapsing with the aromatic proton resonance signals of the indole ring. However, the ¹³C-NMR spectrum was much more informative because of two new acetylene carbon signals. In compounds **391a** and **391b**, there are two alkyne carbon resonance signals at around 70 – 80 ppm. However, the ¹³C-NMR spectra of compounds **393a** and **393b** show two additional alkyne carbon resonance signals at around 85 – 100 ppm. These data show the incorporation of the second alkynyl substituent to the carbonyl group. In addition to these, in the IR spectrum, the C=O stretching frequency is shifted to the lower frequency (1607 cm⁻¹) because of the α,β -unsaturated nature of the alkynyl group in compound.

After the synthesis of α,β -unsaturated alkynyl ketones, the next step was the derivatization of dialkynyl ketones **393a** with various substituents. Sonogashira cross-coupling reaction of aryl halides with terminal alkynes is an effective approach to the synthesis of functionalized alkynes as mentioned in the previous section. For Sonogashira coupling reaction, we used a palladium catalyst and a copper(I) cocatalyst, in which the palladium has the function to promote the cross-

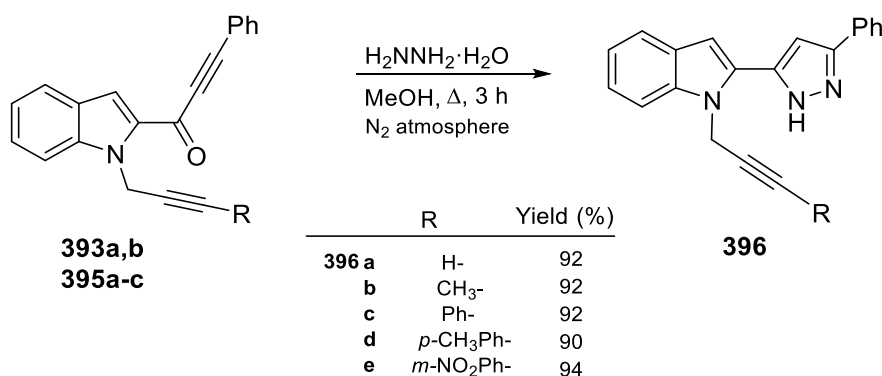


Scheme 89. Derivatization of α,β -unsaturated alkynyl ketones

coupling of an aryl fragment in the presence of triphenylphosphine and diisopropylamine (DIPA) as the base. Three halosubstituted aromatic compounds were smoothly coupled with alkyne derivatives **393a** to give dialkynes **395a-c** substituted at the terminal alkyne carbon atom in high yields and the compounds were characterized by NMR spectra (Scheme 89).

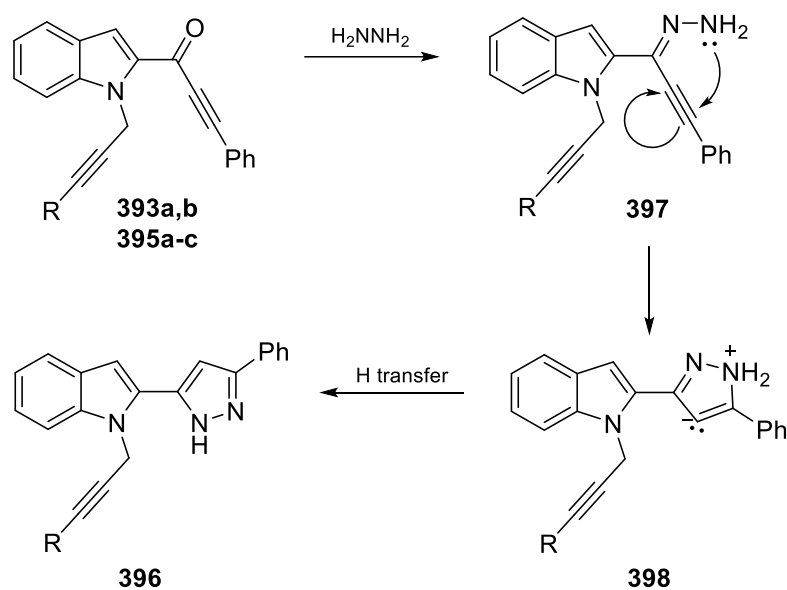
2.2.2.3 Synthesis of *N*-propargyl Substituted 2-Pyrazolo-indole Derivatives

Before the cyclization reactions of the alkyne unit, the next step was the formation of the pyrazole ring. Pyrazole rings were synthesized with different methodologies. They can be synthesized by cyclization or cycloaddition reactions. Among these reactions, the cyclization reactions of 1,3-dicarbonyl compounds with hydrazines is one of the most popular methods to form pyrazoles known as “Knorr pyrazole synthesis”.^{88,134} Another method for the formation of pyrazole and/or substituted pyrazole rings is the cyclization reaction of alkynyl ketones with hydrazine derivatives. The cyclization reaction of 1,3-dicarbonyl compounds with hydrazine molecule generally give the regioisomers of the pyrazoles. However, the cyclization reactions of α,β -unsaturated alkynyl ketones with hydrazines give the regioselectively cyclized pyrazole.¹³⁵ In our synthetic pathway, α,β -unsaturated alkynyl ketones were used as the precursor of the pyrazole rings. For this purpose, compounds **393a,b** and **395a-c** were subjected to the cyclization reaction with hydrazine to form 2-pyrazole-indole derivatives **396a-e** (Scheme 90).



Scheme 90. Synthesis Pyrazole derivatives **396**

During the synthetic pathway, first hydrazine attacks to the carbonyl carbon atom of the α,β -unsaturated alkynyl ketones to form hydrazones **397**. Then, by attack of unpaired electrons of nitrogen atom to the β -position of alkyne unit forms intermediate **398**. In the final step, the proton transfer yields the corresponding pyrazole rings **396** (Scheme 91).¹³⁶ “Michael addition” is the second possible mechanism for the formation of pyrazoles **396** over corresponding enones.

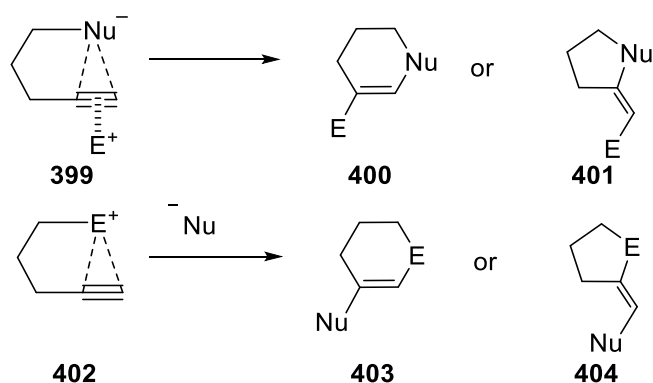


Scheme 91. Mechanism of the formation of pyrazoles **396**.

Characterization was done by means of spectroscopic data. The main indicator of the formation of pyrazole rings was the disappearance of the carbonyl and alkyne carbons resonance signals in the ^{13}C -NMR spectra. The carbonyl resonance signals of α,β -unsaturated alkynyl ketones at around 165 – 182 ppm disappeared by the formation of imine which resonate at the higher fields. In addition to this, alkyne carbon resonance signals of α,β -unsaturated alkynyl ketones at around 80 – 100 ppm also disappeared in the ^{13}C -NMR spectra of compounds **396a-e**. In the ^1H -NMR spectra of compounds, a singlet of the pyrazole rings was observed at around 6.0 – 6.8 ppm. Additionally, mass spectra also fully supported the formation of the corresponding molecules **396**.

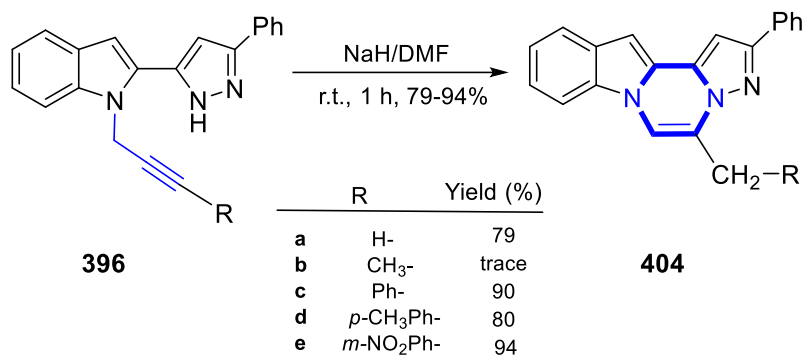
2.2.2.4 NaH Supported Intramolecular Electrophilic Cyclization Reactions of *N*-propargyl Substituted 2-Pyrazolo-indole Derivatives

For alkyne cyclization reactions, two different mechanisms are proposed in the literature. The first one; alkyne **399** can be coordinated by any electrophile which can be then attacked by an internal nucleophile to give an intramolecular (6)-*endo*-dig cyclization product **400** and/or (5)-*exo*-dig cyclization product **401** as shown in Scheme 92. In the second case, an electrophile which is a part of the compound can activate the alkyne followed by attack by a nucleophile can result in the formation of 6-*endo*-dig cyclization product **403** and/or 5-*exo*-dig cyclization product **404**. The nomenclature of the cyclization reactions was described by *Jack E. Baldwin* and known as the “*Baldwin’s rules for the ring closure*”. According to his rules, cyclization is named in terms of the three different point. One of them is the number of the atom on the ring formed which is 5- or 6-. Second point is the hybridization of the ring closure point, which is *sp*-hybridization meaning diagonal structure (*dig*). The third point is the place of the resultant double bond which can be *exo*- meaning out of the ring or *endo*- meaning on the ring (Scheme 92).^{137,138}



Scheme 92. Possible cyclization modes

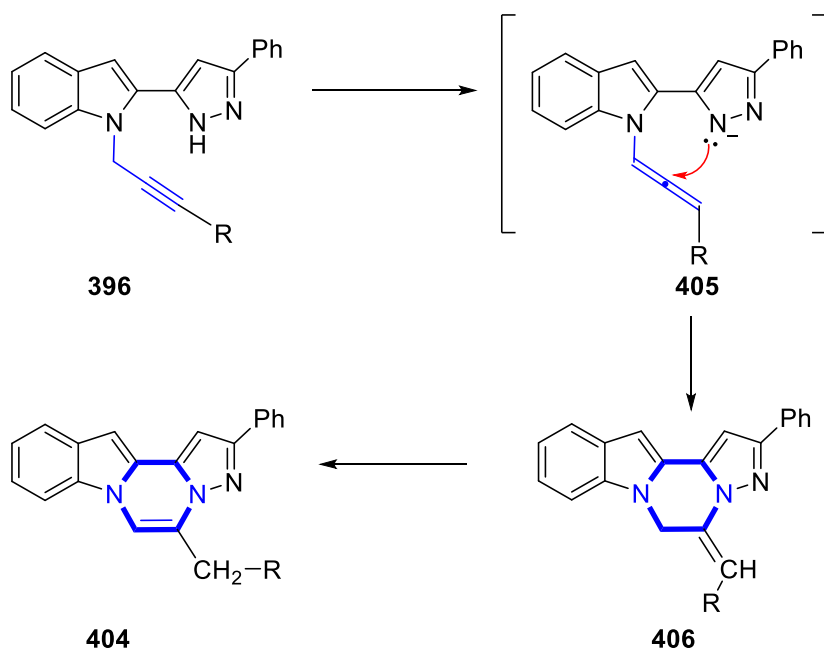
As the next, we decided to perform alkyne cyclization reactions in the presence of NaH. For this purpose, *N*-propargyl substituted 2-pyrazolo-indoles **396a-e** were reacted with NaH as the base in dry DMF at room temperature. During this reactions compounds **396a,c-e** gave the targeted 6-*exo*-dig cyclization products **404a,c-e** while the methyl substituted one, **396b**, did not. As a result of this cyclization



Scheme 93. NaH induced cyclization reactions of **396**

reactions, pyrazolo-pyrazino-indole derivatives **404a,c-e** were synthesized in good yields (Scheme 93).

For the formation of pyrazolo-pyrazino-indole derivatives **404a,c-e** we propose the following reaction mechanism (Scheme 94). Firstly the base abstracts the proton on the pyrazole ring and makes pyrazole ring much more nucleophilic. On the other hand, NaH isomerizes alkyne unit in **396** to the corresponding allene **405**. As the central atom of allene unit is much more electropositive than the other carbon atoms, pyrazole unit exclusively attacks the central carbon atom of allene to gener-

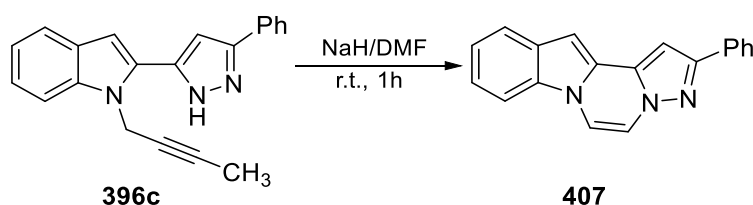


Scheme 94. Mechanism for the formation of pyrazine rings

ate the 6-*exo*-dig cyclization products **406** which are successively isomerized to the *endo*-products **404** (Scheme 94).^{91,102}

Formation of the pyrazine rings were confirmed by the NMR spectral data. In the ¹H-NMR spectra, the resonance signal belonging to the methylene protons at around 5.0 – 6.0 ppm disappeared and new methylene signals appeared at about 4.0 – 4.5 ppm. In the case of unsubstituted alkyne, a new methyl signal was observed. The disappearance of –NH proton resonance belonging to the pyrazole ring nitrogen and formation of a new singlet in the aromatic region also supported the formation of the pyrazine rings. In addition to this, in the ¹³C-NMR spectra of compound **404a,c-e**, the alkyne resonance signals disappeared and new two resonance signal in the sp² region showed the formation of the pyrazine rings.

The methyl substituted alkyne unit, surprisingly, did not form the expected product **404b**. It is only seen in trace amount. Instead of this, the compound **407** was formed where an ethyl group was removed from the compound. The attempts for understanding the mechanism of this conversion is under investigation (Scheme 95).



Scheme 95. Formation of compound **407**

The ¹H-NMR spectrum of the compound **407** showed the removal of the ethyl group from pyrazine ring. This could be easily seen, in other words the disappearance of the substituent out of pyrazine ring could be easily determined from ¹H-NMR spectrum of the compound **407**. The spectrum did not show any signal in the aliphatic region. Furthermore, an AB system arising from the aromatic protons of the pyrazine ring around 7.50 ppm clearly indicated the removal of ethyl group. The HSQC spectrum of the compound **407** also supports the structure (Figure 38).

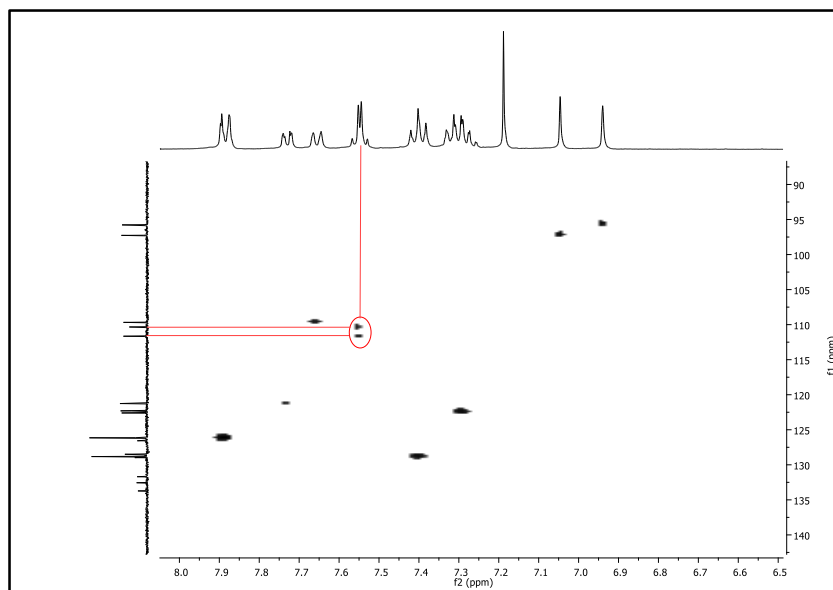
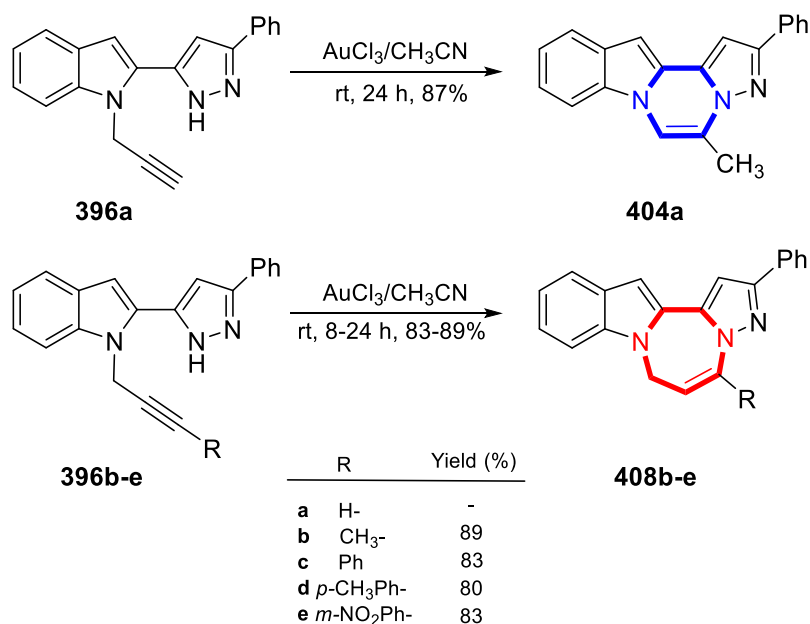


Figure 38. HSQC spectrum of compound **407**

2.2.2.5 Gold Catalyzed Intramolecular Cyclizations of **396**.

Gold is one of the useful catalyst for the alkyne cyclization reaction. Actually, it is called as alkynophilic in some references.¹³⁹ Because of the good ability at coordinating towards alkyne multiple bonds, gold catalyst activates the alkyne functionality as electrophilic and make them reactive towards nucleophilic attacks.¹³⁹ Throughout our synthetic approach, as the next step, the targeted skeletons **349** and **350** were intended to be synthesized by the gold catalyzed alkyne cyclization reactions. As the catalyst, AuCl₃ was used for the intramolecular cyclization reaction of **396a-e** because of the best results were obtained from the Au³⁺ salts as mentioned in the previous section.

Compounds **396a-e** were subjected to the gold catalyzed cyclization reactions with AuCl₃ in CHCl₃ at room temperature (Scheme 96). The reaction of **396a** having a terminal alkyne afforded the cyclization product **404a**. The reaction proceeds via electrophilic activation of the triple bond followed by 6-*exo*-dig heterocyclization and final H-shift leading to the pyrazolo-pyrazino-indole **404a** which is the same product obtained by the NaH-induced cyclization reaction of **396**. On the other

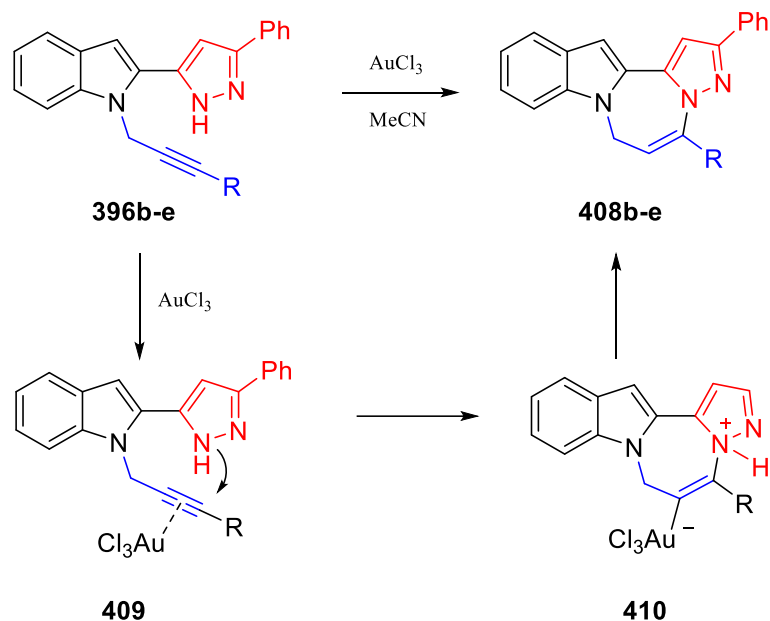


Scheme 96. Gold catalyzed cyclization reactions of **396**.

hand, exclusive formation of 7-endo-dig cyclization products **408b-e** having a pyrazolo-diazepino-indole skeleton was observed by the reaction of internal alkynes **396b-e** with AuCl₃ catalyst under the same reaction conditions (Scheme 96).

The proposed mechanism for the formation of seven-membered rings starts with the coordination of gold catalyst to the alkyne bonds yielding the complex **409** and followed by a nucleophilic attack of the nitrogen atom of the pyrazole ring to form the seven-membered intermediate **410**. The formation of intermediate is followed by the decomplexation of the gold catalyst to give the compound **408b-e** (Scheme 97).

The interesting outcome of these reactions is the reactivity difference between substituted alkynes **396b-e** and unsubstituted alkyne **396a**. It is easily seen that the electronic nature of the substituent responsible for these regioselectivity. The unsubstituted alkyne favors the attacking on the internal alkyne carbon atom, whereas the substituted ones favor the carbon atom which is next to the substituents. It means that in the unsubstituted case, the inner carbon atom gain more



Scheme 97. Mechanism of the gold-catalyzed cyclizations of **396**

electrophilic character of the alkyne unit while in the substituted alkynes the carbon atoms nearby the substituents becomes more electrophilic part of the molecule. To understand this regioselectivity, we performed some calculations. Geometry optimization and frequency calculations of complexes **409a** and **409c** with the catalyst AuCl_3 were performed using the B3LYP hybrid level of the 6-31G(d,p) and LANL2DZ (Au) mixed basis set coupled with DFT. Natural bond orbital analysis was performed at the same level of theory (Figure 39).

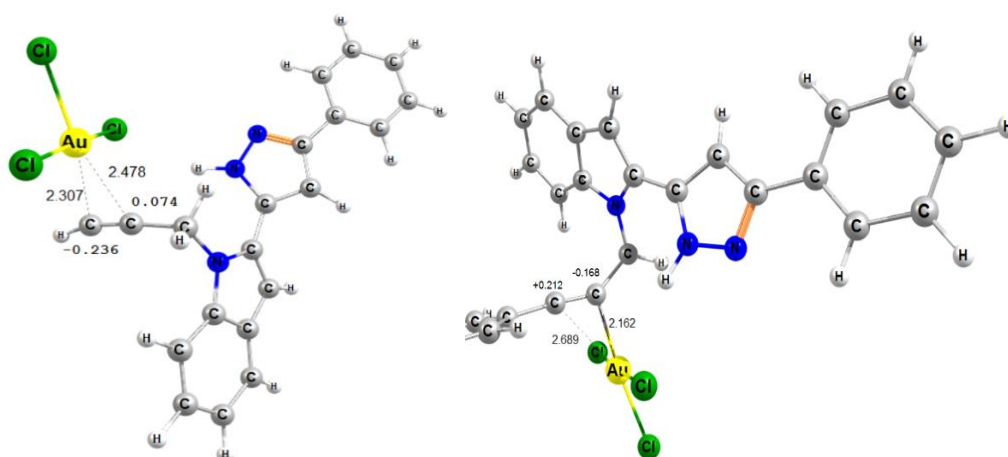


Figure 39. Geometry optimized structures of **409a**+ AuCl_3 and **409c**+ AuCl_3 complexes; NBO charges and distances in Å

In the case of the complex of **409a**+AuCl₃, the distance between the terminal alkyne carbon atom and the gold atom is shorter (2.307 Å) than the distance between the internal alkyne carbon atom and the gold atom, indicating that the positive charge is localized on the internal alkyne carbon atom. Therefore, the pyrazole nitrogen atom attacks exclusively this carbon atom positively charged, forming 6-*exo*-dig cyclization product **404a**. On the other hand, if the terminal alkyne carbon is substituted by a phenyl group, in the complex of the gold atom has a stronger interaction with the C-2 carbon atom (Au-C distance 2.162 Å) and the positive charge is concentrated on C-1 because of the better stabilization of the positive charge by the aromatic ring and methyl group in the case of **409c**. Therefore, alkyne carbon atoms, substituted by phenyl or methyl groups, are exclusively attacked at the C-1 carbon atom, giving rise to the formation of 7-*endo*-dig cyclization products **408b-e**.

The constitution of the cyclization products were determined by the application of 1D- and 2D-NMR spectra. For example, for the cyclization of the methyl substituted alkyne (**396b**), there are two possible reaction pathways. In the first one, nucleophilic part of the molecule can attack on the C-1 carbon atom and form the 6-*exo*-dig cyclization products **411** after the isomerization of the double to the *endo*-product. On the other hand, attacking on the C-2 carbon atom of the alkyne unit will generate the 7-*endo*-dig cyclization product **408** (Figure 40).

In the ¹H-NMR spectrum of the isolated product of gold catalyzed cyclization reaction of **396b**, there is an olefinic proton resonance signal at 5.66 ppm which is

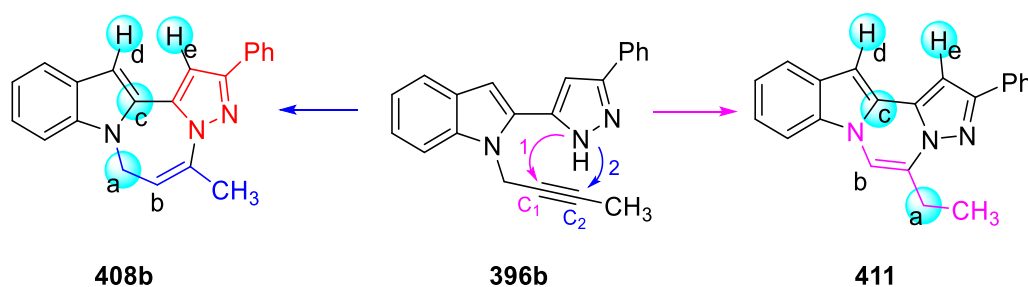


Figure 40. Possible cyclization pathways

split into triplet ($J = 7.2$ Hz) because of adjacent $-\text{CH}_2-$ protons. In the case of formation of **411**, we should observe an ethyl resonance in the aliphatic region.

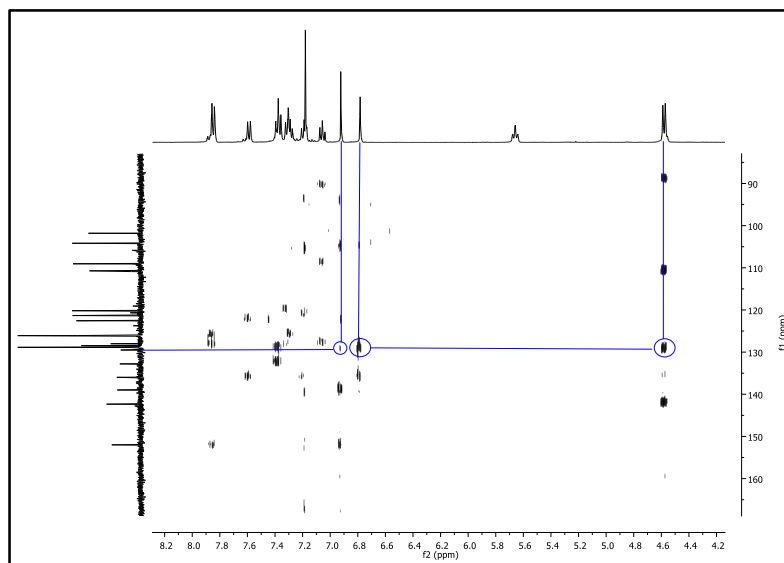


Figure 41. HMBC spectrum of compound **408b**

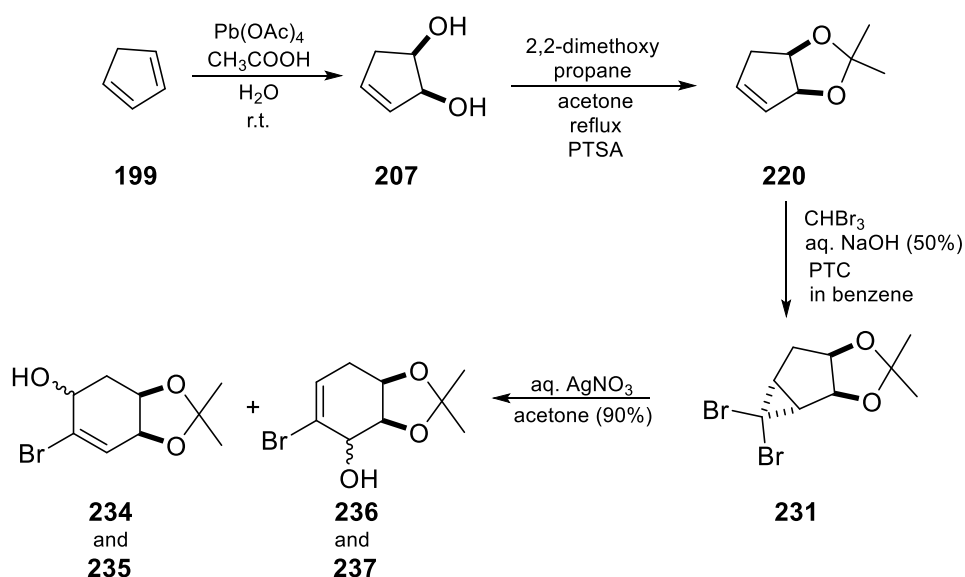
Furthermore, a methyl resonance at 2.35 ppm as singlet supports the formation of a seven-membered cyclization product. In addition to this, the 2D-NMR techniques also support the proposed structure. In the HMBC spectrum of the product **408b**, a correlation between the $-\text{CH}_2-$ protons with the quaternary carbon at 129.4 ppm, labeled as “c” determined by the correlation between proton “d” (H_d) and proton “e” (H_e) (Figure 40), also support the structure.

These results show that the cyclization products have the structure **408b-e**. As a result, the mode of the cyclizations in the internal alkynes, in other words, in the case of substituted alkyne derivatives follow by a nucleophilic attack on the carbon atom next to the substituent because of the localization of the positive charge on this carbon atom according to the theoretical calculations.

CHAPTER 3

CONCLUSION

The aim of this thesis was to develop new methodologies for the synthesis organic compounds having possible potential for biological activities. In the first part, we developed a synthetic strategy for the synthesis at the double bond halogen substituted cyclohexenetriols. For this purpose, cyclopentadiene was first subjected to the *cis*-hydroxylation reaction to get compound **207**. Then, compound **207** was converted to corresponding ketal **220**. Addition of dibromocarbene to the remaining double bond in **220** gave tricyclic carbene addition product **231**. The electrophilic ring opening reaction of compound **231** was achieved in the presence of AgNO_3 by removal one of the bromine atoms from the molecule. This ring

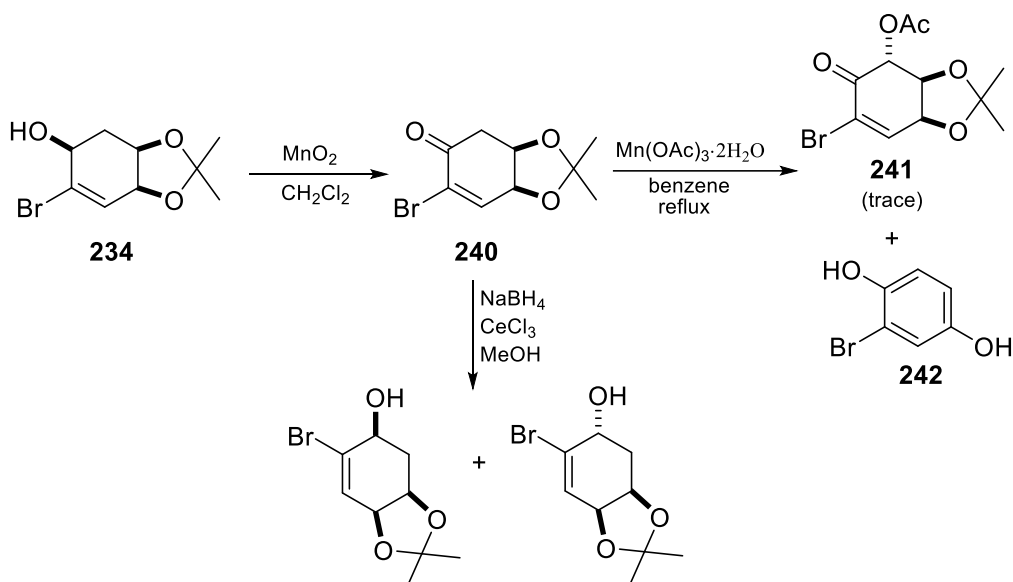


Scheme 98. Synthesis of bromocyclohexenetriol derivatives **234-237**

enlargement procedure resulted in the formation of the constitutional and configurational isomers **234-237** which were separated by the chromatographic methods (Scheme 98).

The allylic oxidation of **234** was performed with MnO_2 to get α,β -unsaturated ketone **240**. For final functionalization of the molecule and to obtain the tetrahydroxylated cyclohexene derivatives, the α -acetoxylation reaction was applied. The desired product **241** was observed in traces. Instead, the aromatic compound **242** was formed in almost quantitative yield (

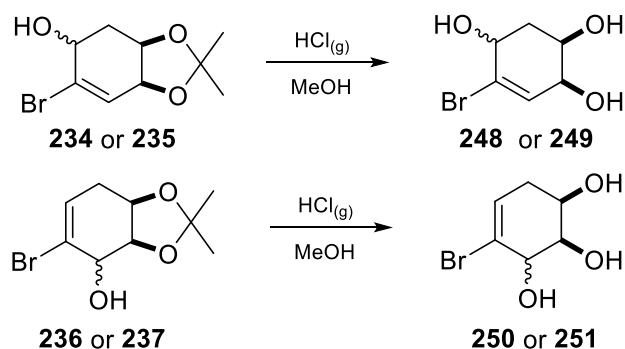
Scheme 99).



Scheme 99. α -Acetoxylation attempt and reduction reaction

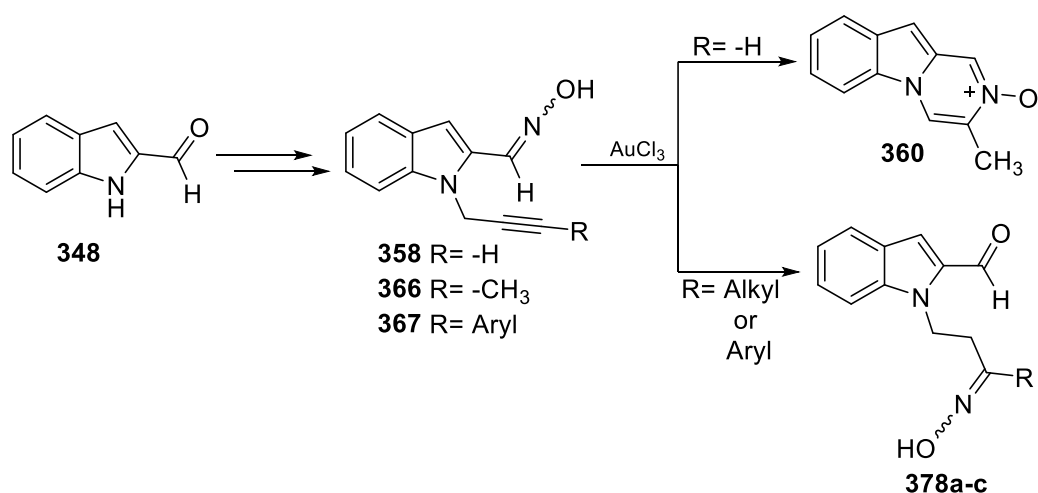
Finally, the protected ketals were hydrolyzed and the corresponding bromocyclohexenetriols **248-251** were obtained and characterized (Scheme 100).

Heterocyclic molecules especially nitrogen containing heterocycles are the common structure among the bioactive molecules. In the second part of the thesis, we concentrated ourselves on the synthesis of *N*-atom containing heterocycles where we mainly used gold-catalyzed alkyne cyclization reactions. Accordingly, we followed two methods for the construction of pyrazine condensed indoles. In



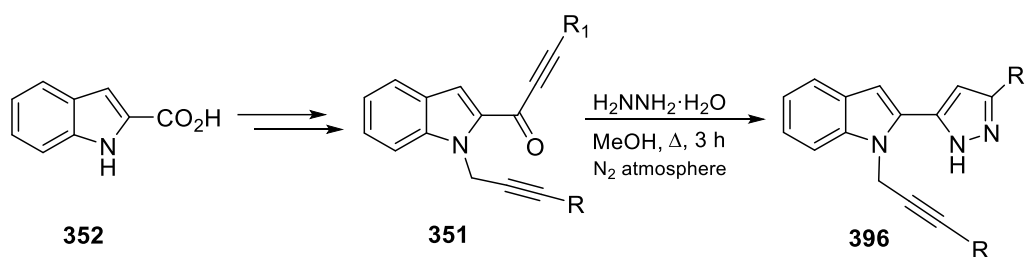
Scheme 100. Deprotection reactions

the first strategy, oximes **347** derived from *N*-propargyl indole-2-carbaldehyde (**348**) were submitted to the gold-catalyzed cyclization reaction. The functionalization of the alkyne moiety was achieved by the Sonagashira cross-coupling reaction. According to the experimental results, unsubstituted alkyne **358** gave 6-*exo*-dig cyclization product, the *N*-oxide molecule **360**. However, the alkyl or aryl substituted derivatives **358**, **366** and **367** formed the rearranged products **378a-c** where the oxime moiety was transferred from one carbon atom next to the indole ring to the carbon atom nearby the substituent. A mechanism for this conversion was proposed. A 7-*endo*-dig cyclization intermediate was proposed as an intermediate. To the best of our knowledge, this reaction is unprecedented in the literature and it was named as “*The oxime-oxime rearrangement*” (Scheme 101).¹³²



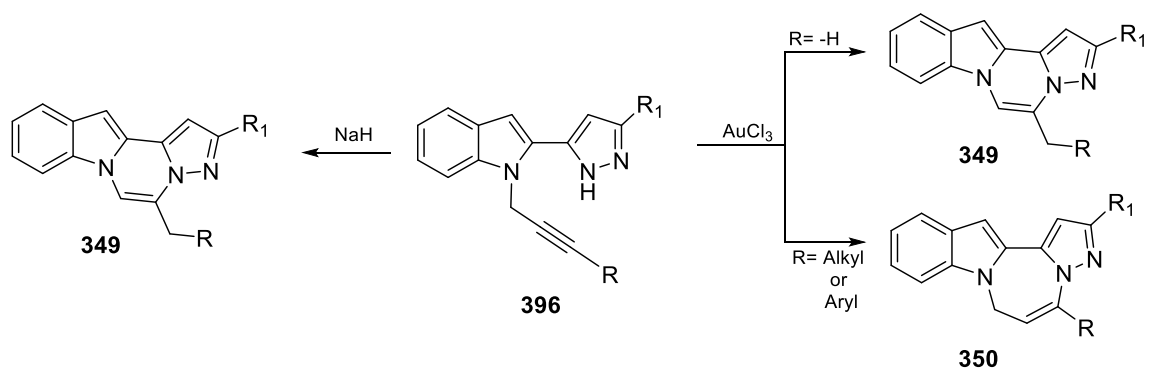
Scheme 101. Gold catalyzed cyclization attempts of oximes **358**, **366** and **367**

In the second part of the heterocyclization reactions, the aim was the investigation of the alkyne cyclization reactions with the pyrazole unit in the presence of a base as well as a gold catalyst. We first prepared pyrazoles **396** starting from indole-2-carboxylic acid (**352**). After introduction of propargyl group with the convenient method, the carboxylic acid moiety was converted into α,β -alkynyl ketones **351**. Furthermore, these α,β -alkynyl ketones **351** were converted to the pyrazole derivatives **396** by reaction with hydrazine (Scheme 102).



Scheme 102. Synthesis of pyrazoles **396** with hydrazine

Formation of the pyrazole derivatives was followed by the application of the cyclization procedures by NaH as the base and gold catalyst. The base-induced cyclization reactions resulted in the formation of 6-*exo*-dig cyclization products **349**. Nevertheless, the gold-catalyzed cyclization reactions, gave 6-*exo*-dig as well as a 7-*endo*-dig cyclization products, the diazepine ring depending on the electronic nature of the substituents attached to the alkyne group. According to the theoretical calculations, the substituents affect the mode of the reaction. In the case of unsubstituted alkyne, the positive charge is localized on the internal alkyne carbon atom after the coordination with the gold catalyst. As a result of this, the nucleophilic attack takes place on this carbon atom and forms the corresponding pyrazine ring. On the other hand, in the case of substituted alkynes, the positive charge is localized on the carbon atom which is nearby the substituent. As a result of this, the nucleophilic attack takes place on this carbon and results in the formation of diazepine derivatives (Scheme 103).¹⁴⁰



Scheme 103. Gold catalyzed cyclization reactions of pyrazoles **396**

CHAPTER 4

EXPERIMENTAL

4.1 General

Nuclear magnetic resonance ($^1\text{H-NMR}$, $^{13}\text{C-NMR}$ and 2D-NMR) spectra were recorded on a Bruker Instrument Avance Series-Spectrospin DPX-400 Ultrashield instrument in CDCl_3 , CD_3OD , CD_3COCD_3 and $\text{DMSO-}d_6$ with TMS as internal reference. Chemical shifts (δ) were expressed in units parts per million (ppm). Spin multiplicities were specified as singlet (s), doublet (d), doublet of doublets (dd), triplet (t) and multiplet (m) and coupling constants (J) were reported in Hertz (Hz).

Infrared spectra were recorded on a Bruker Platinum ATR FT-IR spectrometer and Thermo Scientific Nicolet IS10 ATR FT-IR spectrometer. Band positions were reported in reciprocal centimeters (cm^{-1}).

Gallenkamp electronic melting point apparatus was used to obtain melting points.

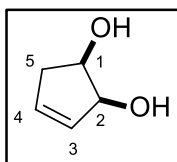
HRMS data were recorded by Agilent Technologies, 6224 TOF LC/MS-T1200 Series applying the electrospray technique. GC-MS data were recorded by Agilent Technology 7890A using Agilent J&W GC HP-5MS, 30m x 0,250mm x 0,25 μm (190915-433:325 $^\circ\text{C}$) column.

Column chromatographic separations were performed by using Merck Silica Gel 60 plates with a particle size of 0.063–0.200 mm. Thin layer chromatography (TLC) was performed by using 0.25 mm silica gel plates purchased from Merck.

Compounds were named by using ChemDraw Ultra 11.0 and ACD NMR. Solvents were purified as reported in the literature.¹⁴¹

4.2 Synthesis of cyclopent-3-ene-1,2-diol (**207**)

To a stirred mixture of $\text{Pb}(\text{OAc})_4$ (142 g, 0.321 mol), AcOH (290 mL, 5.1 mol, and H_2O (12 mL, 0.66 mol) maintained under N_2 atm. in an ice-bath was slowly added freshly distilled cyclopentadiene (**199**) (32.0 g, 0.469 mol) during 30 min. After completion of the addition, the mixture became homogenous and then the ice-bath was removed. After stirring for additional hour, this mixture was poured into the diethyl ether (500 mL). The resulting supernatant liquid was decanted and filtered out over the silica gel and celite. The filtrate was then treated with Na_2CO_3 (150 g) and resulting mixture was stirred vigorously overnight. Then, the precipitate was removed by filtration and washed with diethyl ether (2×100 mL). The combined filtrates were concentrated under reduced pressure to give the mixture of regioisomeric mono-acetylated products associated with diol (\pm)-**206** as a yellow oil.⁶⁸ This mixture was dissolved in MeOH (100 mL) and cooled to 0 °C. NH_3 gas was passed through the solution for 2 h and the reaction flask was closed with a stopper and stirred at room temperature for additional 2 h. After completion of the hydrolysis reaction and removal of the solvent and acetamide under reduced pressure (25 mm Hg), **207** (30.5 g, 0.30 mol) was obtained in 65% yield.

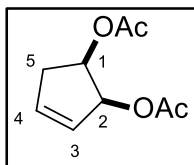


^1H NMR (400 MHz, CDCl_3) δ 5.85 (dt, $J_{3,4} = 5.5$, and $J_{3,2} = 2.7$ Hz, 1H, H-3), 5.71 (dq, $J_{4,3} = 5.6$, and $J_{4,5} = {}^4J_{4,2} = 1.9$ Hz, 1H, H-4), 4.48 (bd, $J_{2,1} = 4.8$ Hz, 1H, H-2), 4.30 – 4.09 (m, 1H, H-1), 3.67 (s, 2H, –OH), 2.51 (ddt, A part of AB system, ${}^2J_{5a,5b} = 17.0$, $J_{5a,1} = 6.3$ and $J_{5a,4} = 1.9$ Hz, 1H, H-5a), 2.28 (bd, B part of AB system, ${}^2J_{5b,5a} = 17.0$ Hz, 1H, H-5b). **^{13}C NMR** (100 MHz, CDCl_3) δ 132.8, 131.6, 75.8, 70.9, 39.4. **IR (ATR, cm^{-1})** 3345, 2933, 1397, 1071, 906, 725.

4.3 Synthesis of cyclopent-3-ene-1,2-diol diacetate (**213**)

Cyclopent-3-ene-1,2-diol (**207**) (5.0 g, 50 mmol) was dissolved in 15 mL of pyridine in a 250 mL round bottom flask which was maintained in an ice-bath. To this solution, excess acetic anhydride (10 mL) was added and stirred. After 30 min.,

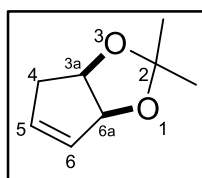
the ice-bath was removed and the solution was stirred overnight. Subsequently, ethyl acetate (50 mL) was added and the solution was extracted with sat. NaHCO_3 (5×50 mL) solution and dried over MgSO_4 . Removal of the organic solvent gave the cyclopent-3-ene-1,2-diyl diacetate (**213**) (9.0 g, 48 mmol) in quantitative yield.



$^1\text{H NMR}$ (400 MHz, CDCl_3) δ 6.02–5.98 (m, 1H, H-3), 5.76 (dq, $J_{4,3} = 6.3$, and $^4J_{4,2} = J_{4,5a} = J_{4,5b} = 2.2$, Hz, 1H, H-4), 5.61 (bd, $J_{2,1} = 6.1$ Hz, 1H, H-2), 5.29 (ddd, $J_{1,5a} = 6.9$, $J_{1,2} = 6.1$, and $J_{1,5b} = 4.5$ Hz, 1H, H-1), 2.65 (ddt, A part of AB system, $J_{5a,5b} = 17.2$, $J_{5a,1} = 6.9$, and $^4J_{5a,3} = 2.3$ Hz, 1H, 5a), 2.43 (ddt, B part of AB system, $J_{5b,5a} = 17.2$, $J_{5b,1} = 4.5$, and $J_{5b,4} = 2.2$ Hz, 1H, 5b), 2.00 (s, 6H, CH_3). **$^{13}\text{C NMR}$** (100 MHz, CDCl_3) δ 170.3, 170.2, 134.7, 128.2, 75.6, 71.2, 36.6, 20.8, 20.7. **IR (ATR, cm^{-1})** 1721, 1229, 1028, 603.¹⁴²

4.4 2,2-Dimethyl-4,6a-dihydro-3aH-cyclopenta[*d*][1,3]dioxole (**220**)

Diol **207** (5.0 g, 50 mmol) was dissolved in a mixture of 50 mL acetone and 2,2-dimethoxypropane (1:4). To this solution, *p*-toluene sulfonic acid (PTSA) (50 mg, 0.26 mmol) was added. The resulting mixture was stirred at room temperature for 1 h. After that, the reaction mixture was heated under the reflux temperature overnight. After cooling of the reaction mixture to room temperature, water (50 mL) was added followed by saturated NaHCO_3 (50 mL) and then the resulting mixture was extracted with ethyl acetate (3×50 mL). The combined organic phases were dried over MgSO_4 . Evaporation of the organic solvent under reduced pressure gave the 2,2-dimethyl-4,6a-dihydro-3aH-cyclopenta[*d*][1,3]dioxole (**220**) (4.90 g, 35 mmol) as a yellow oil in 70% yield.

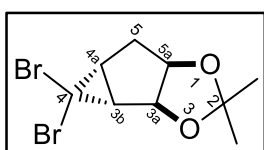


$^1\text{H NMR}$ (400 MHz, CDCl_3) δ 5.76 (dt, $J_{6,5} = 5.8$, and $J_{6,4b} = J_{6,6a} = 1.8$ Hz, 1H, H-6), 5.71 (dq, $J_{5,6} = 5.8$ and $J_{5,4a} = J_{5,4b} = J_{5,6a} = 1.8$ Hz, 1H, H-5), 5.04 (bd, $J_{6a,3a} = 5.9$ Hz, 1H, H-6a), 4.69 (dt, $J_{3a,4b} = 1.8$ and $J_{3a,6a} = J_{3a,4a} = 5.9$ Hz, 1H, H-3a), 2.56 – 2.48 (bd, A part of AB system, $^2J_{4a,4b} = 18.0$ Hz, 1H, H-4a), 2.44 (dq, B part of AB system, $^2J_{4b,4a} = 18.0$ and $J_{4b,3a} = J_{4b,5} = J_{4b,6} = J_{4b,6a} = 1.8$ Hz, 1H, H-4b), 1.34 (s, 3H, CH_3),

1.28 (s, 3H, CH₃). ¹³C NMR (100 MHz, CDCl₃) δ 132.4, 130.7, 109.7, 85.5, 77.7, 38.8, 27.4, 25.6. IR (ATR, cm⁻¹) 2957, 2917, 1733, 1366, 1074.¹⁴³

4.5 4,4-Dibromo-2,2-dimethylhexahydrocyclopropa[3,4]cyclopenta[1,2-*d*][1,3]di-oxole (231)

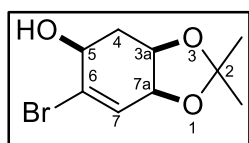
To the vigorously stirred solution of ketal **220** (4.20 g, 30 mmol), benzyltriethylammonium chloride (150 mg, 0.66 mmol), and bromoform (10 mL, 114.5 mmol) in benzene (20 mL), and NaOH (25 mL of 50% w/v aqueous solution) were added in an ice-bath maintained at 0 °C during 30 min. After completion of addition, the resulting mixture stirred an additional hour then ice-bath was removed and the stirring was continued overnight at room temperature. Then, the reaction mixture was partitioned between hexane (100 mL) and brine (100 mL). After separation of this dark mixture, the aqueous phase was extracted with ethyl acetate (3 × 50 mL). The combined organic phases were washed with brine (2 × 50 mL), dried over MgSO₄, and concentrated under reduced pressure. Excess bromoform was removed by vacuum distillation (1 × 10⁻¹ mm Hg) to get the crude product as a brown oil.¹⁴⁴ The crude product was subsequently eluted over silica gel with hexane to obtain the 4,4-dibromo-2,2-dimethylhexahydrocyclopropa[3,4]cyclopenta[1,2-*d*][1,3]dioxole (**231**) as a pale yellow oil (7.67 g, 24.6 mmol, 82%).



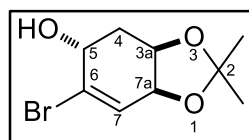
¹H NMR (400 MHz, CDCl₃) δ 4.51 (dt, A-part of AB system, $J_{5a,5a'} = 2.0$ and $J_{5a,3a} = J_{5a,5b'} = 5.7$ Hz, 1H, 5a), 4.43 (d, B-part of AB system, $J_{3a,5a} = 5.7$ Hz, 1H, 3a), 2.42 (d, A-part of AB-system, $J_{3b,4a} = 7.3$ Hz, 1H, 3b), 2.37 (ddd, B-part of AB-system, $J_{4a,3b} = 7.3$, $J_{4a,5a'} = 6.3$, $J_{4a,5b'} = 1.3$ Hz, 1H, 4a), 2.16 (ddd, A-part of AB-system, ${}^2J_{5a',5b'} = 15.4$, $J_{5a',4a} = 6.3$ and $J_{5a',5a} = 2.0$ Hz, 1H, 5a'), 2.08 (ddd, B-part of AB-system, ${}^2J_{5b',5a'} = 15.3$, $J_{5b',5a} = 5.7$ and $J_{5b',4a} = 1.3$ Hz, 1H, 5b'), 1.40 (s, 3H, CH₃), 1.23 (s, 3H, CH₃). ¹³C NMR (100 MHz, CDCl₃) δ 111.8, 85.0, 84.7, 41.6, 38.0, 36.6, 35.2, 27.1, 24.9. IR (ATR, cm⁻¹) 2963, 1716, 1259, 1078, 1014, 793. HRMS Calcd for (C₆H₄Br₂) [M + H]⁺: 234.87525. Found: 234.87688

4.6 (3a*R*,5*S*,7a*S*)-6-bromo-2,2-dimethyl-3a,4,5,7a-tetrahydrobenzo[*d*][1,3]-diox-ol-5-ol (**234**)

Silver nitrate (2.038 g, 12 mmol) was dissolved in water (10 mL) and added to a magnetically stirred solution of cyclopropane **231** (0.935 g, 3 mmol) in 90 mL of acetone. The resulting solution was stirred at room temperature for 8 hours while protecting from the light. After completion of the reaction, precipitate was filtered through a plug of celite which was washed with 200 mL of EtOAc. The resulting mixture was concentrated under reduced pressure. After addition of 50 mL of brine, this mixture was extracted with EtOAc (3 × 30 mL). The combined organic phases were dried over MgSO₄. Evaporation of the organic solvent under reduced pressure gave a mixture of products **234–237** (0.485 g, 65%). The resulting crude products was chromatographed on silica gel eluting with ethyl acetate/hexane (1:20) to give the regio and stereoisomers in the following order; **234** (0.291 g, 60%), **235** (0.034 g, 7%), **236** (0.068 g, 14%) and **237** (0.092 g, 19%). Recrystallization of the main product **234** from CH₂Cl₂-hexane system gave colorless cubic crystals, mp.: 90–92 °C (lit. mp.: 69–70 °C).⁸³

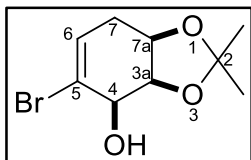


¹H NMR (400 MHz, CDCl₃) δ 6.01 (dd, $J_{7,7a} = 3.2$ and ${}^4J_{7,5} = 1.1$ Hz, 1H, H-7), 4.47 (dd, $J_{7a,3a} = 4.9$ and $J_{7a,7} = 3.2$ Hz, 1H, H-7a), 4.45–4.41 (m, 1H, H-3a), 4.08 (bd, $J_{5,4} = 2.3$ Hz, 1H), 3.23 (s, 1H, –OH), 2.50 (ddd, A-part of AB-system, ${}^2J_{4a,4b} = 15.3$, $J_{4a,3a} = 3.6$ and $J_{4a,5} = 2.3$ Hz, 1H, H-4a), 2.08 (ddd, B-part of AB-system, ${}^2J_{4b,4a} = 15.3$, $J_{4b,3a} = 4.6$, and $J_{4b,5} = 2.1$ Hz, 1H, H-4b), 1.40 (s, 3H, –CH₃), 1.30 (s, 3H, –CH₃). ¹³C NMR (100 MHz, CDCl₃) δ 128.7, 128.2, 110.2, 74.0, 71.9, 69.4, 32.4, 28.1, 26.5. IR (ATR, cm⁻¹) 3487, 2932, 1645, 1382, 1230, 1029. . Elem. Anal. Calcd for C₉H₁₃BrO₃: C, 43.40; H, 5.26. Found: C, 43.32; H, 5.21.

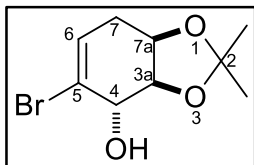


Compound **235**: Colorless fernlike crystals form CH₂Cl₂-hexane system, mp.: 101–103 °C (lit. mp.: 125–126 °C).⁸³ ¹H NMR (400 MHz, CDCl₃) δ 6.04–6.01 (m, 1H, H-7), 4.45–4.38 (m, 2H), 4.32 (ddt, $J = 8.4, 5.5, 1.3$ Hz, 1H, H-5), 2.55 (ddd, $J = 14.1, 5.4, 4.2$ Hz, 1H, H-4a), 1.81 (ddd, $J = 14.1, 8.9, 2.4$ Hz, 1H, H-4b), 1.32 (s, 3H, –CH₃), 1.29

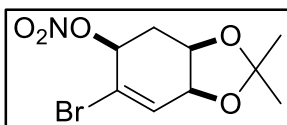
(s, 3H, $-\text{CH}_3$). ^{13}C NMR (100 MHz, CDCl_3) δ 130.6, 129.2, 109.3, 73.3, 72.3, 66.2, 33.8, 27.8, 26.4. **IR** (ATR, cm^{-1}) 3266, 2931, 1638, 1366, 1222, 1016. **Elem. Anal.** Calcd for $\text{C}_9\text{H}_{13}\text{BrO}_3$: C, 43.40; H, 5.26. Found: C, 43.33; H, 5.21.



Compound 236: Colorless cubic crystals form CH_2Cl_2 -hexane system, mp.: 103–105 °C. ^1H NMR (400 MHz, CDCl_3) δ 6.07 (dd, $J_{6,7a'} = 5.7$, and $J_{6,7b'} = 3.2$ Hz, 1H, H-6), 4.62 (dt, $J_{3a,7} = 1.6$ and $J_{3a,4} = J_{3a,7a} = 5.6$, Hz, 1H, H-3a), 4.45 (ddd, $J_{7a,3a} = 5.6$, $J_{7a,7a'} = 2.5$, and $J_{7a,7b'} = 0.5$ Hz, 1H, H-7a), 4.03 – 3.94 (m, 1H, H-4), 2.44 – 2.37 (m, A-part of AB-system, 1H, H-7a'), 2.37 – 2.30 (m, B-part of AB-system, 1H, H-7b'), 2.00 (d, $J = 8.4$ Hz, 1H, $-\text{OH}$), 1.46 (s, 3H, $-\text{CH}_3$), 1.44 (s, 3H, $-\text{CH}_3$). ^{13}C NMR (100 MHz, CDCl_3) δ 128.3, 122.2, 110.5, 100.0, 78.2, 66.8, 31.0, 27.3, 26.5. **IR** (ATR, cm^{-1}) 3448, 3333, 2919, 1688, 1638, 1277, 1031. **Elem. Anal.** Calcd for $\text{C}_9\text{H}_{13}\text{BrO}_3$: C, 43.40; H, 5.26. Found: C, 43.36; H, 5.16.



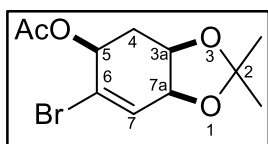
Compound 237: ^1H NMR (400 MHz, CDCl_3) δ 6.47 (ddd, $J_{6,7a'} = 6.2$, $J_{6,7b'} = 3.3$, and $^4J_{6,4} = 0.4$ Hz, 1H, H-6), 5.53 (bd, $J_{4,3a} = 2.3$ Hz, 1H, H-4), 5.30 (s, 1H, $-\text{OH}$), 4.55 (ddd, $J_{7a,3a} = 6.6$, $J_{7a,4b} = 4.4$, and $J_{7a,4a} = 2.5$ Hz, 1H, H-7a), 4.46 (dd, $J_{3a,7a} = 6.6$, and $J_{3a,4} = 2.3$ Hz, 1H, H-3a), 2.56 (ddd, A-part of AB-system, $^2J_{7a',7b} = 17.5$, $J_{7a',6} = 6.2$, and $J_{7a',7a} = 2.5$ Hz, 1H, H-7a'), 2.47 (dddd, B-part of AB-system, $^2J_{7b',7a'} = 17.5$, $J_{7b',7a} = 4.4$, $J_{7b',6} = 3.3$, and $^5J_{7b',4} = 0.6$ Hz, 1H, H-7b), 1.45 (s, 3H, $-\text{CH}_3$), 1.35 (s, 3H, $-\text{CH}_3$).



Compound 238: Colorless cubic crystals form CH_2Cl_2 -hexane system, mp. 120–122 °C: ^1H NMR (400 MHz, CDCl_3) δ 6.30 (d, $J = 3.5$ Hz, 1H), 5.51 (dd, $J = 5.0$, 2.6 Hz, 1H), 4.49 – 4.45 (m, 1H), 4.38 – 4.33 (m, 1H), 2.56 (ddd, A-part of AB-system, $J = 16.0$, 3.8, 2.6 Hz, 1H), 2.23 (ddd, B-part of AB-system, $J = 16.0$, 5.0, 3.1 Hz, 1H), 1.39 (s, 3H), 1.29 (s, 3H). ^{13}C NMR (100 MHz, CDCl_3) δ 134.9, 118.3, 110.7, 77.6, 72.9, 69.2, 29.9, 27.9, 26.4. **IR** (ATR, cm^{-1}) 3726, 3626, 2987, 2929, 1631, 1280, 1058, 855.

4.7 (3a*R*,5*S*,7a*S*)-6-bromo-2,2-dimethyl-3a,4,5,7a-tetrahydrobenzo[*d*][1,3]-diox-ol-5-yl acetate (**239**)

(3a*R*,5*S*,7a*S*)-6-bromo-2,2-dimethyl-3a,4,5,7a-tetrahydrobenzo[*d*][1,3]diox-ol-5-ol (**234**) (50 mg, 0.2 mmol) was dissolved in 5 mL of pyridine in a 25 mL round bottom flask which is maintained in an ice-bath. To this solution, excess acetic anhydride (5 mL) was added. After 30 min, the ice-bath was removed and the solution was stirred overnight. Subsequently, ethyl acetate (50 mL) was added and this solution was extracted with sat. NaHCO₃ (5 × 25 mL) solution. Organic phase was washed with brine and dried over MgSO₄. Removal of the organic solvent gave the (3a*R*,5*S*,7a*S*)-6-bromo-2,2-dimethyl-3a,4,5,7a-tetrahydrobenzo[*d*][1,3]dioxol-5-yl acetate (**239**), mp.: 88–90 °C (55 mg, 95%).

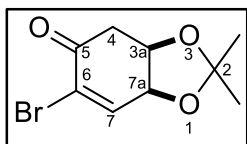


¹H NMR (400 MHz, CDCl₃) δ 6.22 (d, $J_{7,7a} = 3.6$ Hz, 1H, H-7), 5.36 (dd, $J_{5,4b} = 5.3$ and $J_{5,4a} = 4.5$ Hz, 1H, H-5), 4.44 (ddd, $J_{7a,3a} = 5.4$, $J_{7a,7} = 3.6$ Hz, and ${}^4J_{7a,4b} = 1.0$ Hz 1H, H-7a), 4.31 (dt, $J_{3a,4b} = 3.7$ and $J_{3a,4a} = J_{3a,7a} = 5.4$ Hz, 1H, H-3a), 2.26 (ddd, A-part of AB-system, ${}^2J_{4a,4b} = 14.9$, $J_{4a,3a} = 5.4$ and $J_{4a,5} = 4.5$ Hz, 1H, H-4a), 2.13 (ddd, B-part of AB-system, $J_{4b,4a} = 14.9$, $J_{4b,5} = 5.3$ and $J_{4b,3a} = 3.7$ Hz, 1H, H-4b), 2.06 (s, 3H, –COCH₃), 1.40 (s, 3H, –CH₃), 1.30 (s, 3H, –CH₃). ¹³C NMR (100 MHz, CDCl₃) δ 170.1, 130.8, 123.8, 109.8, 72.5, 69.7, 68.0, 30.8, 27.5, 25.9, 20.6. IR (ATR, cm⁻¹) 2987, 2929, 1631, 1280, 854. HRMS Calcd for (C₈H₉BrO₃) [M + H]⁺: 232.98078. Found: 232.98168.

4.8 (3a*R*,7a*S*)-6-bromo-2,2-dimethyl-3a,4-dihydrobenzo[*d*][1,3]dioxol-5(7a*H*)-one (**240**)

(3a*R*,5*S*,7a*S*)-6-bromo-2,2-dimethyl-3a,4,5,7a-tetrahydrobenzo[*d*][1,3]di-oxol-5-ol (**234**) (250 mg, 1.0 mmol) was dissolved in 50 mL of CH₂Cl₂ in a 100 mL round bottom flask. To this solution, activated MnO₂ (0.869 g, 10.0 mmol) was added. The resulting suspension was stirred overnight. After completion of the reaction controlling by TLC, the reaction mixture was filtered through the plug of celite and

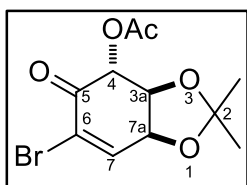
washed with 200 mL of CH₂Cl₂. Removal of the solvent gave the (3a*R*,7a*S*)-6-bromo-2,2-dimethyl-3a,4-dihydrobenzo[*d*][1,3]dioxol-5(7a*H*)-one (**240**) as a white solid (240 mg, 97%) which was recrystallized from CH₂Cl₂-hexane, mp.: 108-109 °C.



¹H NMR (400 MHz, CDCl₃) δ 7.03 (dd, $J_{7,7a} = 3.0$ and ${}^4J_{7,3a} = 1.8$ Hz, 1H, H-7), 4.69 (dd, $J_{7a,3a} = 4.8$ and $J_{7a,7} = 3.0$ Hz, 1H, H-7a), 4.62 (dddd, $J_{3a,7a} = 4.8$, $J_{3a,4b} = 3.6$, $J_{3a,4a} = 2.6$ and ${}^4J_{3a,7} = 1.7$ Hz, 1H, H-3a), 3.11 (dd, A-part of AB-system, ${}^2J_{4a,4b} = 17.4$ and $J_{4a,3a} = 2.6$ Hz, 1H, H-4a), 2.73 (dd, B-part of AB-system, ${}^2J_{4b,4a} = 17.4$ and $J_{4b,3a} = 3.6$ Hz, 1H, H-4b), 1.32 (s, 6H, -CH₃). ¹³C NMR (100 MHz, CDCl₃) δ 187.3, 146.1, 124.3, 110.5, 73.5, 73.0, 38.7, 27.8, 26.5.

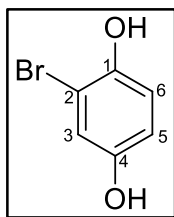
4.9 (3a*S*, 4*R*, 7a*S*)-6-bromo-2,2-dimethyl-5-oxo-3a,4,5,7a-tetrahydrobenzo[*d*]-[1,3]dioxol-4-yl acetate (**241**)

Mn(OAc)₃·2H₂O (0.217 g, 0.82 mmol) was suspended in benzene (50 mL) and the resulting mixture was refluxed for 2 h to remove water by using Dean-Stark apparatus. After cooling to room temperature (3a*R*,7a*S*)-6-bromo-2,2-dimethyl-3a,4-dihydrobenzo[*d*][1,3]dioxol-5(7a*H*)-one (**240**) (0.100 g, 0.41 mmol) was added and the resulting mixture was heated to reflux temperature until the color of the Mn(OAc)₃ was disappeared or the starting material was consumed monitoring by TLC.⁷⁸ Then, NaHCO₃ (50 mL) was added and the resulting mixture was extracted with EtOAc (3 × 50 mL). Organic phases were combined and washed with brine (2 × 50 mL) and dried over MgSO₄. Removal of the organic solvent under reduced pressure afforded the crude mixture which was chromatographed on silica gel eluting with EtOAc-hexane mixture (1:3) to give (3a*S*, 4*R*, 7a*S*)-6-bromo-2,2-dimethyl-5-oxo-3a,4,5,7a-tetrahydrobenzo[*d*]-[1,3]dioxol-4-yl acetate (**241**).



¹H NMR (400 MHz, CDCl₃) δ 7.23 (d, $J_{7,7a} = 4.7$ Hz, 1H, H-7), 5.50 (d, $J_{4,3a} = 8.3$ Hz, 1H, H-4), 4.76 (dd, $J_{7a,3a} = 6.0$ and $J_{7a,7} = 4.7$ Hz, 1H, H-7a), 4.48 (dd, $J_{3a,4} = 8.3$ and $J_{3a,7a} = 6.0$

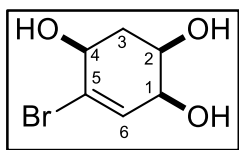
Hz, 1H), 2.15 (s, 3H, -COCH₃), 1.48 (s, 3H, -CH₃), 1.37 (s, 3H, -CH₃).



Compound **242**⁸⁰ mp.: 105–107 °C (Lit. mp.: 110–112 °C). ¹H NMR (400 MHz, CDCl₃) δ 7.01 (d, *J*_{3,5} = 2.9 Hz, 1H, H-3), 6.92 (d, *J*_{6,5} = 8.9 Hz, 1H, H-6), 6.75 (dd, *J*_{5,6} = 8.9 and *J*_{5,3} = 2.9 Hz, 1H, H-5). ¹³C NMR (100 MHz, CDCl₃) δ 149.5, 146.6, 118.6, 116.4, 116.3, 109.9.

4.10 (1*S*,2*R*,4*S*)-5-bromocyclohex-5-ene-1,2,4-triol (**248**)

(3*aR*,5*S*,7*aS*)-6-bromo-2,2-dimethyl-3*a*,4,5,7*a*-tetrahydrobenzo[*d*][1,3]-dioxol-5-ol (**234**) (75 mg, 0.30 mmol) was dissolved in methanol and cooled to 0 °C. At this temperature HCl_(g) was passed through the solution for 30 min. After completion of the reaction, solvent was removed to give (1*S*,2*R*,4*S*)-5-bromocyclohex-5-ene-1,2,4-triol (**248**) in quantitative yield. Recrystallization of the compound **248** from EtOH gave white cubic crystal mp.: 136-138 °C.

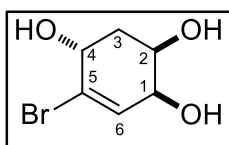


¹H NMR (400 MHz, D₂O) δ 6.21 (dd, *J*_{6,1} = 5.4, and ⁴*J*_{6,4} = 1.1 Hz, 1H, H-6), 4.27 – 4.13 (m, 1H, H-4), 4.03 (quasi triplet, 1H, H-1), 3.77 (dt, *J* = 12.0, 3.4 Hz, 1H, H-2), 2.13 – 2.03 (m, A-part of AB-system, main coupling *J* = 12.0 Hz, 1H, H-3a), 1.84 (td, B-part of AB-system, *J* = 12.0, and *J* = 8.8 Hz, 1H, H-3b). ¹³C NMR (100 MHz, D₂O) δ 131.4, 130.2, 68.7, 67.2, 66.0, 34.0. IR (ATR, cm⁻¹) 3262, 2908, 2852, 1354, 1094, 1059, 1015, 701. Elem. Anal. Calcd for C₆H₉BrO₃: C, 34.47; H, 4.34. Found: C, 34.14; H, 4.27.

4.11 (1*S*,2*R*,4*R*)-5-bromocyclohex-5-ene-1,2,4-triol (**249**)

(3*aR*,5*R*,7*aS*)-6-bromo-2,2-dimethyl-3*a*,4,5,7*a*-tetrahydrobenzo[*d*][1,3]-dioxol-5-ol (**235**) (50 mg, 0.20 mmol) was dissolved in methanol and cooled to 0 °C. At this temperature HCl_(g) was passed through the solution for 30 min. After completion of the reaction, solvent was removed to give (1*S*,2*R*,4*R*)-5-bromocyclohex-5-ene-

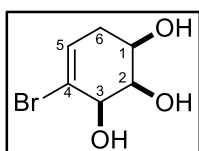
1,2,4-triol (**249**) in quantitative yield. Recrystallization of the compound **249** from EtOH gave white crystal mp.: 130-132 °C.



¹H NMR (400 MHz, D₂O) δ 6.13 (d, $J_{6,1} = 4.3$ Hz, 1H, H-6), 4.30 (t, $J_{4,3a} = J_{4,3b} = 5.1$ Hz, 1H, H-4), 4.11 (quasi triplet, 1H, H-1), 3.99 (dt, $J = 9.4, 3.1$ Hz, 1H, H-2), 2.24 – 2.15 (m, A-part of AB-system, main coupling $J_{3a,3b} = 13.8$ Hz, 1H, H-3a), 1.74 (ddd, B-part of AB-system, $J_{3b,3a} = 13.8, J_{3b,4} = 5.1,$ and $J_{3b,2} = 2.8$ Hz, 1H, H-3b). ¹³C NMR (100 MHz, D₂O) δ 131.6, 128.1, 69.0, 67.4, 65.8, 34.9. IR (ATR, cm⁻¹) 3267, 2915, 1357, 1098, 1058, 1016, 704. Elem. Anal. Calcd for C₆H₉BrO₃: C, 34.47; H, 4.34. Found: C, 34.35; H, 4.23.

4.12 (1R,2R,3R)-4-bromocyclohex-4-ene-1,2,3-triol (**250**)

(3a*S*,4*R*,7a*R*)-5-bromo-2,2-dimethyl-3a,4,7,7a-tetrahydrobenzo[*d*][1,3]-dioxol-4-ol (**236**) (50 mg, 0.20 mmol) was dissolved in methanol and cooled to 0 °C. At this temperature HCl_(g) was passed through the solution for 30 min. After completion of the reaction, solvent was removed to give (1*R*,2*R*,3*R*)-4-bromocyclohex-4-ene-1,2,3-triol (**250**) in quantitative yield. Recrystallization of the compound **250** from EtOH gave white cubic crystal mp.: 156-158 °C.

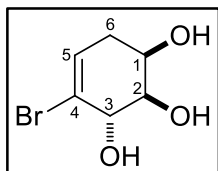


¹H NMR (400 MHz, D₂O) δ 6.05 (t, $J_{5,6a} = J_{5,6b} = 3.6$ Hz, 1H, H-5), 4.19 (bs, 1H, H-3), 3.96 (d, $J_{2,3} = 2.1$ Hz, 1H, H-2), 3.91 (t, $J_{1,6a} = J_{1,6b} = 7.0$ Hz, 1H, H-1), 2.27 – 2.09 (m, AB-system, 2H, H-6a and H-6b). ¹³C NMR (100 MHz, D₂O) δ 128.8, 122.7, 71.6, 70.7, 67.1, 31.0. IR (ATR, cm⁻¹) 3241, 2907, 2423, 1637, 1455, 1014. Elem. Anal. Calcd for C₆H₉BrO₃: C, 34.47; H, 4.34. Found: C, 34.45; H, 4.26.

4.13 (1R,2R,3*S*)-4-bromocyclohex-4-ene-1,2,3-triol (**251**)

(3a*S*,4*S*,7a*R*)-5-bromo-2,2-dimethyl-3a,4,7,7a-tetrahydrobenzo[*d*][1,3]-dioxol-4-ol (**237**) (40 mg, 0.14 mmol) was dissolved in methanol and cooled to 0 °C. At this temperature HCl_(g) was passed through the solution for 30 min. After completion of

the reaction, solvent was removed to give (1*R*,2*R*,3*S*)-4-bromocyclohex-4-ene-1,2,3-triol (**251**) in quantitative yield. Recrystallization of the compound **251** from EtOH gave white crystal mp.: 126-128 °C.

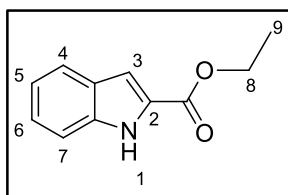


¹H NMR (400 MHz, MeOD) δ 6.34 (t, $J_{5,6a} = J_{5,6b} = 4.0$ Hz, 1H, H-5), 5.66 (d, $J_{3,2} = 4.9$ Hz, 1H, H-3), 4.05 – 3.89 (m, 2H, H1 and H-2), 2.50 – 2.26 (m, 2H, AB-system, H-6a and H-6b). **¹³C NMR** (100 MHz, MeOD) δ 135.8, 114.7, 85.9, 72.3, 67.8, 33.4.

IR (ATR, cm⁻¹) 3252, 2907, 2425, 1638, 1456, 1015. **Elem. Anal.** Calcd for C₆H₉BrO₃: C, 34.47; H, 4.34. Found: C, 34.10; H, 4.26.

4.14 Ethyl-1*H*-indole-2-carboxylate (**353**)

To a stirred solution of indole-2-carboxylic acid (**352**) (3 g, 18.61 mmol) in dry ethanol (50 mL), sulfuric acid (1 mL) was added as the catalyst to perform Fischer esterification reaction. Then, this solution was heated at the reflux temperature, overnight during stirring. After completion of reaction, monitoring by TLC, solvent was removed. To the crude mixture was added NaHCO₃ (50 mL) and the mixture was extracted with ethyl acetate (3 × 30 mL). Organic phases were then combined and dried over MgSO₄. The evaporation of the solvent under reduced pressure gave ethyl 1*H*-indole-2-carboxylate (**353**) as a white solid mp.: 122–123 °C (Lit mp.: 114–115 °C). (3.31 g, 94%).¹²⁴



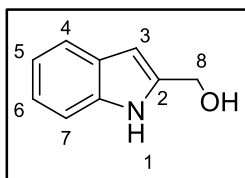
¹H NMR (400 MHz, CDCl₃) δ 9.01 (s, 1H, H-1), 7.69 (dd, $J_{4,5} = 8.0$ and $J_{4,6} = 0.8$ Hz, 1H, H-4), 7.43 (dd, $J_{7,6} = 8.3$ and $J_{7,5} = 0.9$ Hz, 1H, H-7), 7.32 (ddd, $J_{6,7} = 8.3$, $J_{6,5} = 7.0$ and $J_{6,4} = 0.8$ Hz, 1H, H-6), 7.24 (dd, $J_{3,1} = 2.0$ and $J_{3,4} = 0.8$

Hz, 1H, H-3), 7.15 (ddd, $J_{5,4} = 8.0$, $J_{5,6} = 7.0$ and $J_{5,7} = 0.9$ Hz, 1H, H-5), 4.42 (q, $J_{9,10} = 7.2$ Hz, 2H, H-9), 1.42 (t, $J_{10,9} = 7.2$ Hz, 3H, H-10). **¹³C NMR** (100 MHz, CDCl₃): δ 159.6, 134.4, 133.5, 124.9, 122.8, 120.1, 118.3, 109.4, 106.3, 58.6, 11.9.

IR (ATR, cm⁻¹) 3290, 3274, 2923, 1698, 1455, 1161, 1119, 740.

4.15 1*H*-indol-2-ylmethanol (**354**)

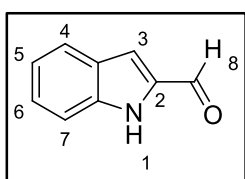
To a chilled solution of ethyl 1*H*-indole-2-carboxylate (**353**) (3.4 g, 17.97 mmol) in dry THF (40 mL), the solid LiAlH₄ (1.37 g, 36 mmol) was gradually added by controlling the gas releasing. After all LiAlH₄ was added, the reaction mixture was stirred in ice bath for 1 h. Then, the ice bath was removed and stirring was continued for additional 1 h. After completion of the reaction controlling by TLC, sat. NH₄Cl was carefully added to quench excess of LiAlH₄. The reaction medium was extracted with EtOAc (3 × 25 mL) and the combined organic phases were washed with brine and dried over MgSO₄. The evaporation of the solvent gave 1*H*-indol-2-ylmethanol (**354**) (2.54 g, 96%) as a white solid.¹⁴⁵ mp.: 75–76 °C.



¹H NMR (400 MHz, CDCl₃) δ 8.32 (s, 1H, H-1), 7.50 (bd, $J_{4,5}$ = 7.8 Hz, 1H, H-4), 7.23 (bd, $J_{7,6}$ = 8.0 Hz, 1H, H-7), 7.11 (ddd, $J_{6,7}$ = 8.0, $J_{6,5}$ = 7.1 and $J_{6,4}$ = 1.2 Hz, 1H, H-6), 7.03 (ddd, $J_{5,4}$ = 7.8, $J_{5,6}$ = 7.1 and $J_{5,7}$ = 1.0 Hz, 1H, H-5), 6.31 (d, $J_{3,4}$ = 0.8 Hz, 1H, H-3), 4.69 (s, 2H, H-8). **¹³C NMR** (100 MHz, CDCl₃) δ 137.6, 136.4, 128.0, 122.2, 120.7, 120.0, 111.1, 100.6, 58.5. **IR (ATR, cm⁻¹):** 3393, 3374, 3238, 1455, 1289, 1006, 735.

4.16 1*H*-indole-2-carboxaldehyde (**355**)

To a stirred solution of 1*H*-indol-2-ylmethanol (**354**) (2.46 g, 16.7 mmol) in acetone (50 mL) in the presence of molecular sieve (4Å) MnO₂ (10 eq, 14.52 g, 167 mmol) was added and the mixture was stirred overnight at room temperature. After the completion of the reaction, the mixture was filtered over pad of celite by using vacuum filtration and washed with plenty of DCM. The filtrated solution was evaporated to obtain 1*H*-indole-2-carbaldehyde (**355**) (2.26 g, 93 %) as a white solid, mp.: 75–76 °C (lit mp.: 75–76 °C).¹²⁵

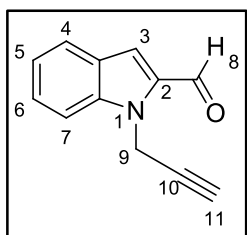


¹H NMR (400 MHz, CDCl₃) δ 9.85 (s, 1H, H-8), 9.00 (s, 1H, H-1), 7.76 (d, $J_{4,5}$ = 8.1 Hz, 1H, H-4), 7.48 – 7.37 (m, 2H, H-7 and H-6), 7.29 (d, $J_{3,4}$ = 1.2 Hz, 1H, H-3), 7.19 (ddd, $J_{5,4}$ =

8.1, $J_{5,6} = 6.7$ and $J_{5,7} = 1.1$ Hz, 1H, H-5). ^{13}C NMR (100 MHz, CDCl_3) δ 182.1, 138.0, 136.0, 127.4, 123.4, 121.3, 114.9, 112.5. IR (ATR, cm^{-1}) 2988, 2900, 1651, 1066, 821, 741.

4.17 1-Prop-2-ynyl-1H-indole-2-carbaldehyde (357)

To a stirred solution of 1H-indole-2-carbaldehyde (**355**) (2.64 g, 18.2 mmol) in dry DMF (20 mL), solid NaH was added (0.48 g, 20 mmol) piecewise. After a while, at the end of releasing of H_2 gas, propargyl bromide (**356**) (80 wt. % in toluene) (2.4 mL, 21.8 mmol) was diluted with 1:3 ratio of dry DMF and added to the stirring solution over 30 min. After the completion of the reaction (6 h), water (100 mL) was added and the mixture was extracted with EtOAc (3×30 mL). The collected organic phases were washed with brine, water, and dried over MgSO_4 . Removal of the solvent gave 1-prop-2-ynyl-1H-indole-2-carbaldehyde (**357**) (2.56 g, 97%) as a pale yellow solid. mp.: 101-103 °C (Lit. mp.: 137-138 °C).^{146,127}

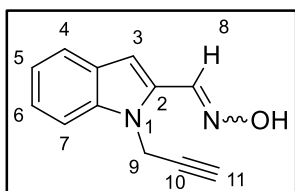


^1H NMR (400 MHz, CDCl_3) δ 9.81 (s, 1H, H-8), 7.68 (dt, $J_{4,5} = 8.0$, and $J_{4,6} = J_{4,3} = 0.9$ Hz, 1H, H-4), 7.47 (dd, $J_{7,6} = 8.4$ and $J_{7,5} = 1.0$ Hz, 1H, H-7), 7.40 (ddd, $J_{6,7} = 8.4$, $J_{6,5} = 7.0$ and $J_{6,4} = 0.9$ Hz, 1H, H-6), 7.22 (d, $J_{3,4} = 0.9$ Hz, 1H, H-3), 7.15 (ddd, $J_{5,4} = 8.0$, $J_{5,6} = 7.0$ and $J_{5,7} = 1.0$ Hz, 1H, H-5), 5.39 (d, $^4J_{9,11} = 2.5$ Hz, 2H, H-9), 2.20 (t, $^4J_{11,9} = 2.5$ Hz, 1H, H-11). ^{13}C NMR (100 MHz, CDCl_3) δ 182.6, 140.1, 134.5, 127.4, 126.6, 123.5, 121.5, 118.7, 110.8, 78.2, 72.5, 33.9. IR (ATR, cm^{-1}) 3238, 2923, 2851, 2120, 1661, 1478, 1461, 1162, 1123, 1110, 757, 728. HRMS calcd for $\text{C}_{12}\text{H}_9\text{NO}$ $[\text{M}+\text{H}]^+$: 184,0777. Found: 184,07569.

4.18 (E/Z)-1-(1-prop-2-ynyl-1H-indol-2-yl)ethanone oxime (358 and 359)

A solution of the propargyl aldehyde **357** (2.13 g, 11.63 mmol) in ethanol (20 mL) was reacted with $\text{NH}_2\text{OH}\cdot\text{HCl}$ (750 mg, 11.64 mmol) and anhydrous Na_2CO_3 (616 mg, 5.8 mmol) in EtOH (10 mL) at reflux temperature for 4 h. After completion of the reaction, evaporation of the solvent under the reduced pressure gave a mixture

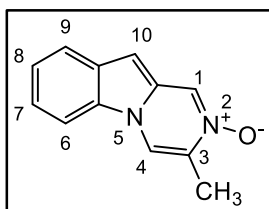
of *E*- and *Z*-isomers of the oxime **358** and **359**. The $^1\text{H-NMR}$ spectral analysis showed the formation of an oxime mixture (93%) consisting of a mixture of *E*- and *Z*-isomers **358** and **359** in a ratio of 5:1. The *E*-isomer was separated by column chromatography on silica gel eluting with hexane/EtOAc (3:1). Pale yellow solid, mp.: 92-94 °C.



$^1\text{H-NMR}$ (400 MHz, CDCl_3) δ 8.19 (s, 1H, H-8), 7.54 (bd, $J_{4,5} = 8.0$ Hz, 1H, H-4), 7.36 (dd, $J_{7,6} = 8.3$ Hz, and $J_{7,5} = 1.0$ Hz, 1H, H-7), 7.25 (ddd, $J_{6,7} = 8.3$, $J_{6,5} = 7.1$, and $J_{6,4} = 1.0$ Hz, 1H, H-6), 7.07 (ddd, $J_{5,4} = 8.0$, $J_{5,6} = 7.1$, and $J_{5,7} = 1.0$ Hz, 1H, H-5), 6.67 (bs, 1H, H-3), 5.21 (d, $J_{9,11} = 2.5$ Hz, 2H, CH_2), 2.19 (t, $J_{11,9} = 2.5$ Hz, 1H, $\text{C}\equiv\text{CH}$). $^{13}\text{C-NMR}$ (100 MHz, CDCl_3) δ 144.2, 139.0, 130.3, 127.6, 124.3, 121.7, 120.7, 109.9, 109.4, 78.7, 72.1, 34.7. **IR** (ATR, cm^{-1}) 3383, 3253, 2120, 1609, 1456, 1163, 1150, 950, 938, 750. **HRMS** calcd for $\text{C}_{12}\text{H}_{10}\text{N}_2\text{O}$ $[\text{M}+\text{H}]^+$: 199.0855; found: 199.08659.

4.19 3-Methylpyrazino[1,2-*a*]indole-2-oxide (**360**)

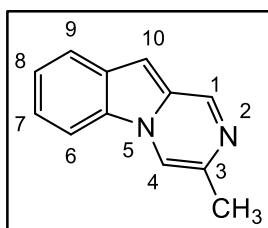
To a solution of 140 mg (0.7 mmol) of (*E/Z*)-1-(prop-2-yn-1-yl)-1H-indole-2-carbaldehyde oxime (**358** and **359**) in 10 mL CHCl_3 , 6 mg of AuCl_3 (3% mmol) was added to this solution as catalyst. The mixture was stirred for 4 h at room temperature. After completion of the reaction monitoring by TLC, evaporation of solvent under reduced pressure gave the crude product. The residue was purified by silica gel eluting with EtOAc:EtOH (90:15) to give 3-methylpyrazino[1,2-*a*]indole 2-oxide (**360**) as pale brown solid, mp.: 191-194 °C (37 mg, 26%, isolated yield).



$^1\text{H-NMR}$ (400 MHz, CDCl_3) δ 8.60 (s, 1H), 8.10 (s, 1H), 7.8–7.75 (m, 2H, arom.), 7.43–7.37 (m, 2H, arom.), 6.81 (s, 1H), 2.48 (s, 3H, CH_3). $^{13}\text{C-NMR}$ (100 MHz, CDCl_3) δ 171.8, 129.8, 128.7, 123.9, 122.4, 121.5, 117.6, 110.1, 100.0, 94.2, 83.0, 29.7. **IR** (ATR, cm^{-1}) 2919, 2849, 1466, 1176, 742, 671. **HRMS** calcd for $\text{C}_{12}\text{H}_{10}\text{N}_2\text{O}$ $[\text{M}+\text{H}]^+$: 199.0862. Found: 199.08659.

4.20 3-Methylpyrazino[1,2-*a*]indole (364)

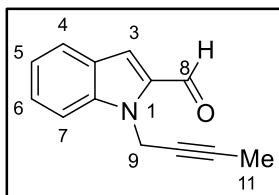
was taken. To a solution of 1-(prop-2-yn-1-yl)-1*H*-indole-2-carbaldehyde (**357**) (520 mg, 2.84 mmol) in MeOH (30 mL), K₂CO₃ (430 mg, 3.12 mmol) was added. After addition of 5 mL of NH₃ (24%), the mixture was heated at reflux temperature for 12 h. After completion of the reaction monitoring by TLC, the solvent was removed under reduced pressure. The residue was extracted with EtOAc (3 × 30 mL). After combination of the organic phases, the solution was dried over MgSO₄, and the solvent was removed under reduced pressure. The crude product was then purified by column chromatography on silica gel eluting with hexane:EtOAc (3:1). 3-Methylpyrazino[1,2-*a*]indole (**364**) was isolated as pale yellow solid mp.: 162–164 °C (Lit mp.: 173 °C) (76%).¹⁰⁰



¹H NMR (400 MHz, CDCl₃) δ 8.99 (d, *J*_{1,10} = 1.2 Hz, 1H, H-1), 7.98 (bs, 1H, H-4), 7.94 – 7.85 (m, 2H), 7.46 – 7.34 (m, 2H), 6.96 (s, 1H, H-10), 2.51 (d, *J*_{1a,4} = 1.0 Hz, 3H, H-1a). ¹³C NMR (100 MHz, CDCl₃) δ 146.4, 132.3, 129.3, 129.0, 128.4, 123.5, 122.3, 122.1, 113.4, 110.8, 94.8, 20.7.

4.21 1-But-2-ynyl-1*H*-indole-2-carbaldehyde (366)

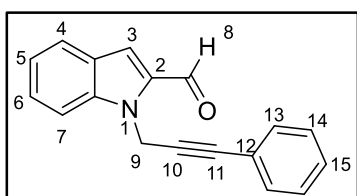
To a stirring solution of indole-2-carbaldehyde (**357**) (1.45 g, 10 mmol) in dry DMF NaH (0.312 g, 13 mmol) was added over a period of 30 min. After completion of addition, a solution of 1-bromobut-2-yne (**365**) (0.96 mL, 11 mmol) in dry DMF (5 mL) was slowly added and the mixture was stirred for 4 h. Water (50 mL) was added and the resulting solution was extracted with EtOAc (3 × 50 mL). The collected organic layers were washed with brine and dried over MgSO₄. Evaporation of the solvent under the reduced pressure gave the crude product **366** (1.87 g, 95%). The residue was purified by silica gel column chromatography eluting with hexane/EtOAc (3:1) afforded target product **366** as a pale yellow solid (1.10 g, 56%) from CH₂Cl₂/n-hexane, mp.: 80-81 °C.



¹H NMR (¹H NMR (400 MHz, CDCl₃) δ 9.89 (s, 1H, CHO), 7.75 (bd, $J_{4,5} = 8.1$ Hz, 1H, H-4), 7.55 (bd, $J_{7,6} = 8.3$ Hz, 1H, H-7), 7.46 (ddd, $J_{6,7} = 8.3$, $J_{6,5} = 6.8$, and $J_{6,4} = 1.0$ Hz, 1H, H-6), 7.28 (bs, 1H, H-3), 7.21 (ddd, $J_{5,4} = 8.0$, $J_{5,6} = 6.8$, and $J_{5,7} = 0.7$ Hz, 1H, H-5), 5.39 (q, $J_{9,11} = 2.4$ Hz, 1H, CH₂), 1.75 (t, $J_{11,9} = 2.4$ Hz, 1H, CH₃). **¹³C NMR** (100 MHz, CDCl₃) δ 182.7, 140.2, 134.6, 127.2, 126.6, 123.5, 121.3, 118.3, 111.1, 80.2, 73.7, 34.3, 3.5. **IR** (ATR, cm⁻¹) 2920, 2851, 1661, 1610, 1478, 1344, 1135, 739. **HRMS** calcd for C₁₃H₁₁NO [M+H]⁺: 198.0928. Found: 198.09134.

4.22 1-(3-Phenylprop-2-ynyl)-1H-indole-2-carbaldehyde (367a)

CuI (3,8 mg, 0,02 mmol), Pd(OAc)₂ (4,5 mg, 0,02 mmol), and PPh₃ (13,1 mg, 0,05 mmol) were placed in a two necked round bottom flask and nitrogen gas was passed over the reaction medium before starting the reaction. In another flask, 1-prop-2-ynyl-1H-indole-2-carbaldehyde (**357**) (0.360 g, 1.97 mmol) and iodobenzene (0.24 mL, 2,18 mmol) and DIPA (1 mL, 7 mmol) were dissolved in THF (20 mL), and then added to the reaction medium. After that, the solution was stirred at reflux temperature for 1.5 h. After the reaction was completed, the reaction medium was extracted with 0,1 N HCl and EtOAc (3 × 50 mL). Organic layers were combined and washed with brine, dried over MgSO₄ and concentrated under reduced pressure to give the crude product (0.437 g, 86%). The crude product was eluted over silica gel column with hexane:ethyl acetate (3:1) mixture to isolate 1-(3-phenylprop-2-ynyl)-1H-indole-2-carbaldehyde (**367a**) as yellow solid (0.357 g, 70%), mp.: 77-78 °C.¹⁰⁰

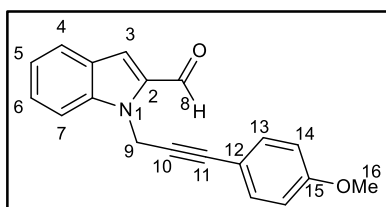


¹H NMR (400 MHz, CDCl₃) δ 9.89 (s, 1H, CHO), 7.75 (dt, $J_{4,5} = 8.0$ and $J_{4,6} = J_{4,3} = 0.9$ Hz, 1H, H-4), 7.62 (dd, $J_{7,6} = 8.4$ and $J_{7,5} = 0.9$ Hz, 1H, H-7), 7.46 (ddd, $J_{6,7} = 8.4$, $J_{6,5} = 7.0$, and $J_{6,4} = 0.9$ Hz, 1H, H-6), 7.35 – 7.33 (m, 2H, arom.), 7.28 (d, $J_{3,4} = 0.9$ Hz, 1H, H-3), 7.26 – 7.19 (m, 4H, arom.), 5.66 (s, 2H, CH₂). **¹³C NMR** (100 MHz, CDCl₃) δ 182.7, 140.3, 134.6, 131.8, 128.4, 128.2, 127.3, 126.7, 123.5, 122.4, 121.5, 118.6, 111.1, 84.2, 83.7,

34.8. **IR** (ATR, cm^{-1}) 2917, 2849, 1663, 1523, 1459, 1346, 1149, 1127, 731. **HRMS** calcd for $\text{C}_{18}\text{H}_{13}\text{NO}$ $[\text{M}+\text{H}]^+$: 260.1061. Found: 260.10699.

4.23 1-[3-(4-Methoxyphenyl)prop-2-ynyl]-1*H*-indole-2-carb-aldehyde (**367b**)

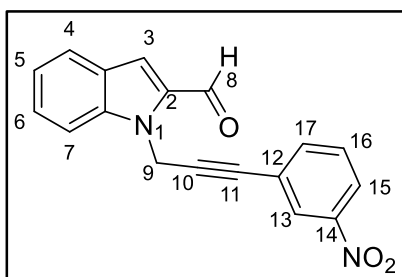
CuI (7.6 mg, 0.04 mmol), Pd(OAc)₂ (9 mg, 0.04 mmol), PPh₃ (27 mg, 0.1 mmol) were placed in a two necked round bottom flask and nitrogen gas was passed over the reaction medium before starting the reaction. In another flask, 1-prop-2-ynyl-1*H*-indole-2-carbaldehyde (**357**) (366 mg, 2 mmol), 4-iodoanisole (514 mg, 2.18 mmol) and DIPA (2 ml, 14 mmol) were dissolved in THF (30 mL), and then added to the reaction medium. After that, the solution was stirred at reflux temperature for 3 hours. After the reaction was completed, the reaction medium was extracted with 0.1 N HCl (30 mL) and EtOAc (3 × 30 mL). Organic layers were combined and washed with water and brine, dried over MgSO₄ and concentrated under reduced pressure (0.503 g, 87%). The crude product was eluted over silica gel column with hexane:ethyl acetate (3:1) mixture to give 1-[3-(4-methoxyphenyl)prop-2-ynyl]-1*H*-indole-2-carbaldehyde (**367b**) as yellow solid, mp.: 73-74 °C (0.269 g, 46.4%). (Lit. m.p. 72 °C).¹⁰⁰



¹H NMR (400 MHz, CDCl₃) δ 9.82 (s, 1H), 7.67 (dd, $J_{4,5} = 8.0$, $J_{4,6} = 1.0$ Hz, 1H, H-4), 7.55 (dd, $J_{7,6} = 8.4$, $J_{7,5} = 0.9$ Hz, 1H, H-7), 7.38 (ddd, $J_{6,7} = 8.4$, $J_{6,5} = 7.0$, and $J_{6,4} = 0.9$ Hz, 1H, H-6), 7.21 – 7.19 (m, 3H, H-3 and 2 arom.), 7.13 (ddd, $J_{5,4} = 8.0$, $J_{5,6} = 7.0$, and $J_{5,7} = 0.9$ Hz, 1H, H-5), 6.69 – 6.67 (m, 2H, arom.), 5.57 (s, 2H, CH₂), 3.67 (s, 3H, OCH₃). **¹³C NMR** (100 MHz, CDCl₃) δ 182.7, 159.7, 140.3, 134.6, 133.3, 127.3, 126.7, 123.5, 121.4, 118.5, 114.5, 113.8, 111.2, 84.1, 82.3, 55.3, 34.8. **IR** (ATR, cm^{-1}) 2915, 1662, 1605, 1568, 1509, 1250, 844. **HRMS** calcd for $\text{C}_{19}\text{H}_{15}\text{NO}_2$ $[\text{M}+\text{H}]^+$: 290.1227. Found: 290.11756.

4.24 1-[3-(3-nitrophenyl)prop-2-ynyl]-1*H*-indole-2-carbaldehyde (**367c**)

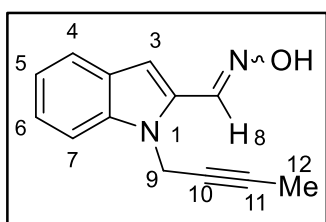
CuI (7.6 mg, 0.04 mmol), Pd(OAc)₂ (9 mg, 0.04 mmol), PPh₃ (27 mg, 0.1 mmol) were placed in a two necked round bottom flask and nitrogen gas was passed over the reaction medium before starting to the reaction. In another flask, 1-prop-2-ynyl-1*H*-indole-2-carbaldehyde (**357**) (366 mg, 2 mmol), 1-bromo-3-nitrobenzene (440 mg, 2.18 mmol) and DIPA (2 mL, 14 mmol) were dissolved in THF (30 mL), and then added to the reaction medium. After that, the solution was stirred at reflux temperature for 6 h. After the reaction was completed, the reaction medium was extracted with 0.1 N HCl (30 mL) and EtOAc (3 × 30 mL). Organic layers were combined and washed with water and brine, dried over MgSO₄ and concentrated under reduced pressure (0.505 g, 83%). The crude product was eluted over silica gel column with hexane:ethyl acetate (3:1) mixture to isolate 1-[3-(3-nitrophenyl)prop-2-ynyl]-1*H*-indole-2-carbaldehyde (**367c**) as a yellow solid, mp.: 121-122 (0.365 g, 60%).



¹H NMR (400 MHz, CDCl₃) δ 9.93 (s, 1H, H-8), 8.19 (dd, *J*₁₃₋₁₇ = 1.9, *J*₁₃₋₁₅ = 1.3 Hz, 1H, H-13), 8.12 (ddd, *J*₁₅₋₁₆ = 8.0, *J*₁₅₋₁₇ = 1.9, *J*₁₅₋₁₃ = 1.3 Hz, 1H, H-15), 7.78 (d, *J*₄₋₅ = 8.0 Hz, 1H, H-4), 7.65 (dt, *J*₁₇₋₁₆ = 8.0, *J*_{17-13, 17-15} = 1.9 Hz, 1H, H-17), 7.60 (dd, *J*₇₋₆ = 8.4, *J*₇₋₅ = 0.7 Hz, 1H, H-7), 7.51 (ddd, *J*₆₋₇ = 8.4, *J*₆₋₅ = 7.0, *J*₆₋₄ = 1.0 Hz, 1H, H-6), 7.44 (t, *J*_{16-15, 16-17} = 8.0 Hz, 1H, H-16), 7.34 (d, *J*₃₋₄ = 0.7 Hz, 1H, H-3), 7.25 (ddd, *J*₅₋₄ = 8.0, *J*₅₋₆ = 7.0, *J*₅₋₇ = 0.7 Hz, 1H, H-5), 5.71 (s, 2H, H-9). **¹³C NMR** (100 MHz, CDCl₃) δ 181.0, 146.2, 138.4, 135.7, 132.7, 127.5, 125.8, 124.9, 124.9, 122.4, 121.9, 121.4, 119.9, 117.1, 108.9, 84.7, 79.9, 32.8. **IR** (ATR, cm⁻¹) 3272, 2917, 1667, 1525, 1346, 738. **HRMS** calcd for C₁₈H₁₂N₂O₃ [M-H]⁻: 303,0800. Found: 303,07752.

4.25 (*E/Z*)-1-(1-prop-2-ynyl-1*H*-indol-2-yl)ethanone oxime (**376a**).

A solution of the methylpropargyl aldehyde (**367a**) (1.97 g, 10.0 mmol) in ethanol (20 mL) was reacted with $\text{NH}_2\text{OH}\cdot\text{HCl}$ (644 mg, 10.0 mmol) and anhydrous Na_2CO_3 (530 mg, 5.0 mmol) in EtOH (10 mL) at reflux temperature for 6 h. After monitoring the completion of the reaction by TLC, solvent was removed under reduced pressure. Water (50 mL) was added and the mixture was extracted with EtOAc (3×50 mL). Organic layers were combined and dried over MgSO_4 . Evaporation of the solvent under the reduced pressure gave a mixture of *E*- and *Z*-isomers of the oxime **376a**. The ^1H NMR spectral analysis showed the formation of an oxime mixture (1.98 g, 93%) consisting of a mixture of *E*- and *Z*-isomers in a ratio of 94/6. The *E*-isomer **376a** was separated by column chromatography on silica gel eluting with hexane/EtOAc (3:1). Pale yellow solid, mp.: 115-117 °C. *E*-Isomer (Isolated yield 66%).

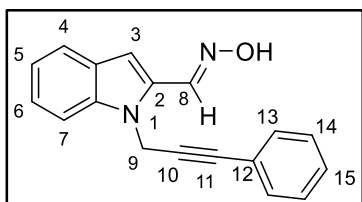


E-Isomer. ^1H NMR (400 MHz, CDCl_3) δ 8.19 (s, 1H, H-8), 7.54 (bd, $J_{4,5} = 8.0$ Hz, 1H, H-4), 7.36 (dd, $J_{7,6} = 8.3$ Hz, and $J_{7,5} = 1.0$ Hz, 1H, H-7), 7.25 (ddd, $J_{6,7} = 8.3$, $J_{6,5} = 7.1$, and $J_{6,4} = 1.0$ Hz, 1H, H-6), 7.07 (ddd, $J_{5,4} = 8.0$, $J_{5,6} = 7.1$, and $J_{5,7} = 1.0$ Hz, 1H, H-5), 6.67 (bs, 1H, H-3), 5.21 (quasi q, $J_{9,11} = 2.5$ Hz, 2H, CH_2), 2.19 (t, $J_{11,9} = 2.5$ Hz, 1H, $\text{C}\equiv\text{CH}$). ^{13}C -NMR (100 MHz, CDCl_3) δ 144.2, 139.0, 130.3, 127.6, 124.3, 121.7, 120.7, 109.9, 109.4, 78.7, 72.1, 34.7. IR (ATR, cm^{-1}) 3383, 3253, 1609, 1456, 1163, 1150, 950, 938, 750. HRMS calcd for $\text{C}_{12}\text{H}_{10}\text{N}_2\text{O}$ $[\text{M}+\text{H}]^+$: 199.0855. Found: 199.08659.

4.26 1-(3-Phenylprop-2-ynyl)-1*H*-indole-2-carbaldehyde oxime (**376b**)

A solution of 1-(3-phenylprop-2-ynyl)-1*H*-indole-2-carbaldehyde (**367b**) (0.9 g, 3.47 mmol) in EtOH (30 mL) was added to mixture of $\text{NH}_2\text{OH}\cdot\text{HCl}$ (224 mg, 3.47 mmol) and anhydrous Na_2CO_3 (183 mg, 1.74 mmol) in EtOH (10 mL). The reaction mixture was heated at refluxed temperature for 4 h. After monitoring the completion of the reaction by TLC, solvent was removed under reduced pressure. Water (30 mL) was added and the mixture was extracted with EtOAc (3×50 mL). Organic

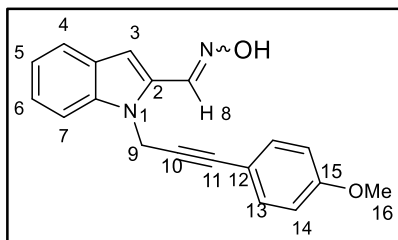
layers were combined and dried over MgSO₄. Evaporation of the solvent under the reduced pressure gave a mixture of *E*- and *Z*-isomers of the oxime **376b** (917 mg (96%), in a ratio of 84/16. The *E*-isomer **11i** was separated by column chromatography eluting with hexane/EtOAc (3:1) as a pale yellow solid, 505 mg (53%), mp.: 126-128 °C.



E-Isomer: ¹H NMR (400 MHz, CDCl₃) δ 8.30 (s, 1H, H-8), 8.02 (bs, 1H, OH), 7.61 (bd, *J*_{4,5} = 8.0 Hz, 1H, H-4), 7.50 (bd, *J*_{7,6} = 8.2 Hz, 1H, H-7), 7.35 (dd, *J*_{13,14} = 7.5 and *J*_{13,15} = 2.0 Hz, 2H, H-13), 7.30 (ddd, *J*_{6,7} = 8.2, *J*_{6,5} = 7.1, and *J*_{6,4} = 1.1 Hz, 1H, H-6), 7.25 – 7.18 (m, 3H, H-14 and H-15), 7.14 (ddd, *J*_{5,4} = 8.0, *J*_{5,6} = 7.1, and *J*_{5,7} = 0.8 Hz, 1H, H-5), 6.76 (s, 1H, H-3), 5.47 (s, 2H, H-9). ¹³C NMR (100 MHz, CDCl₃) δ 144.1, 139.1, 131.8, 130.4, 128.4, 128.2, 127.6, 124.1, 122.5, 121.5, 120.6, 110.1, 109.0, 84.1, 77.0, 35.5. IR (ATR, cm⁻¹) 3305, 3054, 1441, 1313, 1254, 957, 750. HRMS calcd for C₁₈H₁₄N₂O [M+H]⁺: 275.1229; found: 275.11789.

4.27 1-[3-(4-Methoxyphenyl)prop-2-ynyl]-1*H*-indole-2-carbaldehyde oxime (**376c**)

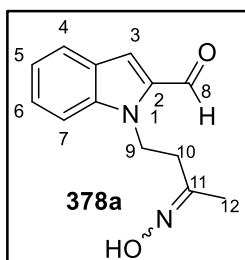
A solution methoxyphenylpropargyl aldehyde **367c** (0.349 g, 1.21 mmol) in ethanol (20 mL) was reacted with NH₂OH·HCl (80 mg, 1.24 mmol) and anhydrous Na₂CO₃ (183 mg, 0.62 mmol) at reflux temperature for 4 h. After monitoring the completion of the reaction by TLC, solvent was removed under reduced pressure. Water was added (30 mL) and the mixture was extracted with EtOAc (3 × 50 mL). Organic layers were combined and dried over MgSO₄. Evaporation of the solvent under the reduced pressure gave a mixture of *E*- and *Z*-isomers of the oxime **376c** (302 mg (82%), in a ratio of 87/13. The *E*-isomer **376c** was separated by column chromatography eluting with hexane/EtOAc (3:1) to give a pale yellow solid, (164 mg, 45%), mp.: 132-134 °C



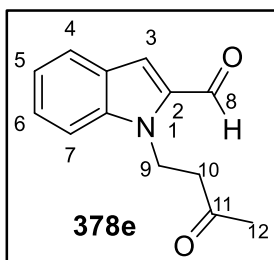
E-Isomer: $^1\text{H NMR}$ (400 MHz, CDCl_3) δ 8.29 (s, 1H, H-8), 7.63 (bd, $J_{4,5} = 7.9$ Hz, 1H, H-4), 7.55 (bd, $J_{7,6} = 7.9$ Hz, 1H, H-7), 7.33 (ddd, $J_{6,7} = 7.9$, $J_{6,5} = 7.5$, and $J_{6,4} = 1.1$ Hz, 1H, H-6), 7.30 (bd, $J_{13,14} = 9.0$ Hz, 2H, H-13), 7.15 (ddd, $J_{5,4} = 7.9$, $J_{5,6} = 7.5$, and $J_{5,7} = 0.9$ Hz, 1H, H-5), 6.78 (d, $J_{14,13} = 9.0$ Hz, 2H, H-14), 6.76 (s, 1H, H-3), 5.53 (s, 2H, CH_2), 3.78 (s, 3H, OCH_3). $^{13}\text{C NMR}$ (100 MHz, CDCl_3) δ 159.7, 143.9, 139.0, 133.4, 130.6, 127.7, 124.1, 121.6, 120.7, 114.6, 113.9, 110.2, 108.5, 84.2, 82.8, 55.3, 35.5. **IR (ATR, cm^{-1})** 3250, 2922, 2852, 1598, 1455, 1246, 1170, 742. **HRMS** calcd for $\text{C}_{19}\text{H}_{16}\text{N}_2\text{O}_2$ $[\text{M}+\text{H}]^+$: 305.1345. Found: 305.12845.

4.28 1-[(3*E/Z*)-3-(hydroxyimino)butyl]-1*H*-indole-2-carbaldehyde (**378a**)

A solution of (*Z/E*)-1-(but-2-yn-1-yl)-1*H*-indole-2-carbaldehyde oxime (**376a**) (126 mg, 0.6 mmol) in 15 mL CHCl_3 , was added $\text{HAuCl}_4 \cdot 2\text{H}_2\text{O}$ (7 mg, 3 mmol%). This mixture was stirred at room temperature for 48 h. After completion of the reaction monitoring by TLC, evaporation of solvent under reduced pressure gave an inseparable mixture of *E/Z*-isomers of **378a** in a ratio of 62:38. Attempted purification of the mixture of *E/Z*-isomers by column chromatography eluting with 3:1 hexane: ethyl acetate afforded ketone **378e** derived of the corresponding oximes (**378a**) as a brown solid (30 mg, 22%).



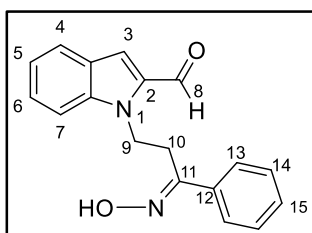
E-Isomer: $^1\text{H NMR}$ (400 MHz, CDCl_3) δ 9.88 (s, 1H, CHO), 7.74 (bd, $J_{4,5} = 8.0$ Hz, 1H, H-4), 7.54 (bd, $J_{7,6} = 8.3$ Hz, 1H, H-7), 7.47–7.37 (m, 1H, H-6), 7.29 (s, 1H, H-3), 7.17 (ddd, $J_{5,4} = 8.0$, $J_{5,6} = 6.0$, and $J_{5,7} = 1.5$ Hz, 1H, H-5), 4.75 (quasi t, A-part of A_2X_2 -system, 2H, CH_2), 2.68 (quasi t, B-part of A_2X_2 -system, 2H, CH_2), 1.94 (s, 3H, CH_3); *Z*-Isomer: $^1\text{H NMR}$ (400 MHz, CDCl_3) δ 9.89 (s, 1H, CHO), 7.73 (bd, $J_{4,5} = 8.0$ Hz, 1H, H-4), 7.44 (bd, $J_{7,6} = 8.1$ Hz, 1H, H-7), 7.43–7.37 (m, 1H, H-6), 7.43 (s, 1H, H-3), 7.17 (ddd, $J_{5,4} = 8.0$, $J_{5,6} = 6.0$, and $J_{5,7} = 1.5$ Hz, 1H, H-5), 4.77 (quasi t, A-part of A_2X_2 -system, 2H, CH_2), 2.84 (quasi t, B-part of A_2X_2 -system, 2H, CH_2), 1.81 (s, 3H, CH_3).



Ketone Form: $^1\text{H NMR}$ (400 MHz, CDCl_3) δ 9.87 (s, 1H, H-8), 7.73 (bd, $J_{4,5} = 8.0$ Hz, 1H, H-4), 7.51 (bd, $J_{7,6} = 8.3$ Hz, 1H, H-7), 7.43 (ddd, $J_{6,7} = 8.3$, $J_{6,5} = 7.0$, and $J_{6,4} = 1.2$ Hz, 1H, H-6), 7.29 (d, $J_{3,4} = 0.6$ Hz, 1H, H-3), 7.18 (ddd, $J_{5,4} = 8.0$, $J_{5,6} = 7.0$, and $J_{5,7} = 0.9$ Hz, 1H, H-5), 4.78 (dd, $J_{9,12} = 7.2$, $J_{9a,9b} = 7.0$ Hz, 1H, H-9), 2.96 (t, $J_{12,9} = 7.2$ Hz, 1H, H-12), 2.15 (s, 1H). $^{13}\text{C NMR}$ (100 MHz, CDCl_3) δ 206.5, 182.5, 140.1, 135.2, 127.2, 126.4, 123.4, 121.2, 118.5, 110.7, 43.9, 39.6, 30.3. **IR** (ATR, cm^{-1}) 3268, 2919, 1708, 1664, 1354, 667. **HRMS** calcd for $\text{C}_{13}\text{H}_{14}\text{N}_2\text{O}_2$ $[\text{M}+\text{H}]^+$: 216,1010. Found: 231,10191.

4.29 1-[(3*E/Z*)-3-(hydroxyimino)-3-phenylpropyl]-1*H*-indole-2-carbaldehyde (378b)

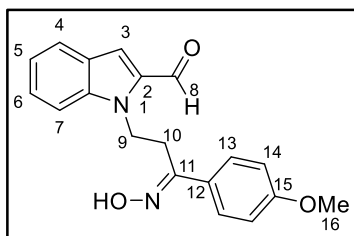
A solution of (*Z/E*)-1-(3-phenylprop-2-yn-1-yl)-1*H*-indole-2-carbaldehyde oxime (**376b**) (80 mg, 0.3 mmol) in 15 mL CHCl_3 , was added $\text{HAuCl}_4 \cdot 2\text{H}_2\text{O}$ (4 mg, 3 mmol%). This mixture was stirred at room temperature for 72 h. After completion of the reaction monitoring by TLC, evaporation of solvent under reduced pressure gave the crude oxime mixture **378b** (42 mg, 49%) in a ratio of 80/20. The residue was chromatographed on a short silica gel column eluting with n-hexane/EtOAc (3:1) to afford *E*-isomers of **378b**.



E-Isomer. $^1\text{H NMR}$ (400 MHz, CDCl_3) δ 9.89 (s, 1H, H-8), 7.72–7.66 (m, 3H, H-4 and H-13), 7.59 (dd, $J_{7,5} = 8.4$, and $J_{7,6} = 0.8$ Hz, 1H, H-7), 7.42 (ddd, $J_{6,7} = 8.4$, $J_{6,5} = 7.0$, and $J_{6,4} = 1.2$ Hz, 1H, H-6), 7.38 – 7.33 (m, 3H, H-14 and H-15), 7.24 (d, $J_{3,4} = 0.5$ Hz, 1H, H-3), 7.17 (ddd, $J_{5,4} = 8.0$, $J_{5,6} = 7.0$, and $J_{5,7} = 0.8$ Hz, 1H, H-5), 4.86 (quasi t, A-part of A_2X_2 -system, 2H, CH_2), 3.30 (quasi t, B-part of A_2X_2 -system, 2H, CH_2). $^{13}\text{C NMR}$ (100 MHz, CDCl_3) δ 182.6, 157.0, 140.4, 135.1, 131.8, 129.4, 128.5, 127.2, 126.4, 126.2, 123.3, 121.1, 118.2, 110.9, 41.3, 27.8. **IR** (ATR, cm^{-1}) 3283, 3054, 1643, 1456, 1313, 955, 748. **HRMS** calcd for $\text{C}_{18}\text{H}_{16}\text{N}_2\text{O}_2$ $[\text{M}+\text{H}]^+$: 293.1309. Found: 293.12845.

4.30 1-[(3Z)-3-(hydroxyimino)-3-(4-methoxyphenyl)propyl]-1H-indole-2-carbaldehyde (378c)

A solution of (*E/Z*)-1-(3-(4-methoxyphenyl)prop-2-yn-1-yl)-1H-indole-2-carbaldehyde oxime (**376c**) (180 mg, 0.6 mmol) in 15 mL CHCl₃ was added H₂AuCl₄·2H₂O (7 mg, 3 mmol%). This mixture was stirred 48 h in room temperature. After completion of the reaction monitoring by TLC, evaporation of solvent under reduced pressure gave the crude product of **378c** (67 mg, 35%). The residue was chromatographed on a short silica gel column eluting with n-hexane/EtOAc (3:1) to afford a mixture of *E/Z*-isomers of corresponding oxime **378c** (67 mg, 35%) as a pale brown solid in a ratio of 77/23 of *E*- and *Z*-isomers.

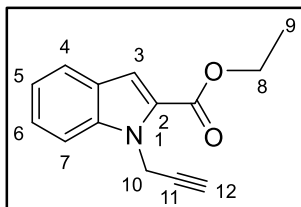


E-Isomer: ¹H NMR (400 MHz, CDCl₃) δ 9.86 (s, 1H, CHO), 7.71 (bd, *J*_{4,5} = 8.0 Hz, 1H, H-4), 7.67 (bd, *J*_{7,6} = 8.5 Hz, 1H, H-7), 7.51 (d, *J* = 8.9 Hz, 2H, arom.), 7.39 (ddd, *J*_{6,7} = 8.5, *J*_{6,5} = 6.8, and *J*_{6,4} = 1.1 Hz, 1H, H-6), 7.25 (d, *J*_{3,4} = 0.6 Hz, 1H, H-3), 7.17 (ddd, *J*_{5,4} = 8.0, *J*_{5,6} = 6.8, and *J*_{5,7} = 1.0 Hz, 1H, H-5), 6.91 (d, *J* = 8.9 Hz, 2H, arom.), 4.74 (quasi t, A-part of A₂X₂-system, 2H, CH₂), 3.83 (s, 3H, H-16), 3.03 (quasi t, B-part of A₂X₂-system, 2H, CH₂). ¹³C NMR (100 MHz, CDCl₃) δ 182.9, 168.4, 130.7, 127.7, 126.3, 123.5, 122.0, 121.9, 121.4, 120.6, 119.1, 114.1, 114.1, 110.8, 100.0, 55.5, 42.3, 29.7. IR (ATR, cm⁻¹) 3300, 2918, 2849, 1667, 1599, 1509, 1250, 1167, 1027, 741. HRMS calcd for C₁₉H₁₈N₂O₃ [M+H]⁺: 323.1435. Found: 323.13902.

4.31 Ethyl 1-(prop-2-yn-1-yl)-1H-indole-2-carboxylate (390a)

A stirred solution of ethyl 1H-indole-2-carboxylate (**353**) (4.0 g, 21.14 mmol) in dry DMF (20 mL) was added solid NaH (0.528 g, 22 mmol) piecewise. After a while, at the end of releasing of H₂ gas, propargyl bromide (**356**) (80 wt. % in toluene) (2.45 mL, 22 mmol) was diluted with 1:3 ratio of dry DMF and added to the stirring solution over 30 min period. After completion of the reaction (4 h), water was added and the resulting mixture was extracted with ethyl acetate and

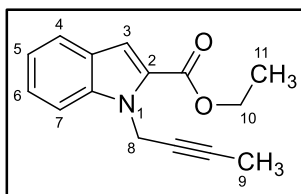
brine solution. The organic extracts were combined and dried over with MgSO_4 and filtrated. After the evaporation of the solvent, the product ethyl-1-(prop-2-yn-1-yl)-1*H*-indole-2-carboxylate (**390a**) was obtained as a white powdered solid (4.51 g, 19.9 mmol, 94%). mp.: 64–65 °C.¹⁴⁷



¹H NMR (400 MHz, CDCl_3) δ 7.60 (bd, $J_{4,5} = 8.0$ Hz, 1H, H-4), 7.41 (bd, $J_{7,6} = 8.4$ Hz, 1H, H-7), 7.31 (ddd, $J_{6,7} = 8.4$, $J_{6,5} = 7.0$, $J_{6,4} = 1.0$ Hz, 1H, H-6), 7.26 (d, $J_{3,4} = 0.7$ Hz, 1H, H-3), 7.10 (ddd, $J_{5,4} = 8.0$, $J_{5,6} = 7.0$, $J_{5,6} = 1.0$ Hz, 1H, H-5), 5.35 (d, $J_{10,12} = 2.5$ Hz, 2H, H-10), 4.31 (q, $J_{8,9} = 7.14$ Hz, 2H, H-8), 2.17 (t, $J_{12,10} = 2.5$ Hz, 1H, H-12), 1.33 (t, $J_{9,8} = 7.14$ Hz, 3H, H-9). **¹³C NMR** (100 MHz, CDCl_3) δ 162.0, 139.0, 127.0, 126.3, 125.5, 122.8, 121.2, 111.4, 110.5, 78.8, 72.0, 60.8, 33.9, 14.3.

4.32 Ethyl 1-(but-2-yn-1-yl)-1*H*-indole-2-carboxylate (**390b**).

A stirred solution of ethyl-1*H*-indole-2-carboxylate (**353**) (4.0 g, 21.14 mmol) in dry DMF (20 mL) was added solid NaH (0.528 g, 22 mmol) piecewise. After a while, at the end of releasing of H_2 gas, 1-bromobut-2-yne (**365**) (1.86 mL, 21 mmol) was diluted with 1:3 ratio of dry DMF and added to the stirring solution over 30 min. After completion of the reaction (2 h), water was added (100 mL) and the mixture was extracted with ethyl acetate (3×30 mL). The collected organic phases were washed with brine, dried over MgSO_4 , and filtrated. After evaporation of the solvent, the product, ethyl 1-(but-2-yn-1-yl)-1*H*-indole-2-carboxylate (**390b**), was obtained as a white solid (4.56 g, 90%) from petroleum ether. mp.: 66–68 °C.

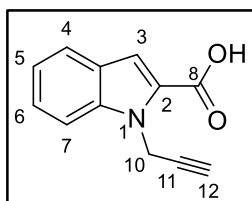


¹H NMR (400 MHz, CDCl_3) δ 7.68 (dt, $J_{4,5} = 8.0$, $J_{4,6} = J_{4,3} = 0.9$ Hz 1H, H-4), 7.51 (d, $J_{7,6} = 8.3$, and $J_{7,5} = 0.7$ Hz 1H, H-7), 7.38 (ddd, $J_{6,7} = 8.3$, $J_{6,5} = 7.0$, and $J_{6,4} = 0.9$ Hz, 1H, H-6), 7.32 (d, $J_{3,4} = 0.9$ Hz, 1H, H-3), 7.18 (ddd, $J_{5,4} = 8.0$, $J_{5,6} = 7.0$, and $J_{5,7} = 0.7$ Hz, 1H, H-5), 5.38 (q, $^5J_{8,9} = 2.3$ Hz, 2H, - CH_2 , H-8), 4.39 (q, $J_{10,11} = 7.1$ Hz, 2H, - CH_2 , H-10), 1.75 (t, $^5J_{11,10} = 2.4$ Hz, 3H, - CH_3 , H-9), 1.42 (t, $J_{11,10} = 7.1$ Hz, 3H, - CH_3 , H-11). **¹³C NMR** (100 MHz, CDCl_3) δ 162.0,

139.0, 127.0, 126.2, 125.2, 122.6, 120.9, 111.0, 110.8, 79.7, 74.1, 60.7, 34.2, 14.4, 3.6. **IR (ATR)** 1698, 1317, 1195, 766. **HRMS** Calcd for (C₁₅H₁₅NO₂) [M + H]⁺: 242.11756; Found: 242.1174

4.33 1-(Prop-2-yn-1-yl)-1*H*-indole-2-carboxylic acid (**391a**)

A stirred solution of 4.51 g (19.9 mmol) of ethyl-1-(prop-2-yn-1-yl)-1*H*-indole-2-carboxylate (**390a**) in 50 mL MeOH was added 3.02 g (21.85 mmol) of K₂CO₃. This mixture was heated at reflux temperature for 12 h. After completion of the reaction, solvent was evaporated and water (100 mL) was added. The mixture was extracted with EtOAc (3 × 50 mL). The combined organic phases was washed with 1 N HCl and brine and dried over MgSO₄. Evaporation of solvent gave of 1-(prop-2-yn-1-yl)-1*H*-indole-2-carboxylic acid (**391a**) as a white solid from hexane/CH₂Cl₂ (3.52 g, 17.7 mmol, 89%). mp.: 193–195 °C (Lit. mp.: 190–193 °C).¹⁴⁸

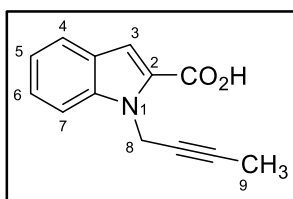


¹H NMR (400 MHz, Acetone) δ 7.60 (dt, $J_{4,5} = 8.0$, $J_{4,3} = 0.9$ Hz, 1H, H-4), 7.51 (dd, $J_{7,6} = 8.4$, $J_{7,5} = 0.8$ Hz, 1H, H-7), 7.28 (ddd, $J_{6,7} = 8.4$, $J_{6,5} = 7.0$, $J_{6,4} = 0.9$ Hz, 1H, H-6), 7.24 (d, $J_{3,4} = 0.9$ Hz, 1H, H-3), 7.06 (ddd, $J_{5,4} = 8.0$, $J_{5,6} = 7.0$, $J_{5,7} = 0.8$ Hz, 1H, H-5), 5.44 (d, $J_{10,12} = 2.5$ Hz, 2H, H-10), 2.63 (t, $J_{12,10} = 2.5$ Hz, 2H, H-12). **¹³C NMR** (100 MHz, Acetone) δ 163.2, 140.1, 127.8, 127.2, 126.1, 123.5, 121.9, 112.2, 111.8, 80.0, 73.4, 34.2.

4.34 1-(But-2-yn-1-yl)-1*H*-indole-2-carboxylic acid (**391b**).

A stirred solution of ethyl 1-(but-2-yn-1-yl)-1*H*-indole-2-carboxylate (**390b**) (4.83 g, 20 mmol) in 50 mL MeOH was added 3.04 g of K₂CO₃ (22 mmol). This mixture was heated at reflux temperature for 12 h. After completion of the reaction, solvent was evaporated. The crude product was added 1 N HCl (reaction medium acidified) and extracted with EtOAc (3 × 50 mL). Organic layers were combined and dried over MgSO₄. Evaporation of solvent gave of 1-(but-2-yn-1-yl)-1*H*-indole-2-

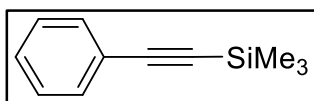
carboxylic acid (**391b**) (3.41 g, 17.7 mmol, 90%) as a white needles from EtOAc/*n*-hexane. mp.: 190–192 °C.



¹H NMR (400 MHz, Acetone-*d*₆) δ 11.31 (bs, 1H, –OH), 7.74 (dt, $J = 8.0, 0.9$ Hz, 1H), 7.64 (dd, $J = 8.4, 0.8$ Hz, 1H), 7.41 (ddd, $J = 8.3, 7.0, 1.0$ Hz, 1H), 7.37 (d, $J = 1.0$ Hz, 1H), 7.20 (ddd, $J = 8.0, 7.0, 0.7$ Hz, 1H), 5.50 (q, $J = 2.4$ Hz, 1H), 1.72 (t, $J = 2.4$ Hz, 1H). **¹³C NMR** (100 MHz, Acetone-*d*₆) δ 163.2, 140.1, 127.8, 127.2, 126.0, 123.4, 121.8, 111.92, 111.88, 79.9, 75.4, 34.5, 3.1. **IR (ATR)** 2851, 2513, 1654, 1518, 1264, 1206, 733. **HRMS** Calcd for (C₁₃H₁₁NO₂) [M + H]⁺: 214.0863; Found: 214.0869.

4.35 Trimethyl(phenylethynyl)silane (**394**)

A solution of phenylacetylene (0.05 mol, 5.5 mL) in diethyl ether (25 mL), *n*-butyllithium (15 mL) was added dropwise at 0 °C. Gas evolution was observed. The mixture was then stirred for 24 h at room temperature. After completion of the reaction, trimethylsilyl chloride (0.05 mol, 6.5 mL) in ether (10 mL) was added dropwise at room temperature, and the solution was stirred for 24 h. To remove the excess of *n*-BuLi, water (25 mL) was added carefully and the solution was extracted with diethyl ether (3 × 25 mL). The combined organic extracts were dried over Na₂SO₄. Evaporation of solvent gave trimethyl(phenylethynyl)silane (**394**) as a colorless liquid (8.3 g, 0.05 mol, 95%).

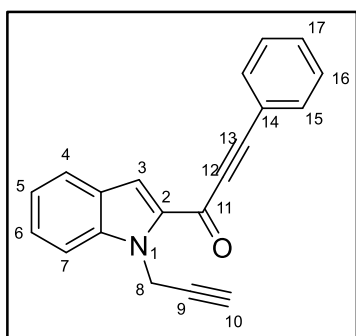


¹H NMR (400 MHz, CDCl₃) δ 7.36 (dd, $J = 6.5, 3.2$ Hz, 2H), 7.17 (dd, $J = 5.1, 2.0$ Hz, 3H), 0.15 (s, 9H). **¹³C NMR** (100 MHz, CDCl₃) δ 131.9, 128.5, 128.2, 123.2, 105.2, 94.1, 0.01.

4.36 3-Phenyl-1-(1-(prop-2-yn-1-yl)-1H-indol-2-yl)prop-2-yn-1-one (**393a**)

A solution of 1-(prop-2-yn-1-yl)-1H-indole-2-carboxylic acid (**391a**) (500 mg, 2.5 mmol) in THF (20 mL) was added triethylamine (100 μ L). The reaction mixture was stirred at room temperature for 30 min. To this solution was then added a

solution of thionyl chloride (800 μL , 11 mmol) in THF (2 mL) dropwise, and the resulting mixture was stirred at room temperature for 3 h. Afterwards the solid was filtered off, and solvent was evaporated. The acyl chloride **392a** was dissolved in chloroform (5 mL) without purification, and trimethyl(phenylethynyl)silane¹³³ (3.0 mmol, 523 mg, 1.2 equiv.) was added to the solution at room temperature. The mixture was then added to a solution of aluminum chloride (450 mg, 3.4 mmol) in chloroform (15 mL) dropwise at 0 $^{\circ}\text{C}$, and the mixture was stirred for 24 h at room temperature. After completion of the reaction (controlled by TLC), water (30 mL) was added, and the solution was extracted with dichloromethane. The combined organic extracts were dried over Na_2SO_4 . The solvent was evaporated to give crude product, which was purified by column chromatography eluting with EtOAc/hexane to give 3-phenyl-1-(1-(prop-2-yn-1-yl)-1*H*-indol-2-yl)prop-2-yn-1-one (**393a**) as a yellow solid (0.45 g, 1.6 mmol, 63%) from EtOAc/*n*-hexane. mp.: 99–101 $^{\circ}\text{C}$.



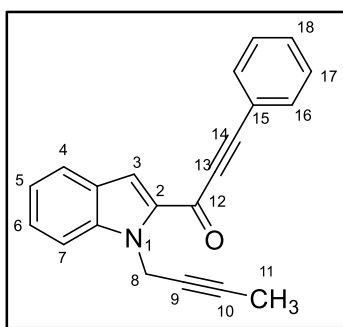
^1H NMR (400 MHz, CDCl_3) δ 7.79 (dt, $J_{4,5} = 8.1$ and $J_{4,6} = J_{4,3} = 1.0$ Hz, 1H, H-4), 7.73 (d, $J_{3,4} = 1.0$ Hz, 1H, H-3) 7.72 (dd, $J_{15,16} = 8.1$, and $J_{15,17} = 1.4$ Hz, 2H, H-15), 7.54 – 7.37 (m, 5H, arom.), 7.22 (ddd, $J_{5,4} = 8.1$, $J_{5,6} = 6.8$, and $J_{5,7} = 1.1$ Hz, 1H, H-5), 5.49 (d, $^4J_{8-10} = 2.5$ Hz, 2H, H-8), 2.28 (t, $^4J_{10-8} = 2.5$ Hz, 1H, H-10). **^{13}C NMR** (100 MHz, CDCl_3) δ 169.5, 140.3,

134.9, 133.0, 130.6, 128.7, 127.4, 126.4, 123.6, 121.7, 120.3, 117.7, 110.8, 90.2, 87.8, 78.4, 72.3, 34.2. **IR (ATR, cm^{-1})** 3270, 2988, 2901, 2199, 2097, 1608. **HRMS** Calcd for ($\text{C}_{20}\text{H}_{13}\text{NO}$) [$\text{M} + \text{H}$] $^{+}$: 284.10699; Found: 284.10725.

4.37 1-(1-(But-2-yn-1-yl)-1*H*-indol-2-yl)-3-phenylprop-2-yn-1-one (**393b**).

A solution of 1-(but-2-yn-1-yl)-1*H*-indole-2-carboxylic acid (**391b**) (500 mg, 2.35 mmol) in THF (20 mL) was added triethylamine (100 μL). This mixture was stirred at room temperature for 30 min. To this solution, a solution of thionyl chloride (800 μL , 11 mmol) in THF (2 mL) was then added dropwise, and the resulting mixture

was stirred at room temperature for 3 h. Afterwards, the formed solid was filtered out, and solvent was evaporated. The resulting acyl chloride **392b** was dissolved in chloroform (5 mL), and trimethyl(phenylethynyl)silane (3.0 mmol, 523 mg, 1.2 equiv.) was added to the solution at room temperature. The mixture was then added to a suspension of aluminum chloride (450 mg, 3.4 mmol) in chloroform (15 mL) dropwise at 0 °C, and the mixture was stirred for 24 h at room temperature. After completion of the reaction, water (30 mL) was added, and the mixture was extracted with dichloromethane. The combined organic extracts were dried over Na₂SO₄. The solvent was evaporated to give crude product, which was purified by column chromatography eluting with EtOAc/hexane (1:5) to give 1-(1-(but-2-yn-1-yl)-1*H*-indol-2-yl)-3-phenylprop-2-yn-1-one (**393b**) as pale yellow needles (0.395 g, 1.33 mmol, 57%). mp.: 150-152 °C.

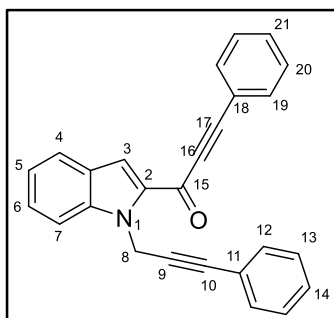


¹H NMR (400 MHz, CDCl₃) δ 7.67 (bd, $J_{4,5} = 8.1$ Hz, 1H, H-4), 7.51 – 7.47 (m, 2H, arom.), 7.39 – 7.31 (m, 4H, arom), 7.28 (ddd, $J_{6,7} = 8.0$, $J_{6,5} = 6.9$, and $J_{6,4} = 1.0$ Hz, 1H, H-6), 7.10 (ddd, $J_{5,4} = 8.1$, $J_{5,6} = 6.9$, and $J_{5,7} = 0.9$ Hz, 1H, H-5), 6.98 (bs, 1H, H-3), 5.00 (q, $^5J_{8,11} = 1.5$ Hz, 2H, H-8), 2.54 (t, $^5J_{11,8} = 1.5$ Hz, 3H, H-11). **¹³C NMR** (100 MHz, CDCl₃) δ 182.2, 139.9, 138.5, 134.3, 132.0, 131.8, 130.2, 129.6, 128.6, 125.2, 124.0, 122.0, 121.4, 110.5, 101.2, 99.8, 89.5, 47.0, 18.4. **IR** (ATR, cm⁻¹): 3056, 2917, 2849, 2197, 1682, 1607, 1148, 741. **HRMS**: calcd for C₂₁H₁₅NO [M-H]⁻: 296.10809; Found: 296.11096.

4.38 3-Phenyl-1-(1-(3-phenylprop-2-yn-1-yl)-1*H*-indol-2-yl)prop-2-yn-1-one (**395a**)

A stirred mixture of CuI (17 mg, 0.09 mmol), PPh₃ (90 mg, 0.34 mmol), and Pd(OAc)₂ (17 mg, 0.08 mmol) was purged with nitrogen for 30 min and heated to 50 °C. Then a solution of 0.312 g (1.1 mmol) of 3-phenyl-1-(1-(prop-2-yn-1-yl)-1*H*-indol-2-yl)prop-2-yn-1-one (**393a**), 0.244 g (1.2 mmol) of iodobenzene, and DIPA (2 mL) in THF (15 mL) was added successively. The mixture was then refluxed for 2 h. After complete conversion (monitored by TLC) solvent was

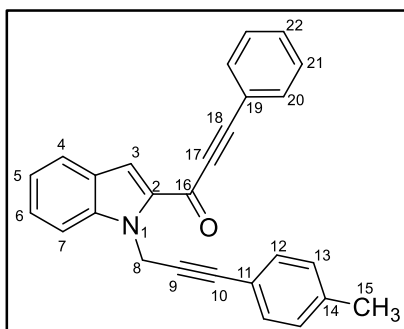
evaporated, and the residue was chromatographed on silica gel eluting with ethyl acetate/hexane (1:4) to give 3-phenyl-1-(1-(3-phenylprop-2-yn-1-yl)-1*H*-indol-2-yl)prop-2-yn-1-one (**395a**) (313 mg, 0.87 mmol, 79%) as a yellow solid, m.p.: 114–116 °C.



¹H NMR (400 MHz, CDCl₃) δ 7.80 (d, *J* = 8.1 Hz, 1H), 7.74 (s, 1H), 7.73 (dd, *J* = 8.0, 1.5 Hz, 3H), 7.65 (d, *J* = 8.5 Hz, 1H), 7.52–7.44 (m, 4H), 7.40–7.38 (m, 2H), 7.30–7.23 (m, 4H), 5.77 (s, 2H); **¹³C NMR** (100 MHz, CDCl₃) δ 169.5, 140.5, 135.0, 133.0, 131.8, 130.6, 128.7, 128.4, 128.2, 127.3, 126.4, 123.5, 122.6, 121.6, 120.4, 117.6, 111.1, 90.1, 87.8, 84.1, 83.9, 35.1; **IR (ATR, cm⁻¹)** 3062, 2986, 2917, 2201, 1609, 1509; **HRMS** Calcd for (C₂₆H₁₇NO) [M + H]⁺: 360.13829; Found: 360.13893.

4.39 3-phenyl-1-(1-(3-(*p*-tolyl)prop-2-yn-1-yl)-1*H*-indol-2-yl)prop-2-yn-1-one (**395b**)

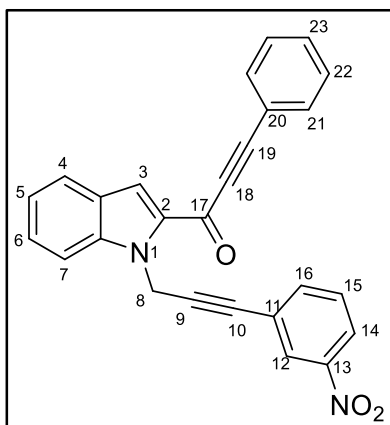
A stirred mixture of CuI (17 mg, 0.09 mmol), PPh₃ (90 mg, 0.34 mmol), and Pd(OAc)₂ (17 mg, 0.08 mmol) was purged with nitrogen for 30 min and heated to 50 °C. Then a solution of 0.312 g (1.1 mmol) of 3-phenyl-1-(1-(prop-2-yn-1-yl)-1*H*-indol-2-yl)prop-2-yn-1-one (**393a**), 0.244 g (1.2 mmol) of *p*-bromotoluene, and DIPA (2 mL) in THF (15 mL) was added successively. The mixture was then refluxed for 2 h at 70 °C. After complete conversion (monitored by TLC) solvent was evaporated, and the residue was chromatographed on silica gel eluting with ethyl acetate/hexane (1:4) to give 3-phenyl-1-(1-(3-(*p*-tolyl)prop-2-yn-1-yl)-1*H*-indol-2-yl)prop-2-yn-1-one (**395b**) (329 mg, 0.88 mmol, 80%) as a yellow colored viscous oil.



¹H NMR (400 MHz, CDCl₃) δ 7.81 (d, *J* = 8.0 Hz, 1H), 7.75 (s, 1H), 7.73 (dd, *J* = 7.9, 1.5 Hz, 3H), 7.66 (d, *J* = 8.5 Hz, 1H), 7.56–7.42 (m, 4H), 7.35–7.21 (m, 3H), 7.09 (d, *J* = 8.0 Hz, 2H), 5.76 (s, 2H), 2.34 (s, 3H); **¹³C NMR** (100 MHz, CDCl₃) δ 169.5, 140.5, 138.5, 135.1, 133.0, 131.6, 130.6, 128.9, 128.7, 127.3, 126.4, 123.5, 121.6, 120.4, 119.5, 117.6, 111.2, 90.1, 87.9, 84.2, 83.3, 35.1, 21.5; **IR (ATR, cm⁻¹)** 3059, 3025, 2987, 2917, 2847, 2201, 1609, 1508; **HRMS** Calcd for (C₂₇H₁₉NO) [M + H]⁺: 374.15394; Found: 374.15698.

4.40 1-(1-(3-(3-nitrophenyl)prop-2-yn-1-yl)-1H-indol-2-yl)-3-phenylprop-2-yn-1-one (395c)

A stirred mixture of CuI (17 mg, 0.09 mmol), PPh₃ (90 mg, 0.34 mmol), and Pd(OAc)₂ (17 mg, 0.08 mmol) was purged with nitrogen for 30 min and heated to 50 °C. Then a solution of 0.312 g (1.1 mmol) of 3-phenyl-1-(1-(prop-2-yn-1-yl)-1H-indol-2-yl)prop-2-yn-1-one (**393a**), 0.299 g (1.2 mmol) of 1-iodo-3-nitrobenzene, and DIPA (2 mL) in THF (15 mL) was added successively. The mixture was then refluxed for 4 h at 70 °C. After complete conversion (monitored by TLC) solvent was evaporated, and the residue was chromatographed on silica gel eluting with ethyl acetate/hexane (1:4) to give 1-(1-(3-(3-nitrophenyl)prop-2-yn-1-yl)-1H-indol-2-yl)-3-phenylprop-2-yn-1-one (**395c**) (384 mg, 0.95 mmol, 86%) as a powder yellow solid from EtOAc/n-hexane, mp.: 115–117 °C.

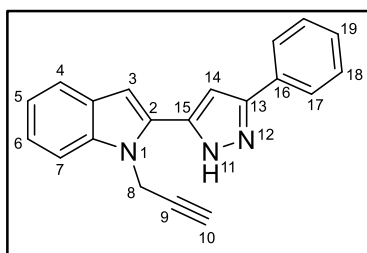


¹H NMR (400 MHz, CDCl₃) δ 8.19 (d, *J* = 1.6 Hz, 1H), 8.12 (dd, *J* = 8.3, 1.3 Hz, 1H), 7.79 (d, *J* = 8.0 Hz, 1H), 7.73 (s, 1H), 7.70 (dd, *J* = 7.6, 1.6 Hz, 2H), 7.63 (d, *J* = 7.7 Hz, 1H), 7.58 (d, *J* = 8.4 Hz, 1H), 7.52–7.47 (m, 2H), 7.46–7.41 (m, 3H), 7.25 (t, *J* = 7.5 Hz, 1H), 5.76 (s, 2H); **¹³C NMR** (100 MHz, CDCl₃) δ 169.5, 148.0, 140.4, 137.6, 135.0, 133.0, 130.7, 129.2, 128.7, 127.5, 126.7, 126.4,

124.3, 123.7, 123.1, 121.8, 120.2, 117.8, 110.7, 90.4, 87.7, 86.8, 81.6, 34.9; **IR** (ATR, cm^{-1}) 2988, 2968, 2901, 2355, 2191, 1607, 1522; **HRMS** Calcd for ($\text{C}_{26}\text{H}_{16}\text{N}_2\text{O}_3$) $[\text{M} + \text{H}]^+$: 405.12337; Found: 405.12613.

4.41 2-(3-phenyl-1*H*-pyrazol-5-yl)-1-(prop-2-yn-1-yl)-1*H*-indole (396a)

A solution of methanol (15 mL) and 3-phenyl-1-(1-(prop-2-yn-1-yl)-1*H*-indol-2-yl)prop-2-yn-1-one (**353a**) (0.142 g, 0.5 mmol) at reflux temperature was added hydrazine monohydrate (1 mL) dropwise under nitrogen atmosphere. After 3 h, water was added, and the mixture was extracted with ethyl acetate (3×20 mL). The combined extracts were dried over MgSO_4 , and evaporated under the reduced pressure. The resulting crude product was chromatographed on silica gel eluting with ethyl acetate/hexane (1:4) to give 2-(3-phenyl-1*H*-pyrazol-5-yl)-1-(prop-2-yn-1-yl)-1*H*-indole (**396a**) (137 mg, 0.46 mmol, 92%) as a yellow solid from DCM/n-hexane, mp.: 164–166 °C.

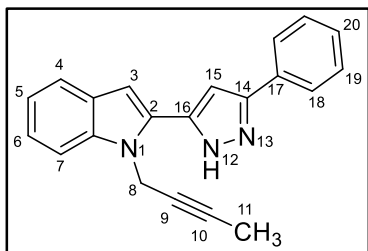


^1H NMR (400 MHz, Acetone) δ 7.83 (d, $J_{17,18} = 7.1$ Hz, 2H, H-17), 7.52 (m, 2H, arom.), 7.46 – 7.38 (m, 2H, arom.), 7.34 (m, 1H, arom.), 7.18 (ddd, $J = 8.1, 7.1,$ and 1.0 Hz, 1H, H-6), 7.10 (s, 1H, H-3), 7.05 (t, $J = 7.3$ Hz, 1H, H-5), 6.84 (s, 1H, H-14), 5.52 (d, $^4J_{8,10} = 2.0$ Hz, 2H, H-8), 4.54 (bs, 1H, H-11) 2.71 (t, $^4J_{10,8} = 2.0$ Hz, 1H, H-10). **^{13}C NMR** (100 MHz, Acetone) δ 145.5, 143.8, 137.8, 132.1, 130.3, 129.0, 128.33, 128.31, 125.5, 122.1, 120.5, 120.2, 110.2, 102.2, 102.1, 79.5, 72.7, 33.8. **IR** (ATR, cm^{-1}) 3272, 3269, 2972, 2901, 1454, 1075. **HRMS** Calcd for ($\text{C}_{20}\text{H}_{15}\text{N}_3$) $[\text{M} + \text{H}]^+$: 298.1339; Found: 298.1343.

4.42 1-(but-2-yn-1-yl)-2-(3-phenyl-1*H*-pyrazol-5-yl)-1*H*-indole (396b)

A solution of methanol (15 mL) and 1-(1-(but-2-yn-1-yl)-1*H*-indol-2-yl)-3-phenylprop-2-yn-1-one (**393b**) (0.148 g, 0.5 mmol) at reflux temperature was added hydrazine monohydrate (1 mL) dropwise under nitrogen atmosphere. After 2 h,

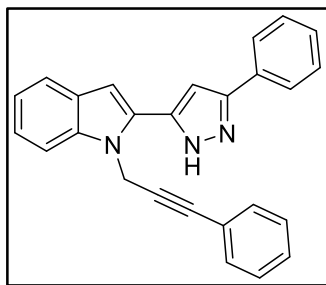
water was added, and the mixture was extracted with ethyl acetate (3 × 20 mL). The combined extracts were dried over MgSO₄, and evaporated under the reduced pressure. The resulting crude product was chromatographed on silica gel eluting with ethyl acetate/hexane (1:5) to give 1-(but-2-yn-1-yl)-2-(3-phenyl-1*H*-pyrazol-5-yl)-1*H*-indole (**396b**) (128 mg, 0.41 mmol, 92%) as a pale yellow solid, mp.: 120–121 °C.



¹H NMR (400 MHz, CDCl₃) δ 9.32 (s, 1H, –NH), 7.66 (d, *J* = 7.4 Hz, 2H, arom.), 7.50 (d, *J*_{4,5} = 8.0 Hz, 1H, H-4), 7.37 (d, *J*_{7,6} = 8.3 Hz, 1H, H-7), 7.32 (t, *J* = 7.4 Hz, 2H, arom.), 7.27 (d, *J* = 6.9 Hz, 1H, arom.), 7.20 (ddd, *J*_{5,4} = 8.0, *J*_{5,6} = 7.0, and *J*_{5,7} = 0.9 Hz, 1H, H-5), 7.07 (t, *J* = 7.4 Hz, 1H, arom.), 6.84 (s, 1H, H-3), 6.67 (s, 1H, pyrazole), 4.97 (d, *J* = 1.5 Hz, 2H, CH₂), 1.68 (t, *J* = 2.0 Hz, 3H, CH₃). **¹³C NMR** (100 MHz, CDCl₃) δ 148.2, 141.5, 137.6, 130.6, 130.2, 129.0, 128.7, 127.8, 125.8, 122.7, 121.0, 120.4, 110.3, 110.0, 102.9, 80.8, 74.4, 34.4, 3.6. **IR (ATR, cm⁻¹)** 3055, 2918, 2851, 1456, 1335, 788. **HRMS** Calcd for (C₂₀H₁₅N₃) [M + H]⁺: 312.1483; Found: 312.1495.

4.43 2-(3-Phenyl-1*H*-pyrazol-5-yl)-1-(3-phenylprop-2-yn-1-yl)-1*H*-indole (**396c**)

To a solution of methanol (15 mL) and 3-phenyl-1-(1-(3-phenylprop-2-yn-1-yl)-1*H*-indol-2-yl)prop-2-yn-1-one (**395a**), (0.175 g, 0.5 mmol) at reflux temperature was added hydrazine monohydrate (1 mL) dropwise under nitrogen atmosphere. After 2.5 h, water was added, and the mixture was extracted with ethyl acetate (3 × 20 mL). The combined extracts were dried over MgSO₄, and evaporated under the reduced pressure. The resulting crude product was chromatographed on silica gel eluting with ethyl acetate/hexane (1:5) to give 2-(3-phenyl-1*H*-pyrazol-5-yl)-1-(3-phenylprop-2-yn-1-yl)-1*H*-indole (**396c**) (176 mg, 0.47 mmol, 94%) as a cubic yellow solid from hexane-DCM, mp.: 189–191 °C.

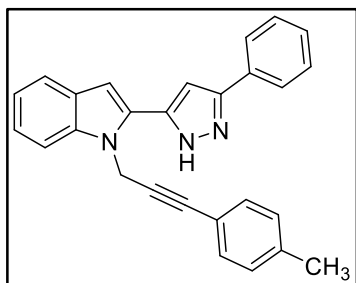


¹H NMR (400 MHz, Acetone) δ 12.78 (bs, 1H, -NH), 7.92 (d, $J = 7.4$ Hz, 2H, arom.), 7.69 (d, $J = 8.2$ Hz, 1H, H-4), 7.64 (d, $J = 7.9$ Hz, 1H, H-7), 7.52 (t, $J = 7.4$ Hz, 2H, arom.), 7.42 (t, $J = 7.2$ Hz, 1H, arom.), 7.38 – 7.25 (m, 6H, arom.), 7.22 (s, 1H, H-3), 7.14 (t, $J = 7.4$ Hz, 1H, arom), 6.94 (s, 1H, pyrazole), 5.85 (bs, 1H, CH₂).

¹³C NMR (100 MHz, CDCl₃) δ 147.9, 147.8, 137.7, 131.8, 130.7, 130.4, 129.0, 128.7, 128.5, 128.2, 128.0, 125.8, 122.7, 122.4, 121.0, 120.5, 110.2, 103.1, 103.0, 84.5, 84.3, 34.9. **IR** (ATR, cm⁻¹) 3650, 2988, 2972, 2901, 1456, 1076. **HRMS** Calcd for (C₂₆H₁₉N₃) [M + H]⁺: 274.16517; Found: 374.16830.

4.44 2-(3-Phenyl-1H-pyrazol-5-yl)-1-(3-(p-tolyl)prop-2-yn-1-yl)-1H-indole (396d)

To a solution of methanol (15 mL) and 3-phenyl-1-(1-(3-(p-tolyl)prop-2-yn-1-yl)-1H-indol-2-yl)prop-2-yn-1-one (**395b**), (0.187 g, 0.5 mmol) at reflux temperature was added hydrazine monohydrate (1 mL) dropwise under nitrogen atmosphere. After 2 h, water was added, and the mixture was extracted with ethyl acetate (3 × 20 mL). The combined extracts were dried over MgSO₄, and evaporated under the reduced pressure. The resulting crude product was chromatographed on silica gel eluting with ethyl acetate/hexane (1:4) to give 2-(3-phenyl-1H-pyrazol-5-yl)-1-(3-(p-tolyl)prop-2-yn-1-yl)-1H-indole (**396d**) (178 mg, 0.46 mmol, 92%) as a powder white solid from DCM/n-hexane, m.p.: 208–210 °C.



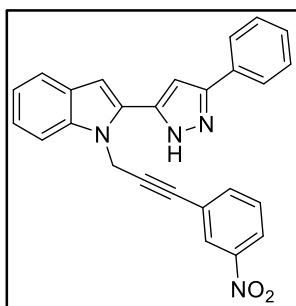
¹H NMR (400 MHz, Acetone) δ 12.73 (bs, 1H, -NH), 7.83 (d, $J = 7.5$ Hz, 1H, arom.), 7.59 (d, $J = 8.3$ Hz, 1H, H-4), 7.55 (d, $J = 7.8$ Hz, 1H, H-7), 7.43 (t, $J = 7.5$ Hz, 1H, arom.), 7.32 (t, $J = 7.3$ Hz, 1H, arom.), 7.22 – 7.11 (m, 4H, arom), 7.08 – 6.98 (m, 3H, arom), 6.85 (d, $^4J = 0.6$ Hz, 1H, pyrazole), 5.73 (bs, 1H, CH₂), 2.20 (s, 3H, CH₃).

¹³C NMR (100 MHz, Acetone) δ 138.5, 137.9, 131.4(2C), 129.1(2C), 129.0, 128.3, 128.2(2C), 125.4(2C), 122.1, 120.5, 120.1, 119.7, 110.2,

102.2, 102.0, 84.5, 83.4, 34.6, 20.4. **IR** (ATR, cm^{-1}) 3680, 2988, 2901, 1456, 1075. **HRMS** Calcd for ($\text{C}_{27}\text{H}_{21}\text{N}_3$) $[\text{M} + \text{H}]^+$: 388.1808; Found: 388.1812.

4.45 1-(3-(3-Nitrophenyl)prop-2-yn-1-yl)-2-(3-phenyl-1H-pyrazol-5-yl)-1H-indole (396e)

A solution of methanol (15 mL) and 1-(1-(3-(3-nitrophenyl)prop-2-yn-1-yl)-1H-indol-2-yl)-3-phenylprop-2-yn-1-one (**395c**), (0.202 g, 0.5 mmol) at reflux temperature was added hydrazine monohydrate (1 mL) dropwise at 70 °C under nitrogen atmosphere. After 4 h, water was added, and the mixture was extracted with ethyl acetate (3×20 mL). The combined extracts were dried over MgSO_4 , and evaporated under the reduced pressure. The resulting crude product was chromatographed on silica gel eluting with ethyl acetate/hexane (1:2) to give 1-(3-(3-nitrophenyl)prop-2-yn-1-yl)-2-(3-phenyl-1H-pyrazol-5-yl)-1H-indole (**396e**) (193 mg, 0.43 mmol, 92%) as a yellow solid, mp.: 199–201 °C.

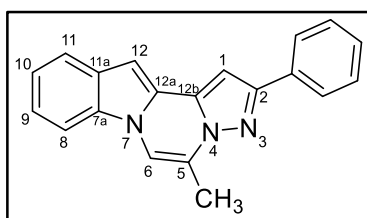


^1H NMR (400 MHz, Acetone) δ 8.11 (ddd, $J = 8.3, 2.3, 1.0$ Hz, 1H, arom.), 8.08 – 8.05 (m, 1H, arom.), 7.86 – 7.80 (m, 2H, arom.), 7.67 (dt, $J = 7.8, 1.4$ Hz, 1H, H-4), 7.61 (d, $J = 8.3$ Hz, 1H, arom.), 7.57 – 7.51 (m, 2H), 7.46 – 7.39 (m, 2H), 7.33 (tt, $J = 7.4, 1.2$ Hz, 1H), 7.20 (ddd, $J = 8.2, 7.1, 1.1$ Hz, 1H), 7.06 (td, $J = 7.6, 0.8$ Hz, 1H), 5.82 (s, 2H, CH_2). **^{13}C NMR** (100 MHz, Acetone) δ 148.2, 137.9, 137.4, 132.7, 130.1, 130.0, 129.0, 128.4, 128.3, 126.0, 125.5(2C), 124.3, 123.1, 122.2, 120.53, 120.51, 120.3, 110.1, 102.3, 102.2, 88.0, 81.0, 34.6. **IR** (ATR, cm^{-1}) 3680, 3059, 2974, 2926, 2893, 1523, 1347. **HRMS** Calcd for ($\text{C}_{26}\text{H}_{18}\text{N}_4\text{O}_2$) $[\text{M} + \text{H}]^+$: 419.15025; Found: 419.15322.

4.46 5-Methyl-2-phenylpyrazolo[5',1':3,4]pyrazino[1,2-*a*]indole (404a)

A solution of 2-(3-phenyl-1H-pyrazol-5-yl)-1-(prop-2-yn-1-yl)-1H-indole (**396a**) (0.119 g, 0.4 mmol) in DMF (10 mL) under nitrogen atmosphere was added sodium

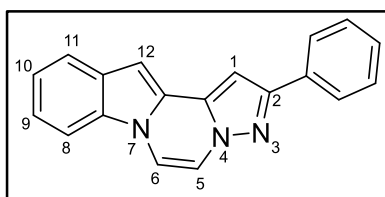
hydride (10.5 mg, 1.1 eq.) at room temperature. The reaction mixture was stirred for 10-15 min. After complete conversion, water was added, and the resulting mixture was extracted with ethyl acetate (3 × 20 mL). The combined extracts were dried over MgSO₄, and evaporated to give crude product which was subsequently chromatographed on silica gel eluting with ethyl acetate/hexane (1:4) to give 5-methyl-2-phenylpyrazolo[5',1':3,4]pyrazino[1,2-*a*]indole (**404a**) (0.101 g, 0.34 mmol, 87%) as a white solid from EtOAc/n-hexane, mp.: 125–127 °C.



¹H NMR (400 MHz, CDCl₃) δ 7.91–7.86 (m, 2H), 7.70–7.67 (m, 1H), 7.58–7.56 (m, 1H), 7.37 (bt, *J* = 7.5 Hz, 2H), 7.29 (tt, *J* = 7.4, 1.2 Hz, 1H), 7.28 (d, *J* = 1.1 Hz, 1H), 7.25–7.21 (m, 2H), 7.00 (s, 1H), 6.83 (bs, 1H), 2.56 (d, *J* = 1.1 Hz, 3H); **¹³C NMR** (100 MHz, CDCl₃) δ 152.5, 133.7, 133.0, 131.1, 128.8, 128.6, 128.3, 126.5, 126.2, 122.2, 121.7, 121.1, 120.4, 109.7, 107.3, 97.4, 94.4, 14.9; **IR (ATR, cm⁻¹)** 2988, 2968, 2922, 2901, 2358, 1507, 1456, 1078; **HRMS** Calcd for (C₂₀H₁₅N₃) [M + H]⁺: 298.1339; Found: 298.1348.

4.47 2-phenylpyrazolo[5',1':3,4]pyrazino[1,2-*a*]indole (**407**)

A solution of 1-(but-2-yn-1-yl)-2-(3-phenyl-1*H*-pyrazol-5-yl)-1*H*-indole (**396b**) (0.123 g, 0.4 mmol) in DMF (10 mL) under nitrogen atmosphere was added sodium hydride (10.5 mg, 1.1 eq.) at room temperature. The reaction mixture was stirred for 10-15 min. After complete conversion, water was added, and the resulting mixture was extracted with ethyl acetate (3 × 20 mL). The combined extracts were dried over MgSO₄, and evaporated to give the crude product which was subsequently chromatographed on silica gel eluting with ethyl acetate/hexane (1:4) to give 2-phenylpyrazolo[5',1':3,4]pyrazino[1,2-*a*]indole (**407**) (102 mg, 0.36 mmol, 90%) as a white solid, mp.: 218–220 °C.

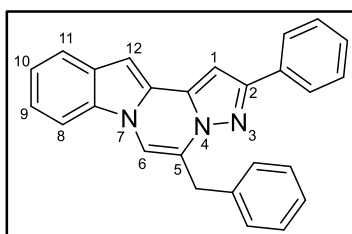


¹H NMR (400 MHz, CDCl₃) δ 7.91 – 7.85 (m, 2H, arom.), 7.73 (dd, *J* = 6.7, 1.6 Hz, 1H, H-11), 7.65 (bd, *J* = 7.9 Hz, 1H, H-8), 7.56 (d, A part of the AB system, *J* = 6.1 Hz, 1H, H-6), 7.54 (d, B part of

the AB system, $J = 6.1$ Hz, 1H, H-5), 7.40 (t, $J = 7.5$ Hz, 2H, arom.), 7.35 - 7.23 (m, 3H, arom.), 7.05 (s, 1H, H-12), 6.94 (s, 1H, H-1). ^{13}C NMR (100 MHz, CDCl_3) δ 153.1, 133.7, 132.6, 131.7, 129.0, 128.8, 128.5, 126.6, 126.2, 122.6, 122.3, 121.3, 111.7, 110.3, 109.7, 97.3, 95.8. IR (ATR, cm^{-1}) 3099, 3050, 2990, 2901. HRMS Calcd for $(\text{C}_{19}\text{H}_{13}\text{N}_3)$ $[\text{M} + \text{H}]^+$: 284.11822; Found: 284.11867.

4.48 5-Benzyl-2-phenylpyrazolo[5',1':3,4]pyrazino[1,2-*a*]indole (404c)

A solution of 2-(3-phenyl-1H-pyrazol-5-yl)-1-(3-phenylprop-2-yn-1-yl)-1H-indole (**396c**) (0.149 g, 0.4 mmol) in DMF (10 mL) under nitrogen atmosphere was added sodium hydride (10.5 mg, 1.1 eq.) at room temperature. The reaction mixture was stirred for 10-15 min. After complete conversion, water was added, and the resulting mixture was extracted with ethyl acetate (3×20 mL). The combined extracts were dried over MgSO_4 , and evaporated to give the crude product which was subsequently chromatographed on silica gel eluting with ethyl acetate/hexane (1:4) to give 5-benzyl-2-phenylpyrazolo[5',1':3,4]pyrazino[1,2-*a*]indole (**404c**) (135 mg, 0.36 mmol, 90%) as a white solid, mp.: 141 - 143 °C.

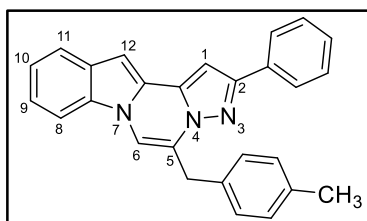


^1H NMR (400 MHz, CDCl_3) δ 7.87 (d, $J = 7.2$ Hz, 2H, arom.), 7.65 (dd, $J = 5.8, 2.5$ Hz, 1H), 7.41 - 7.35 (m, 5H), 7.29 (t, $J = 7.6$ Hz, 3H), 7.24 - 7.14 (m, 3H), 6.97 (d, $J = 7.4$ Hz, 2H), 6.80 (s, 1H), 4.31 (s, 2H, CH_2). ^{13}C NMR (100 MHz, CDCl_3) δ 150.7, 135.2,

132.0, 131.4, 129.7, 128.1, 127.9, 127.16, 127.13, 126.7, 125.5, 124.8, 124.6, 122.6, 120.7, 120.2, 119.5, 108.1, 106.7, 95.8, 93.0, 33.1. IR (ATR, cm^{-1}) 3093, 3062, 3025, 2956, 2920, 2847, 1451, 1069. HRMS Calcd for $(\text{C}_{26}\text{H}_{19}\text{N}_3)$ $[\text{M} + \text{H}]^+$: 374.16517; Found: 374.16611.

4.49 5-(4-methylbenzyl)-2-phenylpyrazolo[5',1':3,4]pyrazino[1,2-*a*]indole (404d)

A solution of 2-(3-phenyl-1*H*-pyrazol-5-yl)-1-(3-(*p*-tolyl)prop-2-yn-1-yl)-1*H*-indole (**396d**) (0.155 g, 0.4 mmol) in DMF (10 mL) under nitrogen atmosphere was added sodium hydride (10.5 mg, 1.1 equiv.) at room temperature. The reaction mixture was stirred for 10-15 min. After complete conversion, water was added, and the resulting mixture was extracted with ethyl acetate (3 × 20 mL). The combined extracts were dried over MgSO₄, and evaporated to give the crude product which was subsequently chromatographed on silica gel eluting with ethyl acetate/hexane (1:10) to give 5-(4-methylbenzyl)-2-phenylpyrazolo[5',1':3,4]pyrazino[1,2-*a*]indole (**404d**) (124 mg, 0.32 mmol, 80%) as a white solid, mp.: 163–165 °C.

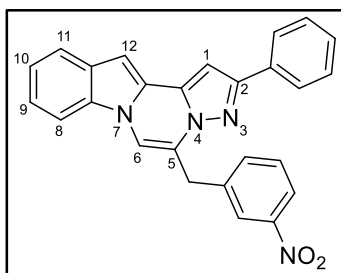


¹H NMR (400 MHz, CDCl₃) δ 7.91 - 7.88 (m, 2H, arom.), 7.70 - 7.66 (m, 1H, H-11), 7.50 - 7.45 (m, 1H, H-8), 7.39 (t, *J* = 7.5 Hz, 2H, arom.), 7.32 - 7.25 (m, A part of the AA'BB' system, and 3H, arom.), 7.24 - 7.17 (m, 2H, arom.), 7.12 (m, B part of the AA'BB' system, 2H, arom.), 7.05 (s, 1H, H-12), 7.03 (bs, 1H, H-1), 6.86 (bs, 1H, H-6), 4.32 (s, 2H, CH₂), 2.30 (s, 3H, CH₃). **¹³C NMR** (100 MHz, CDCl₃) δ 152.3, 136.6, 133.6, 133.6, 133.0, 131.3, 129.6, 129.4, 128.7, 128.3, 126.4, 126.21, 126.17, 124.5, 122.2, 121.7, 121.0, 109.7, 108.2, 97.4, 94.5, 34.2, 21.1. **IR (ATR, cm⁻¹)** 3053, 3020, 2956, 2917, 2847, 1456. **HRMS** Calcd for (C₂₇H₂₁N₃) [M + H]⁺: 388.18082; Found: 388.18153.

4.50 5-(3-nitrobenzyl)-2-phenylpyrazolo[5',1':3,4]pyrazino[1,2-*a*]indole (404e)

A solution of 1-(3-(3-nitrophenyl)prop-2-yn-1-yl)-2-(3-phenyl-1*H*-pyrazol-5-yl)-1*H*-indole (**396e**) (0.167 g, 0.4 mmol) in DMF (10 mL) under nitrogen atmosphere was added sodium hydride (10.5 mg, 1.1 eq.) at room temperature. The reaction mixture was stirred for 10-15 min. After complete conversion, water was added,

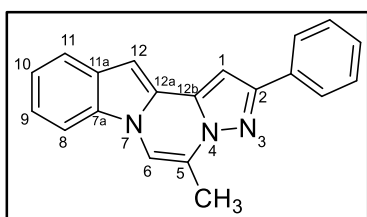
and the resulting mixture was extracted with ethyl acetate (3 × 20 mL). The combined extracts were dried over MgSO₄, and evaporated to give the crude product which was subsequently chromatographed on silica gel eluting with ethyl acetate/hexane (1:4) to give 5-(3-nitrobenzyl)-2-phenylpyrazolo[5',1':3,4]pyrazino[1,2-*a*]indole (**404e**) (155 mg, 0.37 mmol, 93%) as a yellow solid, mp.: 219–221 °C.



¹H NMR (400 MHz, CDCl₃) δ 8.39 (t, *J* = 1.9 Hz, 1H, arom.), 8.07 (dd, *J* = 7.8, 1.9 Hz, 1H, arom.), 7.88 (d, *J* = 7.2 Hz, 2H, arom.), 7.80 (d, *J* = 7.8 Hz, 1H, arom.), 7.76 – 7.69 (m, 1H, arom.), 7.62 (d, *J* = 7.2 Hz, 1H, arom.), 7.45 (t, *J* = 7.8 Hz, 1H, arom.), 7.43 – 7.37 (m, 3H, arom.), 7.34 – 7.24 (m, 3H, arom.), 7.07 (s, 1H, H-12), 6.92 (s, 1H, H-1). **¹³C NMR** (100 MHz, CDCl₃) δ 152.6, 148.4, 139.5, 135.5, 133.7, 132.7, 131.4, 129.4, 128.8, 128.5, 126.3, 126.1, 126.1, 124.5, 122.6, 122.2, 122.15, 121.23, 121.2, 109.7, 108.5, 97.6, 95.2, 34.6. **IR (ATR, cm⁻¹)** 2971, 2920, 2847, 1526, 1456, 1346. **HRMS** Calcd for (C₂₆H₁₈N₄O₂) [M + H]⁺: 419.15025; Found: 419.14975.

4.51 5-methyl-2-phenylpyrazolo[5',1':3,4]pyrazino[1,2-*a*]indole (**404a**)

A solution of 2-(3-phenyl-1*H*-pyrazol-5-yl)-1-(prop-2-yn-1-yl)-1*H*-indole (**396a**) (0.118 g, 0.4 mmol) in acetonitrile (10 mL) under nitrogen atmosphere was added dropwise a solution of gold trichloride (3 mg, 2.5 mmol %) in acetonitrile (1 mL) at room temperature. The reaction mixture was stirred for 24 h. After completion of the reaction monitored by TLC, the solvent was evaporated. The residue was chromatographed on silica gel eluting with ethyl acetate/hexane (1:4) to give 5-methyl-2-phenylpyrazolo[5',1':3,4]pyrazino[1,2-*a*]indole (**404a**) (103 mg, 0.35 mmol, 87%) as a white solid, from EtOAc/*n*-hexane mp.: 125–127 °C.

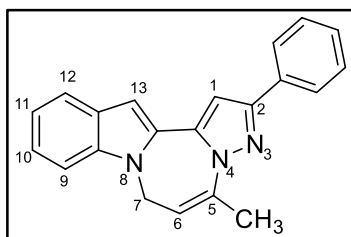


¹H NMR (400 MHz, CDCl₃) δ 7.91–7.86 (m, 2H), 7.70–7.67 (m, 1H), 7.58–7.56 (m, 1H), 7.37 (bt, *J* = 7.5 Hz, 2H), 7.29 (tt, *J* = 7.4, 1.2 Hz, 1H), 7.28 (d, *J* = 1.1 Hz, 1H), 7.25–7.21 (m, 2H), 7.00 (s, 1H), 6.83

(bs, 1H), 2.56 (d, $J = 1.1$ Hz, 3H); ^{13}C NMR (100 MHz, CDCl_3) δ 152.5, 133.7, 133.0, 131.1, 128.8, 128.6, 128.3, 126.5, 126.2, 122.2, 121.7, 121.1, 120.4, 109.7, 107.3, 97.4, 94.4, 14.9; IR (ATR, cm^{-1}) 2988, 2968, 2922, 2901, 2358, 1507, 1456, 1078; HRMS Calcd for ($\text{C}_{20}\text{H}_{15}\text{N}_3$) $[\text{M} + \text{H}]^+$: 298.13387; Found: 298.13805.

4.52 5-Methyl-2-phenyl-7H-pyrazolo[5',1':3,4][1,4]diazepino[1,2-a]indole (408b)

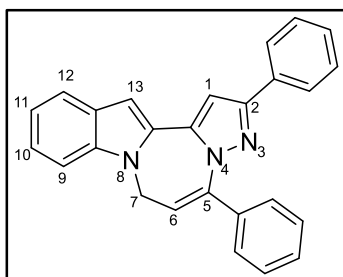
A solution of 1-(but-2-yn-1-yl)-2-(3-phenyl-1H-pyrazol-5-yl)-1H-indole (**396b**) (0.125 g, 0.4 mmol) in acetonitrile (10 mL) under nitrogen atmosphere was added dropwise a solution of gold trichloride (3 mg, 2.5 mmol%) in acetonitrile (1 mL) at room temperature. The reaction mixture was stirred for 12 h. After completion of the reaction monitored by TLC, the solvent was evaporated. The residue was chromatographed on silica gel eluting with ethyl acetate/hexane (1:5) to give 5-methyl-2-phenyl-7H-pyrazolo[5',1':3,4][1,4]diazepino[1,2-a]indole (**408b**) (111 mg, 0.36 mmol, 89%) as a white solid, mp.: 109–111 °C.



^1H NMR (400 MHz, CDCl_3) δ 7.87 – 7.82 (m, 2H, arom.), 7.59 (dt, $J_{12-11} = 8.0$, and $J_{12-10} = J_{12-13} = 1.0$ Hz, 1H, H-12), 7.41 – 7.35 (m, 2H, arom.), 7.34 – 7.27 (m, 2H, arom.), 7.19 (ddd, $J_{10-9} = 8.2$, $J_{10-11} = 7.0$, and $J_{10-12} = 1.0$ Hz, 1H, H-10), 7.06 (ddd, $J_{11-12} = 8.0$, $J_{11-10} = 7.0$, and $J_{11-9} = 1.0$ Hz, 1H, H-11), 6.93 (s, 1H, H-13), 6.79 (s, 1H, H-1), 5.66 (tq, $J = 7.2, 1.2$ Hz, 1H, H-6), 4.59 (d, $J = 7.2$ Hz, 1H, CH_2), 2.35 (d, $J = 1.0$ Hz, 3H, CH_3). ^{13}C NMR (101 MHz, CDCl_3) δ 151.8, 142.2, 138.9, 135.8, 132.6, 129.4, 128.7, 128.3, 127.9, 125.9, 122.4, 121.2, 120.0, 110.6, 108.9, 104.0, 101.7, 39.1, 21.0. IR (ATR, cm^{-1}) 2959, 2918, 2850, 1710, 1455, 734, 692. HRMS Calcd for ($\text{C}_{21}\text{H}_{17}\text{N}_3$) $[\text{M} + \text{H}]^+$: 312.14952; Found: 312.14935.

4.53 2,5-diphenyl-7H-pyrazolo[5',1':3,4][1,4]diazepino[1,2-a]indole (408c)

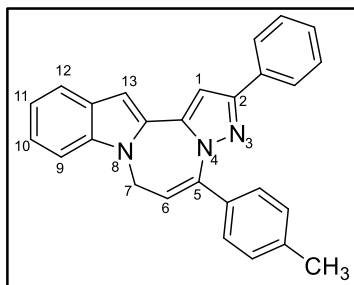
A solution of 2-(3-phenyl-1H-pyrazol-5-yl)-1-(3-phenylprop-2-yn-1-yl)-1H-indole (**396c**) (0.149 g, 0.4 mmol) in acetonitrile (10 mL) under nitrogen atmosphere was added dropwise a solution of gold trichloride (3 mg, 2.5 mmol%) in acetonitrile (1 mL) at room temperature. The reaction mixture was stirred for 8 h. After completion of the reaction monitored by TLC, the solvent was evaporated. The residue was chromatographed on silica gel eluting with ethyl acetate/hexane (1:4) to give 2,5-diphenyl-7H-pyrazolo[5',1':3,4][1,4]diazepino[1,2-a]indole (**408c**) (123 mg, 0.33 mmol, 83%) as a powdered white solid from EtOAc/n-hexane, mp.: 211–213 °C.



¹H NMR (400 MHz, CDCl₃) δ 7.90 – 7.84 (m, 2H, arom.), 7.73 (d, J = 7.9 Hz, 1H, arom.), 7.48 – 7.35 (m, 9H, arom.), 7.34 – 7.29 (m, 1H, arom.) 7.18 (t, J = 7.4 Hz, 1H, arom.), 7.10 (s, 1H, H-13), 6.98 (s, 1H, H-1), 6.15 (t, J = 7.6 Hz, 1H, H-6), 4.85 (d, J = 7.6 Hz, 2H, H-7). **¹³C NMR** (100 MHz, CDCl₃) δ 152.2, 145.7, 140.3, 136.5, 135.9, 132.5, 129.13, 129.11, 128.6, 128.4, 128.3, 128.1, 127.8, 126.1, 122.6, 121.3, 120.1, 113.9, 108.9, 104.3, 101.9, 39.1. **IR (ATR, cm⁻¹)** 3650, 2988, 2971, 2918, 2901, 2358, 1456, 1076. **HRMS** Calcd for (C₂₆H₁₉N₃) [M + H]⁺: 374.16517; Found: 374.16797.

4.54 2-phenyl-5-(p-tolyl)-7H-pyrazolo[5',1':3,4][1,4]diazepino[1,2-a]indole (408d)

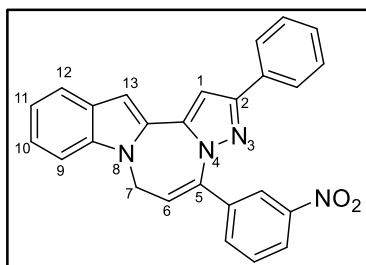
A solution of 2-(3-phenyl-1H-pyrazol-5-yl)-1-(3-(p-tolyl)prop-2-yn-1-yl)-1H-indole (**396d**) (0.155 g, 0.4 mmol) in acetonitrile (10 mL) under nitrogen atmosphere was added dropwise a solution of gold trichloride (3 mg, 2.5 mmol%) in acetonitrile (1 mL) at room temperature. The reaction mixture was stirred for 8 h. After completion of the reaction monitored by TLC, the solvent was evaporated. The residue was chromatographed on silica gel eluting with ethyl acetate/hexane (1:4) to give 2-phenyl-5-(p-tolyl)-7H-pyrazolo[5',1':3,4][1,4]diazepino[1,2-a]indole (**408d**) (124 mg, 0.32 mmol, 80%) as a white solid, mp.: 142–144 °C.



¹H NMR (400 MHz, CDCl₃) δ 7.79 – 7.74 (m, 2H, arom.), 7.61 (d, $J = 7.9$ Hz, 1H, H-12), 7.37 – 7.29 (m, 3H, arom.), 7.28 – 7.25 (m, 1H, arom.), 7.23 – 7.15 (m, 5H, arom.), 7.09 – 7.04 (m, 3H, arom.), 6.97 (s, 1H, H-13), 6.85 (s, 1H, H-1), 6.00 (t, $J = 7.6$ Hz, 1H, H-6), 4.72 (d, $J = 7.6$ Hz, 2H, H-7), 2.28 (s, 3H, CH₃). **¹³C NMR** (100 MHz, CDCl₃) δ 152.1, 145.7, 140.2, 139.1, 135.9, 133.7, 132.6, 129.2, 128.8, 128.6, 128.3, 128.2, 127.8, 126.1, 122.5, 121.3, 120.1, 113.1, 108.9, 104.3, 101.8, 39.1, 21.3. **IR (ATR, cm⁻¹)** 3680, 2988, 2971, 2901, 2356, 1456, 1243, 1080. **HRMS** Calcd for (C₂₇H₂₁N₃) [M + H]⁺: 388.18082; Found: 388.18366.

4.55 5-(3-nitrophenyl)-2-phenyl-7H-pyrazolo[5',1':3,4][1,4]diazepino[1,2-a]indole (408e)

A solution of 1-(3-(3-nitrophenyl)prop-2-yn-1-yl)-2-(3-phenyl-1*H*-pyrazol-5-yl)-1*H*-indole (**396e**) (0.167 g, 0.4 mmol) in acetonitrile (10 mL) under nitrogen atmosphere was added dropwise a solution of gold trichloride (3 mg 2.5 mmol%) in acetonitrile (1 mL) at room temperature. The reaction mixture was stirred for 8 h. After completion of the reaction monitored by TLC, the solvent was evaporated. The residue was chromatographed on silica gel eluting with ethyl acetate/hexane (1:4) to give 5-(3-nitrophenyl)-2-phenyl-7*H*-pyrazolo[5',1':3,4][1,4]diazepino[1,2-*a*]indole (**408e**) (138 mg, 0.33 mmol, 83%) as a yellow solid, mp.: 118–120 °C.



¹H NMR (400 MHz, CDCl₃) δ 8.25 (t, $J = 1.7$ Hz, 1H, arom.), 8.17 (dt, $J = 8.1$, and 1.0 Hz, 1H, arom.), 7.75 – 7.70 (m, 2H, arom.), 7.64 (d, $J = 7.9$ Hz, 1H, arom.), 7.57 (d, $J = 7.8$ Hz, 1H, arom.), 7.50 – 7.40 (m, 1H, arom.), 7.39 – 7.28 (m, 4H, arom.), 7.24 (t, $J = 7.7$ Hz, 1H, arom.), 7.10 (t, $J = 7.5$ Hz, 1H, arom.), 7.03 (s, 1H, H-13), 6.91 (s, 1H, H-1), 6.17 (t, $J = 7.4$ Hz, 1H, H-6), 4.81 (d, $J = 7.5$ Hz, 2H, H-7). **¹³C NMR** (100 MHz, CDCl₃) δ 152.9, 148.2, 143.7, 140.3, 138.2, 136.0, 134.4, 134.2, 132.2, 129.0, 128.7, 128.6, 127.8, 126.1, 123.9, 123.3, 122.9, 121.4, 120.3, 115.4, 108.9,

104.7, 102.4, 39.0. **IR (ATR, cm⁻¹)** 3680, 2988, 2971, 2901, 2357, 1526, 1455, 1348, 1080. **HRMS** Calcd for (C₂₆H₁₈N₄O₂) [M + H]⁺: 419.15025; Found: 419.15305.

REFERENCES

- (1) Balci, M.; Sütbeyaz, Y.; Secen, H. *Tetrahedron* **1990**, *46*, 3715–3742.
- (2) Gultekin, M. S.; Celik, M.; Balci, M. *Curr. Org. Chem.* **2004**, *8*, 1159–1186.
- (3) Posternak, T. *The cyclitols*; Holden-Day: San Fransisco, 1965.
- (4) Balci, Metin; Sütbeyaz, Yaşar; Seçen, H. *Tetrahedron* **1990**, *46*, 3715–3742.
- (5) Mehta, G.; Ramesh, S. S. *Tetrahedron Lett.* **2001**, *42*, 1987–1990.
- (6) Scherer, J. *J. Lie Ann. Chem.* **1850**, *73*, 322–328.
- (7) Kılbaş, B.; Balci, M. *Tetrahedron* **2011**, *67*, 2355–2389.
- (8) Baran, A.; Balci, M. *J. Org. Chem.* **2009**, *74*, 88–95.
- (9) McCasland, G. E.; Naumann, M. O.; Durham, L. J. *J. Org. Chem.* **1968**, *33*, 4220–4227.
- (10) Salamci, E.; Sec, H.; Su, Y.; Balci, M. *J. Org. Chem.* **1997**, *3263*, 2453–2457.
- (11) Aydın, G.; Savran, T.; Aktaş, F.; Baran, A.; Balci, M. *Org. Biomol. Chem.* **2013**, *11*, 1511–1524.
- (12) Kübler, K. *Arch. Pharm. (Weinheim)*. **1908**, *246*, 620.
- (13) Dangschat, G.; Fisher, H. O. L. *Naturwissenschaften* **1939**, *27*, 756–757.
- (14) Dangschat, G.; Fischer, H. O. L.; MacDonald, D. L. *Carbohydr. Res.* **1987**, *164*, 343–355.
- (15) Nakajima, M.; Tomida, I.; Takei, S. *Chem. Ber.* **1957**, 246–250.
- (16) Knapp, S.; Ornaf, R. M.; Rodriques, K. E. *J. Am. Chem. Soc.* **1983**, *105*, 5494–5495.

- (17) Sütbeyaz, Y.; Seçen, H.; Balci, M. *J. Chem. Soc. Chem. Commun.* **1988**, 25, 1330–1331.
- (18) Ackermann, L.; El Tom, D.; Fürstner, A. *Tetrahedron* **2000**, 56, 2195–2202.
- (19) Kelebekli, L.; Kara, Y.; Balci, M. *Carbohydr. Res.* **2005**, 340, 1940–1948.
- (20) Müller, H. *J. Chem. Soc. Trans.* **1907**, 91, 1780–1793.
- (21) McCasland, G. E.; Horswill, E. C. *J. Am. Chem. Soc.* **1953**, 75, 4020–4026.
- (22) Nagabhushan, T. L. *Can. J. Chem.* **1970**, 48, 383–384.
- (23) Aleksejczyk, R. A.; Berchtold, G. A.; Braun, A. G. *J. Am. Chem. Soc.* **1985**, 107, 2554–2555.
- (24) Seçen, H.; Sütbeyaz, Y.; Balci, M. *Tetrahedron Lett.* **1990**, 31, 1323–1326.
- (25) Akiyama, T.; Shima, H.; Ohnari, M.; Okazaki, T.; Ozaki, S. *Bull. Chem. Soc. Jpn.* **1993**, 66, 3760–3767.
- (26) Cerè, V.; Mantovani, G.; Peri, F.; Pollicino, S.; Ricci, A. *Tetrahedron* **2000**, 56, 1225–1231.
- (27) Cantekin, S.; Çalışkan, R.; Şahin, E.; Balci, M. *Helv. Chim. Acta* **2007**, 90, 2227–2235.
- (28) Reeves, J. M.; McCasland, G. E. *J. Am. Chem. Soc.* **1955**, 7, 1812–1814.
- (29) Yurev, Y.; Zefirov, N. S. *Obs. Khim.* **1961**, 685–686.
- (30) Seçen, H.; Maraş, A.; Sütbeyaz, Y.; Balci, M. *Synth. Commun.* **1992**, 22, 2613–2619.
- (31) Yoshizaki, H.; Bäckvall, J.-E. *J. Org. Chem.* **1998**, 63, 9339–9341.
- (32) Lang, M.; Ziegler, T. *European J. Org. Chem.* **2007**, 5, 768–776.
- (33) Angyal, S. J.; Gilham, P. T. *J. Chem. Soc.* **1958**, 375–379.
- (34) Criegee, R.; Becher, P.; Criegee, R.; Becher, P. *Chem. Ber.* **1957**, 90, 2516–2521.

- (35) Carless, H. A. J.; Oak, O. Z. *Tetrahedron Lett.* **1989**, *30*, 1719–1720.
- (36) Carless, H. A. J.; Oak, O. Z. *J. Chem. Soc. Chem. Commun.* **1991**, 61–62.
- (37) Carless, H. a. J.; Busia, K.; Dove, Y.; Malik, S. S. *J. Chem. Soc. Perkin Trans. 1* **1993**, *8*, 2505.
- (38) Kara, Y.; Balçı, M.; Bourne, S. A.; Watson, W. H. *Tetrahedron Lett.* **1994**, *35*, 3349–3352.
- (39) Hudlicky, T.; Price, J. D.; Olivo, H. F. *Synlett* **1991**, *9*, 645–646.
- (40) Takano, S.; Yoshimitsu, T.; Ogasawara, K. *J. Org. Chem.* **1994**, *59*, 54–57.
- (41) Amberg, W.; Bennani, Y. L.; Chadha, R. K.; Crispino, G. A.; Davis, W. D.; Hartung, J.; Jeong, K. S.; Ogino, Y.; Shibata, T.; Sharpless, K. B. *J. Org. Chem.* **1993**, *58*, 844–849.
- (42) Maras, A.; Secen, H.; Sutbeyaz, Y.; Balci, M. *Turk. J. Chem.* **1996**, *20*, 341–344.
- (43) Finn, K. J.; Collins, J.; Hudlicky, T. *Tetrahedron* **2006**, *62*, 7471–7476.
- (44) Plouvier, V. *C. R. Hebd. Seances Acad. Sci.* **1962**, 360–362.
- (45) Mgani, Q. a; Klunder, A. J. .; Nkunya, M. H. .; Zwanenburg, B. *Tetrahedron Lett.* **1995**, *36*, 4661–4664.
- (46) Freeman, S.; Hudlicky, T. *Bioorg. Med. Chem. Lett.* **2004**, *14*, 1209–1212.
- (47) Ekmekci, Z.; Balci, M. *European J. Org. Chem.* **2012**, *26*, 4988–4995.
- (48) Cantekin, S. The Development of The Novel Synthesis for Conduritols, Middle East Technical University, 2006.
- (49) Baran, A. Halokonduritoller ve gala-Quersitolün Yeni Yöntemle Sentezi, 2003.
- (50) Legler, G. *Affinity labeling; Methods in Enzymology*; Elsevier, 1977; Vol. 46.
- (51) Guo, Z.; Haines, A. H.; Pyke, S. M.; Pyke, S. G.; Taylor, R. J. K. *Carbohydr.*

- Res.* **1994**, *264*, 147–153.
- (52) Hudlicky, T.; Luna, H.; Olivo, H. F.; Andersen, C.; Nugent, T.; Price, J. D. *J. Chem. Soc. Perkin Trans. 1* **1991**, 2907.
- (53) Jung, P.; Motherwell, W.; Williams, A. *Chem. Commun.* **1997**, *14*, 1283–1284.
- (54) Baran, A.; Kazaz, C.; Seçen, H.; Sütbeyaz, Y. *Tetrahedron* **2003**, *59*, 3643–3648.
- (55) Baran, A.; Kazaz, C.; Seçen, H.; Sec, H. *Tetrahedron* **2004**, *60*, 861–866.
- (56) Cantekin, S.; Baran, A.; Çalışkan, R.; Balci, M. *Carbohydr. Res.* **2009**, *344*, 426–431.
- (57) ITUO, K.; FUMIO, Y.; TOSHIKAZU, N.; TADASHI, F.; YOSHIHISA, N.; HIDEKI, T. Inhibitory Agent of An Increase in Blood Sugar Level. EP0474358 (A2), March 11, 1992.
- (58) Billington, D. C.; Perron-Sierra, F.; Picard, I.; Beaubras, S.; Duhault, J.; Espinal, J.; Challal, S. *Bioorg. Med. Chem. Lett.* **1994**, *4*, 2307–2312.
- (59) Mehta, G.; Lakshminath, S. *Tetrahedron Lett.* **2000**, *41*, 3509–3512.
- (60) Fellows, L. E.; Nash, R. J. *Sci. Prog.* **1990**, *74*, 245–255.
- (61) Falshaw, A.; Hart, J. B.; Tyler, P. C. *Carbohydr. Res.* **2000**, *329*, 301–308.
- (62) Pandey, S.; Sree, A.; Dash, S. S.; Sethi, D. P. *BMC Microbiol.* **2013**, *13*, 55.
- (63) Hudlicky, T.; Olivo, H. F. *J. Am. Chem. Soc.* **1992**, *114*, 9694–9696.
- (64) Lambert, W. T.; Hanson, G. H.; Benayoud, F.; Burke, S. D. *J. Org. Chem.* **2005**, *70*, 9382–9398.
- (65) Datema, R.; Romero, P. A.; Legler, G.; Schwarz, R. T. *Proc. Natl. Acad. Sci.* **1982**, *79*, 6787–6791.
- (66) Legler, G.; Bieberich, E. *Arch. Biochem. Biophys.* **1988**, *260*, 437–442.
- (67) Brutcher, F. V.; Vara, F. J.; Moore, A. E. *J. Am. Chem. Soc.* **1956**, *78*, 5695–

5696.

- (68) Banwell, M. G.; Ebenbeck, W.; Edwards, A. J. *J. Chem. Soc. Perkin Trans. I* **2001**, 114–117.
- (69) Karplus, M. *J. Am. Chem. Soc.* **1963**, *85*, 2870–2871.
- (70) Balci, M. *Basic ¹H- and ¹³C-NMR Spectroscopy*; Elsevier, 2005.
- (71) Schenck, G. O.; Eggert, H.; Denk, W. *Justus Liebigs Ann. Chem.* **1953**, *584*, 177–198.
- (72) Hoffmann, H. M. R. *Angew. Chemie Int. Ed. English* **1969**, *8*, 556–577.
- (73) Harding, L. B.; Goddard, W. A. *J. Am. Chem. Soc.* **1980**, *102*, 439–449.
- (74) Balcı, M. In *Organik Kimya Reaksiyon Mekanizmaları*; TÜBA: Ankara, 2009; pp. 297–352.
- (75) Makosza, M.; Wawrzyniewicz, M. *Tetrahedron Lett.* **1969**, *10*, 4659–4662.
- (76) Skell, P. S.; Woodworth, R. C. *J. Am. Chem. Soc.* **1956**, *78*, 4496–4497.
- (77) Wong, H. N. C.; Hon, M. Y.; Tse, C. W.; Yip, Y. C.; Tank, J.; Hudlicky, T. *Chem. Rev.* **1989**, *89*, 165–198.
- (78) Tanyeli, C.; Turkut, E.; Akhmedov, İ. M. *Tetrahedron: Asymmetry* **2004**, *15*, 1729–1733.
- (79) Ikawa, T.; Kaneko, H.; Masuda, S.; Ishitsubo, E.; Tokiwa, H.; Akai, S. *Org. Biomol. Chem.* **2015**, *13*, 520–526.
- (80) Zysman-Colman, E.; Arias, K.; Siegel, J. S. *Can. J. Chem.* **2009**, *87*, 440–447.
- (81) Luche, J. L. *J. Am. Chem. Soc.* **1978**, *100*, 2226–2227.
- (82) Gemal, A. L.; Luche, J. L. *J. Am. Chem. Soc.* **1981**, *103*, 5454–5459.
- (83) Paquette, L. A.; Kuo, L. H.; Doyon, J. *J. Am. Chem. Soc.* **1997**, *119*, 3038–3047.
- (84) Wilkinson, compiled by A. D. M. and A. In *IUPAC Compendium of*

Chemical Terminology - The Gold Book; XML on-line corrected version: <http://goldbook.iupac.org> (2006-) created by M. Nic, J. Jirat, B. K. updates compiled by A. J., Ed.; Blackwell Scientific Publications: Oxford (1997), 2014; p. 673.

- (85) Encyclopedia Britannica, Encyclopedia Britannica Online The official website: <http://global.britannica.com/science/heterocyclic-compound> (accessed Oct 11, 2015).
- (86) Eicher, T.; Hauptmann, S.; Speicher, A. *The Chemistry of Heterocycles: Structure, Reactions, Syntheses, and Applications*; 2nd Ed.; Wiley-VCH Verlag GmbH & Co. KGaA: Weinheim, 2003.
- (87) Bartoli, G.; Dalpozzo, R.; Nardi, M. *Chem. Soc. Rev.* **2014**, *43*, 4728–4750.
- (88) Alvarez-Builla, J.; Vaquero, J. J.; Barluenga, J. *Modern Heterocyclic Chemistry*; Wiley-VCH: Weinheim, Germany, 2011.
- (89) Robinson, B. *Chem. Rev.* **1963**, *63*, 373–401.
- (90) Butler, M.; Cabrera, G. M. *J. Mol. Struct.* **2013**, *1043*, 37–42.
- (91) Basceken, S.; Balci, M. *J. Org. Chem.* **2015**, *80*, 3806–3814.
- (92) Yang, C.-G.; Liu, G.; Jiang, B. *J. Org. Chem.* **2002**, *67*, 9392–9396.
- (93) Reybier, K.; Nguyen, T. H. Y.; Ibrahim, H.; Perio, P.; Montrose, A.; Fabre, P.-L.; Nepveu, F. *Bioelectrochemistry* **2012**, *88*, 57–64.
- (94) Bognár, B.; Kálai, T.; Hideg, K. *Synthesis (Stuttg.)* **2008**, 2439–2445.
- (95) Flament, I.; Stoll, M. *Helv. Chim. Acta* **1967**, *50*, 1754–1758.
- (96) Blake, K. W.; Porter, A. E. A.; Sammes, P. G. *J. Chem. Soc. Perkin Trans. I* **1972**, 2494.
- (97) Chandrasekhar, S.; Gopalaiah, K. *Tetrahedron Lett.* **2001**, *42*, 8123–8125.
- (98) Palacios, F.; Retana, A. M. O.; Gil, J. I.; Munain, R. L. *Org. Lett.* **2002**, *4*, 2405–2408.

- (99) Buchi, G.; Galindo, J. *J. Org. Chem.* **1991**, *56*, 2605–2606.
- (100) Abbiati, G.; Arcadi, A.; Bellinazzi, A.; Beccalli, E.; Rossi, E.; Zanzola, S.; Organica, C.; Marchesini, A. *J. Org. Chem.* **2005**, *70*, 4088–4095.
- (101) Smith, S. G.; Sanchez, R.; Zhou, M.-M. *Chem. Biol.* **2014**, *21*, 573–583.
- (102) Menges, N.; Sari, O.; Abdullayev, Y.; Erdem, S. S.; Balci, M. *J. Org. Chem.* **2013**, *78*, 5184–5195.
- (103) Jones, G. B.; Davey, C. L.; Jenkins, T. C.; Kamal, A.; Kneale, G. G.; Neidle, S.; Webster, G. D.; Thurston, D. E. *Anticancer. Drug Des.* **1990**, *5*, 249–264.
- (104) Hsu, M.; Schutt, A.; Holly, M.; Slice, L.; Sherman, M.; Richman, D.; Potash, M.; Volsky, D. *Science (80-.)*. **1991**, *254*, 1799–1802.
- (105) Wu, J.; Tung, J. S.; Thorsett, E. D.; Pleiss, M. A.; Nissen, J. S.; Neitz, J.; Latimer, L. H.; John, V.; Freedman, S.; Britton, T. C.; Audia, J. E.; Reel, J. K.; Mabry, T. E.; Dressman, B. A.; Cwi, C. L.; Droste, J. J.; Henry, S. S.; Mcdaniel, S. L.; Scott, W. L.; Stucky, R. D.; Porter, W. J. Preparation of cycloalkyl, lactam, lactone and related compounds for inhibiting β -amyloid peptide release and/or its synthesis. WO 9828268, 1998.
- (106) Neubert, T.; Numa, M.; Ernst, J.; Clemens, J.; Krenitsky, P.; Liu, M.; Fleck, B.; Woody, L.; Zuccola, H.; Stamos, D. *Bioorg. Med. Chem. Lett.* **2015**, *25*, 1338–1342.
- (107) Reeder, E.; Sternbach, L. H. *J. Org. Chem.* **1961**, *26*, 4936–4941.
- (108) Evans, B. E.; Rittle, K. E.; Bock, M. G. *J. Med. Chem.* **1988**, *31*, 2235–2246.
- (109) Dömling, a; Ugi, I. *Angew. Chem. Int. Ed. Engl.* **2000**, *39*, 3168–3210.
- (110) Keating, T. A.; Armstrong, R. W. *J. Am. Chem. Soc.* **1996**, *118*, 2574–2583.
- (111) Keating, T. A.; Armstrong, R. W. *J. Org. Chem.* **1996**, *61*, 8935–8939.
- (112) Maleki, A. *Tetrahedron Lett.* **2013**, *54*, 2055–2059.
- (113) Zhou, Y.; Li, J.; Ji, X.; Zhou, W.; Zhang, X.; Qian, W.; Jiang, H.; Liu, H. *J. Org. Chem.* **2011**, *76*, 1239–1249.

- (114) Tiwari, R. K.; Singh, D.; Singh, J.; Yadav, V.; Pathak, A. K.; Dabur, R.; Chhillar, A. K.; Singh, R.; Sharma, G. L.; Chandra, R.; Verma, A. K. *Bioorg. Med. Chem. Lett.* **2006**, *16*, 413–416.
- (115) Romagnoli, R.; Baraldi, P. G.; Carrion, M. D.; Cara, C. L.; Casolari, A.; Hamel, E.; Fabbri, E.; Gambari, R. *Lett. Drug Des. Discov.* **2010**, *7*, 476–486.
- (116) He, Z.; Bae, M.; Wu, J.; Jamison, T. F. *Angew. Chem. Int. Ed. Engl.* **2014**, *53*, 14451–14455.
- (117) Arban, R.; Bianchi, F.; Buson, A.; Cremonesi, S.; Di Fabio, R.; Gentile, G.; Micheli, F.; Pasquarello, A.; Pozzan, A.; Tarsi, L.; Terreni, S.; Tonelli, F. *Bioorg. Med. Chem. Lett.* **2010**, *20*, 5044–5049.
- (118) Haruta, M. *Nature* **2005**, *437*, 1098–1099.
- (119) Shen, H. C. *Tetrahedron* **2008**, *64*, 7847–7870.
- (120) Hashmi, A. S. K. *Chem. Rev.* **2007**, *107*, 3180–3211.
- (121) Jiménez-Núñez, E.; Echavarren, A. M. *Chem. Rev.* **2008**, *108*, 3326–3350.
- (122) Staben, S. T.; Kennedy-Smith, J. J.; Toste, F. D. *Angew. Chem. Int. Ed. Engl.* **2004**, *43*, 5350–5352.
- (123) Fischer, E.; Speier, A. *Berichte der Dtsch. Chem. Gesellschaft* **1895**, *28*, 3252–3258.
- (124) Kuuloja, N.; Tois, J.; Franzén, R. *Tetrahedron Asymmetry* **2011**, *22*, 468–475.
- (125) Echavarren, A. M. *J. Org. Chem.* **1990**, *55*, 4255–4260.
- (126) Broggini, G.; Bruche, L.; Zecchi, G.; Pilati, T. *J. Chem. Soc. Perkin Trans. I* **1990**, 533–539.
- (127) Bashiardes, G.; Safir, I.; Barbot, F. *Synlett* **2007**, *2007*, 1707–1710.
- (128) Karabatsos, G. J.; Taller, R. A. *Tetrahedron* **1968**, *24*, 3347–3360.

- (129) Devinsky, F.; Lacko, I.; Nagy, A.; Krasnec, L. *Chem. Zvesti* **1978**, *32*, 106–115.
- (130) Wiley, R. H.; Slaymaker, S. C. *J. Am. Chem. Soc.* **1957**, *79*, 2233–2236.
- (131) Sonogashira, K.; Tohda, Y.; Hagihara, N. *Tetrahedron Lett.* **1975**, *16*, 4467–4470.
- (132) Guven, S.; Ozer, M. S.; Kaya, S.; Menges, N.; Balci, M. *Org. Lett.* **2015**, *17*, 2660–2663.
- (133) Hanack, M.; Haßdenteufel, J. R. *Chem. Ber.* **1982**, *115*, 764–771.
- (134) Knorr, L. *Berichte der Dtsch. Chem. Gesellschaft* **1883**, *16*, 2597–2599.
- (135) Bishop, B.; Brands, K.; Gibb, A.; Kennedy, D. *Synthesis (Stuttg.)* **2004**, 43–52.
- (136) Kong, Y.; Tang, M.; Wang, Y. *Org. Lett.* **2014**, *16*, 576–579.
- (137) Baldwin, J. E. *J. Chem. Soc. Chem. Commun.* **1976**, *18*, 734.
- (138) Gilmore, K.; Alabugin, I. V. *Chem. Rev.* **2011**, *111*, 6513–6556.
- (139) Hashmi, a. S. K.; Toste, F. D. *Modern Gold Catalyzed Synthesis*; Hashmi, A. S. K., Toste, F. D., Ed.; First Edit.; Wiley-VCH: Weinheim, Germany, 2012.
- (140) Bascenken, S.; Kaya, S.; Balci, M. *J. Org. Chem.* **2015**, *80*, 12552–12561.
- (141) Furniss, B. S.; Hannaford, A. J.; Smith, P. W. G.; Tatchell, A. R. *Vogel's Textbook of Practical organic chemistry*; 5th Ed.; John Wiley & Sons, 1989.
- (142) Wang, Z.-M.; Kakiuchi, K.; Sharpless, K. B. *J. Org. Chem.* **1994**, *59*, 6895–6897.
- (143) Hancock, a J.; Greenwald, S. M.; Sable, H. Z. *J. Lipid Res.* **1975**, *16*, 300–307.
- (144) Matveenko, M.; Kokas, O. J.; Banwell, M. G.; Willis, A. C. **2007**, 2006–2008.

- (145) Tsotinis, A.; Afroudakis, P. a.; Davidson, K.; Prashar, A.; Sugden, D. *J. Med. Chem.* **2007**, *50*, 6436–6440.
- (146) Jones, G. B.; Moody, C. J.; Padwa, A.; Kassir, J. M. *J. Chem. Soc. Perkin Trans. I* **1991**, 1721–1727.
- (147) Verniest, G.; Padwa, A. *Org. Lett.* **2008**, *10*, 4379–4382.
- (148) Defossa, E.; Heinelt, U.; Klingler, O.; Zoller, G.; Al-Obeidi, F. A.; Walser, A.; Wildgoose, P.; Matter, H. PCT Int. Appl. WO 9933800 A1 19990708, 1999.
- (148) Gaussian 09, Revision **D.01**, Frisch, M. J.; Trucks, G. W.; Schlegel, H. B.; Scuseria, G. E.; Robb, M. A.; Cheeseman, J. R.; Scalmani, G.; Barone, V.; Mennucci, B.; Petersson, G. A.; Nakatsuji, H.; Caricato, M.; Li, X.; Hratchian, H. P.; Izmaylov, A. F.; Bloino, J.; Zheng, G.; Sonnenberg, J. L.; Hada, M.; Ehara, M.; Toyota, K.; Fukuda, R.; Hasegawa, J.; Ishida, M.; Nakajima, T.; Honda, Y.; Kitao, O.; Nakai, H.; Vreven, T.; Montgomery, J. A., Jr.; Peralta, J. E.; Ogliaro, F.; Bearpark, M.; Heyd, J. J.; Brothers, E.; Kudin, K. N.; Staroverov, V. N.; Kobayashi, R.; Normand, J.; Raghavachari, K.; Rendell, A.; Burant, J. C.; Iyengar, S. S.; Tomasi, J.; Cossi, M.; Rega, N.; Millam, M. J.; Klene, M.; Knox, J. E.; Cross, J. B.; Bakken, V.; Adamo, C.; Jaramillo, J.; Gomperts, R.; Stratmann, R. E.; Yazyev, O.; Austin, A. J.; Cammi, R.; Pomelli, C.; Ochterski, J. W.; Martin, R. L.; Morokuma, K.; Zakrzewski, V. G.; Voth, G. A.; Salvador, P.; Dannenberg, J. J.; Dapprich, S.; Daniels, A. D.; Farkas, Ö.; Foresman, J. B.; Ortiz, J. V.; Cioslowski, J.; Fox, D. J. Gaussian, Inc., Wallingford CT, 2009.
- (149) Becke, A. D. *J. Chem. Phys.* 1993, *98*, 5648–5652. (b) Becke, A. D. *J. Chem. Phys.* 1993, *98*, 1372–1377. (c) Lee, C.; Yang, W.; Parr, R. G. *Phys. Rev. B* 1988, *37*, 785–789.
- (150) Hay P. J., Wadt W. R. *J. Chem. Phys.* **1985**, *82*, 299 – 310
- (151) Reed, A. E.; Curtiss, L. A.; Weinhold, F. *Chem. Rev.* **1988**, *88*, 889.
- (152) Foster, J. P.; Weinhold, F. *J. Am. Chem. Soc.* **1980**, *102*, 7211.

APPENDIX A

SPECTRAL DATA

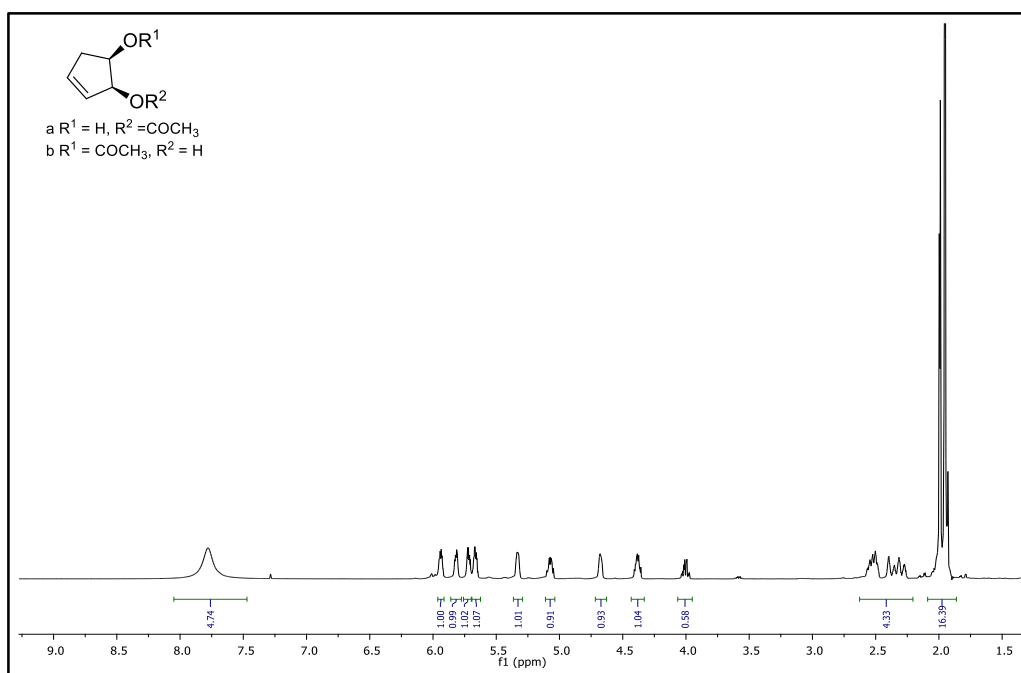


Figure 42. ¹H-NMR Spectrum of Crude Mixture of *cis*-hydroxylation Reaction

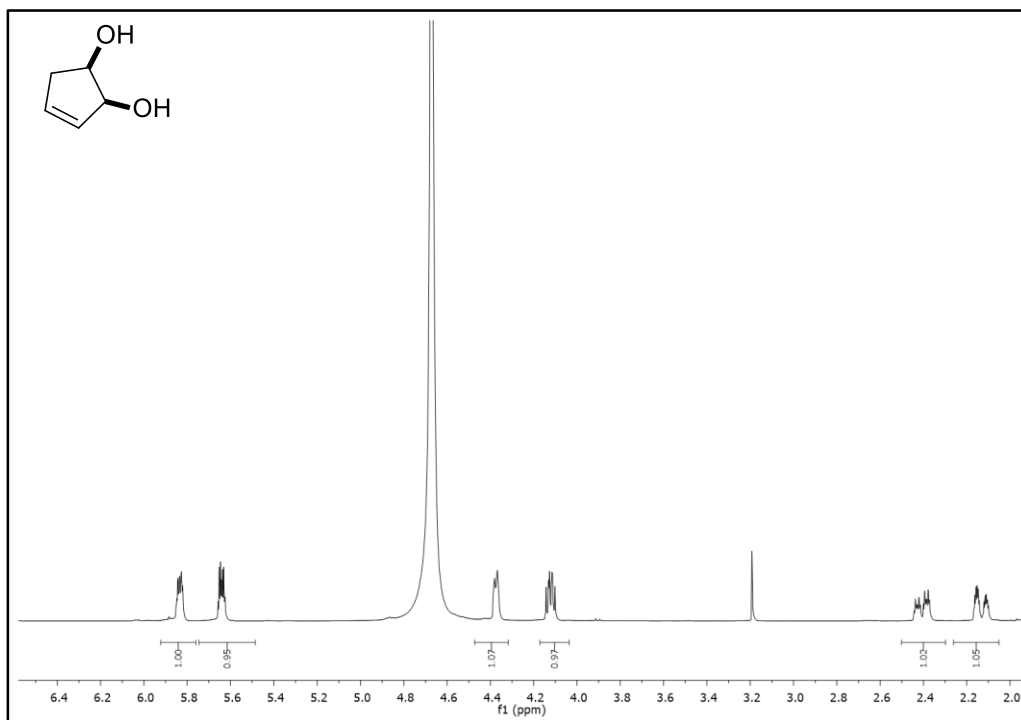


Figure 43. ^1H -NMR Spectrum of Compound **207**

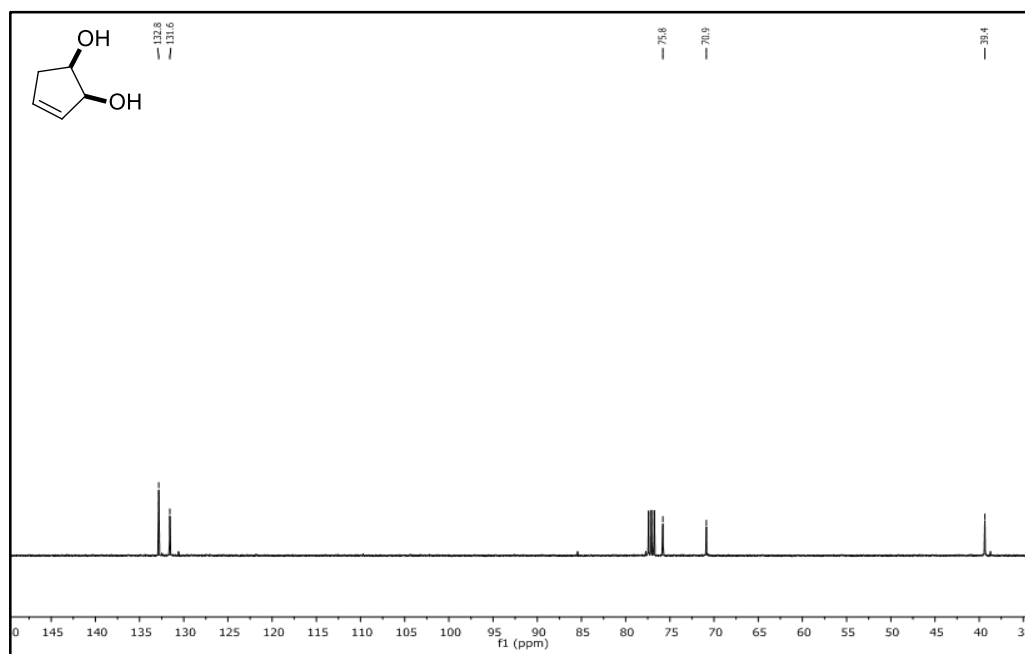


Figure 44. ^{13}C -NMR Spectrum of Compound **207**

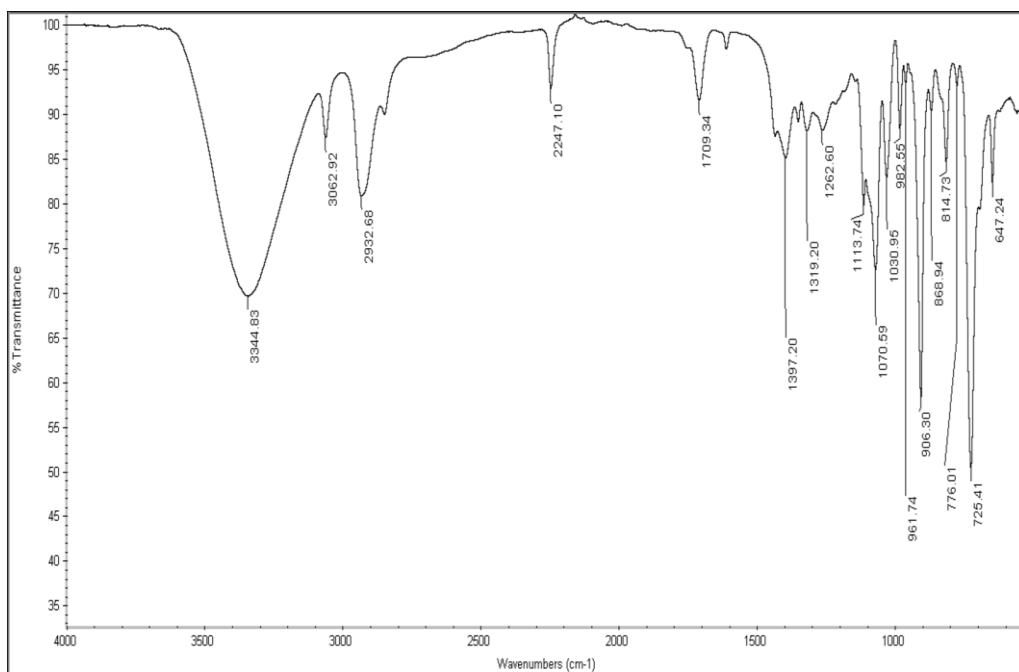


Figure 45. IR Spectrum of Compound 207

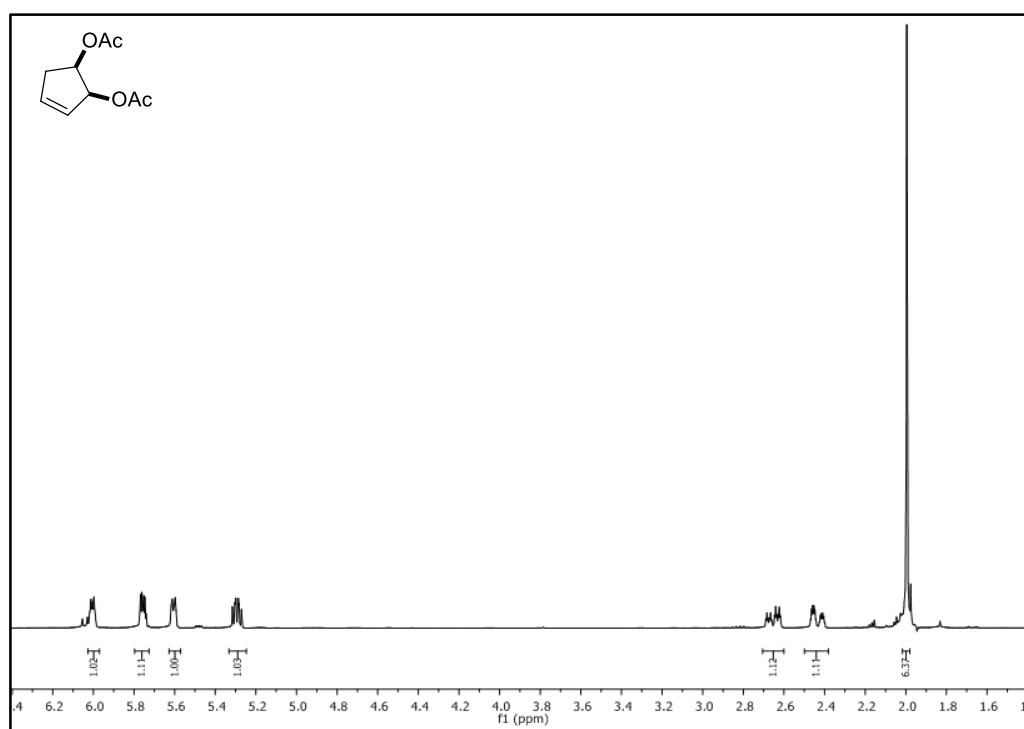


Figure 46. ¹H-NMR Spectrum of Compound 213

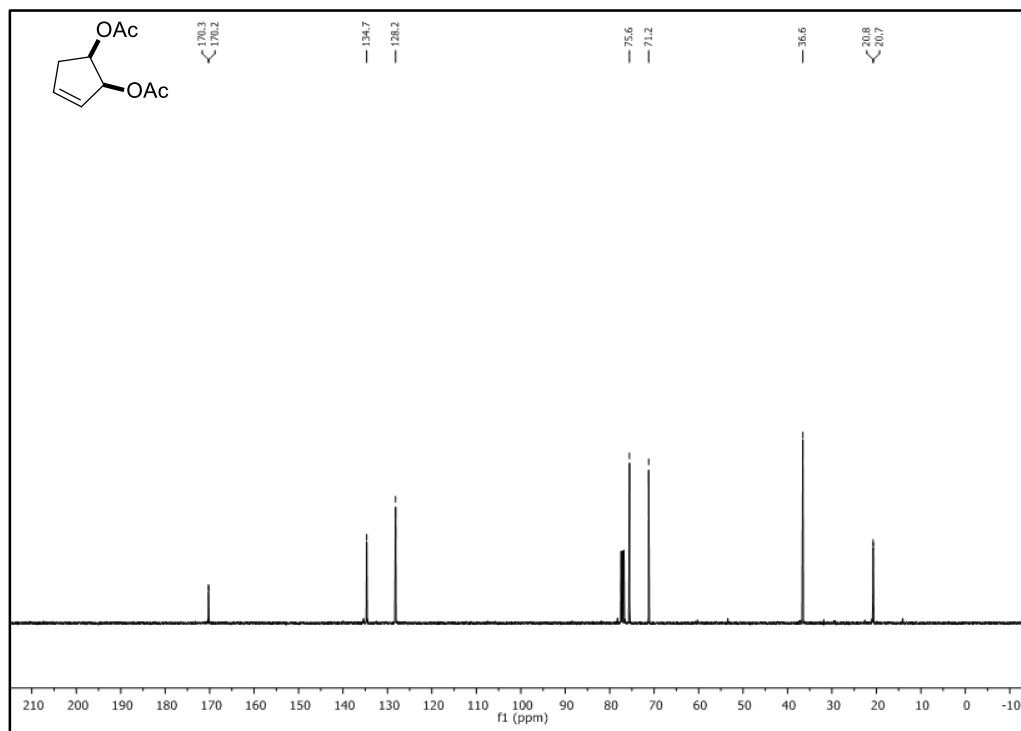


Figure 47. ^{13}C -NMR Spectrum of Compound **213**

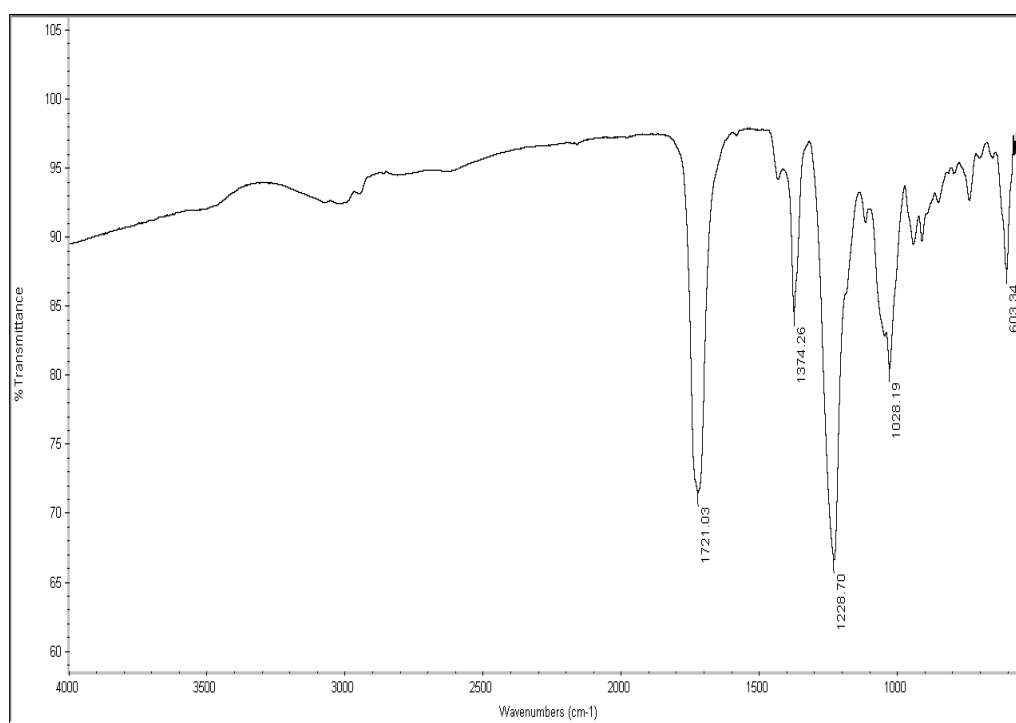


Figure 48. IR Spectrum of Compound **213**

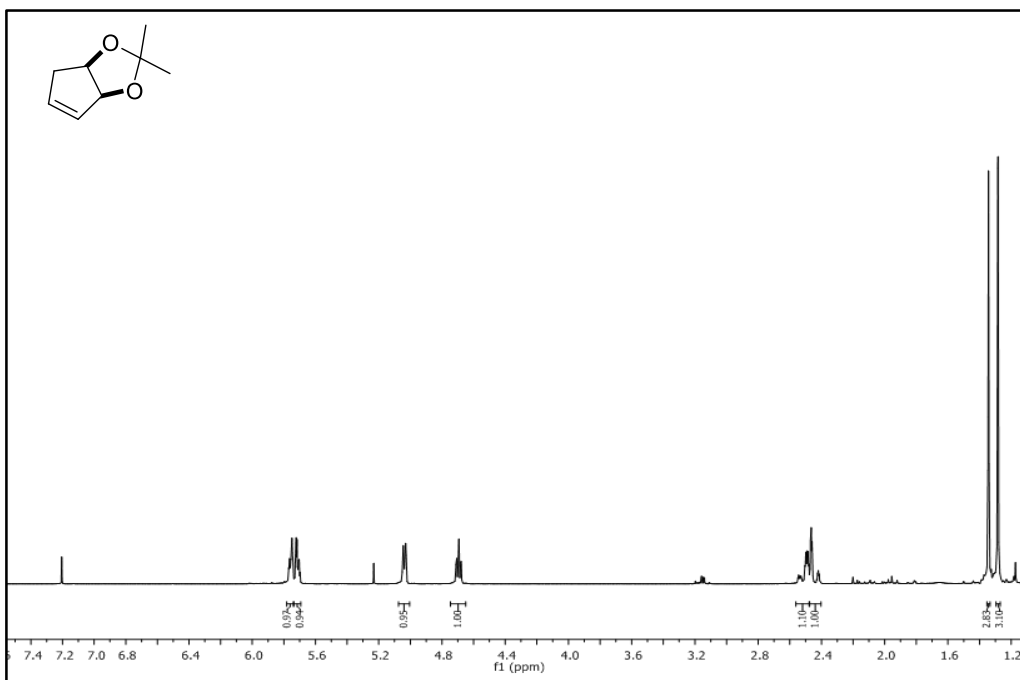


Figure 49. ^1H -NMR Spectrum of Compound 220

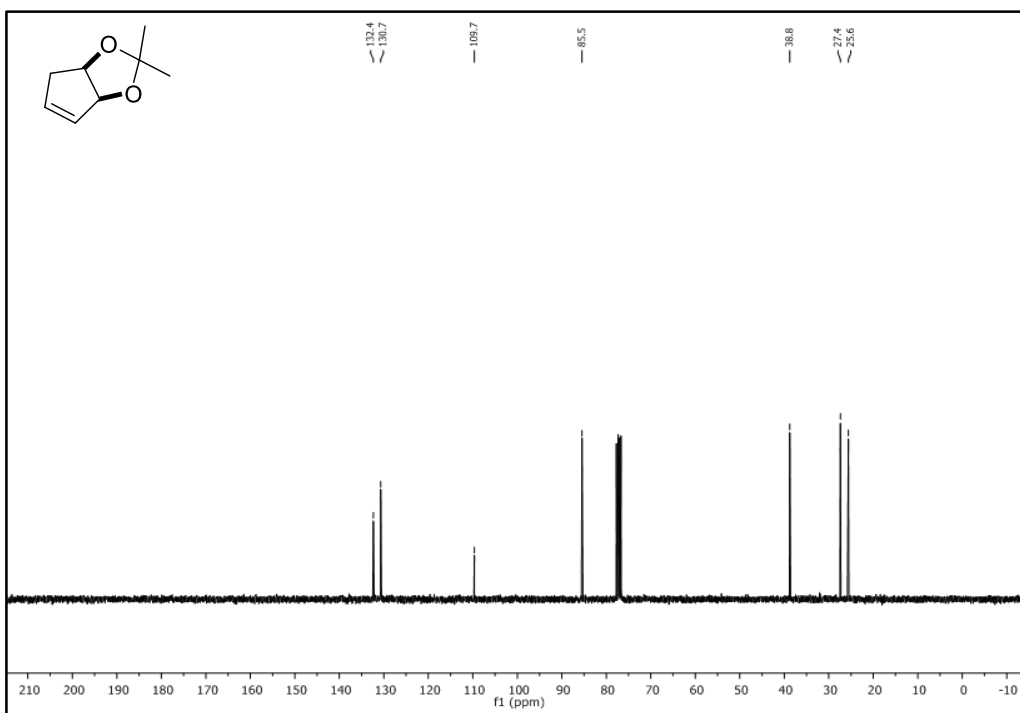


Figure 50. ^{13}C -NMR Spectrum of Compound 220

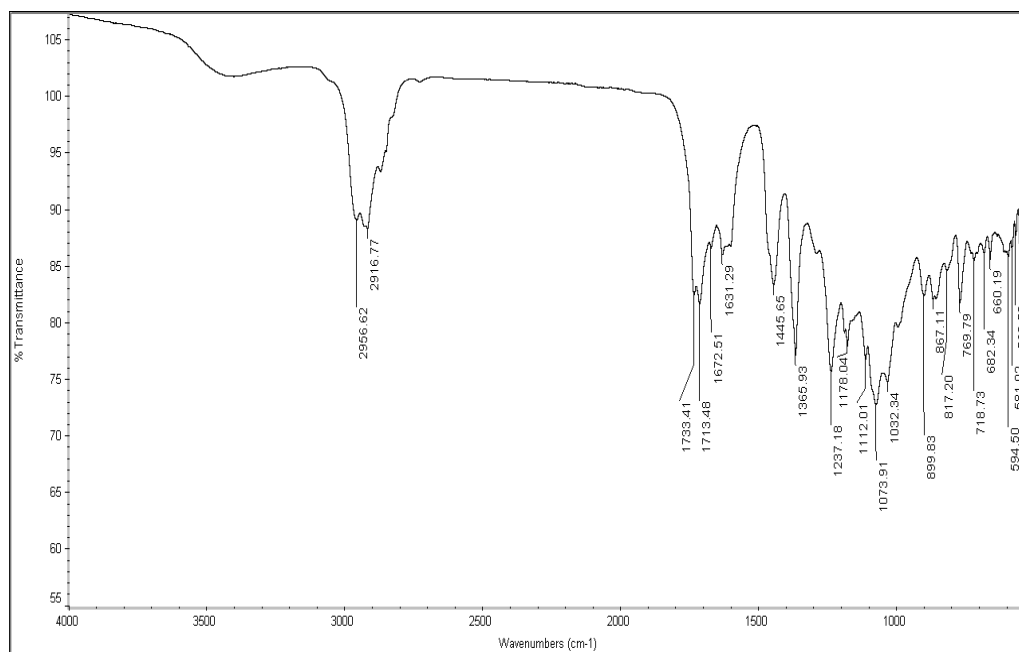


Figure 51. IR Spectrum of Compound **220**

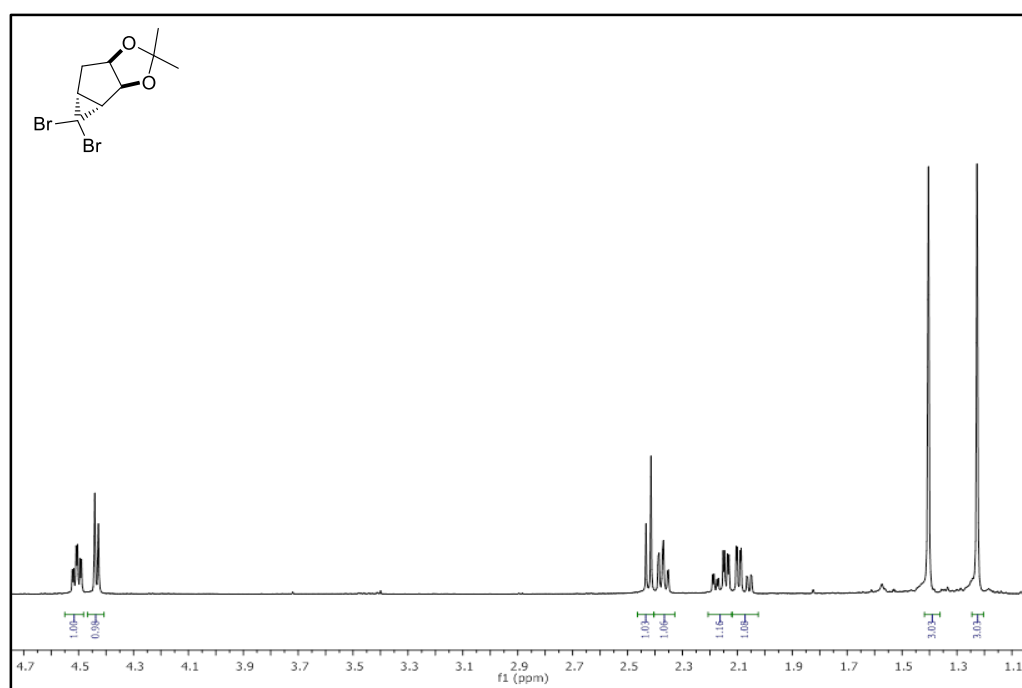


Figure 52. ¹H-NMR Spectrum of Compound **231**

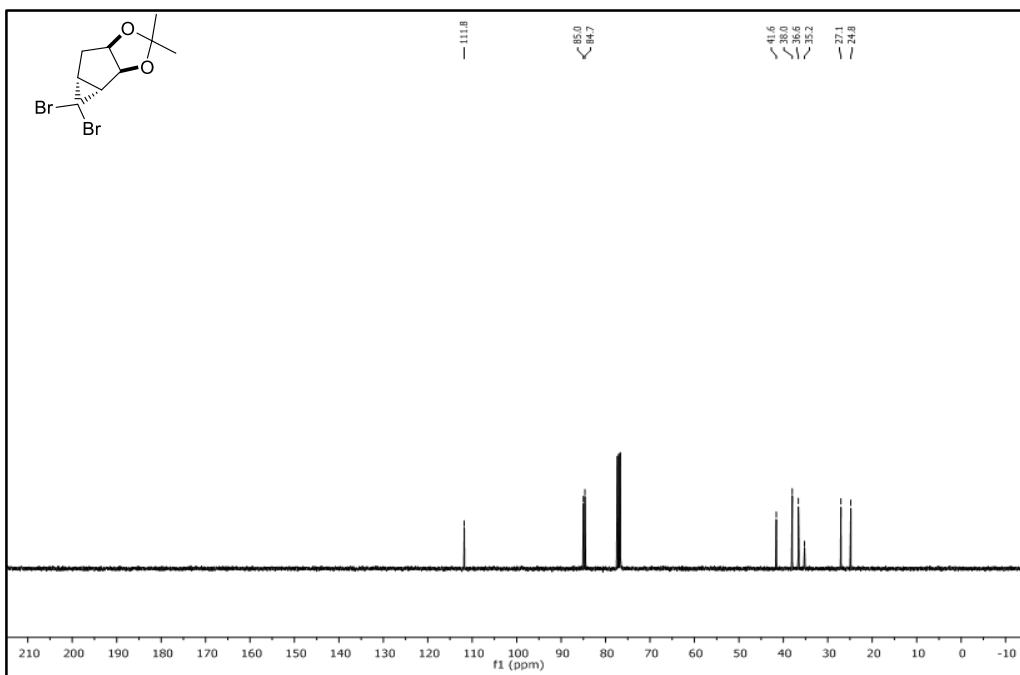


Figure 53. $^{13}\text{C-NMR}$ Spectrum of Compound 231

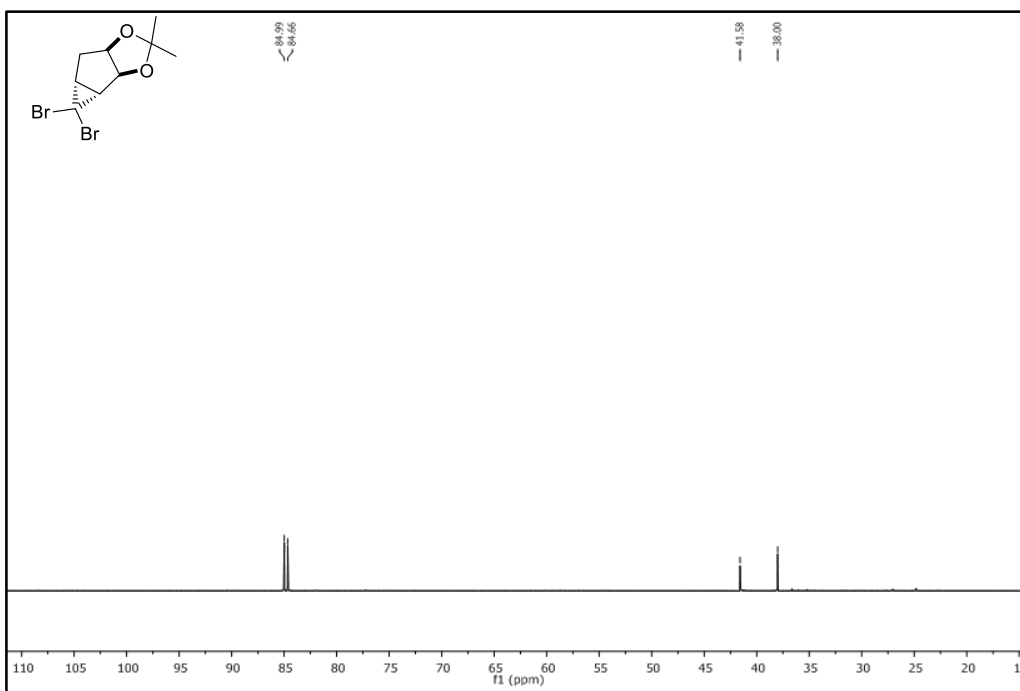


Figure 54. DEPT-90 Spectrum of Compound 231

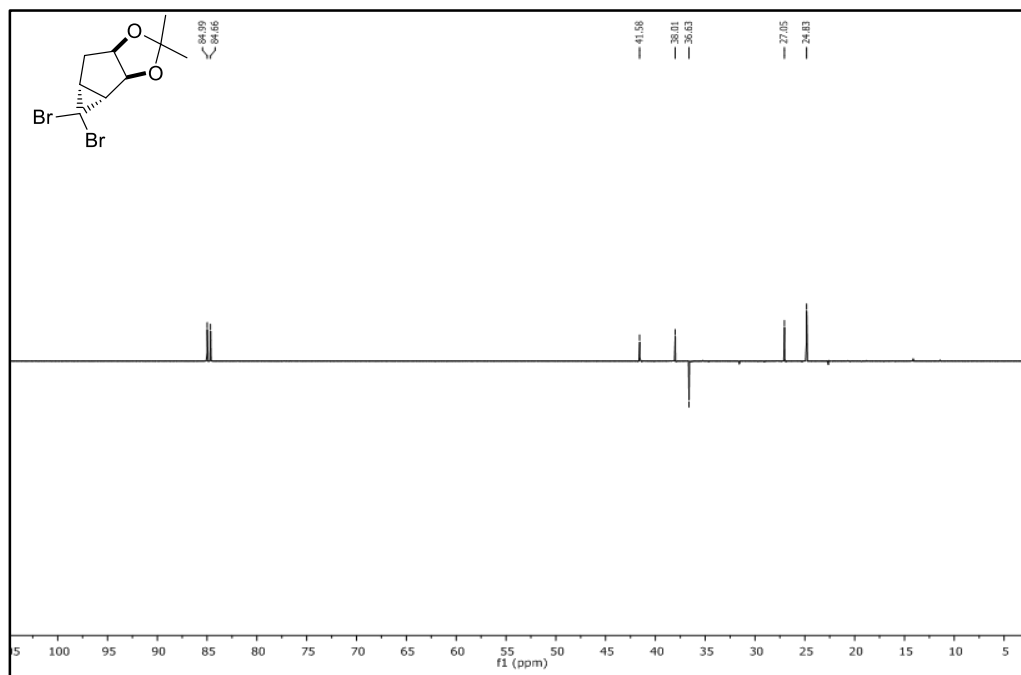


Figure 55. DEPT-135 Spectrum of Compound **231**

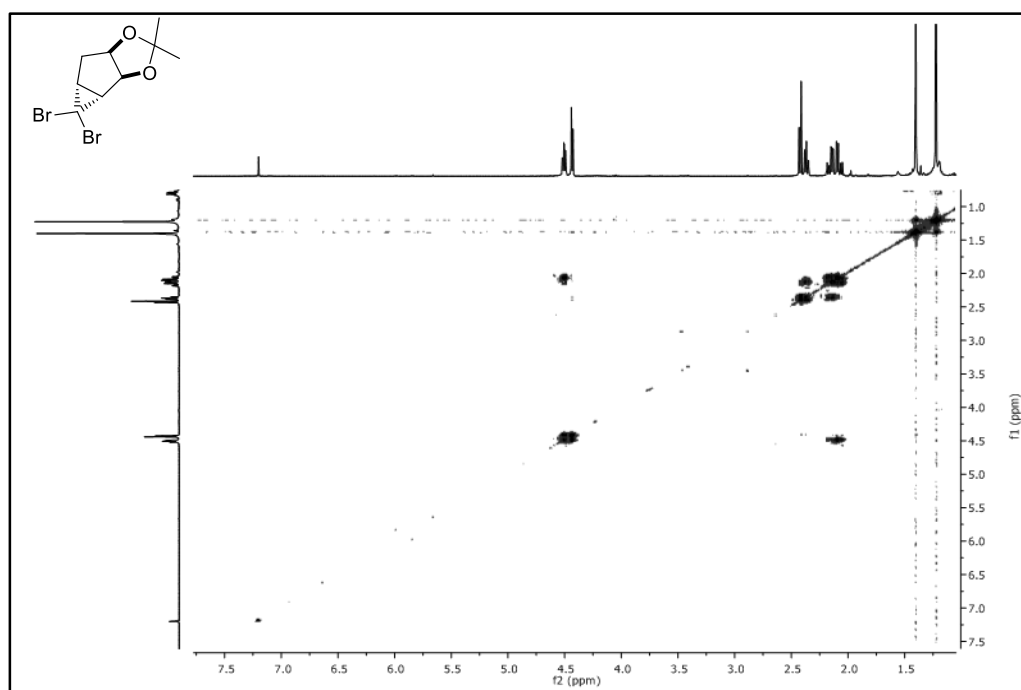


Figure 56. COSY Spectrum of Compound **231**

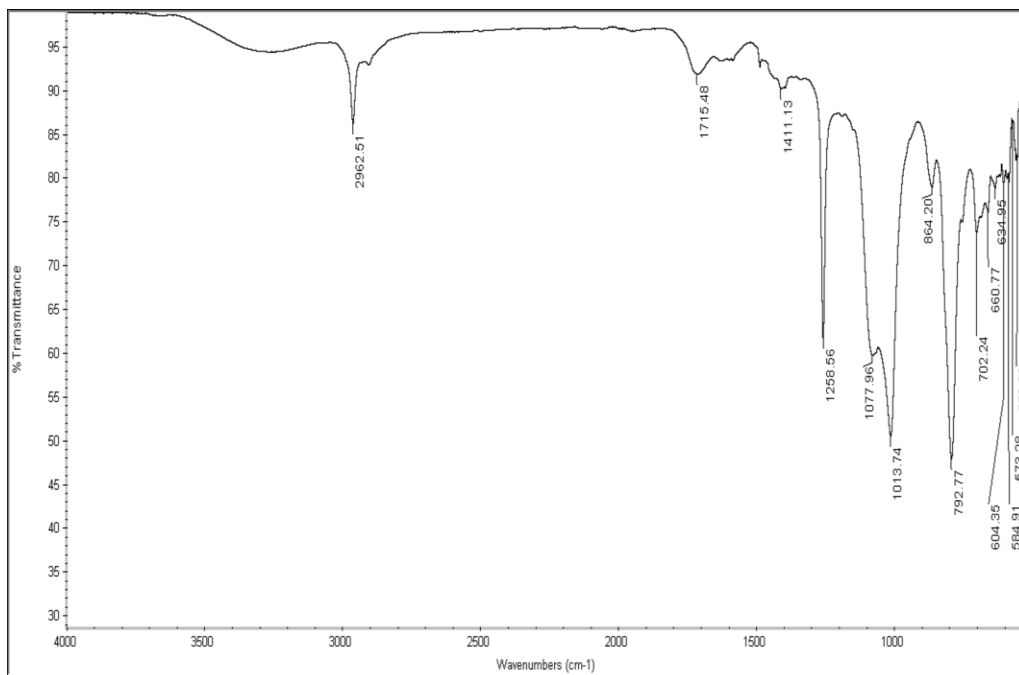


Figure 57. IR Spectrum of Compound 231

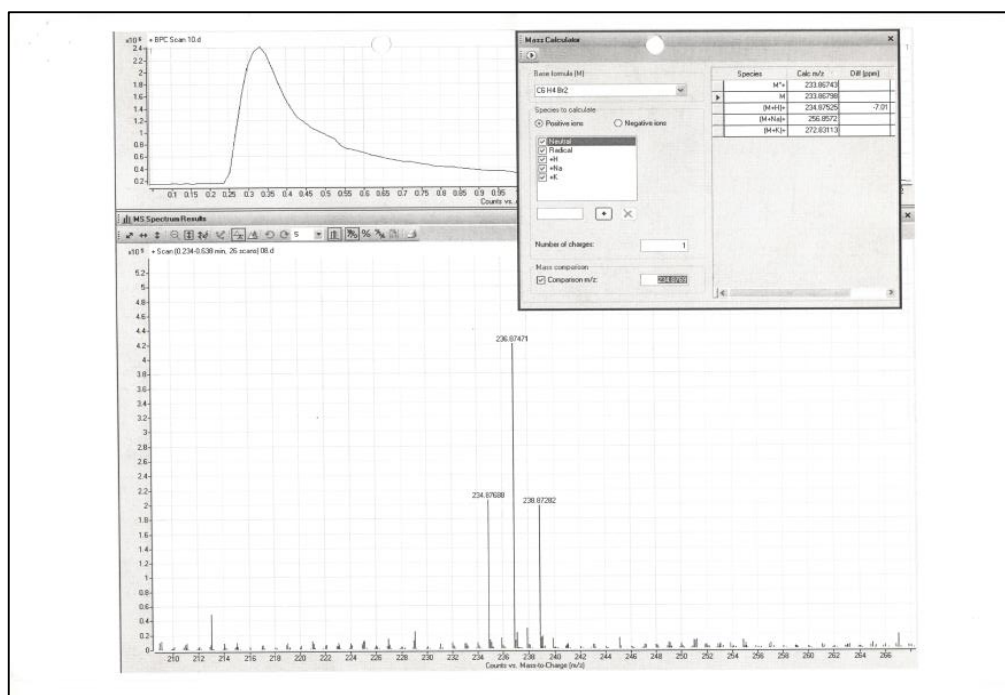


Figure 58. HRMS Spectrum of Compound 231

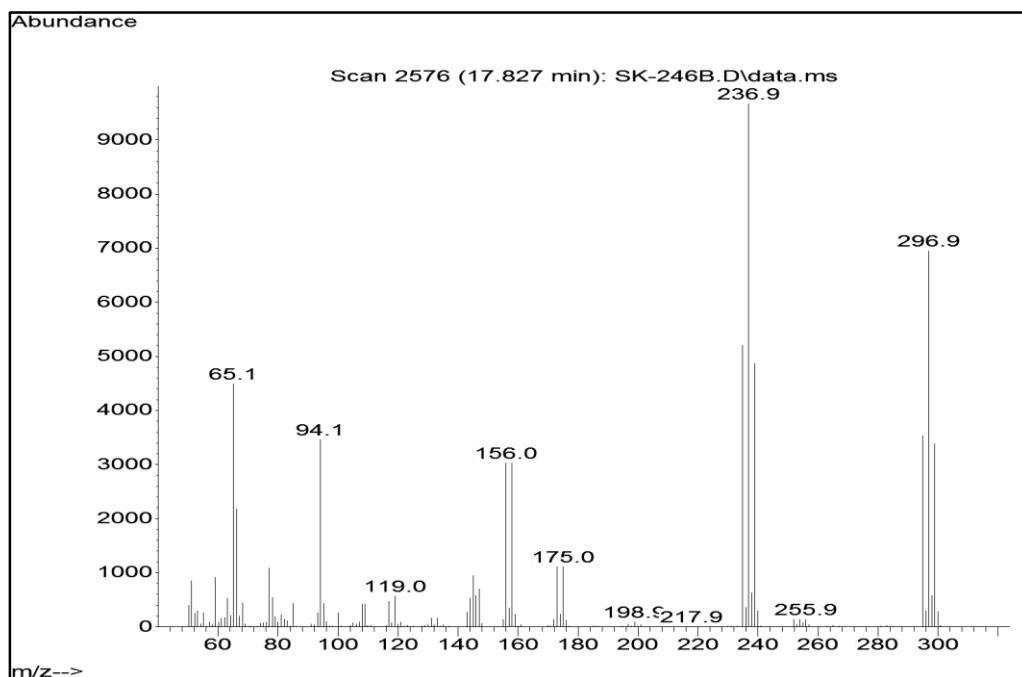


Figure 59. GC-MS Spectrum of Compound **231**

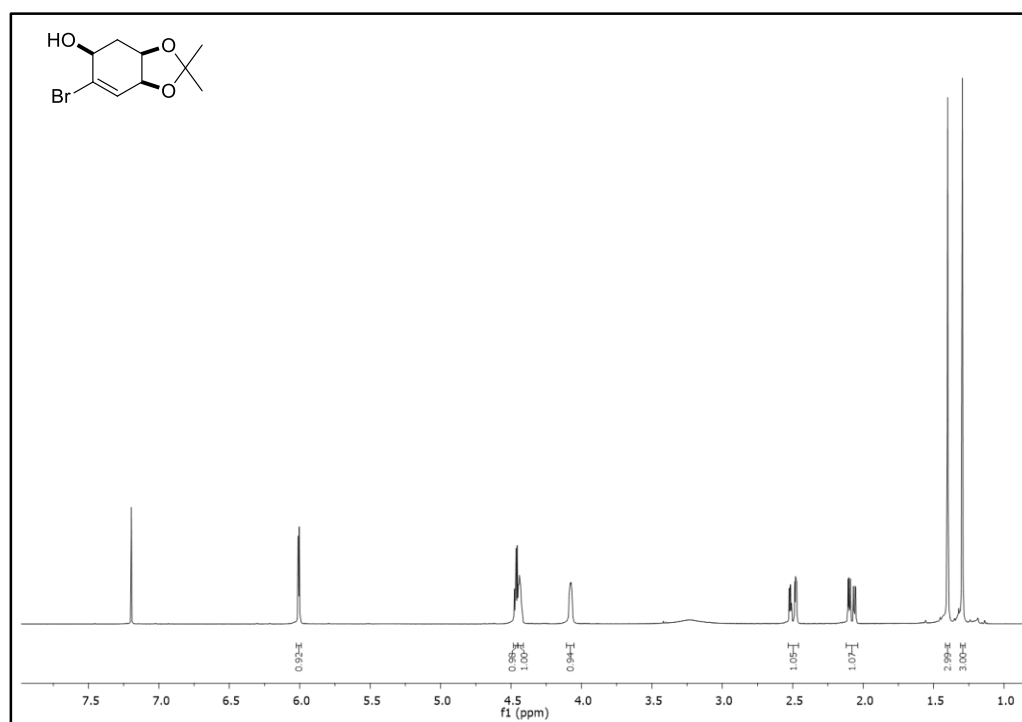


Figure 60. $^1\text{H-NMR}$ Spectrum of Compound **234**

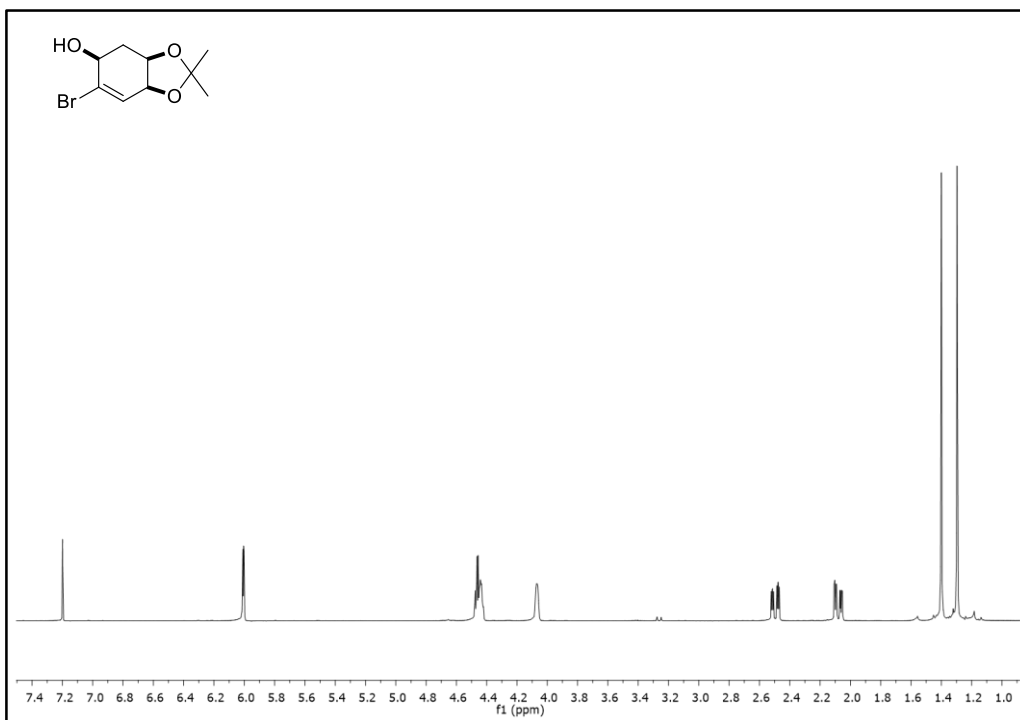


Figure 61. ¹H-NMR Spectrum of D₂O Exchange Reaction of Compound 234

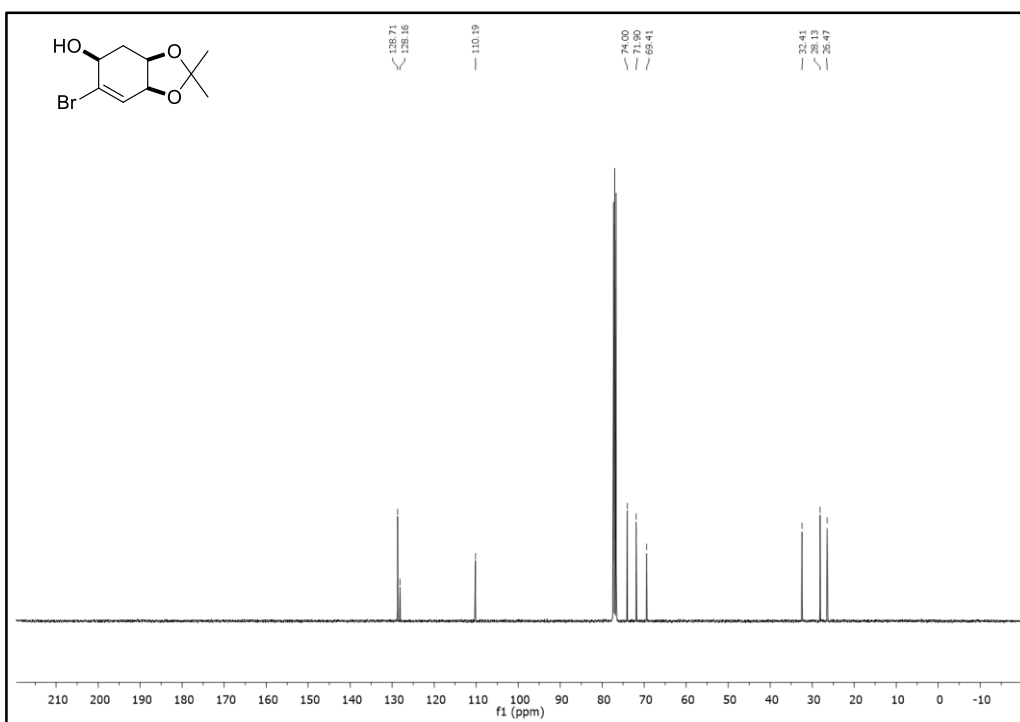


Figure 62. ¹³C-NMR Spectrum of Compound 234

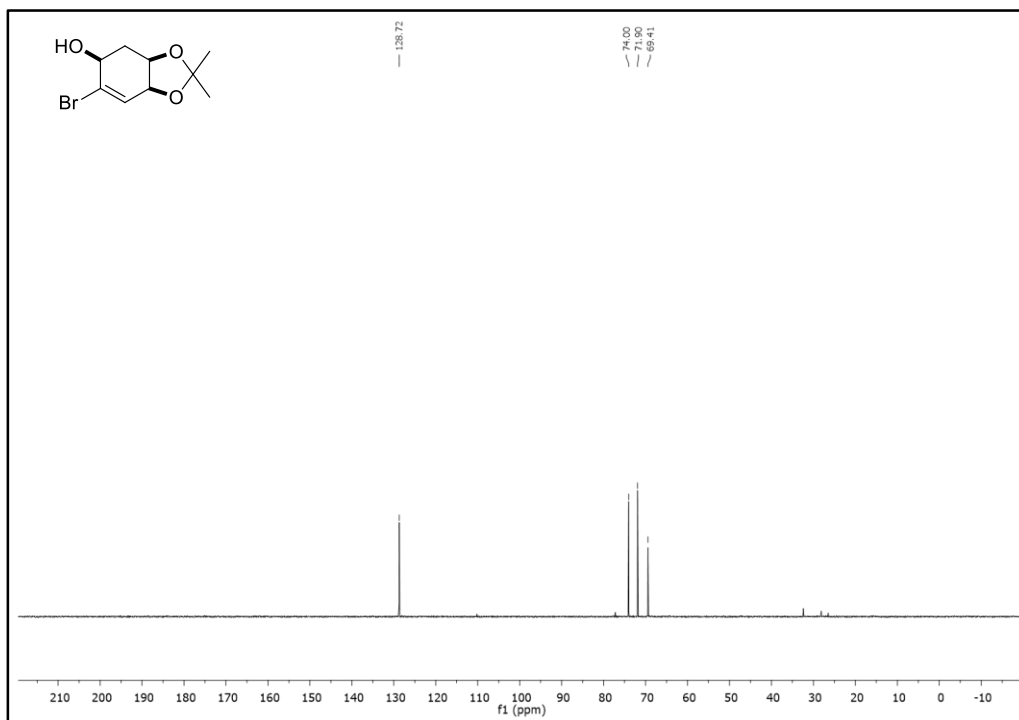


Figure 63. DEPT-90 Spectrum of Compound **234**

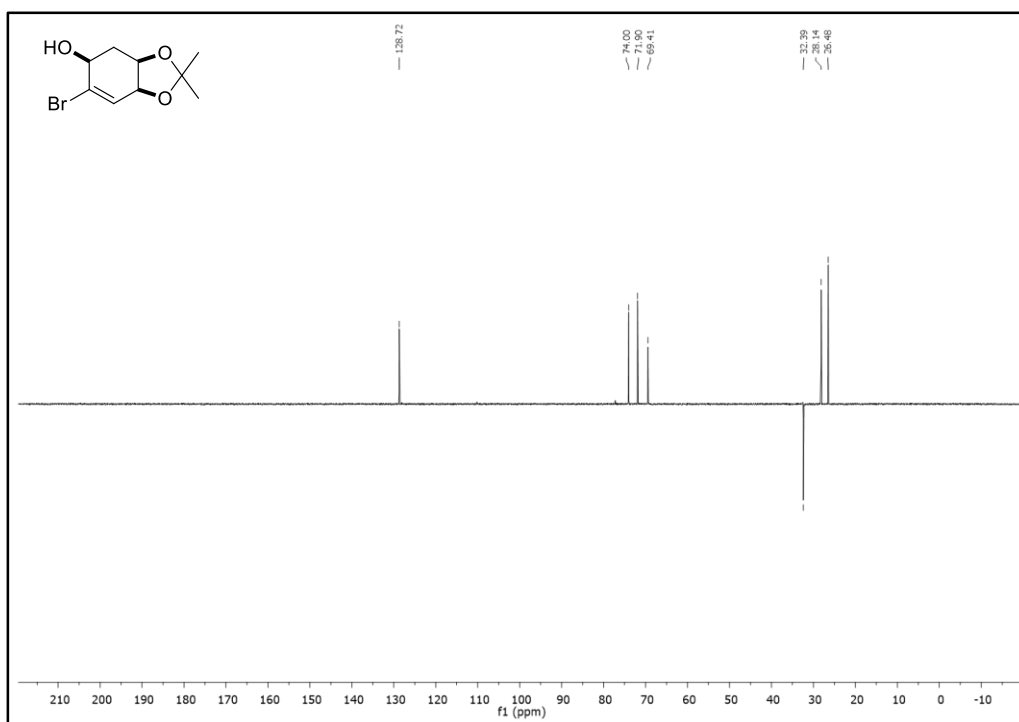


Figure 64. DEPT-135 Spectrum of Compound **234**

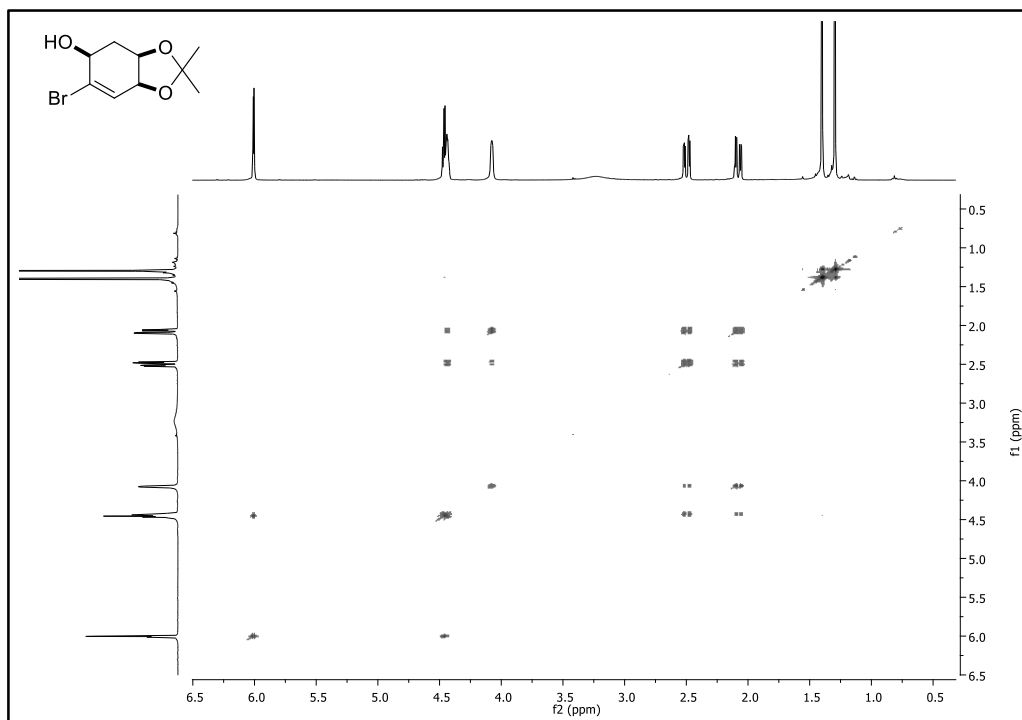


Figure 65. COSY Spectrum of Compound **234**

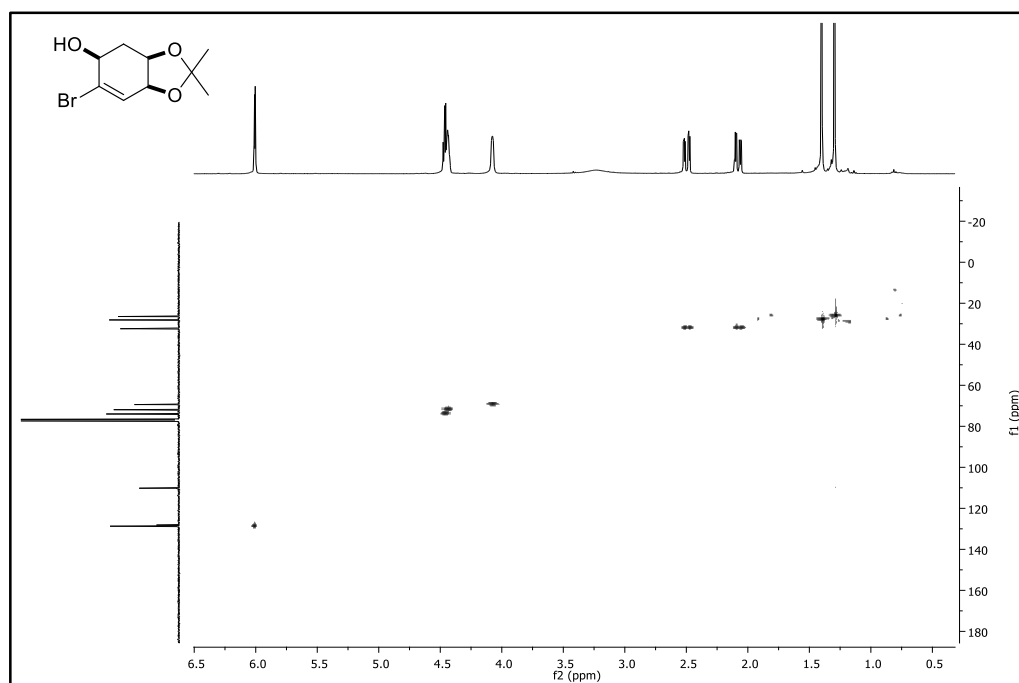


Figure 66. HSQC Spectrum of Compound **234**

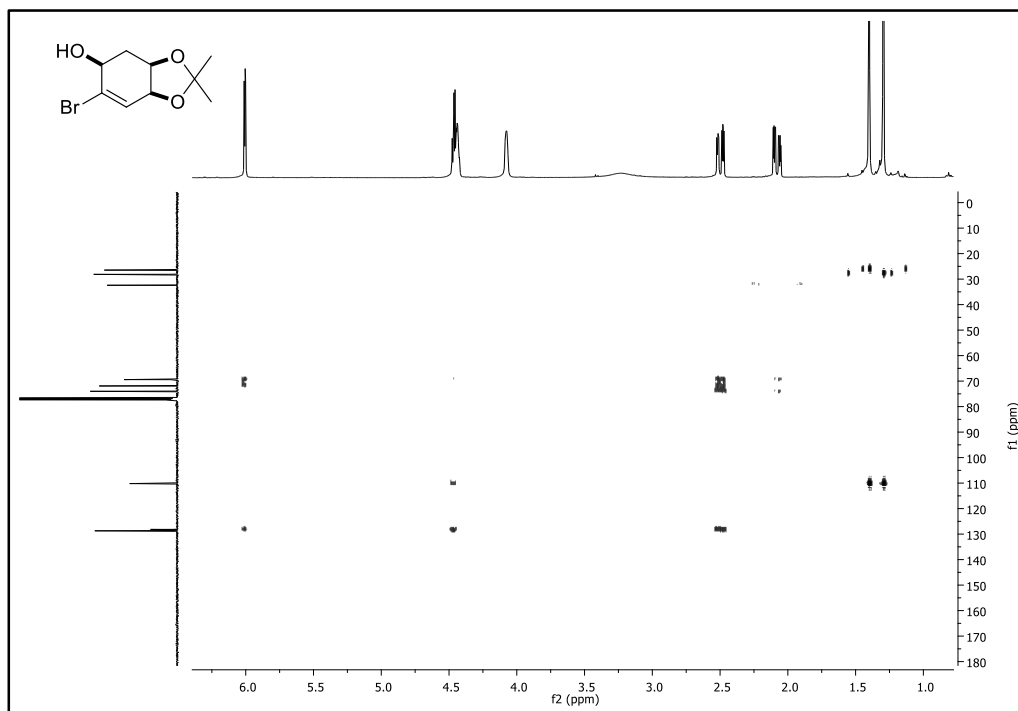


Figure 67. HMBC Spectrum of Compound 234

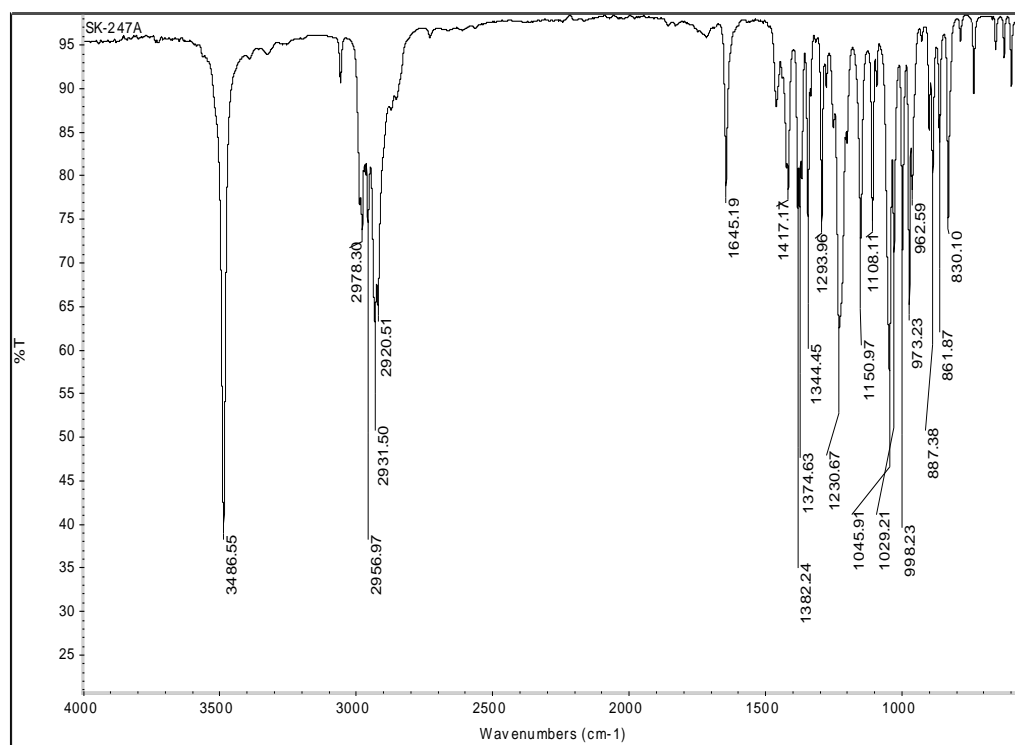
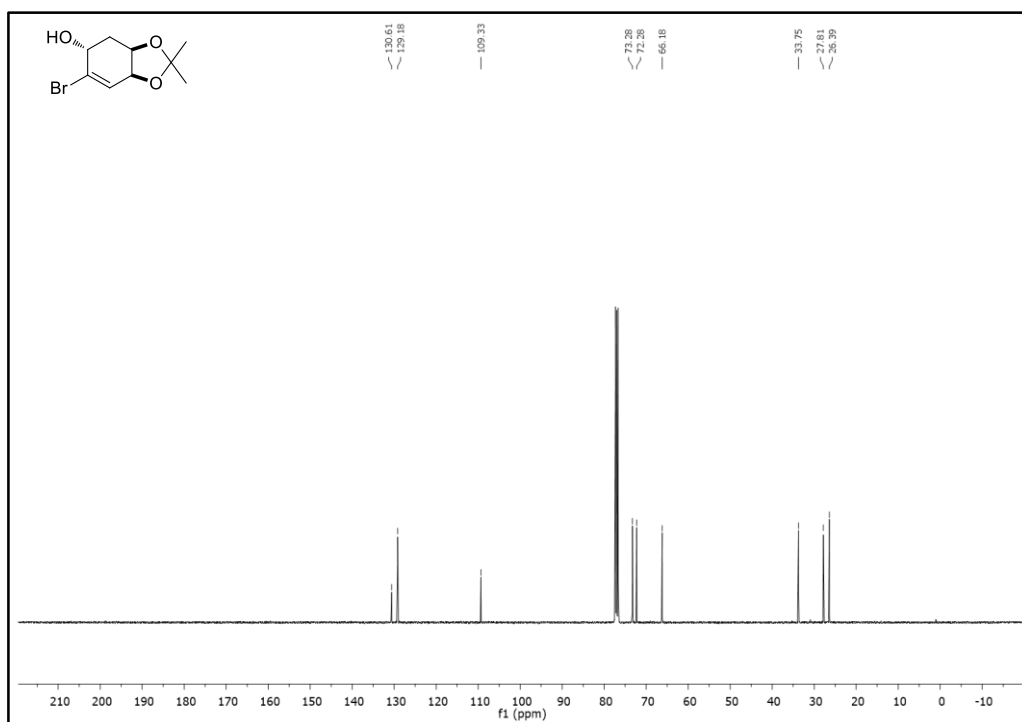
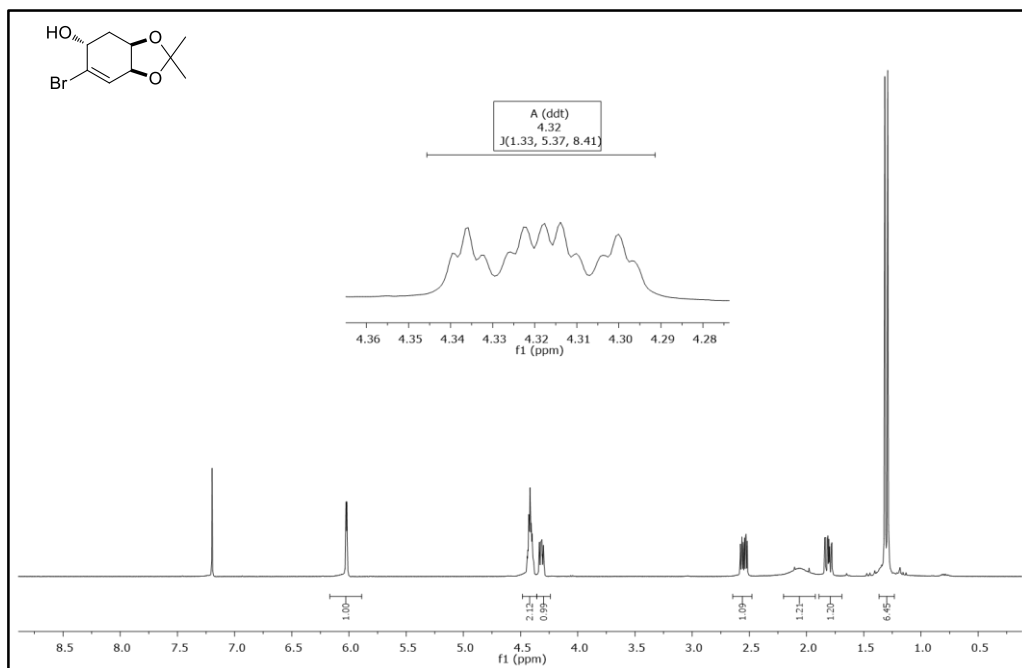


Figure 27. IR Spectrum of Compound 234



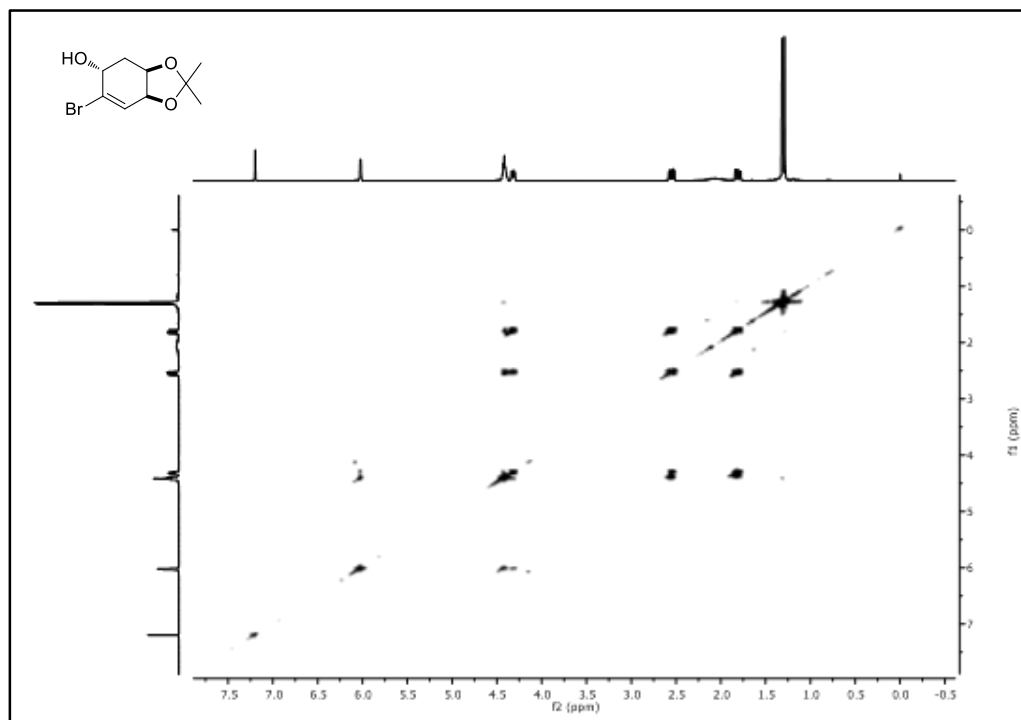


Figure 70. COSY Spectrum of Compound 235

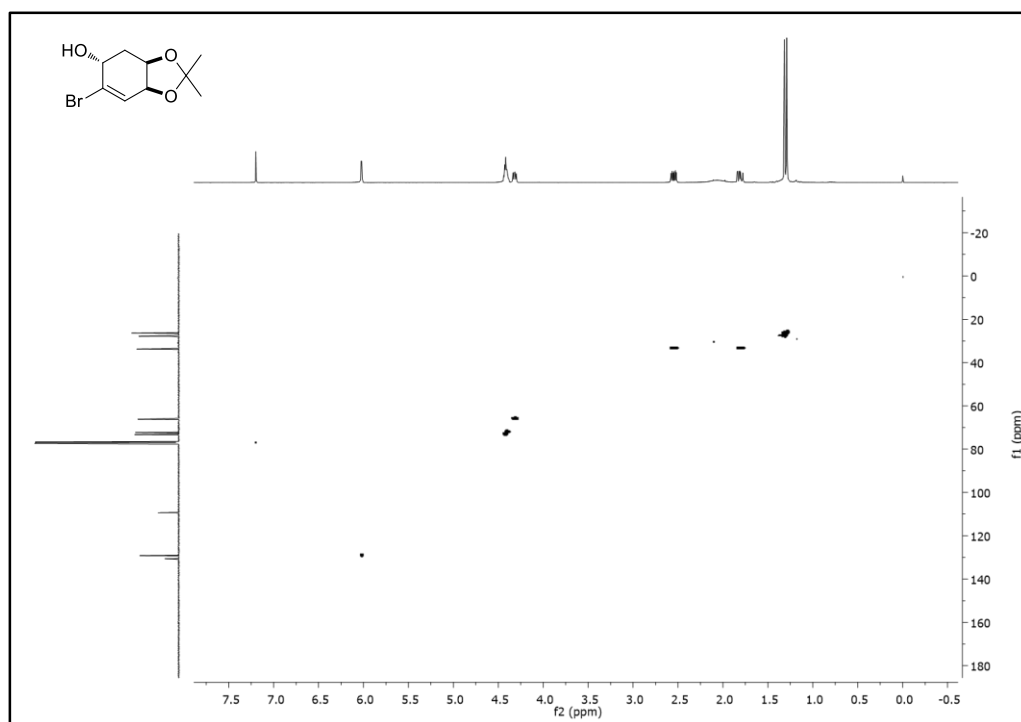


Figure 71. HSQC Spectrum of Compound 235

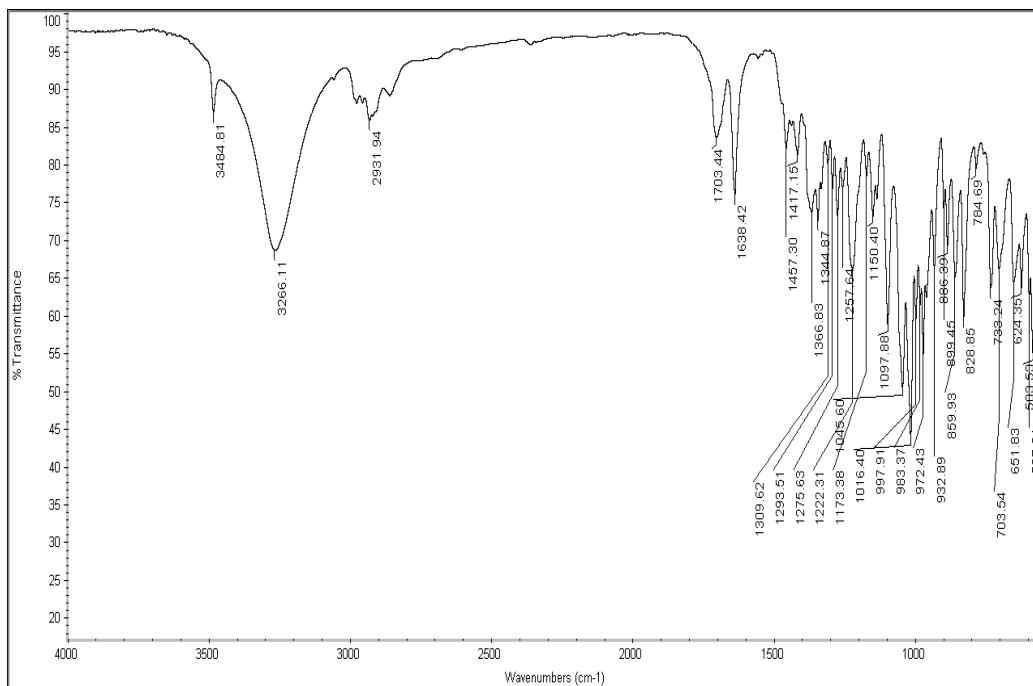


Figure 72. IR Spectrum of Compound 235

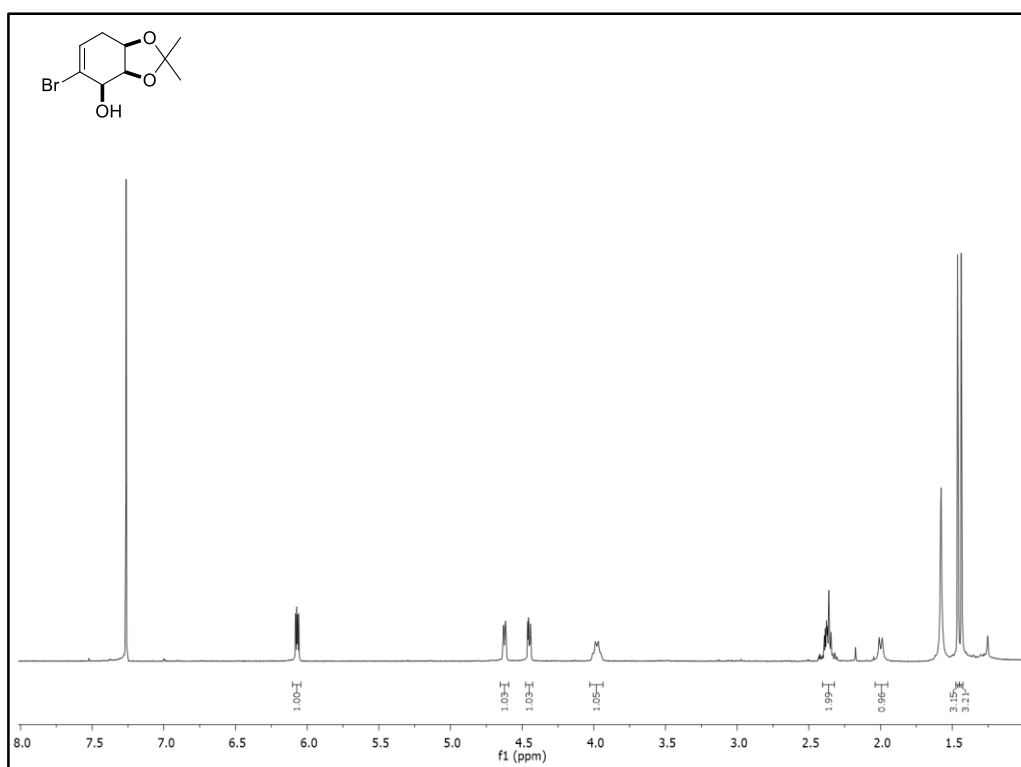


Figure 73. ¹H-NMR Spectrum of Compound 236

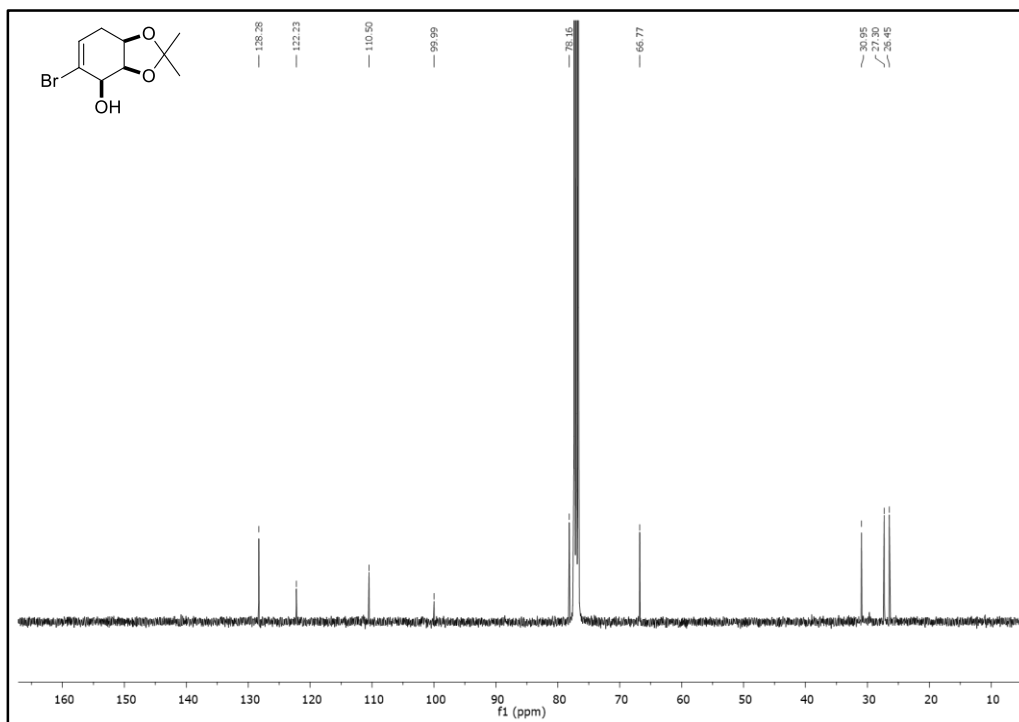


Figure 74. $^{13}\text{C-NMR}$ Spectrum of Compound 236

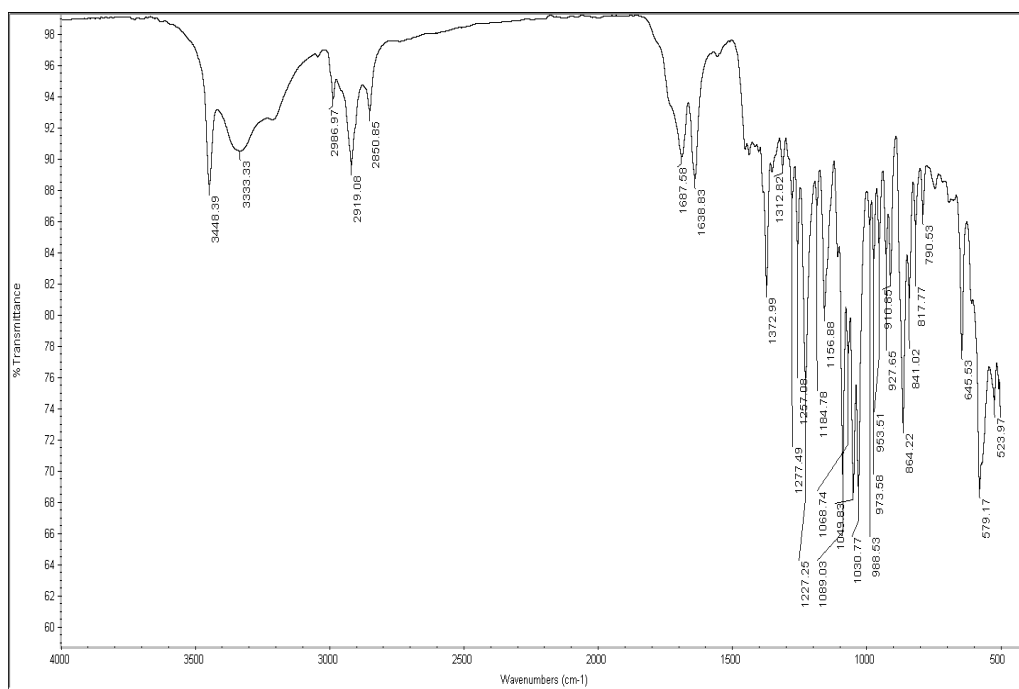


Figure 75. IR Spectrum of Compound 236

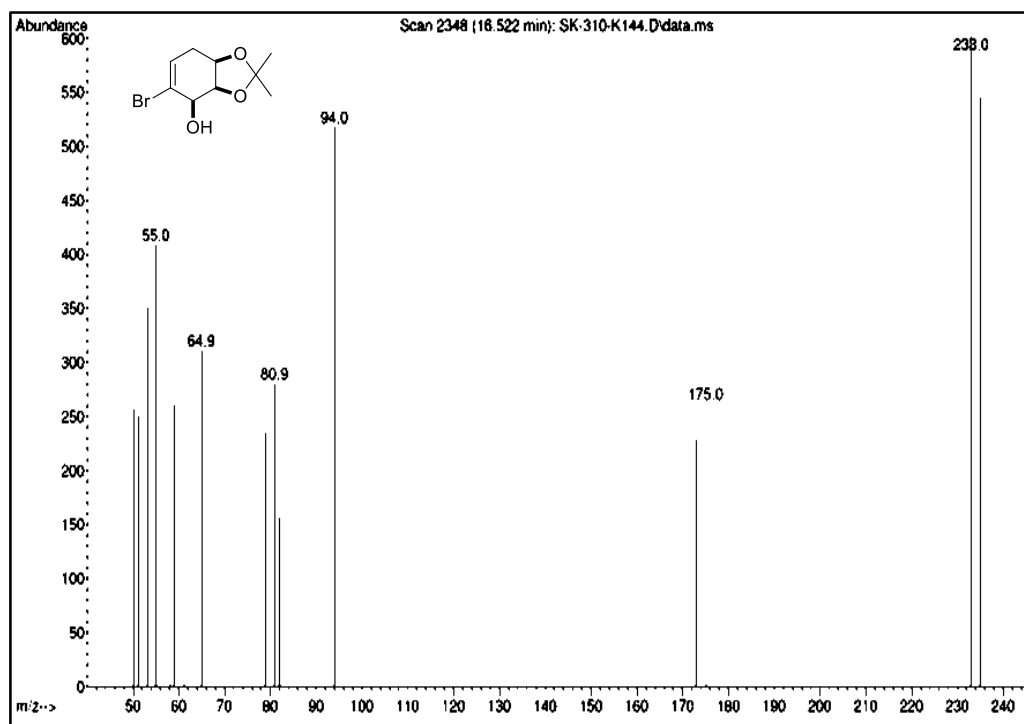


Figure 76. Mass Spectrum of Compound 236

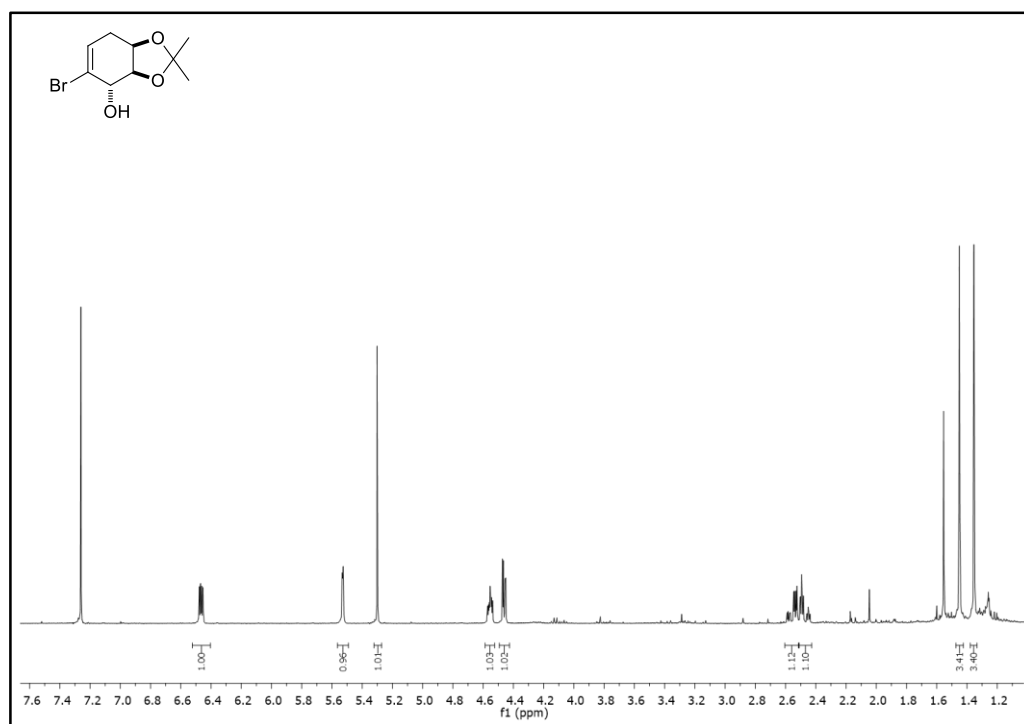


Figure 77. ¹H-NMR Spectrum of Compound 237

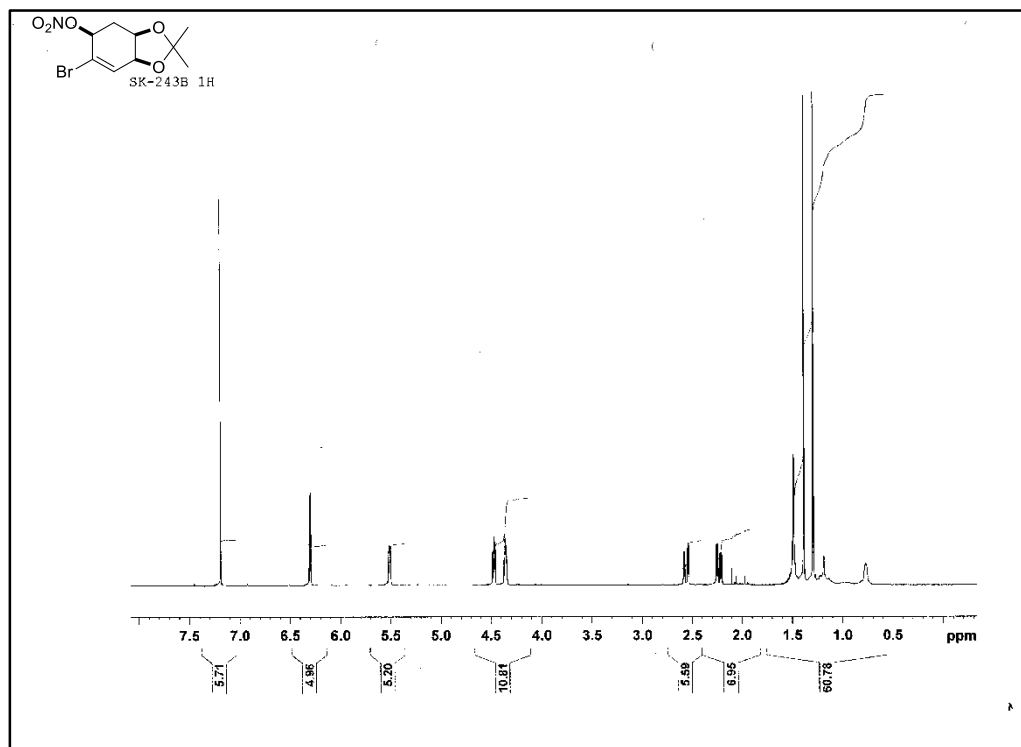


Figure 78. ¹H-NMR Spectrum of Compound 238

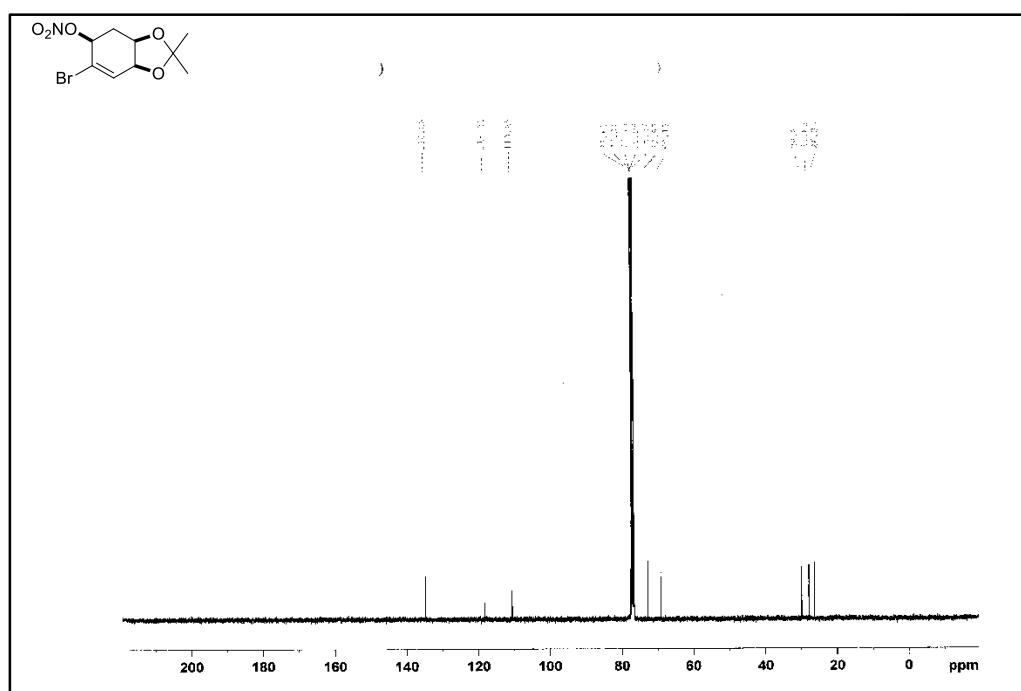


Figure 79. ¹³C-NMR Spectrum of Compound 238

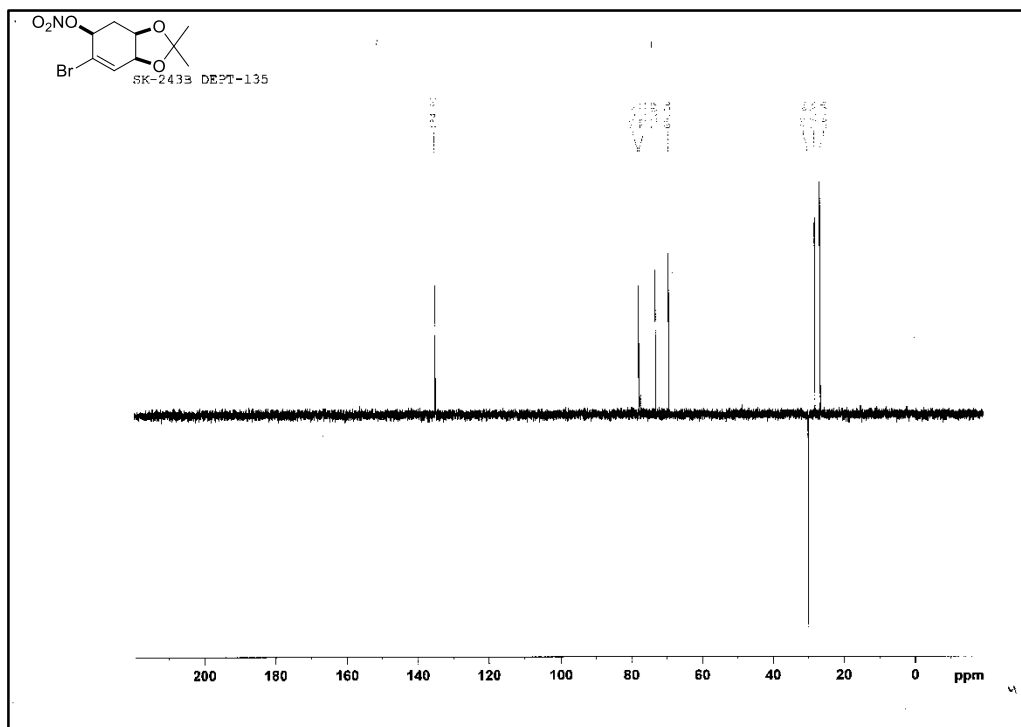


Figure 80. DEPT-135 Spectrum of Compound 238

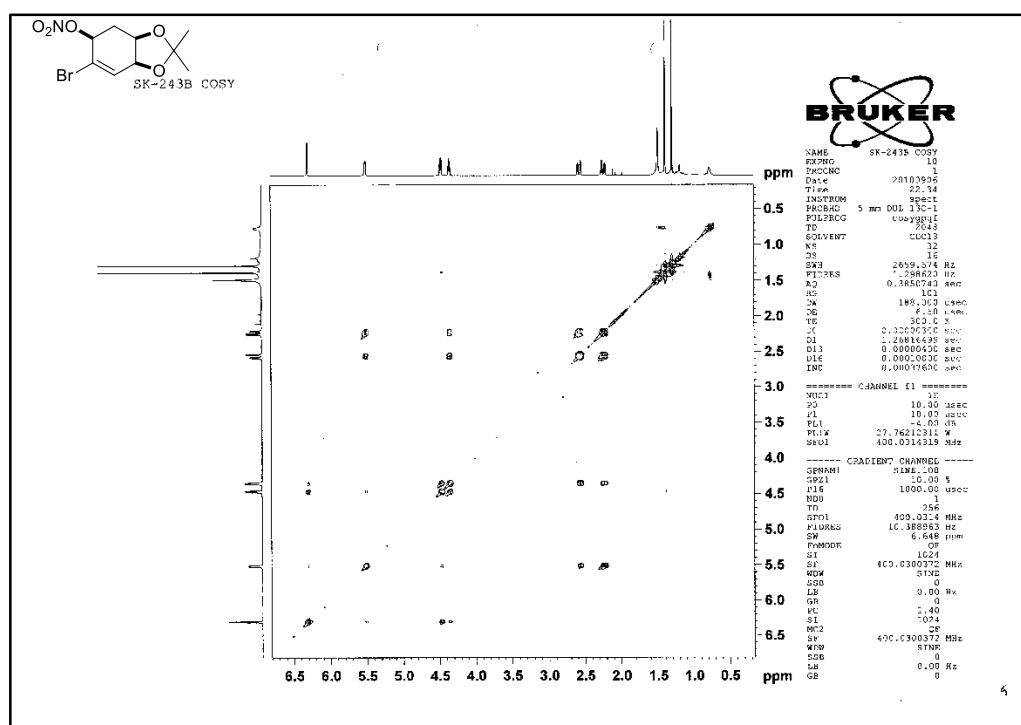


Figure 81. COSY Spectrum of Compound 238

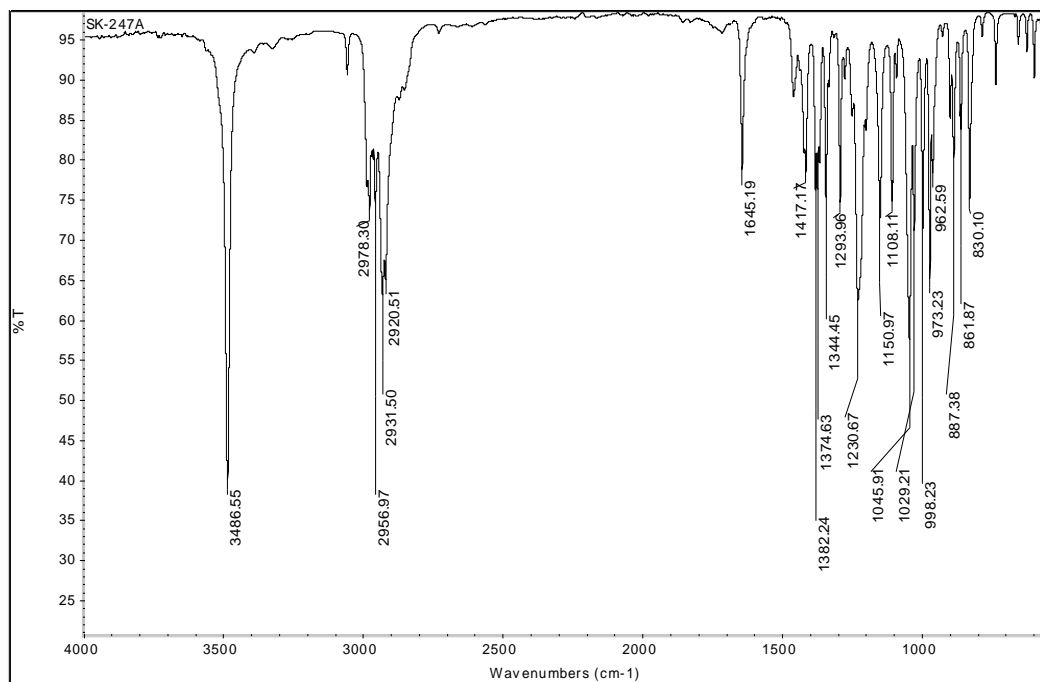


Figure 84. IR Spectrum of Compound 238

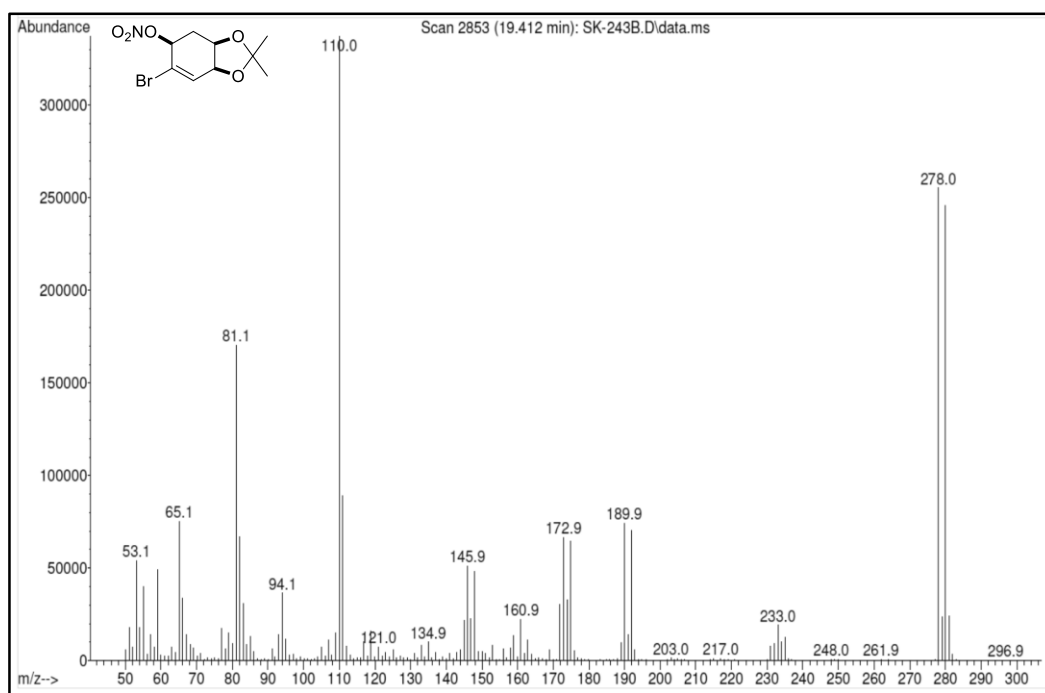


Figure 85. Mass Spectrum of Compound 238

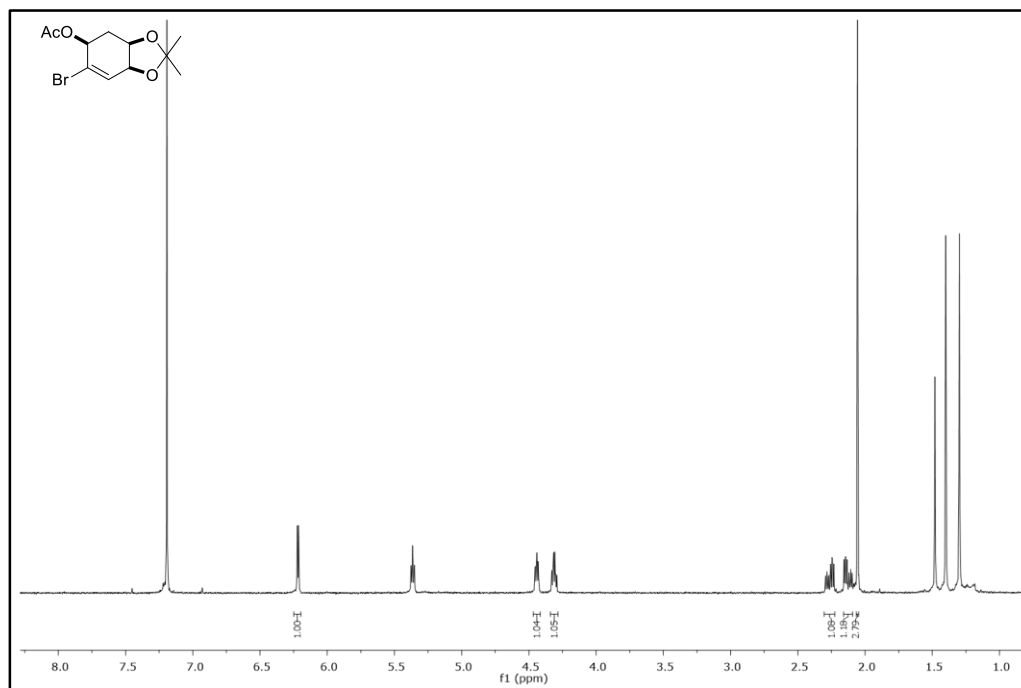


Figure 86. ¹H-NMR Spectrum of Compound 239

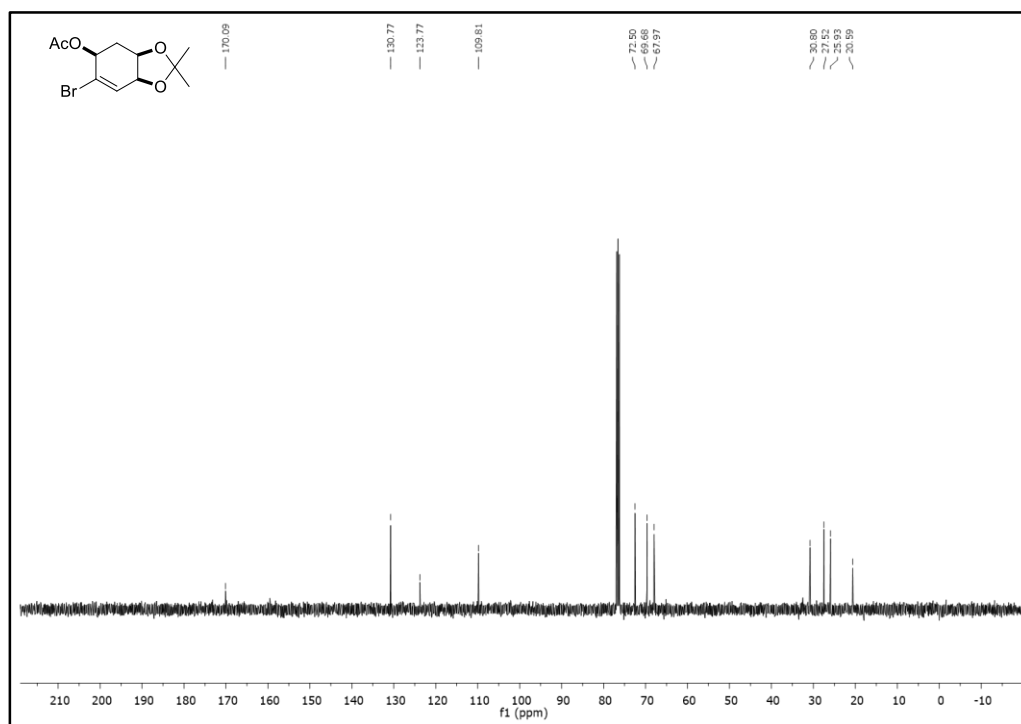


Figure 87. ¹³C-NMR Spectrum of Compound 239

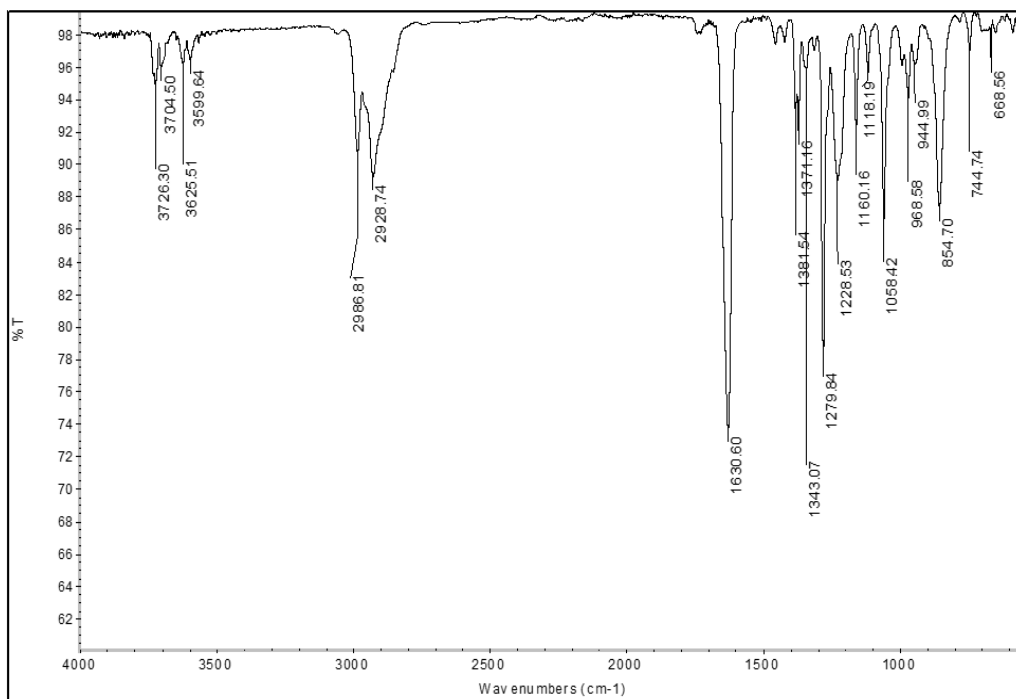


Figure 88. IR Spectrum of Compound 239

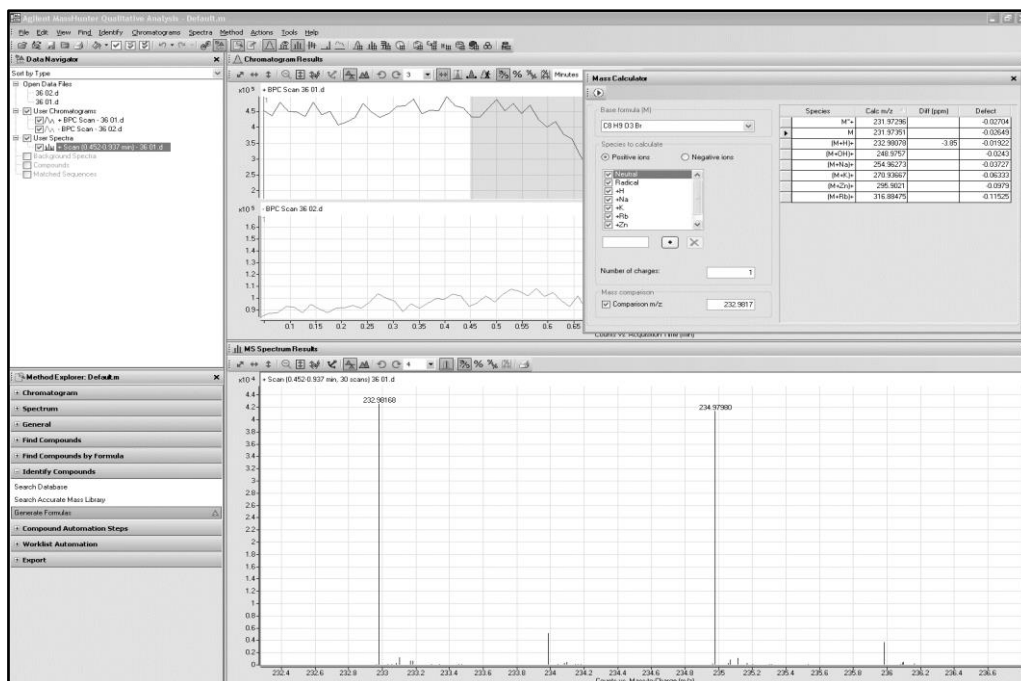


Figure 89. HRMS Spectrum of Compound 239

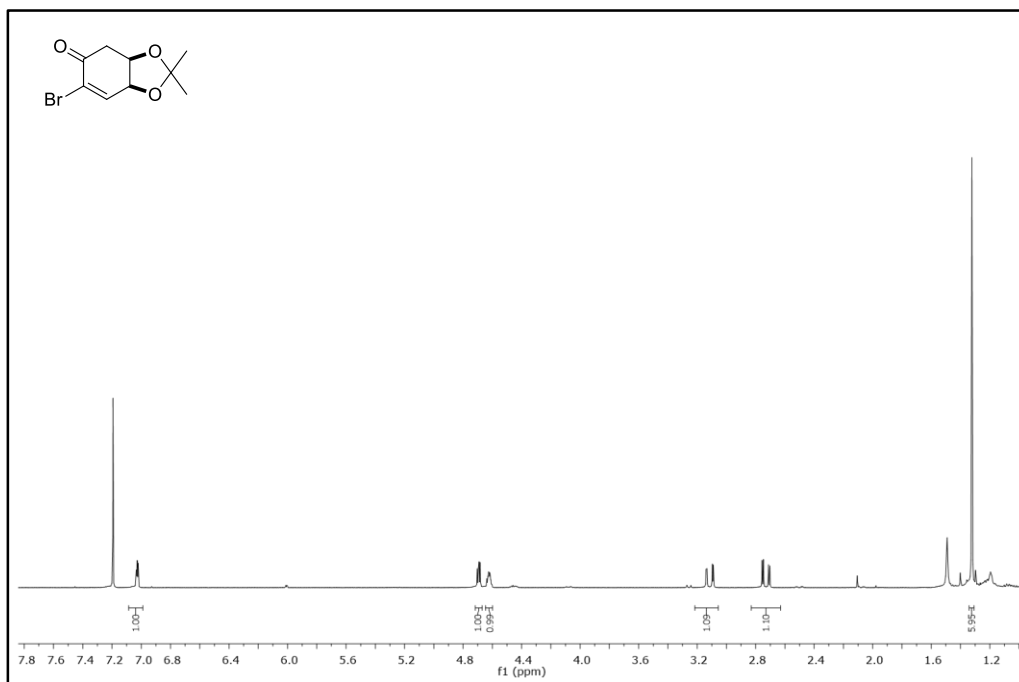


Figure 90. ¹H-NMR Spectrum of Compound 240

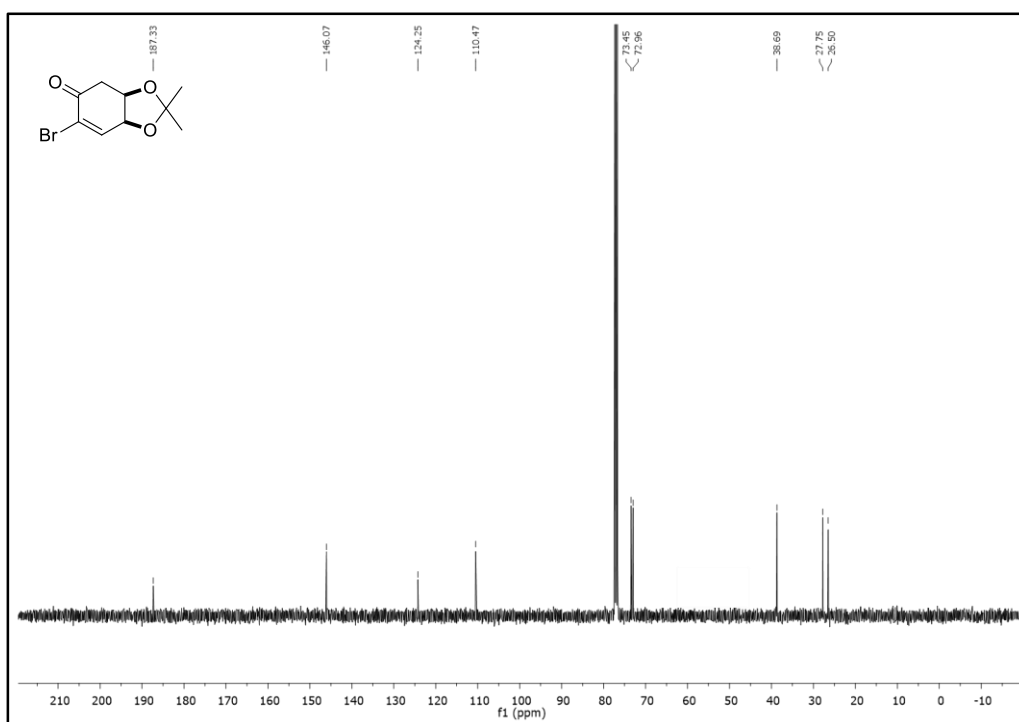


Figure 91. ¹³C-NMR Spectrum of Compound 240

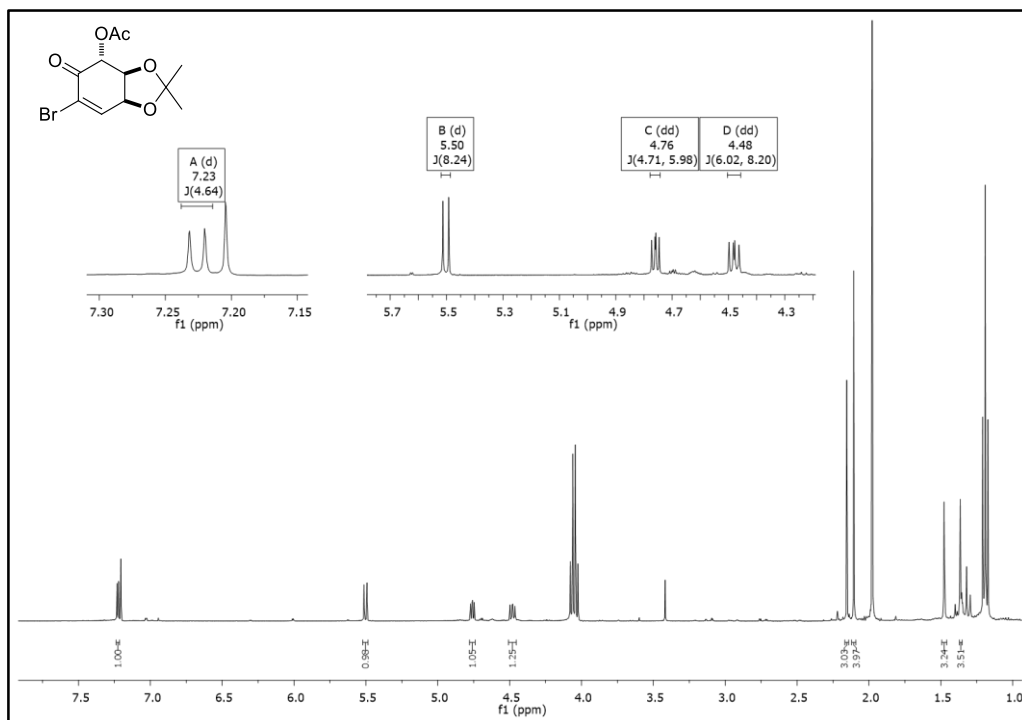


Figure 92. ¹H-NMR Spectrum of Compound 241

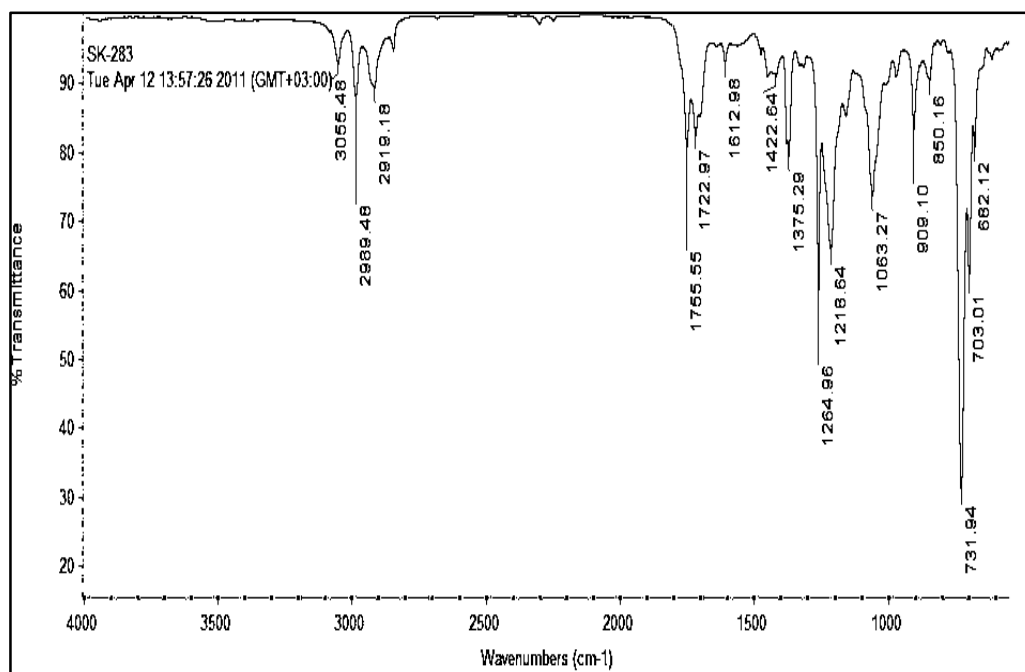


Figure 93. IR Spectrum of Compound 241

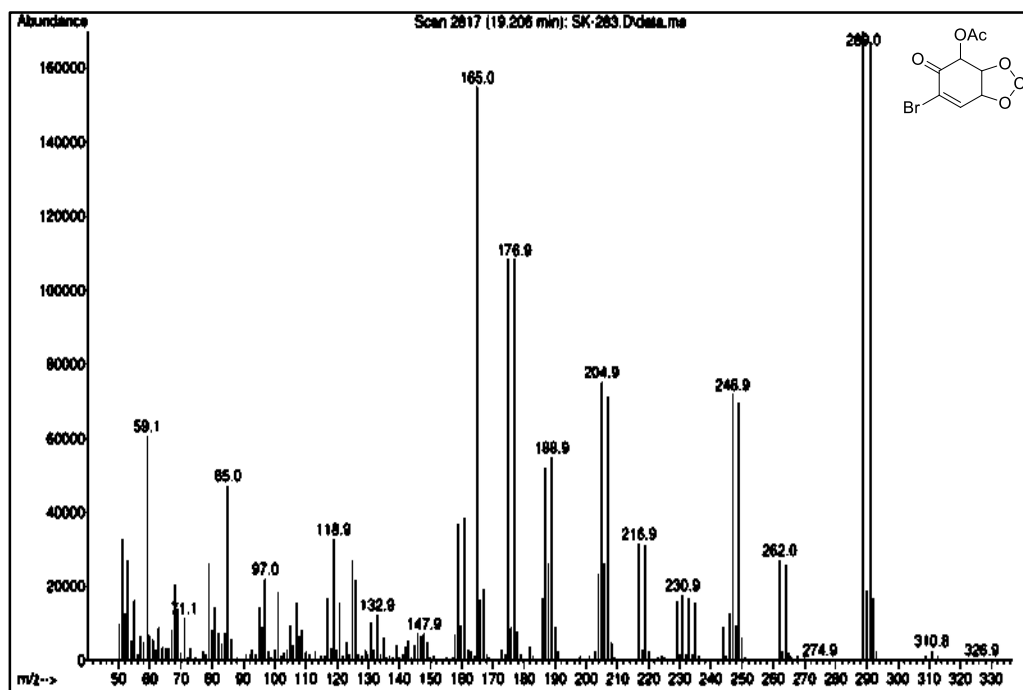


Figure 94. Mass Spectrum of Compound 241

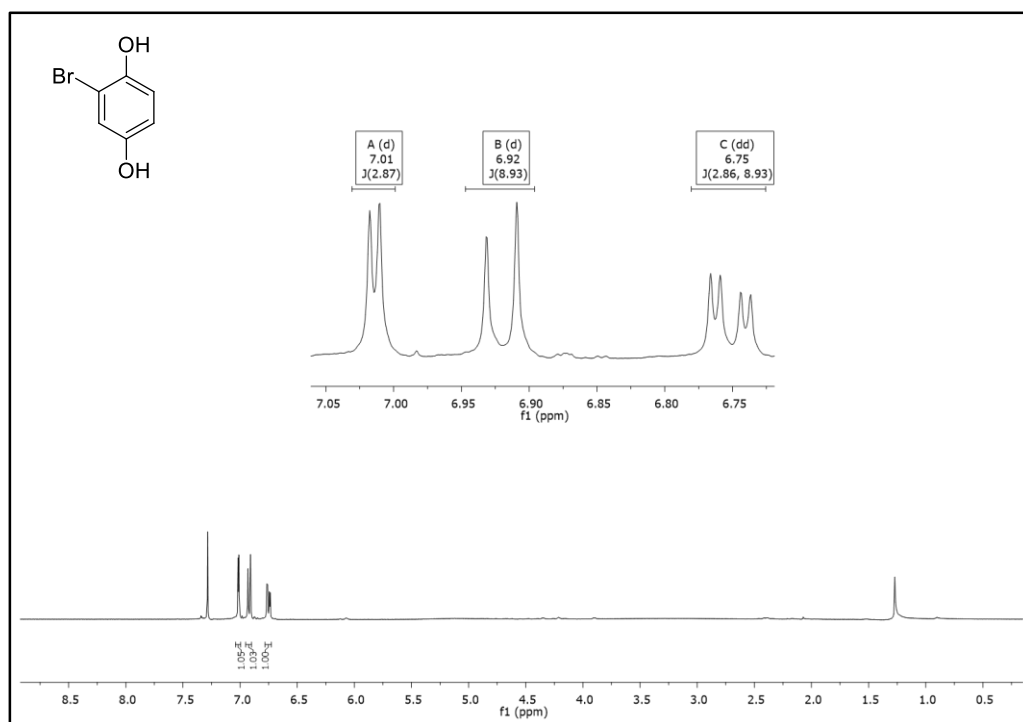


Figure 95. ¹H-NMR Spectrum of Compound 242

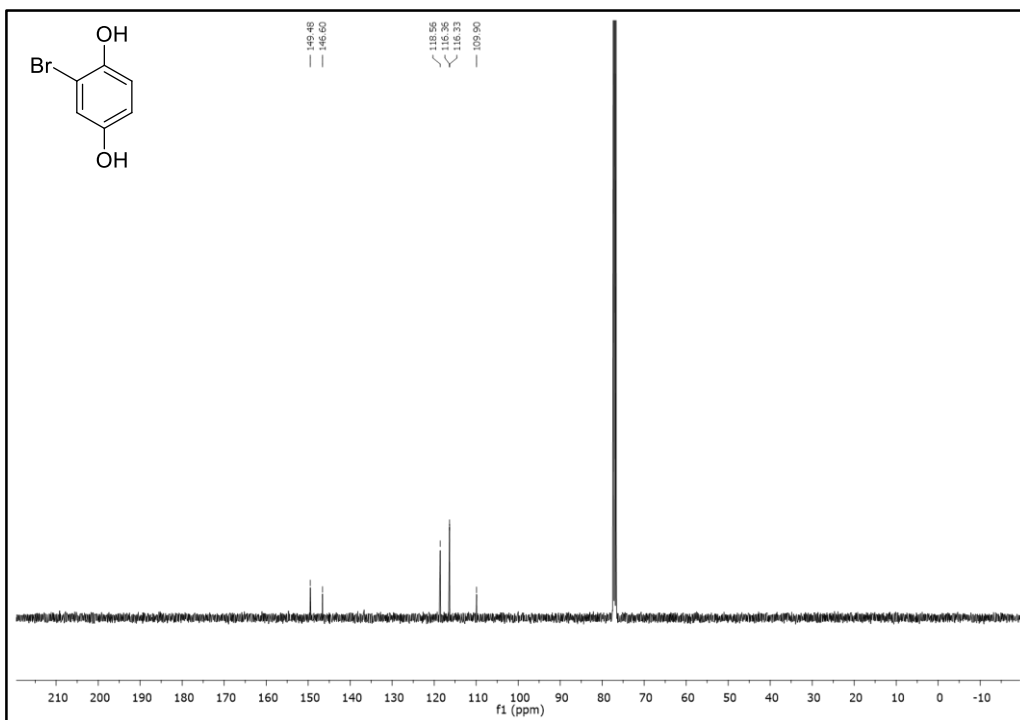


Figure 96. ¹H-NMR Spectrum of Compound 242

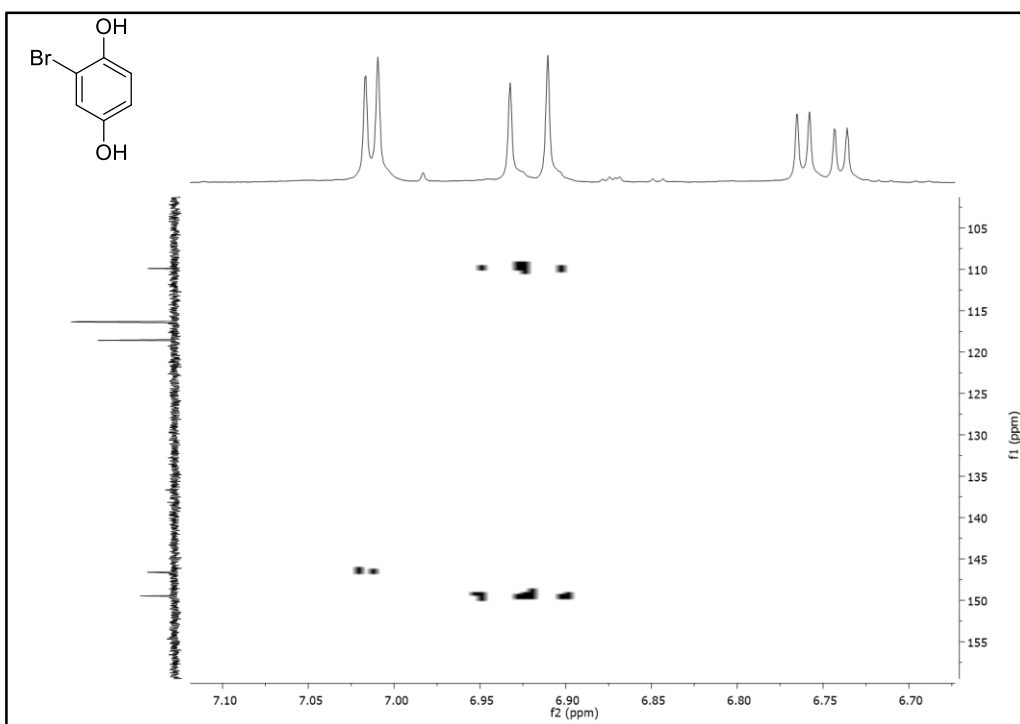


Figure 97. HMBC Spectrum of Compound 242

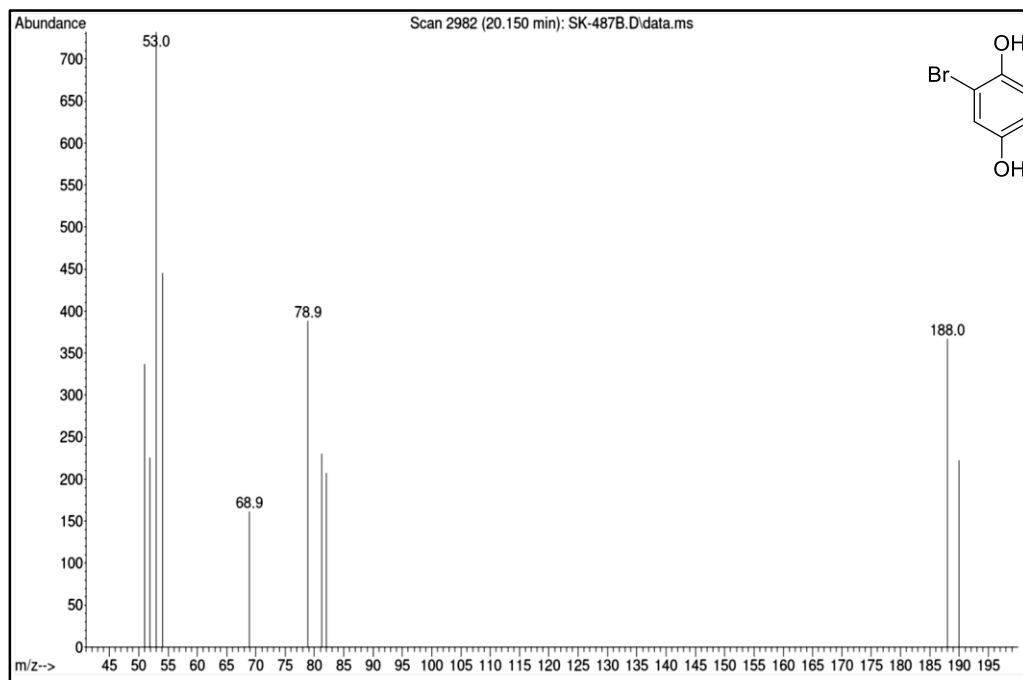


Figure 98. Mass Spectrum of Compound 242

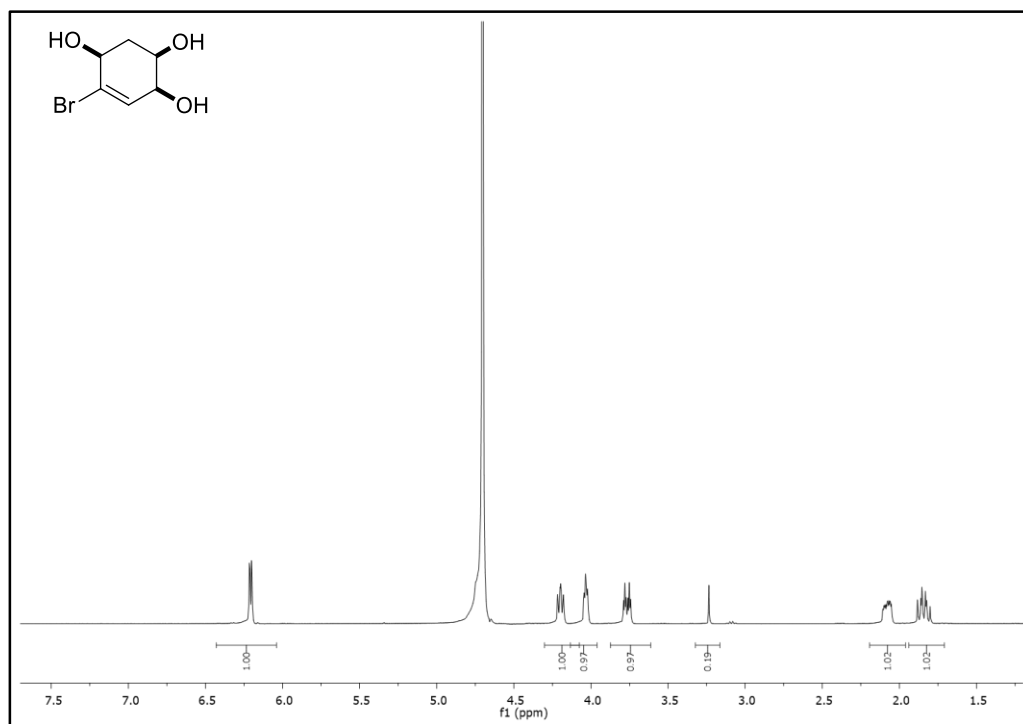


Figure 99. $^1\text{H-NMR}$ Spectrum of Compound 248

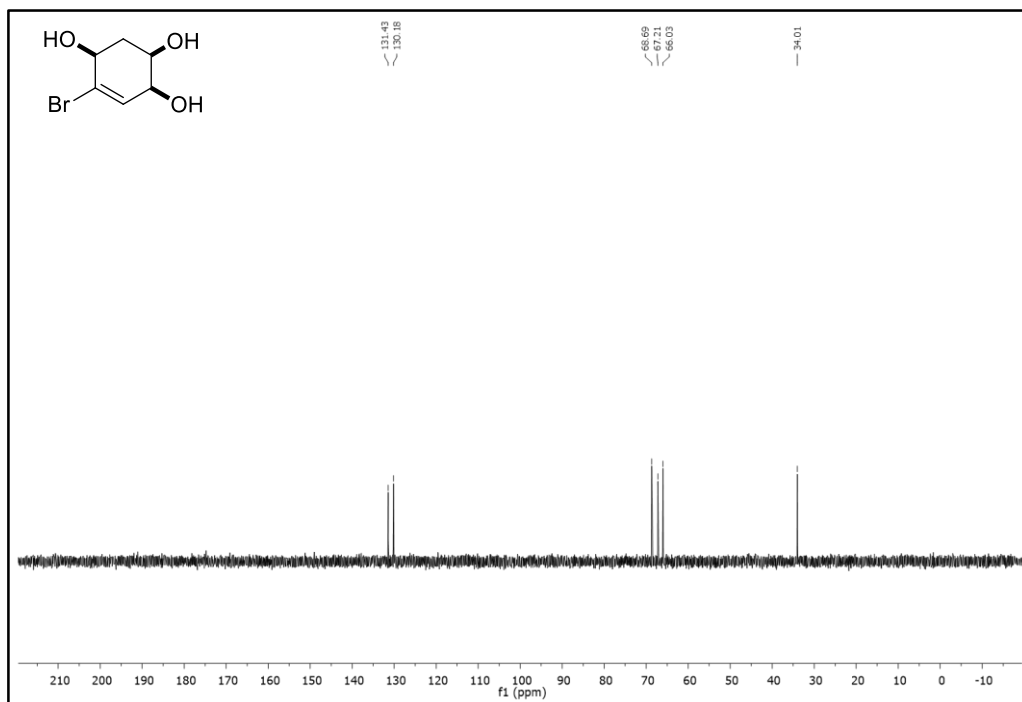


Figure 100. ¹³C-NMR Spectrum of Compound **248**

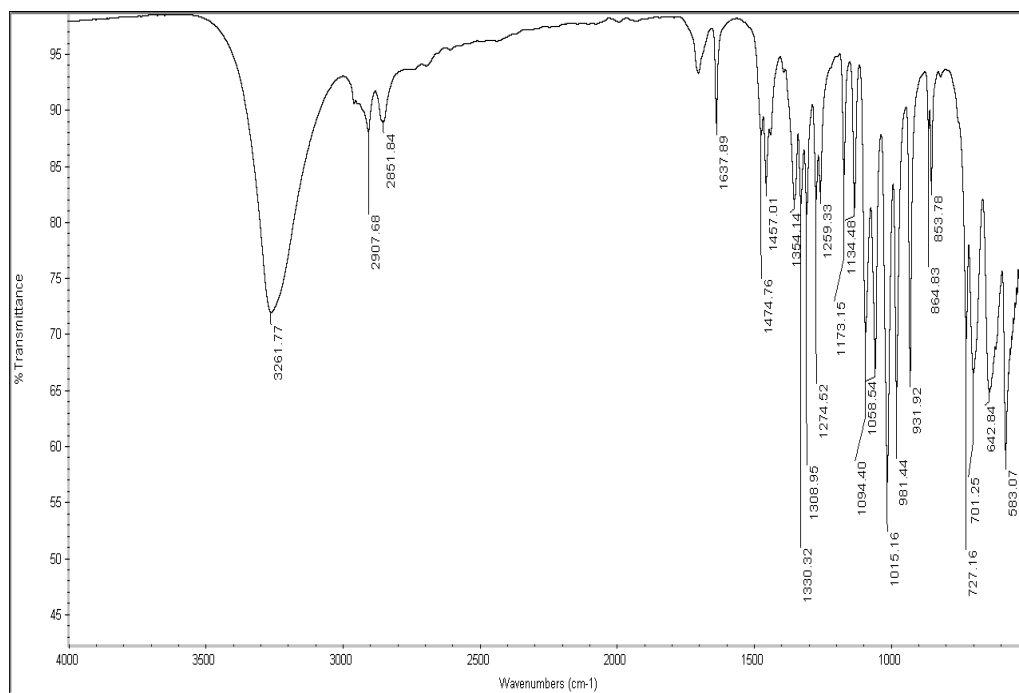


Figure 101. IR Spectrum of Compound **248**

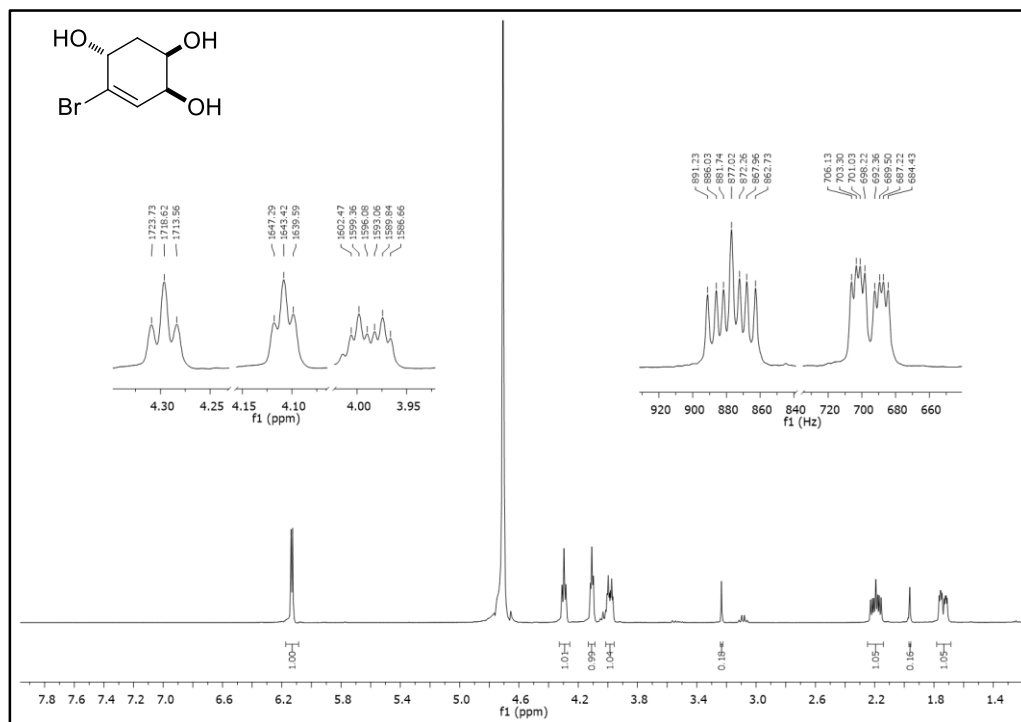


Figure 102. ¹H-NMR Spectrum of Compound 249

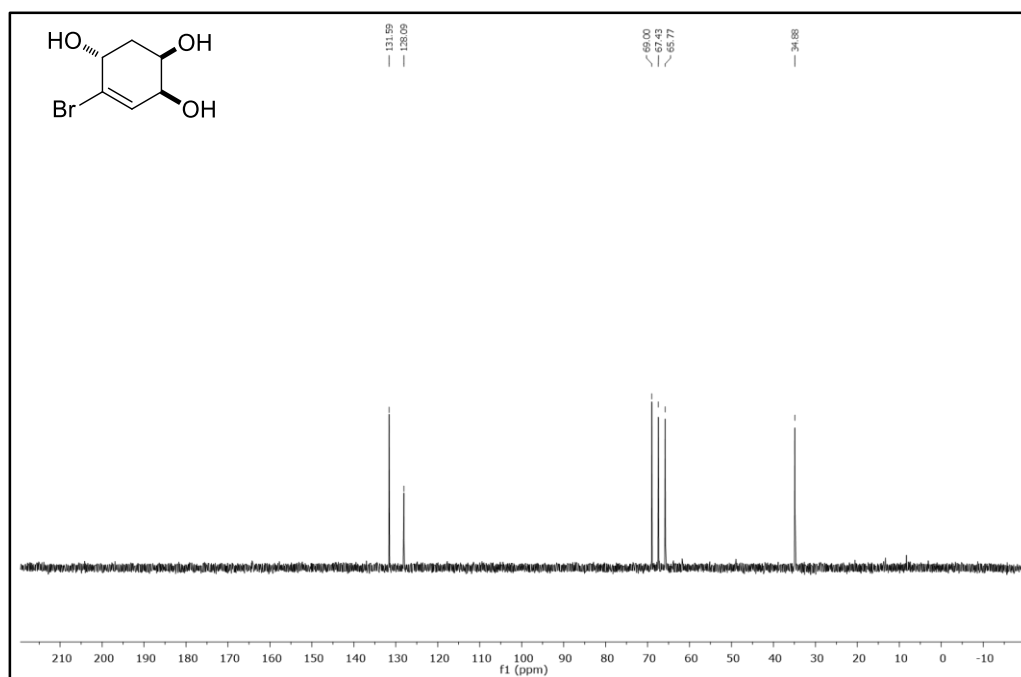


Figure 103. ¹³C-NMR Spectrum of Compound 249

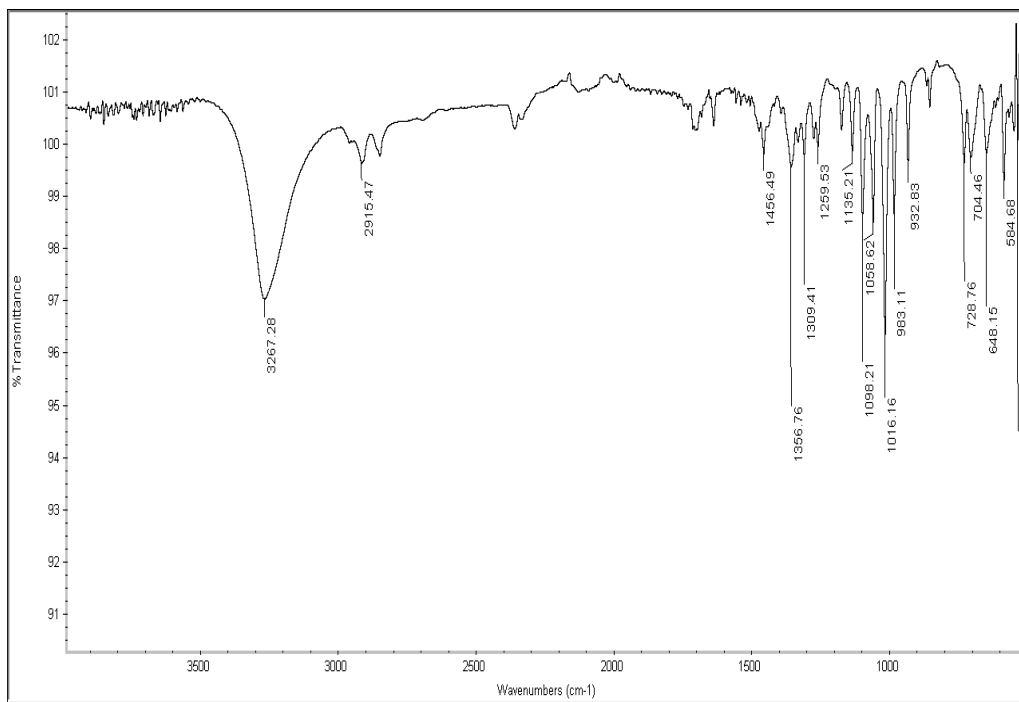


Figure 104. IR Spectrum of Compound 249

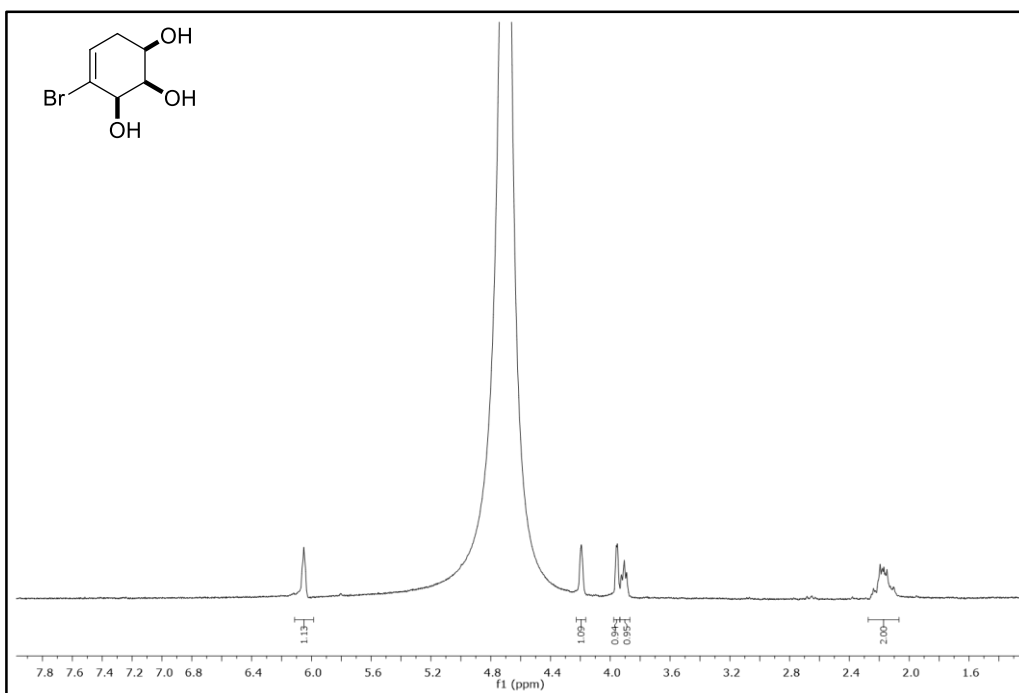


Figure 105. ¹H-NMR Spectrum of Compound 250

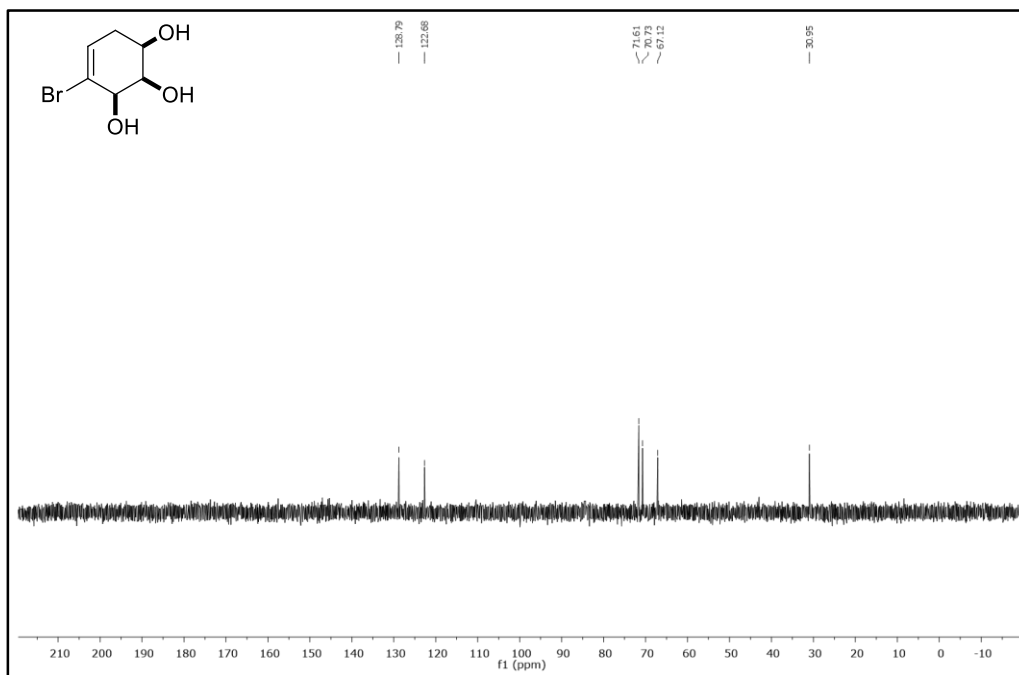


Figure 106. ^{13}C -NMR Spectrum of Compound 250

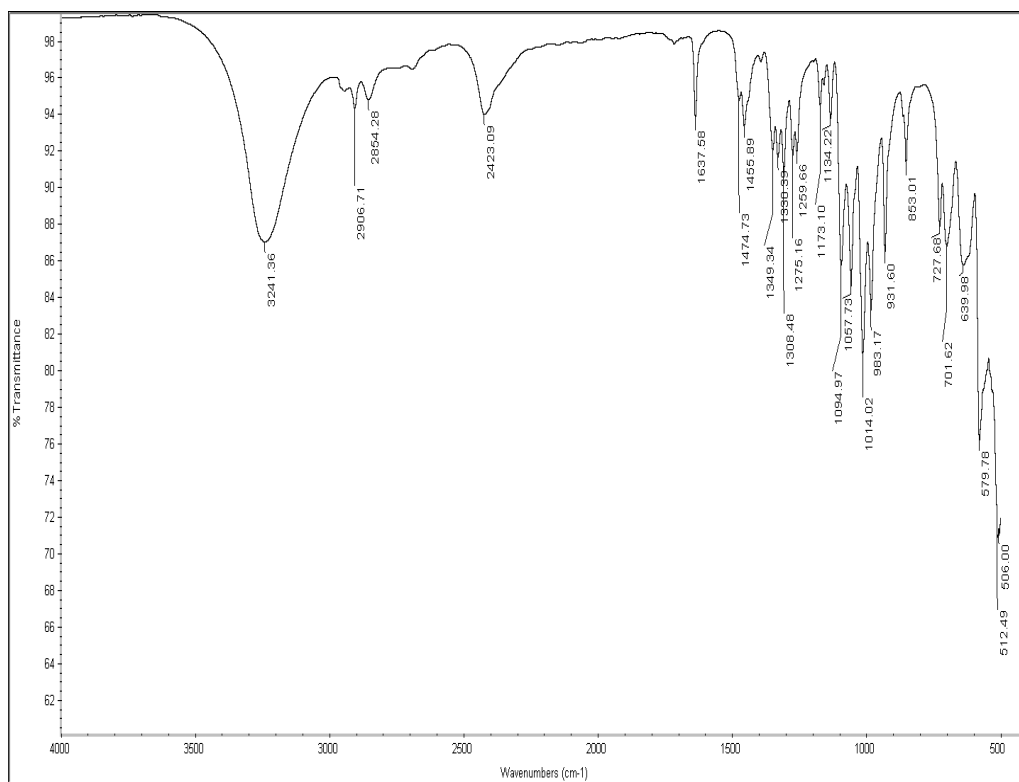


Figure 107. IR Spectrum of Compound 250

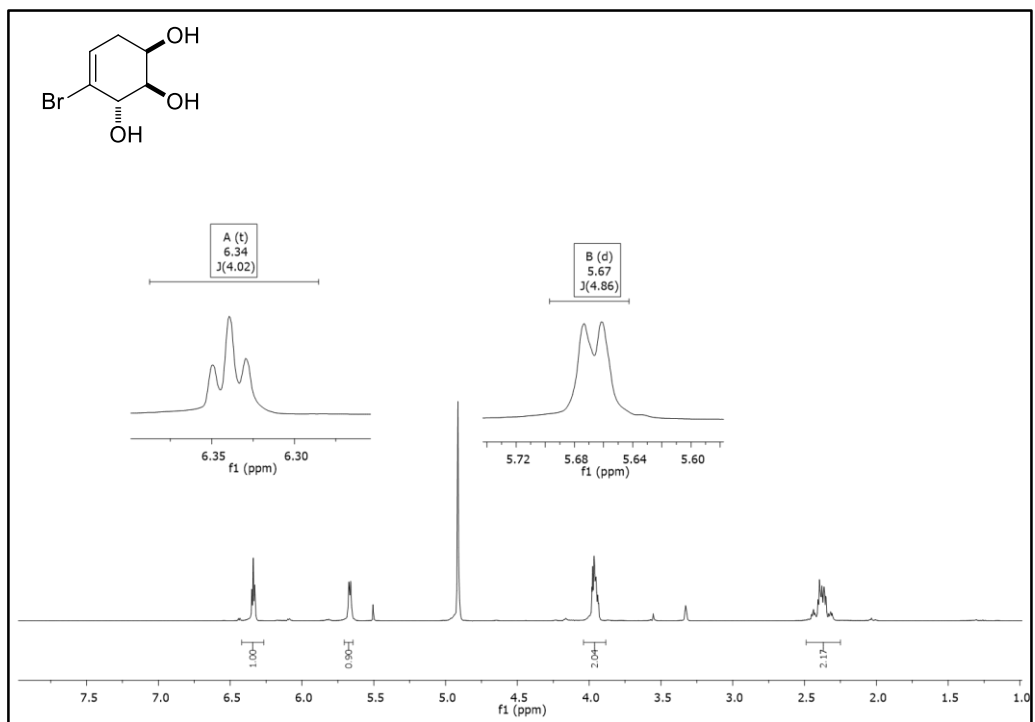


Figure 108. ^1H -NMR Spectrum of Compound **251**

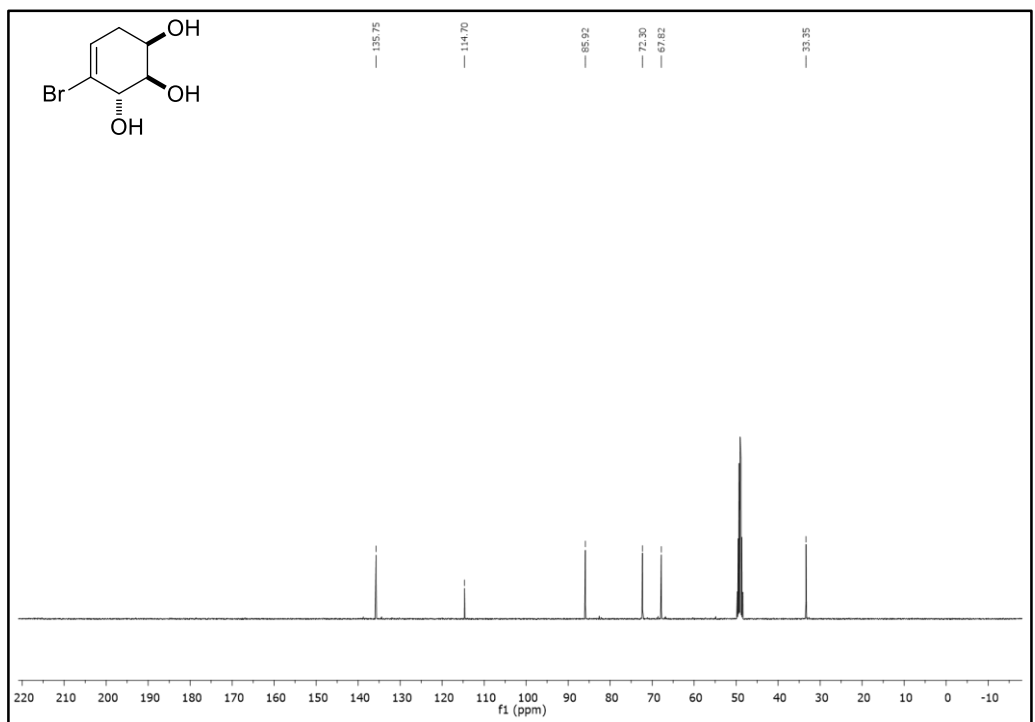


Figure 109. ^{13}C -NMR Spectrum of Compound **251**

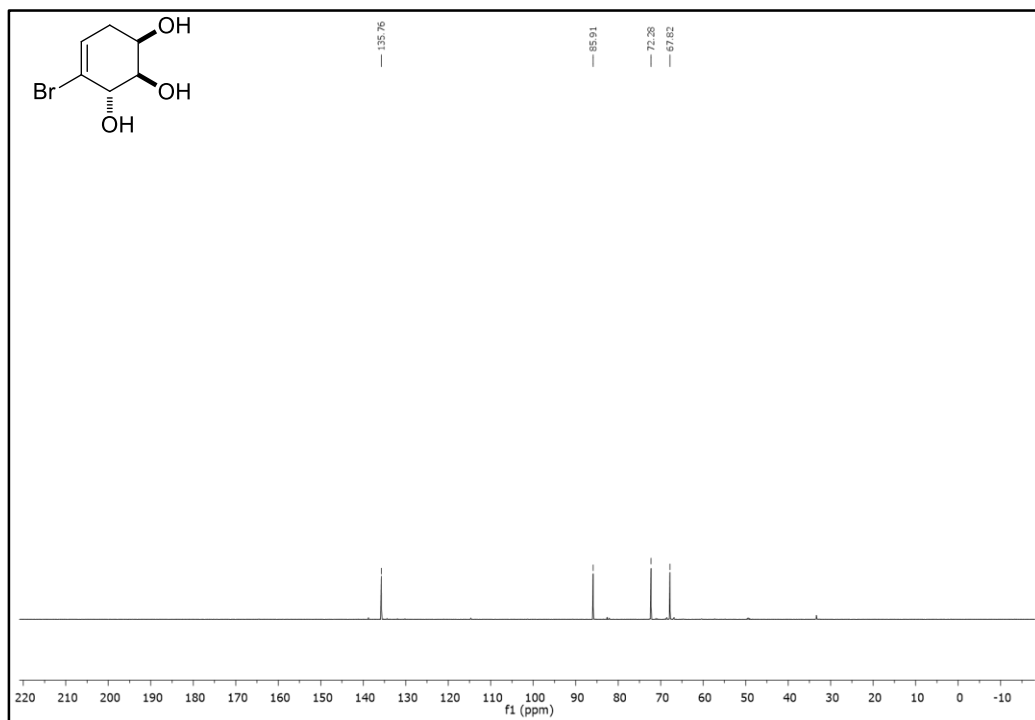


Figure 110. DEPT-90 Spectrum of Compound **251**

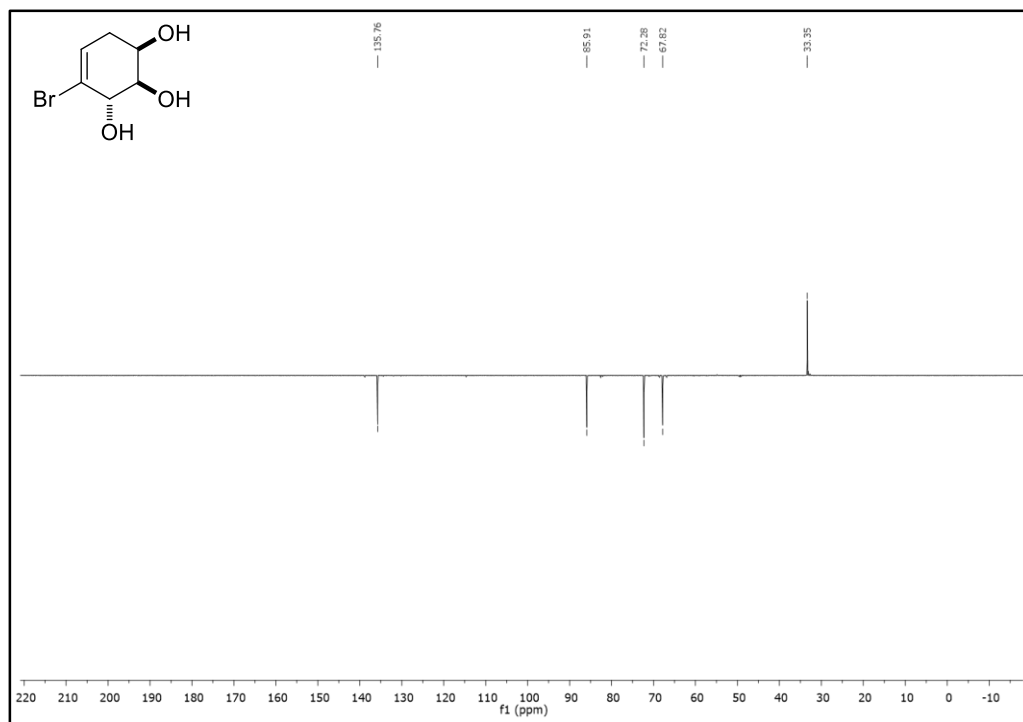


Figure 111. DEPT-135 Spectrum of Compound **251**

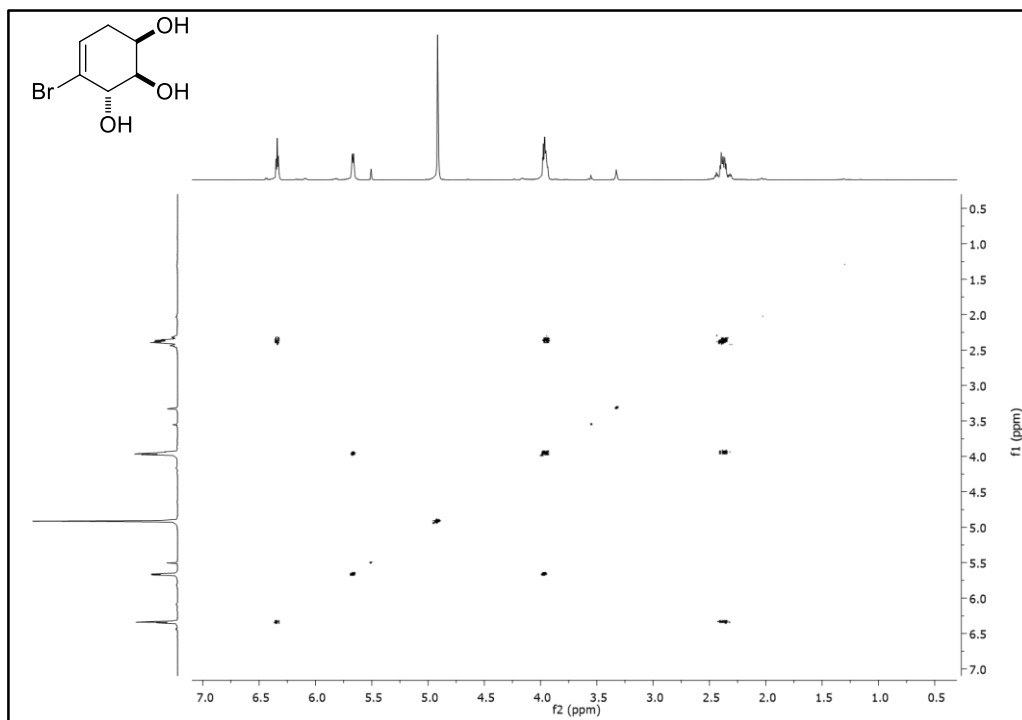


Figure 112. COSY Spectrum of Compound **251**

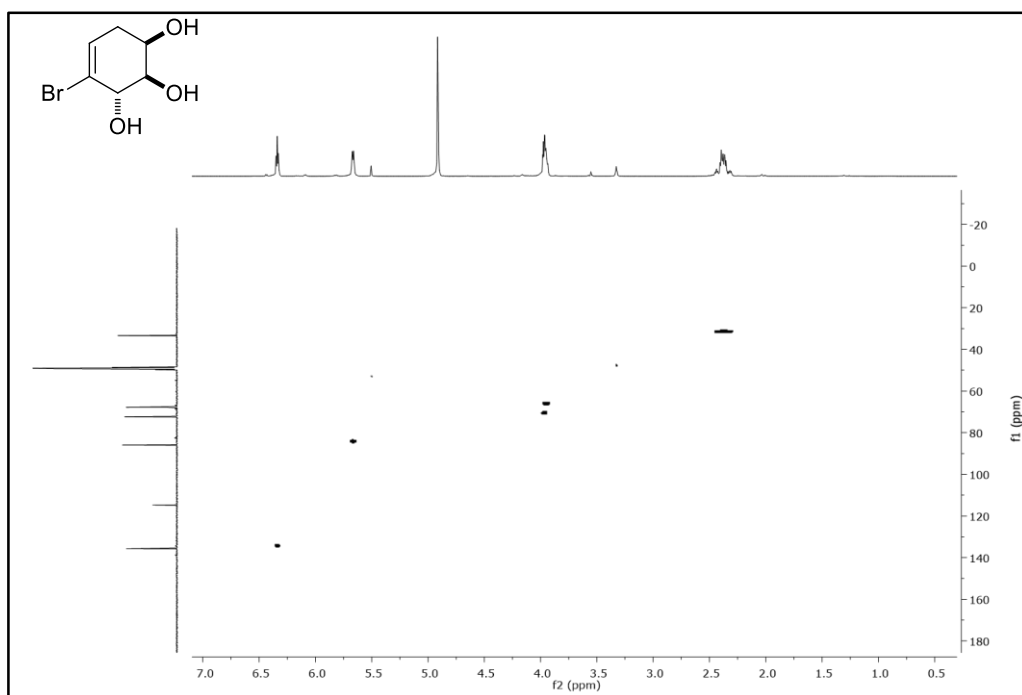


Figure 113. HSQC Spectrum of Compound **251**

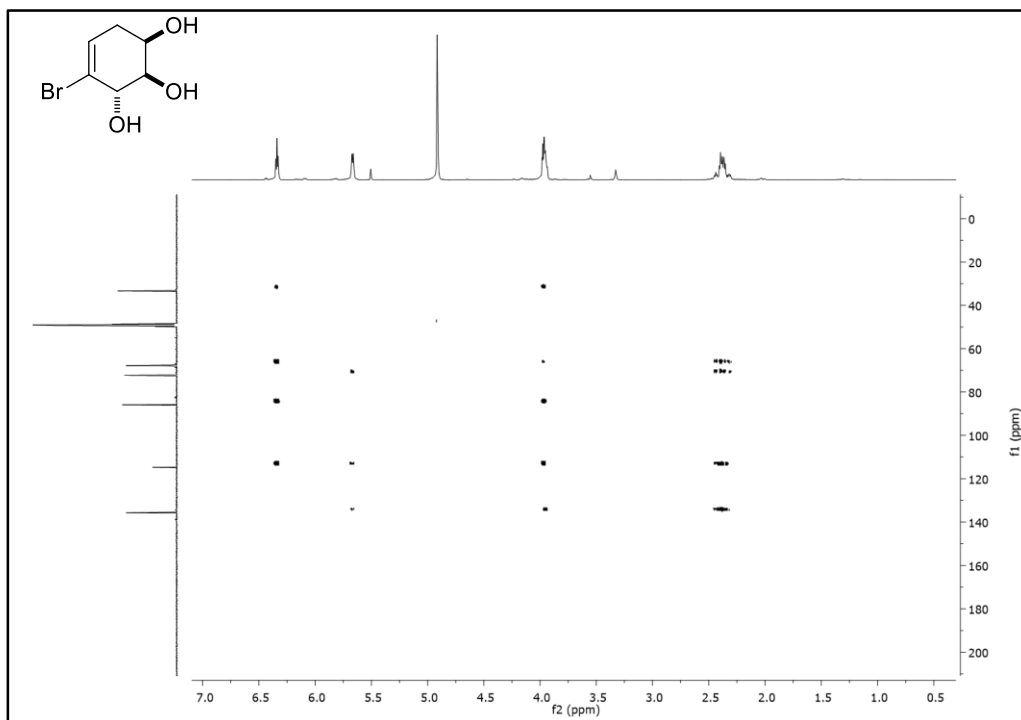


Figure 114. HMBC Spectrum of Compound **251**

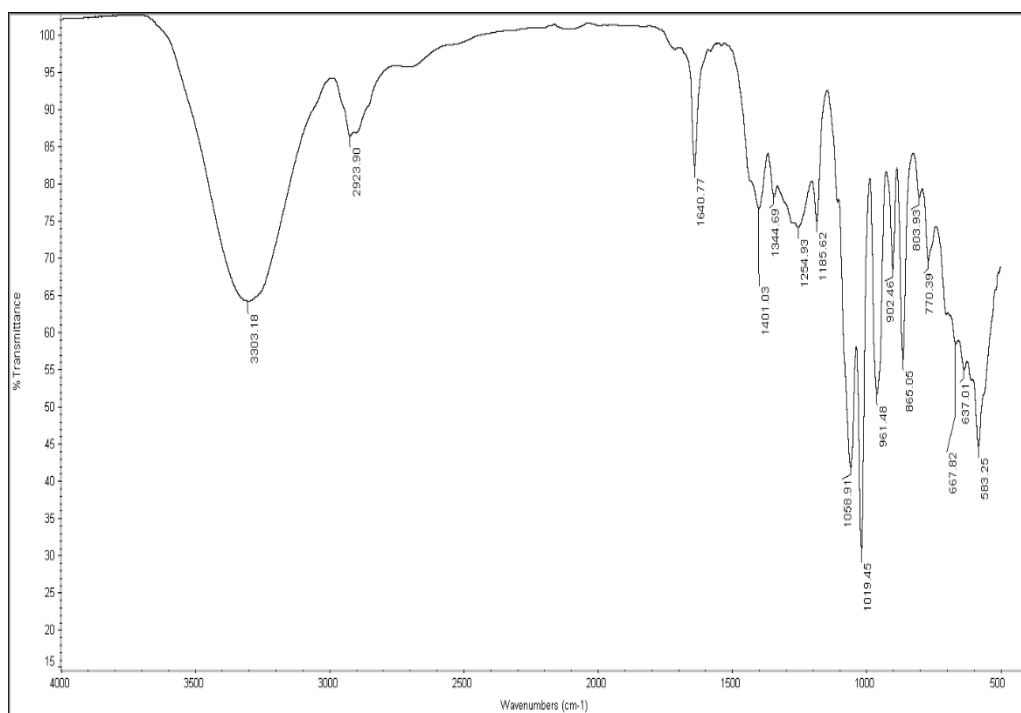


Figure 115. IR Spectrum of Compound **251**

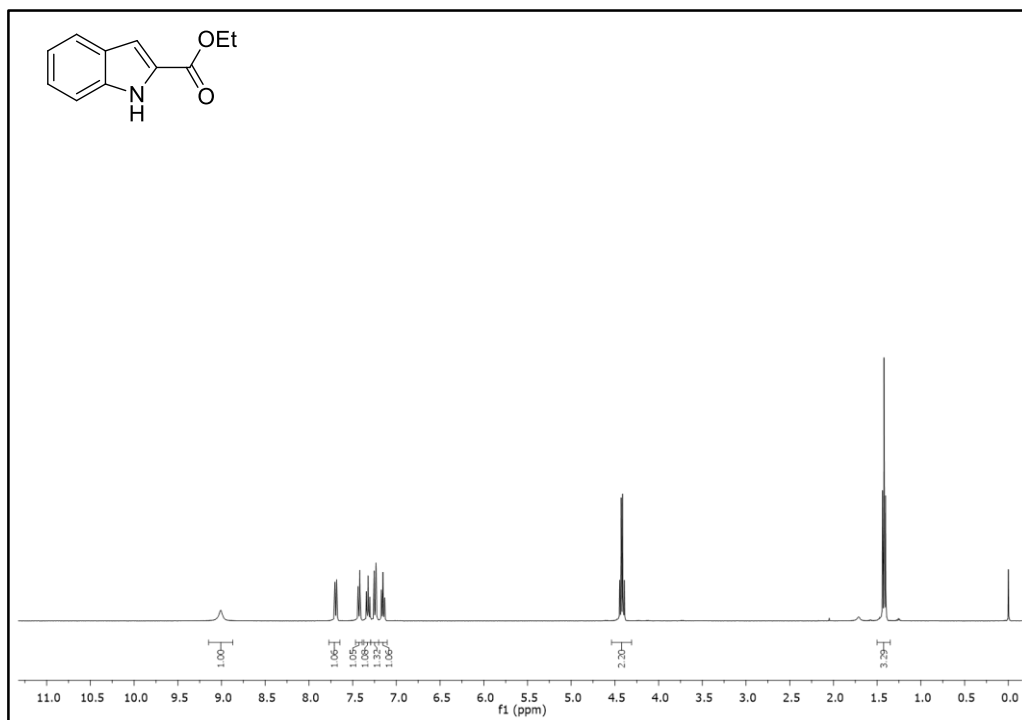


Figure 116. ¹H-NMR Spectrum of Compound **353**

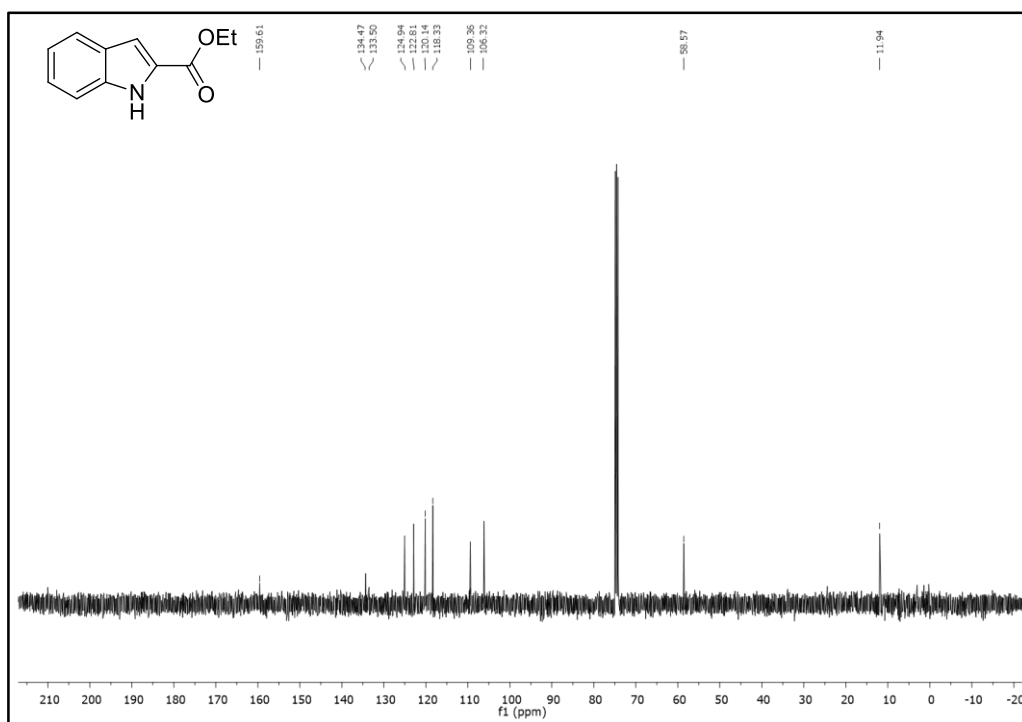


Figure 117. ¹³C-NMR Spectrum of Compound **353**

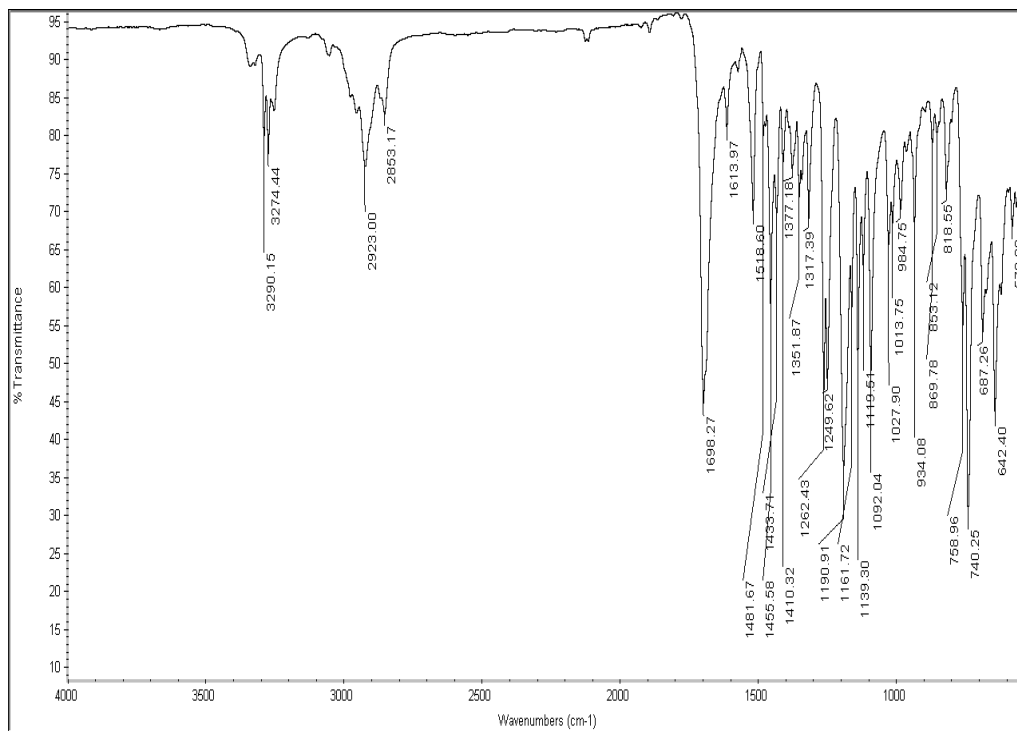


Figure 118. IR Spectrum of Compound 353

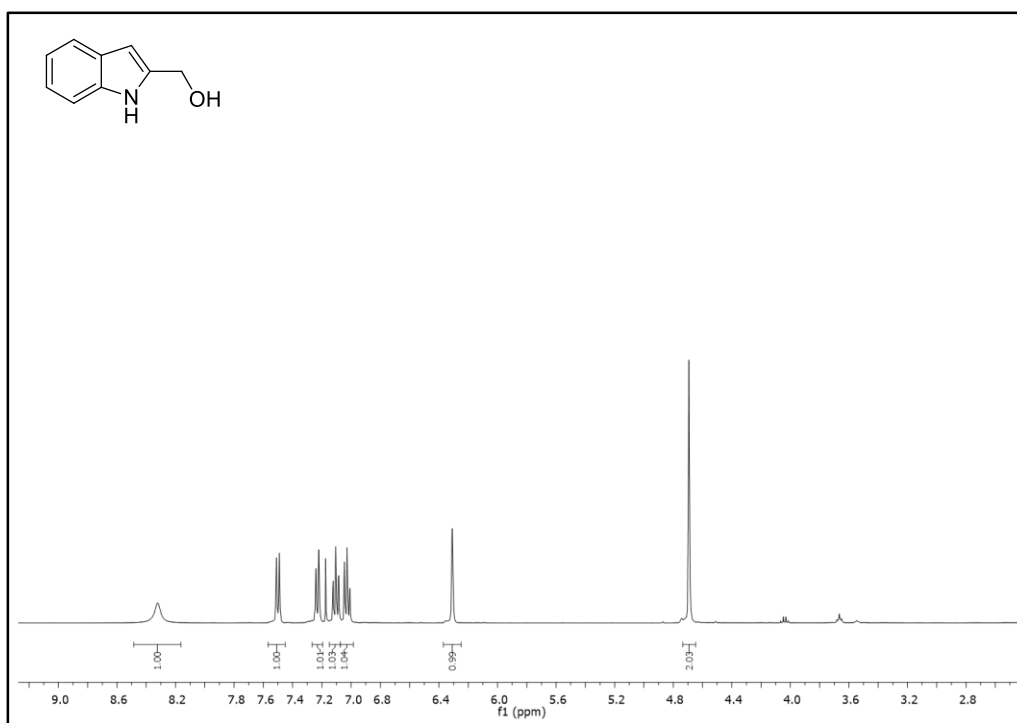


Figure 119. ¹H-NMR Spectrum of Compound 354

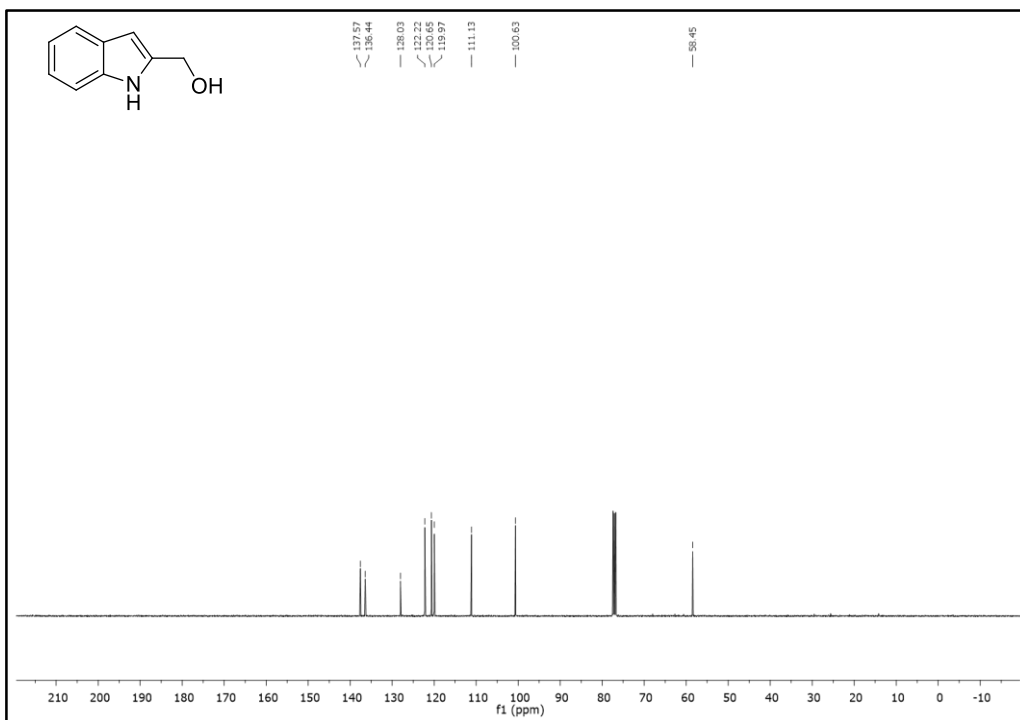


Figure 120. ¹³C-NMR Spectrum of Compound 354

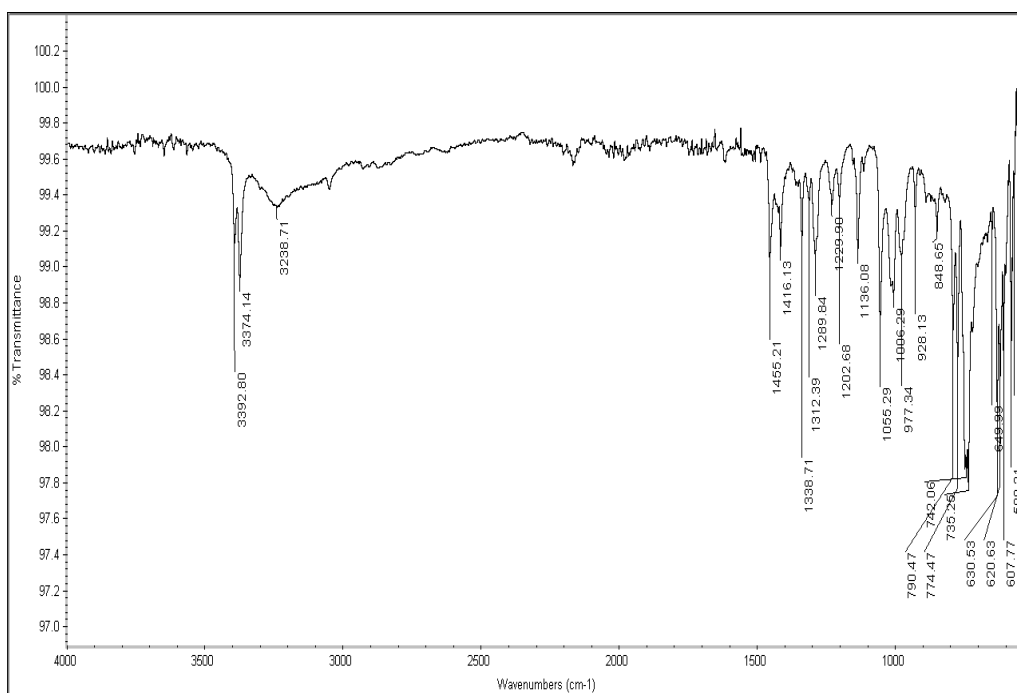


Figure 121. IR Spectrum of Compound 354

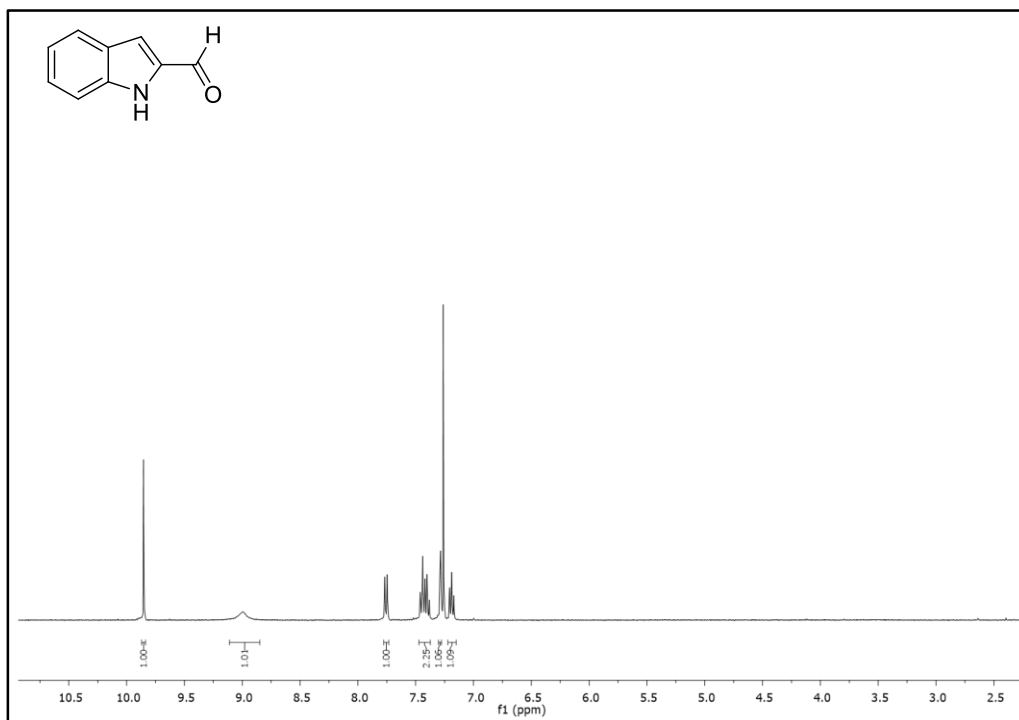


Figure 122. ¹H-NMR Spectrum of Compound 355

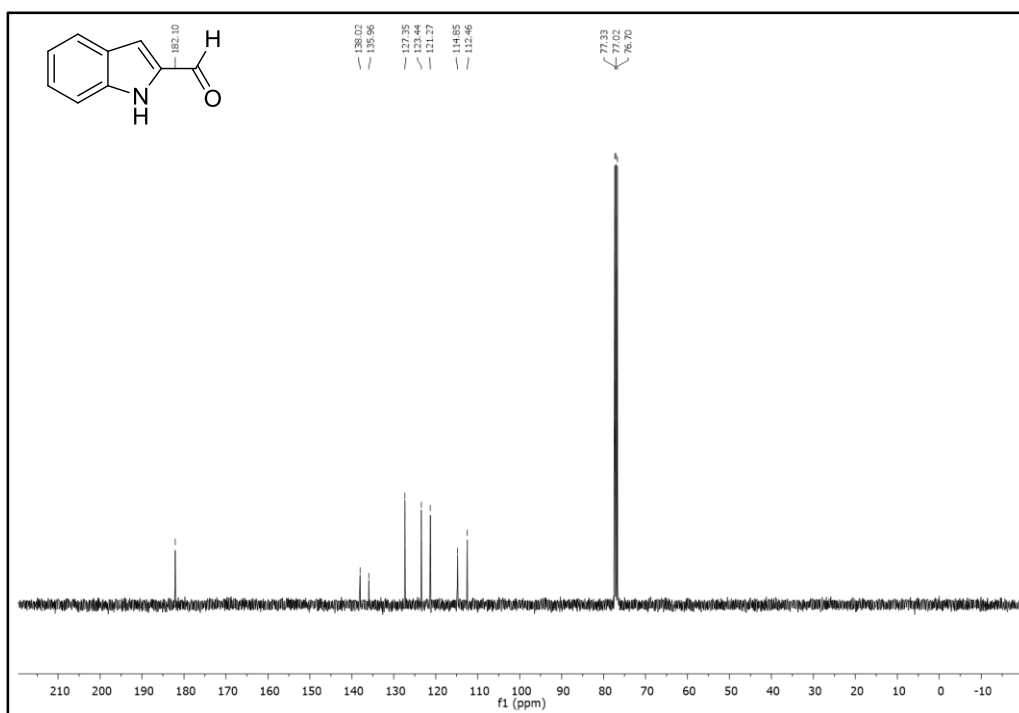


Figure 123. ¹³C-NMR Spectrum of Compound 355

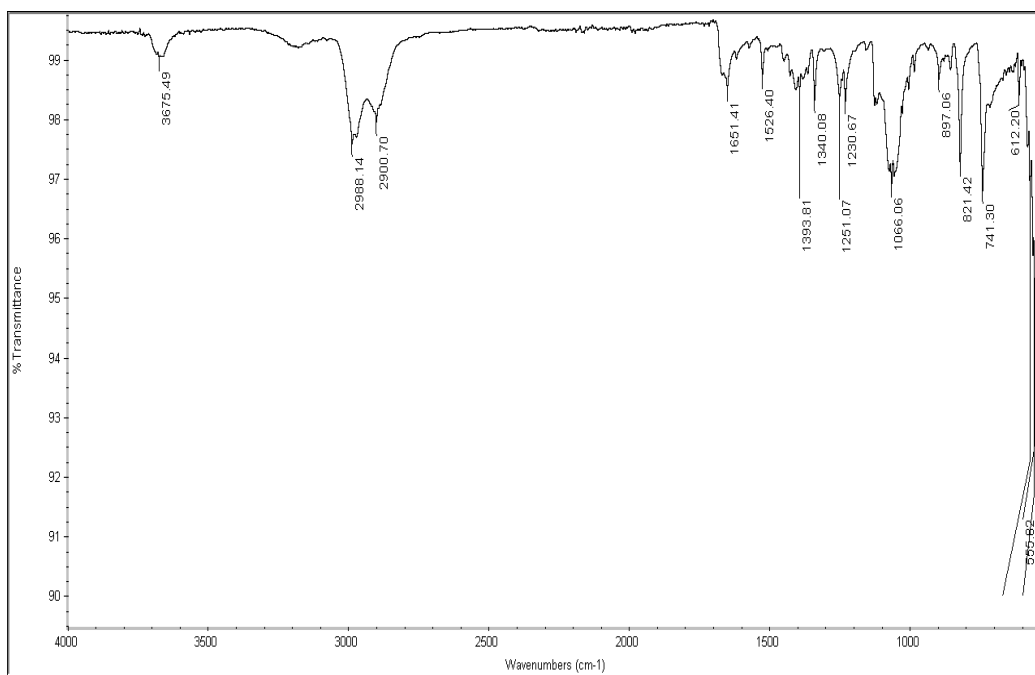


Figure 124. IR Spectrum of Compound 355

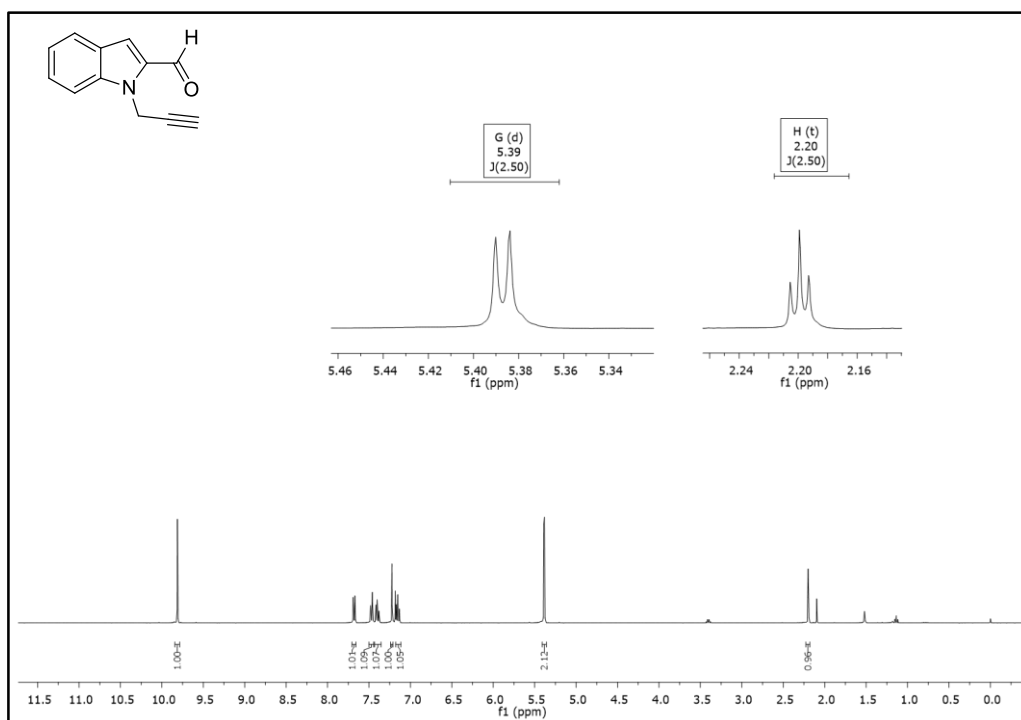


Figure 125. ¹H-NMR Spectrum of Compound 357

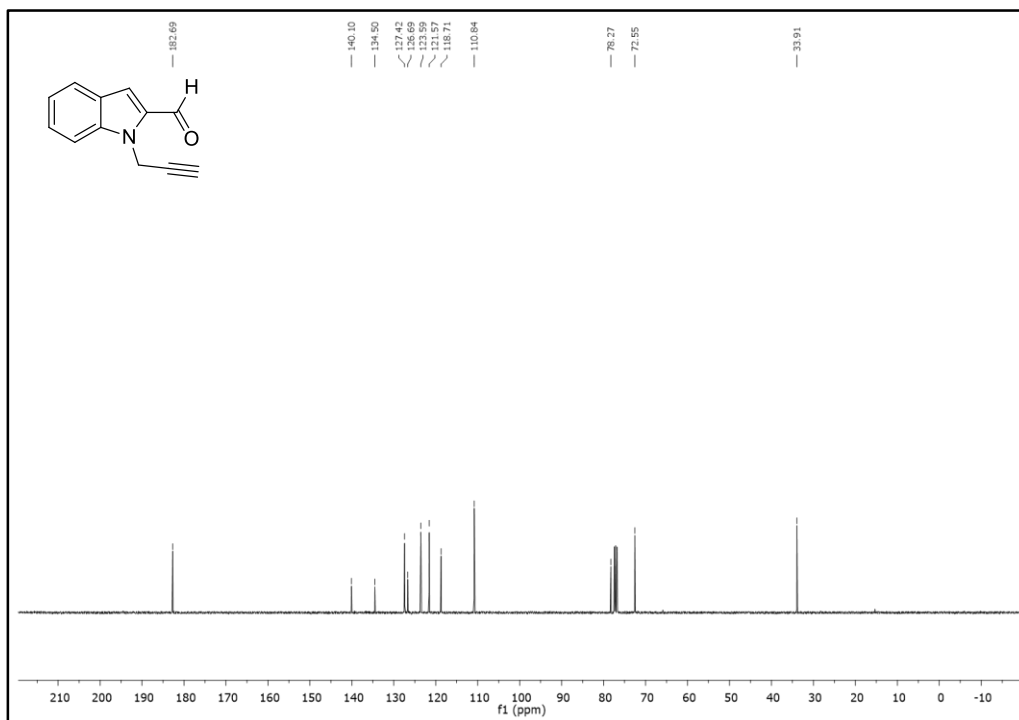


Figure 126. ¹³C-NMR Spectrum of Compound **357**

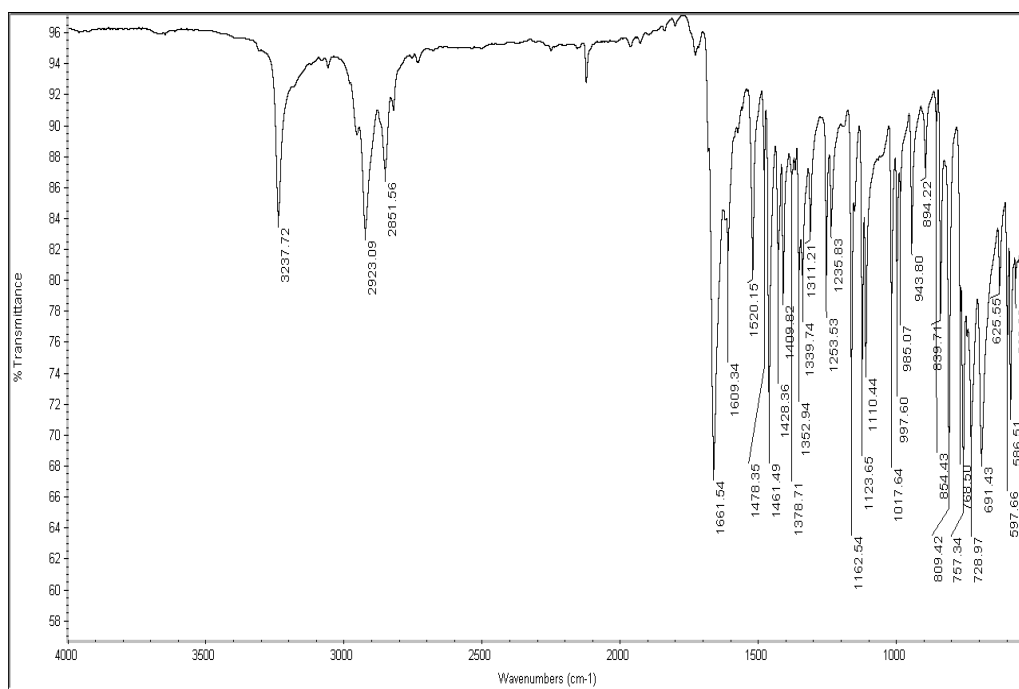


Figure 127. IR Spectrum of Compound **357**

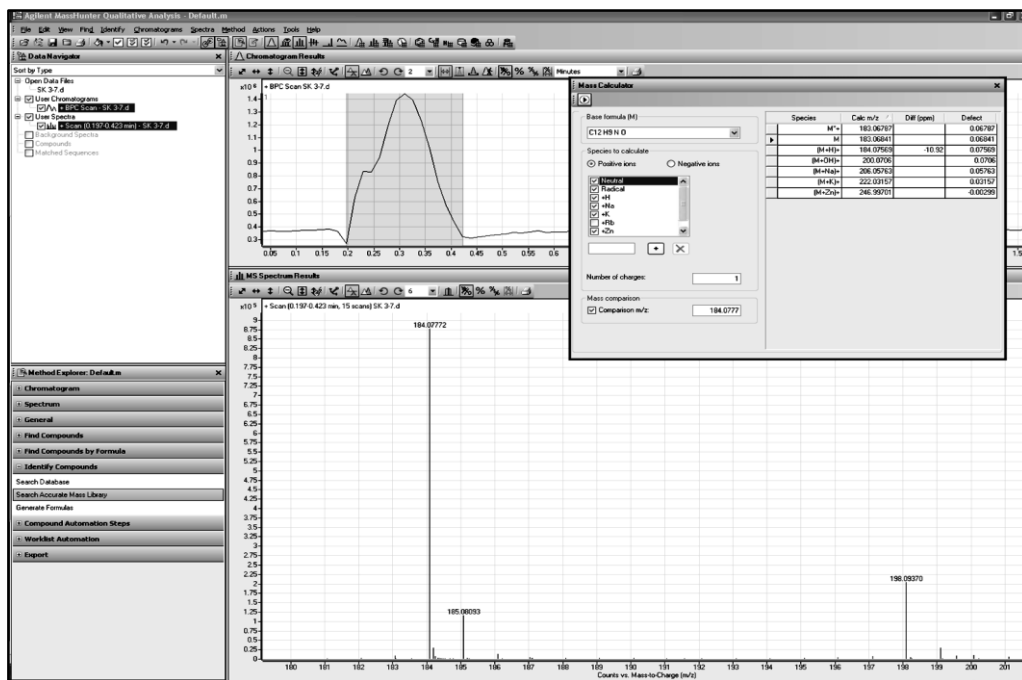


Figure 128. HRMS Spectrum of Compound 357

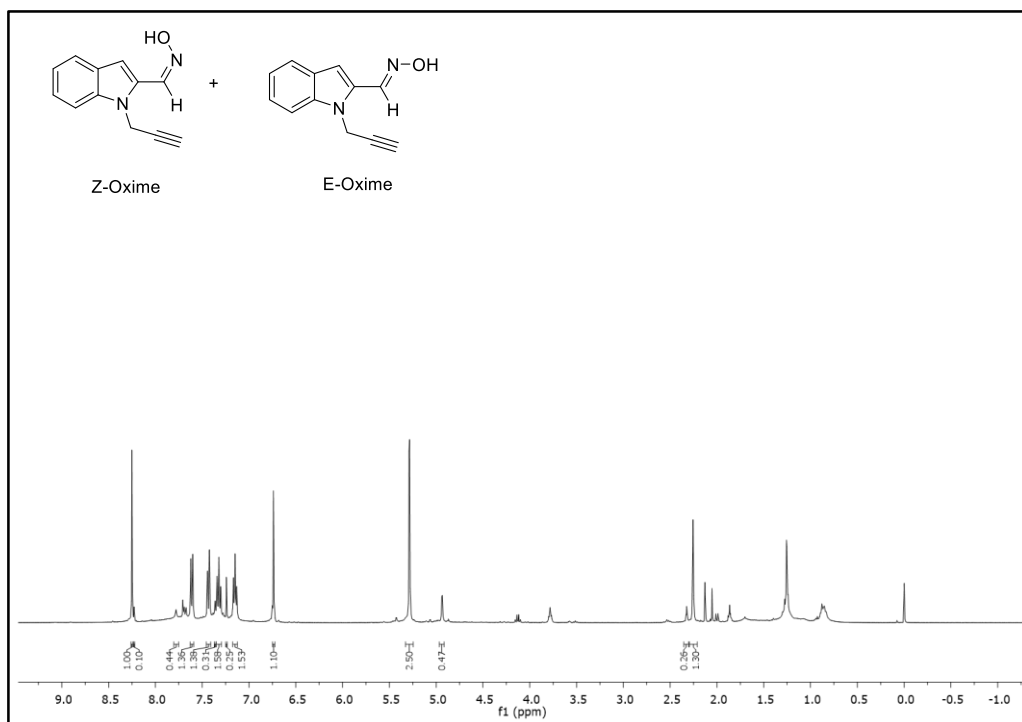


Figure 129. Crude ¹H-NMR Spectrum of Compounds 358 and 359

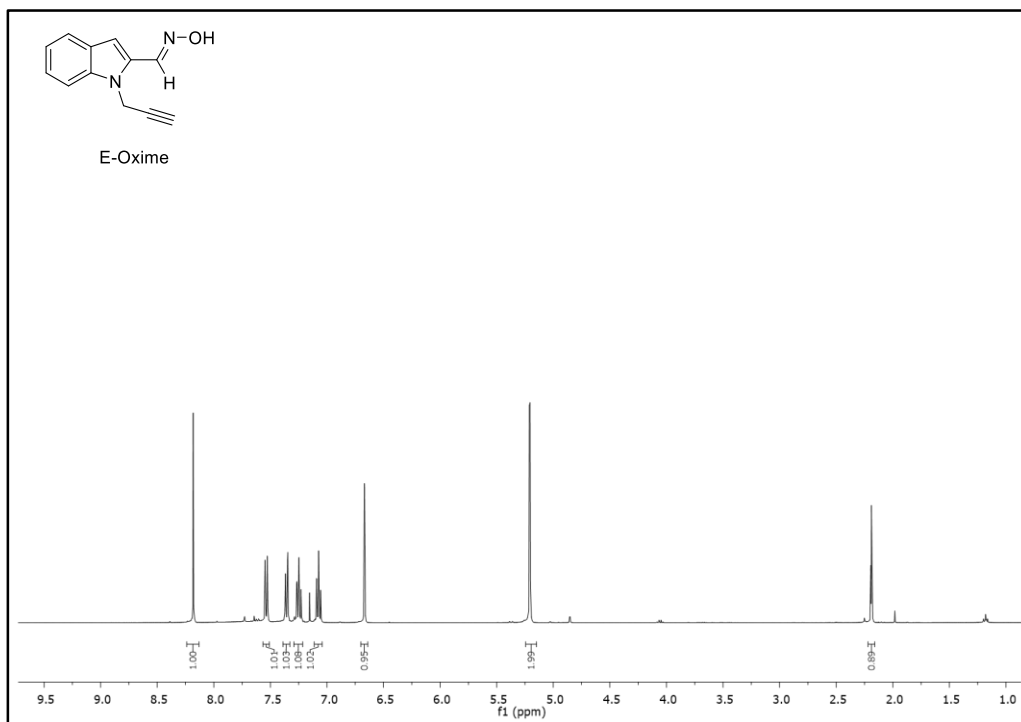


Figure 130. ^1H -NMR Spectrum of Compound 359

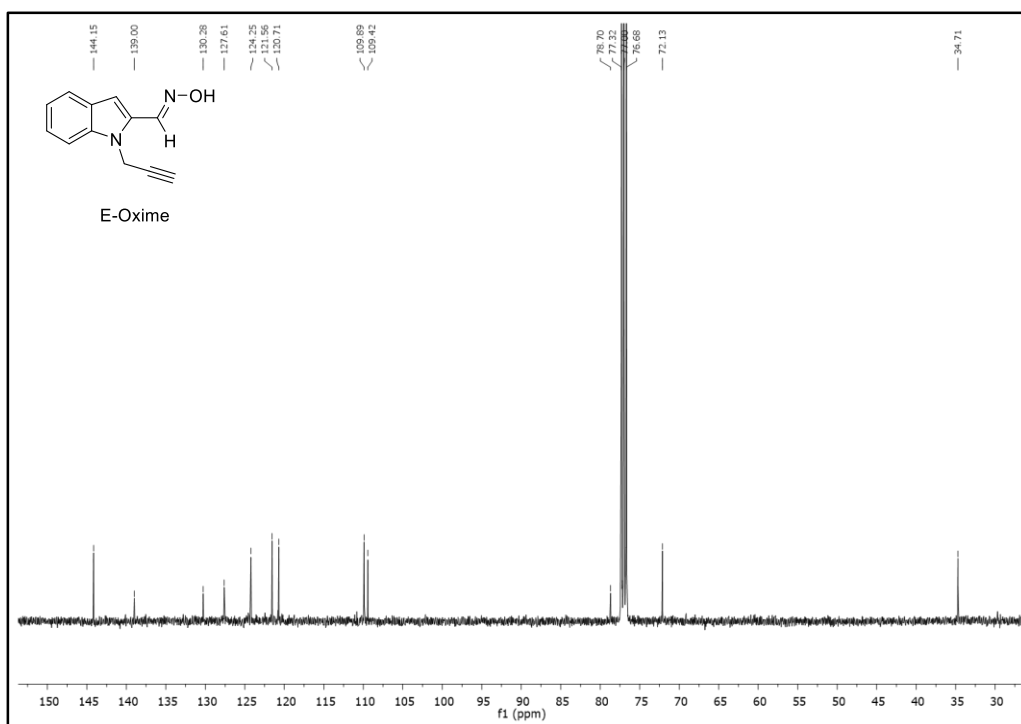


Figure 131. ^{13}C -NMR Spectrum of Compound 359

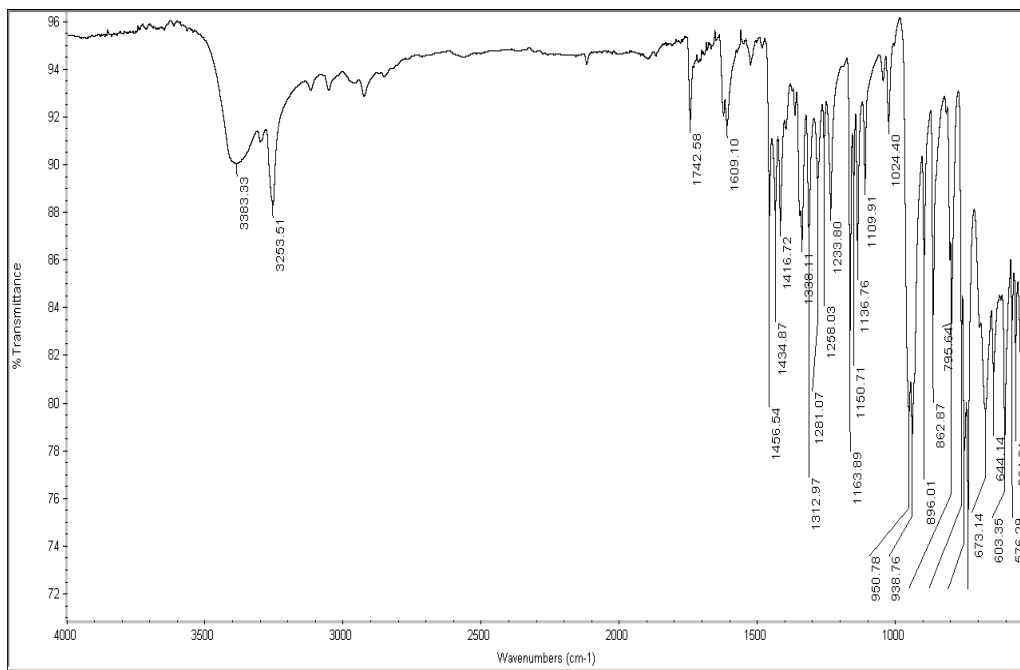


Figure 132. IR Spectrum of Compound 359

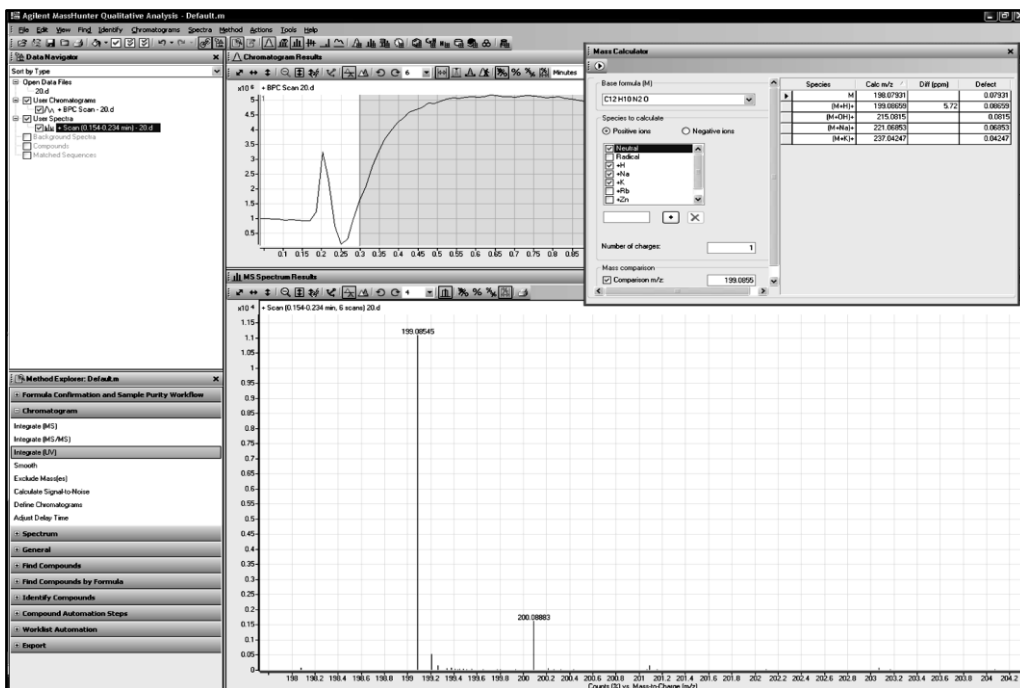


Figure 133. HRMS Spectrum of Compound 359

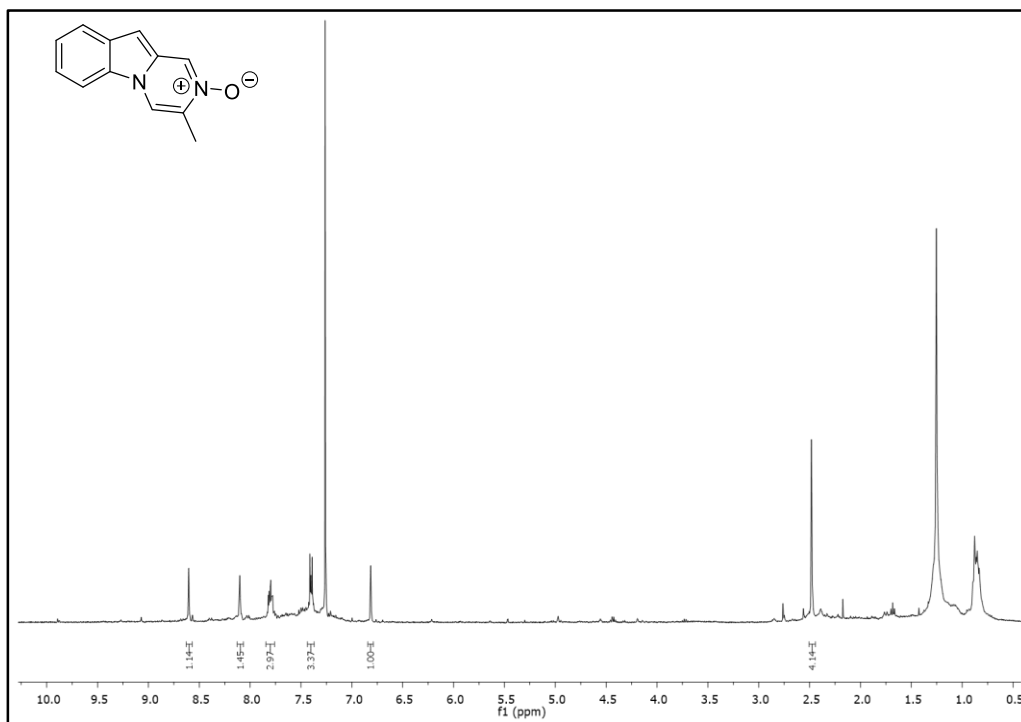


Figure 134. ¹H-NMR Spectrum of Compound 360

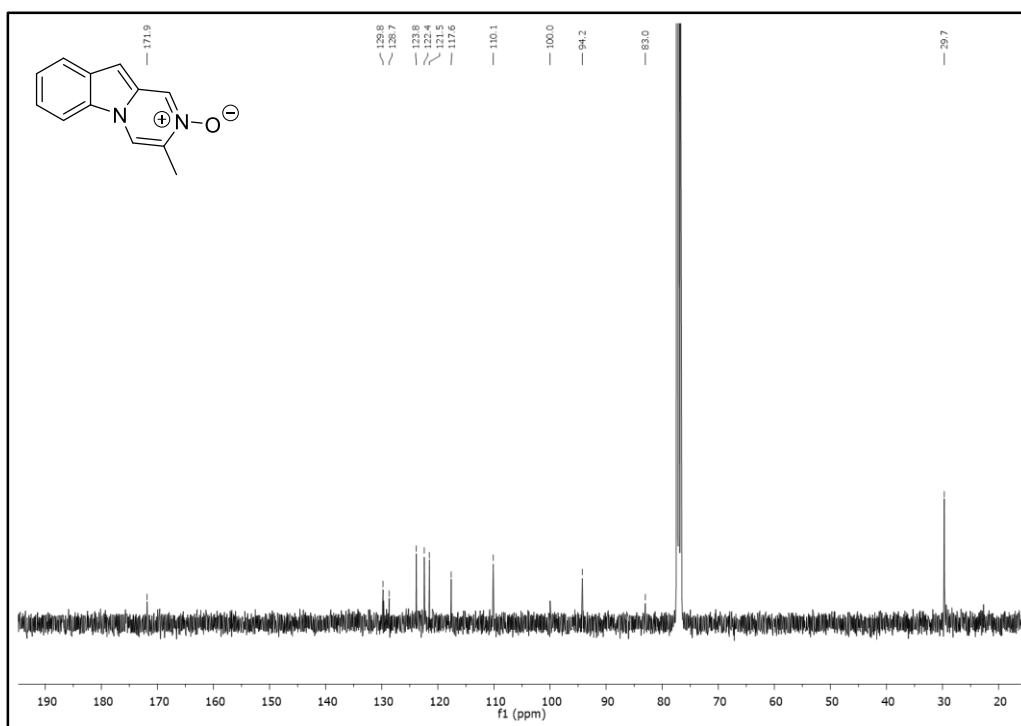


Figure 135. ¹³C-NMR Spectrum of Compound 360

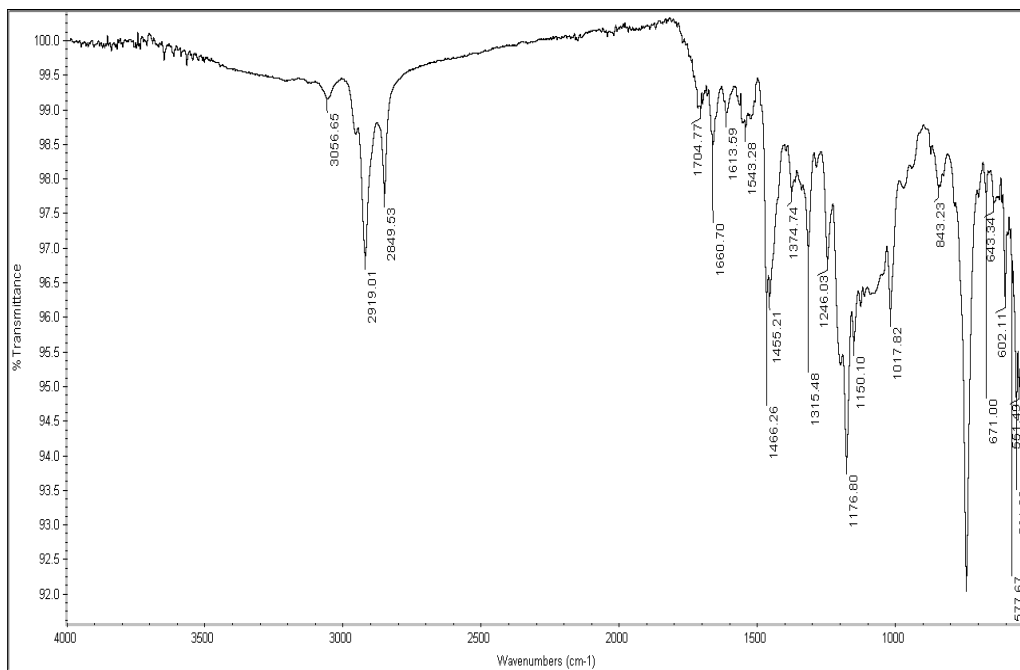


Figure 136. IR Spectrum of Compound 360

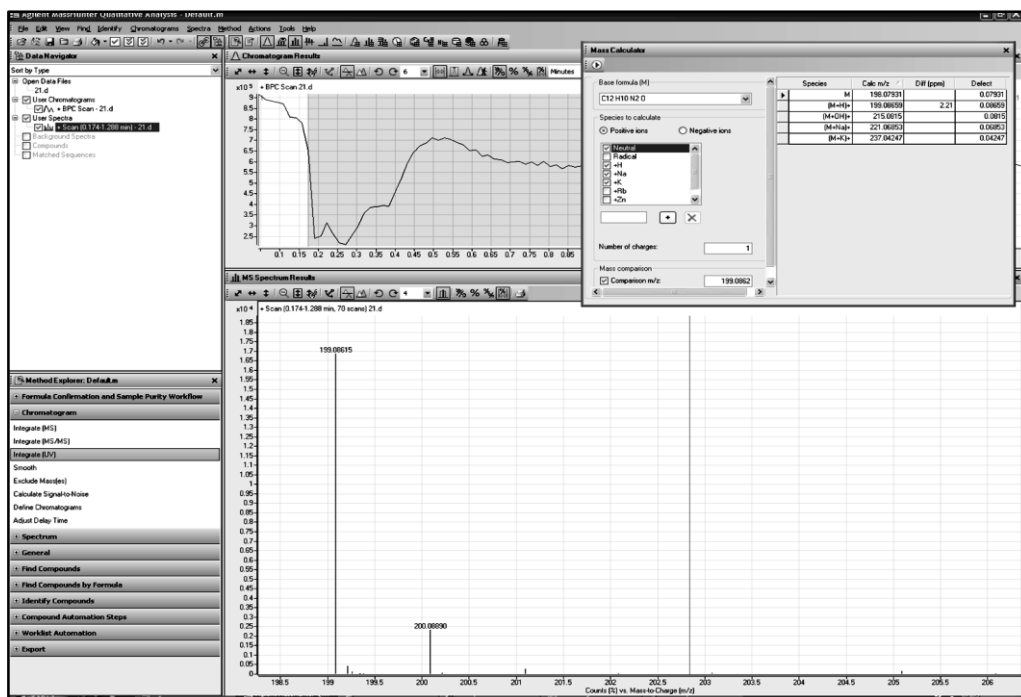


Figure 137. HRMS Spectrum of Compound 360

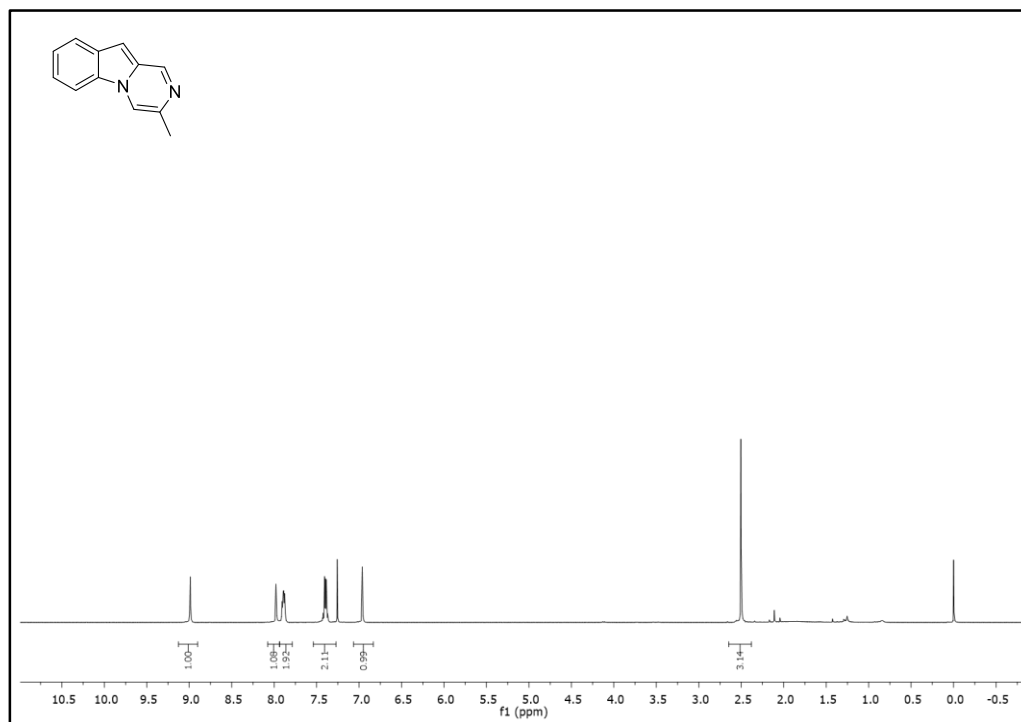


Figure 138. ¹H-NMR Spectrum of Compound 360

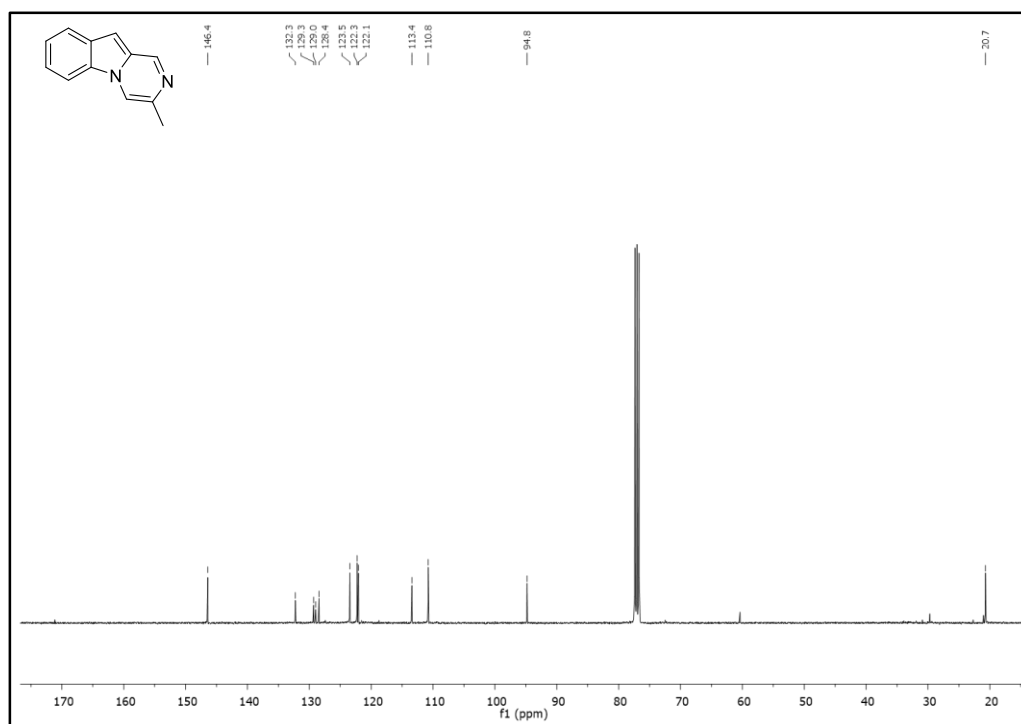


Figure 139. ¹³C-NMR Spectrum of Compound 360

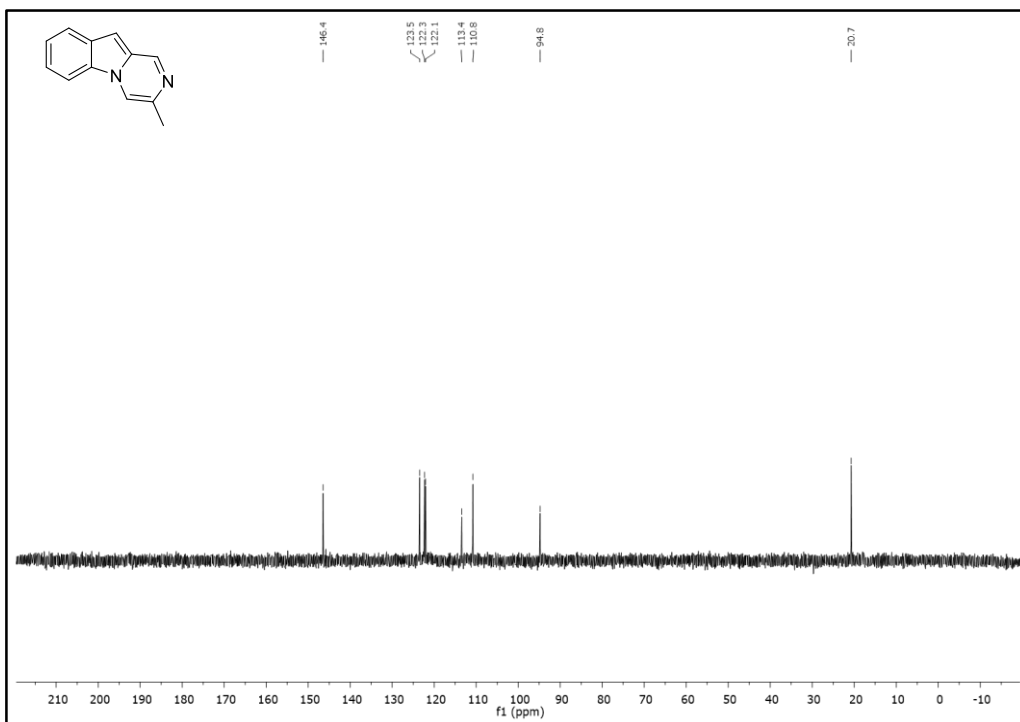


Figure 140. DEPT-135 Spectrum of Compound **360**

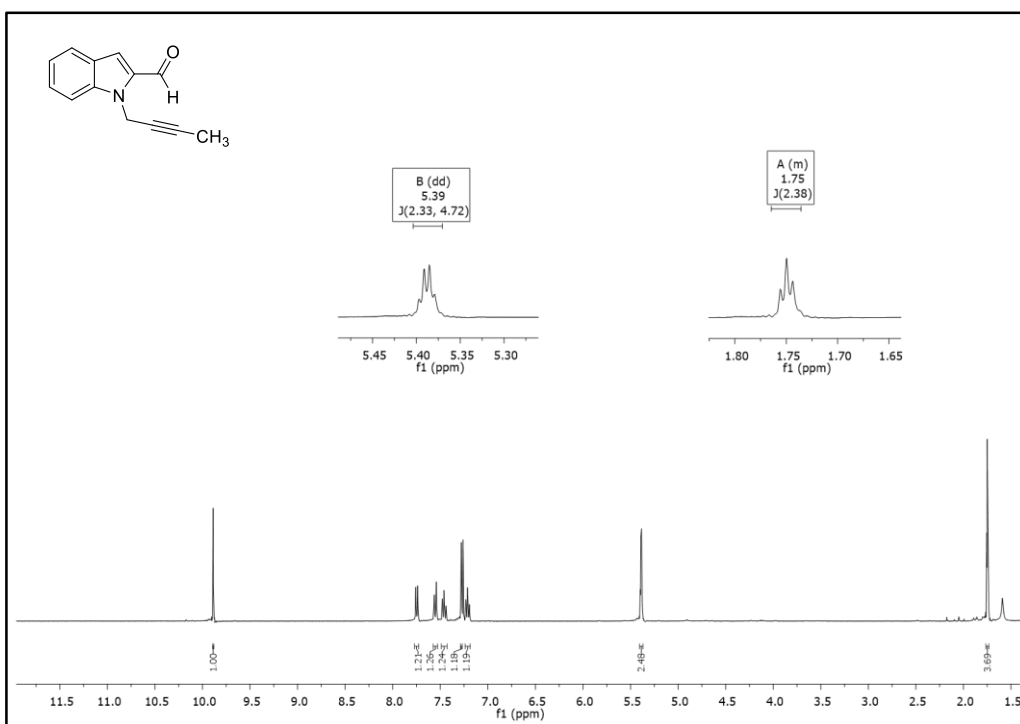


Figure 141. ^1H -NMR Spectrum of Compound **366**

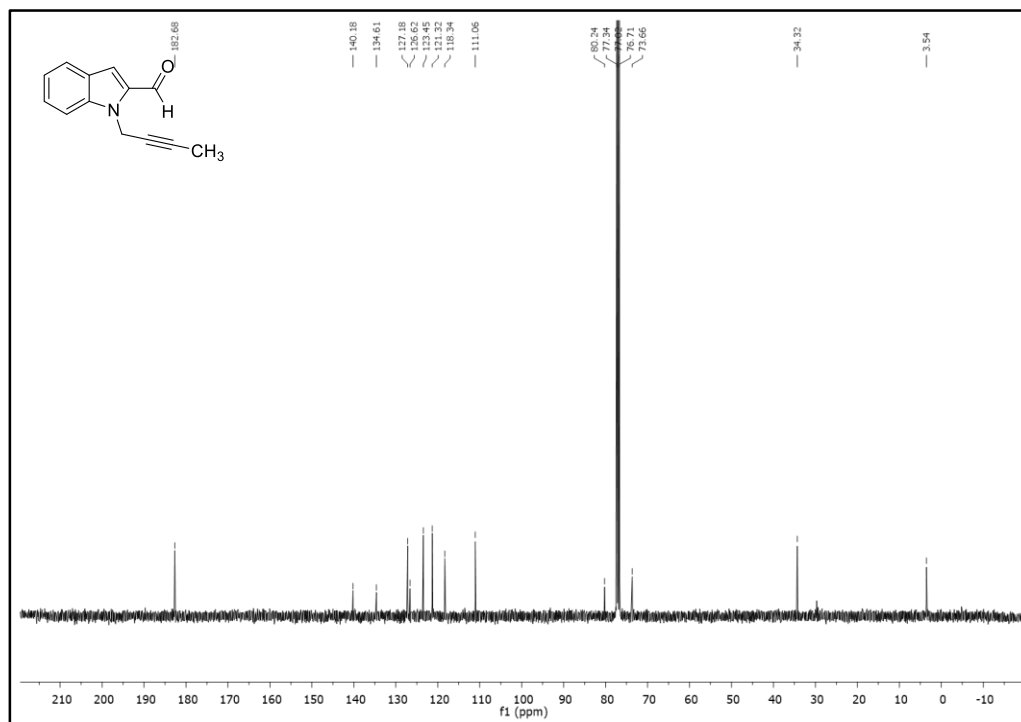


Figure 142. ¹³C-NMR Spectrum of Compound 366

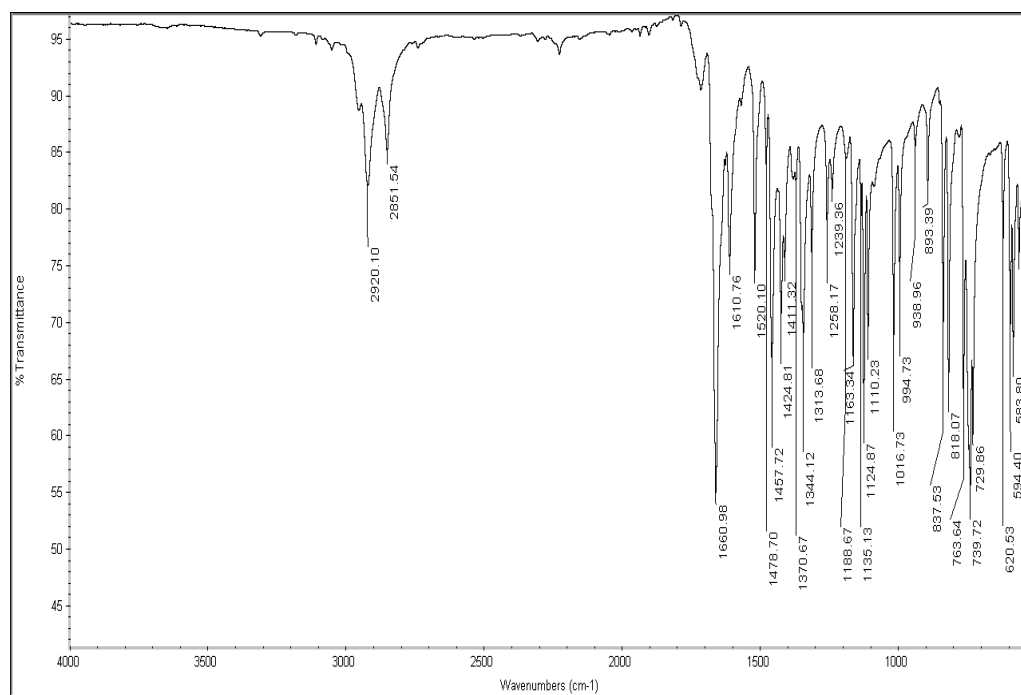


Figure 143. IR Spectrum of Compound 366

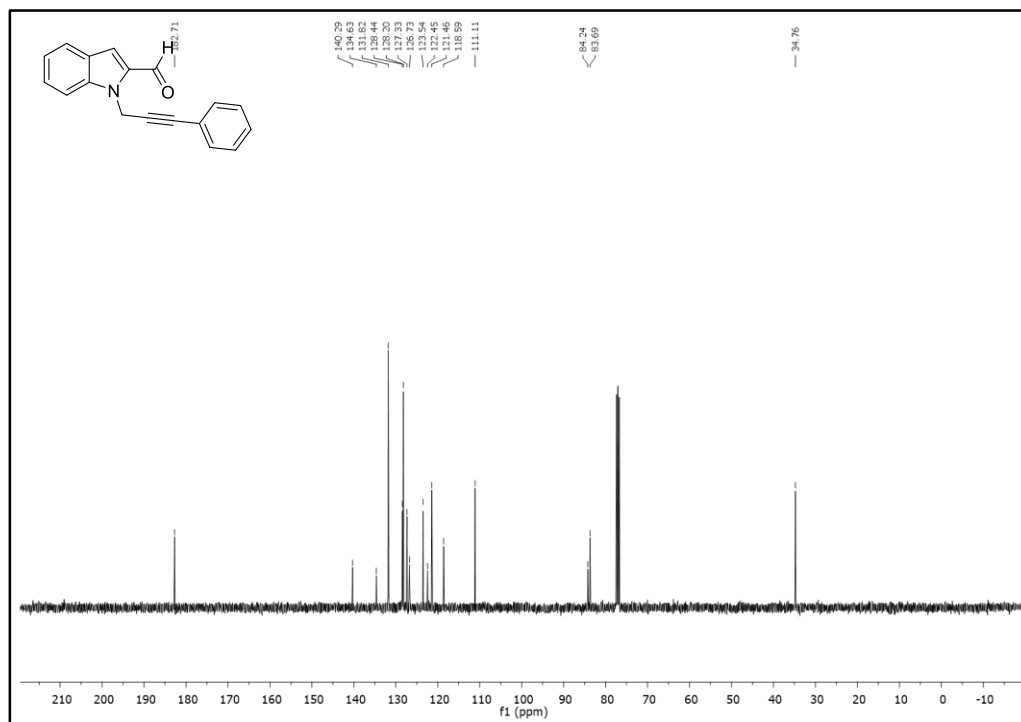


Figure 146. ¹³C-NMR Spectrum of Compound 367a

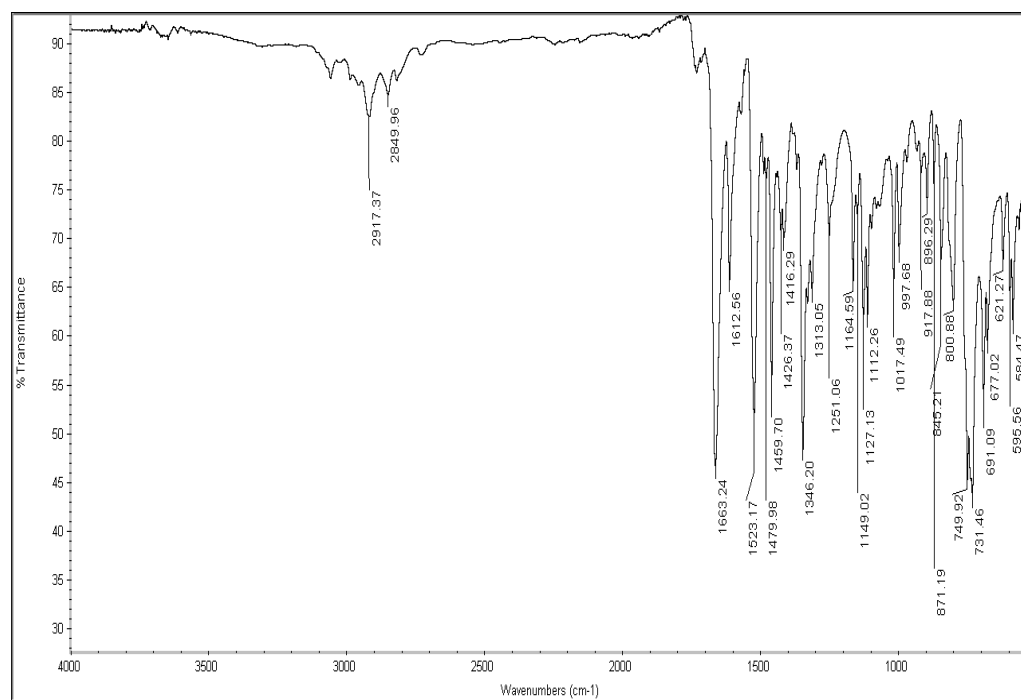


Figure 147. IR Spectrum of Compound 367a

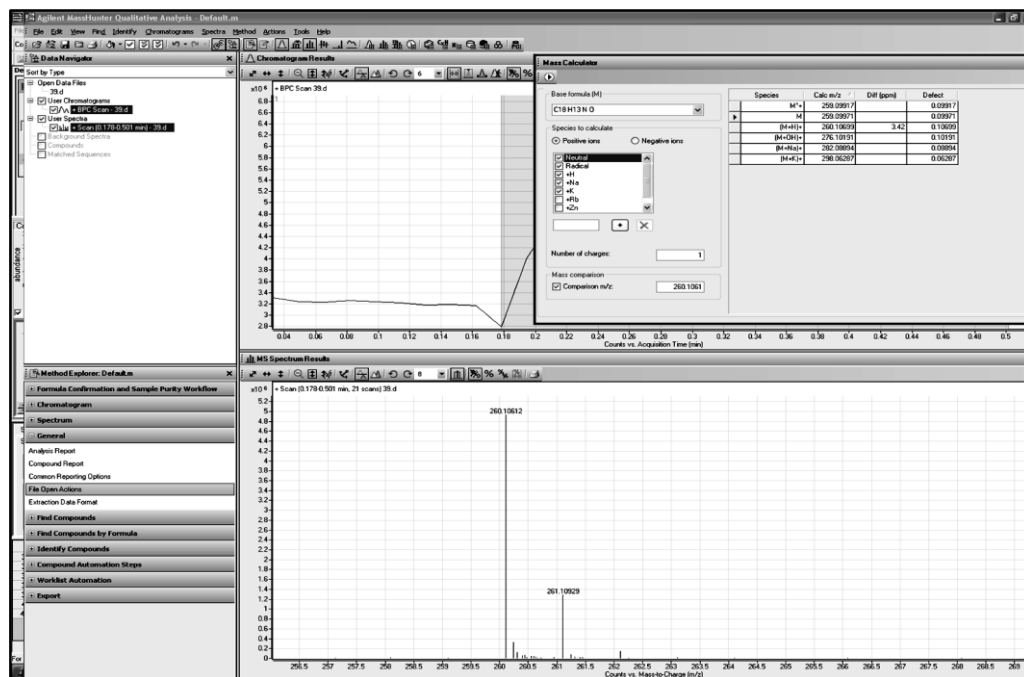


Figure 148. HRMS Spectrum of Compound 367a

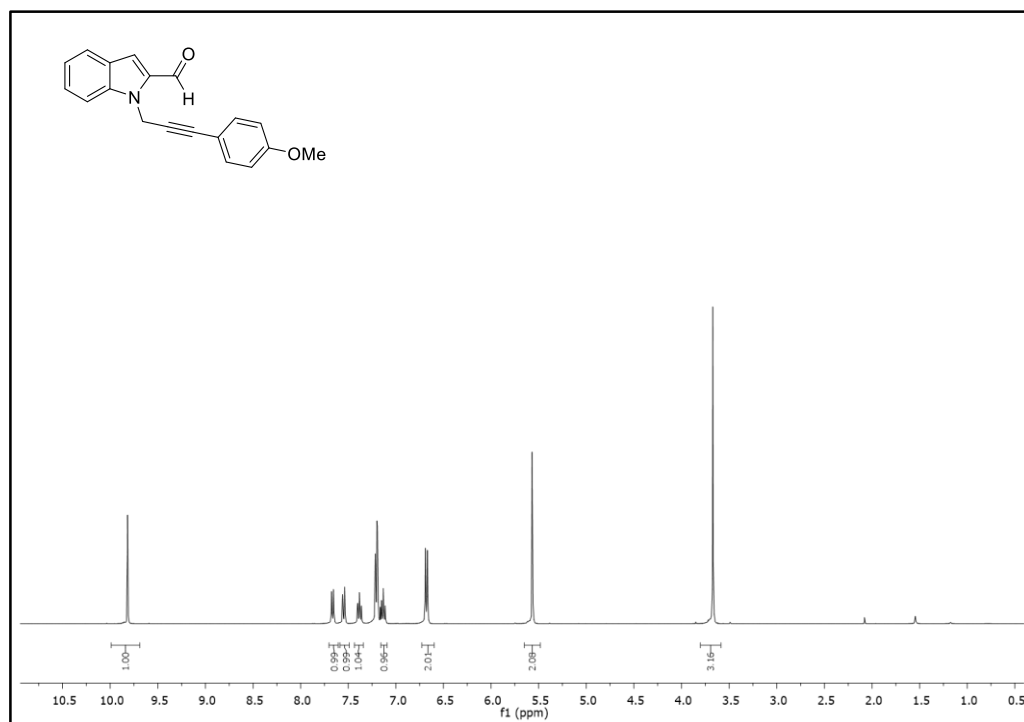


Figure 149. ¹H-NMR Spectrum of Compound 367b

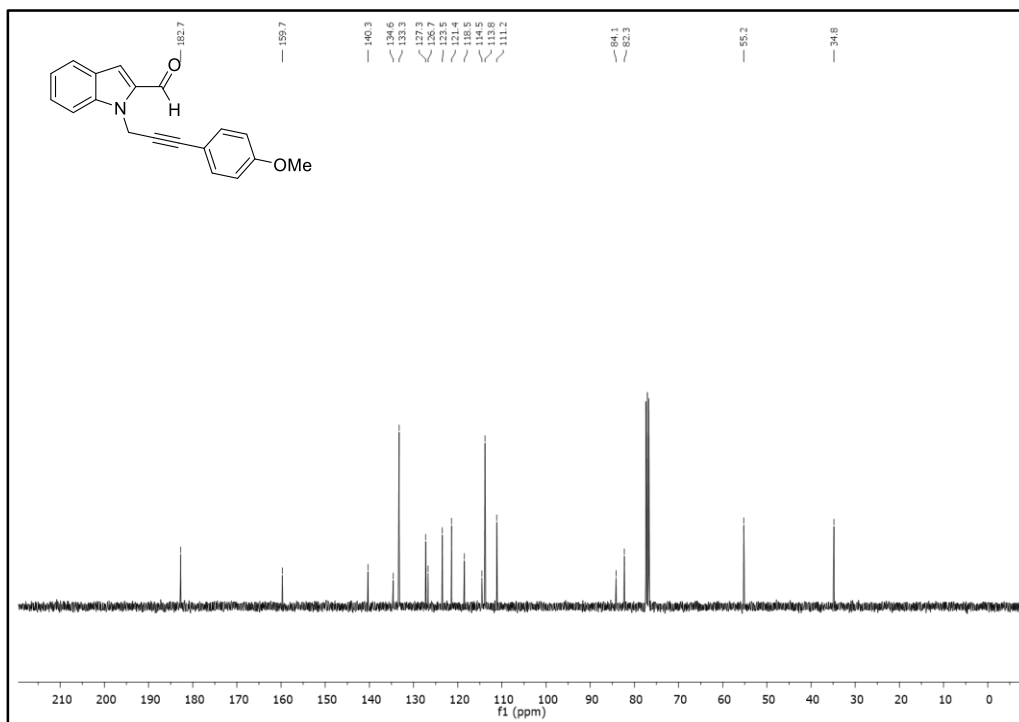


Figure 150. ¹³C-NMR Spectrum of Compound **367b**

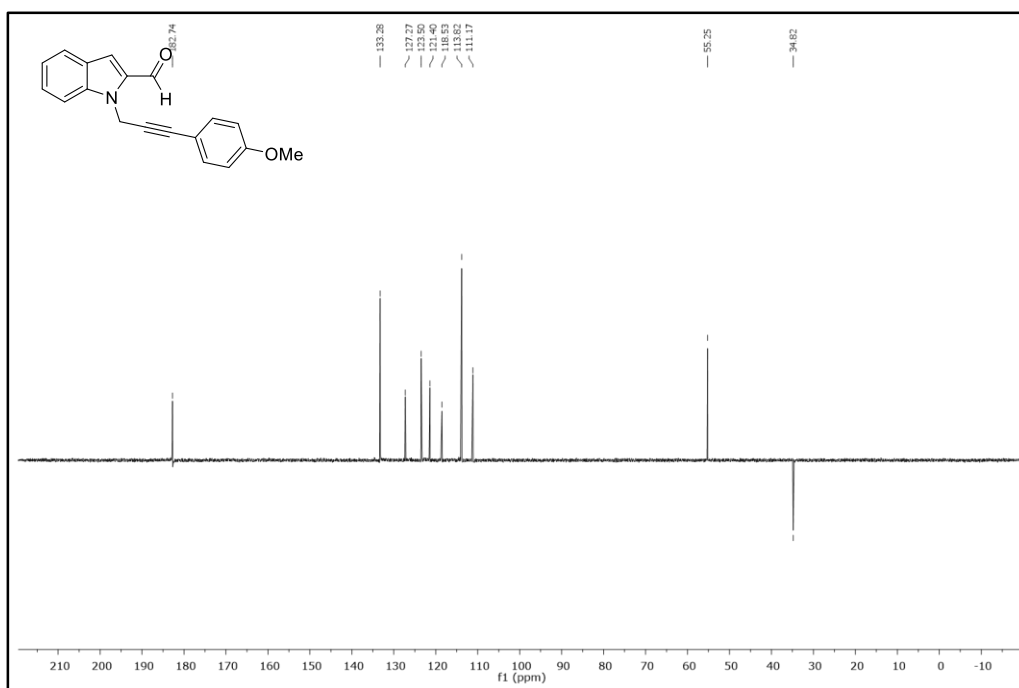


Figure 151. DEPT-135 Spectrum of Compound **367b**

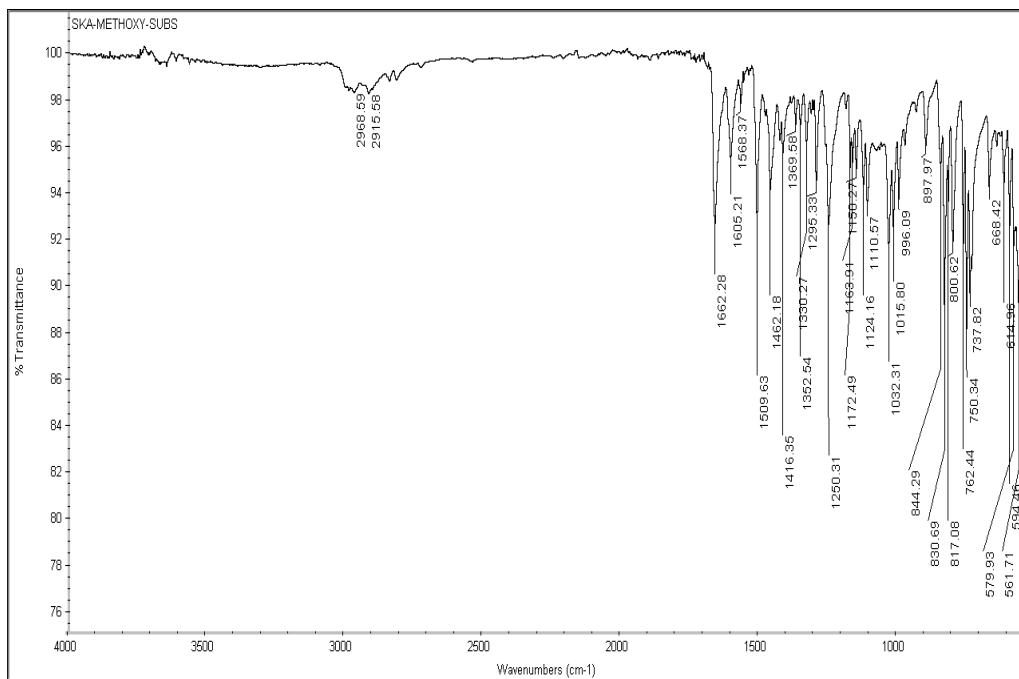


Figure 152. IR Spectrum of Compound 367b

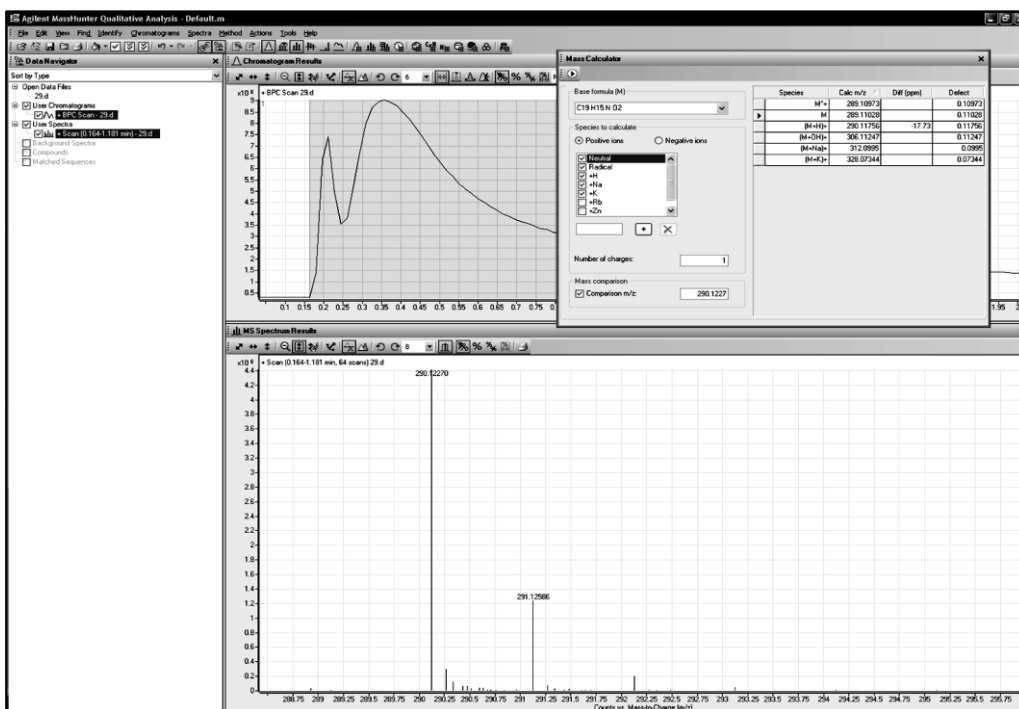


Figure 153. HRMS Spectrum of Compound 367b

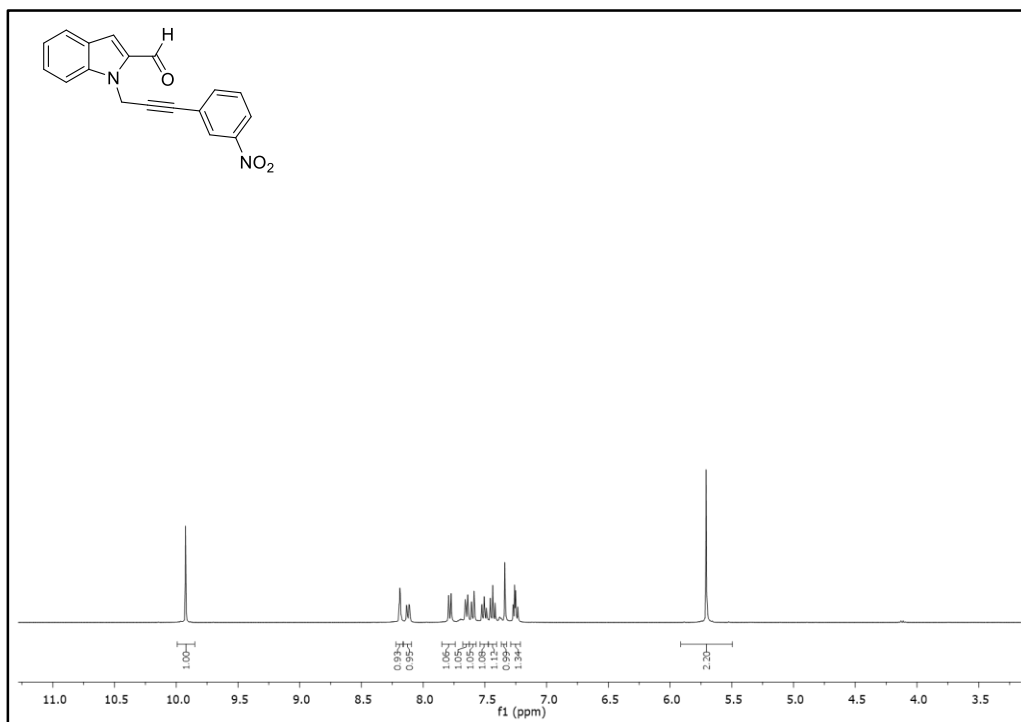


Figure 154. ¹H-NMR Spectrum of Compound 367c

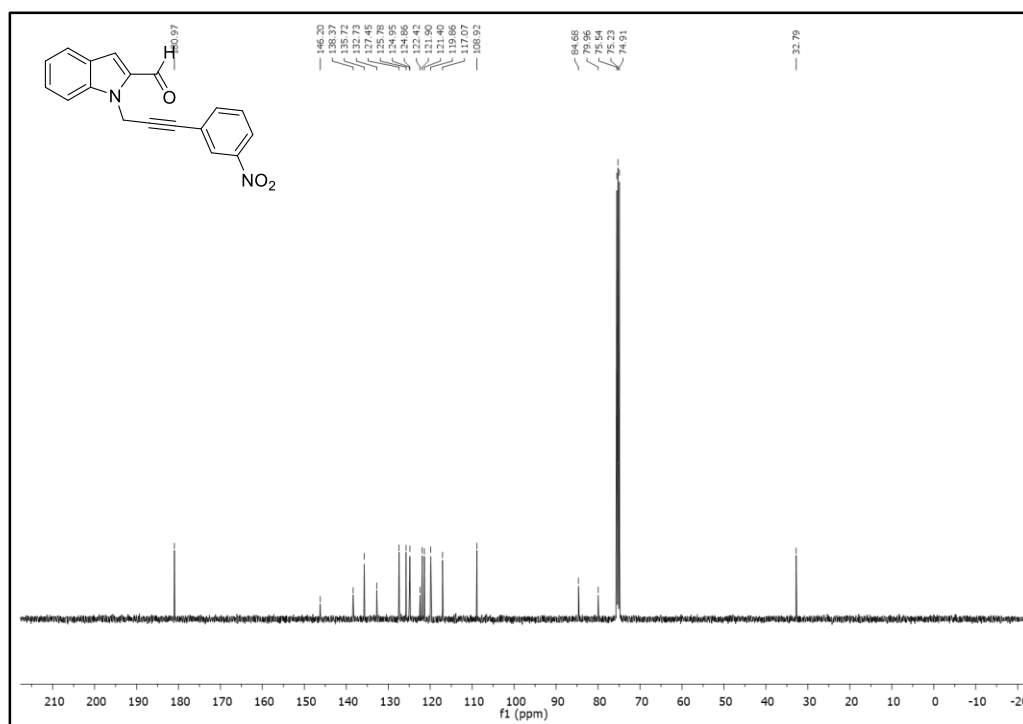


Figure 155. ¹³C-NMR Spectrum of Compound 367c

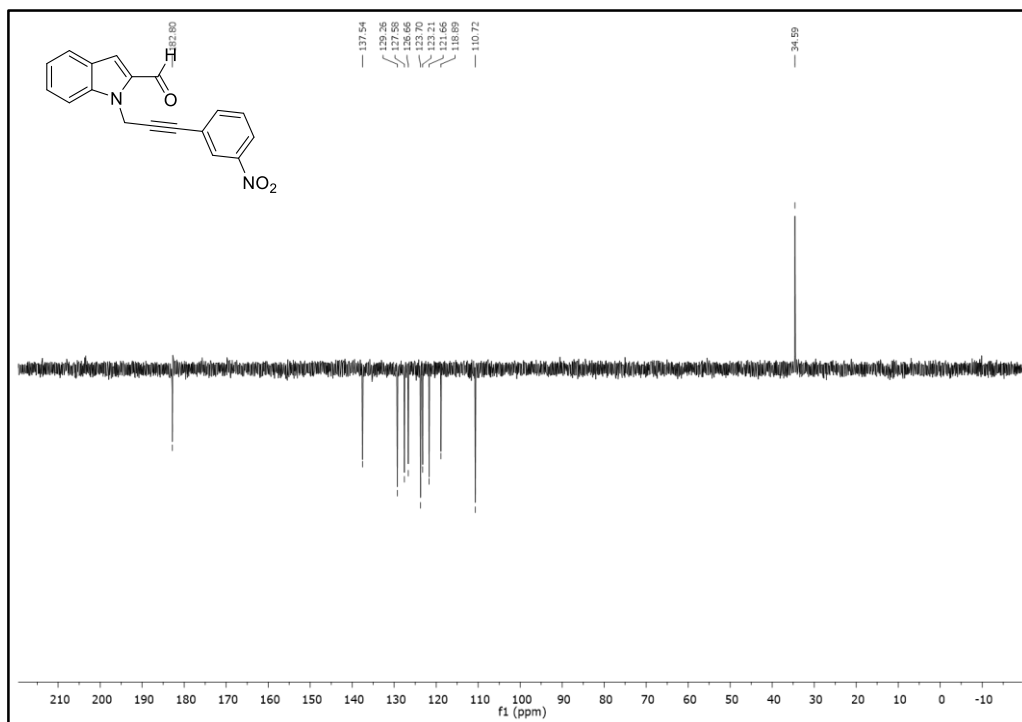


Figure 156. DEPT-135 Spectrum of Compound 367c

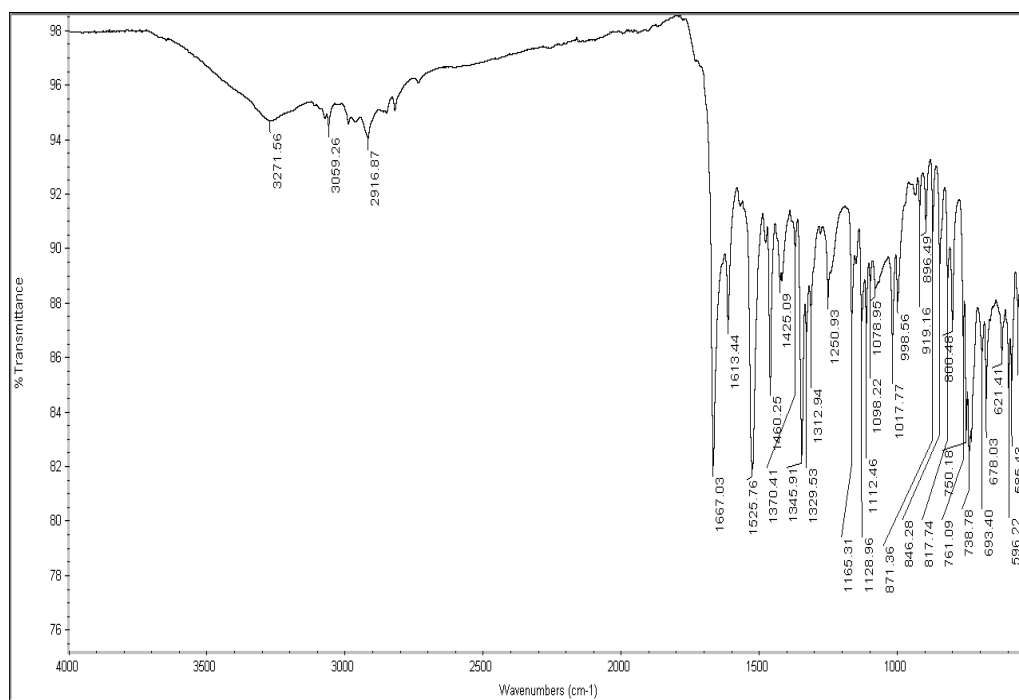


Figure 157. IR Spectrum of Compound 367c

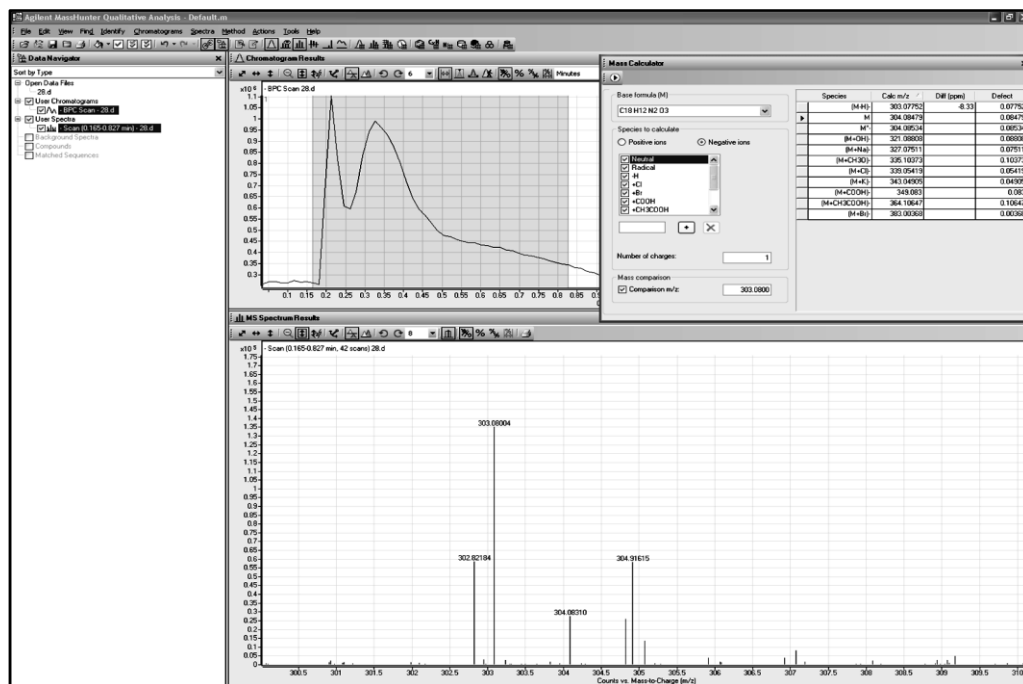


Figure 158. HRMS Spectrum of Compound 367c

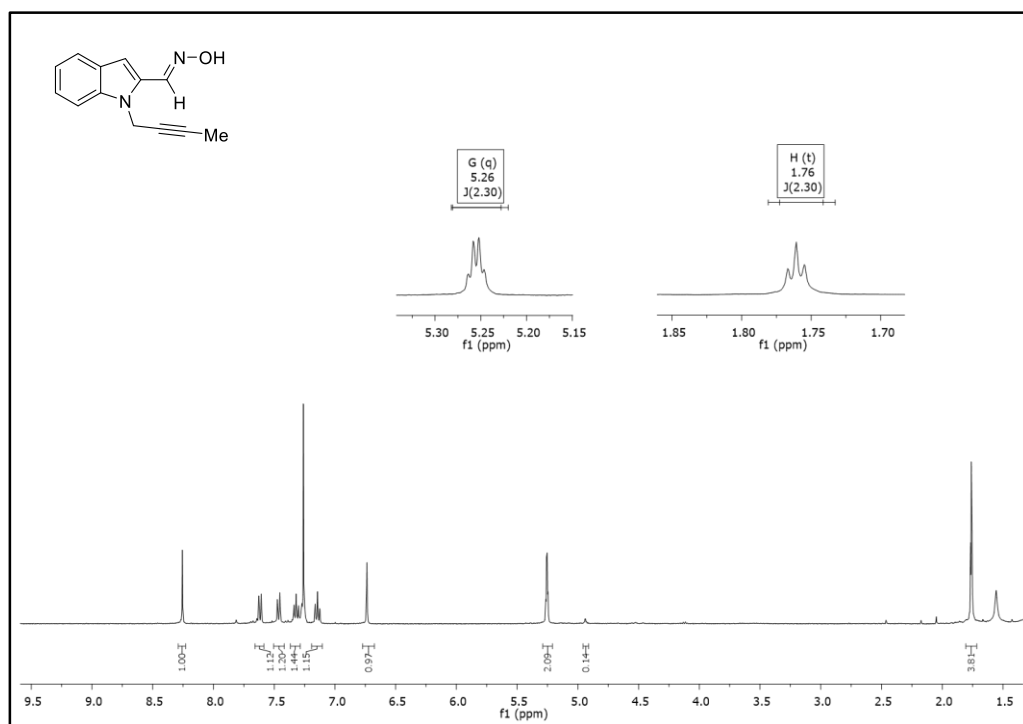


Figure 159. ¹H-NMR Spectrum of Compound 376a (*E*-isomer)

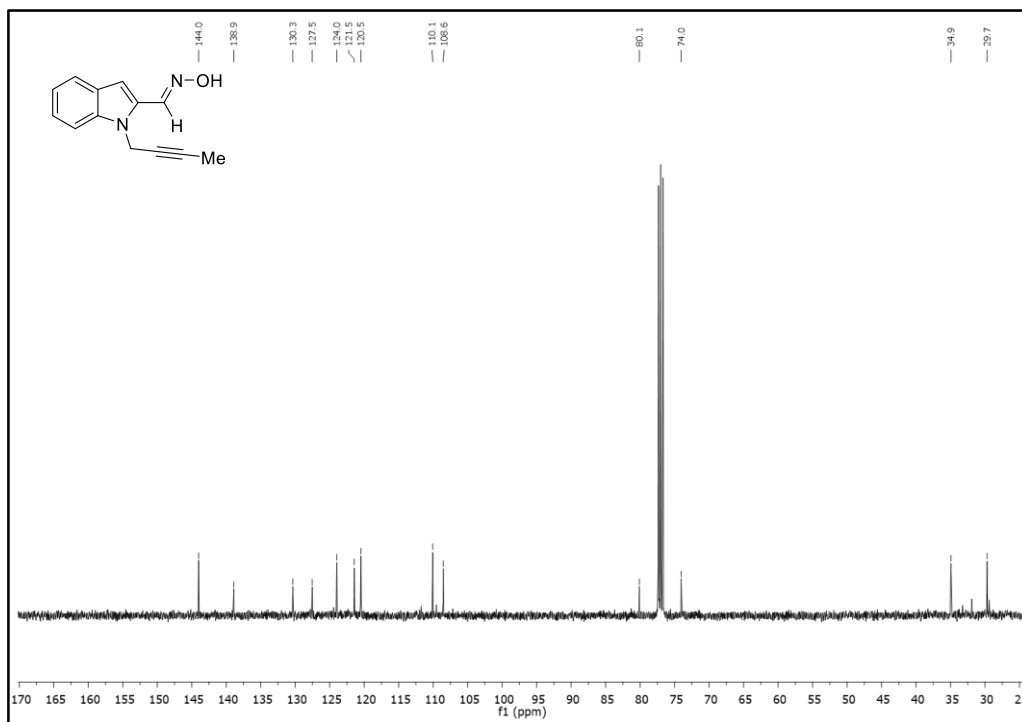


Figure 160. ¹³C-NMR Spectrum of Compound 376a (*E*-isomer)

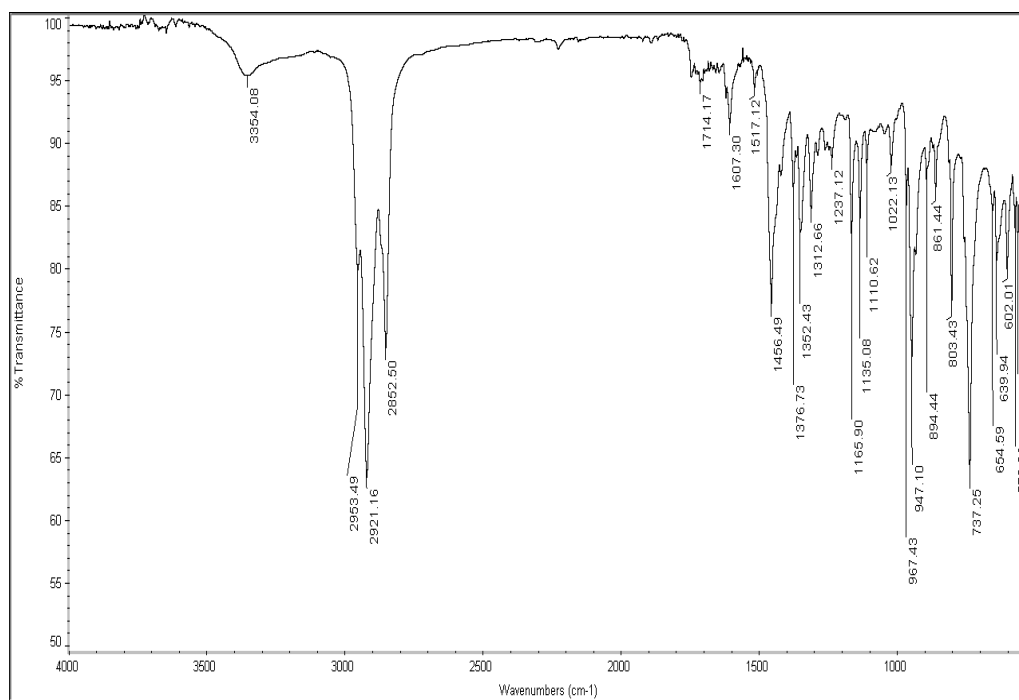


Figure 161. IR Spectrum of Compound 376a (*E*-isomer)

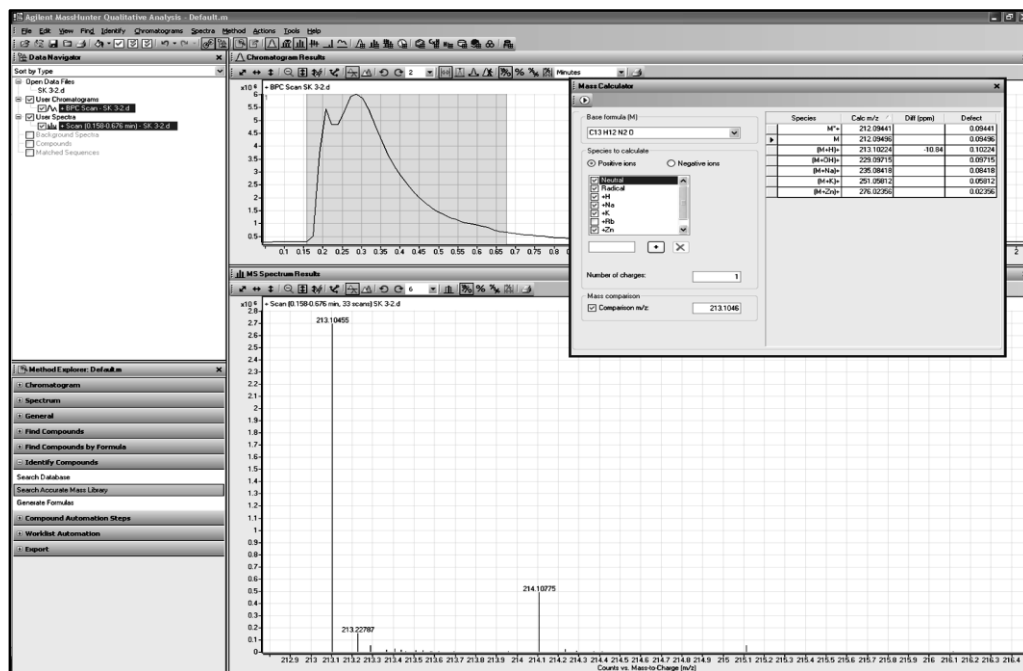


Figure 162. HRMS Spectrum of Compound 376a (*E*-isomer)

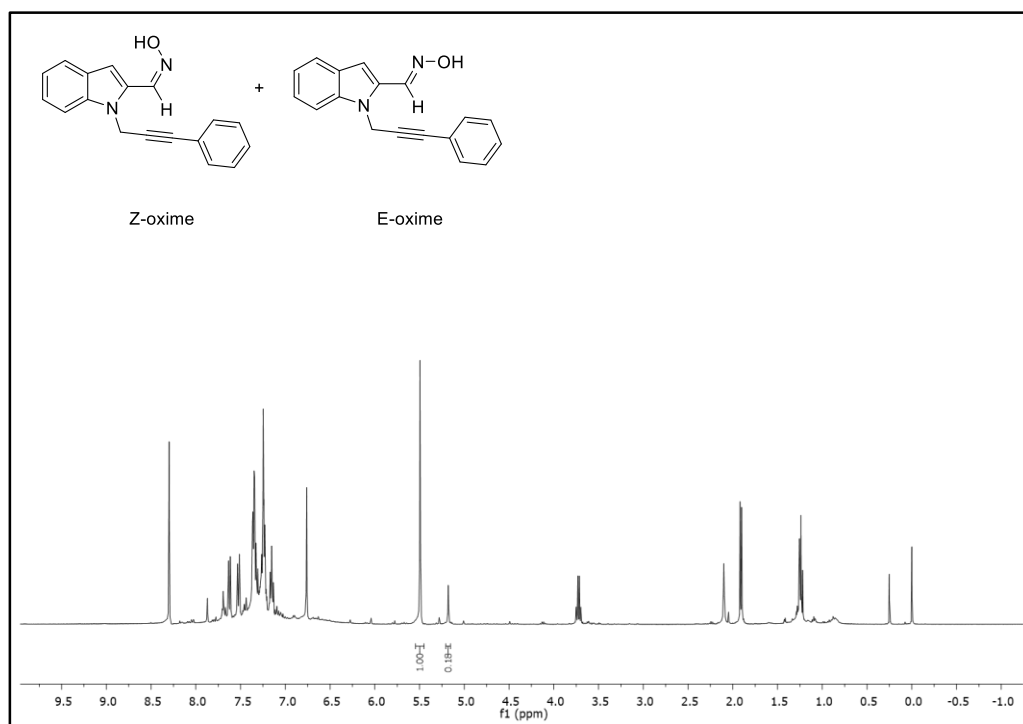


Figure 163. ¹H-NMR Spectrum of Crude Mixture of 376a (*E*- and *Z*-isomer)

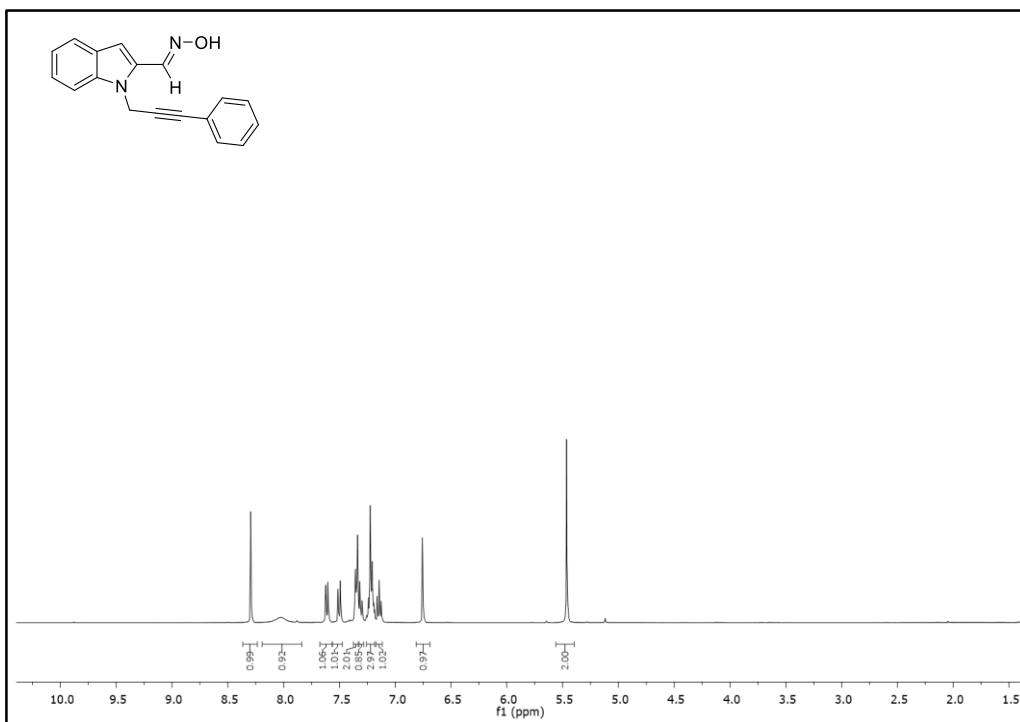


Figure 164. ¹H-NMR Spectrum of Compound **376b** (*E*-isomer)

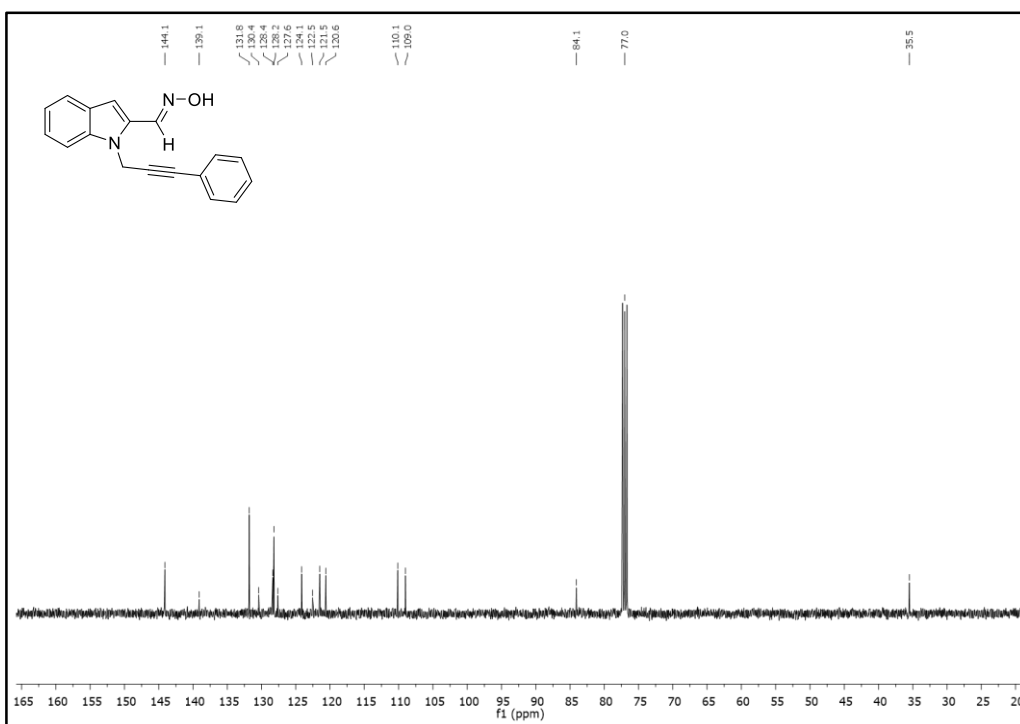


Figure 165. ¹³C-NMR Spectrum of Compound **376b** (*E*-isomer)

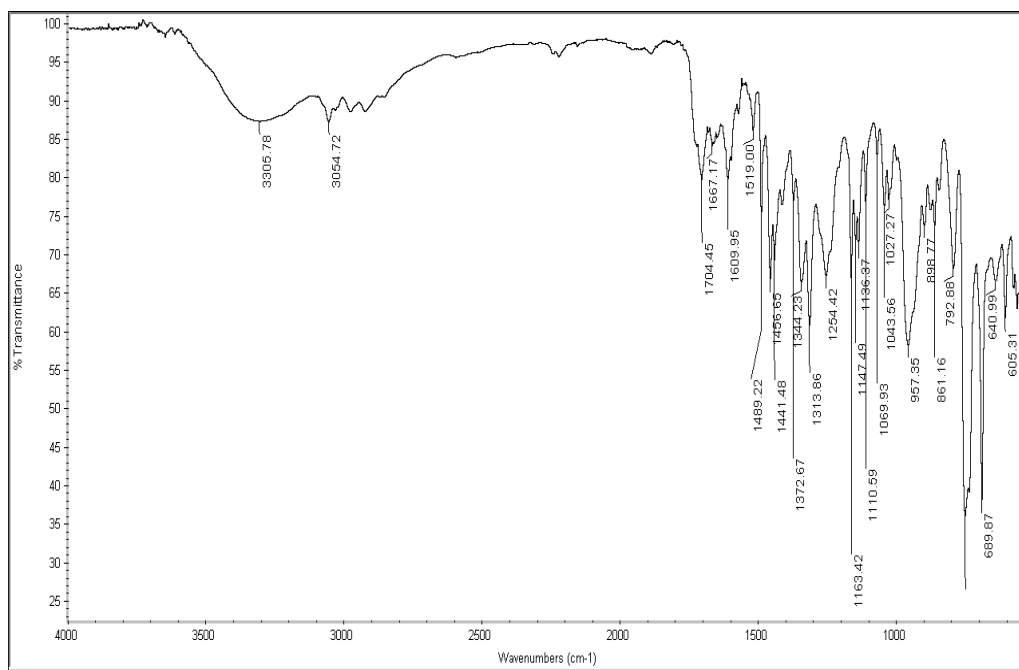


Figure 166. IR Spectrum of Compound 376b (*E*-isomer)

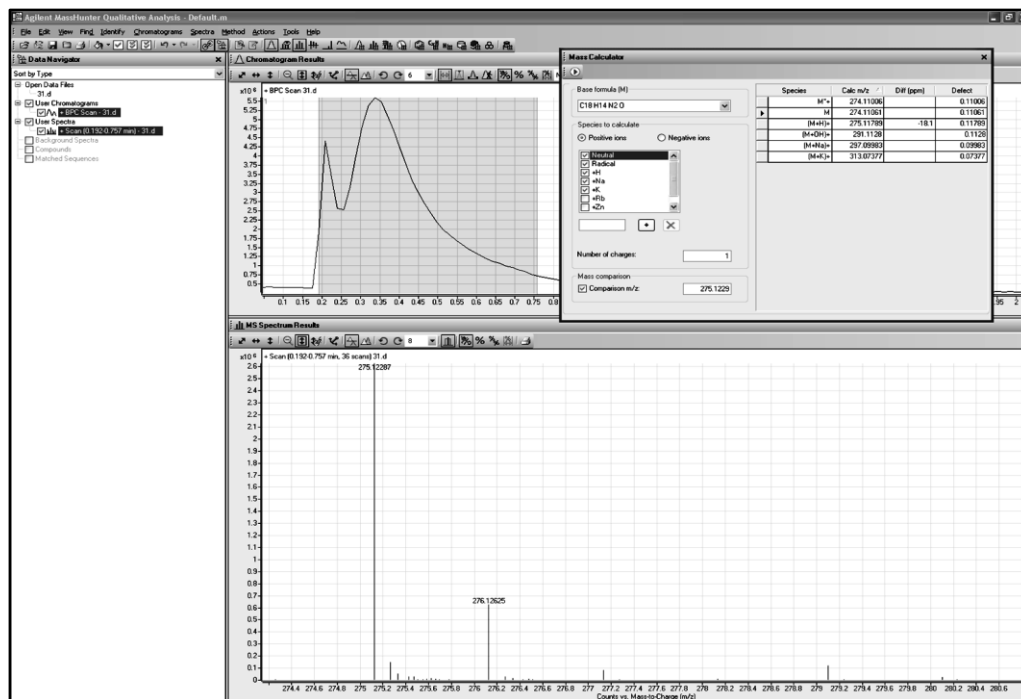


Figure 167. HRMS Spectrum of Compound 376b (*E*-isomer)

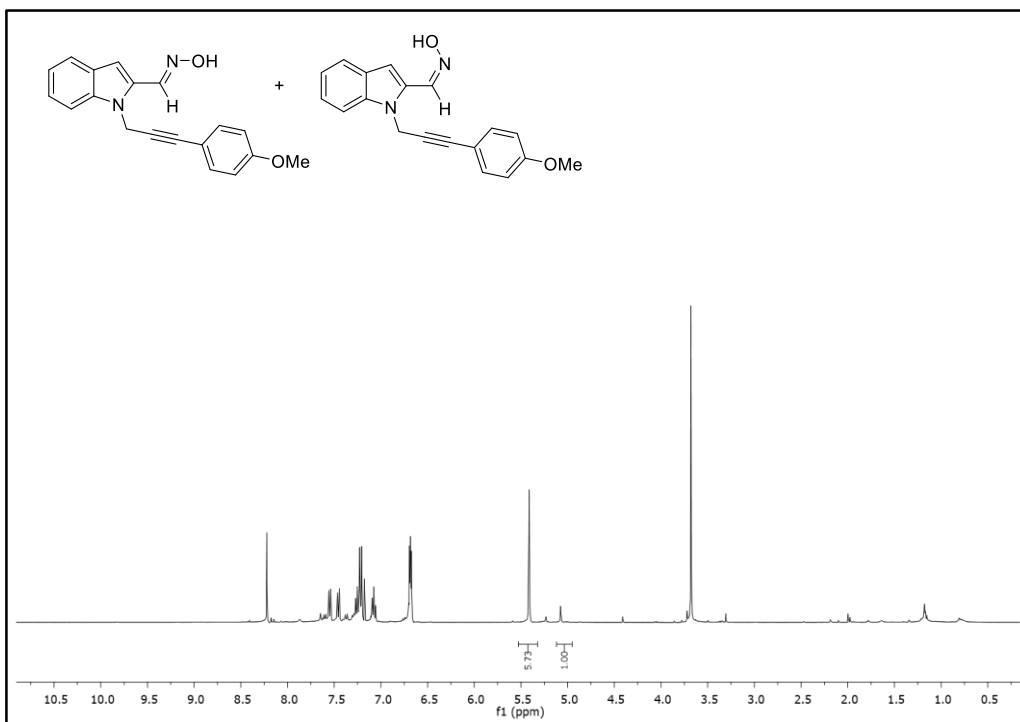


Figure 168. ¹H-NMR Spectrum of Crude Mixture of **376c** (*E*- and *Z*-isomer)

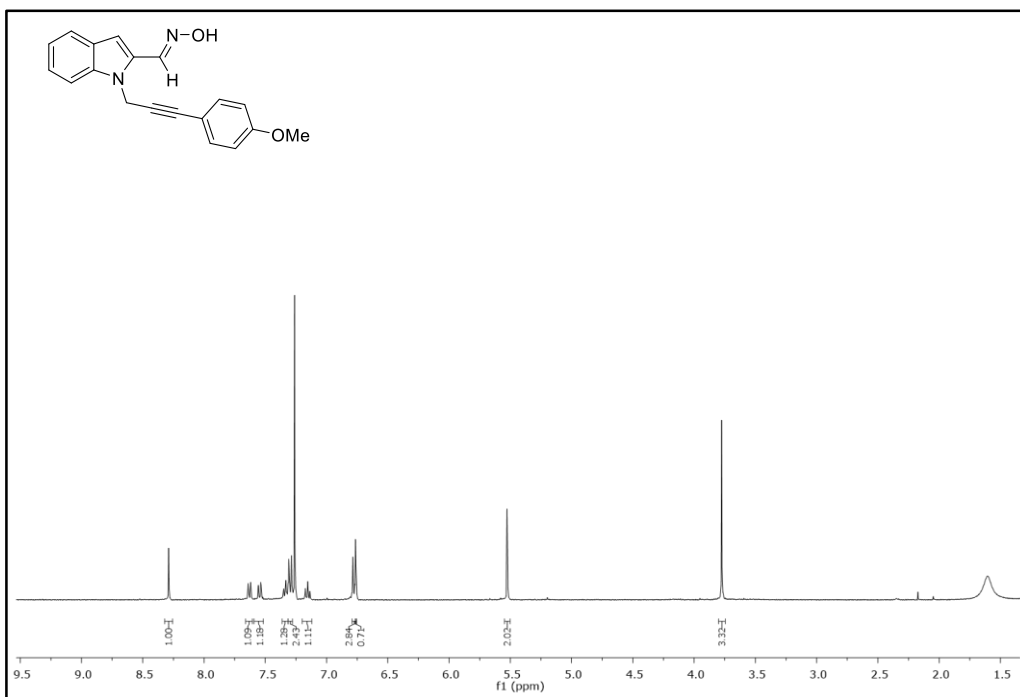


Figure 169. ¹H-NMR Spectrum of Compound **376c** (*E*-isomer)

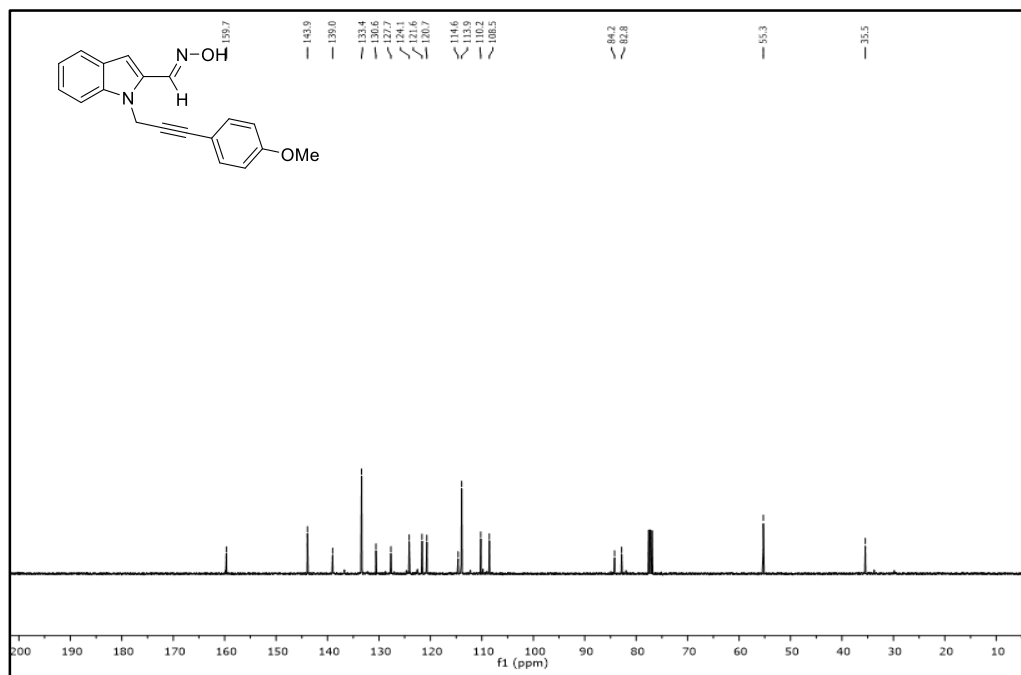


Figure 170. ¹³C-NMR Spectrum of Compound **376c** (*E*-isomer)

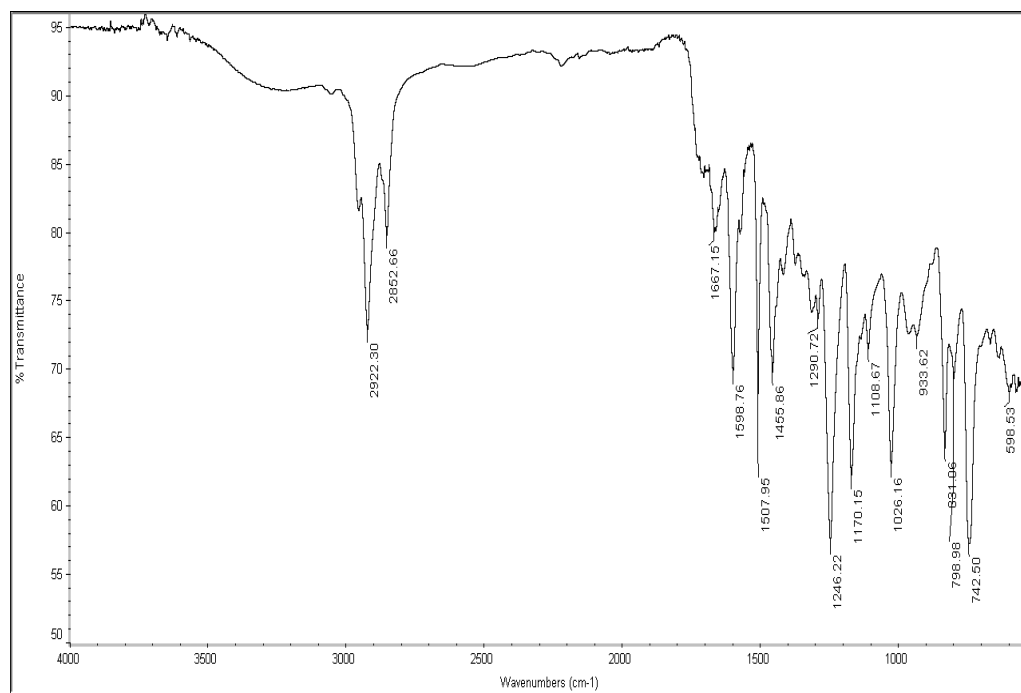


Figure 171. IR Spectrum of Compound **376c** (*E*-isomer)

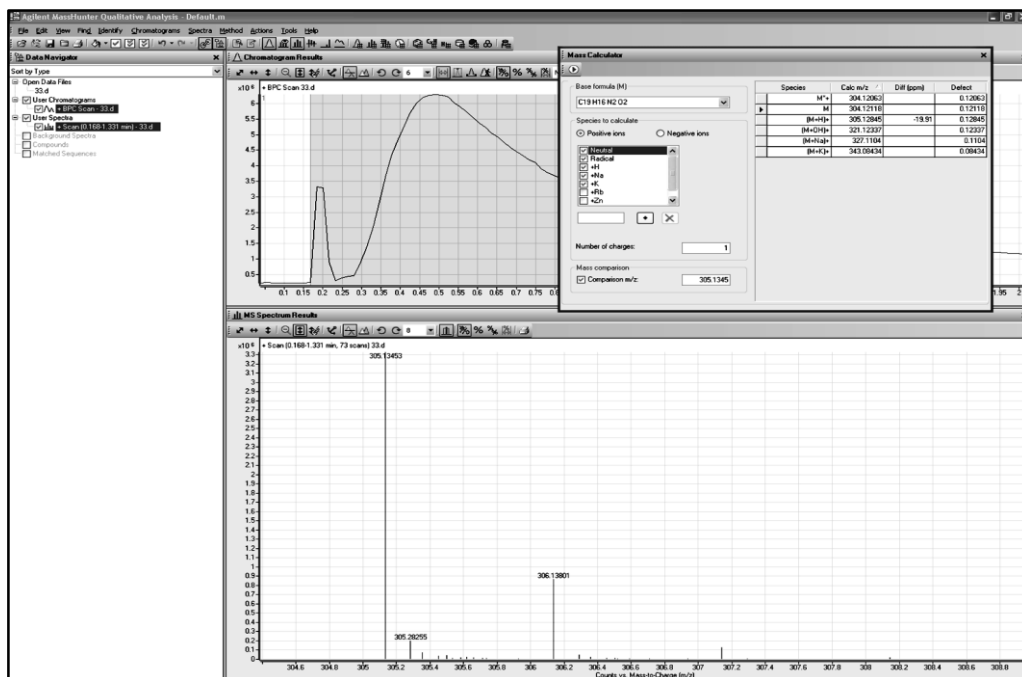


Figure 172. HRMS Spectrum of Compound **376c** (*E*-isomer)

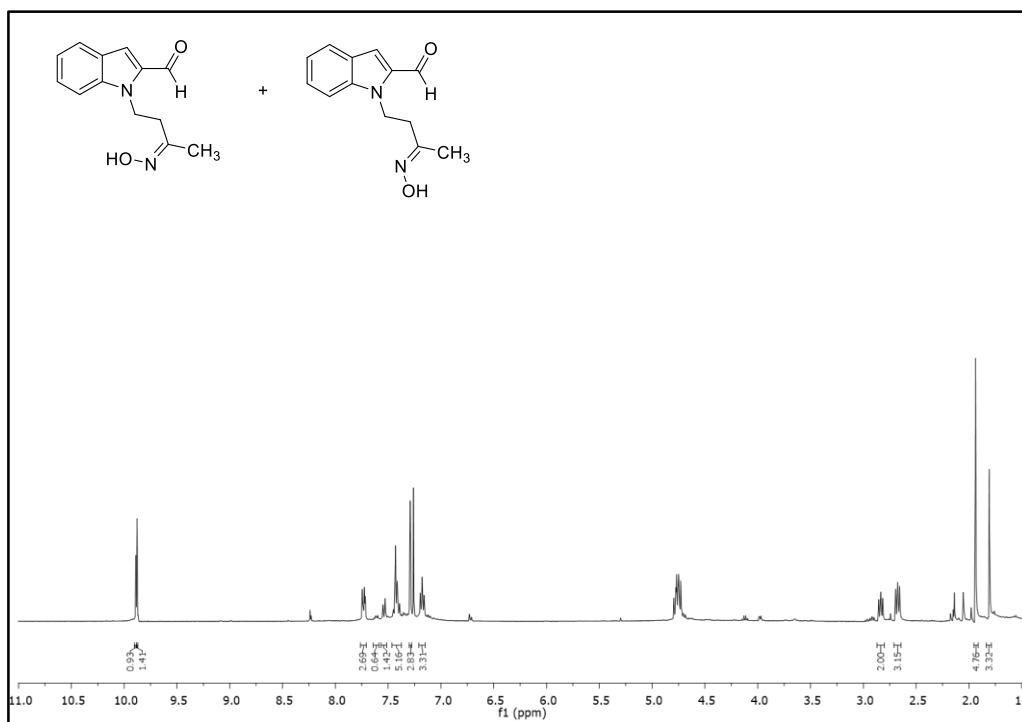


Figure 173. ¹H-NMR Spectrum of Crude Mixture of **378a** (*E*- and *Z*-isomer)

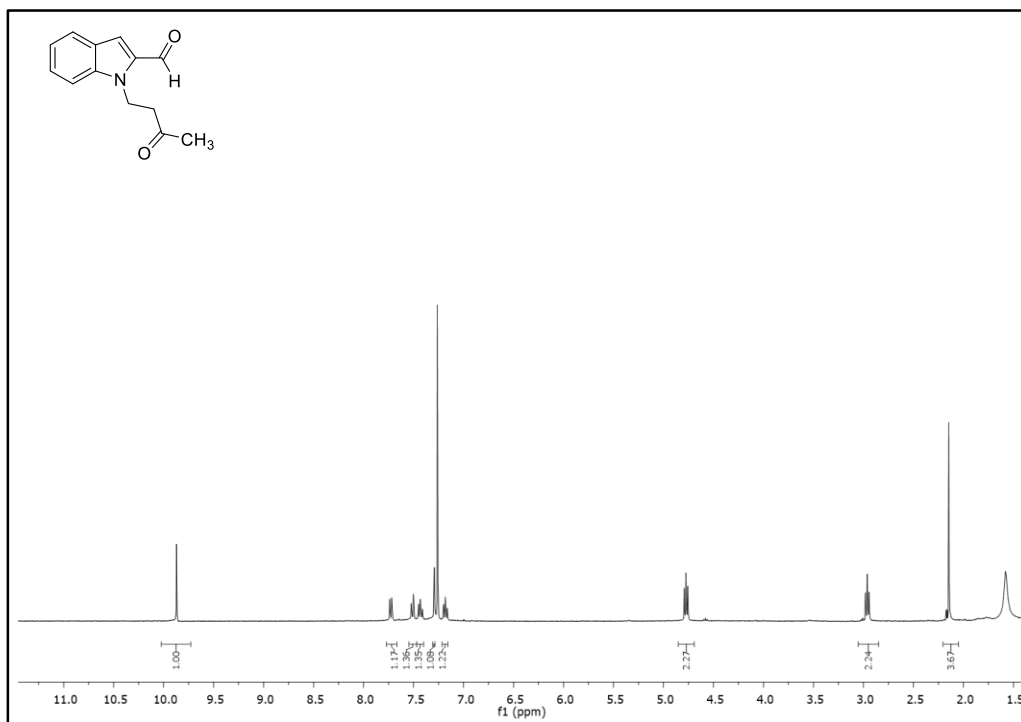


Figure 174. ¹H-NMR Spectrum of Compound 378e

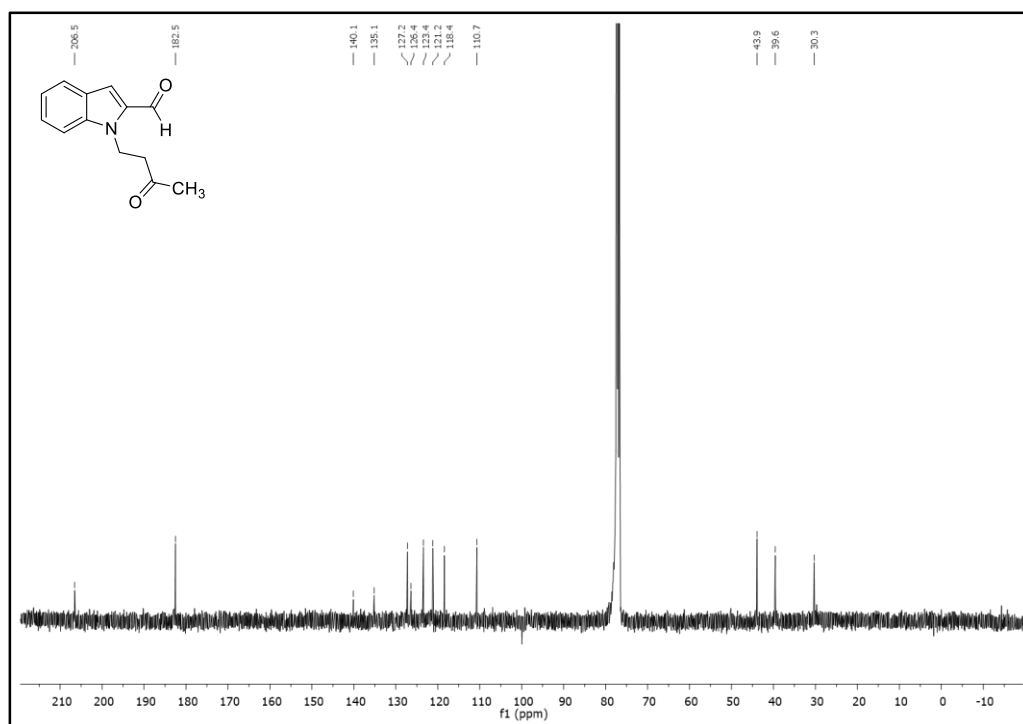


Figure 175. ¹³C-NMR Spectrum of Compound 378e

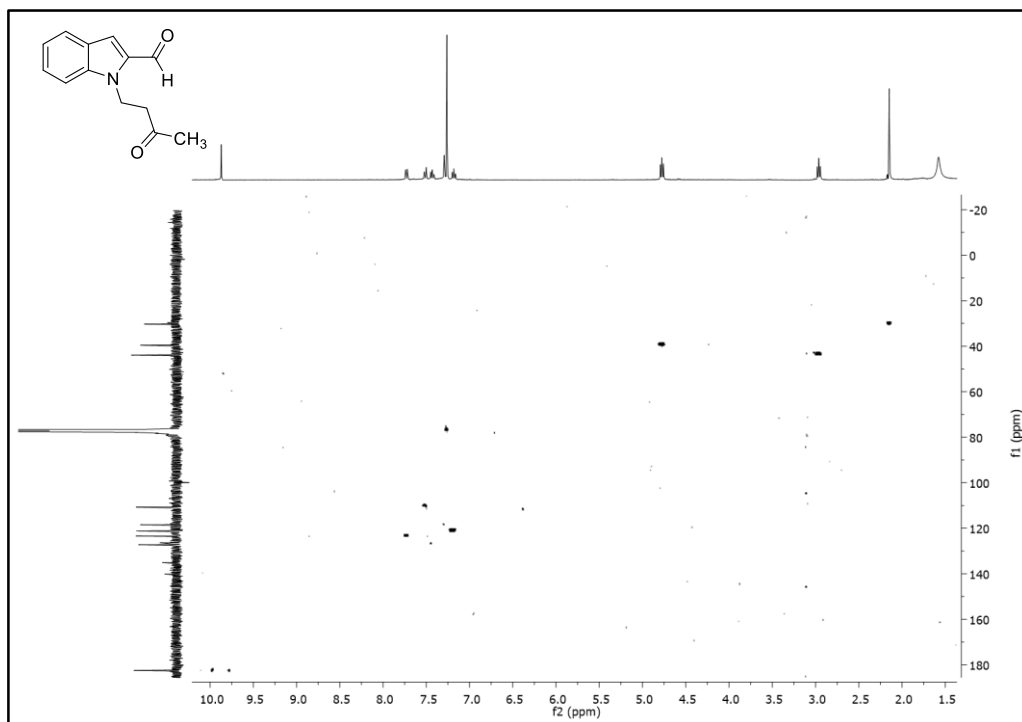


Figure 176. HSQC Spectrum of Compound 378e

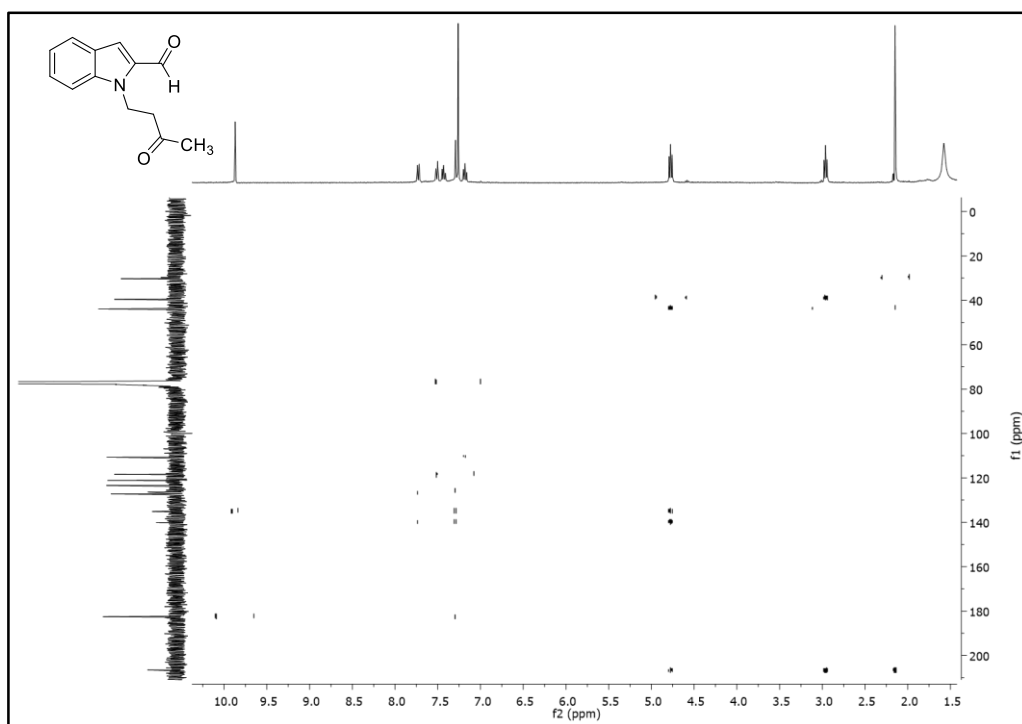


Figure 177. HMBC Spectrum of Compound 378e

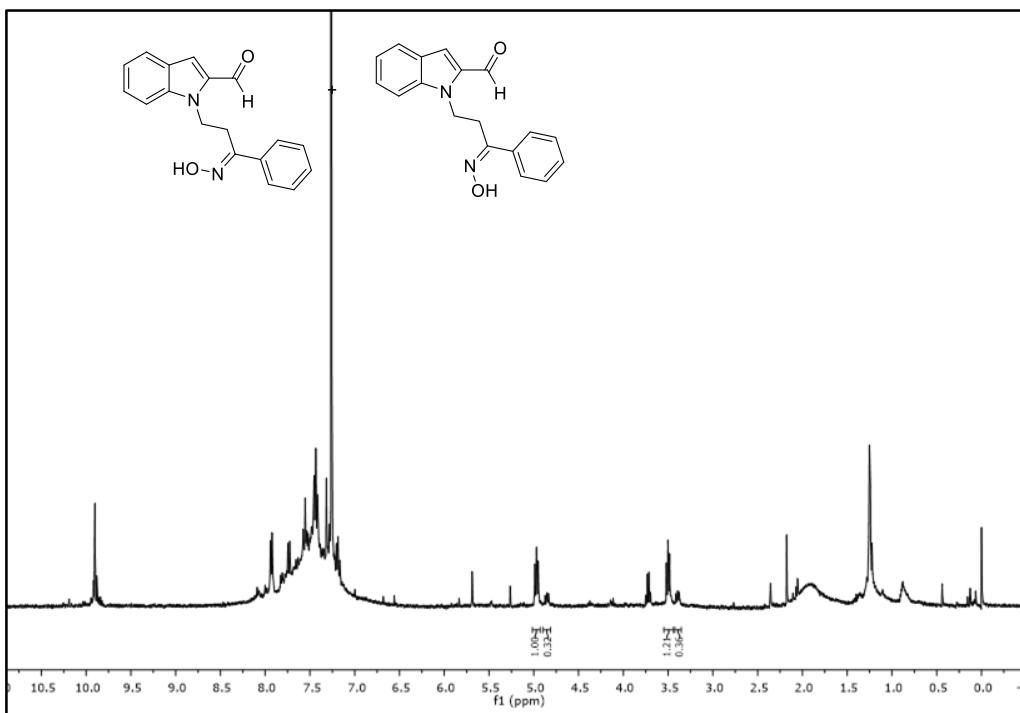


Figure 180. ¹H-NMR Spectrum of Crude Mixture of **378b** (*E*- and *Z*-isomer)

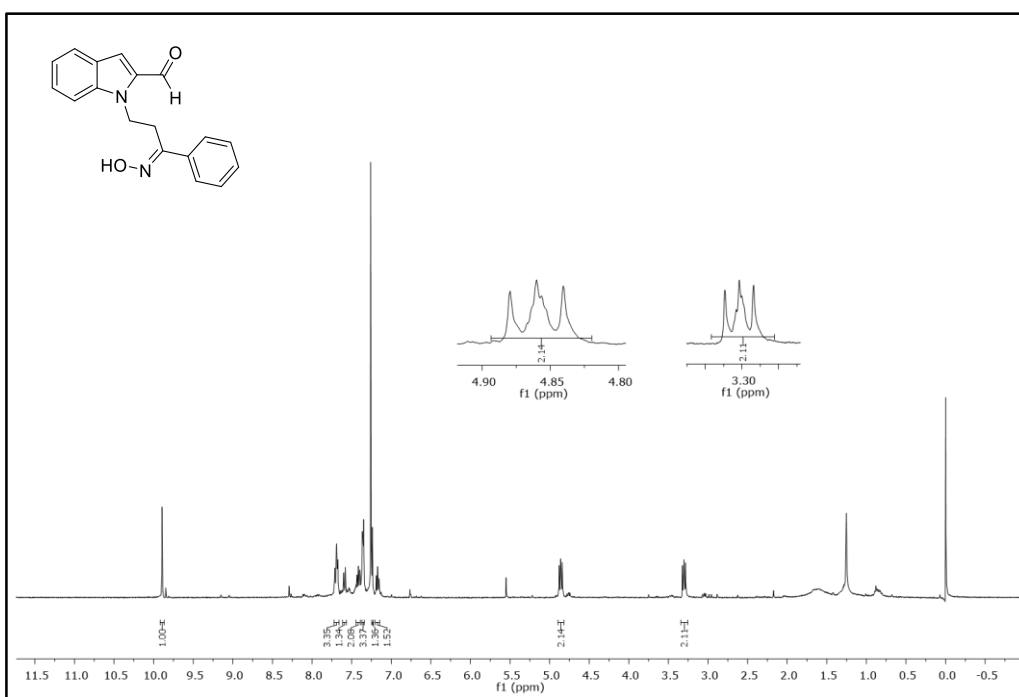


Figure 181. ¹H-NMR Spectrum of Compound **378b** (*E*-isomer)

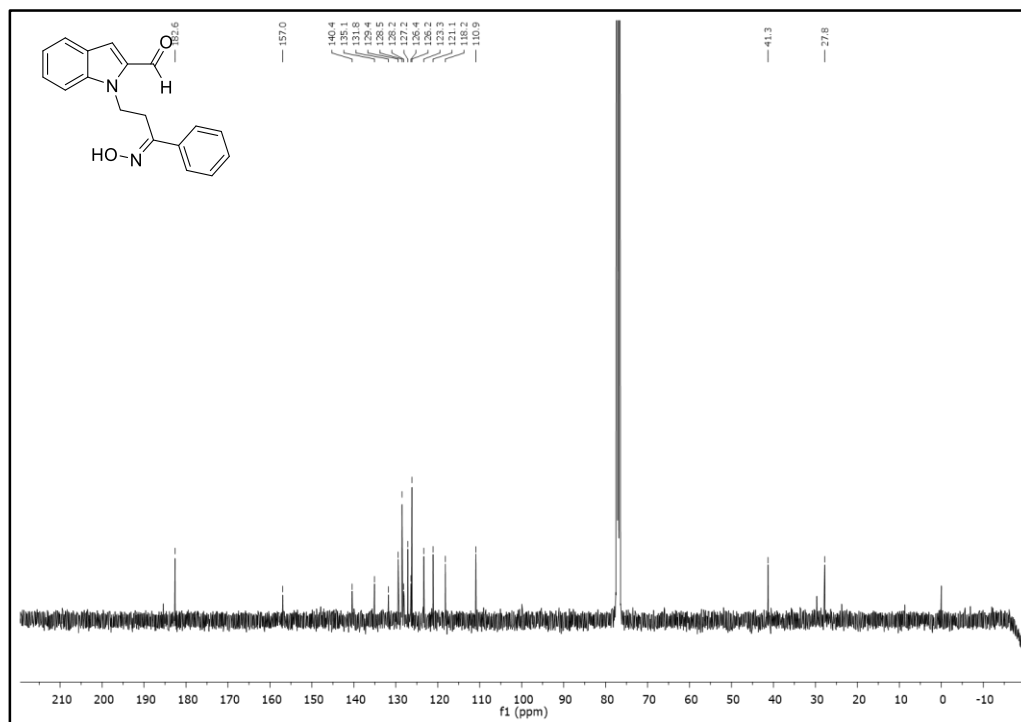


Figure 182. ¹³C-NMR Spectrum of Compound 378b (*E*-isomer)

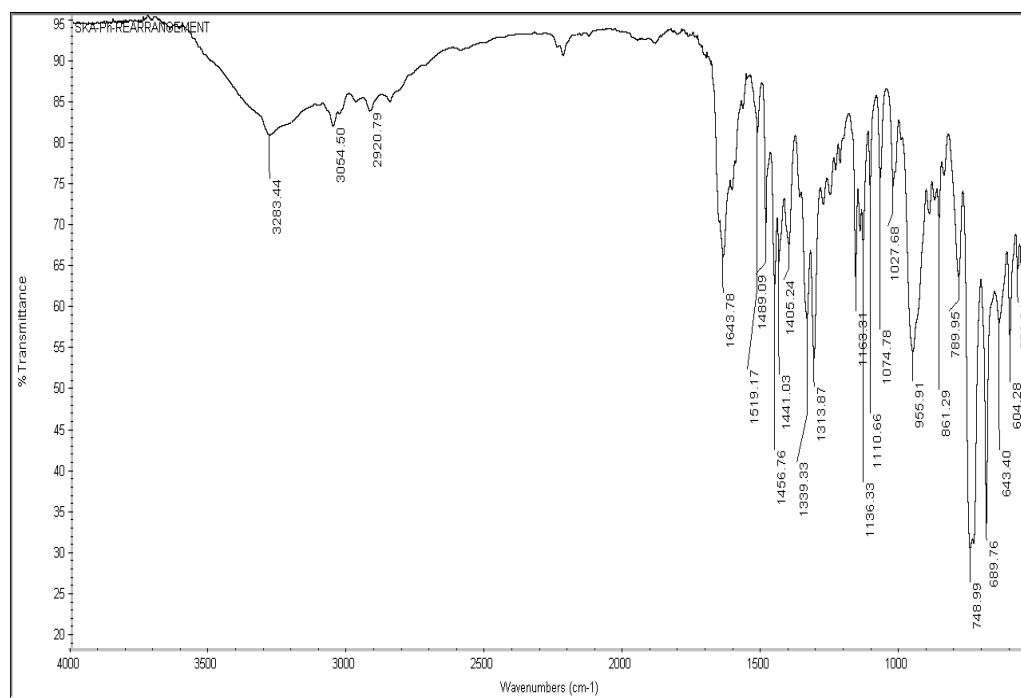


Figure 183. IR Spectrum of Compound 378b (*E*-isomer)

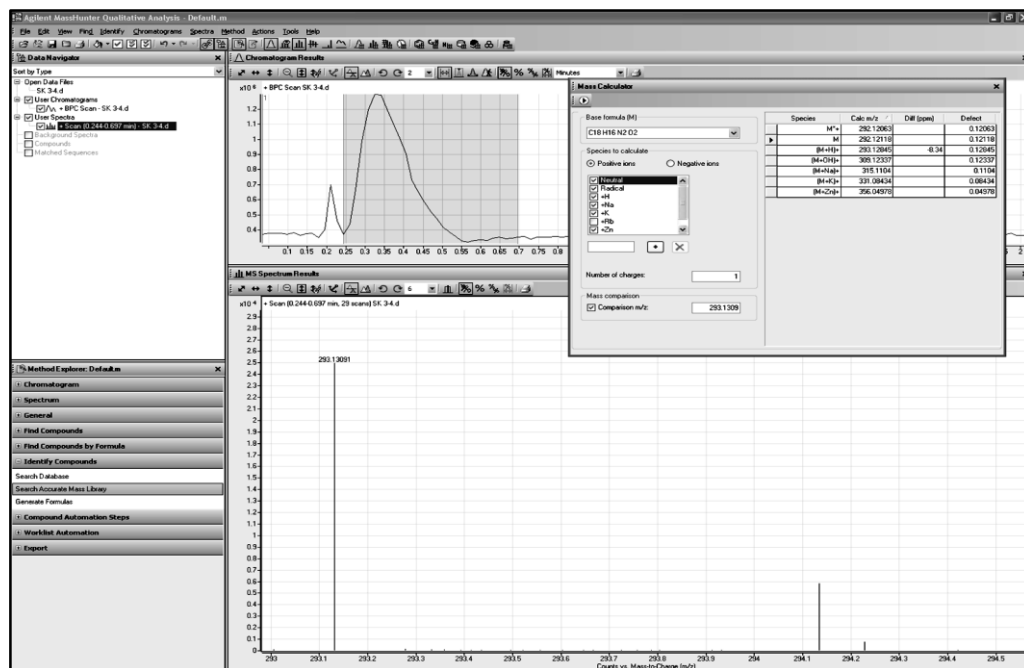


Figure 184. HRMS Spectrum of Compound **378b** (*E*-isomer)

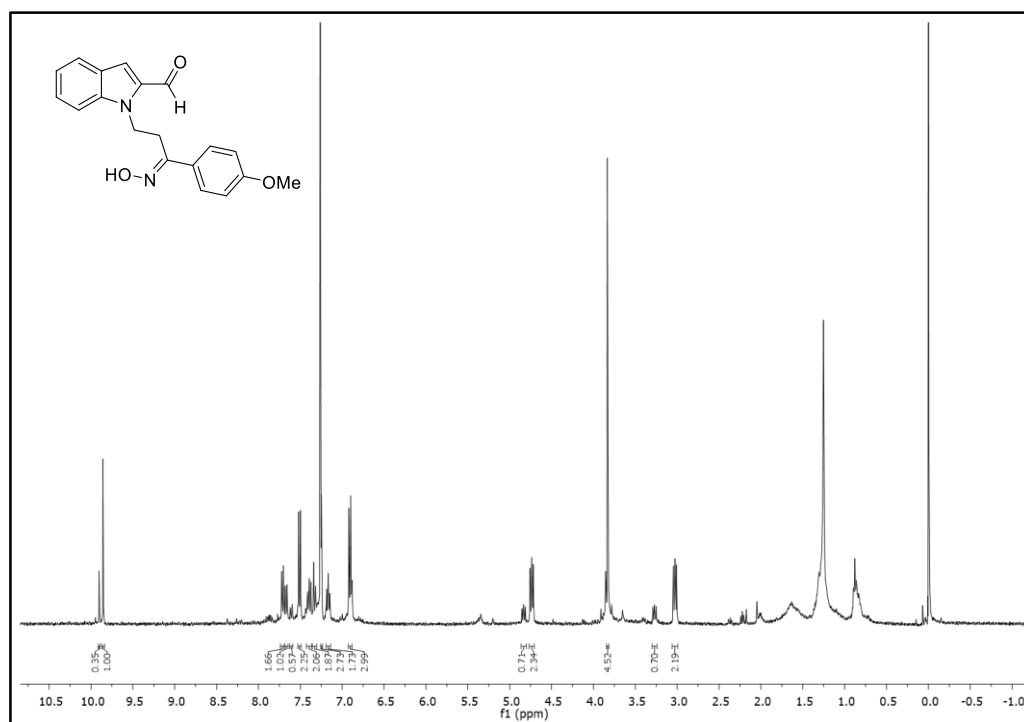


Figure 185. ¹H-NMR Spectrum of Compound **378c** (*E*-isomer)

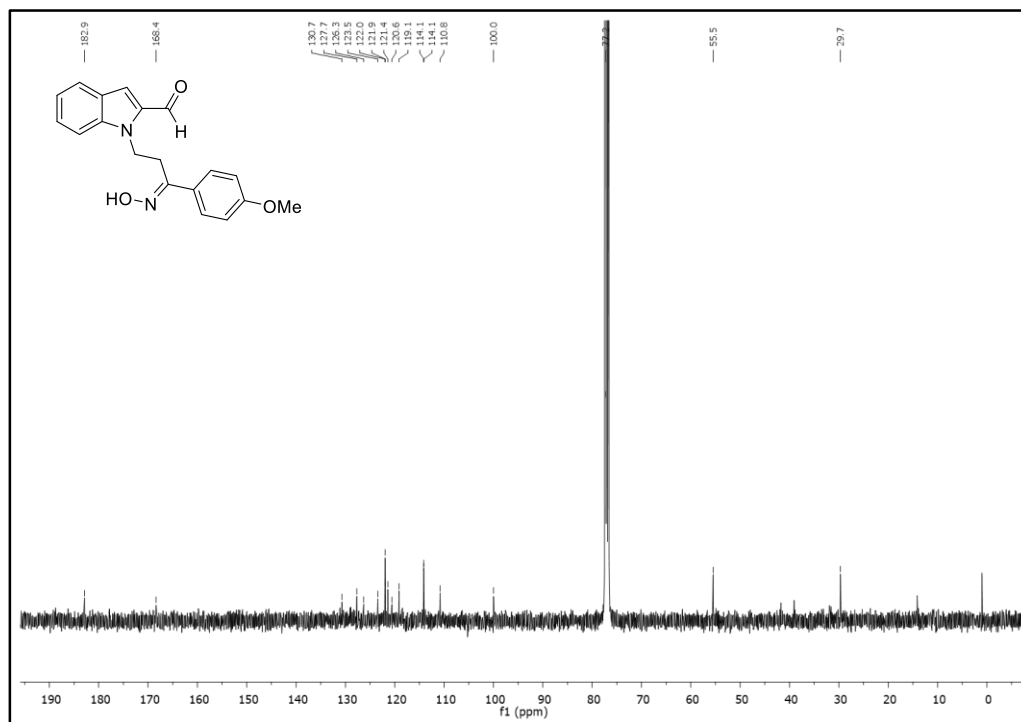


Figure 186. ¹³C-NMR Spectrum of Compound **378c** (*E*-isomer)

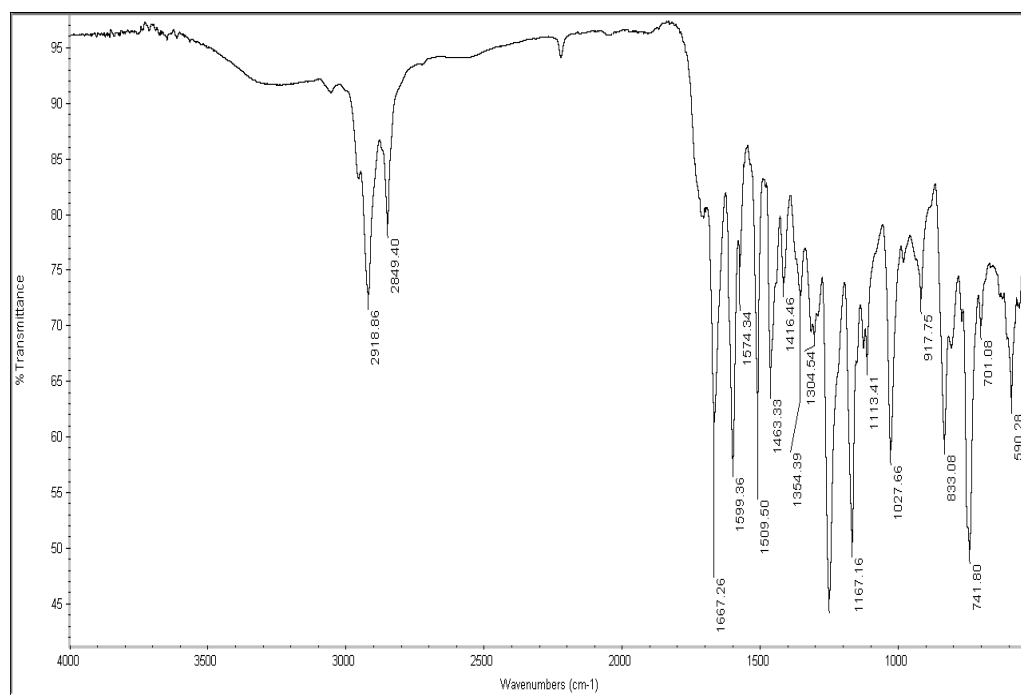


Figure 187. IR Spectrum of Compound **378c** (*E*-isomer)

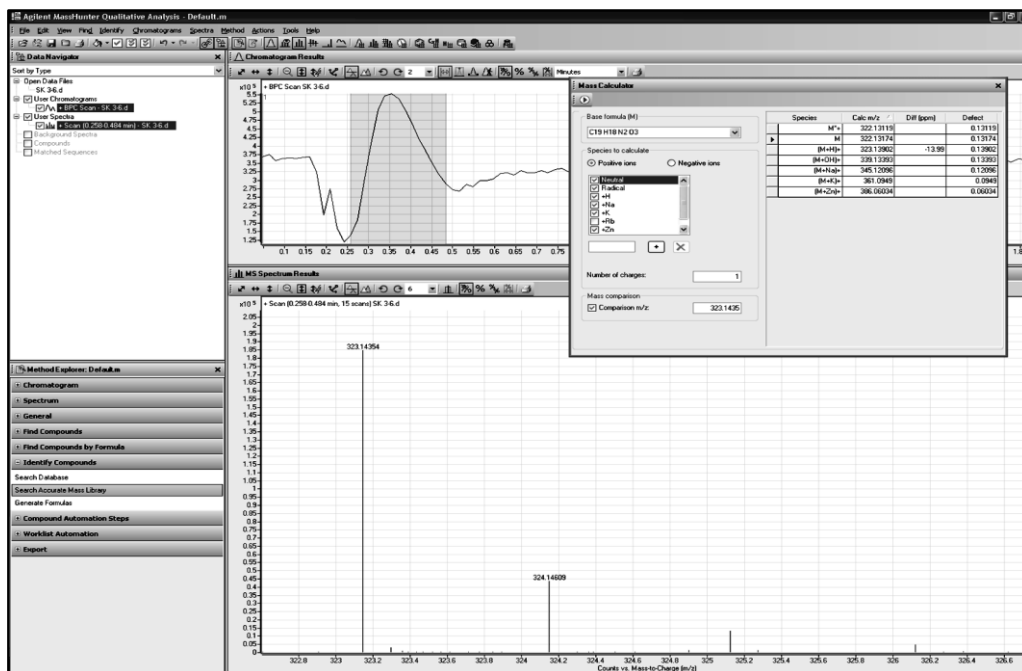


Figure 188. HRMS Spectrum of Compound 378c (*E*-isomer)

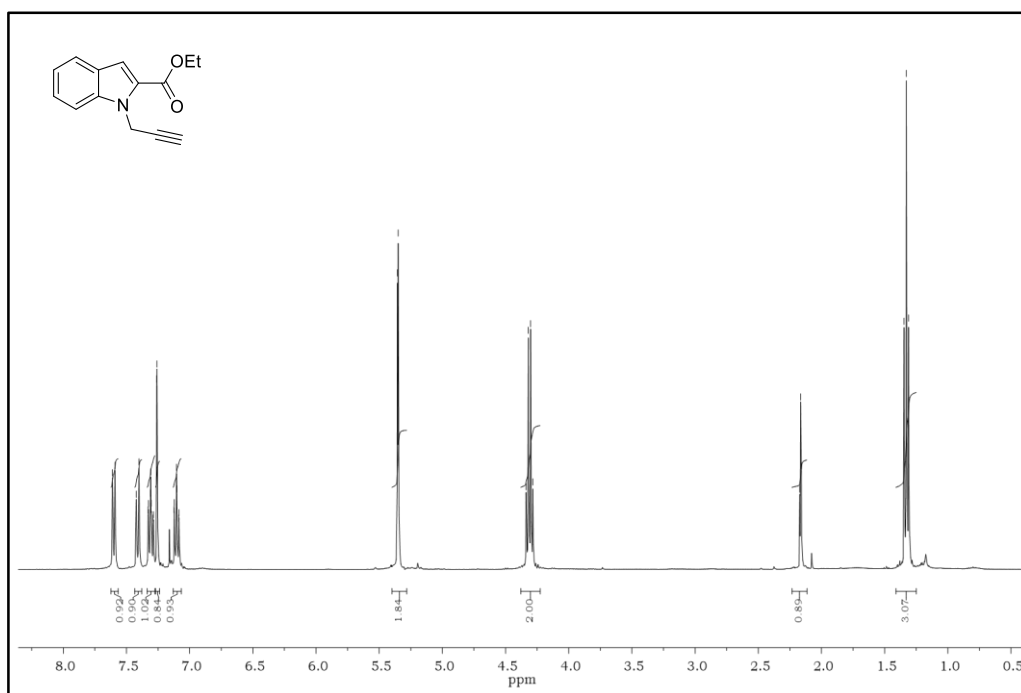


Figure 189. ¹H-NMR Spectrum of Compound 390a

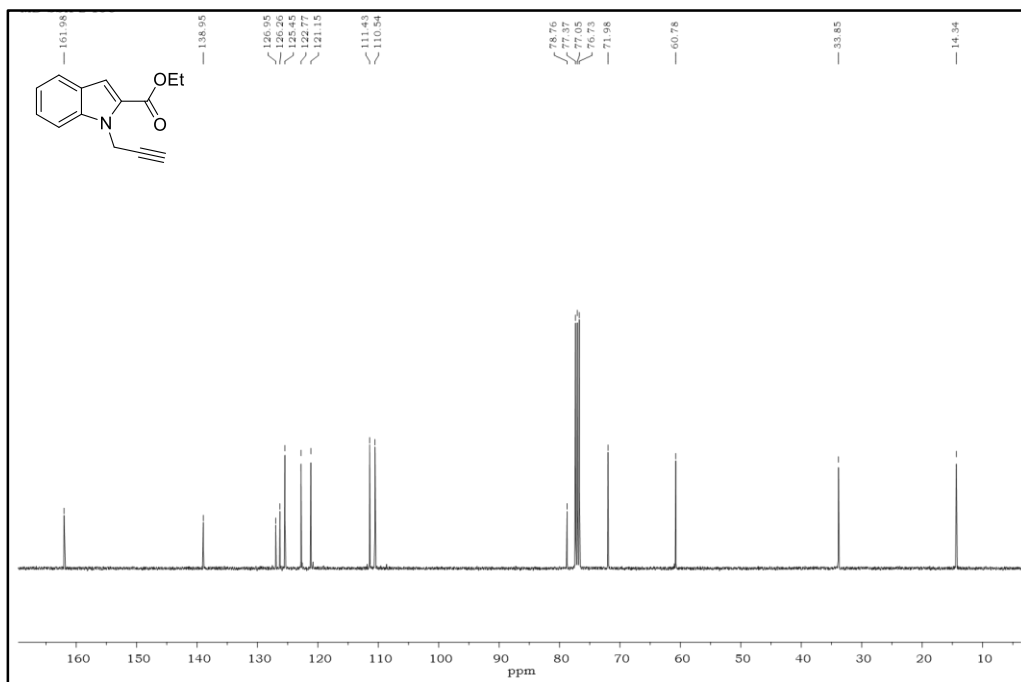


Figure 190. ¹³C-NMR Spectrum of Compound **390a**

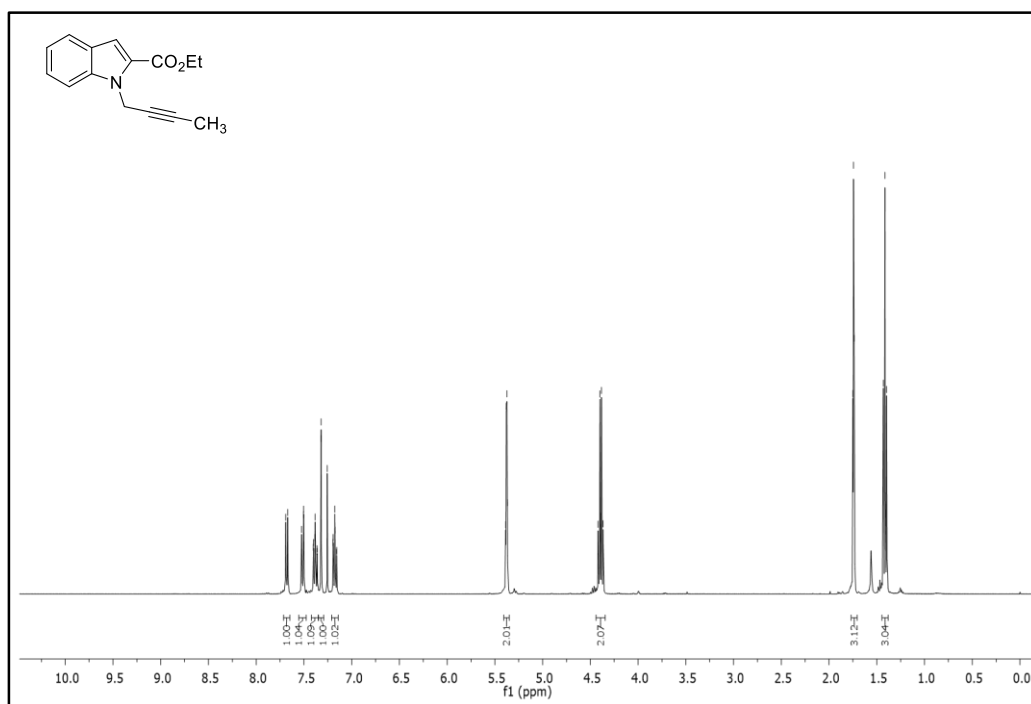


Figure 191. ¹H-NMR Spectrum of Compound **390b**

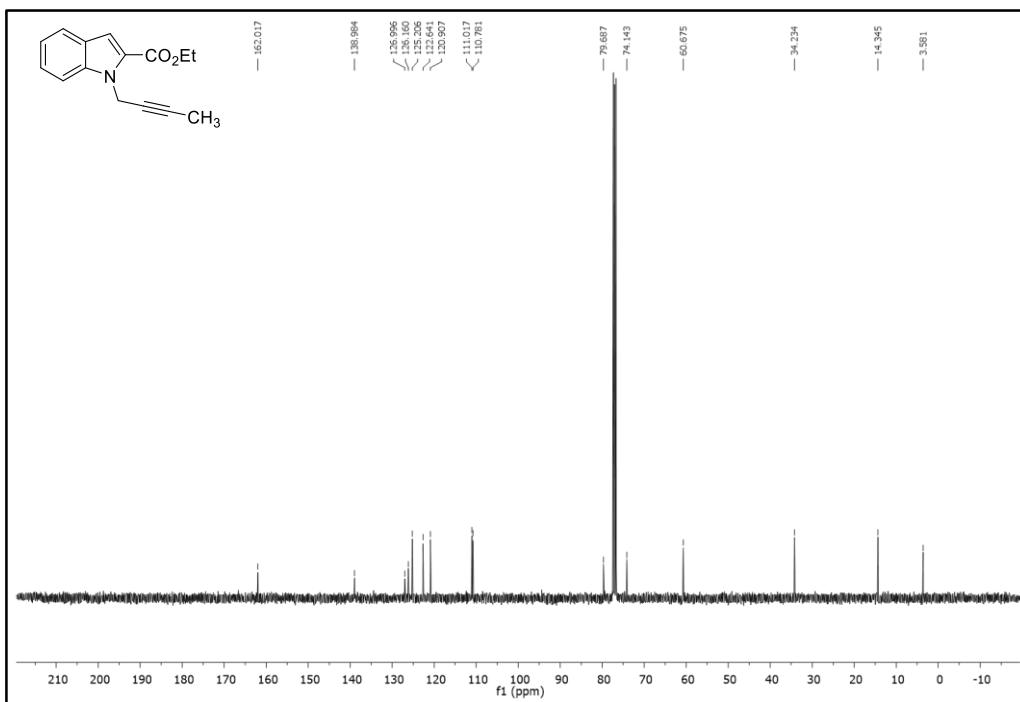


Figure 192. ¹³C-NMR Spectrum of Compound **390b**

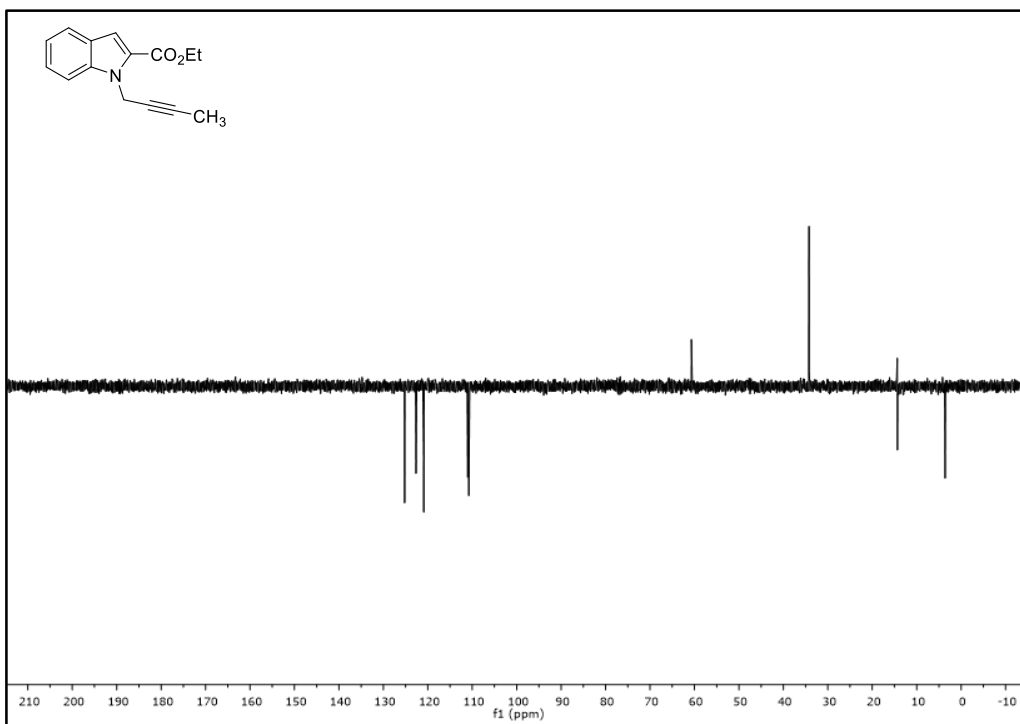


Figure 193. DEPT-135 Spectrum of Compound **390b**

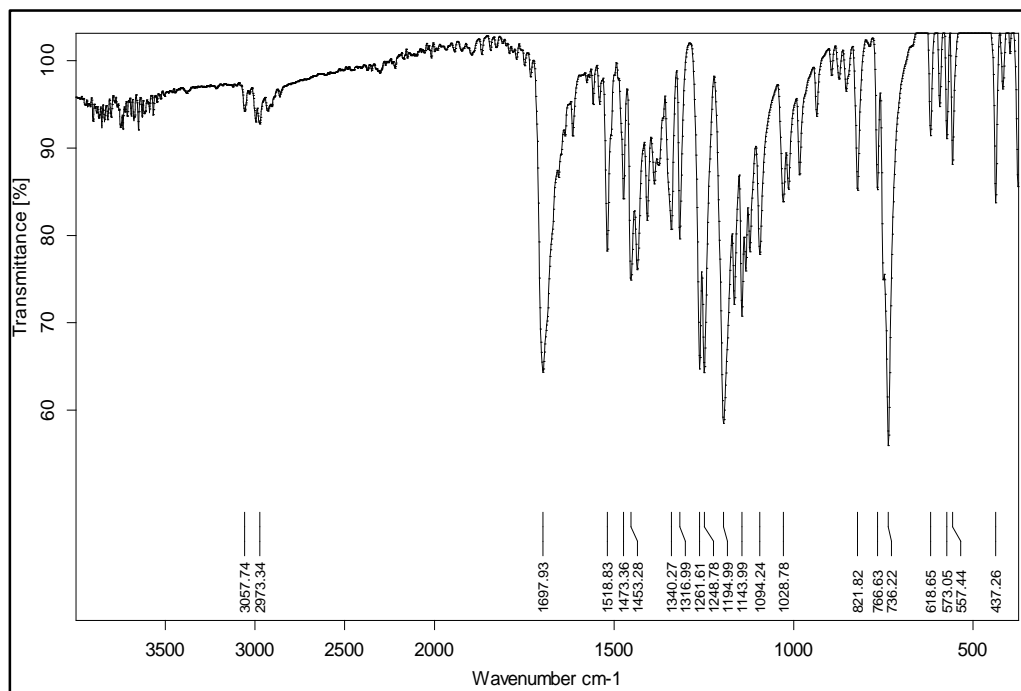


Figure 194. IR Spectrum of Compound 390b

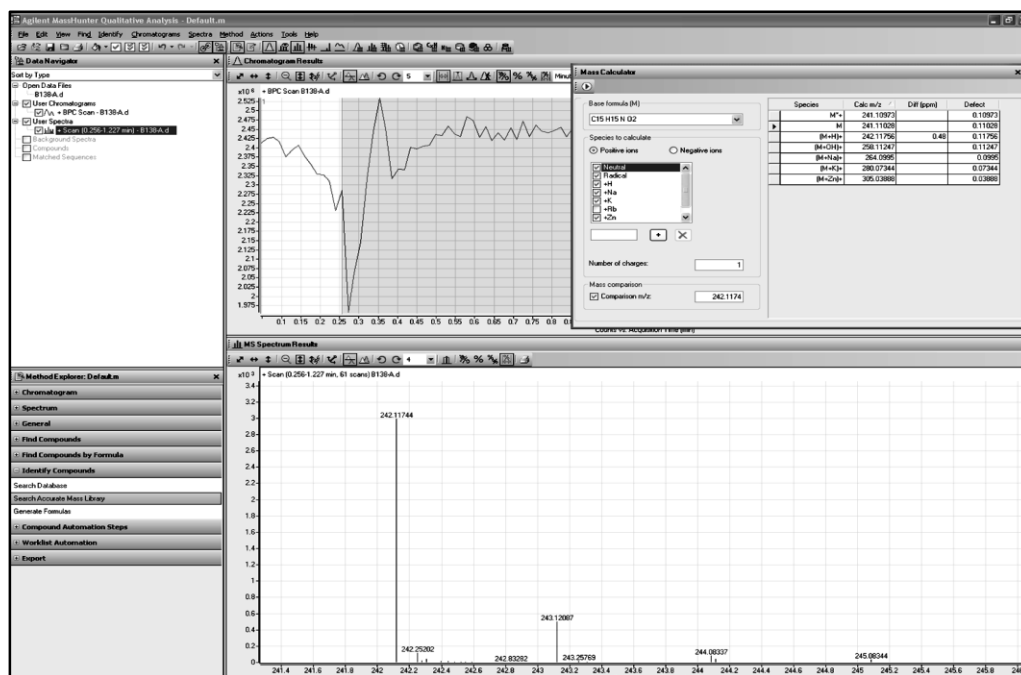


Figure 195. HRMS Spectrum of Compound 390b

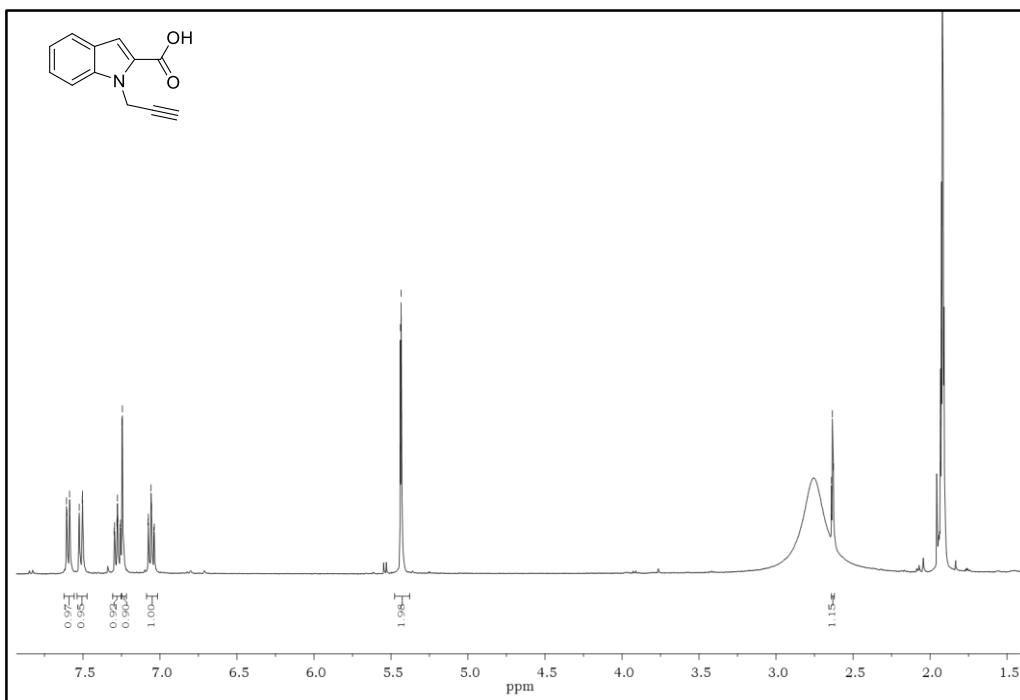


Figure 196. ¹H-NMR Spectrum of Compound 391a

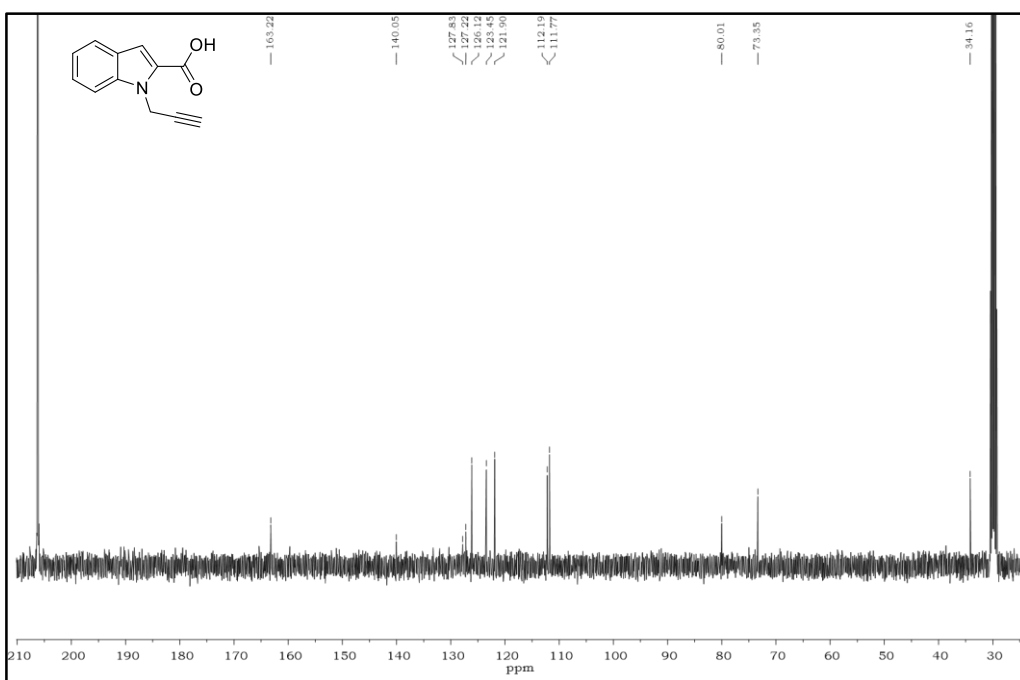


Figure 197. ¹³C-NMR Spectrum of Compound 391a

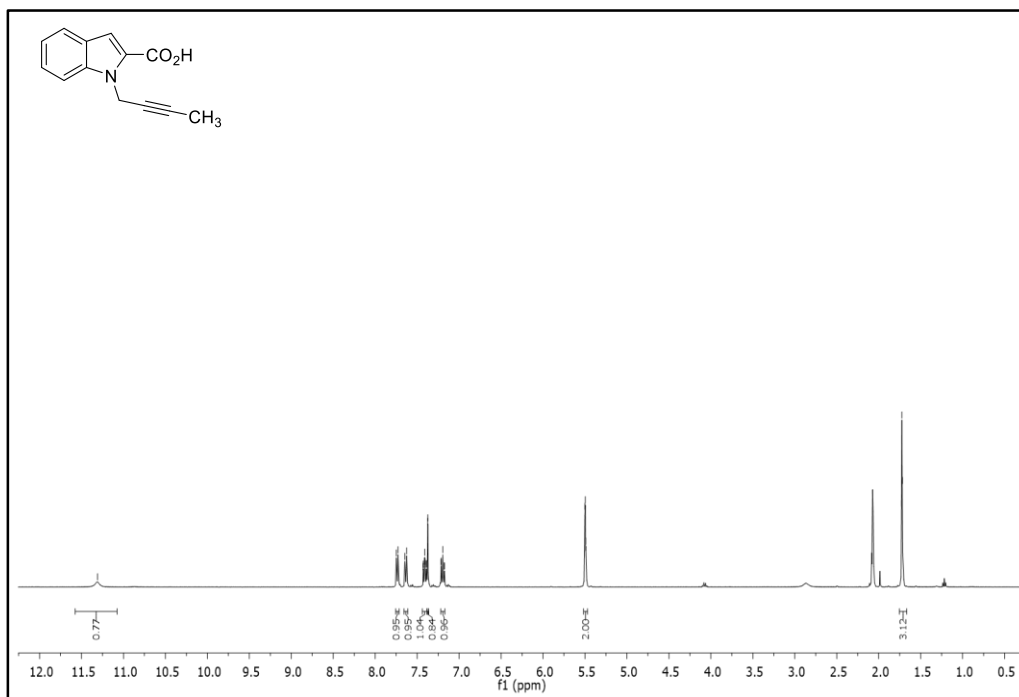


Figure 198. ¹H-NMR Spectrum of Compound 391b

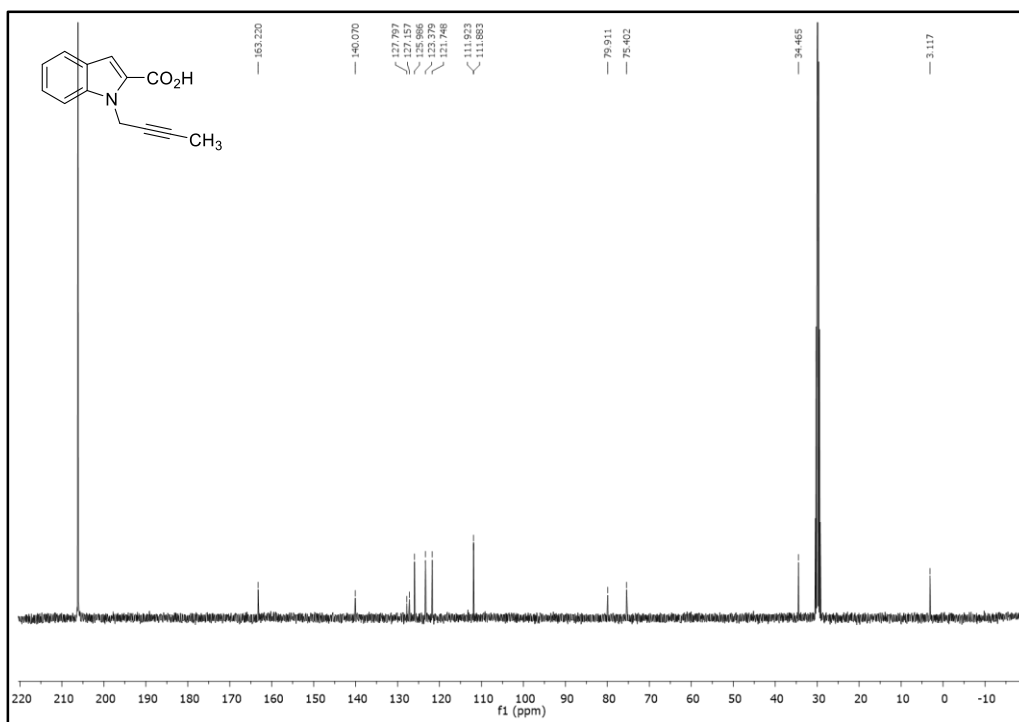


Figure 199. ¹³C-NMR Spectrum of Compound 391b

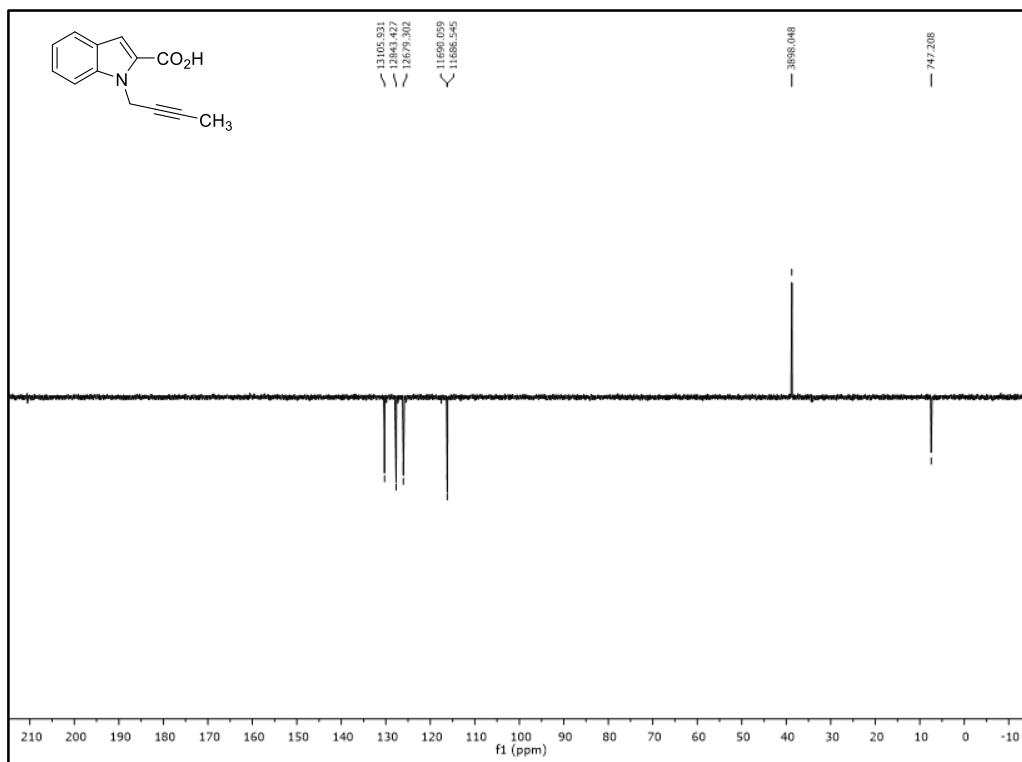


Figure 200. DEPT-135 Spectrum of Compound **391b**

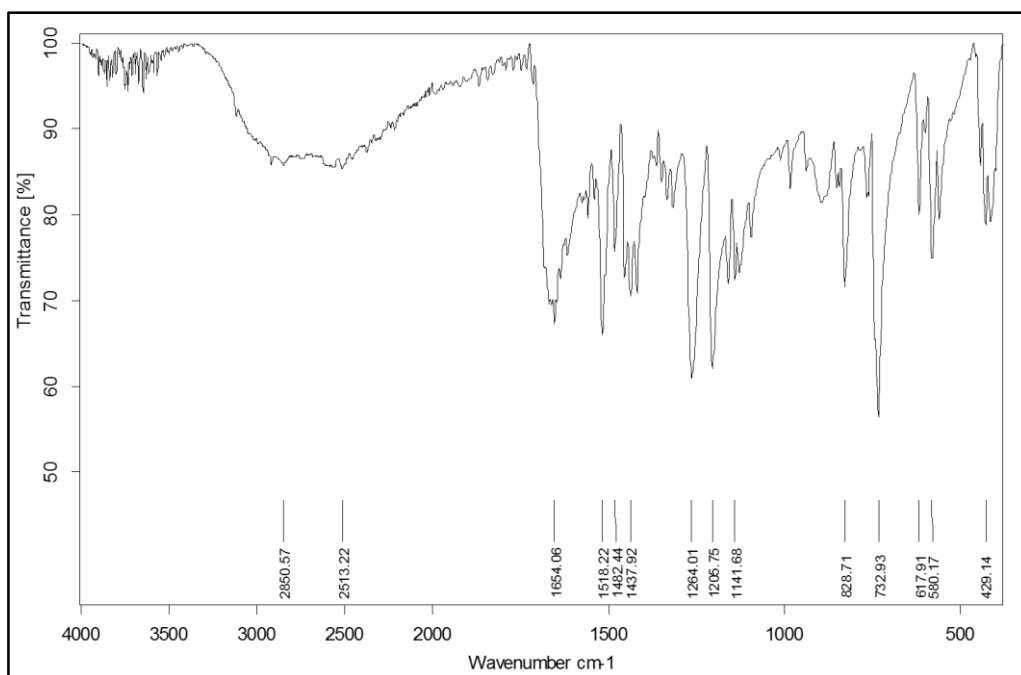


Figure 201. IR Spectrum of Compound **391b**

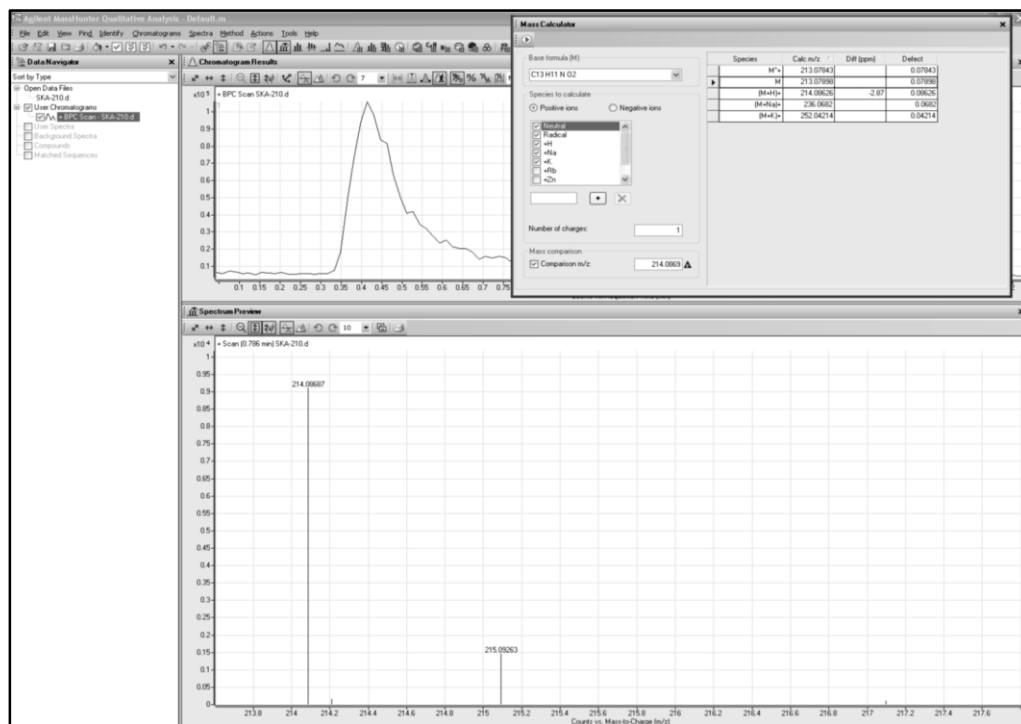


Figure 202. HRMS Spectrum of Compound 391b

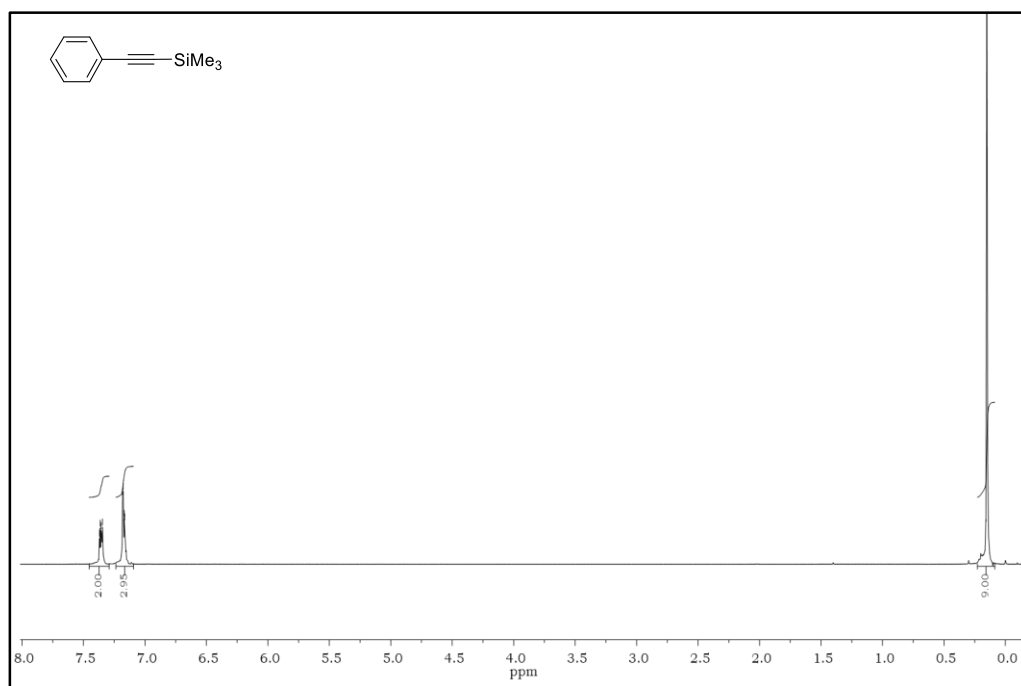


Figure 203. ¹H-NMR Spectrum of Compound 394

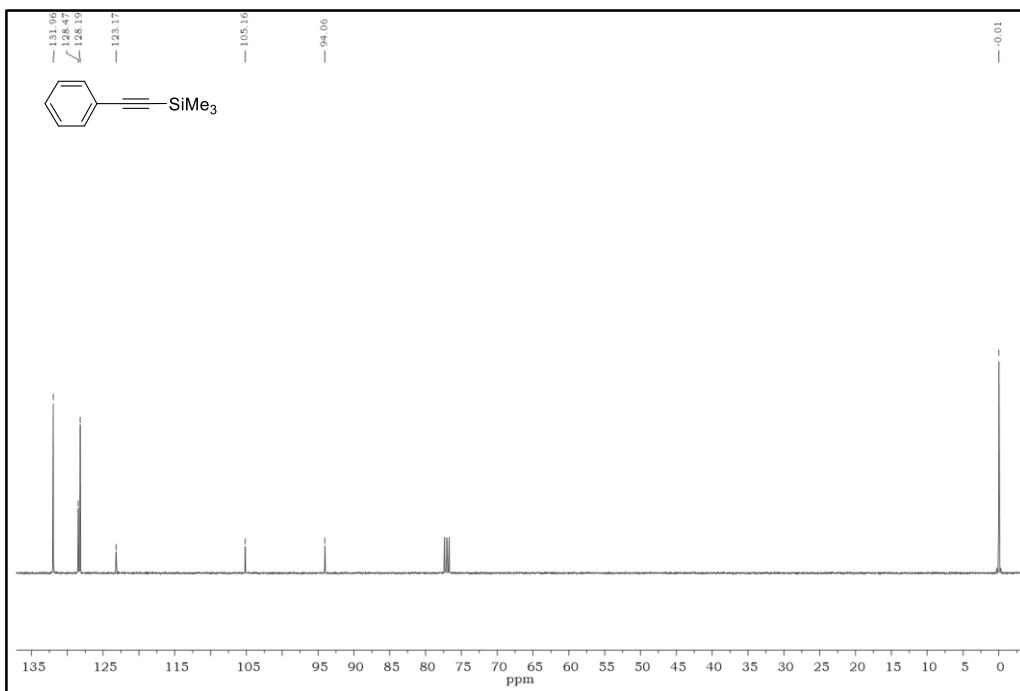


Figure 204. ^{13}C -NMR Spectrum of Compound **394**

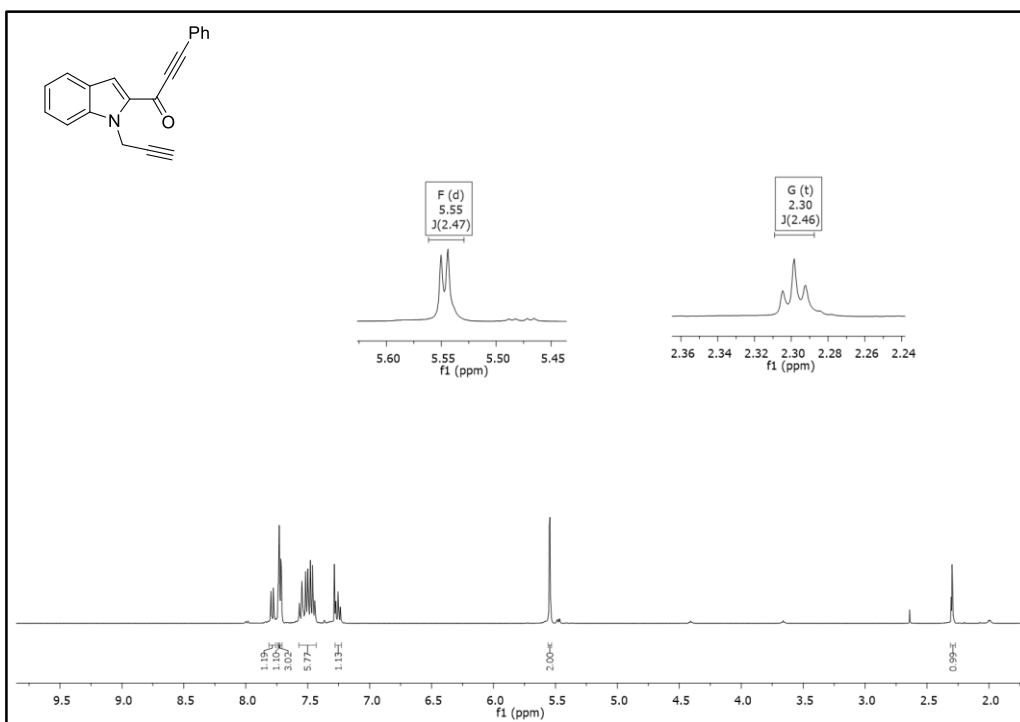


Figure 205. ^1H -NMR Spectrum of Compound **393a**

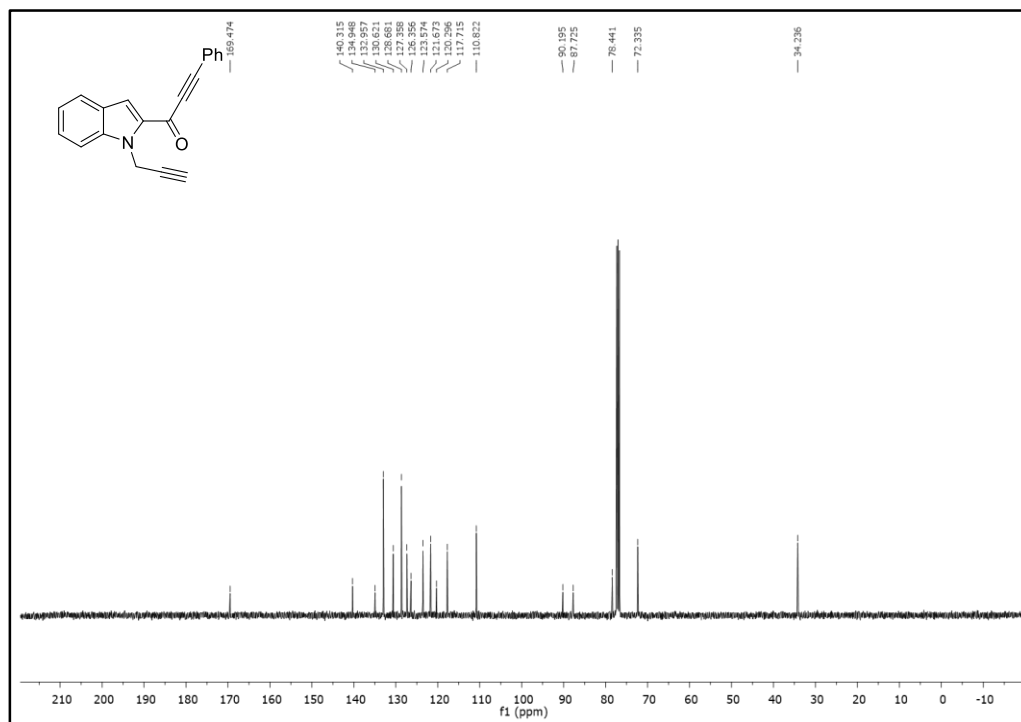


Figure 206. ¹³C-NMR Spectrum of Compound 393a

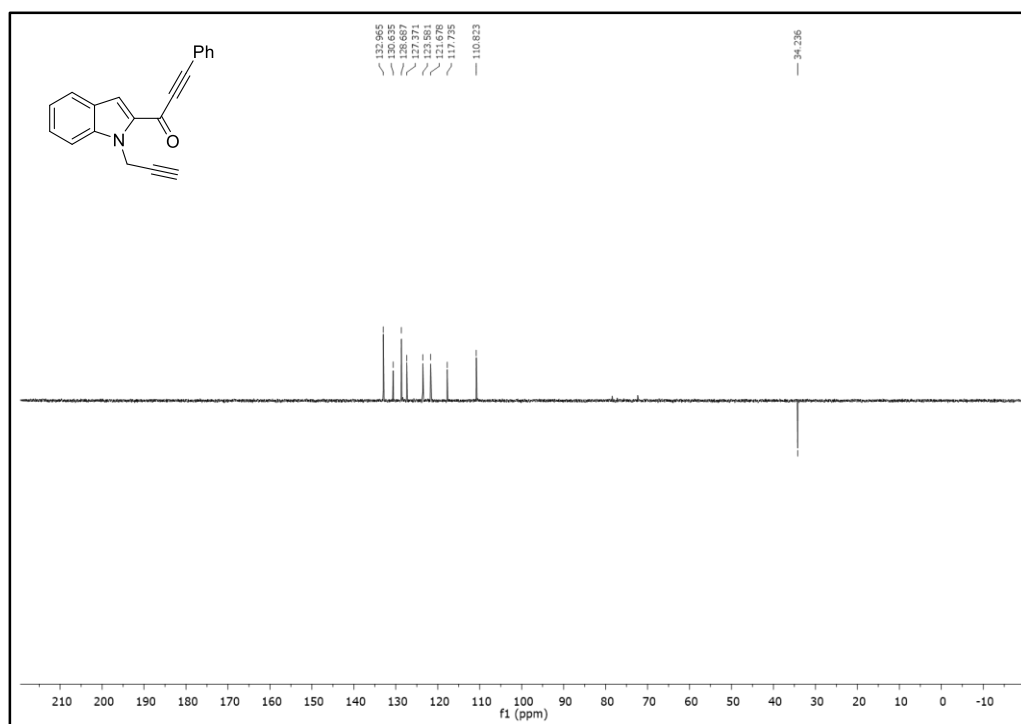


Figure 207. DEPT-135 Spectrum of Compound 393a

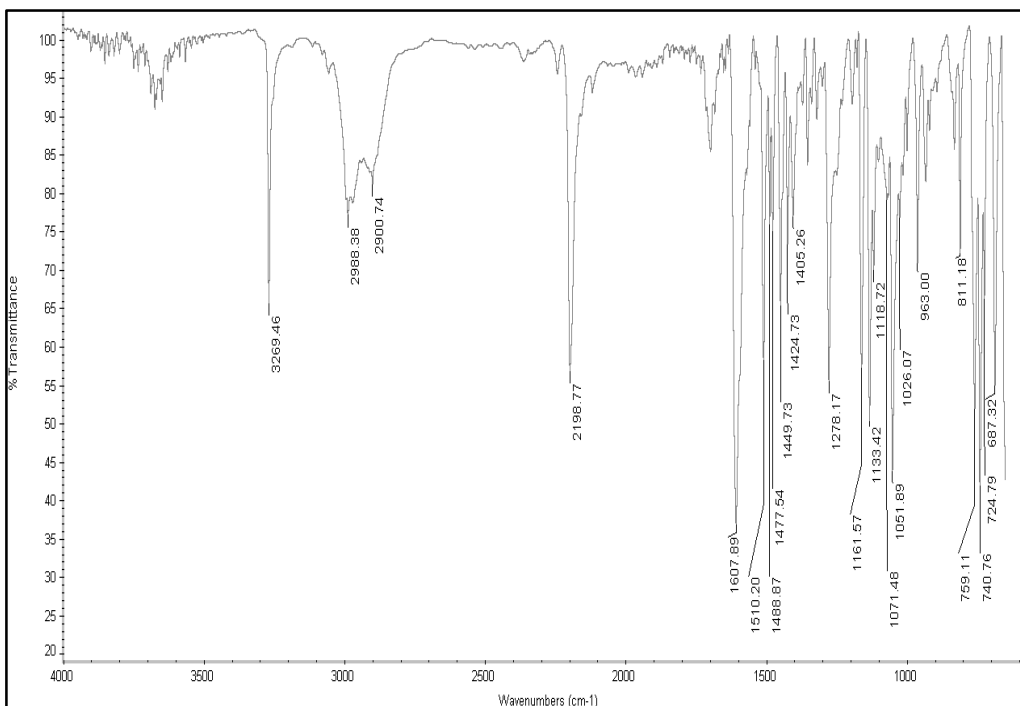


Figure 208. IR Spectrum of Compound 393a

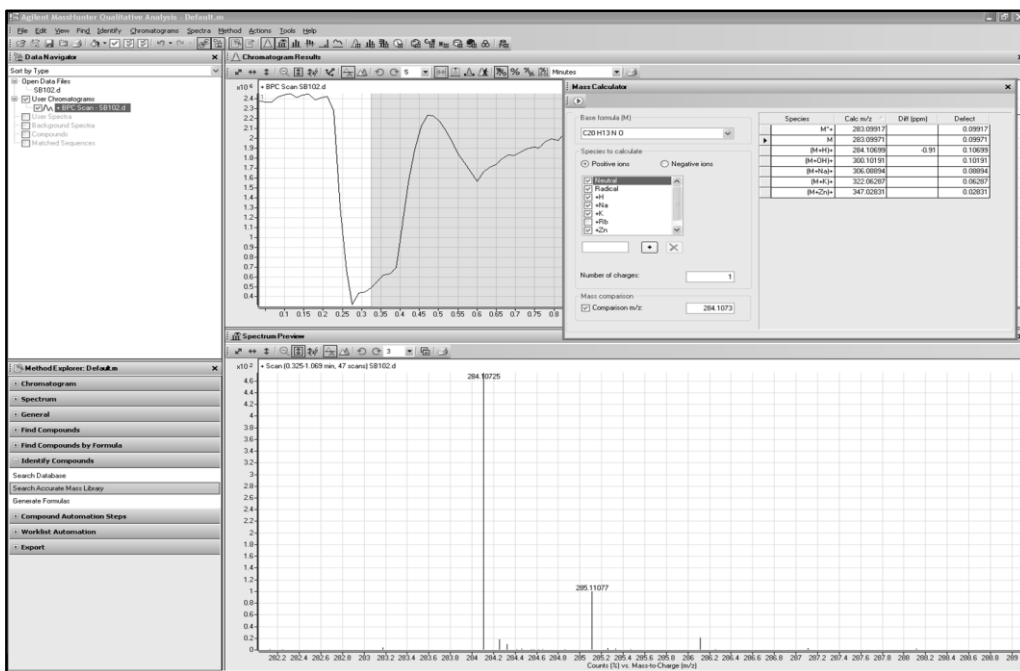
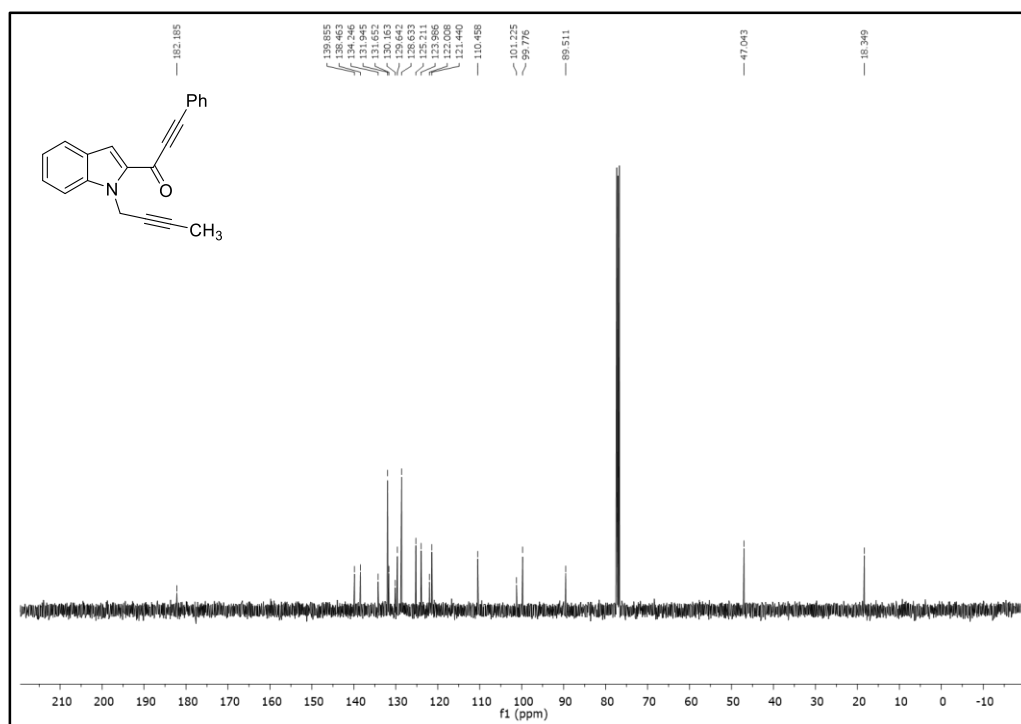
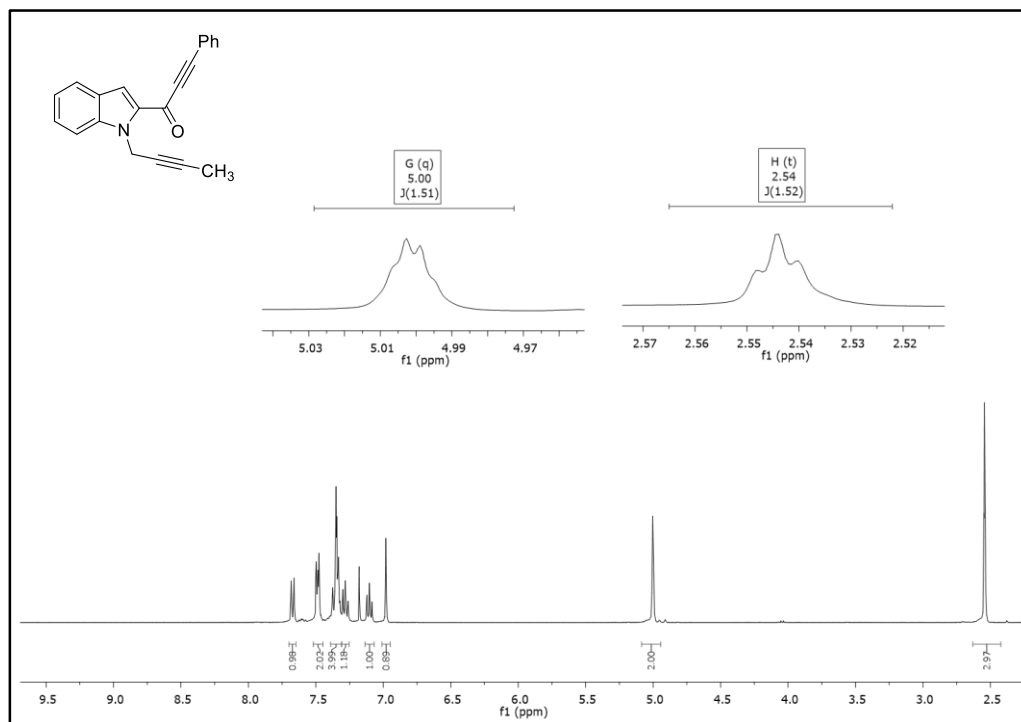


Figure 209. HRMS Spectrum of Compound 393a



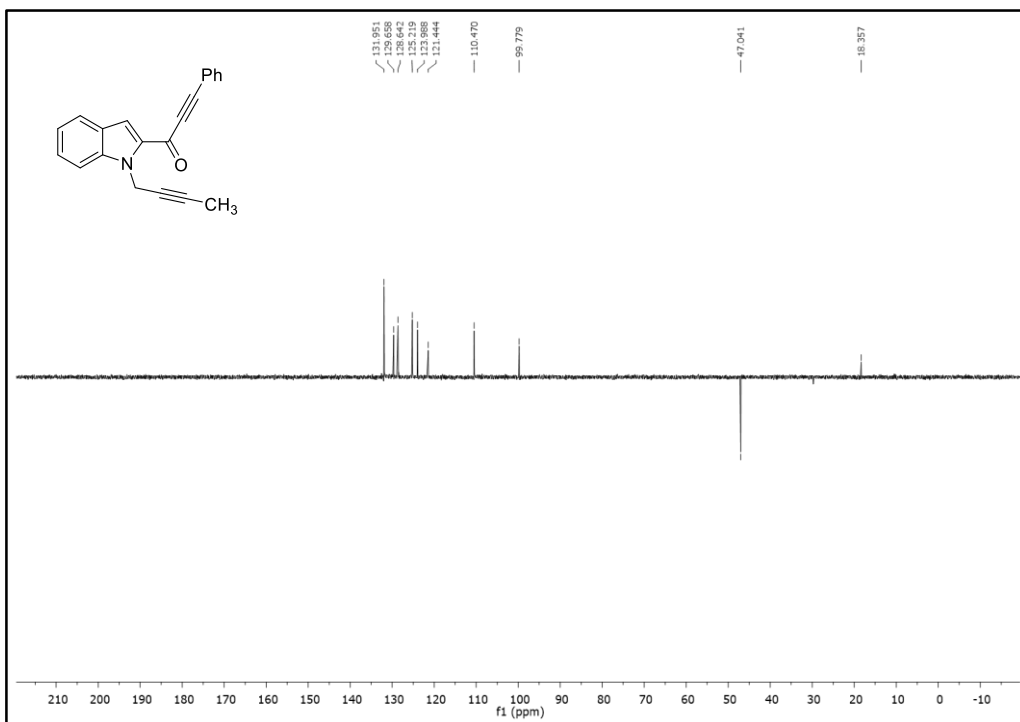


Figure 212. DEPT-135 Spectrum of Compound 393b

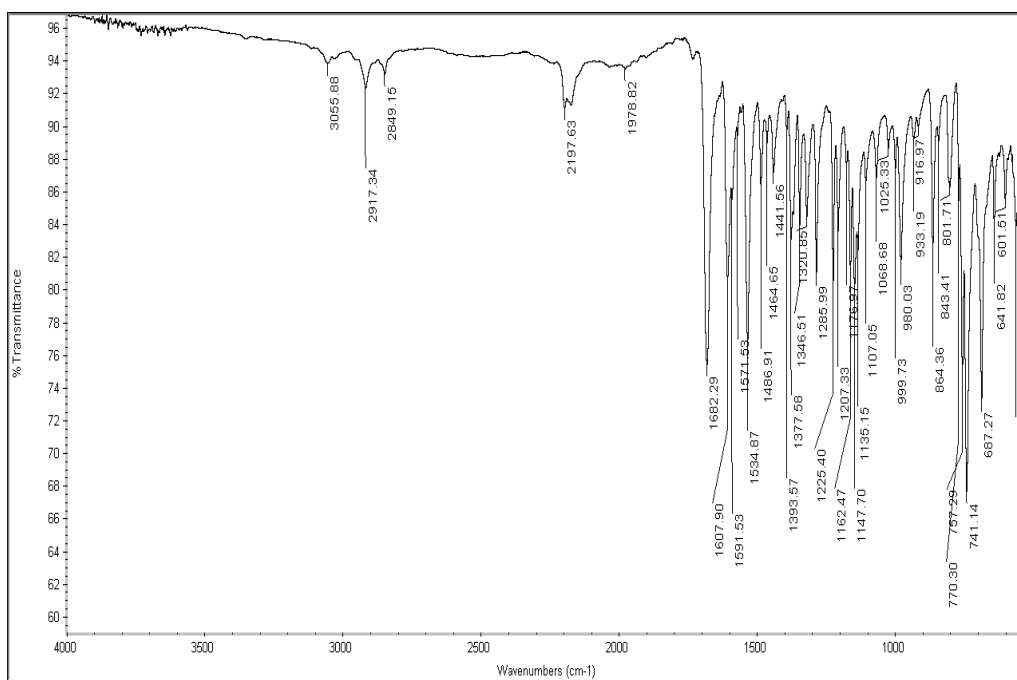


Figure 213. IR Spectrum of Compound 393b

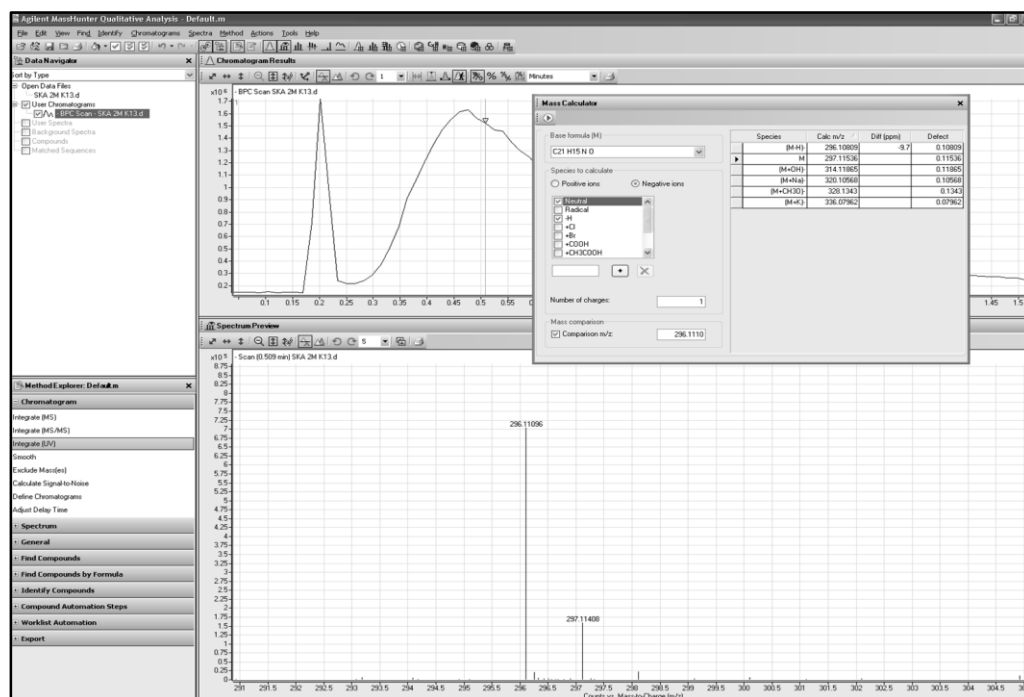


Figure 214. HRMS Spectrum of Compound 393b

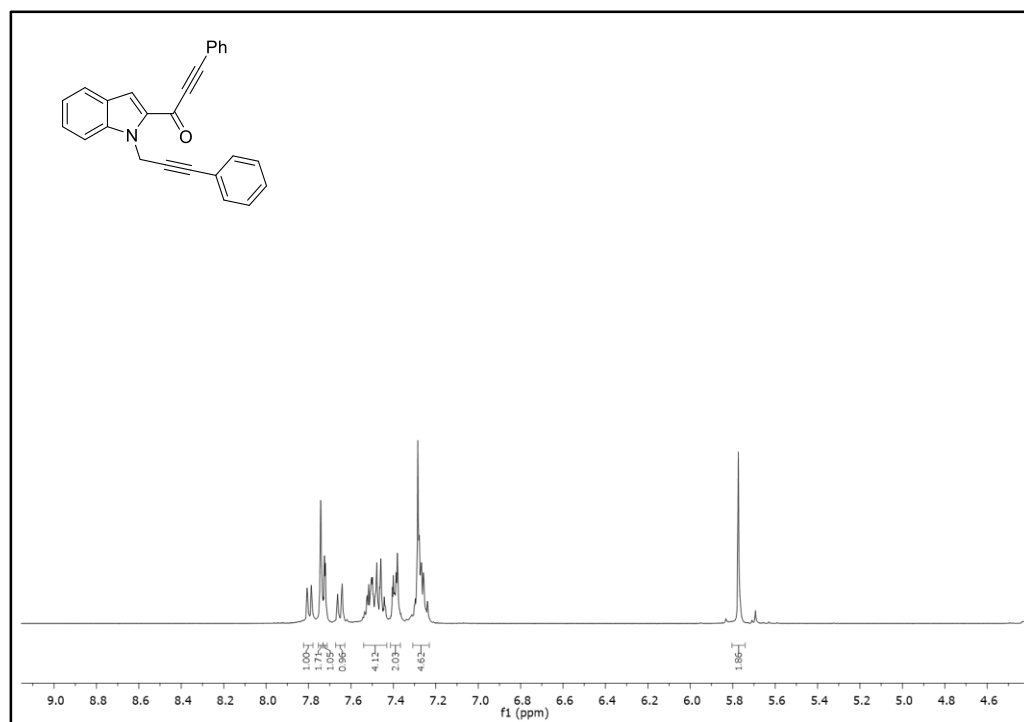


Figure 215. ¹H-NMR Spectrum of Compound 395a

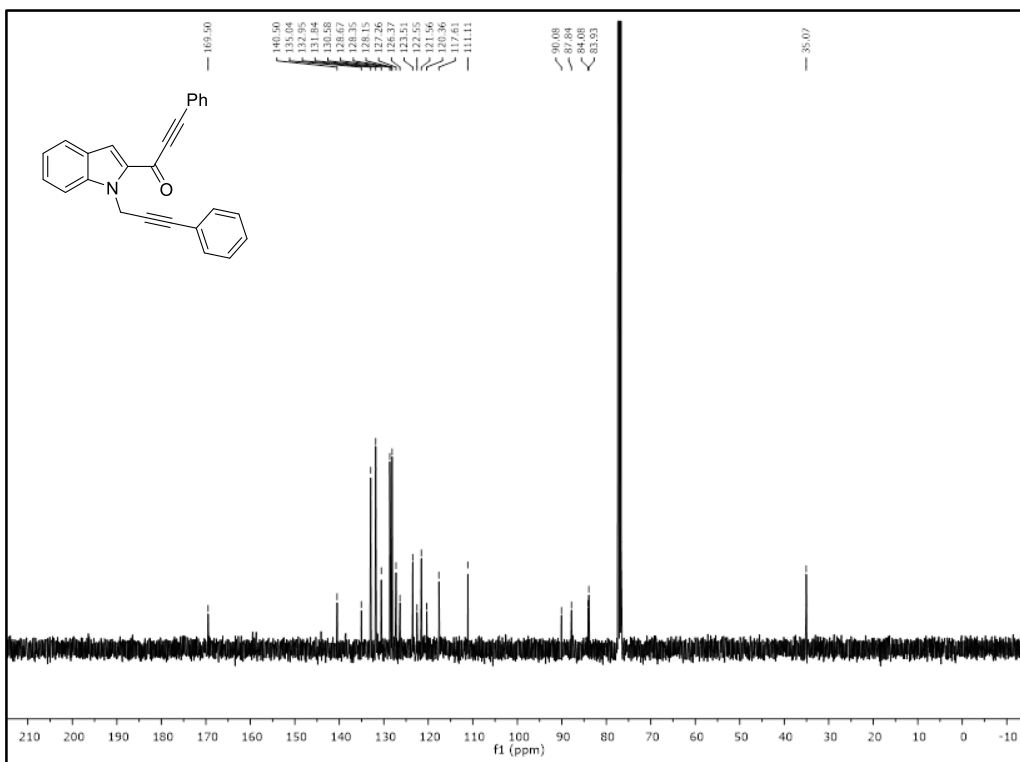


Figure 216. ^{13}C -NMR Spectrum of Compound 395a

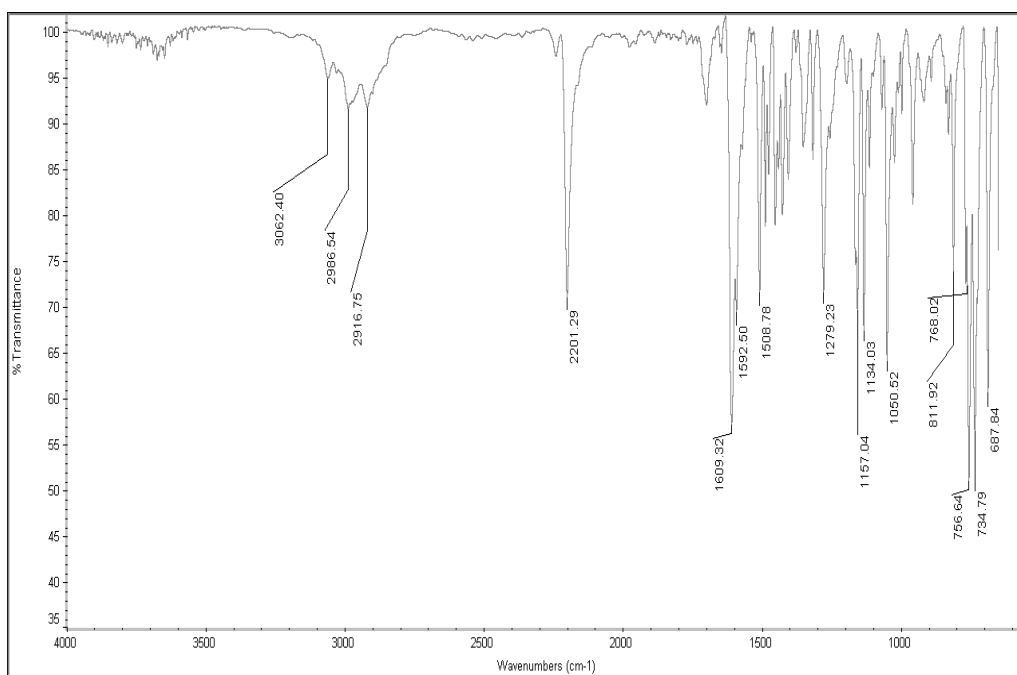


Figure 217. IR Spectrum of Compound 395a

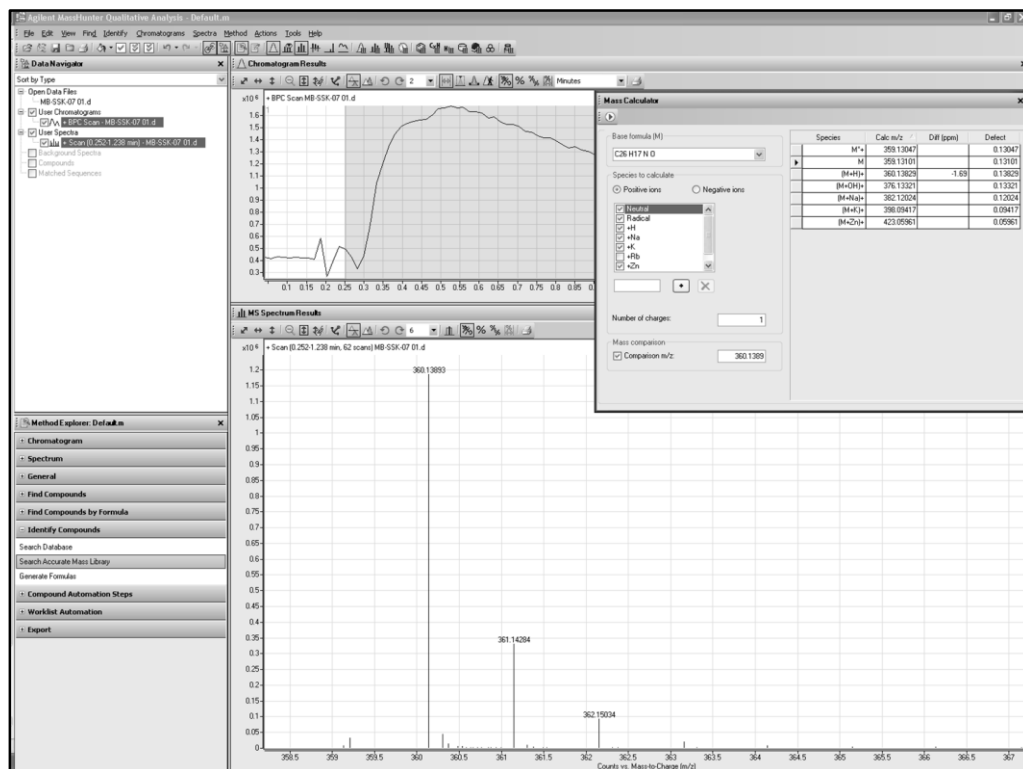


Figure 218. HRMS Spectrum of Compound 395a

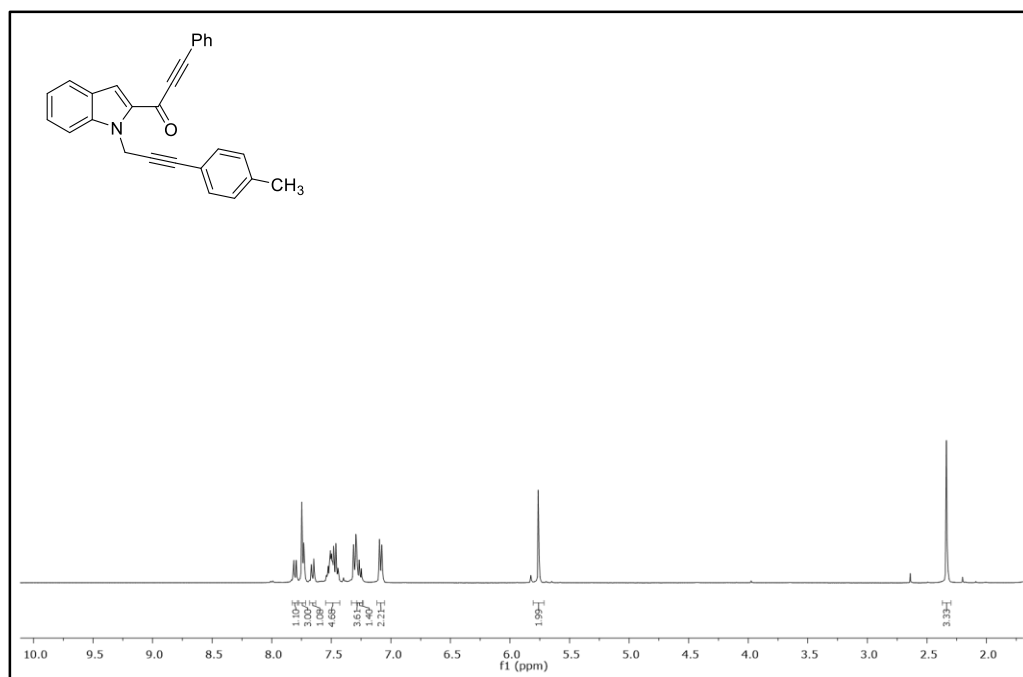


Figure 219. ¹H-NMR Spectrum of Compound 395b

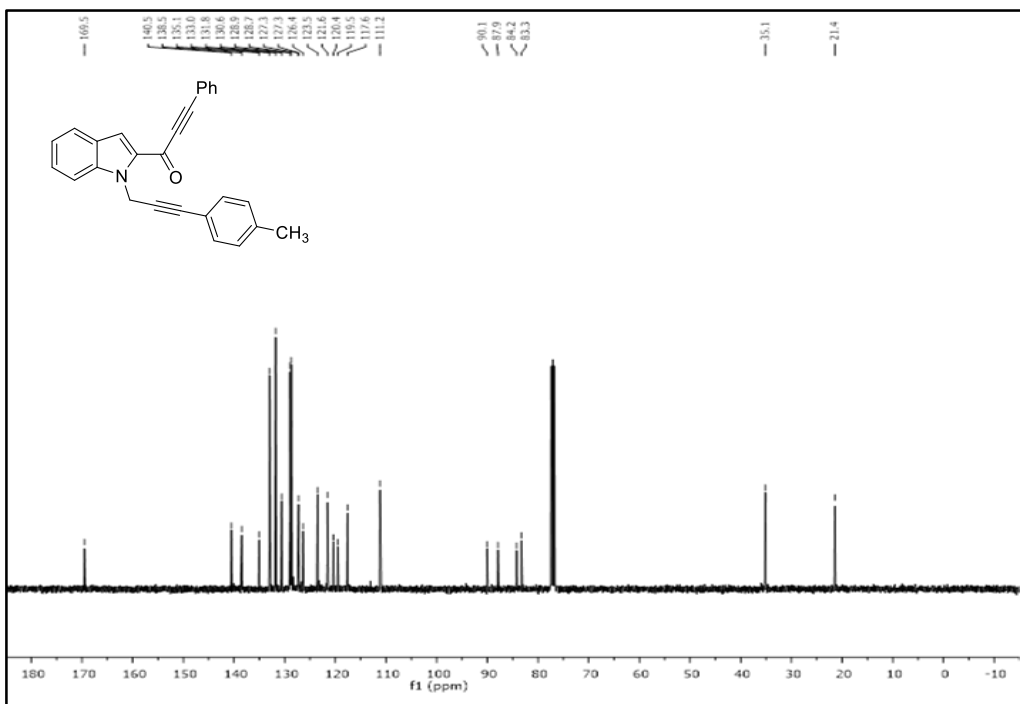


Figure 220. ^{13}C -NMR Spectrum of Compound **395b**

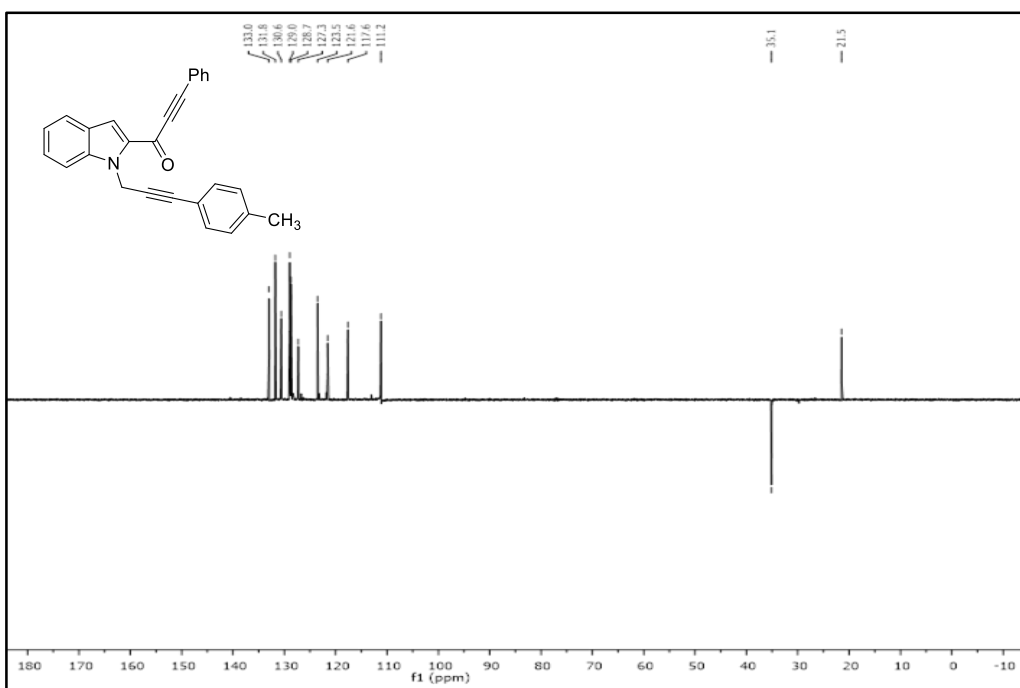


Figure 221. DEPT-135 Spectrum of Compound **395b**

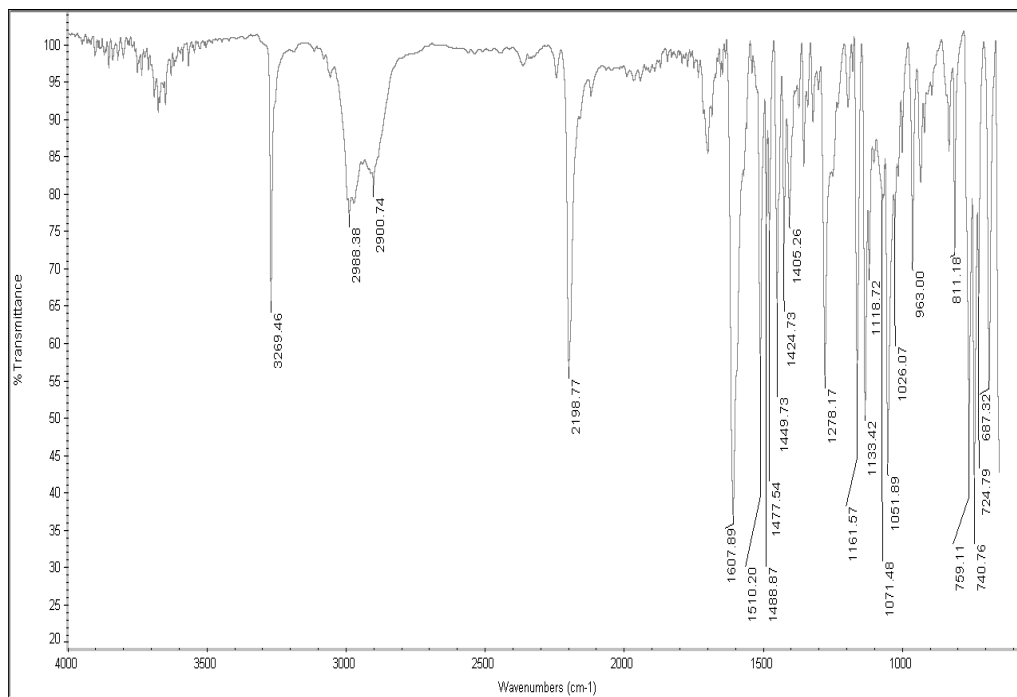


Figure 222. IR Spectrum of Compound 395b

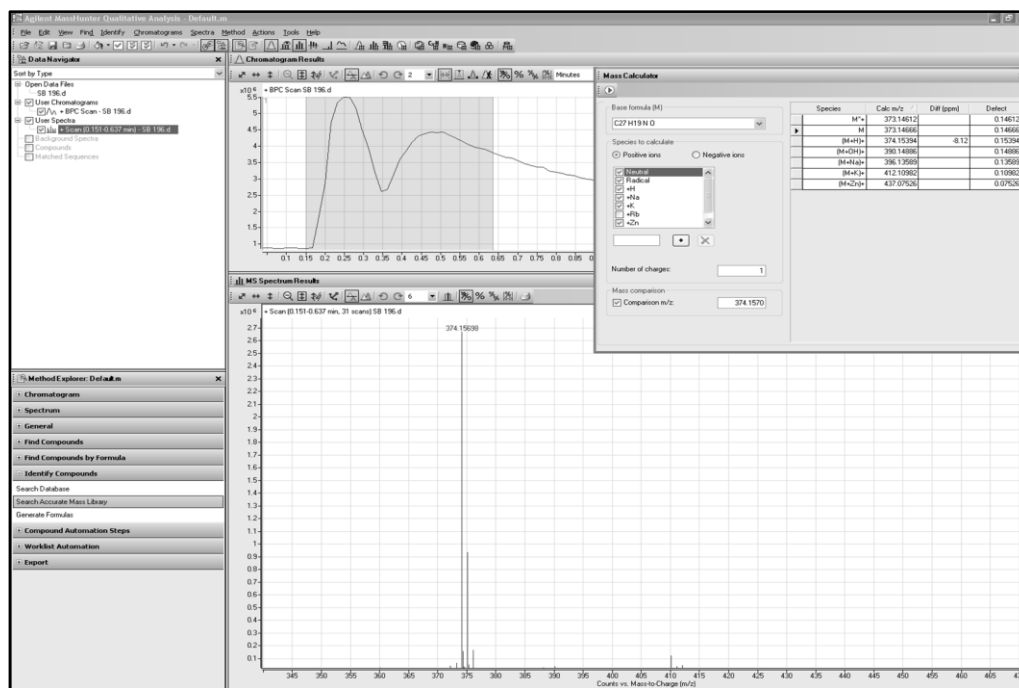


Figure 223. HRMS Spectrum of Compound 395b

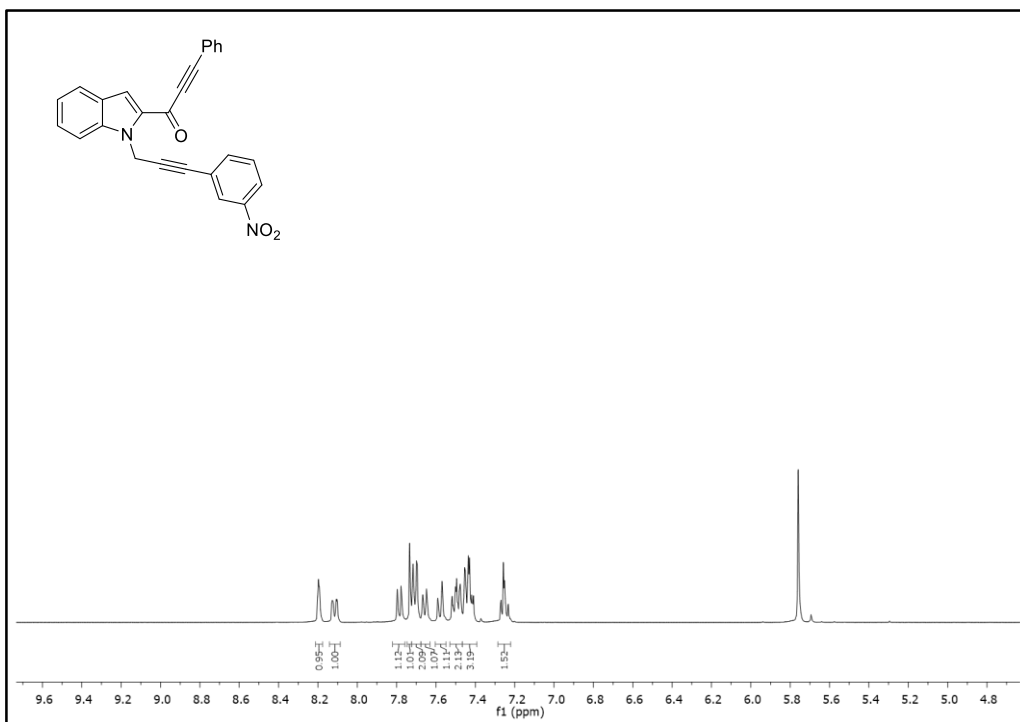


Figure 224. ¹H-NMR Spectrum of Compound 395c

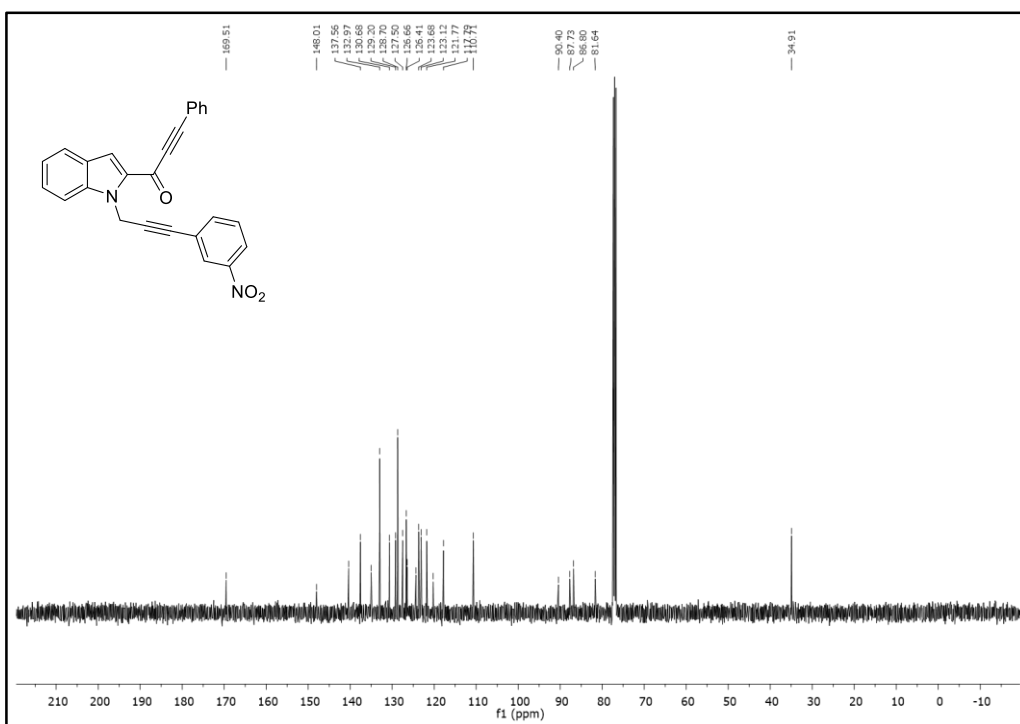


Figure 225. ¹³C-NMR Spectrum of Compound 395c

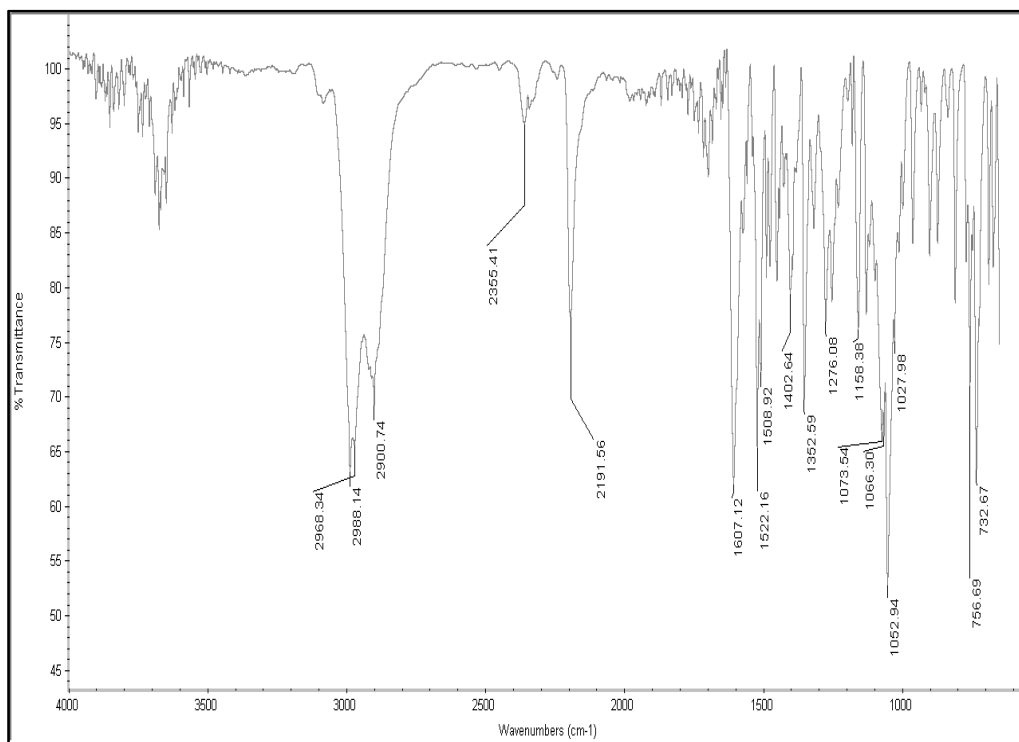


Figure 226. IR Spectrum of Compound 395c

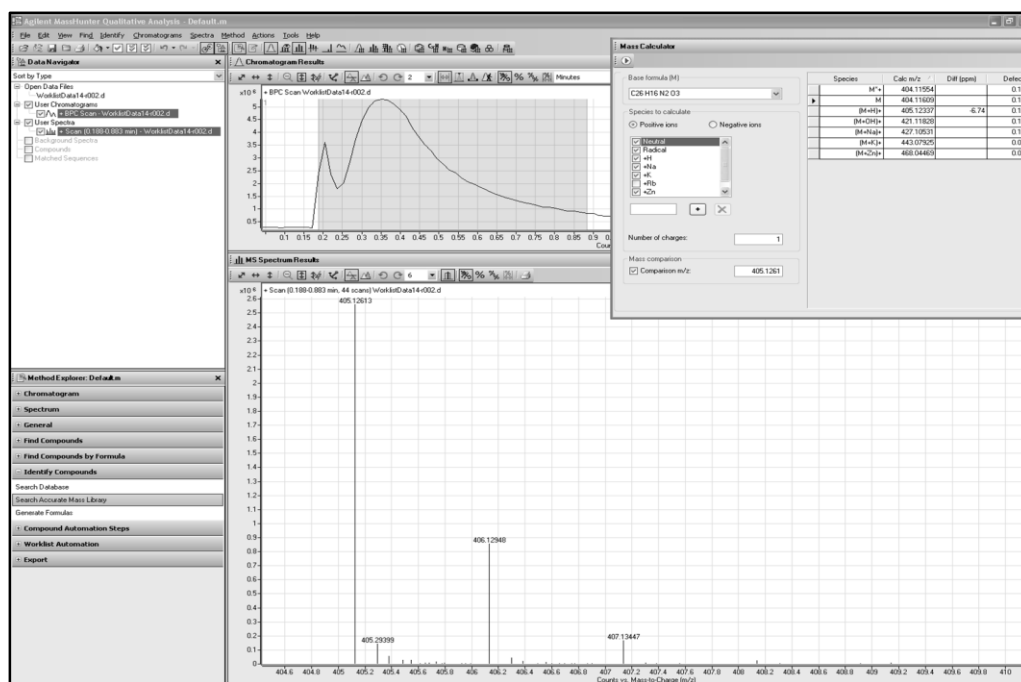


Figure 227. HRMS Spectrum of Compound 395c

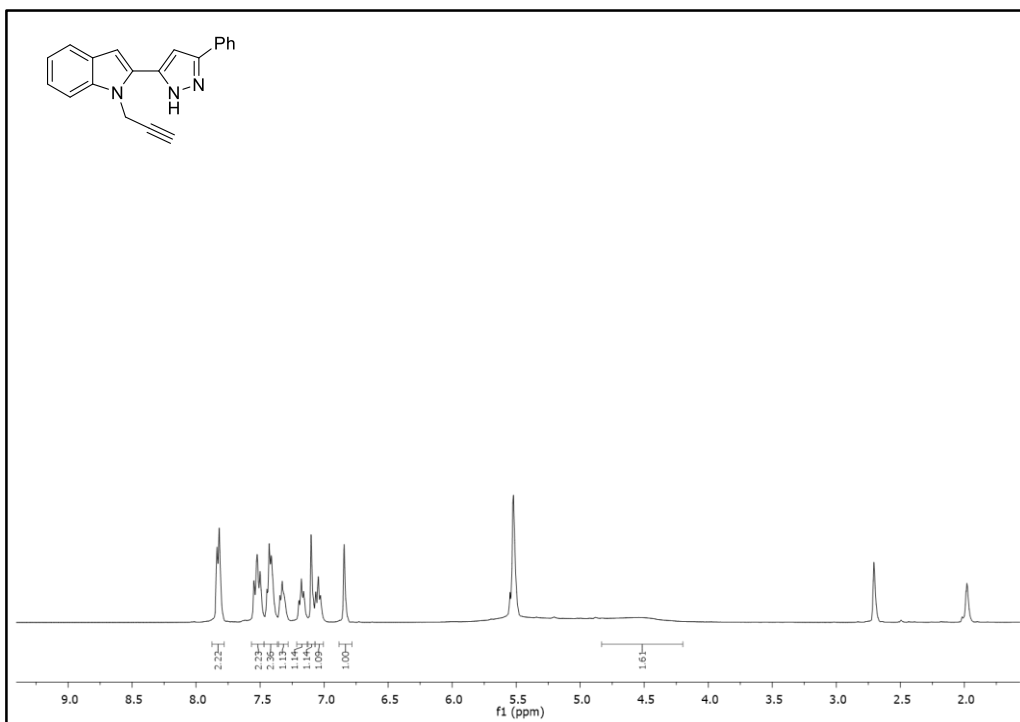


Figure 228. ¹H-NMR Spectrum of Compound 396a

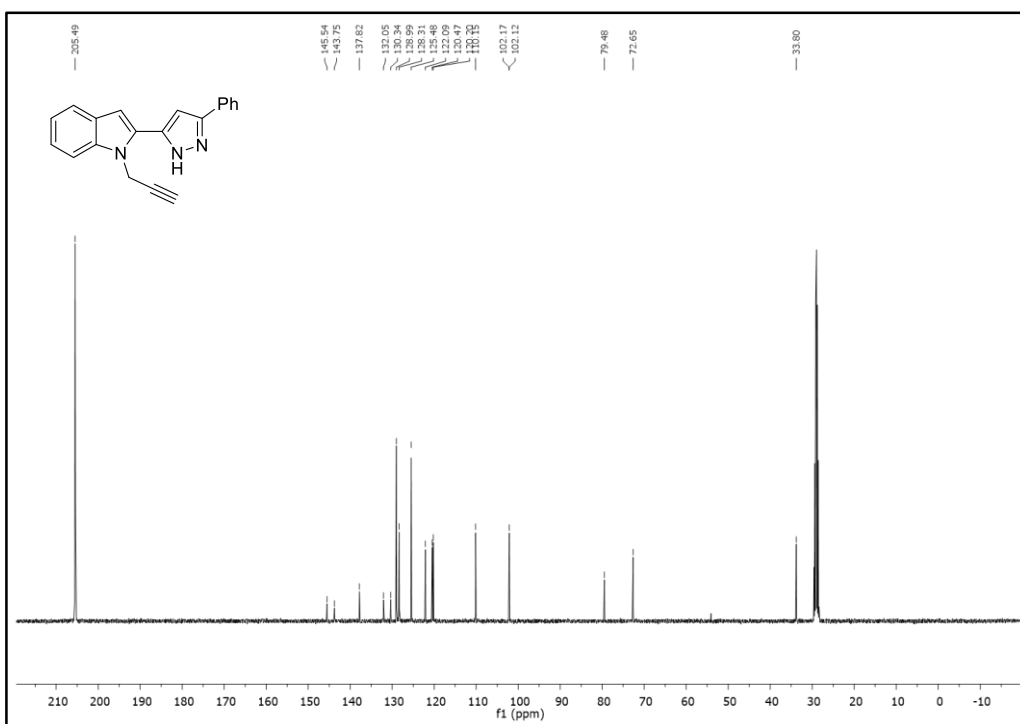


Figure 229. ¹³C-NMR Spectrum of Compound 396a

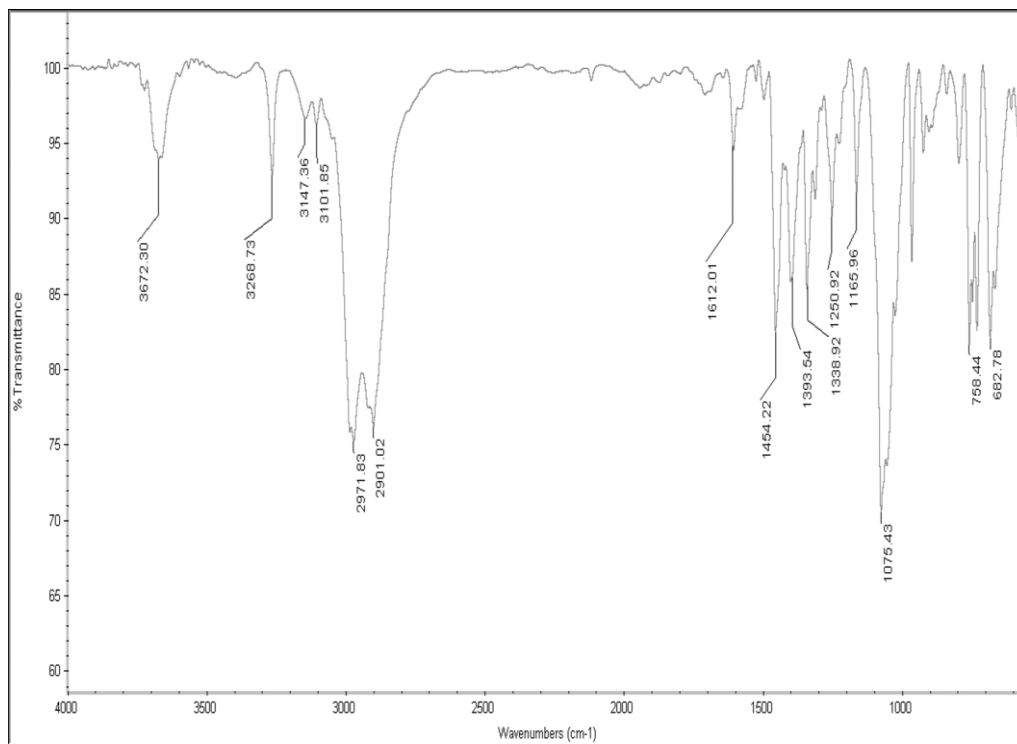


Figure 230. IR Spectrum of Compound 396a

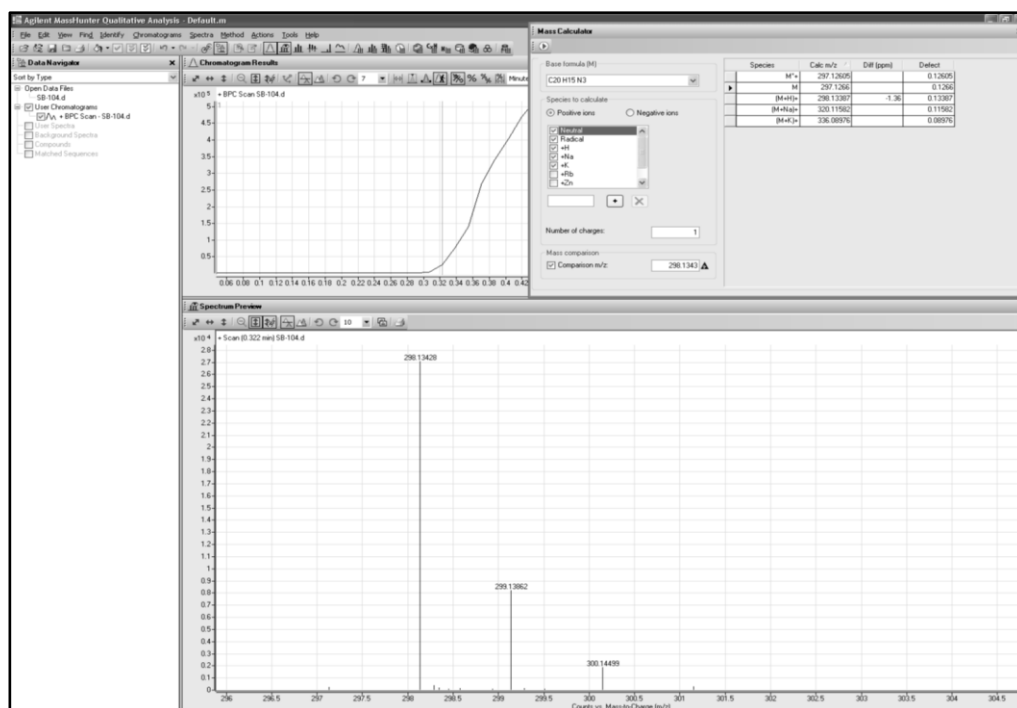


Figure 231. HRMS Spectrum of Compound 396a

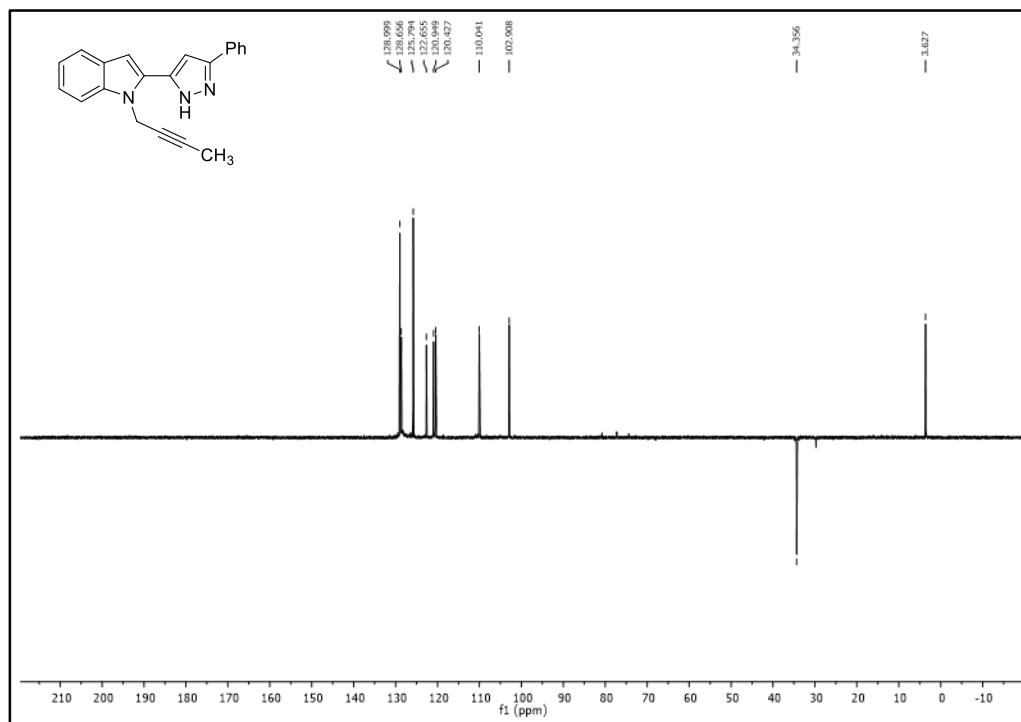


Figure 234. DEPT-135 Spectrum of Compound **396b**

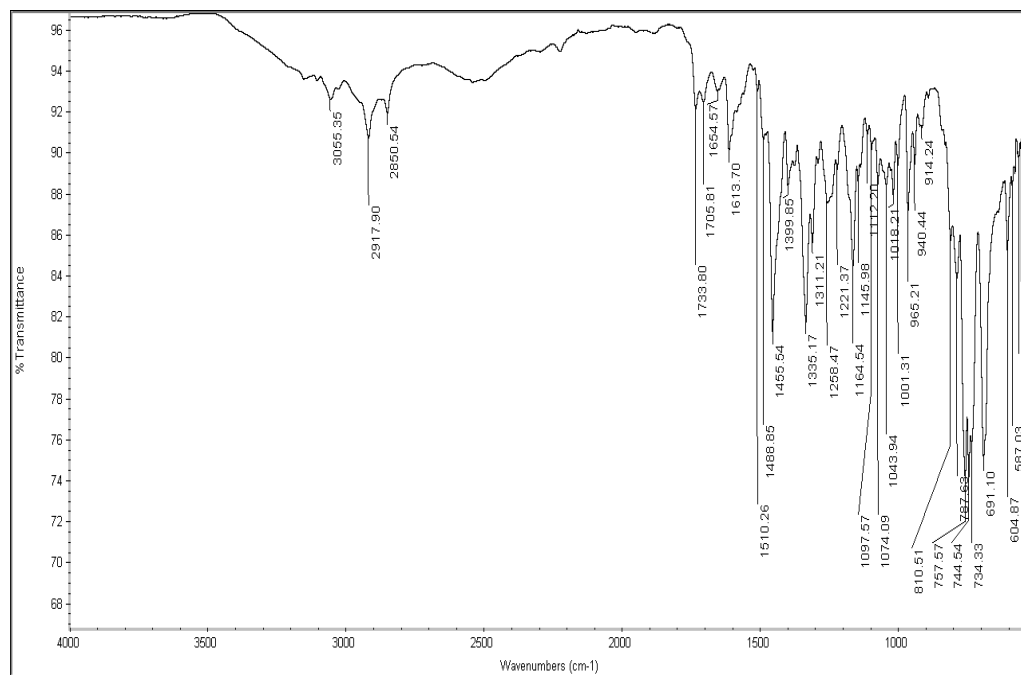


Figure 235. IR Spectrum of Compound **396b**

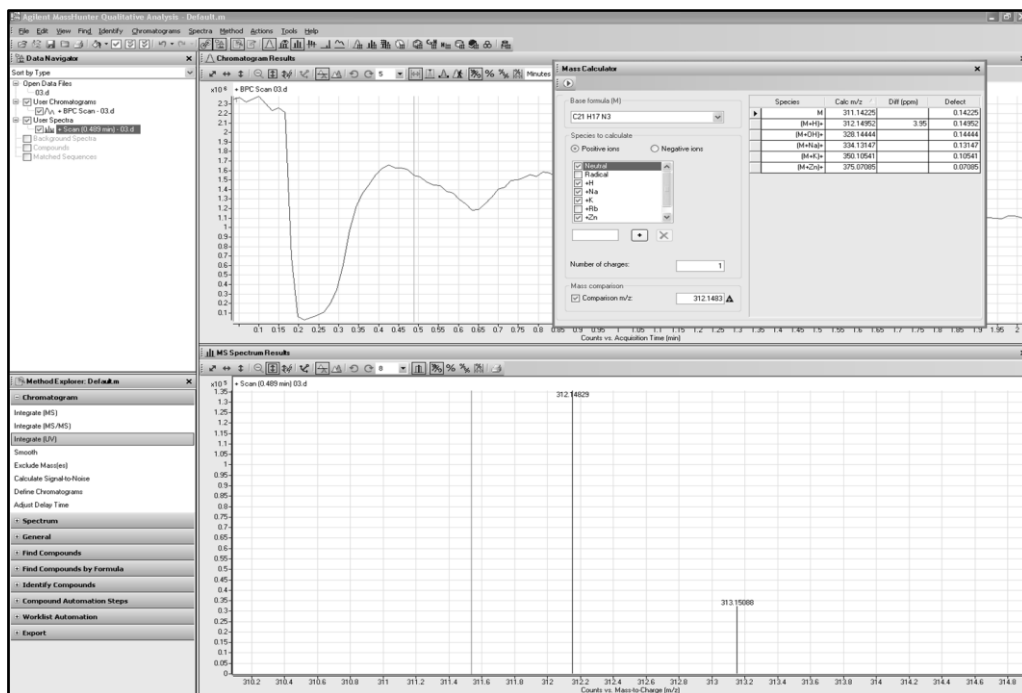


Figure 236. HRMS Spectrum of Compound 396b

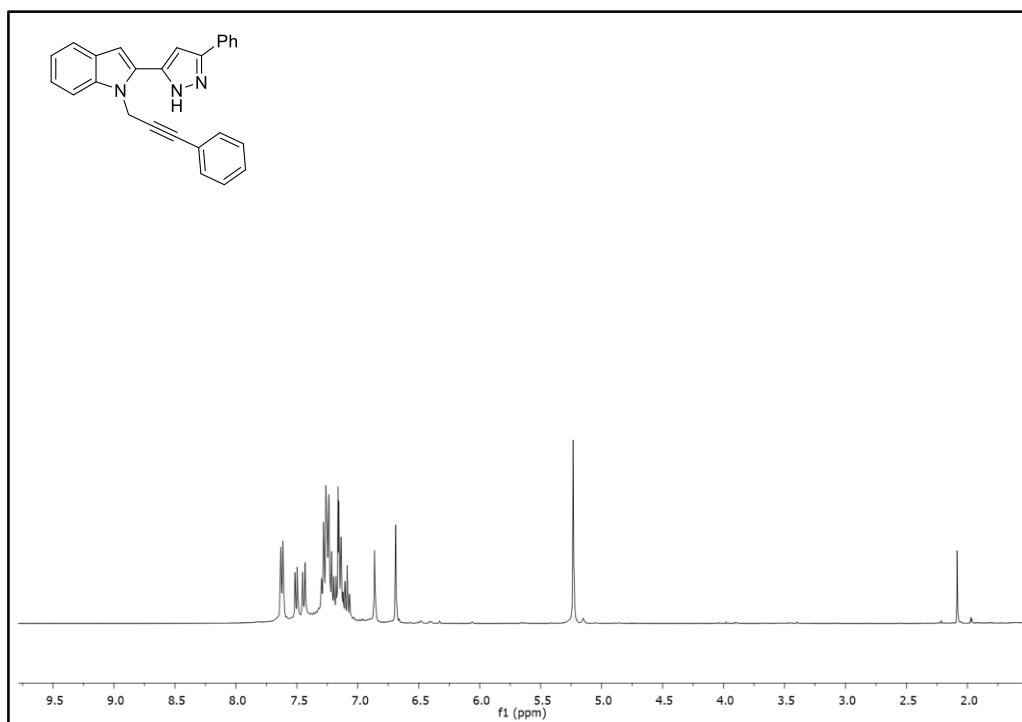


Figure 237. ¹H-NMR Spectrum of Compound 396c

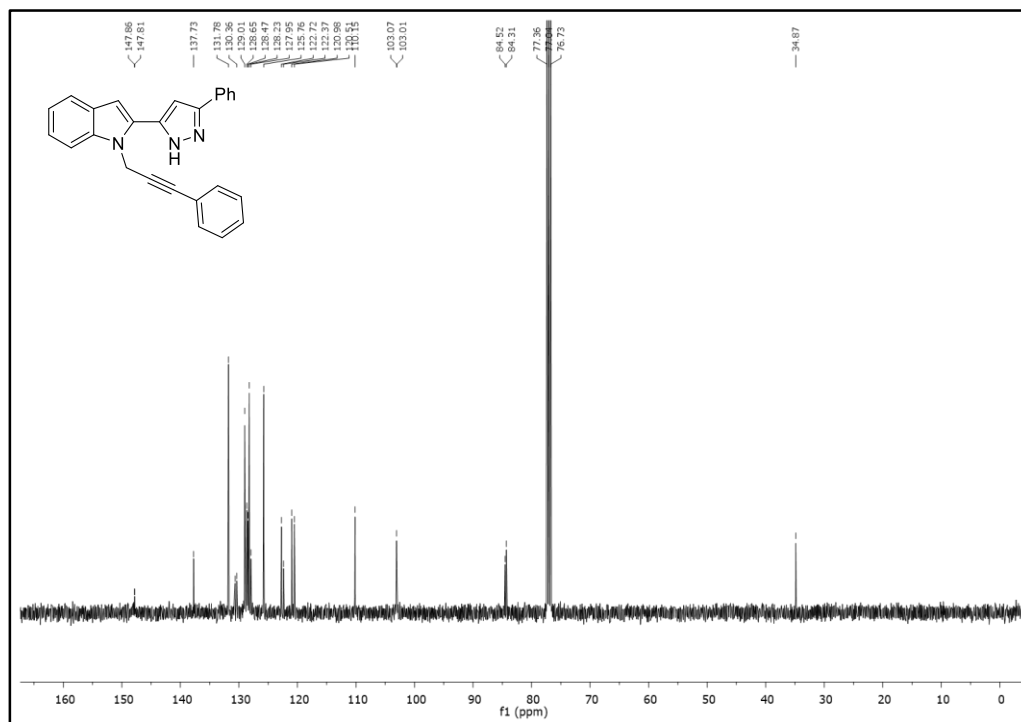


Figure 238. ¹³C-NMR Spectrum of Compound 396c

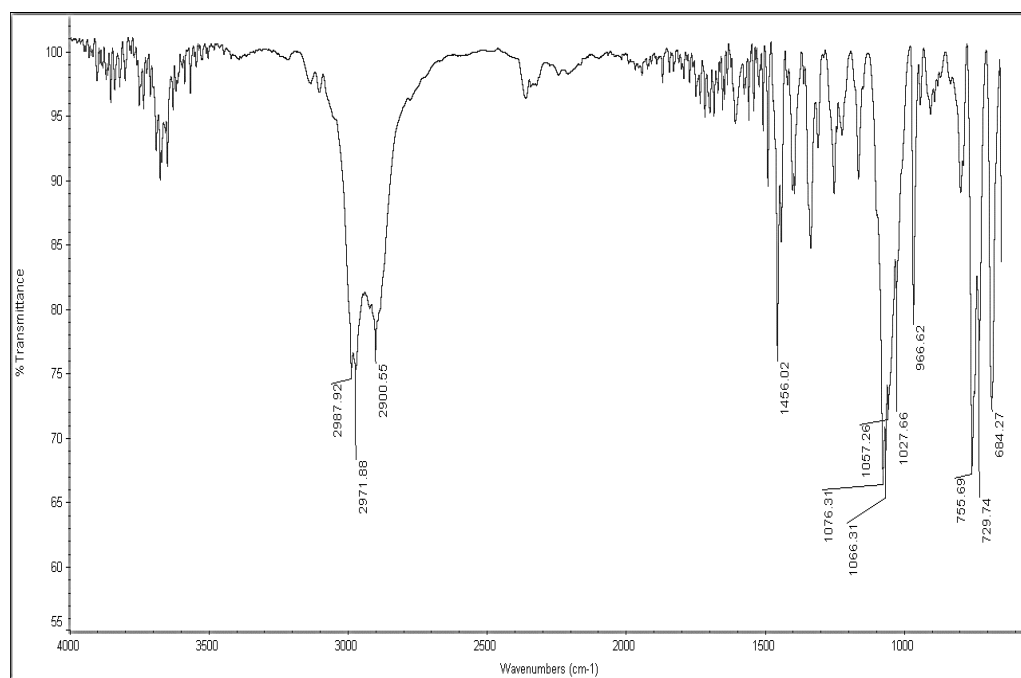


Figure 239. IR Spectrum of Compound 396c

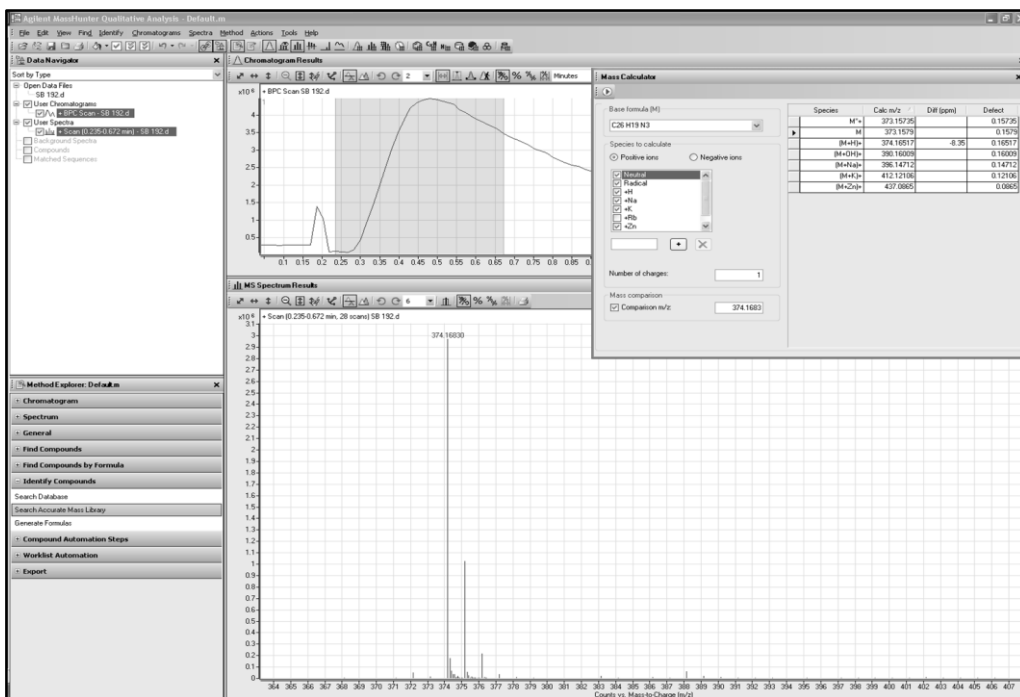


Figure 240. HRMS Spectrum of Compound 396c

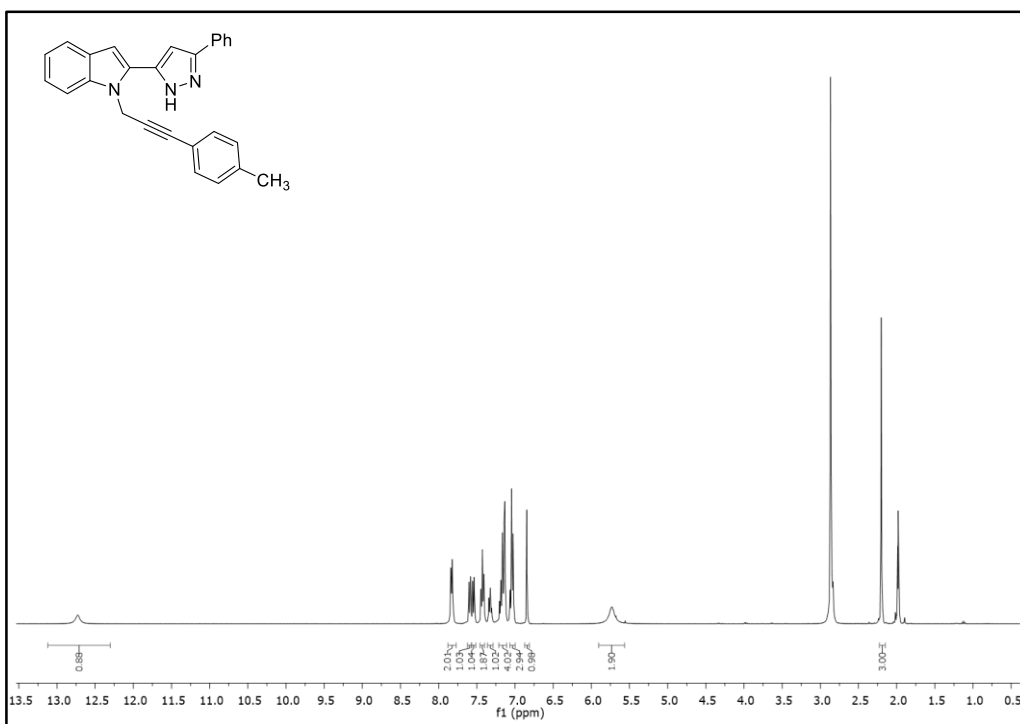


Figure 241. ¹H-NMR Spectrum of Compound 396d

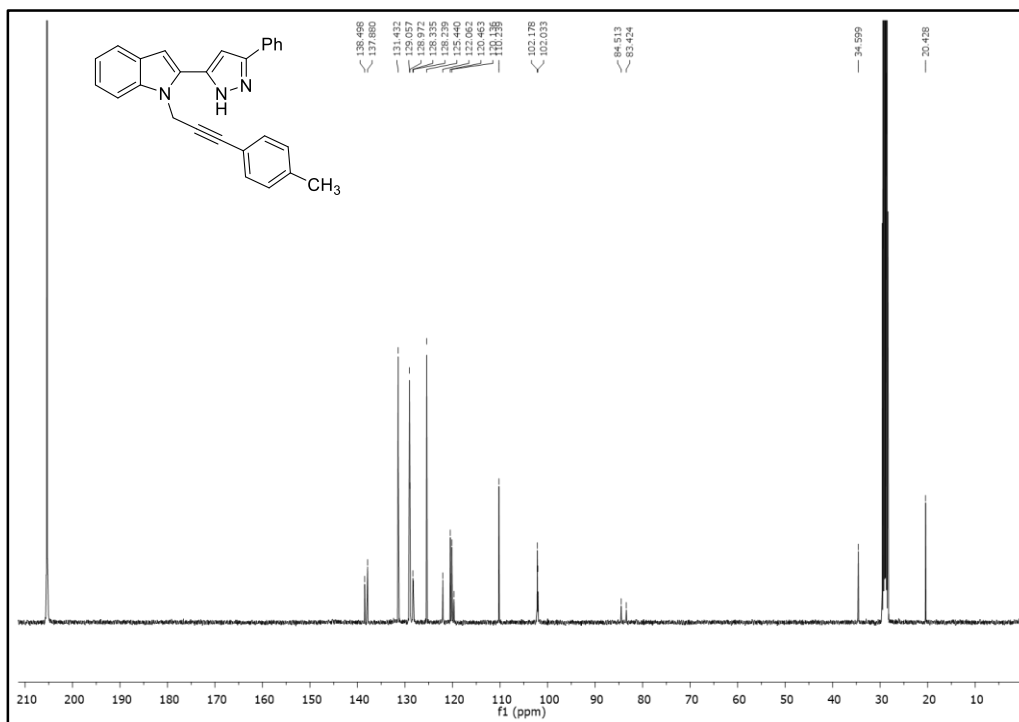


Figure 242. ¹³C-NMR Spectrum of Compound 396d

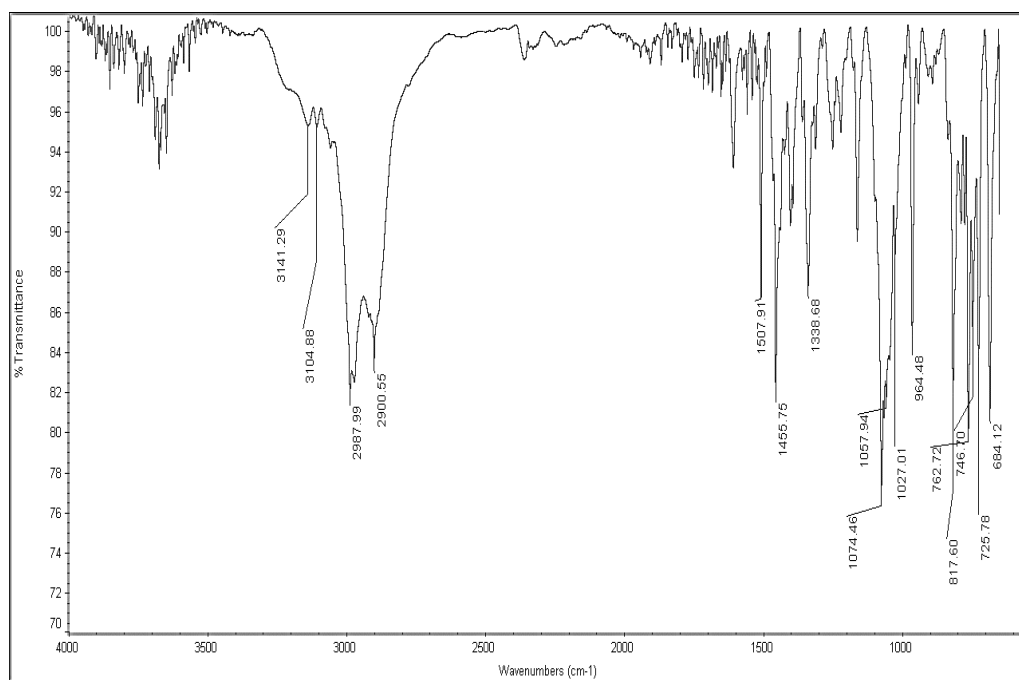


Figure 243. IR Spectrum of Compound 396d

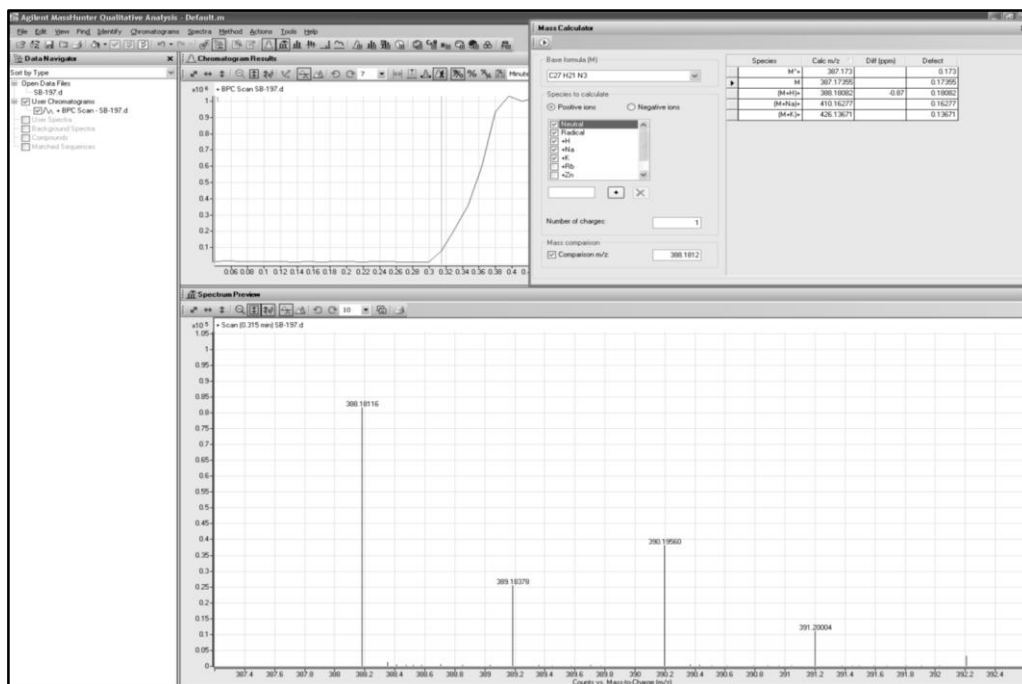


Figure 244. HRMS Spectrum of Compound 396d

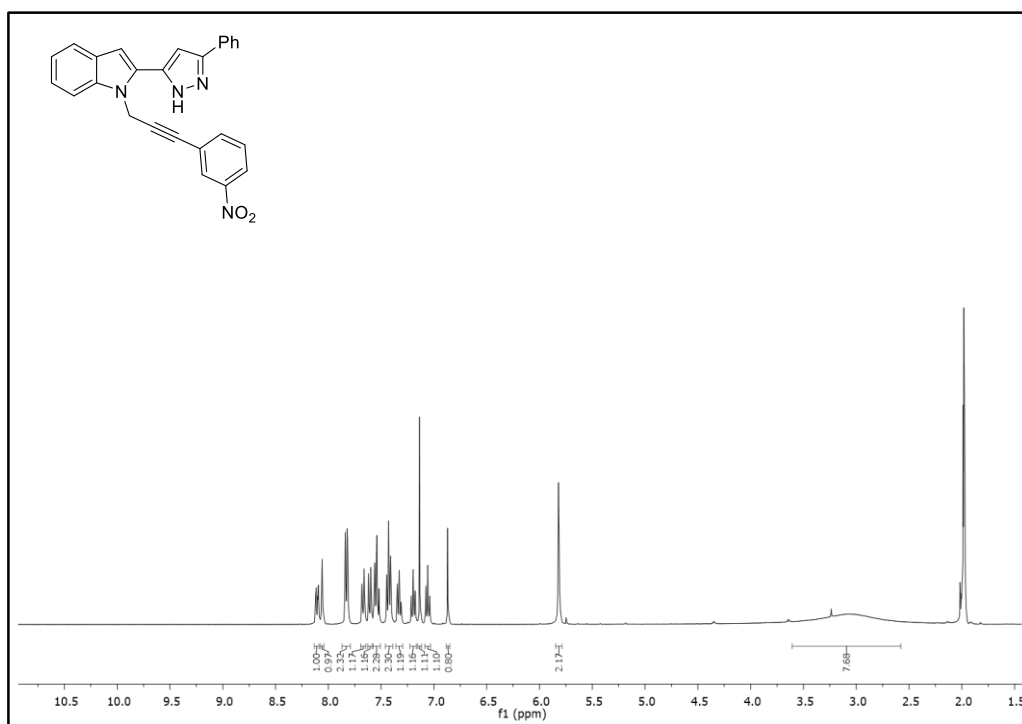


Figure 245. ¹H-NMR Spectrum of Compound 396e

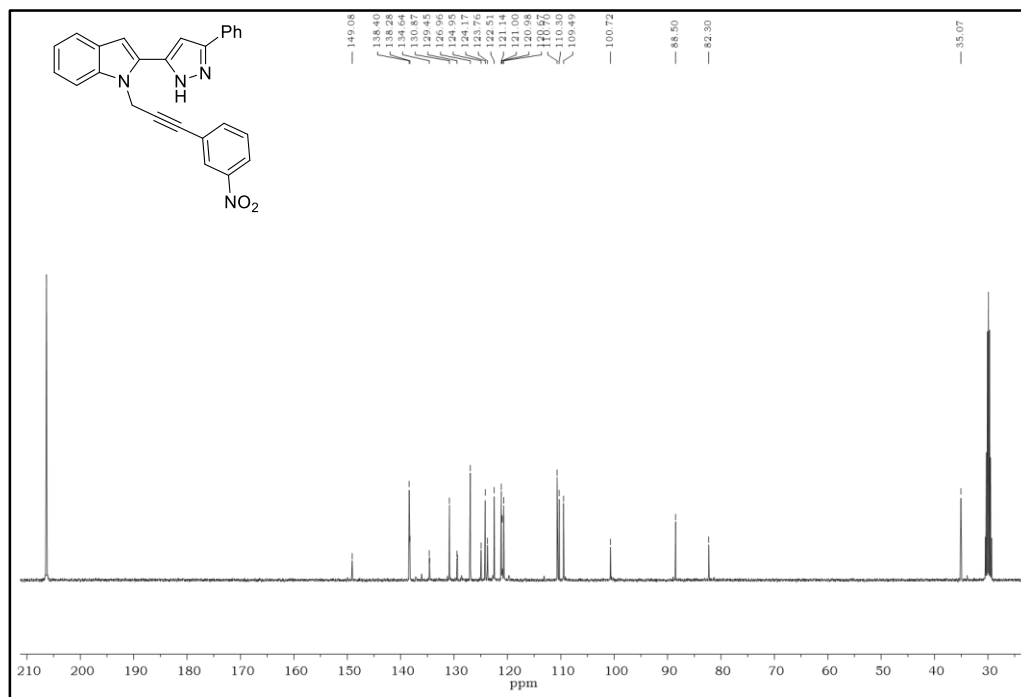


Figure 246. ¹³C-NMR Spectrum of Compound 396e

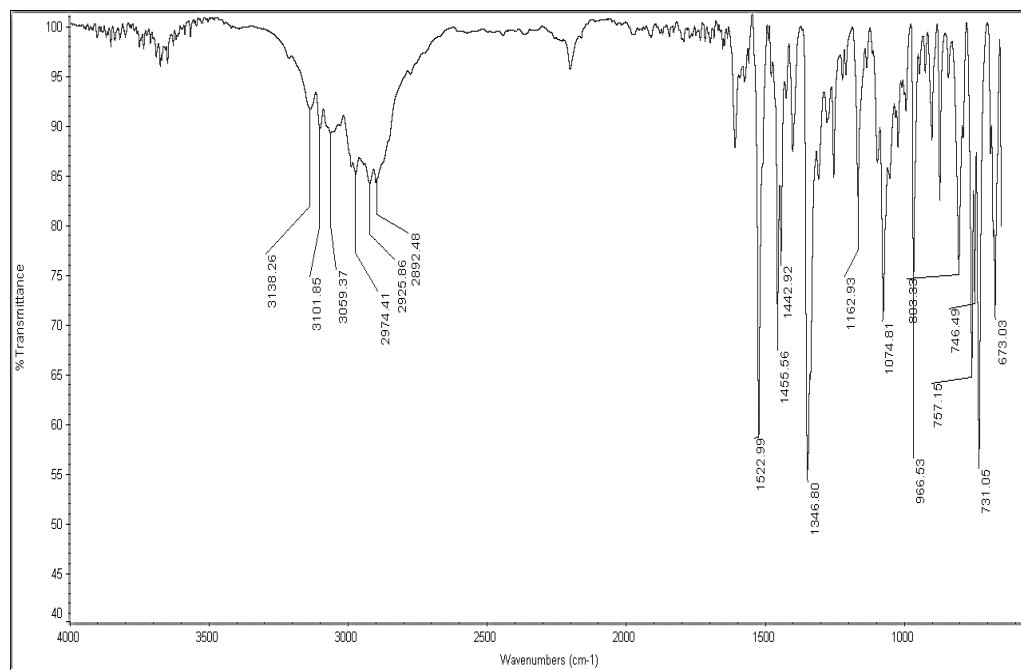


Figure 247. IR Spectrum of Compound 396e

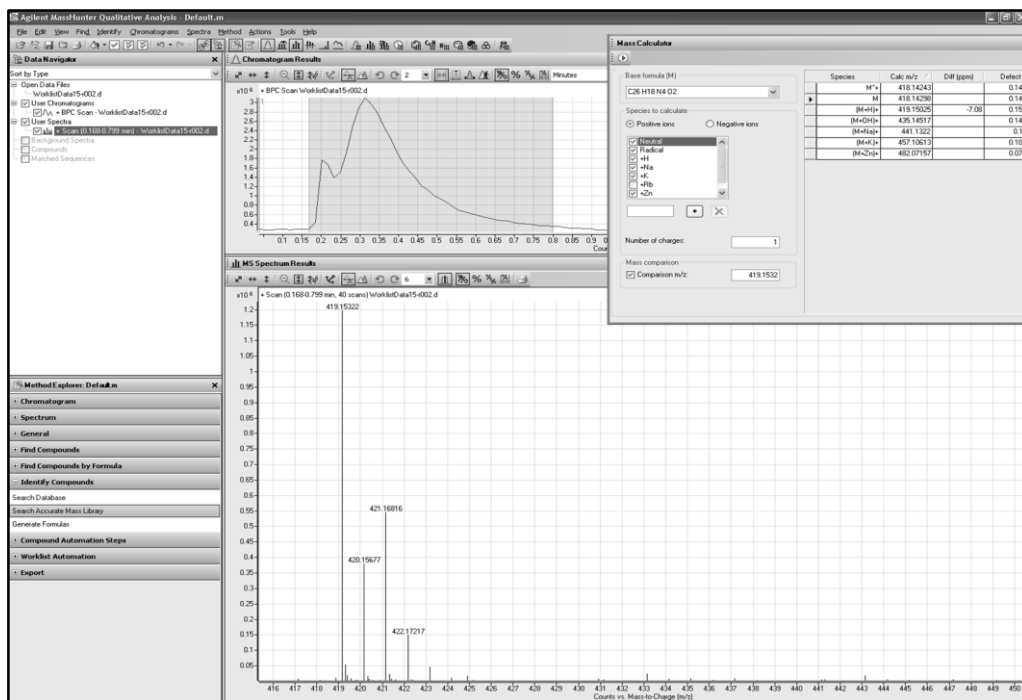


Figure 248. HRMS Spectrum of Compound 396e

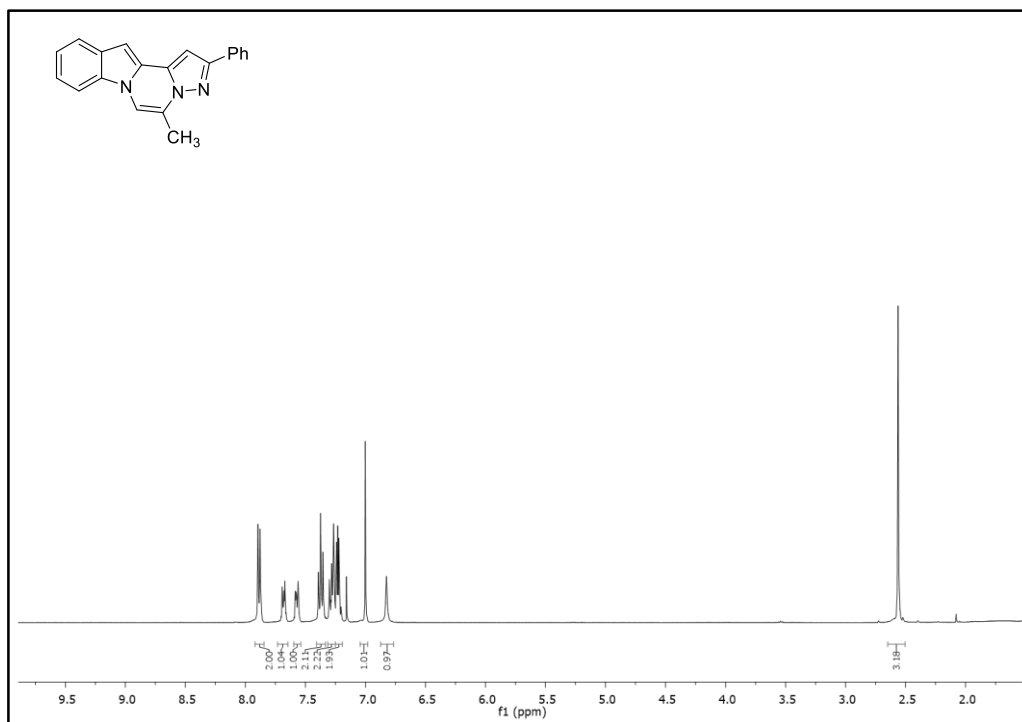


Figure 249. ¹H-NMR Spectrum of Compound 404a

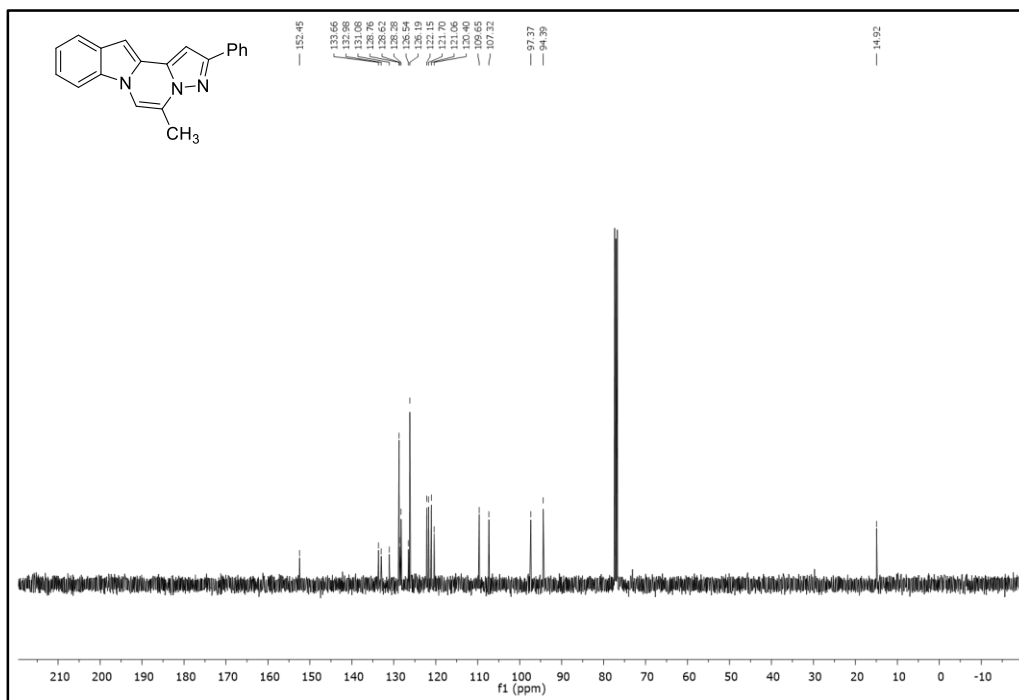


Figure 250. ^{13}C -NMR Spectrum of Compound 404a

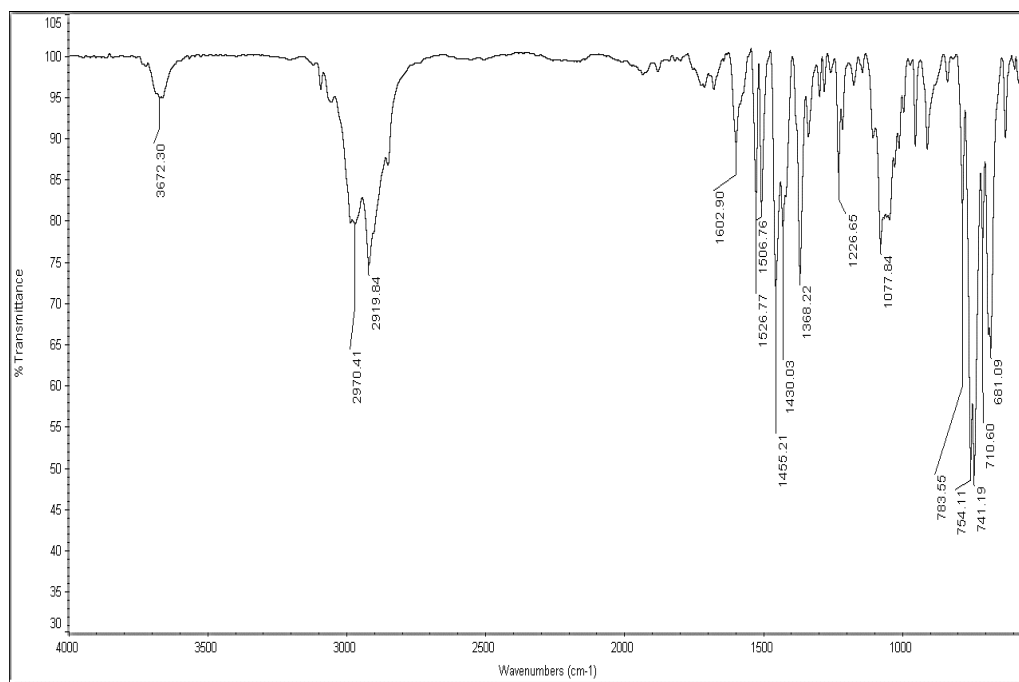


Figure 251. IR Spectrum of Compound 404a

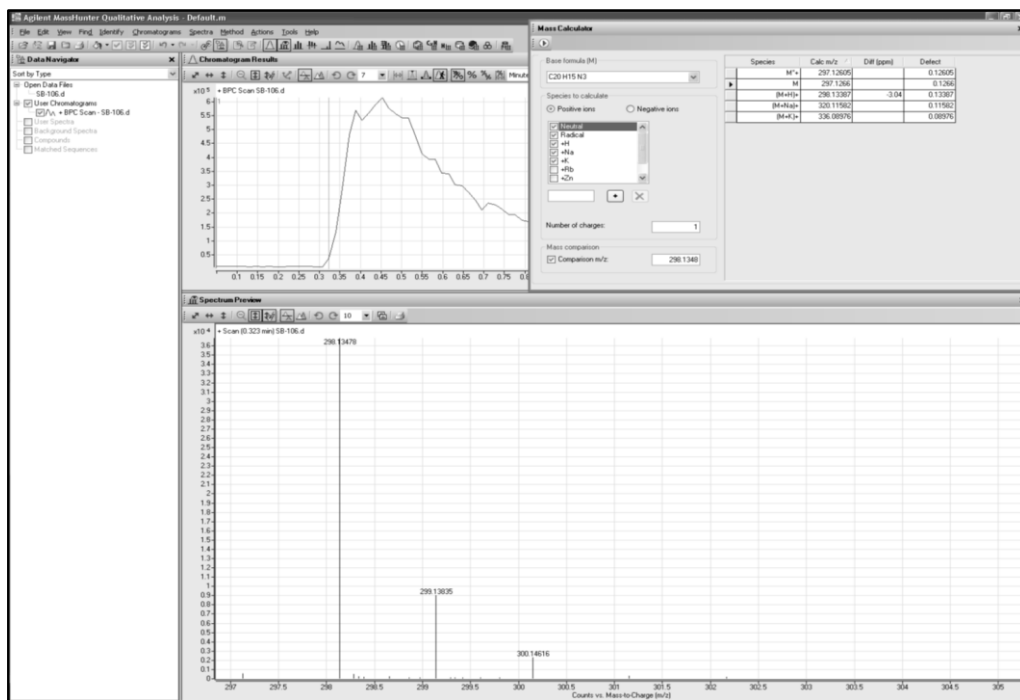


Figure 252. HRMS Spectrum of Compound **404a**

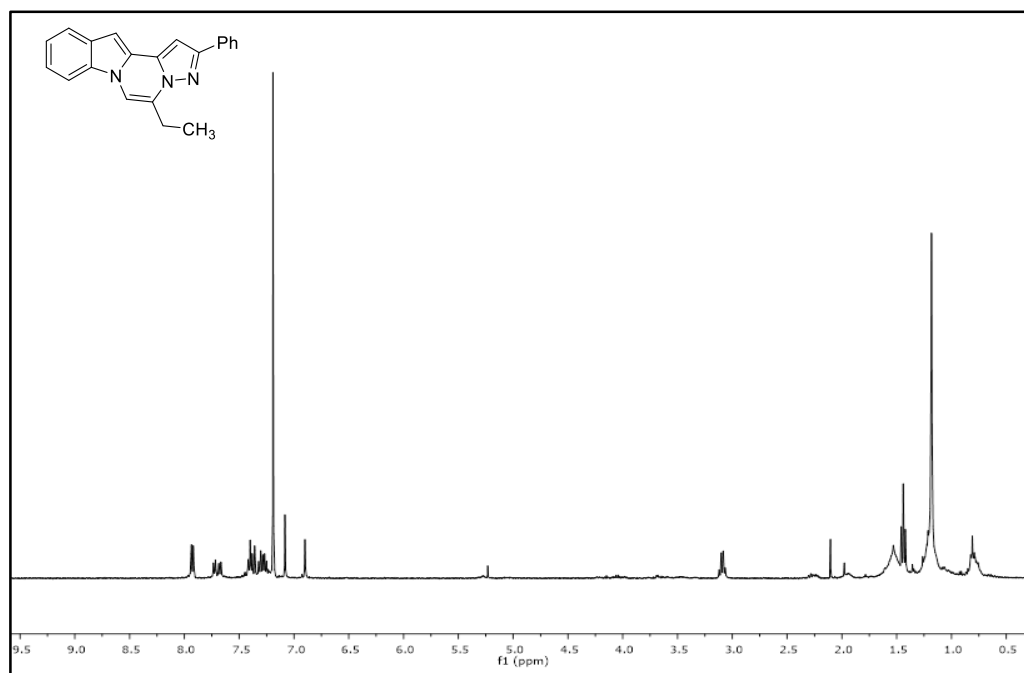


Figure 253. ¹H-NMR Spectrum of Compound **404b**

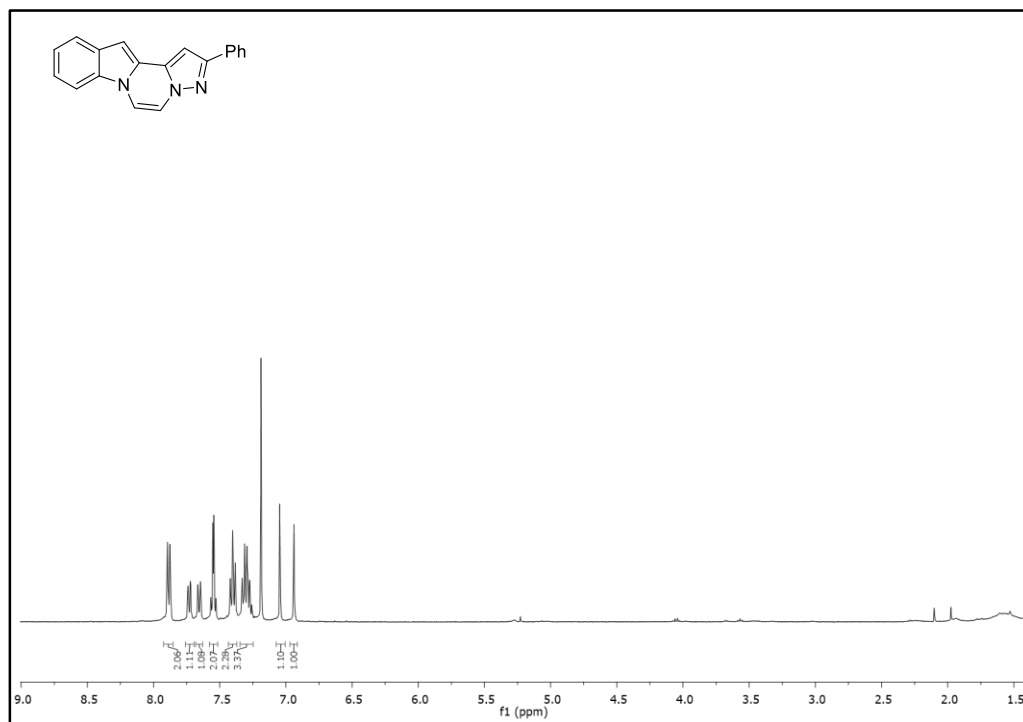


Figure 254. ¹H-NMR Spectrum of Compound 407

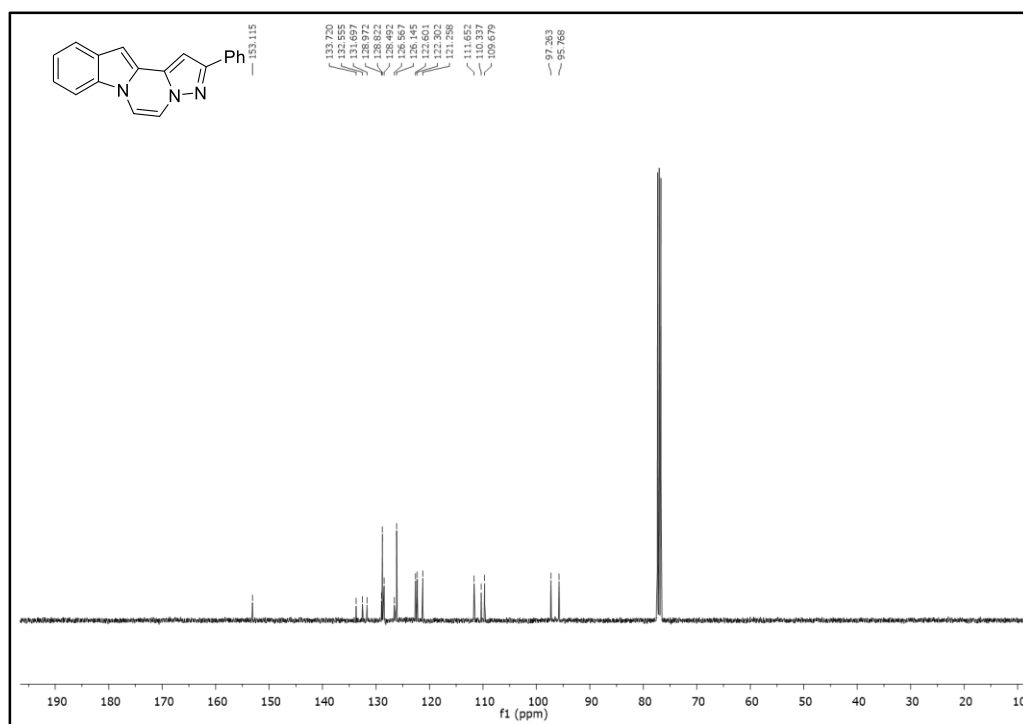


Figure 255. ¹³C-NMR Spectrum of Compound 407

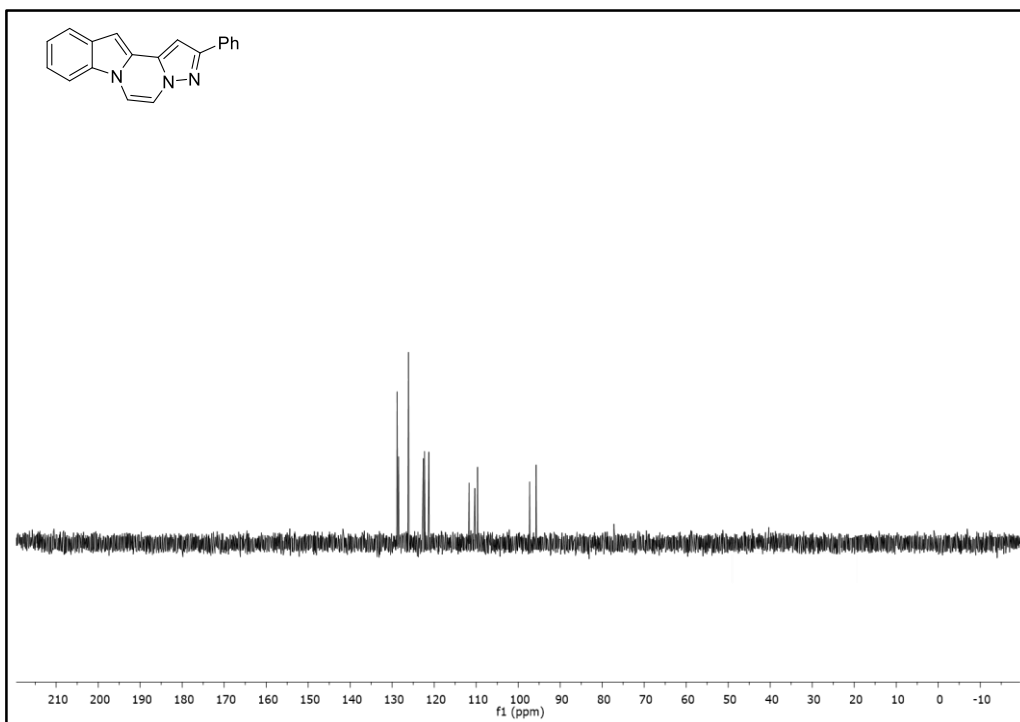


Figure 256. DEPT-135 Spectrum of Compound **407**

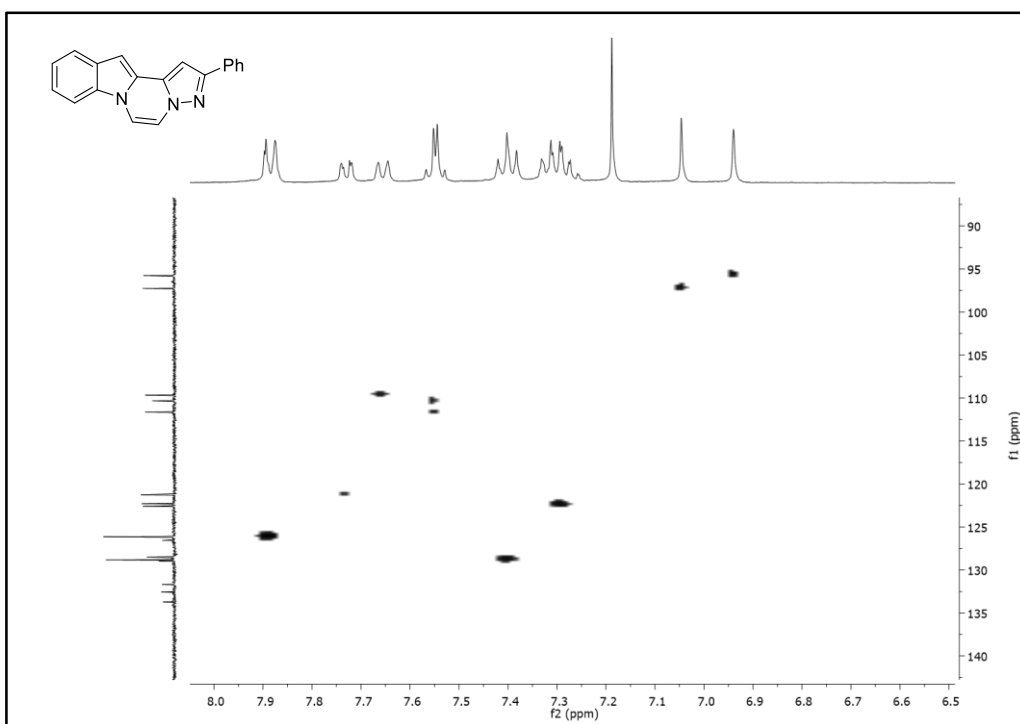


Figure 257. HSQC Spectrum of Compound **407**

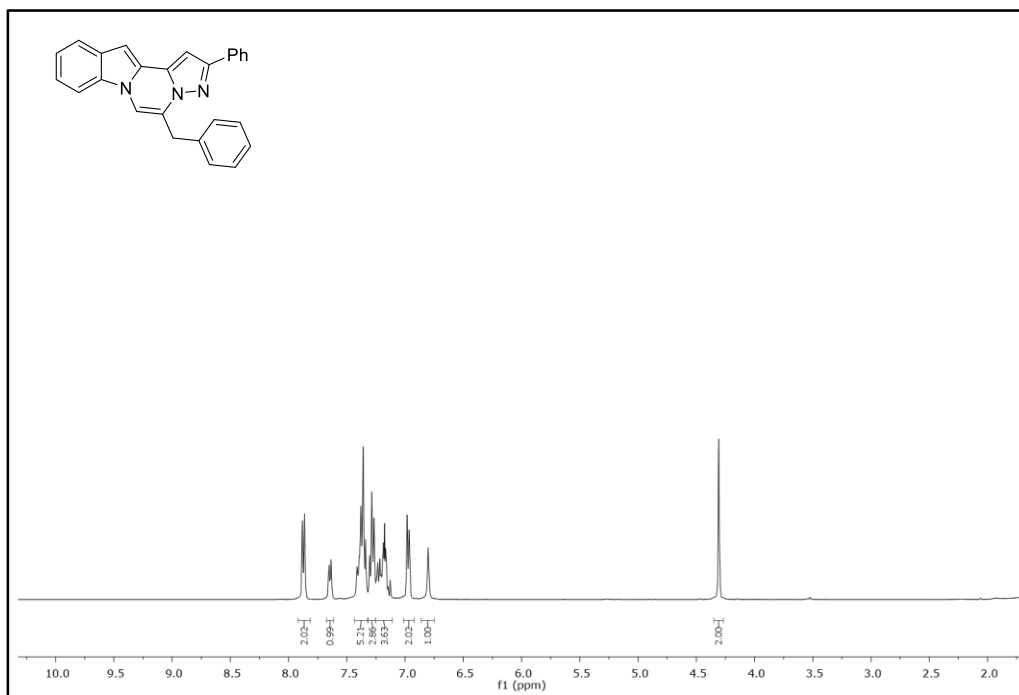


Figure 258. ¹H-NMR Spectrum of Compound **404c**

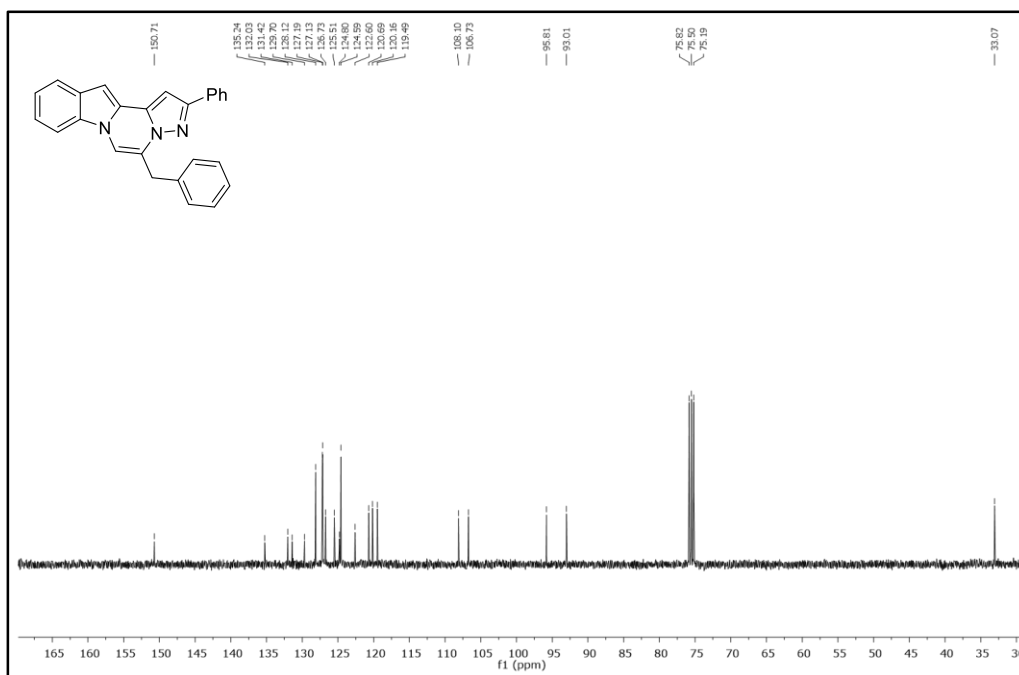


Figure 259. ¹³C-NMR Spectrum of Compound **404c**

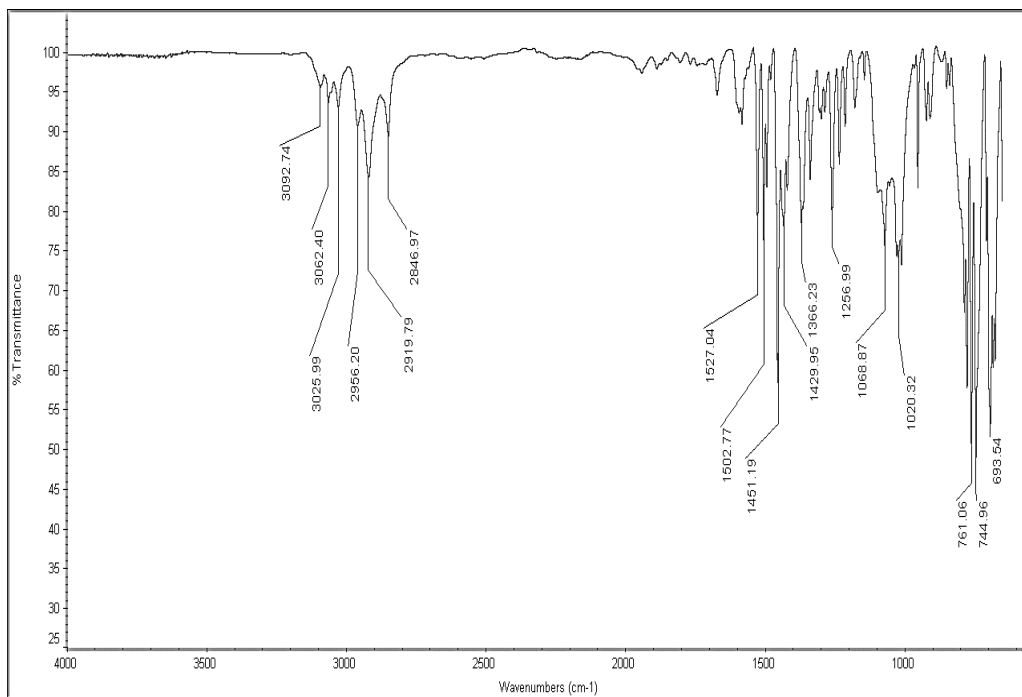


Figure 260. IR Spectrum of Compound 404c

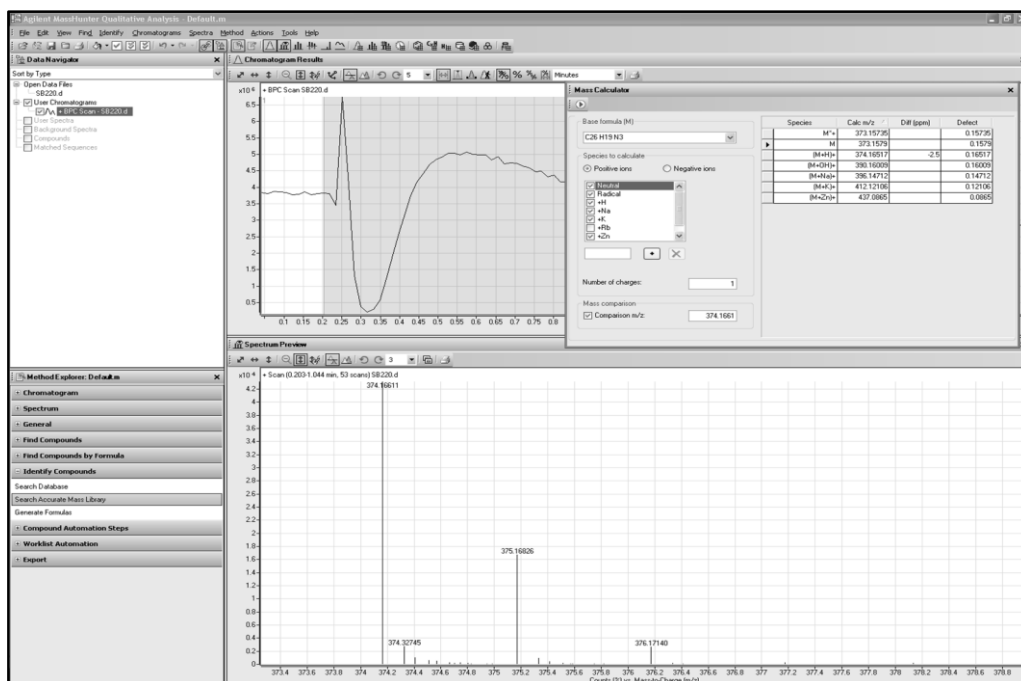


Figure 261. HRMS Spectrum of Compound 404c

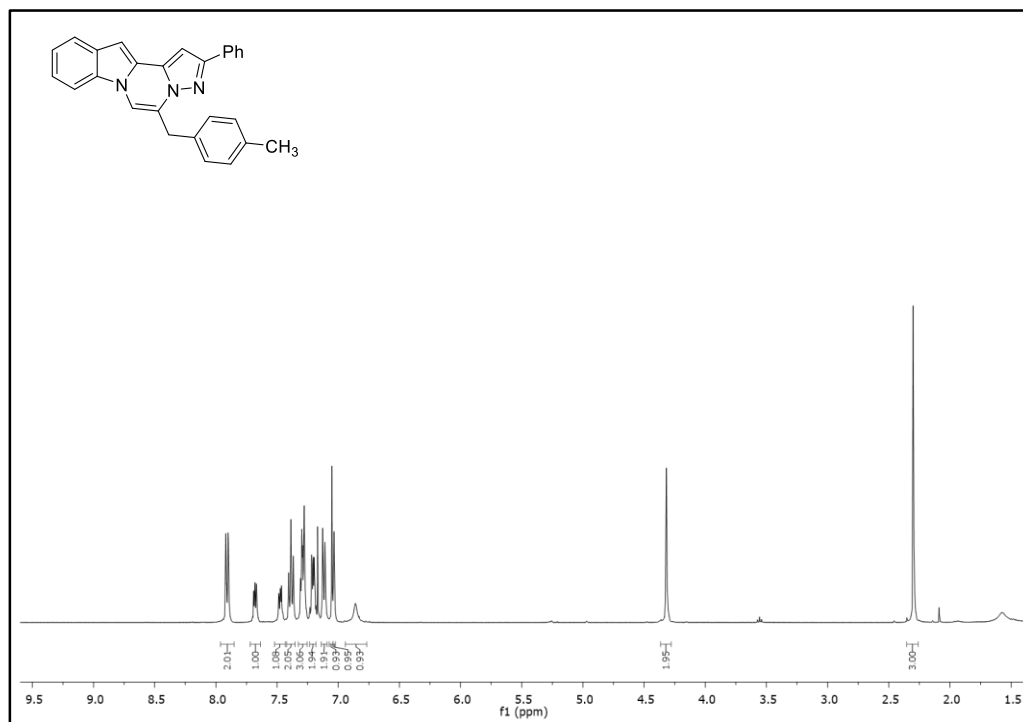


Figure 262. ¹H-NMR Spectrum of Compound 404d

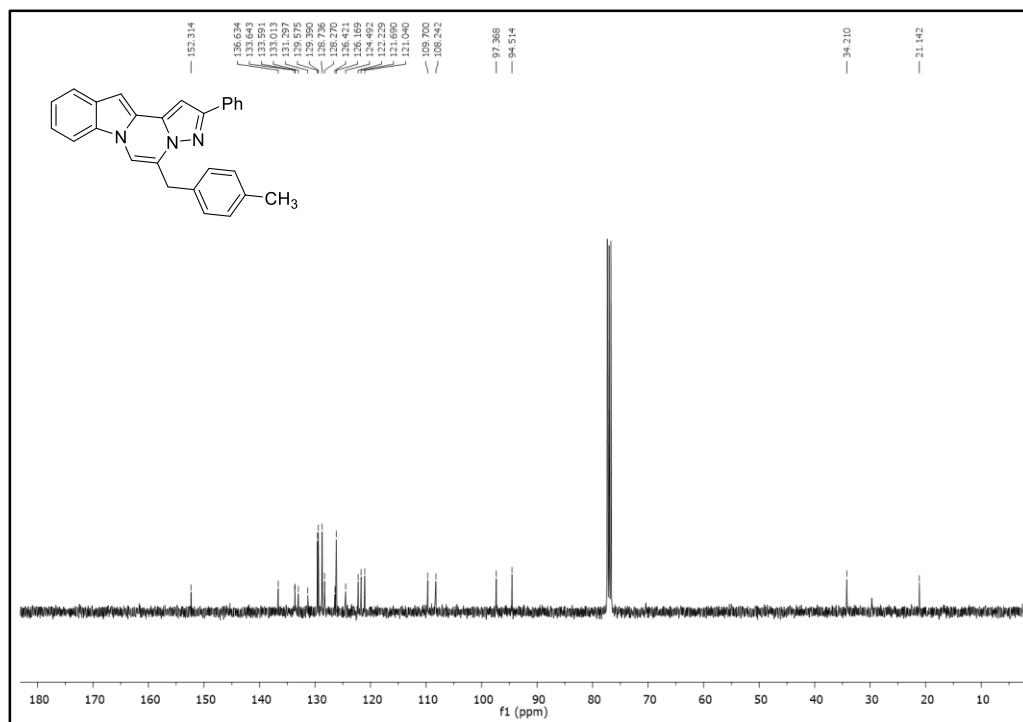


Figure 263. ¹³C-NMR Spectrum of Compound 404d

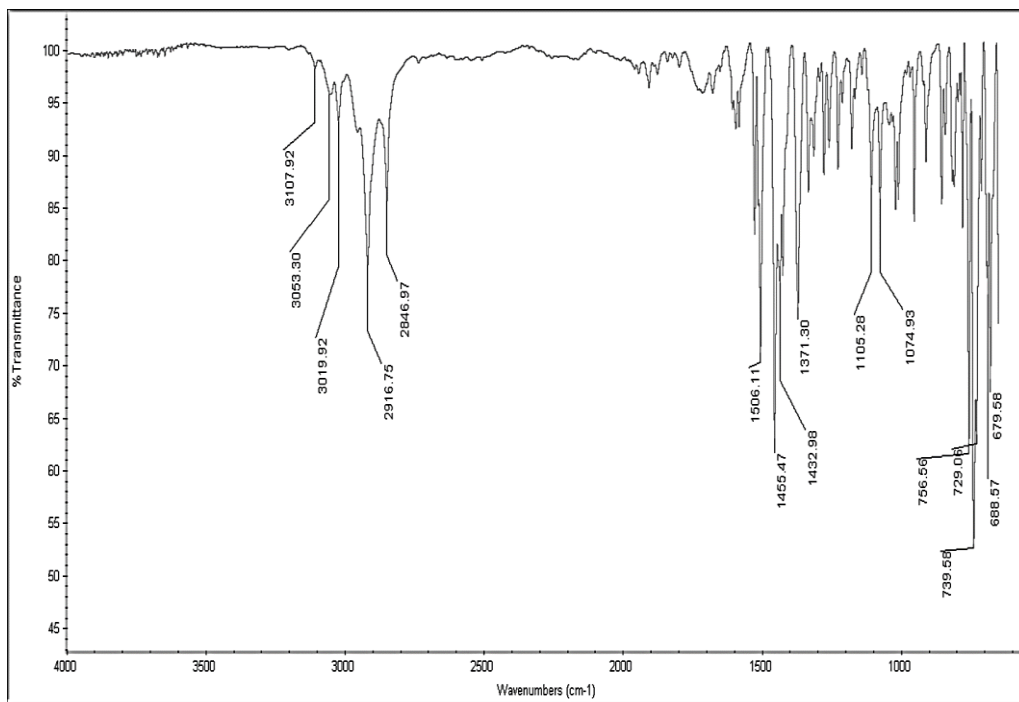


Figure 264. IR Spectrum of Compound 404d

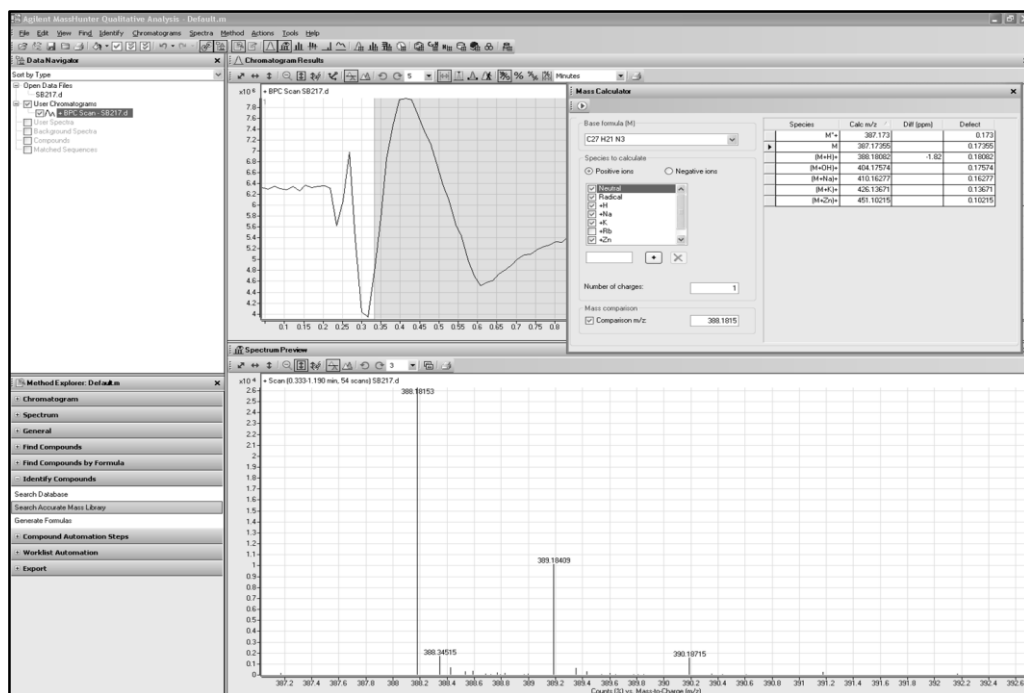
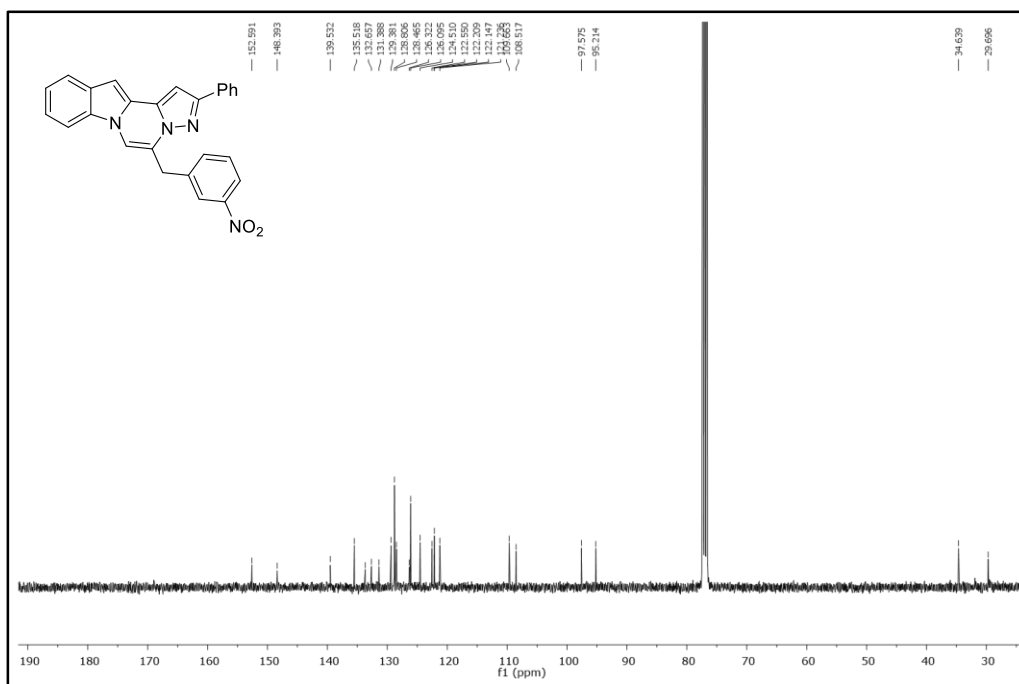
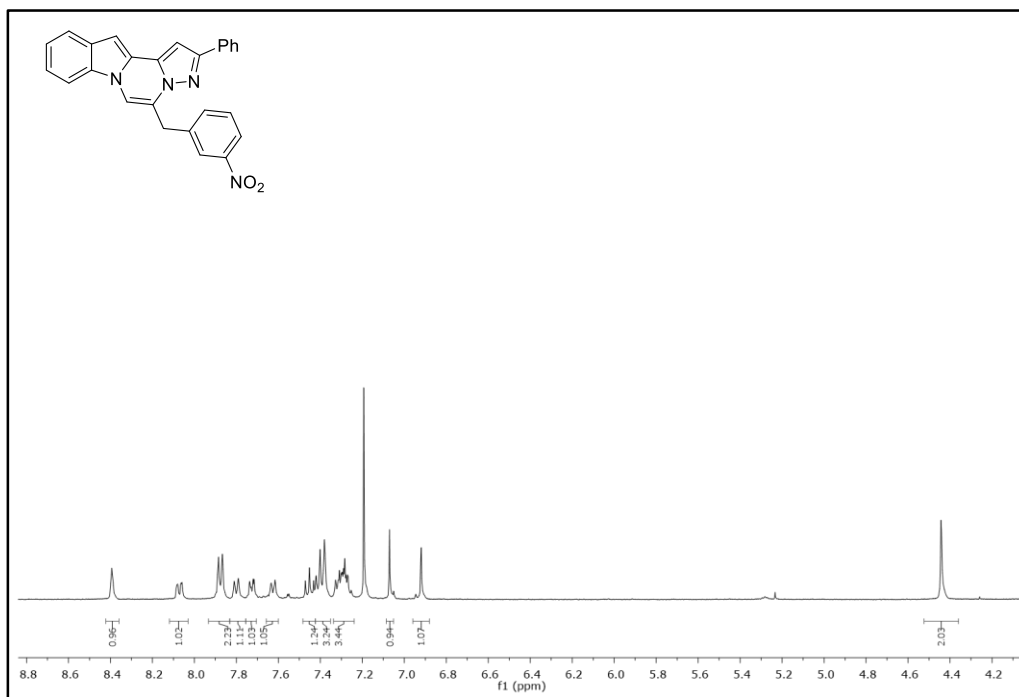


Figure 265. HRMS Spectrum of Compound 404d



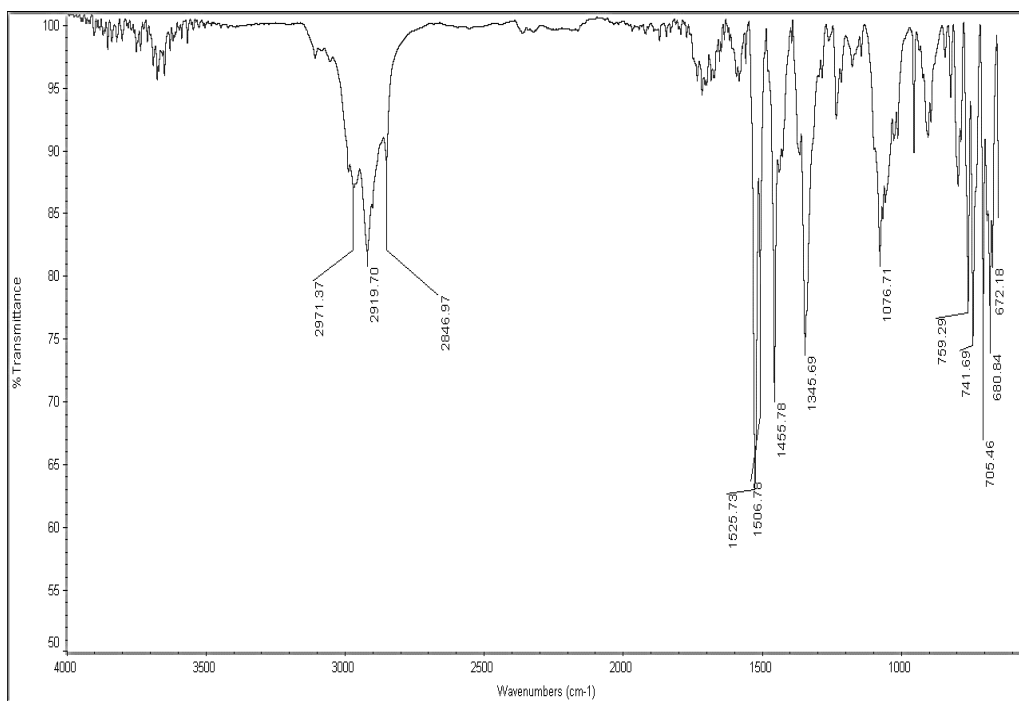


Figure 268. IR Spectrum of Compound **404e**

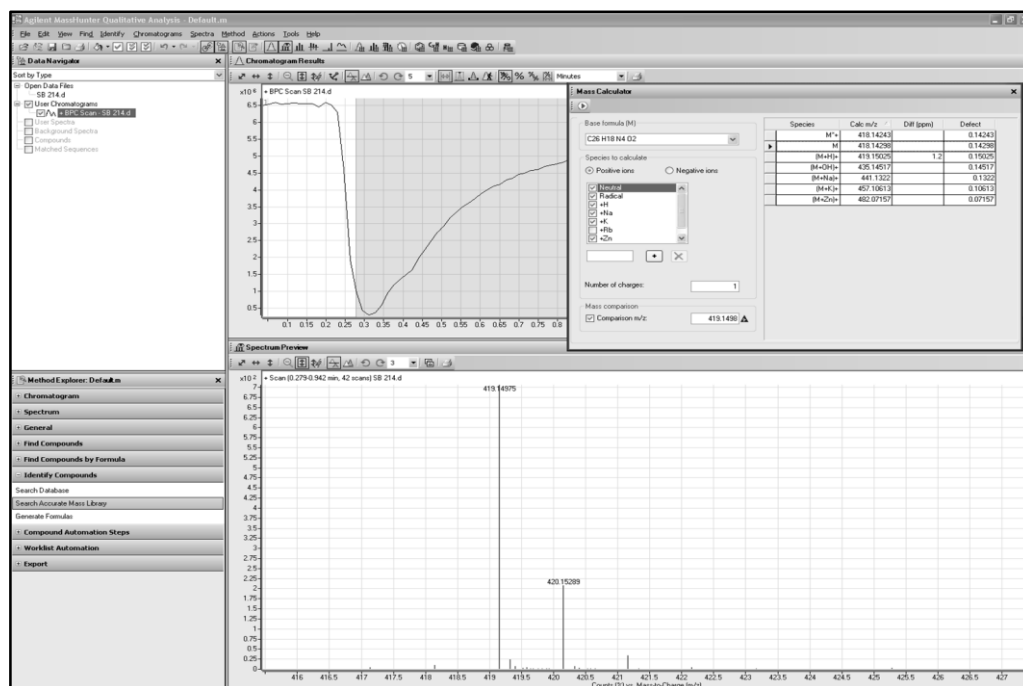


Figure 269. HRMS Spectrum of Compound **404e**

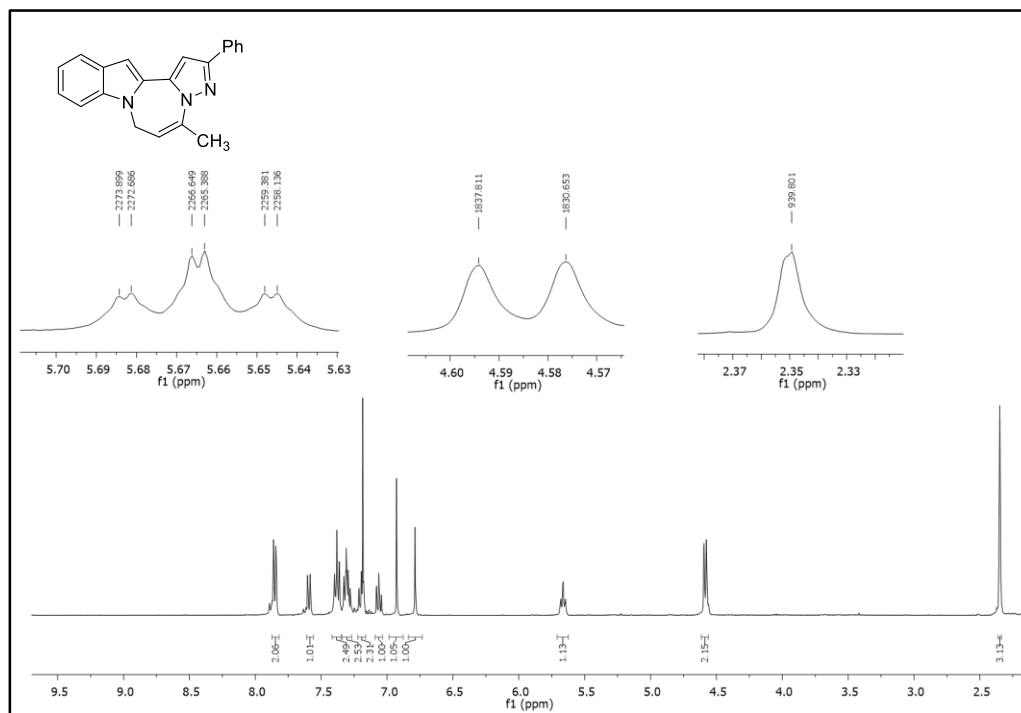


Figure 270. ¹H-NMR Spectrum of Compound **408b**

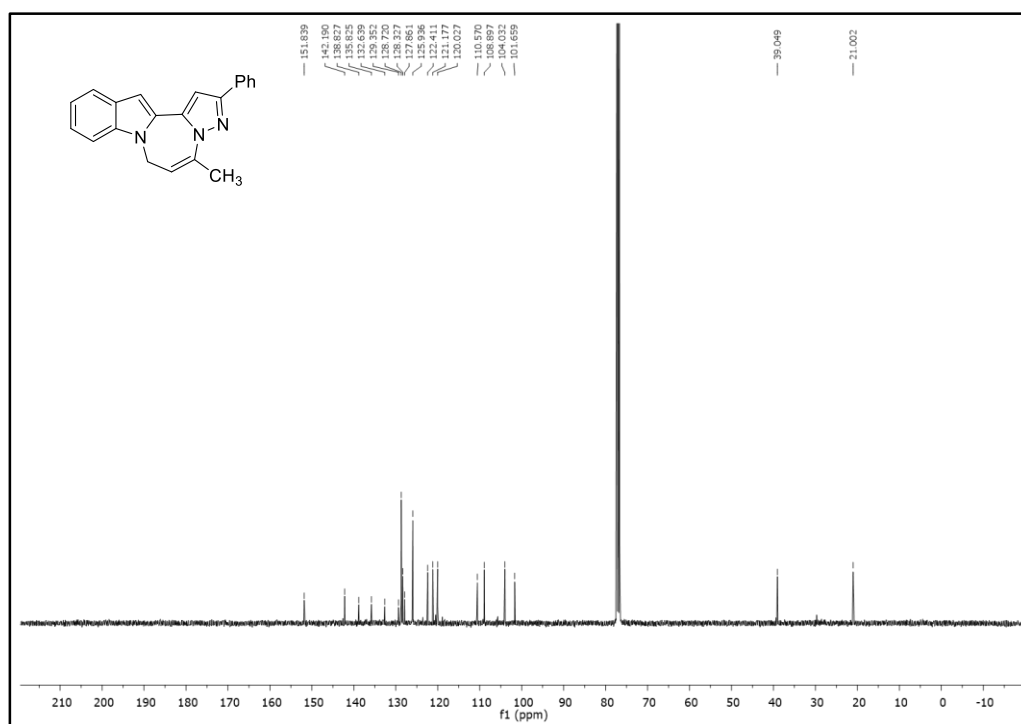


Figure 271. ¹³C-NMR Spectrum of Compound **408b**

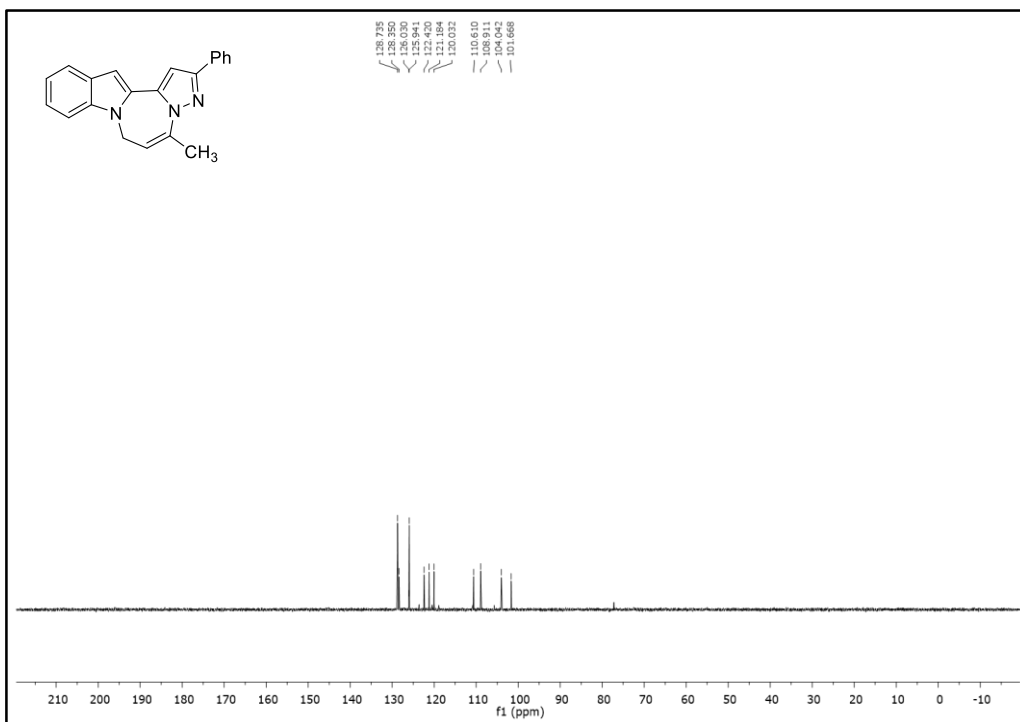


Figure 272. DEPT-90 Spectrum of Compound 408b

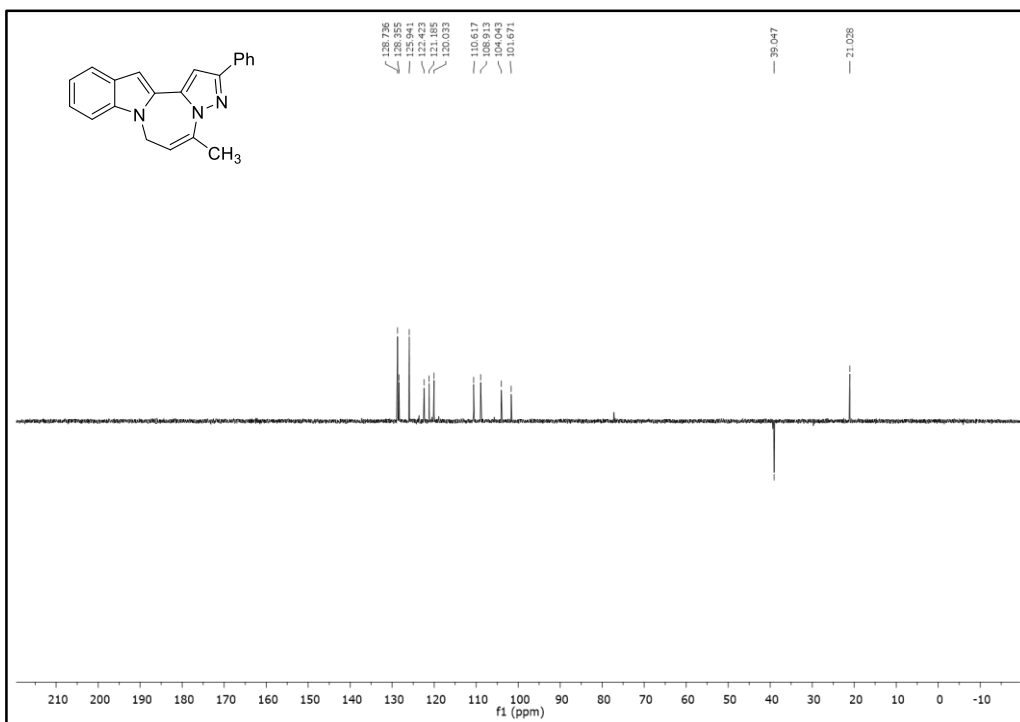


Figure 273. DEPT-135 Spectrum of Compound 408b

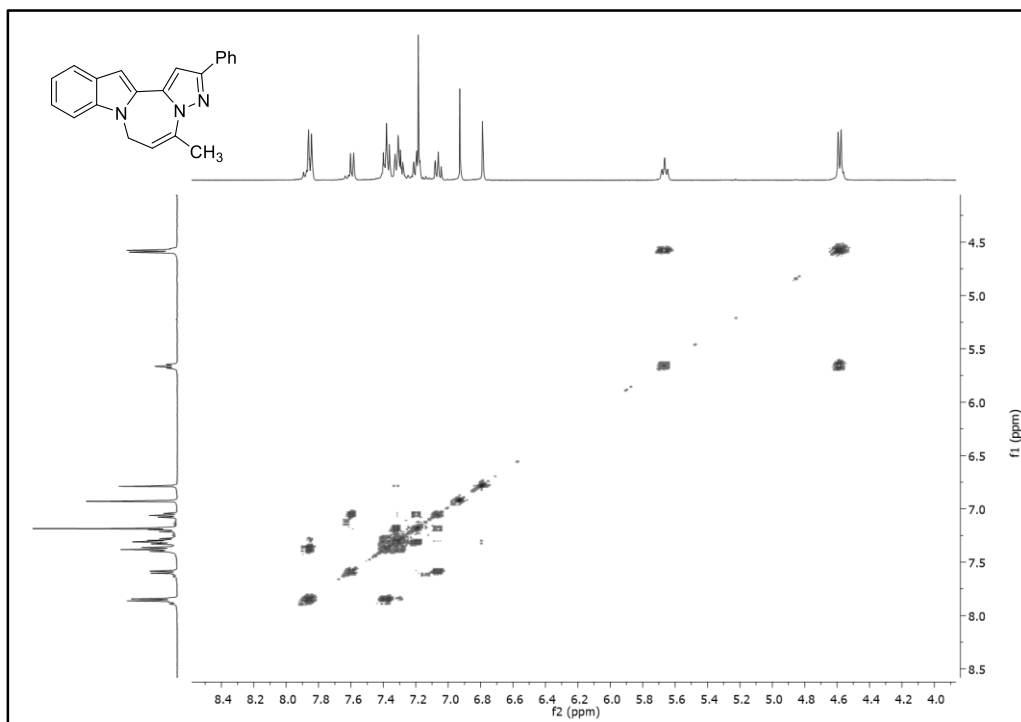


Figure 274. COSY Spectrum of Compound **408b**

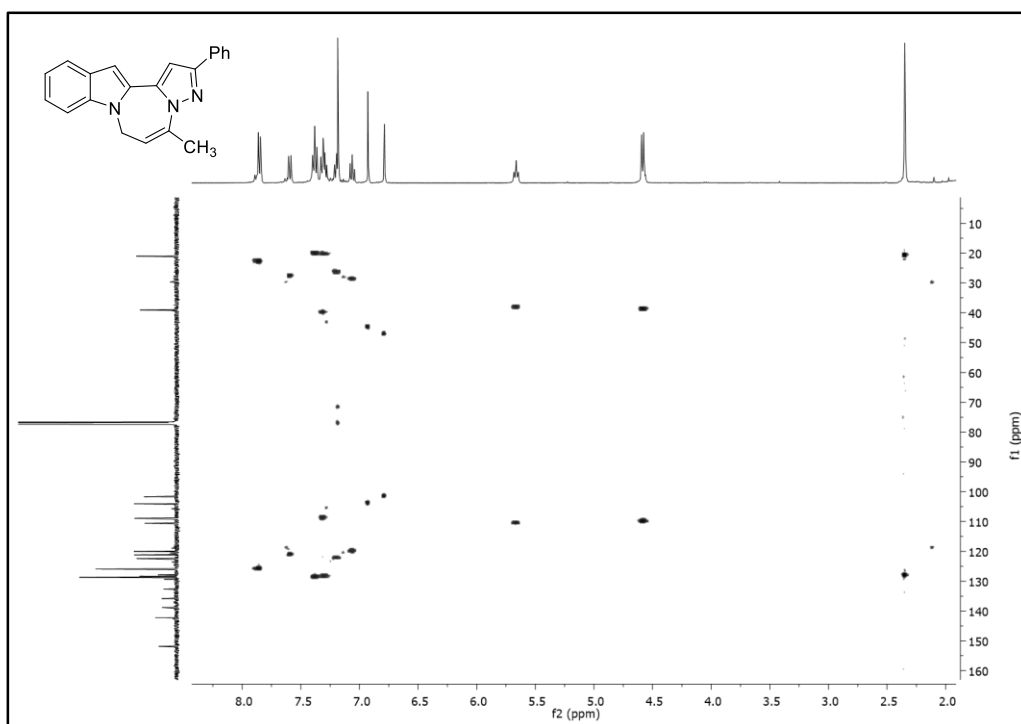


Figure 275. HSQC Spectrum of Compound **408b**

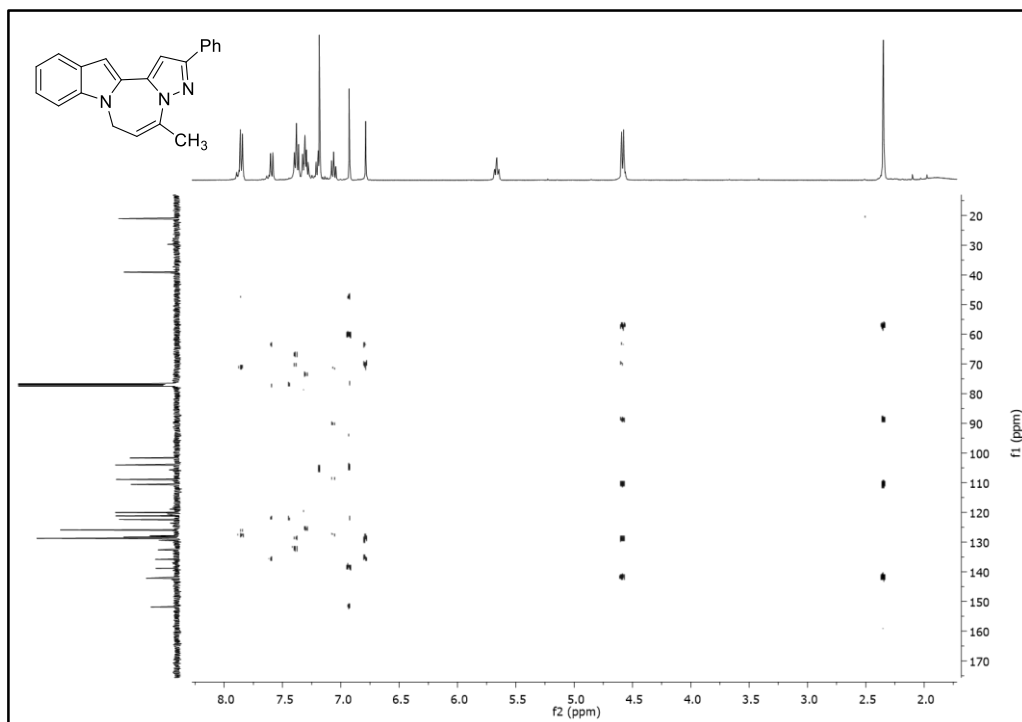


Figure 276. HMBC Spectrum of Compound **408b**

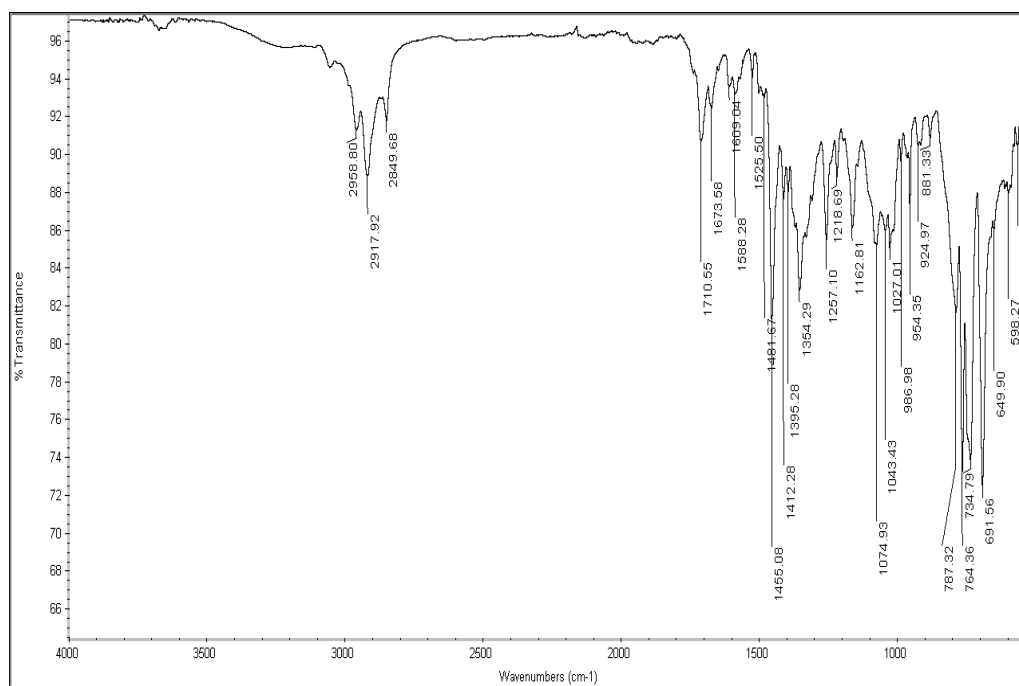


Figure 277. IR Spectrum of Compound **408b**

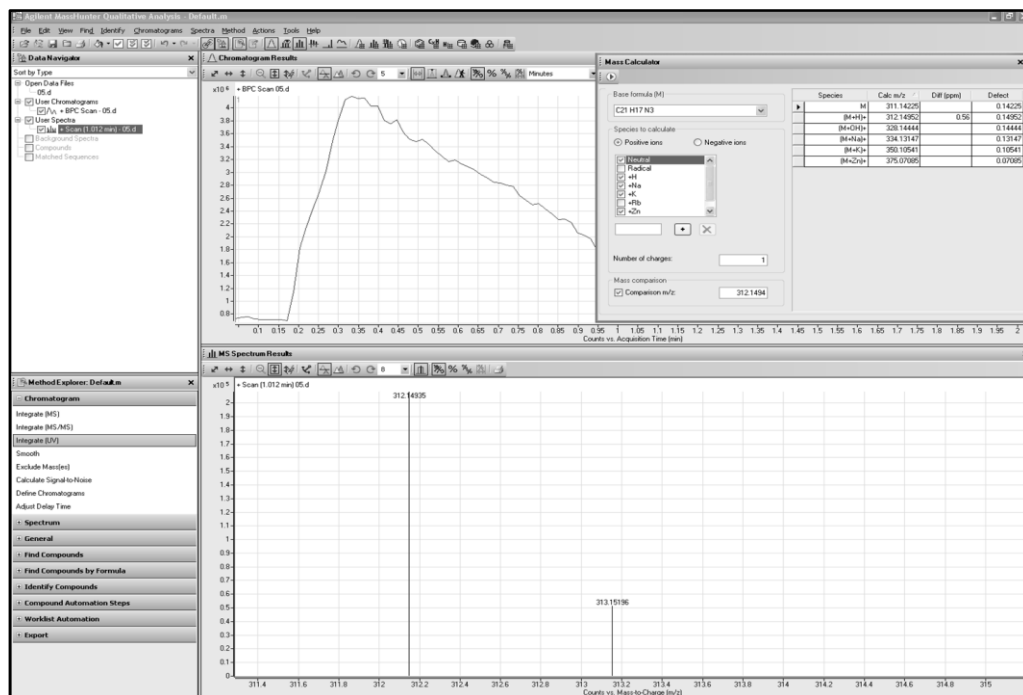


Figure 278. HMBC Spectrum of Compound 408b

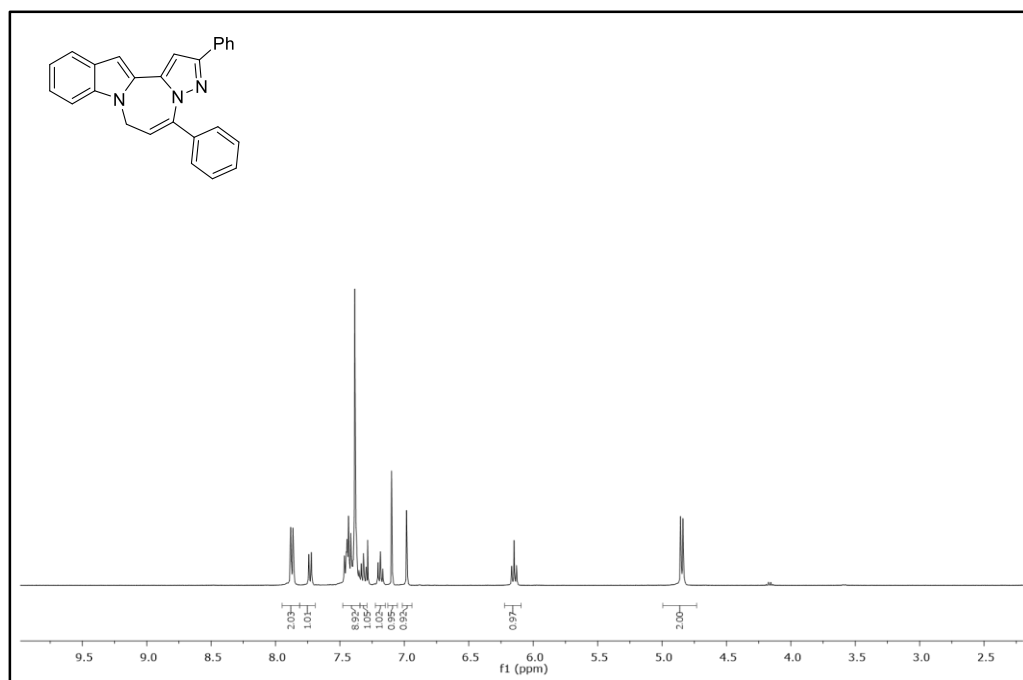


Figure 279. ¹H-NMR Spectrum of Compound 408c

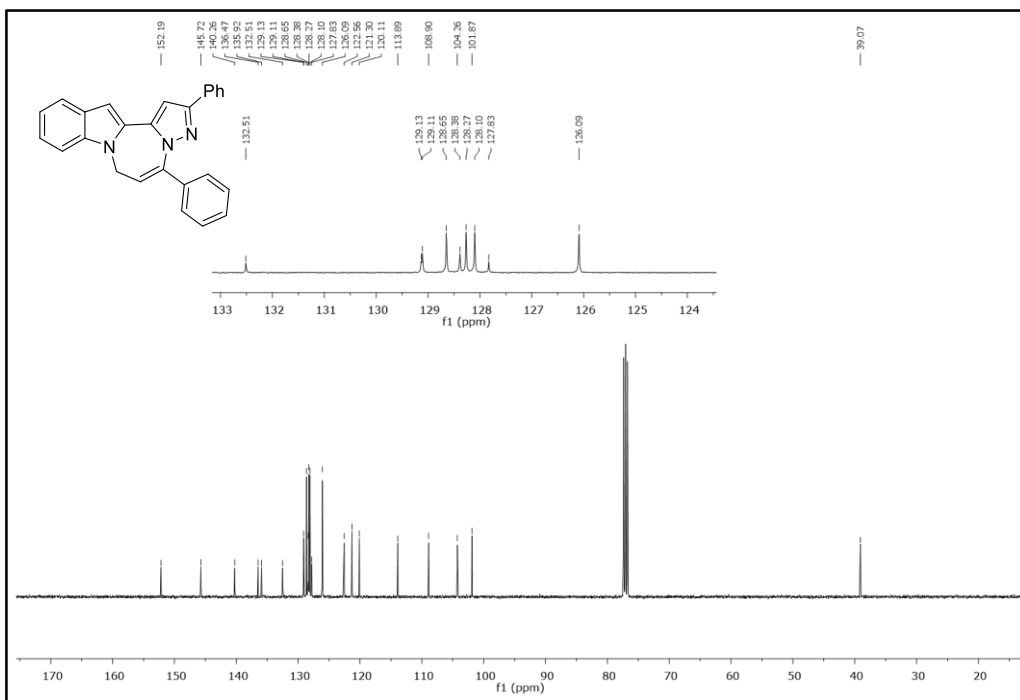


Figure 280. ¹³C-NMR Spectrum of Compound 408c

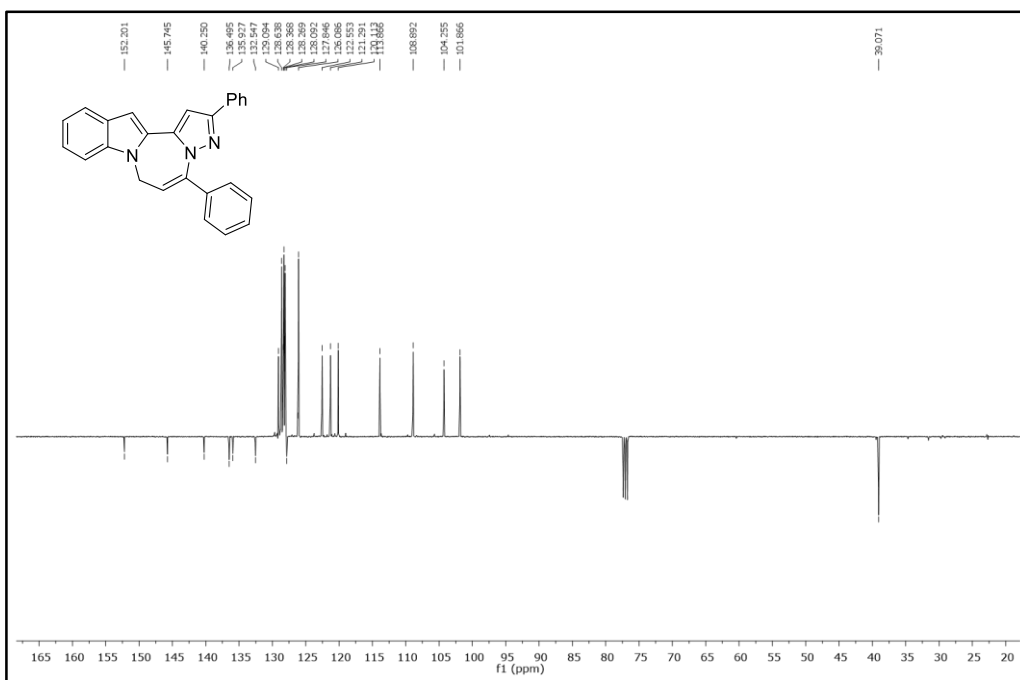


Figure 281. APT Spectrum of Compound 408c

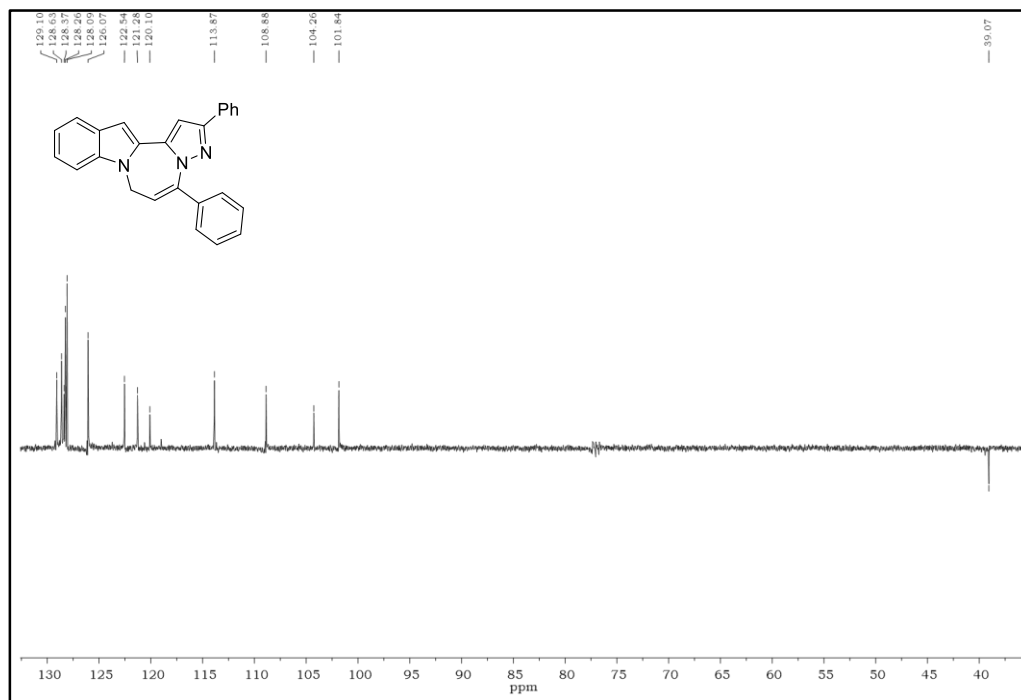


Figure 282. DEPT-135 Spectrum of Compound **408c**

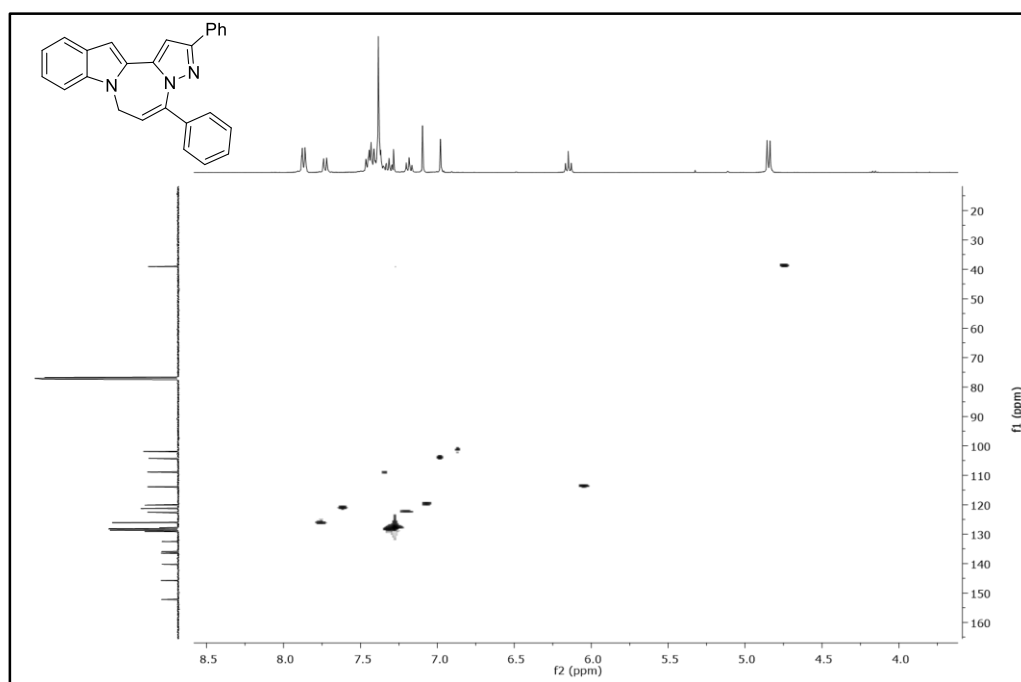


Figure 283. HSQC Spectrum of Compound **408c**

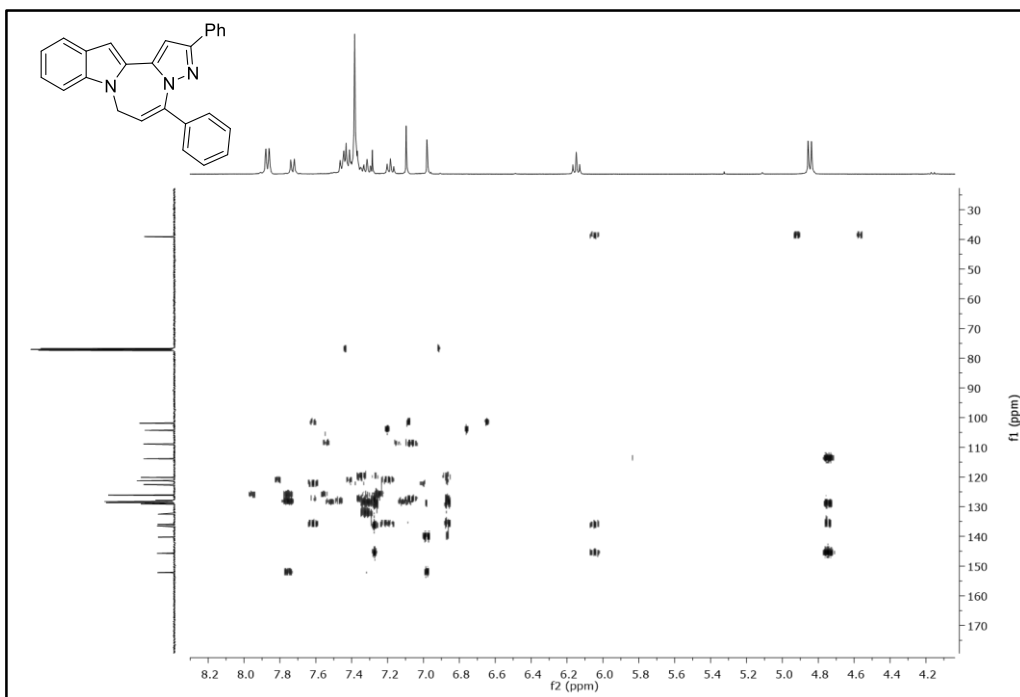


Figure 284. HMBC Spectrum of Compound **408c**

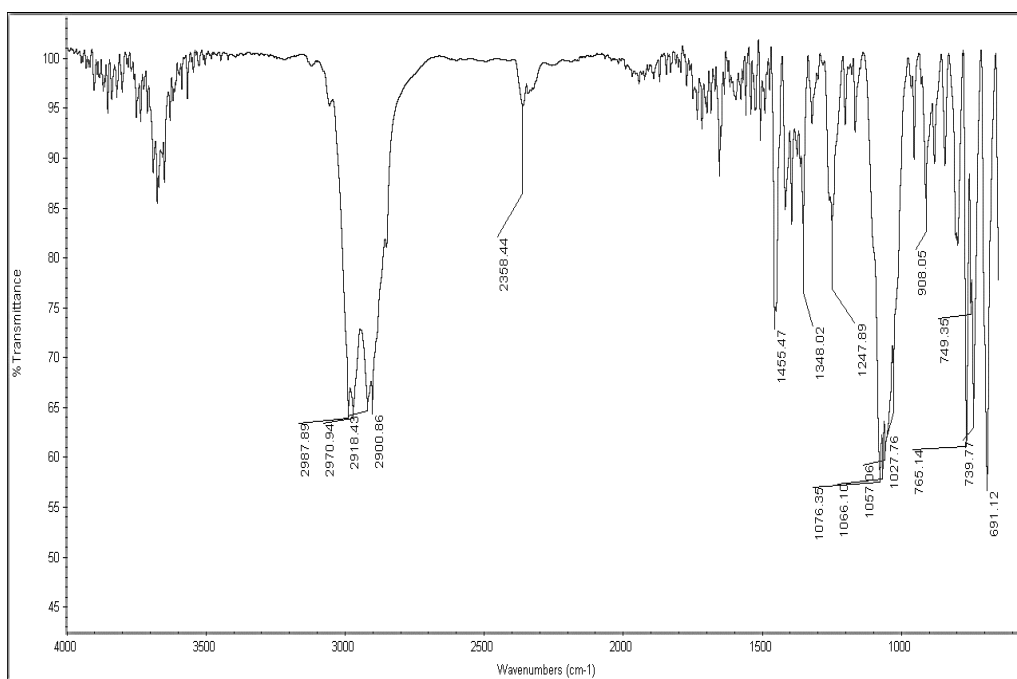


Figure 285. IR Spectrum of Compound **408c**

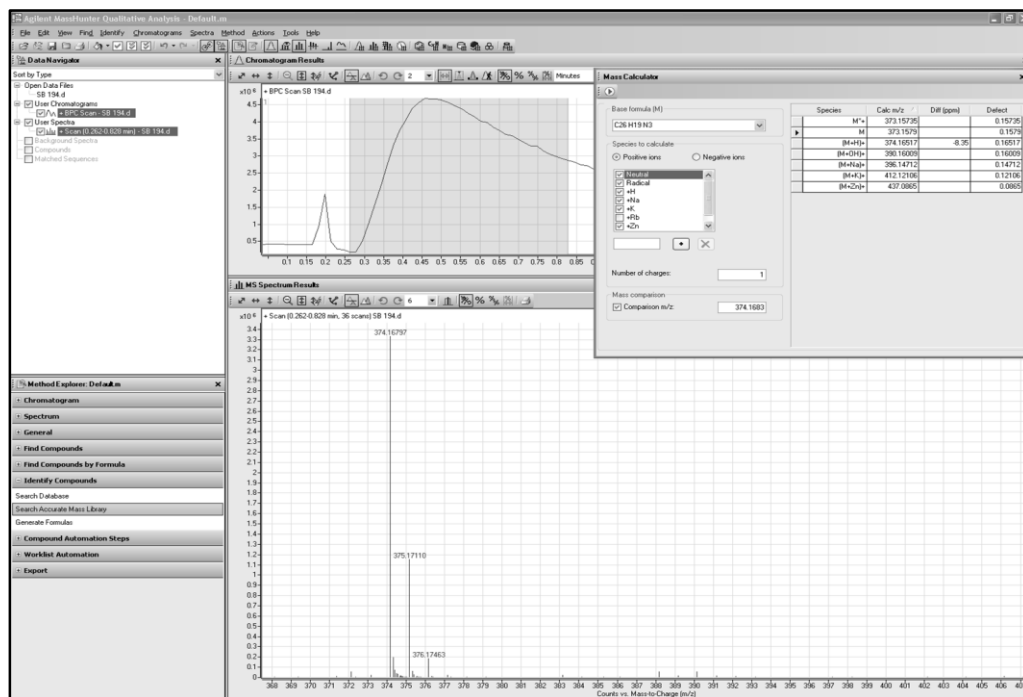


Figure 286. HRMS Spectrum of Compound 408c

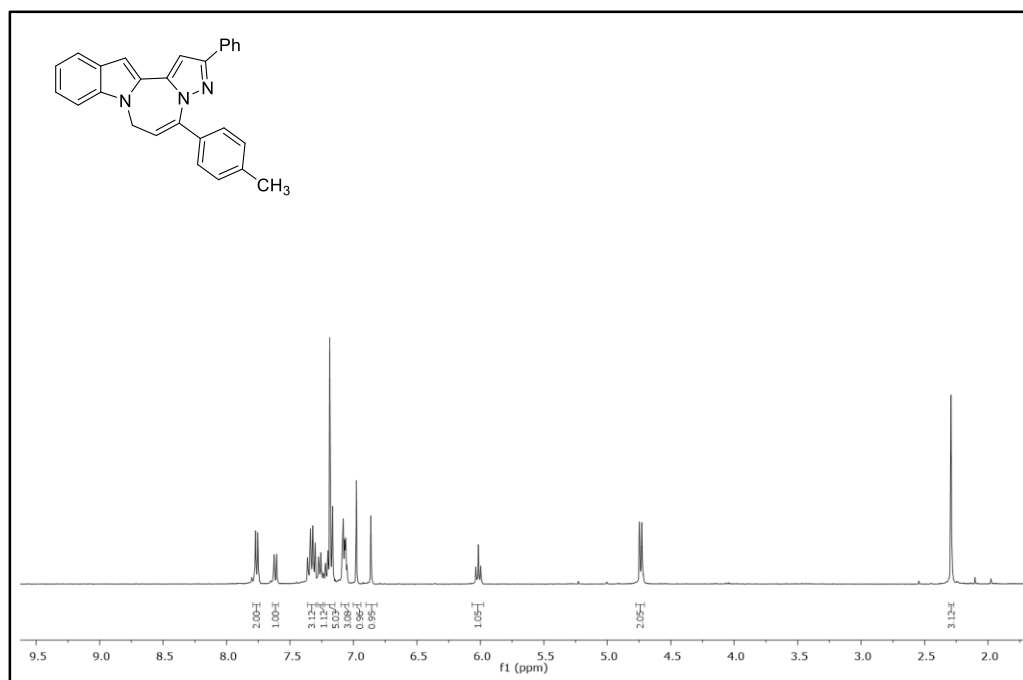


Figure 287. ¹H-NMR Spectrum of Compound 408d

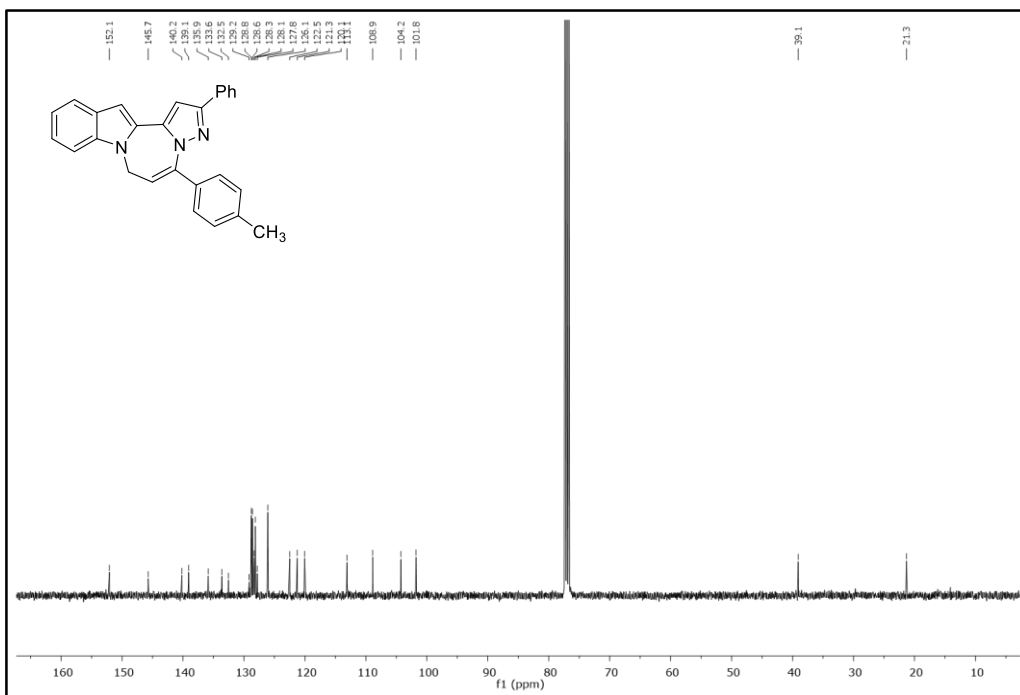


Figure 288. ¹³C-NMR Spectrum of Compound 408d

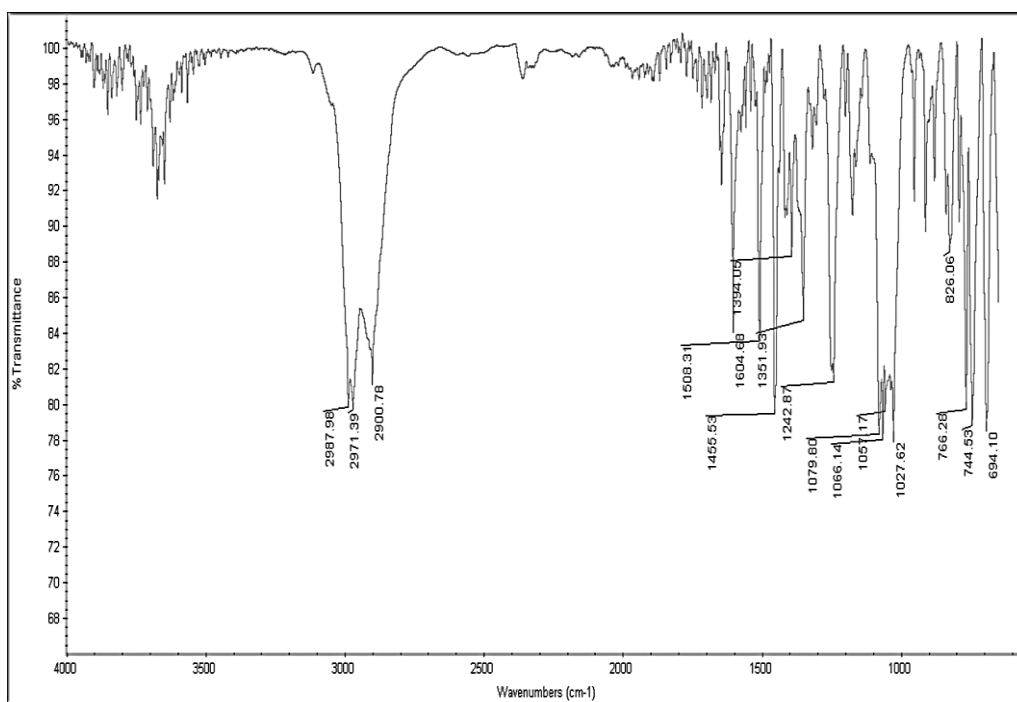


Figure 289. IR Spectrum of Compound 408d

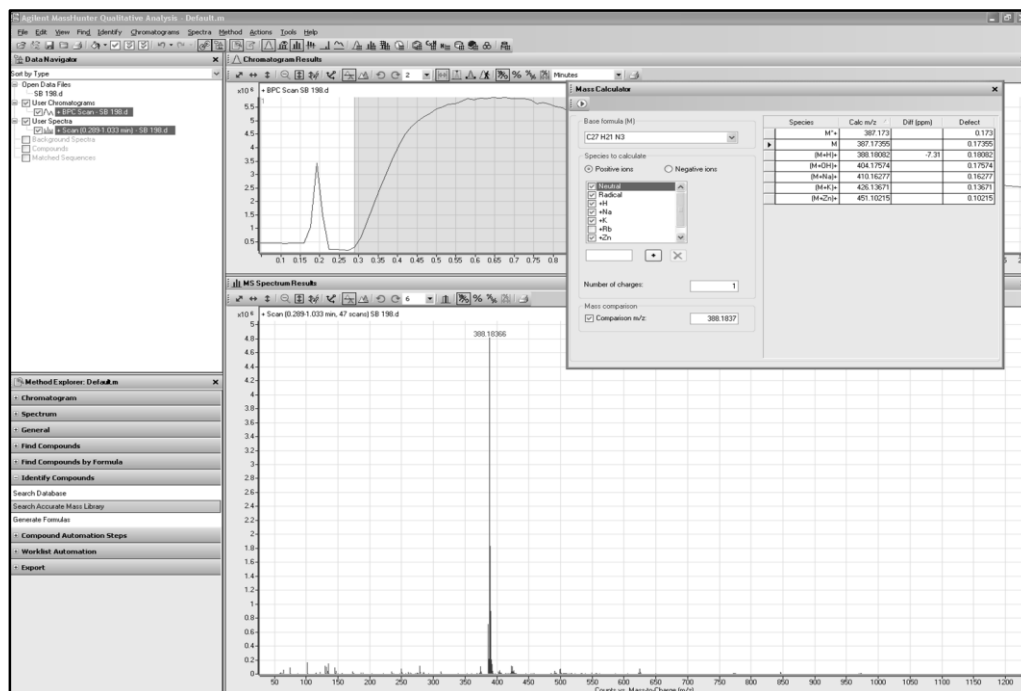


Figure 290. HRMS Spectrum of Compound 408d

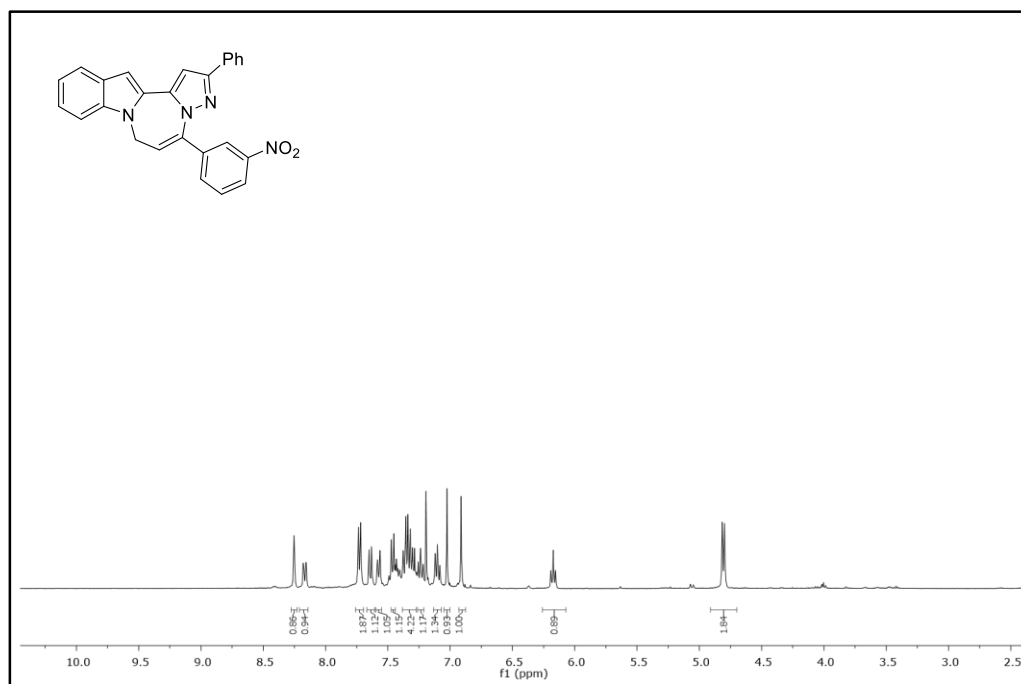


Figure 291. ¹H-NMR Spectrum of Compound 408e

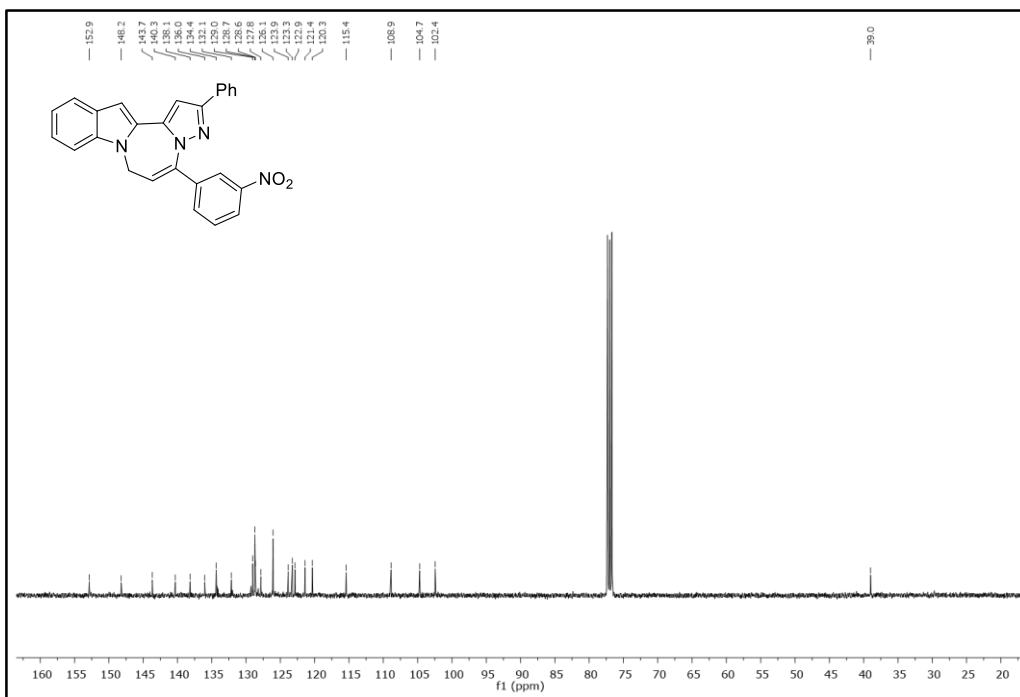


Figure 292. ¹³C-NMR Spectrum of Compound **408e**

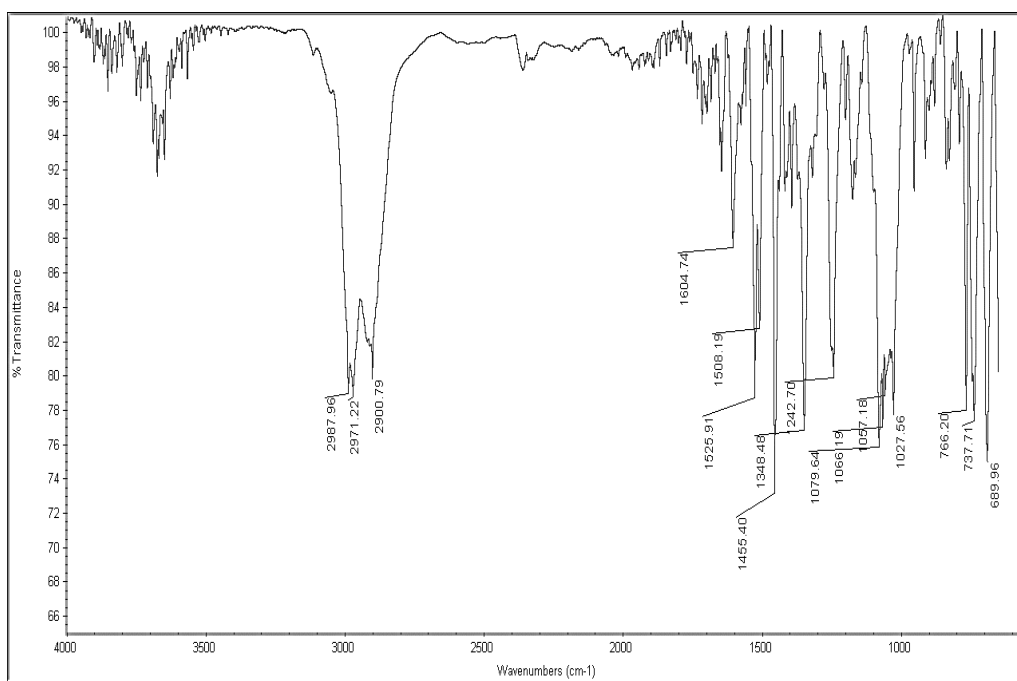


Figure 293. IR Spectrum of Compound **408e**

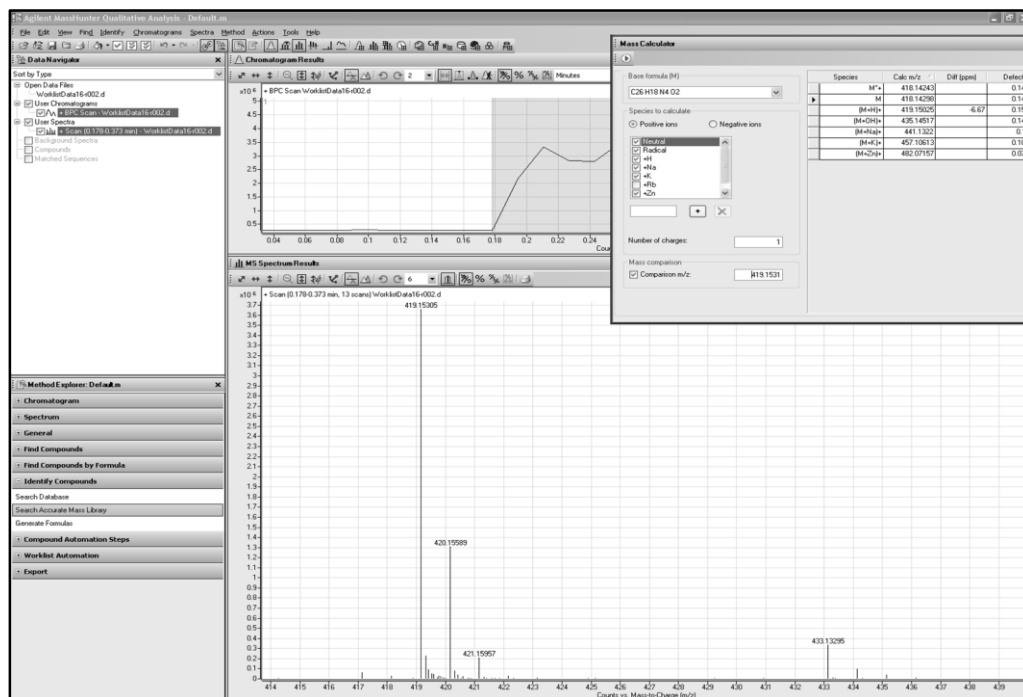


Figure 294. HRMS Spectrum of Compound 408e

APPENDIX B

CARTESIAN COORDINATES FOR THE OPTIMIZED STRUCTURES

Methodology

All of the calculations were performed with using Gaussian 09¹⁴⁸ program package. Geometry optimizations and frequency calculations of structure **1** and **2** were performed with using the B3LYP¹⁴⁹ (Becke-3-parameter-Lee-Yang-Parr) hybrid level within 6-31G(d,p) and LANL2DZ¹⁵⁰ (Au) mixed basis set coupled with DFT. Natural bond orbital (NBO)^{151,152} analysis was performed at the same level of theory to obtain the charge distribution of the structures.

Structure 207

		X	Y	Z

C	0	-0.583683	-0.626358	0.524881
C	0	-0.039371	0.850755	0.500115
C	0	1.460284	0.731709	0.152563
H	0	-0.754384	-0.953192	1.557619
H	0	-0.200432	1.344435	1.467468
H	0	1.739753	1.481075	-0.596730

H	0	2.089336	0.910532	1.034847
C	0	1.612796	-0.688235	-0.339931
C	0	0.514253	-1.423295	-0.135348
C	0	2.533697	-1.057218	-0.782416
C	0	0.394300	-2.474424	-0.380498
O	0	-0.666033	1.608536	-0.532010
H	0	-1.623189	1.545688	-0.397666
O	0	-1.863463	-0.755368	-0.100402
H	0	-1.728785	-0.689701	-1.057018

Structure 231

	X	Y	Z

C	1.210270	0.320126	-0.785454
C	1.617833	1.054383	0.530178
C	0.723190	0.515983	1.680083
C	-0.176258	-0.563190	1.090277
C	0.121382	-0.686112	-0.417423
H	0.877943	0.999608	-1.575613
H	1.551046	2.141720	0.443313
H	1.363564	0.089628	2.456854
H	0.135629	1.317535	2.139369
H	-0.414183	-1.431865	1.696514

H	0.131133	-1.633545	-0.946428
C	-1.190585	-0.171624	0.066773
Br	-2.696233	-1.378829	-0.109702
Br	-1.716448	1.683975	-0.172973
C	3.364900	-0.341117	-0.182306
O	2.999063	0.730301	0.695352
O	2.399488	-0.310950	-1.241360
C	3.329931	-1.687017	0.550710
H	3.605404	-2.493541	-0.135434
H	4.038099	-1.676466	1.384568
H	2.332586	-1.897474	0.943936
C	4.735839	-0.036106	-0.768109
H	5.484556	-0.002669	0.028246
H	5.019964	-0.810522	-1.486269
H	4.710670	0.930707	-1.275737

Structure 234

	X	Y	Z

C	1.053855	-0.068351	-1.454107
C	1.440838	1.211505	-0.708771
C	0.274844	2.156051	-0.457540

C	-0.889560	1.470573	0.275844
C	-1.189395	0.122547	-0.353902
C	-0.343026	-0.551746	-1.135650
H	0.599696	3.019369	0.131723
H	2.253013	1.729240	-1.237485
H	1.181825	0.025703	-2.538707
H	-0.068757	2.533667	-1.428865
Br	-2.912632	-0.591351	0.044343
H	-0.617347	-1.519031	-1.547207
O	1.931329	0.686801	0.539174
O	2.040924	-1.008815	-1.005971
C	2.537853	-0.594362	0.282545
C	4.054920	-0.459589	0.187541
H	4.469624	-0.158260	1.153851
H	4.497227	-1.416016	-0.105617
H	4.323062	0.289417	-0.562456
C	2.087950	-1.562134	1.370595
H	2.517511	-2.551411	1.190249
H	2.420723	-1.210320	2.352023
H	0.998659	-1.646809	1.370810
H	-1.781472	2.100533	0.210122
O	-0.631275	1.347571	1.674388
H	0.250868	0.949783	1.759506

Structure 235

	X	Y	Z

C	-1.155403	0.129632	1.352738
C	-1.458169	1.311805	0.425831
C	-0.242673	2.138224	0.043717
C	0.912757	1.305639	-0.519381
C	1.099492	0.032141	0.278837
C	0.201324	-0.491769	1.111959
H	-0.520294	2.905801	-0.684696
H	-2.220165	1.959613	0.883498
H	-1.270265	0.389391	2.411347
H	0.691833	1.017966	-1.558246
H	0.123977	2.657630	0.937168
Br	2.755027	-0.872540	-0.055574
H	0.391493	-1.434443	1.617341
O	2.058271	2.154794	-0.490915
H	2.817921	1.659128	-0.830423
O	-1.998703	0.658517	-0.727515
O	-2.200964	-0.798244	1.036771
C	-2.684124	-0.525059	-0.298285
C	-4.189084	-0.281078	-0.214796

H	-4.593516	-0.077718	-1.210699
H	-4.690949	-1.160322	0.199432
H	-4.398391	0.574072	0.433665
C	-2.311852	-1.661464	-1.243029
H	-2.791554	-2.590114	-0.921129
H	-2.640032	-1.428928	-2.260541
H	-1.228432	-1.802160	-1.243912

Structure 236

		X	Y	Z

C	0	-1.012294	0.350341	1.208845
C	0	-1.544232	1.441033	0.237183
C	0	-0.456018	2.360030	-0.332228
C	0	0.769254	1.577432	-0.737574
C	0	1.202978	0.586524	0.043849
H	0	-0.870549	2.902553	-1.186953
H	0	-2.321694	2.044762	0.724406
H	0	-1.463606	0.439690	2.205153
H	0	-0.203918	3.116671	0.426659
Br	0	2.723599	-0.452703	-0.418740
O	0	-2.115230	0.695883	-0.841233
O	0	-1.403944	-0.887837	0.613264

C	0	-2.395182	-0.627055	-0.391042
C	0	-3.796770	-0.711630	0.221492
H	0	-4.551707	-0.474975	-0.533868
H	0	-3.981088	-1.719229	0.605049
H	0	-3.904348	-0.004340	1.049578
C	0	-2.187127	-1.590204	-1.547587
H	0	-2.334778	-2.620271	-1.211489
H	0	-2.902005	-1.375785	-2.346656
H	0	-1.172157	-1.479767	-1.935118
H	0	1.265890	1.810639	-1.673666
C	0	0.524535	0.316166	1.380878
O	0	0.913432	-0.873105	2.030032
H	0	0.520503	-1.614939	1.544482
H	0	0.808572	1.124249	2.068921

Structure 237

	X	Y	Z

C	0.983599	0.860906	-0.806243
C	1.481085	1.209933	0.628183
C	0.374973	1.528699	1.641213
C	-0.827837	0.633615	1.471855
C	-1.229550	0.288556	0.248434

H	0.791588	1.424790	2.647630
H	2.193075	2.044580	0.590495
H	1.374297	1.574253	-1.542701
H	0.077320	2.578722	1.521305
Br	-2.760440	-0.816063	-0.034827
O	2.152584	0.021064	1.056356
O	1.489512	-0.448187	-1.054374
C	2.515588	-0.733720	-0.098087
C	3.881523	-0.290470	-0.633696
H	4.657512	-0.473227	0.115409
H	4.127857	-0.845628	-1.543443
H	3.879330	0.777014	-0.874366
C	2.461193	-2.211935	0.248895
H	2.670937	-2.814821	-0.638910
H	3.203681	-2.445304	1.016973
H	1.465794	-2.459751	0.623530
H	-1.352094	0.277244	2.353457
C	-0.542740	0.816796	-0.987469
H	-0.755449	0.177004	-1.850526
O	-0.942180	2.170040	-1.266857
H	-1.904768	2.189716	-1.359422

Structure *cis*-238

	X	Y	Z

C	-0.766965	0.735980	-0.382273
C	-0.686013	-0.765018	-0.181176
C	0.454401	-1.453671	-0.272059
C	1.758726	-0.802449	-0.633155
C	1.693788	0.709600	-0.901775
C	0.585911	1.392316	-0.094748
Br	-2.330830	-1.652748	0.175180
O	2.687721	-0.886193	0.453346
C	3.662166	0.141012	0.247204
O	2.981503	1.174327	-0.506400
C	4.078595	0.684113	1.605791
C	4.843903	-0.370713	-0.577311
O	-1.704746	1.325186	0.551772
N	-2.992876	1.667022	0.024868
O	-3.755997	2.004305	0.893139
O	-3.160035	1.607500	-1.175267
H	-1.116589	0.959878	-1.394339
H	0.463579	-2.529582	-0.130120
H	2.174593	-1.321863	-1.511253

H	1.565554	0.916280	-1.971493
H	0.540860	2.457619	-0.337795
H	0.804587	1.295776	0.972631
H	4.777447	1.515225	1.477283
H	4.566858	-0.099982	2.191532
H	3.200802	1.038305	2.150820
H	5.380782	-1.148526	-0.026368
H	4.503650	-0.785778	-1.530087
H	5.532436	0.451631	-0.791866

Structure *trans*-238

	X	Y	Z

C	-0.637257	0.796886	-0.229204
C	-0.481885	-0.696004	-0.405044
C	0.630757	-1.267959	-0.869638
C	1.858256	-0.487943	-1.281916
C	1.759149	1.016834	-1.005099
C	0.351313	1.582700	-1.095959
Br	-1.984158	-1.745787	0.117143
O	2.998842	-0.881017	-0.508622
C	3.228749	0.094704	0.533227

O	2.233499	1.110294	0.338563
C	3.012845	-0.530014	1.904804
C	4.632435	0.666998	0.348407
O	-1.959070	1.221861	-0.653644
N	-2.879246	1.570431	0.385892
O	-3.981600	1.788844	-0.049204
O	-2.470217	1.627070	1.526220
H	-0.517861	1.056486	0.824807
H	0.708394	-2.348978	-0.939873
H	2.095257	-0.701372	-2.331001
H	2.423802	1.569545	-1.684836
H	0.020212	1.542296	-2.139915
H	0.347491	2.632259	-0.787293
H	3.132796	0.225743	2.686610
H	3.742696	-1.327244	2.071114
H	2.007334	-0.951873	1.969887
H	5.373893	-0.135259	0.401565
H	4.721496	1.153366	-0.626949
H	4.846932	1.400933	1.130655

Structure 241

	X	Y	Z

C	-1.566893	-0.715901	-0.133570
C	-0.749642	-1.769511	-0.276173
C	0.700740	-1.643881	-0.637552
C	1.214841	-0.226947	-0.932900
C	0.445449	0.864885	-0.177225
C	-1.083185	0.688784	-0.259368
O	-1.824500	1.645698	-0.348232
Br	-3.417004	-0.939914	0.192989
O	1.517592	-2.053515	0.462881
C	2.813709	-1.477134	0.250039
O	2.574947	-0.274646	-0.518438
C	3.401308	-1.115477	1.605330
C	3.711888	-2.411687	-0.559017
O	0.840539	2.106000	-0.736133
O	1.066646	4.300644	-0.660582
C	0.797527	3.295910	-0.050739
C	0.467794	3.268649	1.425676
H	-1.136909	-2.778163	-0.165768
H	0.892667	-2.293371	-1.505587
H	1.178814	0.010911	-2.001268

H	0.709976	0.794129	0.885415
H	4.358720	-0.605227	1.471044
H	3.562533	-2.018477	2.200704
H	2.719366	-0.454468	2.145590
H	3.907063	-3.329427	0.003135
H	3.244212	-2.674385	-1.511980
H	4.663010	-1.917070	-0.774509
H	-0.521643	2.840492	1.605456
H	1.209452	2.686158	1.983347
H	0.484866	4.296287	1.786842

Structure 358 + AlCl₃

	X	Y	Z

C	-3.796706	-0.431020	-0.086327
C	-4.792071	0.584019	-0.093280
C	-6.133127	0.229731	0.138825
C	-6.445893	-1.103132	0.367568
C	-5.443281	-2.093723	0.369646
C	-4.107405	-1.774617	0.144902
C	-2.777966	1.555811	-0.499958
C	-4.123924	1.819317	-0.357973
H	-6.908415	0.990256	0.137063

H	-7.476672	-1.391164	0.549610
H	-5.715885	-3.127904	0.556304
H	-3.345589	-2.548100	0.164581
N	-2.571476	0.176733	-0.344194
C	-1.333684	-0.539677	-0.568005
H	-1.554746	-1.577749	-0.829509
H	-0.781291	-0.097047	-1.399350
C	-0.471133	-0.518551	0.630954
C	0.212742	-0.519835	1.653464
H	-4.571097	2.801862	-0.417715
Au	2.000251	-0.350818	0.194533
Cl	1.569503	-2.438759	-0.874629
Cl	4.052883	-0.178692	-0.929182
Cl	2.431510	1.727417	1.292397
H	0.540225	-0.501978	2.672642
C	-1.727414	2.531384	-0.694365
H	-2.034306	3.561011	-0.885572
N	-0.483188	2.220880	-0.591181
O	0.341259	3.315662	-0.779869
H	1.203460	2.989224	-0.468224

Structure 358

	X	Y	Z

C	-3.809030	-0.642226	0.120640
C	-3.488525	0.650297	-0.351801
C	-2.168620	1.048375	-0.541229
C	-1.163827	0.115219	-0.251049
C	-1.465540	-1.188608	0.235323
C	-2.811524	-1.561810	0.416721
N	0.210751	0.229610	-0.362853
C	-0.215759	-1.847506	0.430185
H	-4.851429	-0.914488	0.256065
H	-4.289435	1.351359	-0.567142
H	-1.935841	2.049856	-0.887861
H	-3.061636	-2.553424	0.783134
H	-0.055781	-2.856514	0.785171
C	0.789268	-0.966878	0.066125
C	2.199860	-1.286267	0.113441
H	2.446269	-2.278844	0.497068
C	0.893632	1.455520	-0.772191
H	1.898848	1.187719	-1.101681
H	0.358980	1.869804	-1.635145
C	0.976917	2.465763	0.290990

C	1.051860	3.309798	1.153492
H	1.115181	4.044739	1.923541
N	3.141733	-0.495721	-0.262518
O	4.394642	-1.114523	-0.095217
H	5.018040	-0.431309	-0.377702

Structure of TS1

	X	Y	Z

C	-4.054535	0.044494	0.138509
C	-3.481009	1.331652	0.058524
C	-2.102529	1.509843	-0.026566
C	-1.296131	0.363449	-0.025049
C	-1.859728	-0.944736	0.036275
C	-3.256265	-1.092459	0.128012
N	0.085432	0.239364	-0.077963
O	-0.768891	-1.866898	-0.015785
H	-5.133766	-0.053762	0.205565
H	-4.127582	2.204081	0.063588
H	-1.683052	2.508749	-0.087733
H	-3.699835	-2.082436	0.184988
H	-0.820047	-2.945916	0.035958
C	0.391937	-1.126181	-0.101136

C	1.764116	-1.581902	-0.086409
H	2.003237	-2.644557	-0.049603
N	2.646670	-0.656350	-0.052020
O	3.948990	-0.866108	0.093413
H	4.238918	0.121705	0.234030
C	0.974262	1.348546	-0.454315
H	0.506833	2.273384	-0.104858
H	1.024495	1.404573	-1.551940
C	2.359187	1.316229	0.076254
C	3.487981	1.764612	0.373693
H	4.023805	2.662044	0.620529

Structure of Intermediate

	X	Y	Z

C	4.070508	0.009025	-0.095630
C	3.522526	1.306520	-0.000549
C	2.145015	1.509234	0.058209
C	1.324839	0.376800	0.019330
C	1.856900	-0.946609	-0.058974
C	3.253343	-1.115105	-0.126109
N	-0.053363	0.269137	0.036081
C	0.747328	-1.849034	-0.042772

H	5.148898	-0.108662	-0.142191
H	4.187141	2.164766	0.026345
H	1.733119	2.511182	0.129691
H	3.683082	-2.110340	-0.194371
H	0.778551	-2.927993	-0.100227
C	-0.400231	-1.075326	0.033445
C	-1.778153	-1.437937	0.091715
H	-2.097485	-2.470746	0.128613
N	-2.754581	-0.540114	0.052361
O	-3.995985	-0.867111	0.029129
H	-4.371233	1.373892	-0.624809
C	-1.031190	1.277114	0.403099
H	-0.773759	2.231632	-0.061941
H	-1.019889	1.422308	1.495516
C	-2.421779	0.873724	-0.036453
C	-3.371233	1.731255	-0.413722
H	-3.152182	2.789704	-0.498289

Structure TS2

	X	Y	Z

C	4.063376	0.017349	0.039199
C	3.510100	1.314794	-0.080697

C	2.134410	1.511109	-0.117083
C	1.320181	0.373776	-0.039422
C	1.852447	-0.946849	0.080956
C	3.254703	-1.106443	0.124080
N	-0.054704	0.268392	-0.034629
C	0.753650	-1.853567	0.128975
H	5.143040	-0.095002	0.068648
H	4.172851	2.172773	-0.138621
H	1.710743	2.507636	-0.194369
H	3.690453	-2.096625	0.220115
H	0.795466	-2.929703	0.219556
C	-0.407453	-1.094668	0.045028
C	-1.774934	-1.474600	-0.047472
H	-2.081484	-2.512348	-0.044028
N	-2.770019	-0.579938	-0.110113
O	-4.015779	-0.886515	-0.172739
C	-1.074901	1.223388	-0.255239
H	-0.915050	1.825368	-1.150067
H	-1.742027	2.419468	0.245423
C	-2.398618	0.778806	-0.007842
C	-3.182142	1.873666	0.409082
H	-2.960279	2.282354	1.392690
H	-4.219322	1.998458	0.098377

Structure 360

	X	Y	Z

C	4.090899	0.104492	0.000070
C	3.503296	1.391465	0.000097
C	2.121575	1.547437	0.000030
C	1.342054	0.385534	-0.000104
C	1.907024	-0.924281	-0.000073
C	3.314219	-1.044869	0.000000
C	-0.039081	0.235001	-0.000095
C	0.838243	-1.868956	-0.000015
H	5.173562	0.019247	0.000106
H	4.140149	2.270465	0.000180
H	1.675402	2.537361	0.000098
H	3.778382	-2.026651	0.000002
H	0.916702	-2.946322	0.000068
C	-0.344920	-1.144322	-0.000065
C	-1.711399	-1.502158	0.000034
H	-2.047100	-2.529810	-0.000034
N	-2.682397	-0.580434	-0.000010
O	-3.927336	-0.901145	0.000171
C	-1.043544	1.169721	-0.000046

H	-0.747842	2.210980	-0.000060
H	-3.132101	2.789218	0.000202
C	-2.351702	0.807509	-0.000139
C	-3.501690	1.760678	0.000036
H	-4.136269	1.604374	0.877557
H	-4.136169	1.604833	-0.877695

Structure 376b + AIC13

	X	Y	Z

C	3.122894	-0.257437	-1.007821
C	4.443874	-0.179331	-0.488667
C	5.370032	0.687047	-1.097392
C	4.960329	1.448092	-2.183271
C	3.640861	1.362308	-2.675692
C	2.701289	0.514073	-2.098147
C	3.261107	-1.675301	0.746684
C	4.501536	-1.082418	0.616082
H	6.386850	0.756355	-0.721664
H	5.663458	2.121035	-2.664839
H	3.350690	1.969872	-3.527746
H	1.686492	0.459302	-2.480167
H	2.415189	-1.184441	-0.254339

C	0.995763	-1.431075	-0.420077
H	0.772413	-1.608417	-1.476577
H	0.716432	-2.318457	0.151169
C	0.161352	-0.270433	0.041108
C	0.174661	0.849659	0.601106
C	0.103862	2.100886	1.226084
C	-0.242672	2.188086	2.597822
C	0.384331	3.275832	0.484386
C	-0.303528	3.432846	3.207743
H	-0.478277	1.277986	3.138189
C	0.326635	4.510856	1.113032
H	0.644090	3.187416	-0.564914
C	-0.016959	4.587922	2.469138
H	-0.576627	3.510829	4.254929
H	0.542208	5.415490	0.554117
H	-0.065551	5.558620	2.953978
H	5.359848	-1.297845	1.237834
Au	-1.964810	-0.354229	-0.449470
Cl	-1.320660	0.159356	-2.692120
Cl	-4.217140	-0.679204	-1.106262
Cl	-2.496066	-0.855894	1.816435
C	2.926887	-2.674797	1.739552
H	3.735354	-2.908989	2.444691

N	1.789618	-3.269716	1.811783
O	1.635506	-4.203109	2.806589
H	2.467131	-4.268362	3.317375

Structure 409a + AuCl₃

	X	Y	Z

C	-0.388163	3.789310	-0.246438
C	0.646165	4.559749	0.345509
C	0.439510	5.934800	0.547871
C	-0.772173	6.495871	0.163510
C	-1.785652	5.710313	-0.419246
C	-1.611830	4.344759	-0.629622
C	1.368090	2.405908	0.196143
C	1.732948	3.664584	0.612850
H	1.217087	6.546408	0.995841
H	-0.944951	7.557043	0.314410
H	-2.723135	6.175657	-0.707515
H	-2.404532	3.747099	-1.069898
N	0.073849	2.478854	-0.351387
C	-0.702308	1.382433	-0.877724
H	-1.263258	1.693721	-1.765648
H	-0.037793	0.565979	-1.174744

C	-1.646341	0.918204	0.160693
C	-2.399247	0.648920	1.095688
C	2.185461	1.198695	0.200372
C	3.515713	1.055782	-0.161274
C	3.831027	-0.308987	0.064761
N	1.779954	-0.050716	0.601982
H	4.143119	1.833487	-0.568525
H	0.911585	-0.334571	1.042487
N	2.762437	-0.965160	0.535661
C	5.106122	-1.011102	-0.161131
C	6.260605	-0.309363	-0.540700
C	5.187164	-2.404110	0.004448
C	7.464333	-0.980786	-0.751350
H	6.223328	0.768721	-0.666500
C	6.390965	-3.071831	-0.204732
H	4.296244	-2.949172	0.297075
C	7.534984	-2.364682	-0.584431
H	8.348056	-0.420792	-1.043985
H	6.436470	-4.149221	-0.072949
H	8.472641	-2.887873	-0.748298
H	2.681595	3.908387	1.069054
Au	-2.419286	-1.435854	0.107361
Cl	-3.929273	-0.715190	-1.585620

Cl	-2.723424	-3.676757	-0.504430
Cl	-0.858601	-2.048400	1.810014
H	-2.998722	0.671866	1.983328

Structure 409c + AuCl₃

	X	Y	Z

C	-0.304287	3.200545	-1.134549
C	0.517182	4.224538	-0.591612
C	0.053647	5.550739	-0.613004
C	-1.196448	5.818196	-1.158600
C	-1.997271	4.785793	-1.685965
C	-1.566155	3.461984	-1.680176
C	1.602082	2.239071	-0.359639
C	1.707629	3.588467	-0.112092
H	0.665288	6.352737	-0.209901
H	-1.565008	6.839394	-1.181645
H	-2.968707	5.025978	-2.107500
H	-2.188870	2.672002	-2.089275
N	0.378303	1.998266	-1.010508
C	-0.177484	0.721355	-1.371130
H	-0.677958	0.781041	-2.344027
H	0.623953	-0.013249	-1.467335

C	-1.200470	0.237880	-0.372034
C	-1.943632	0.615798	0.565769
C	-2.789716	0.925025	1.634005
C	-2.324907	0.782667	2.966968
C	-4.111206	1.376252	1.383413
C	-3.170021	1.094387	4.021311
H	-1.318521	0.416671	3.138338
C	-4.941502	1.683575	2.450249
H	-4.452399	1.464895	0.357848
C	-4.471444	1.544614	3.763206
H	-2.824956	0.985122	5.044041
H	-5.954488	2.027035	2.268811
H	-5.128135	1.785409	4.594036
C	2.608232	1.221468	-0.083617
C	3.986690	1.324881	-0.200890
C	4.505011	0.084270	0.248143
N	2.379410	-0.039105	0.408807
H	4.521409	2.175022	-0.595267
H	1.507275	-0.474027	0.691508
N	3.510060	-0.733528	0.618475
C	5.908229	-0.356958	0.327768
C	6.962194	0.522829	0.036842
C	6.215756	-1.676290	0.701157

C	8.287614	0.096612	0.114924
H	6.748619	1.548877	-0.247898
C	7.540126	-2.098859	0.780260
H	5.402963	-2.358741	0.924873
C	8.582824	-1.215778	0.486963
H	9.090148	0.792259	-0.113953
H	7.759976	-3.122699	1.069767
H	9.615260	-1.547879	0.547727
H	2.548647	4.060462	0.375068
Au	-1.757532	-1.848031	-0.494286
Cl	-3.301609	-1.220059	-2.192032
Cl	-2.205037	-4.151134	-0.811440
Cl	-0.148055	-2.306081	1.213466

APPENDIX C

ABSOLUTE ENERGIES OF OPTIMIZED STRUCTURES IN GAS PHASE [DFT(B3LYP)/6-31+G(D,P)]

Table 3: TS1

TS1					
	E(RB3LYP)	Thermal Correction to Gibbs Free Energy	Total	Activation Barrier	Heat of Reaction
Reactant	- 647,943391596	0,15231	- 647,79108		
TS	- 647,902751073	0,15403	- 647,74872	26,58735	- 24,92123
Product	- 647,990048705	0,15925	- 647,83080		

Table 4. TS2

TS2				
	E(RB3LYP)	Thermal Correction to Gibbs Free Energy	Total	Heat of Reaction
Reactant	-647,990049170	0,15925	-647,83080	
TS	-647,871751211	0,15330	-647,71845	70,49709
Product	-648,012987553	0,15899	-647,85399	

CURRICULUM VITAE

Personal Information

Surname; Name: Kaya, Serdal
Nationality: Turkish (TC)
Date and Place of Birth: 30 March 1982, Ankara
Marital Status: Married
Email: serdalkaya@gmail.com; kserdal@metu.edu.tr

Education

Degree	Institution	Year of graduation
PhD	METU	2015
BS	Selcuk University	2006

Foreign Language

English (fluent)

Work Experience

Year	Place	Enrollment
2008–Present	METU	Research and Teaching Assistant

Publications

1. Guven, S., Ozer, M.S., **Kaya, S.**, Menges, N., Balci, M., “Gold Catalyzed Oxime-Oxime Rearrangement”, *Org. Lett.* **2015**, 17, 2660–2663.
2. Basceken, S., **Kaya, S.**, Balci, M., “Gold-catalyzed and NaH-supported Cyclization Reactions of *N*-Propargylated Indole Derivatives with Pyrazole and Pyrrole Rings: Synthesis of Pyrazolo-diazepino-indole, Pyrazolo-pyrazino-indole, and Pyrrolo-pyrazino-indole”, *J. Org. Chem.* **2015**, 80, 12552–12561.

International Conference Proceedings

1. **Kaya, S.**, Basceken, S., Balci, M., Trans Mediterranean Colloquium on Heterocyclic Chemistry, TRAMECH VIII, “Synthesis of pyrazolo-pyrazino- and pyrazolo-diazepino-indole derivatives via alkyne cyclization reactions”, Antalya, Turkey, 2015 (Poster Presentation)
2. Tan, M., **Kaya, S.**, Balci, M., Trans Mediterranean Colloquium on Heterocyclic Chemistry, TRAMECH VIII, “Synthesis of pyrazino[1,2-a:4,3-a']diindole skeleton: Propargylation and cyclization reactions of 2,2'-bisindole”, Antalya, Turkey, 2015 (Poster Presentation)
3. **Kaya, S.**, Mengeş, N., Balcı, M., Anatolian Conference on Synthetic Organic Chemistry, “Oxime-Oxime Rearrangement via Gold Catalyzed Alkyne Cyclization Reactions of N-Alkyne Substituted Indole Derivatives”, Antalya, 2015, (Poster Presentation)
4. **Kaya, S.**, Mengeş, N., Balcı, M., 13. Ibn Sina International Conference on Pure and Applied Heterocyclic Chemistry, “Gold Catalyzed Alkyne Cyclization Reactions of N-Alkyne Substituted Indole Derivatives: Oxime-Oxime Rearrangement”, Hurghada, Egypt, 2015, (Oral Presentation)
5. **Kaya, S.**, Kılbaş, B., Balcı M., 1. International Chemical and Chemical Engineering Conference, “A New Insight to Synthesize Haloconduritol Derivatives”, Baku, Azerbaijan, 2013 (Poster Presentation)

National Conference Proceedings

1. **Kaya, S.**, Sarı, Ö., Balcı, M., 1. Uluslararası Katılımlı Ulusal Hesaplamalı Kimya Çalıştayı, “İndol Kondense Pirazin-N-Oksit Halkasının Oluşturulması ve Reaksiyon Mekanizmasının DFT Yöntemi ile Modellenmesi” Van, Turkey, 2014, (Poster Presentation)
2. **Kaya, S.**, Mengeş, N., Balcı, M., 2. Ulusal Organik Kimya Kongresi, “N-Sübstitüe İndol Türevlerinin Elektrofilik Halkalaşma Reaksiyonları: Pirazinoindol-N-oksit Sentezi ve Oksim-Oksim Düzenlenmesi”, Ankara, Turkey, 2014 (Poster Presentation)
3. Özer, M.S., Güven, S., **Kaya, S.**, Balcı, M., 2. Ulusal Organik Kimya Kongresi, “Organik Kimyada Yeni Bir Düzenlenme: Oksim-Oksim Düzenlenmesi”, Ankara, Turkey, 2014, (Oral Presentation)
4. **Kaya, S.**, Menges, N., Balcı, M., 2. İlaç Kimyası, Üretimi, Teknolojisi ve Standardizasyonu Kongresi, “N-Sübstitüe İndol Türevlerinin Elektrofilik Halkalaşma Reaksiyonları”, Antalya, Turkey, 2014 (Poster Presentation)
5. Şeybek, A.F., **Kaya, S.**, Balcı, M., 2. İlaç Kimyası, Üretimi, Teknolojisi ve Standardizasyonu Kongresi, “İndol Halkasına Kondense Pirazin ve Oksazin Bileşiklerinin Sentezlenmesi”, Antalya, Turkey, 2014 (Poster Presentation)
6. **Kaya, S.**, Kılbaş, B., Balcı, M., 1. İlaç Kimyası, Üretimi, Teknolojisi ve Standardizasyonu Kongresi, “A New Methods to Synthesize Haloconduritol

- Derivatives: The Potential Alpha-Glycosidase Inhibitor”, Antalya, Turkey, 2013 (Poster Presentation)
7. Şeybek, A.F., **Kaya, S.**, Balcı, M., 1. İlaç Kimyası, Üretimi, Teknolojisi ve Standardizasyonu Kongresi, “İndol Halkasına Kondense Olmuş 6- ve 7- Üyeli Azot Atomu İçeren Heterohalkalı Sistemlerin Tasarlanması Üzerine Yapılan Çalışmalar”, Antalya, Turkey, 2013 (Poster Presentation)
 8. Çokol, N.K., **Kaya, S.**, Balcı, M., 1. İlaç Kimyası, Üretimi, Teknolojisi ve Standardizasyonu Kongresi, “Yeni Bir Yöntemle Bis-Aminoinositol Sentezi”, Antalya, Turkey, 2013 (Poster Presentation)
 9. Çokol, N.K., **Kaya, S.**, Balcı, M., 26. Uluslararası Katılımlı Ulusal Kimya Kongresi, “Yeni Bir Yöntemle Bis-aminoinositol Sentezi”, Muğla, Turkey, 2012 (Oral Presentation)
 10. Şeybek, A.F., **Kaya, S.**, Balcı, M., 26. Uluslararası Katılımlı Ulusal Kimya Kongresi, “İndol Halkasına Kondense Olmuş 6- ve 7- Üyeli Azot Atomu İçeren Heterohalkalı Sistemlerin Tasarlanması Üzerine Yapılan Çalışmalar”, Muğla, Turkey, 2012 (Poster Presentation)
 11. **Kaya, S.**, Kılbaş, B., Balcı, M., 25. Uluslararası Katılımlı Ulusal Kimya Kongresi, “Bromosikloheksentriol Sentezi: Quercitol Sentezi için Anahtar Bileşik”, Erzurum, Turkey, 2011, (Poster Presentation)
 12. Çokol, N.K., **Kaya, S.**, Balcı, M., 25. Uluslararası Katılımlı Ulusal Kimya Kongresi, “Yeni Bir Yöntemle Bis-aminoinositol Sentezi”, Erzurum, Turkey, 2011, (Poster Presentation)
 13. Korkmaz, N., **Kaya, S.**, Balcı, M., 24. Ulusal Kimya Kongresi, “Yeni Bir Yöntemle Aminokonduritol Sentezi”, Zonguldak, Turkey, 2010, (Poster Presentation)
 14. **Kaya, S.**, Kılbaş, B., Balcı, M., 24. Ulusal Kimya Kongresi, “Halokonduritol Sentezinde Yeni Bir Yöntem”, Zonguldak, Turkey, 2010, (Poster Presentation)
 15. Doğan, Ş.D., Altun, Y., Kaya, S., Balcı, M., 24. Ulusal Kimya Kongresi, “Polihidroksisiklopentan Türevlerinin Sentezi İçin Yeni Bir Yöntem”, Zonguldak, Turkey, 2010, (Poster Presentation)
 16. **Kaya, S.**, Kılbaş, B., Balcı, M., 23. Ulusal Kimya Kongresi, “Yeni Halokonduritol Türevlerinin Sentezi”, Sivas, Turkey, 2009, (Poster Presentation)